frontiers | Research Topics

Respiratory RNA viruses: Molecular mechanisms of viral replication and pathogenicity

Edited by
Wei Wei, Qiang Ding and Shijian Zhang

Published in
Frontiers in Microbiology

ISSN 1664-8714
ISBN 978-2-8325-4803-5
DOI 10.3389/978-2-8325-4803-5

About Frontiers

Frontiers is more than just an open access publisher of scholarly articles: it is a pioneering approach to the world of academia, radically improving the way scholarly research is managed. The grand vision of Frontiers is a world where all people have an equal opportunity to seek, share and generate knowledge. Frontiers provides immediate and permanent online open access to all its publications, but this alone is not enough to realize our grand goals.

Frontiers journal series

The Frontiers journal series is a multi-tier and interdisciplinary set of open-access, online journals, promising a paradigm shift from the current review, selection and dissemination processes in academic publishing. All Frontiers journals are driven by researchers for researchers; therefore, they constitute a service to the scholarly community. At the same time, the *Frontiers journal series* operates on a revolutionary invention, the tiered publishing system, initially addressing specific communities of scholars, and gradually climbing up to broader public understanding, thus serving the interests of the lay society, too.

Dedication to quality

Each Frontiers article is a landmark of the highest quality, thanks to genuinely collaborative interactions between authors and review editors, who include some of the world's best academicians. Research must be certified by peers before entering a stream of knowledge that may eventually reach the public - and shape society; therefore, Frontiers only applies the most rigorous and unbiased reviews. Frontiers revolutionizes research publishing by freely delivering the most outstanding research, evaluated with no bias from both the academic and social point of view. By applying the most advanced information technologies, Frontiers is catapulting scholarly publishing into a new generation.

What are Frontiers Research Topics?

Frontiers Research Topics are very popular trademarks of the *Frontiers journals series*: they are collections of at least ten articles, all centered on a particular subject. With their unique mix of varied contributions from Original Research to Review Articles, Frontiers Research Topics unify the most influential researchers, the latest key findings and historical advances in a hot research area.

Find out more on how to host your own Frontiers Research Topic or contribute to one as an author by contacting the Frontiers editorial office: frontiersin.org/about/contact

Respiratory RNA viruses: Molecular mechanisms of viral replication and pathogenicity

Topic editors

Wei Wei — First Affiliated Hospital of Jilin University, China

Qiang Ding — Tsinghua University, China

Shijian Zhang — Dana–Farber Cancer Institute, United States

Citation

Wei, W., Ding, Q., Zhang, S., eds. (2024). *Respiratory RNA viruses: Molecular mechanisms of viral replication and pathogenicity*. Lausanne: Frontiers Media SA.

doi: 10.3389/978-2-8325-4803-5

Table of contents

05 Variable number tandem repeats of a 9-base insertion in the N-terminal domain of severe acute respiratory syndrome coronavirus 2 spike gene
Tetsuya Akaishi, Kei Fujiwara and Tadashi Ishii

14 Altered cell function and increased replication of rhinoviruses and EV-D68 in airway epithelia of asthma patients
Manel Essaidi-Laziosi, Léna Royston, Bernadett Boda, Francisco Javier Pérez-Rodriguez, Isabelle Piuz, Nicolas Hulo, Laurent Kaiser, Sophie Clément, Song Huang, Samuel Constant and Caroline Tapparel

25 pH-dependent endocytosis mechanisms for influenza A and SARS-coronavirus
Amar Aganovic

35 COVID-19 and the cardiovascular system: a study of pathophysiology and interpopulation variability
Yifan Zhao, Xiaorong Han, Cheng Li, Yucheng Liu, Jiayu Cheng, Binay Kumar Adhikari and Yonggang Wang

45 The RSV F p27 peptide: current knowledge, important questions
Wanderson Rezende, Hadley E. Neal, Rebecca E. Dutch and Pedro A. Piedra

53 Genetic characterization and whole-genome sequencing-based genetic analysis of influenza virus in Jining City during 2021–2022
Libo Li, Tiantian Liu, Qingchuan Wang, Yi Ding, Yajuan Jiang, Zengding Wu, Xiaoyu Wang, Huixin Dou, Yongjian Jia and Boyan Jiao

66 Human beta defensin-3 mediated activation of β-catenin during human respiratory syncytial virus infection: interaction of HBD3 with LDL receptor-related protein 5
Swechha M. Pokharel, Indira Mohanty, Charles Mariasoosai, Tanya A. Miura, Lisette A. Maddison, Senthil Natesan and Santanu Bose

83 Respiratory viruses interacting with cells: the importance of electrostatics
Daniel Lauster, Klaus Osterrieder, Rainer Haag, Matthias Ballauff and Andreas Herrmann

97 Construction of an infectious cloning system of porcine reproductive and respiratory syndrome virus and identification of glycoprotein 5 as a potential determinant of virulence and pathogenicity
Yuqing Wei, Guo Dai, Mei Huang, Lianghai Wen, Rui Ai Chen and Ding Xiang Liu

109 Novel receptor, mutation, vaccine, and establishment of coping mode for SARS-CoV-2: current status and future
Zhaomu Zeng, Xiuchao Geng, Xichao Wen, Yueyue Chen, Yixi Zhu, Zishu Dong, Liangchao Hao, Tingting Wang, Jifeng Yang, Ruobing Zhang, Kebin Zheng, Zhiwei Sun and Yuhao Zhang

131 Characterization of host substrates of SARS-CoV-2 main protease
Ivonne Melano, Yan-Chung Lo and Wen-Chi Su

138 Diverse roles of lung macrophages in the immune response to influenza A virus
Haoning Li, Aoxue Wang, Yuying Zhang and Fanhua Wei

149 Inhaled nitric oxide: can it serve as a savior for COVID-19 and related respiratory and cardiovascular diseases?
Yifan Zhao, Cheng Li, Shuai Zhang, Jiayu Cheng, Yucheng Liu, Xiaorong Han, Yinghui Wang and Yonggang Wang

158 Porcine epidemic diarrhea virus causes diarrhea by activating EGFR to regulates NHE3 activity and mobility on plasma membrane
YiLing Zhang, Shujuan Zhang, Zhiwei Sun, Xiangyang Liu, Guisong Liao, Zheng Niu, ZiFei Kan, ShaSha Xu, JingYi Zhang, Hong Zou, Xingcui Zhang and ZhenHui Song

170 Psoriasis comorbidity management in the COVID era: a pressing challenge
Yang Song, Lei Yao, Shanshan Li and Junfeng Zhou

178 The domestication of SARS-CoV-2 into a seasonal infection by viral variants
Ryley D. McClelland, Yi-Chan James Lin, Tyce N. Culp, Ryan Noyce, David Evans, Tom C. Hobman, Vanessa Meier-Stephenson and David J. Marchant

184 Molecular biology of canine parainfluenza virus V protein and its potential applications in tumor immunotherapy
Huai Cheng, Hewei Zhang, Huanchang Cai, Min Liu, Shubo Wen and Jingqiang Ren

199 Classification, replication, and transcription of *Nidovirales*
Ying Liao, Huan Wang, Huiyu Liao, Yingjie Sun, Lei Tan, Cuiping Song, Xusheng Qiu and Chan Ding

frontiers | Frontiers in Microbiology

TYPE Original Research
PUBLISHED 04 January 2023
DOI 10.3389/fmicb.2022.1089399

OPEN ACCESS

EDITED BY
Wei Wei,
First Affiliated Hospital of Jilin University, China

REVIEWED BY
Rajesh Pandey,
CSIR-Institute of Genomics and Integrative Biology (CSIR-IGIB), India
Guan-Zhu Han,
Nanjing Normal University, China

*CORRESPONDENCE
Tetsuya Akaishi
✉ t-akaishi@med.tohoku.ac.jp

SPECIALTY SECTION
This article was submitted to Virology, a section of the journal Frontiers in Microbiology

RECEIVED 04 November 2022
ACCEPTED 12 December 2022
PUBLISHED 04 January 2023

CITATION
Akaishi T, Fujiwara K and Ishii T (2023) Variable number tandem repeats of a 9-base insertion in the N-terminal domain of severe acute respiratory syndrome coronavirus 2 spike gene.
Front. Microbiol. 13:1089399.
doi: 10.3389/fmicb.2022.1089399

Variable number tandem repeats of a 9-base insertion in the N-terminal domain of severe acute respiratory syndrome coronavirus 2 spike gene

Tetsuya Akaishi[1,2]*, Kei Fujiwara[3] and Tadashi Ishii[1,2]

[1]Department of Education and Support for Regional Medicine, Tohoku University, Sendai, Japan, [2]COVID-19 Testing Center, Tohoku University, Sendai, Japan, [3]Department of Gastroenterology and Metabolism, Nagoya City University, Nagoya, Japan

Introduction: The world is still struggling against the pandemic of coronavirus disease 2019 (COVID-19), caused by severe acute respiratory syndrome coronavirus 2 (SARS-CoV-2), in 2022. The pandemic has been facilitated by the intermittent emergence of variant strains, which has been explained and classified mainly by the patterns of point mutations of the spike (*S*) gene. However, the profiles of insertions/deletions (indels) in SARS-CoV-2 genomes during the pandemic remain largely unevaluated yet.

Methods: In this study, we first screened for the genome regions of polymorphic indel sites by performing multiple sequence alignment; then, NCBI BLAST search and GISAID database search were performed to comprehensively investigate the indel profiles at the polymorphic indel hotspot and elucidate the emergence and spread of the indels in time and geographical distribution.

Results: A polymorphic indel hotspot was identified in the N-terminal domain of the *S* gene at approximately 22,200 nucleotide position, corresponding to 210–215 amino acid positions of SARS-CoV-2 S protein. This polymorphic hotspot was comprised of adjacent 3-base deletion (5′-ATT-3′; Spike_N211del) and 9-base insertion (5′-AGCCAGAAG-3′; Spike_ins214EPE). By performing NCBI BLAST search and GISAID database search, we identified several types of tandem repeats of the 9-base insertion, creating an 18-base insertion (Spike_ins214EPEEPE, Spike_ins214EPDEPE). The results of the searches suggested that the two-cycle tandem repeats of the 9-base insertion were created in November 2021 in Central Europe, whereas the emergence of the original one-cycle 9-base insertion (Spike_ins214EPE) would date back to the middle of 2020 and was away from the Central Europe. The identified 18-base insertions based on 2-cycle tandem repeat of the 9-base insertion were collected between November 2021 and April 2022, suggesting that these mutations could not survive and have been already eliminated.

Discussion: The GISAID database search implied that this polymorphic indel hotspot to be with one of the highest tolerability for incorporating indels in SARS-CoV-2 S gene. In summary, the present study identified a variable number of tandem repeat of 9-base insertion in the N-terminal domain of SARS-CoV-2 S gene, and the repeat could have occurred at different time from the insertion of the original 9-base insertion.

KEYWORDS

BLAST search, insertions/deletions, GISAID, N-terminal domain, variable number tandem repeats, spike gene, severe acute respiratory syndrome coronavirus 2

1. Introduction

The pandemic of coronavirus disease 2019 (COVID-19), caused by severe acute respiratory syndrome coronavirus 2 (SARS-CoV-2), is still ongoing worldwide still in end of 2022 (Alexandridi et al., 2022; Biancolella et al., 2022). The pandemic has been sustained in the last 3 years, driven by the intermittent emergence of consequential variant strains (Papanikolaou et al., 2022; Viana et al., 2022). By now, the lineages of the variant strains have been classified mainly based on the types of point mutations in the spike (*S*) gene of the virus. This is reasonable because SARS-CoV-2 Sprotein has been known to play major roles in binding to the receptor angiotensin-converting enzyme 2 (ACE2) and also as the target antigen of most neutralizing antibodies (Liu et al., 2020; Zhang et al., 2020; Min and Sun, 2021). Recently, the genomes of many SARS-related coronavirus species, including SARS-CoV-2 from humans, have reported to incorporate many mutation hotspots with relatively long and highly divergent insertions/deletions (indels; Akaishi, 2022b; Akaishi et al., 2022b), which are not common in many of other virus families (Willemsen and Zwart, 2019; Akaishi, 2022a). These indel hotspots with highly divergent RNA sequences in SARS-related coronavirus species were identified to be clustered in several specific genome positions, including the non-structural protein 2 (Nsp2) and Nsp3 of the open-reading frame 1a (*ORF1a*), N-terminal domain (NTD) of *S* gene, and *ORF8* gene (Akaishi et al., 2022a). Many of these divergent and complex indel hotspots are away from the known genomic recombination sites in the viruses (Alexandridi et al., 2022; Lytras et al., 2022). However, the genomic regions and patterns of highly polymorphic indel sites in the genomes of SARS-CoV-2 from humans have not been enough evaluated until now. Moreover, the geographical distributions and prevailing periods of each indel pattern remains largely unevaluated. Therefore, in this report, we searched for the polymorphic indel hotspots in the genomes of SARS-CoV-2 collected from humans and estimated the time period and geographical locations of the emergence of such polymorphic indels. Furthermore, we are going to report an insertion site with variable number tandem repeat of 9-base insertion, found in the NTD of the SARS-CoV-2 *S* gene.

2. Materials and methods

2.1. Initially evaluated genome sequences

In this study, a total of 20 SARS-CoV-2 genome sequences from different timings and countries were initially collected to search for the presence of polymorphic indel sites, which were randomly selected from the NCBI GenBank Database in October 2022, based on the sample collection time and geographic distribution. These sequences were first used to preliminarily search for the location of the polymorphic site across the SARS-CoV-2 genome in the last 3 years. The list of the initially collected 20 sequences is shown in Table 1 (Holland et al., 2020; Wu et al., 2020; Wilkinson et al., 2021; De Marco et al., 2022).

2.2. Multiple sequence alignment

By using the initially collected 20 virus genome sequences, multiple sequence alignment was performed by using Molecular Evolutionary Genetics Analysis Version 11 (MEGA11) software (Tamura et al., 2021). The Multiple Sequence Comparison by Log-Expectation (MUSCLE) program was run to align the whole genome sequences. As for the alignment parameters, gap opening penalty score was set with −400 and gap extension penalty score was set with 0. The presence of polymorphic indel sites were manually searched across the whole genomes using the aligned sequences. Polymorphism of the indel site was determined if more than two patterns of indels at the indel site, including the nearby sequences of ±10 bases, were observed. Point mutation patterns in the indel sites were not considered to decide the polymorphism of the indels.

2.3. Basic Local Alignment Search Tool (BLAST) search

The identified sites of polymorphic RNA sequences based on sequence alignment were further evaluated by performing sequence search with NCBI basic local alignment search tool (BLAST) to know the numbers of registered sequences with 100% sequence identity with each of the identified polymorphic RNA sequence.[1] Sequences those are 100% identical to the reference sequence were determined when they achieved 100% both for with the query cover rate and percent sequence identity. To pick up other types of overlooked polymorphic RNA sequence patterns, the identified sequences upon highly similar sequence search method (megablast) with <100% sequence identity were further checked manually and visually one by one.

Furthermore, to search for other patterns of polymorphic sequence which are not included in the initially recruited 20

1 https://blast.ncbi.nlm.nih.gov/Blast.cgi

TABLE 1 List of the initially recruited 20 SARS-CoV-2 strains.

GenBank accession ID	Collection date	Country	Sequence names
MN908947	December 2019	China	Wuhan-Hu-1 (original)
ON507065	January 17, 2022	Italy	SARS-CoV-2/human/ITA/ID6_170122/2022
MT339039	May 17, 2020	United States	SARS-CoV-2/human/United States/AZ-ASU2922/2020
MT844030	July 20, 2020	Brazil	SARS-CoV-2/human/BRA/RJ-DCVN4/2020
OP699312	October 09, 2021	United States	SARS-CoV-2/human/United States/WA-S21827/2021
OW981938	May 07, 2022	Switzerland	hCoV-19/Switzerland/SG-ETHZ-674753/2022
OL989090	April 26, 2021	Philippines	SARS-CoV-2/human/PHL/210430–1/2021
OP355305	January 15, 2022	India	SARS-CoV-2/Homosapiens/IND/EPI_ISL_11887846/2022
OL989098	July 05, 2021	Argentina	SARS-CoV-2/human/ARG/210711–54/2021
OP024160	March 03, 2022	Japan	SARS-CoV-2/human/JPN/HiroC311c/2022
ON513706	January 17, 2022	United States	SARS-CoV-2/human/United States/TG996464/2022
ON819429	January 07, 2022	Australia	SARS-CoV-2/human/AUS/QIMR01/2022
OM945722	February 11, 2022	Turkey	SARS-CoV-2/human/TUR/ERAGEM-OM-1104/2022
ON032859	January 25, 2022	Russia	SARS-CoV-2/human/RUS/Altufjevo/2022
OM640073	January 19, 2022	Austria	SARS-CoV-2/human/AUT/SKV-316/2022
OM773467	January 19, 2022	South Africa	SARS-CoV-2/human/South Africa/NHLS-UCT-LA-Z842/2022
OP107796	July 01, 2022	Brazil	SARS-CoV-2/human/BRA/LACENAL-270228624/2022
OP279916	July 15, 2022	South Africa	SARS-CoV-2/human/ZAF/NHLS-UCT-LA-ZB06/2022
OP430898	2022	Germany	SARS-CoV-2/human/DEU/C63/2022
ON966115	March 31, 2022	Thailand	SARS-CoV-2/human/THA/BKK-ST023.8/2022

The initially recruited 20 SARS-CoV-2 sequences were randomly selected from NCBI GenBank Database, according to the sample collection time and geographical distribution. The countries of the sequences were selected to cover all of the five continents. These initially selected 20 sequences were aligned to screen for the presence of polymorphic indel sites in the genomes of SARS-CoV-2, developed during the COVID-19 pandemic since 2019.

sequences or are failed to be picked up by the megablast search, several patterns of hypothetical virtual sequences were prepared by gradually shortening the bases with deletion by 3 nucleotides or duplicating the bases with insertion up to 3 tandem repeats. For the collected sequences with indel polymorphisms, recombination analyses were performed using the Recombination Detection Program Version 5 (RDP5) to detect potential recombination sites across the whole virus genomes (Martin et al., 2021).

2.4. Global Initiative on Sharing All Influenza Data (GISAID) database search

Next, to investigate the prevalence of each observed indel type at the identified polymorphic indel site, the registered virus genome sequences worldwide were accessed *via* the Global Initiative on Sharing All Influenza Data (GISAID; Elbe and Buckland-Merrett, 2017; Shu and McCauley, 2017; Khare et al., 2021). A total of 14,066,931 genome sequences, which were registered and available up to December 1, 2022, were evaluated in the present study. The associated EPI_SET Identifier ID is specified in the subsequent data availability statement.

3. Results

3.1. Identified polymorphic site

First, the presence and location of polymorphic indel sites were screened with the initially recruited 20 virus genome sequences, which identified only one polymorphic indel site in the S1-NTD at approximately 22,190–22,210 nucleotide positions of the overall 29,903 nucleotides of SARS-CoV-2 Wuhan-Hu-1 genome. The aligned sequences around the identified polymorphic indel site with some of the randomly selected first 20 sequences are shown in Figure 1, together with the aligned sequences of some of the additional sequences detected by BLAST search. This indel site was comprised of two adjacent but distinct indels: 3-base deletion (5′-ATT-3′) and 9-base insertion (5’-AGCCAGAAG-3′). Among the initially recruited 20 sequences, both of the 3-base deletion and 9-base insertion were confirmed in the same 5 sequences, all of which were sampled and sequenced in 2022. These 5 sequences were distributed across the countries worldwide (United States, Japan, Italy, Australia, and Turkey). Sequences with these mutations accounted for 35.7% of the randomly selected sequences sampled in 2022 ($n = 5/14$ sequences). The estimated prevalence of these 3-base deletion and 9-base insertion among

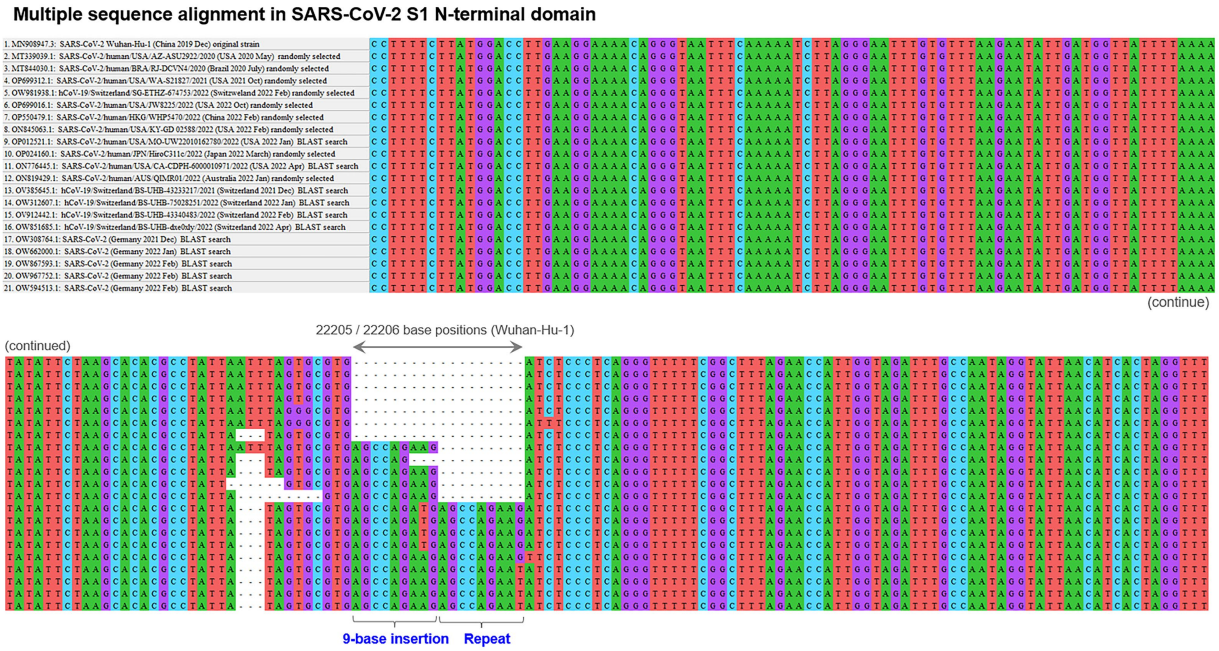

FIGURE 1
Polymorphic insertion/deletion hotspot in SARS-CoV-2 S1-NTD. The result of the multiple sequence alignment with some of the initially recruited sequences by random selection based on geographical distribution and other additional sequences identified with subsequent BLAST searches. This polymorphic indel site was comprised of two adjacent distinct indels: 3-base deletion and 9-base insertion. The combination of these 3-base deletion and 9-base insertion was confirmed in 5 of the randomly selected initial 20 sequences. Further BLAST searches with virtual RNA sequences of different indel patterns revealed the presence of SARS-CoV-2 strains with a 2-cycle tandem repeat of the 9-base insertion in the past. BLAST, basic local alignment search tool; S1-NTD, N-terminal domain of S1 gene; SARS-CoV-2, severe acute respiratory syndrome coronavirus 2.

the viruses worldwide in 2022 was approximately 20–50%, suggesting the rapid spread of the combination of these two indels all over the globe in the early 2022. To be noted here, more than half of the randomly selected virus strains in 2022 ($n = 9/14$ sequences) still preserved the original reference RNA sequences (i.e., sequence of Wuhan-Hu-1) in this polymorphic indel hotspot site.

3.2. BLAST search results for the polymorphic indels

Based on the finding of polymorphic indels basically comprised of 3-base deletion and 9-base insertion in the SARS-CoV-2 S1-NTD, NCBI BLAST search was performed for the identified sequences and other conceivable non-lethal virtual sequences. The search with a virtual sequence conceived from 2-cycle tandem repeat of the 9-base insertion identified a total of 1,257 registered sequences, 5 of which were from Germany and the others were from Switzerland. The presence of two different cycles of tandem repeat of the 9-base insertion exhibited the presence of variable number tandem repeats (VNTD) in RNA sequence of the SARS-CoV-2 genomes. The detailed sequences close to this polymorphic indel hotspot among the initially recruited and additionally identified sequences are shown in Figure 2A, together with the number of the identified sequences with 100% sequence identity to the entered search sequence based on the BLAST search. Recombination analysis using RDP5 was performed with these collected sequences, which did not detect any potential recombination signals across the whole virus genomes.

The identified sequences including both of the 3-base deletion (Spike_N211del) and one-cycle of 9-base insertion (Spike_ins214EPE) distributed across the countries worldwide (e.g., Germany, Switzerland, United Kingdom, Russia, United States, Kenya, Gambia, Australia, Denmark, New Zealand, India, Brazil, Myanmar, Korea, and Japan) in all five continents, as shown in Figure 2B. Based on the BLAST search, the exact time and geographical location of the emergence of Spike_ins214EPE mutation could not be determined. Meanwhile, the origin in time and location of the 18-base insertion, based on 2-cycle tandem repeat of the 9-base insertion, was more obvious because the number of the sequence was much smaller with 1,257 registered sequences. The geographical distribution of the 18-base insertion by the BLAST search result is shown in Figure 2C, most of which were collected in Switzerland since the late November 2021.

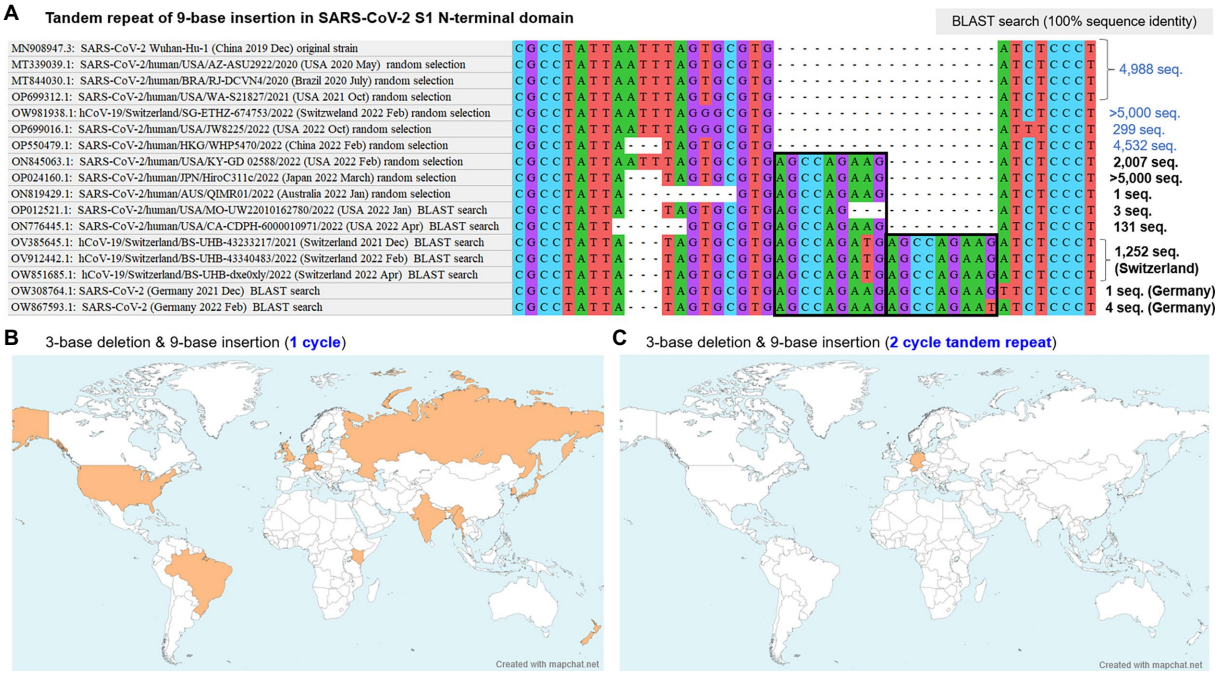

FIGURE 2
BLAST search results and geographic distribution of two-cycle tandem repeat of the 9-base insertion. **(A)** The aligned sequences at the identified polymorphic indel hotspot in SARS-CoV-2 S1-NTD are shown, together with the numbers of identified sequences with 100% sequence identity for each sequence based on the NCBI BLAST search. Both of the one-cycle and two-cycle tandem repeat of the 9-base insertion were dated from the November 2021 in Switzerland. The two-cycle tandem repeat did not spread across the globe, whereas the one-cycle 9-base insertion rapidly spread across the globe in 2022, estimated to account for 20–50% of the overall SARS-CoV-2 sampled from humans in 2022. **(B,C)** Geographic distributions of the one-cycle and two-cycles of the 9-base insertion with the nearby 3-base deletion. Although both cycles were suggested to originate in November 2021 in central Europe, the former rapidly spread across the globe, whereas the latter was limited in Switzerland. BLAST, basic local alignment search tool; S1-NTD, N-terminal domain of S1 gene; SARS-CoV-2, severe acute respiratory syndrome coronavirus 2.

3.3. GISAID database search results for the polymorphic indels

To further investigate the exact time and location of the emergence of the 9-base insertion (Spike_ins214EPE) and its 2-cycle tandem repeats (Spike_ins214EPEEPE and Spike_ins214EPDEPE), we decided to perform the sequence search *via* the GISAID database. The obtained numbers of the identified sequences are listed in Table 2. More than 95% of the sequences with insertions at 214 amino acid position in the S protein were with a 9-base insertion (ins214EPE), which accounted for 13.84% of all registered sequences worldwide by November 2022. The first sample with this 9-base insertion in the GISAID database was collected in May 2020 in the United States. Regarding the 18-base insertion, we could identify two types in the GISAID database (214EPDEPE, 214EPEEPE). The first sample with ins214EPDEPE was collected in November 2021 in Switzerland, and that with ins214EPEEPE was collected in December 2021 in Brazil. The finding of the different seasons and geographical locations of the 9-base insertion and its two-cycle tandem repeat suggests that the observed set of VNTR were not created all at once, but developed gradually in different seasons at different places.

Finally, to confirm that the finding of polymorphic insertion at the 214 amino acid position in the S protein is truly site-specific and it not common in other amino acid positions, the site-specific numbers of registered sequences in the GISAID database with insertions or deletions at each amino acid position in the S1-NTD and receptor-binding domain (RBD) of SARS-CoV-2 *S* gene are shown with line graphs in Figure 3. As can be seen, the 214 amino acid position in the S protein showed the highest peak of sequences with insertions in the evaluated 400 amino acid positions (i.e., 130–530 amino acid positions). This hotspot was also a hotspot for the point mutations in the previous variants of concern (VOCs), suggesting that this amino acid position has some potential roles for the survival of the virus and mutations at this position including indels would often function as beneficial mutations for the virus. Another notable finding of the line graphs was the asymmetrical distributions between the S1-NTD and the S1 RBD, although the frequency of point mutations in the previous VOCs was not apparently different between the two domains or even higher in the S1 RBD. This finding may suggest the different tolerability for incorporating indels between the two domains, with a lower tolerability in the S1 RBD compared to the S1-NTD.

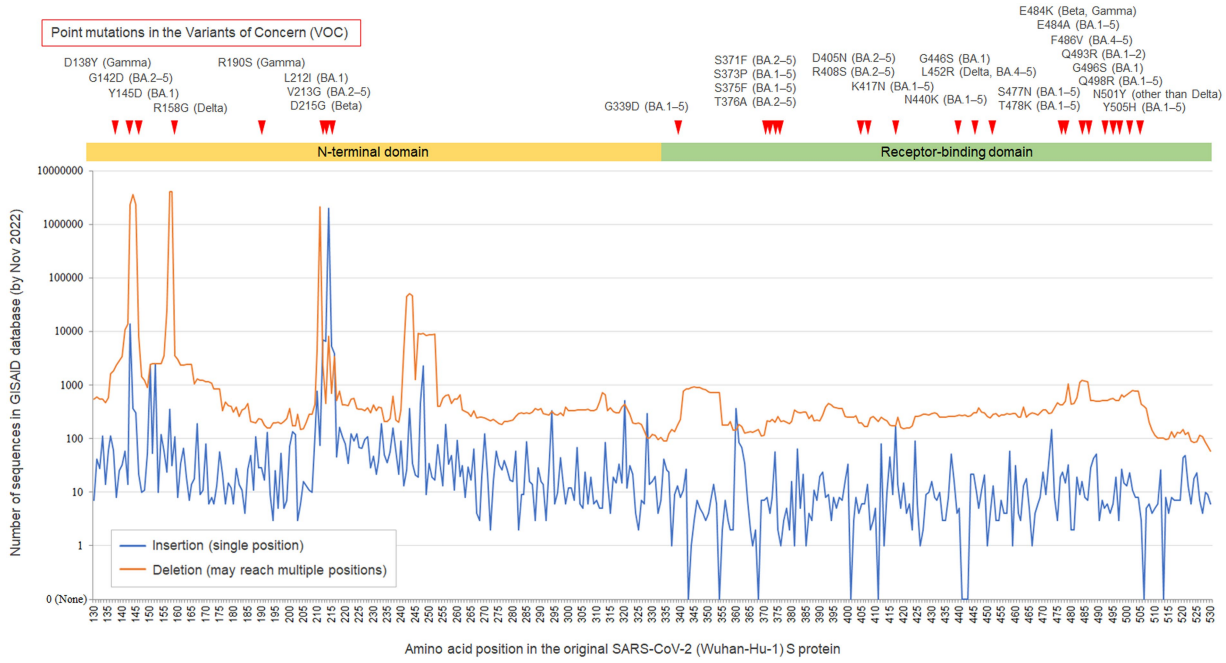

FIGURE 3
GISAID database search for the insertions/deletions in the N-terminal domain and receptor-binding domain of SARS-CoV-2 spike gene. The line graphs show the numbers of sequences sampled from humans with insertions/deletions (indels) at each amino acid position in the N-terminal domain (NTD) and receptor-binding domain (RBD) of the SARS-CoV-2 spike gene, which were registered in the GISAID database by December 01, 2022. The observed variable numbers tandem repeat of this study matches to the peak of insertion at 214 amino acid position of the S1-NTD. The asymmetrical line graphs suggest the different tolerability for incorporating indels between the SARS-CoV-2 S1-NTD and the S1-RBD, with a lower tolerability in the S1 RBD. The Y-axis scale is logarithmic.

4. Discussion

In this study, the presence of highly polymorphic indel hotspot in SARS-CoV-2 genomes, sampled from humans during the pandemic of COVID-19, was identified in the S1-NTD. This polymorphic indel site was comprised of the combination of adjacent 3-base deletion and nearby 9-base insertion. Furthermore, the NCBI BLAST search and GISAID database search identified several derivatives of the 9-base insertion, some of which were 18-base insertions based on two-cycle repeats of the 9-base insertion. The two-cycle tandem repeats of the 9-base insertion were suggested to have emerged in November 2021, possibly in the Central Europe including Switzerland and Germany, whereas the original one-cycle 9-base insertion could have dated back to the middle of 2020 away from the Central Europe. The two-cycle tandem repeat types have not been identified in samples collected after the April 2022, suggesting that this type of mutation could have already eliminated. Meanwhile, the one-cycle 9-base insertion type is still prevailing, known as Spike_214EPE insertion, which is one of the characteristic mutations of the Omicron variant BA.1 (Dhawan et al., 2022; Singh et al., 2022).

One of the notable findings of the present study was that it implied the possible importance of paying attention to mutations in genomic regions other than the SARS-CoV-2 S1 RBD, including S1-NTD, in monitoring and classifying the emerging consequential variant strains. Although the exact role of highly polymorphic indel site in the SARS-CoV-2 evolution and the emergence of VOCs remains undetermined, the high tolerability of S1-NTD for incorporating indels may suggest that the occurrence of polymorphic indels in this domain may be beneficial for the virus *via* some unknown mechanisms like escaping from host immunity. Another notable finding was that this study suggested the potential roles of indels and tandem repeats of inserted sequences, in addition to point mutations, in the process of SARS-CoV-2 genomic evolution. From before, VNTR has been broadly identified in the DNA sequences of the genomes in many organisms, including animals and wide variety of bacteria (Chang et al., 2007; Bilgin Sonay et al., 2015; Bakhtiari et al., 2021), but the reports of VNTR in virus genomes are currently limited (Sun et al., 1995; Avarre et al., 2011). Therefore, the process of emergence, prevalence, and potential role in virus evolution of VNTR remain largely unknown at present. The obtained results suggested that the one-cycle and two-cycle tandem repeat of the 9-base insertion emerged at different seasons in remote areas. This finding may suggest the possibility that previously inserted nucleotides in the virus genome are likely to be repeated and exhibit VNTR. While most of the extraordinarily long indels involving dozens of bases in coding regions would be deleterious

TABLE 2 Numbers of the registered genome sequences with each insertion type at Spike_214 amino acid position in GISAID database.

Insertion types	*n* (%)	Collected seasons and places
Any types of insertion at Spike_214 amino acid position	2,032,091/14,066,931 (14.45%)	March 2020 (Slovenia) – Present (worldwide)
18-base insertion (Spike_214EPDEPE)	1,259/14,066,931 (0.009%)	November 2021 (Switzerland) – April 2022 (Switzerland)
18-base insertion (Spike_214EPEEPE)	82/14,066,931 (0.0006%)	December 2021 (Brazil) – February 2022 (Brazil)
15-base insertion (Spike_214EPEEP)	0/14,066,931 (0.00%)	n.a.
12-base insertion (Spike_214EPEE)	0/14,066,931 (0.00%)	n.a.
9-base insertion (Spike_214EPE)	1,947,137/14,066,931 (13.84%)	May 2020 (United States) – Present (worldwide)
9-base insertion (Spike_214EPK)	1,133/14,066,931 (0.008%)	December 2021 (United Kingdom) – Aug 2022 (United States)
9-base insertion (Spike_214EPD)	284/14,066,931 (0.002%)	December 2021 (United Kingdom) – March 2022 (United States)
9-base insertion (Spike_214EPQ)	82/14,066,931 (0.0006%)	December 2021 (South Africa) – April 2022 (worldwide)
9-base insertion (Spike_214EPV, 214EPG)	26/14,066,931 (0.0002%)	ins214EPV: November 2021 (South Africa) – Aug 2022 (United States)
		ins214EPG: December 2021 (India) – May 2022 (United States)
9-base insertion (Spike_214EPA)	11/14,066,931 (< 0.0001%)	January 2022 (Germany) – March 2022 (Canada)
9-base insertion (Spike_214EPL)	4/14,066,931 (< 0.0001%)	ins214EPL: February 2022 (United Kingdom)
9-base insertion (Spike_214EPstop)	4/14,066,931 (<0.0001%)	January 2022 (United States) – May 2022 (United States)
9-base insertion (Spike_214EPP)	1/14,066,931 (<0.0001%)	January 2022 (United States)
9-base insertion (Spike_214EPF, EPI, EPS, EPM, EPT, EPY, EPH, EPN, EPC, EPW, EPR)	0/14,066,931 (0.00%)	n.a.
6-base insertion (Spike_214EP)	405/14,066,931 (0.003%)	Unknown
3-base insertion (Spike_214E)	361/14,066,931 (0.003%)	Unknown

The amino acids are written in one-letter code. For example, "214EPE" denotes that 9-base insertion with the resultant three amino acids insertion of "glutamic acid – proline – glutamic acid" occurred at the 214 amino acid position of the SARS-CoV-2 spike protein.

and the virus with such mutations will be removed from the population, some of the tandem repeats of relatively short sequences could be non-lethal and survive in the environments, which could partially contribute to the genomic evolution of the virus. Considering from the numbers of identified sequences with the evaluated insertion types, the observed two-cycle tandem repeat of the 9-base insertion (Spike_ins214EPEEPE) and its derivative (Spike_ins214EPDEPE,) may have been non-lethal, although whether the mutations were beneficial or deleterious for the survival of the virus remains uncertain. Studies to elucidate the roles in virus evolution and exact mechanisms of tandem repeat of inserted bases are warranted.

There are several limitations for the present study. First, this study could not determine the exact process of emergence, origin in the environments, and geographical location of the original one-cycle 9-base insertion. Therefore, whether the 9-bases insertion had occurred at one time or had gradually extended by accumulations of 3-base insertion is uncertain. However, because the identified number of the 3-base insertion (Spike_ins214E) or 6-base insertion (Spike_ins214EP) was much smaller than that of the 9-base insertion (Spike_ins214EPE), it could be inferred that the insertion of the nine nucleotides had occurred at once. The environmental origin of the inserted 9-bases (AGCCAGAAG) could not be determined with BLAST search because of its short sequence length. Second, the significance of the observed VNTR for the severity of symptoms in hosts could not be estimated in this study. Determining the severity with the lineages incorporating the 2-cycle tandem repeat seems to be difficult, because the number of the registered sequences with the 18-base insertions was relatively small and the mutations have not been identified later than April 2022, as far as we could search. Lastly, although the BLAST search and GISAID database search could not identify the matched sequences to the two-cycle tandem repeat of 9-base insertion in samples collected after April 2022, this result may not necessarily mean that the tandem repeat insertion had failed to spread and had already been eliminated completely from the environments. As a possibility, the mutation may have subsequently incorporated additional mutations and the BLAST search and GISAID database search in this study could have failed to identify such possible resultant variants.

In summary, the present study identified a polymorphic indel hotspot with different tandem repeat cycles of inserted bases at the 214 amino acid position in SARS-CoV-2 S1-NTD, sampled and sequenced from humans during the COVID-19 pandemic. The obtained results implied the polymorphic patterns of indels could emerge gradually in different seasons at different geographical locations. This finding may imply that tandem repeat may be likely to occur at the indel hotspots and can repeat the previously inserted sequences. Furthermore, the

tolerability for incorporating indels was suggested to be significantly different between the genomic regions and could be distinct from the distribution of tolerability for incorporating point mutations. Further studies are warranted to elucidate the potential roles of polymorphic indels and tandem repeat of insertion in the evolutionary process of viruses including SARS-CoV-2.

Data availability statement

The original contributions presented in the study are included in the article/supplementary material, further inquiries can be directed to the corresponding author.

Author contributions

TA and KF conceived the study, performed the analyses, and drafted the manuscript. TI supervised the study and critically reviewed and revised the manuscript. All authors contributed to the article and approved the submitted version.

Acknowledgments

We gratefully acknowledge all data contributors, i.e., the authors and their originating laboratories responsible for obtaining the specimens, and their submitting laboratories for generating the genetic sequence and metadata and sharing *via* the GISAID Initiative, on which this research is based.

Conflict of interest

The authors declare that the research was conducted in the absence of any commercial or financial relationships that could be construed as a potential conflict of interest.

Publisher's note

References

Akaishi, T. (2022a). Comparison of insertion, deletion, and point mutations in the genomes of human adenovirus HAdvC-2 and SARS-CoV-2. *Tohoku J. Exp. Med.* 258, 23–27. doi: 10.1620/tjem.2022.J049

Akaishi, T. (2022b). Insertion-and-deletion mutations between the genomes of SARS-CoV, SARS-CoV-2, and bat coronavirus RaTG13. *Microbiol. Spectr.* 10:e0071622. doi: 10.1128/spectrum.00716-22

Akaishi, T., Fujiwara, K., and Ishii, T. (2022a). Insertion/deletion hotspots in the Nsp2, Nsp3, S1, and ORF8 genes of SARS-related coronaviruses. *BMC Ecol. Evol.* 22:123. doi: 10.1186/s12862-022-02078-7

Akaishi, T., Horii, A., and Ishii, T. (2022b). Sequence exchange involving dozens of consecutive bases with external origin in SARS-related coronaviruses. *J. Virol.* 96:e0100222. doi: 10.1128/jvi.01002-22

Alexandridi, M., Mazej, J., Palermo, E., and Hiscott, J. (2022). The coronavirus pandemic - 2022: viruses, variants, and vaccines. *Cytokine Growth Factor Rev.* 63, 1–9. doi: 10.1016/j.cytogfr.2022.02.002

Avarre, J. C., Madeira, J. P., Santika, A., Zainun, Z., Baud, M., Cabon, J., et al. (2011). Investigation of cyprinid herpesvirus-3 genetic diversity by a multi-locus variable number of tandem repeats analysis. *J. Virol. Methods* 173, 320–327. doi: 10.1016/j.jviromet.2011.03.002

Bakhtiari, M., Park, J., Ding, Y. C., Shleizer-Burko, S., Neuhausen, S. L., Halldórsson, B. V., et al. (2021). Variable number tandem repeats mediate the expression of proximal genes. *Nat. Commun.* 12:2075. doi: 10.1038/s41467-021-22206-z

Biancolella, M., Colona, V. L., Mehrian-Shai, R., Watt, J. L., Luzzatto, L., Novelli, G., et al. (2022). COVID-19 2022 update: transition of the pandemic to the endemic phase. *Hum. Genomics* 16:19. doi: 10.1186/s40246-022-00392-1

Bilgin Sonay, T., Carvalho, T., Robinson, M. D., Greminger, M. P., Krützen, M., Comas, D., et al. (2015). Tandem repeat variation in human and great ape populations and its impact on gene expression divergence. *Genome Res.* 25, 1591–1599. doi: 10.1101/gr.190868.115

Chang, C. H., Chang, Y. C., Underwood, A., Chiou, C. S., and Kao, C. Y. (2007). VNTRDB: a bacterial variable number tandem repeat locus database. *Nucleic Acids Res.* 35, D416–D421. doi: 10.1093/nar/gkl872

De Marco, C., Veneziano, C., Massacci, A., Pallocca, M., Marascio, N., Quirino, A., et al. (2022). Dynamics of viral infection and evolution of SARS-CoV-2 variants in the Calabria area of southern Italy. *Front. Microbiol.* 13:934993. doi: 10.3389/fmicb.2022.934993

Dhawan, M., Saied, A. A., Mitra, S., Alhumaydhi, F. A., Emran, T. B., and Wilairatana, P. (2022). Omicron variant (B.1.1.529) and its sublineages: what do we know so far amid the emergence of recombinant variants of SARS-CoV-2? *Biomed. Pharmacother.* 154:113522. doi: 10.1016/j.biopha.2022.113522

Elbe, S., and Buckland-Merrett, G. (2017). Data, disease and diplomacy: GISAID's innovative contribution to global health. *Glob. Chall.* 1, 33–46. doi: 10.1002/gch2.1018

Holland, L. A., Kaelin, E. A., Maqsood, R., Estifanos, B., Wu, L. I., Varsani, A., et al. (2020). An 81-nucleotide deletion in SARS-CoV-2 ORF7a identified from sentinel surveillance in Arizona (January to march 2020). *J. Virol.* 94:20. doi: 10.1128/JVI.00711-20

Khare, S., Gurry, C., Freitas, L., Schultz, M. B., Bach, G., Diallo, A., et al. (2021). GISAID's role in pandemic response. *China CDC Wkly* 3, 1049–1051. doi: 10.46234/ccdcw2021.255

Liu, H., Wu, N. C., Yuan, M., Bangaru, S., Torres, J. L., Caniels, T. G., et al. (2020). Cross-neutralization of a SARS-CoV-2 antibody to a functionally conserved site is mediated by avidity. *Immunity* 53, 1272–1280e5. doi: 10.1016/j.immuni.2020.10.023

Lytras, S., Hughes, J., Martin, D., Swanepoel, P., De Klerk, A., Lourens, R., et al. (2022). Exploring the natural origins of SARS-CoV-2 in the light of recombination. *Genome Biol. Evol.* 14:evac018. doi: 10.1093/gbe/evac018

Martin, D. P., Varsani, A., Roumagnac, P., Botha, G., Maslamoney, S., Schwab, T., et al. (2021). RDP5: a computer program for analyzing recombination in, and removing signals of recombination from, nucleotide sequence datasets. *Virus Evol.* 7:veaa087. doi: 10.1093/ve/veaa087

Min, L., and Sun, Q. (2021). Antibodies and vaccines target RBD of SARS-CoV-2. *Front. Mol. Biosci.* 8:671633. doi: 10.3389/fmolb.2021.671633

Papanikolaou, V., Chrysovergis, A., Ragos, V., Tsiambas, E., Katsinis, S., Manoli, A., et al. (2022). From delta to omicron: S1-RBD/S2 mutation/deletion equilibrium in SARS-CoV-2 defined variants. *Gene* 814:146134. doi: 10.1016/j.gene.2021.146134

Shu, Y., and Mccauley, J. (2017). GISAID: global initiative on sharing all influenza data - from vision to reality. *Euro Surveill.* 22:30494. doi: 10.2807/1560-7917.ES.2017.22.13.30494

Singh, P., Negi, S. S., Bhargava, A., Kolla, V. P., and Arora, R. D. (2022). A preliminary genomic analysis of the omicron variants of SARS-CoV-2 in Central India during the third wave of the COVID-19 pandemic. *Arch. Med. Res.* 53, 574–584. doi: 10.1016/j.arcmed.2022.08.006

Sun, H., Jacobs, S. C., Smith, G. L., Dixon, L. K., and Parkhouse, R. M. (1995). African swine fever virus gene j13L encodes a 25-27 kDa virion protein with variable numbers of amino acid repeats. *J. Gen. Virol.* 76, 1117–1127. doi: 10.1099/0022-1317-76-5-1117

Tamura, K., Stecher, G., and Kumar, S. (2021). MEGA11: molecular evolutionary genetics analysis version 11. *Mol. Biol. Evol.* 38, 3022–3027. doi: 10.1093/molbev/msab120

Viana, R., Moyo, S., Amoako, D. G., Tegally, H., Scheepers, C., Althaus, C. L., et al. (2022). Rapid epidemic expansion of the SARS-CoV-2 omicron variant in southern Africa. *Nature* 603, 679–686. doi: 10.1038/s41586-022-04411-y

Wilkinson, E., Giovanetti, M., Tegally, H., San, J. E., Lessells, R., Cuadros, D., et al. (2021). A year of genomic surveillance reveals how the SARS-CoV-2 pandemic unfolded in Africa. *Science* 374, 423–431. doi: 10.1126/science.abj4336

Willemsen, A., and Zwart, M. P. (2019). On the stability of sequences inserted into viral genomes. *Virus Evol.* 5:vez045. doi: 10.1093/ve/vez045

Wu, F., Zhao, S., Yu, B., Chen, Y. M., Wang, W., Song, Z. G., et al. (2020). A new coronavirus associated with human respiratory disease in China. *Nature* 579, 265–269. doi: 10.1038/s41586-020-2008-3

Zhang, H., Penninger, J. M., Li, Y., Zhong, N., and Slutsky, A. S. (2020). Angiotensin-converting enzyme 2 (ACE2) as a SARS-CoV-2 receptor: molecular mechanisms and potential therapeutic target. *Intensive Care Med.* 46, 586–590. doi: 10.1007/s00134-020-05985-9

frontiers | Frontiers in Microbiology

TYPE Original Research
PUBLISHED 01 March 2023
DOI 10.3389/fmicb.2023.1106945

OPEN ACCESS

EDITED BY
Wei Wei,
First Affiliated Hospital of Jilin University,
Jilin University,
China

REVIEWED BY
Zhen Luo,
Jinan University,
China
Tao Wang,
Tianjin University,
China

*CORRESPONDENCE
Caroline Tapparel
caroline.tapparel@unige.ch

SPECIALTY SECTION
This article was submitted to Virology, a section of the journal Frontiers in Microbiology

RECEIVED 24 November 2022
ACCEPTED 18 January 2023
PUBLISHED 01 March 2023

CITATION
Essaidi-Laziosi M, Royston L, Boda B, Pérez-Rodriguez FJ, Piuz I, Hulo N, Kaiser L, Clément S, Huang S, Constant S and Tapparel C (2023) Altered cell function and increased replication of rhinoviruses and EV-D68 in airway epithelia of asthma patients. *Front. Microbiol.* 14:1106945. doi: 10.3389/fmicb.2023.1106945

Altered cell function and increased replication of rhinoviruses and EV-D68 in airway epithelia of asthma patients

Manel Essaidi-Laziosi[1], Léna Royston[1], Bernadett Boda[2], Francisco Javier Pérez-Rodriguez[1,3], Isabelle Piuz[1], Nicolas Hulo[4], Laurent Kaiser[3], Sophie Clément[1], Song Huang[2], Samuel Constant[2] and Caroline Tapparel[1]*

[1]Department of Microbiology and Molecular Medicine, Faculty of Medicine, University of Geneva, Geneva, Switzerland, [2]Epithelix Sàrl, Plan les Ouates, Geneva, Switzerland, [3]Division of Infectious Diseases, Geneva University Hospital, Geneva, Switzerland, [4]Service for Biomathematical and Biostatistical Analyses, Institute of Genetics and Genomics, University of Geneva, Geneva, Switzerland

Introduction: Rhinovirus (RV) infections constitute one of the main triggers of asthma exacerbations and an important burden in pediatric yard. However, the mechanisms underlying this association remain poorly understood.

Methods: In the present study, we compared infections of *in vitro* reconstituted airway epithelia originating from asthmatic versus healthy donors with representative strains of RV-A major group and minor groups, RV-C, RV-B, and the respiratory enterovirus EV-D68.

Results: We found that viral replication was higher in tissues derived from asthmatic donors for all tested viruses. Viral receptor expression was comparable in non-infected tissues from both groups. After infection, ICAM1 and LDLR were upregulated, while CDHR3 was downregulated. Overall, these variations were related to viral replication levels. The presence of the CDHR3 asthma susceptibility allele (rs6967330) was not associated with increased RV-C replication. Regarding the tissue response, a significantly higher interferon (IFN) induction was demonstrated in infected tissues derived from asthmatic donors, which excludes a defect in IFN-response. Unbiased transcriptomic comparison of asthmatic versus control tissues revealed significant modifications, such as alterations of cilia structure and motility, in both infected and non-infected tissues. These observations were supported by a reduced mucociliary clearance and increased mucus secretion in non-infected tissues from asthmatic donors.

Discussion: Altogether, we demonstrated an increased permissiveness and susceptibility to RV and respiratory EV infections in HAE derived from asthmatic patients, which was associated with a global alteration in epithelial cell functions. These results unveil the mechanisms underlying the pathogenesis of asthma exacerbation and suggest interesting therapeutic targets.

KEYWORDS

rhinovirus, enterovirus-D68, asthma, airway epithelial barrier, viral replication

1. Introduction

Rhinoviruses (RVs) are among the most frequent pathogens in human worldwide, involved in more than 50% of common colds. Members of the *Enterovirus* genus, those small non-enveloped positive-stranded RNA viruses are classified into three species: RV-A, RV-B, and RV-C and can be further divided according to their receptor usage. RVs from the major group (most RV-As and all RV-Bs) bind ICAM1 (Greve et al., 1989), RV-As from the minor group bind the low-density

lipoprotein receptor (LDLR; Hofer et al., 1994) and RV-Cs use cadherin related family member 3 receptor (CDHR3), expressed on ciliated airway cells (Bochkov et al., 2015; Everman et al., 2019). Some other non-RV enteroviruses (EVs), including EV-D68, share biological properties with RVs such as acid lability and optimal growth at 33°C and induce respiratory symptoms similar to RVs (Royston and Tapparel, 2016).

It is widely accepted that respiratory and particularly RV infections constitute a major trigger of asthma exacerbations and a risk factor for asthma development (Gern, 2010; Jackson and Gern, 2022). Concerning EV-D68, an association between EV-D68-related symptoms severity and a history of asthma has also been reported (Moss, 2016; Hayashi et al., 2018; Korematsu et al., 2018). The mechanisms linking viral infections to asthma exacerbation remain, however, poorly understood. While upper respiratory tract RV infections are not increased in asthmatic patients, more frequent and more severe lower respiratory tract infections are observed (Corne et al., 2002). How viral infections contribute to these clinical manifestations remains unknown. A dysregulated immune and particularly IFN-response upon infection has been shown in asthmatic patients (Contoli et al., 2006; Edwards et al., 2013; Zhu et al., 2019; Jackson and Gern, 2022; Liew et al., 2022), but remains controversial (Baraldo et al., 2012; Sykes et al., 2014; Da Silva et al., 2017; Hansel et al., 2017; Sopel et al., 2017; Jazaeri et al., 2021; Yang et al., 2021).

RV-As and RV-Cs are more frequently detected in childhood asthma exacerbations than RV-Bs. This could be explained by the difference of virulence between isolates of distinct species, but remains hypothetical (Iwane et al., 2011; Lee et al., 2012). RV-A, B, and C may induce distinct host antiviral responses, possibly through the use of different cellular receptors. A single-nucleotide polymorphism (SNP) in *CDHR3*, the RV-C receptor, is associated with greater risk of asthma hospitalizations in homozygous and heterozygous children (Bonnelykke et al., 2014; Kanazawa et al., 2017; Bonnelykke et al., 2018). This SNP (rs6967330) results in a C529Y amino acid (aa) change in the CDHR3 protein, associated with increased expression at the cell surface upon transfection, favoring RV-Cs infection (Bochkov et al., 2015). Increased expression of the mutated allele was also reported in human bronchial epithelial cells cultured at the air-liquid interface (ALI) (Basnet et al., 2019). Accordingly, the *CDHR3* risk allele was associated with increased RV-C infection incidence in two birth cohorts (Bonnelykke et al., 2018). However, the interaction between RV-C and this receptor and the role of this interaction in asthma exacerbations remains speculative. Recent studies have reported different consequences of *CDHR3* mutation on tissue differentiation, protein subcellular localization, and RV-C binding (Basnet et al., 2019; Everman et al., 2019). Everman and colleagues found that *CDHR3* knockdown affected RV-C binding but not replication and suggested that RV-Cs use a coreceptor for infection (Everman et al., 2019; Lutter and Ravanetti, 2019). Regarding major group RVs, ICAM1 expression is very low in the airways but increases upon inflammation (Bianco et al., 2000). Similarly, LDLR expression may vary in response to inflammation (Zhang et al., 2016). The asthma-associated inflammatory response could enhance the accessibility of viral receptors and improve infectivity (Bochkov and Gern, 2016). However, RV-Bs that are less frequently associated with asthma exacerbations, also use ICAM1 to infect cells. Further research is needed to better define the role of viral receptors in RV-A, RV-B, and RV-C-induced asthma exacerbations.

In this study, we aimed to explore the involvement of different RVs and of EV-D68 in asthma and assess the role of viral receptors and innate immune induction, using human airway epithelia (HAE) and clinical viral isolates. We highlighted overall increased viral replication in tissues from asthmatic patients, but could not link receptor expression or IFN-induction with this phenotype. Unbiased transcriptomic analysis showed basic morphological and physiological differences between tissues from asthmatic versus control donors, even in absence of infection, an observation supported by diminished mucociliary clearance (MCC) and increased mucus secretion in asthma-derived tissues. Our observations suggest an alteration in the mechanical defense of the respiratory mucosae in tissues derived from asthmatic patients, resulting in increased permissiveness and susceptibility to RV or respiratory EV infections.

2. Materials and methods

2.1. Human airway epithelia

HAE ("MucilAir"[1]) were reconstituted from airway cells obtained from patients undergoing surgical nasal polypectomy (for nasal tissues) or lung lobectomy (for bronchial tissues). Patients presenting no atopy, asthma, allergy, or other known respiratory comorbidity were used as controls (Supplementary Table S1). All experimental procedures were explained, and all subjects provided informed consent. The study was conducted according to the Declaration of Helsinki on biomedical research (Hong Kong amendment, 1989), and the research protocol was approved by the local ethics committee (commission cantonale d'éthique de la recherche CCER from Geneva). Cultures are performed in an ALI system according to the procedure previously detailed in (Essaidi-Laziosi et al., 2018). Once differentiated, epithelia contain ciliated, goblet, and basal cells, with a pseudostratified structure and mucociliary clearance functions.

2.2. Viral stocks and tissue infection

Anonymized clinical samples were screened by semi-quantitative real-time PCR (RT-sqPCR; Ambrosioni et al., 2014) and RV/EV were subtyped by sequencing as previously described (Tapparel et al., 2011; Essaidi-Laziosi et al., 2018). A respiratory EV (EV-D68), a major group RV (RV-A16), a minor group RV (RV-A49), and representatives of the B (RV-B48) and C (RV-C15) species were selected. Viral stocks were produced directly in MucilAir to avoid any adaptation in immortalized cells and titrated as described (Essaidi-Laziosi et al., 2020). Serial dilutions were performed in MucilAir to evaluate viral infectious doses within each stock. The viral inoculum was then normalized according to the determined endpoint, which corresponds to the highest inoculum dilution allowing virus replication as described (Essaidi-Laziosi et al., 2020).

Tissues were infected as previously described (Essaidi-Laziosi et al., 2018, 2020). For each virus, the inoculum was normalized based on the infectious titer to contain identical doses of infectious particles (MOI of ~0.001 per accessible cell). Four hours after inoculation, tissues were washed 3 times with PBS. At various times post-infection, 200 µL of medium was applied on the apical surface during 20 min at 33°C for

1 http://www.epithelix.com/products/mucilair

sample collection. Basal medium was collected at the same time and replaced with 500 µL of fresh medium.

2.3. Viral load quantification, gene expression quantification, and *CDHR3* genotyping

RNA was extracted (E.Z.N.A viral RNA kit I, Omega, R687402), and quantified by one-step real-time quantitative PCR (RT-qPCR) with the QuantiTect kit (Qiagen) in a StepOne ABI thermocycler (Essaidi-Laziosi et al., 2018).

Gene expression of the receptors and IFNs at 4dpi was determined by semi-quantitative RT-PCR (RT-sqPCR) on total RNA extracted from tissue lysates using total RNA extraction kit (E.Z.N.A total RNA kit I, Omega, R8334A) and normalized to RNAseP housekeeping gene. IFNλ1 mRNA was amplified using primers and probe (Fwd GGACGCCTTGGAAGAGTCACT, rev AGAAGCCTCAGGTCC CAATTC and probe AGTTGCAGCTCTCCTGTCTTCCCCG) as previously described (Dolganiuc et al., 2012), while mRNAs from CDHR3, ICAM1, LDLR, ISG15, IFNα, IFNβ, and RNAseP were amplified using specific gene expression assay kits (Thermo Fisher Scientific, ref. 4331182, Cat N° Hs00541677_m1, Hs00164932_m1, Hs00181192_m1, Hs01921425, Hs04190680_gH, Hs01077958_s1, and 4403326). Fold changes were calculated after normalization with the RNAseP housekeeping gene with the 2(-Delta Delta C(T)) (Livak and Schmittgen, 2001). Regarding CDHR3 genotyping, the gene was amplified by PCR from extracted DNA and then sequenced using specific primers (Fwd ATTCCTCCAGCCAGAACCCG and Rev. TGTTTCTCACCACATCCGCAG).

2.4. ELISA and Western blot

Interferon lambda (IFNλ1/ λ3, IL-29 /IL-28B) was measured in the basal medium by ELISA (R&D DY1598B-05) according to the manufacturer's instructions.

Western blot assays were performed as previously described (Essaidi-Laziosi et al., 2014). Infected and non-infected tissues from healthy and asthmatic donors were lysed using RIPA buffer (NaCl 150 mM, EDTA 1mM, Tris HCl pH = 7.4 50mM, NP40 1%, SDS 0.1%, and Sodium deoxycholate 1%) containing protease inhibitors (Roche, 04693159001). Cell lysates were clarified and resuspended in SDS-PAGE sample buffer and electrophoresed on 8 or 10% SDS polyacrylamide gel. Gel transfer was made onto a polyvinylidene difluoride membrane (PVDF, Biorad, 1,620,177) using Trans-Blot SD Transfer Cell (Biorad). The membranes were first blocked with 5% skim milk (AppliChem) in TTBS (20 mM Tris HCl, pH 7.5, 500 mM NaCl, and 0.05% Tween 20) at RT for 30 min and then incubated with Anti-ICAM1 (diluted 1/500, Abcam, ab2213), -LDL-R (diluted 1/1,000, R&D systems, AF2148), CDHR3 (diluted 1/500, Sigma-Aldrich, HPA011218), and Actin (diluted 1/1,000 Millipore, MAB1501) primary antibodies overnight at 4°C. The membranes were then washed 3 times with TTBS and incubated at RT for 1 h with corresponding anti-mouse or anti-rabbit horseradish peroxidase (HRP)-coupled secondary antibodies (Cell Signaling). Membranes were washed and viral receptors were detected using an enhanced chemiluminescence solution (ECL, ref. K-12043-D10 Western Bright Sirius Advansta) for 2 min. Immunoblot images were acquired using Fujifilm LAS 4000 luminescence imager.

2.5. Transcriptomic analysis

Infected and non-infected tissues were lysed in 800 µL of trizol (Ambion, 5,596,018) and RNA was extracted according to the manufacturer's instruction. Total RNA was quantified with Qubit (Life Technologies) and RNA integrity was assessed with a Bioanalyzer (Agilent Technologies). The TruSeq Stranded Total RNA kit with Ribo-Zero Gold was used for the library preparation with 150ng of total RNA as input. The 18 libraries were pooled at equimolarity and loaded at 8.5 pM for clustering on a single-read Illumina Flow cell.

Library molarity and quality for all samples were assessed with a Qubit and a Tapestation using a DNA High sensitivity chip (Agilent Technologies). All 100-base sequencing was performed using the TruSeq SBS HS v3 chemistry on an Illumina HiSeq 2,500 sequencer. The sequencing raw data are available at GEO with accession number GSE222129.

Quality control of the resulting reads was done with FastQC and the reads mapped to the Homo sapiens UCSC hg38 genome with the STAR program (version 2.5.2a; Dobin et al., 2013), and count tables containing the number of mapped reads per gene were produced with featureCounts (version 1.6.0). Count tables were then imported into R (version 2.13) to do the differential expression analysis with edgeR (version 3.12.1; Robinson et al., 2010). Data were filtered for genes with weak expression level (average CPM < 1). Library sizes were adjusted with a scaling factor calculated using a trimmed mean of M-values (TMM) between each pair of samples. The common dispersion and tagwise dispersions were estimated with the estimateDisp function. After negative binomial glm fitting the quasi-likelihood (QL), F-test was applied for the testing procedure. The significantly differentially expressed gene lists (FDR < 0.05) obtained with this procedure were then used to do GO enrichment analysis on the cellular component subset of GO term database with ClusterProfiler functions (version 2.4.3) (Yu et al., 2012).

2.6. Mucociliary clearance, mucin measurement with enzyme-linked lectin assay

The mucociliary clearance was monitored using a Sony XCD-U100CR camera connected to an Olympus BX51 microscope with a 5× objective. Polystyrene microbeads of 30 µm diameter (Sigma, 84,135) were added on the apical surface of MucilAir. Microbeads movements were video tracked at 2 frames per second for 30 images at room temperature. Three movies were taken per insert. Average beads movement velocity (µm/s) was calculated with the ImageProPlus 6.0 software.

Mucin secretion was quantified using an Enzyme-linked Lectin Assay (ELLA) in-house protocol detecting the carbohydrate groups of the collected mucus. 96-well plates were coated with 6 µg/mL Lectin from Triticum vulgaris (wheat) (Sigma, L0636) in PBS adjusted at pH 6.8 and incubated 1 h at 37°C. After washing steps with high 0.5M NaCl, 0.1% Tween-20 in PBS, samples, and standards (Mucin from porcine stomach Type II, Sigma, M2378) were incubated 30 min at 37°C. After washing, plates were incubated 30 min at 37°C with a detection solution containing 1µg/mL of Peroxidase conjugated Lectin from Glycine Max (soybean)

(Sigma, L2650), in 0.1% BSA-PBS adjusted at pH 7.4. After the last washing steps, the TMB substrate reagent (3,3′,5,5′-tetramethylbenzidine purchased from ThermoFisher Scientific 34,021) was added and incubated for 10 min in the dark at RT. The reaction was stopped with 2N H_2SO_4 and the plates were read at 450 nm.

2.7. Muc5AC immunohistochemistry

Tissues were fixed using 4% formaldehyde in PBS with Ca^{2+}/Mg^{2+} for 30 min. One epithelium per donor was evaluated for the presence of goblet cells with anti-Muc5AC-specific antibody (Abcam ab3649) and percentage of positive area were assessed. Briefly, inserts were processed for immunohistochemistry using four central transversal paraffin sections of 4 µm. Immunostaining of the slides was performed with the Benchmark automated platform (Ventana-Roche) and the Autostainer Link 48 (Dako) with the detection kit Ultraview DAB (DAB chromogeny).

The sections were pre-treated using heat-mediated antigen retrieval with sodium citrate buffer, pH 6, for 20 min. The sections were then incubated with primary Ab for 1 h at room temperature. A biotinylated secondary Ab (Dako) was used to detect the primary, and visualized using an HRP conjugated ABC system. DAB was used as the chromogen to reveal Muc5AC immune reaction. The sections were then counterstained with hematoxylin and mounted with DPX.

Image analysis using ImagePro Plus software (version 6.2, Media Cybernetics) was conducted to quantify goblet cells on four sections per insert. The whole images of stained sections were scanned and total DAB labeled dark areas were measured using "count and measure object" function based on dark brown color selection. The results are expressed as percentage of Muc5AC stained area of the total surface area of the epithelial sections. Data from the four sections were averaged for one insert.

2.8. Statistics

Results were expressed as scatter plots with the median. Statistical significance was calculated using ordinary one-way ANOVA (no matching), two-way ANOVA (no matching), with multiple comparisons or unpaired *t*-tests, and Spearman's analysis for correlation analyzes using GraphPad Prism 7.02 software.

3. Results

3.1. All tested viruses replicate more robustly in respiratory tissues originating from asthmatic compared to control patients

Viral stocks were prepared and titrated in HAE to avoid cell-adaptation. Viruses (MOI of ~0.001) were applied at the apical surface of the tissues and removed after 4 h by extensive washes. RNA was extracted from apically released viruses and quantified by RT-qPCR as previously described (Essaidi-Laziosi et al., 2018).

Replication was greater for EV-D68 and lower for RV-B48 compared to all other viruses independently of the condition (Figure 1), as previously shown (Essaidi-Laziosi et al., 2018). Interestingly, for all viruses, viral replication was increased in tissues from asthmatic patients compared to controls. This difference was observed independent on the tissue origin [nasal or bronchial (Supplementary Table S1)]. A C529Y mutation in *CDHR3* has been shown to increase asthma susceptibility. We sequenced this allele and found 5/12 (42%) and 6/14 (43%) donors, from the control and asthma groups, respectively, heterozygous for the asthma susceptibility allele and one control donor homozygous. No association between the presence of the susceptibility allele and viral growth could be observed (Supplementary Figure S1).

3.2. RV receptor expression does not account for the increased replication observed in tissues from asthmatic donors

We next assessed whether increased receptor expression could account for the enhanced replication observed in tissues from asthmatic donors. ICAM1, LDLR, and CDHR3 mRNA levels were quantified in non-infected or infected tissues derived from asthmatic or control donors by RT-sqPCR and no significant difference was observed between their basal levels (Figure 2A). This absence of

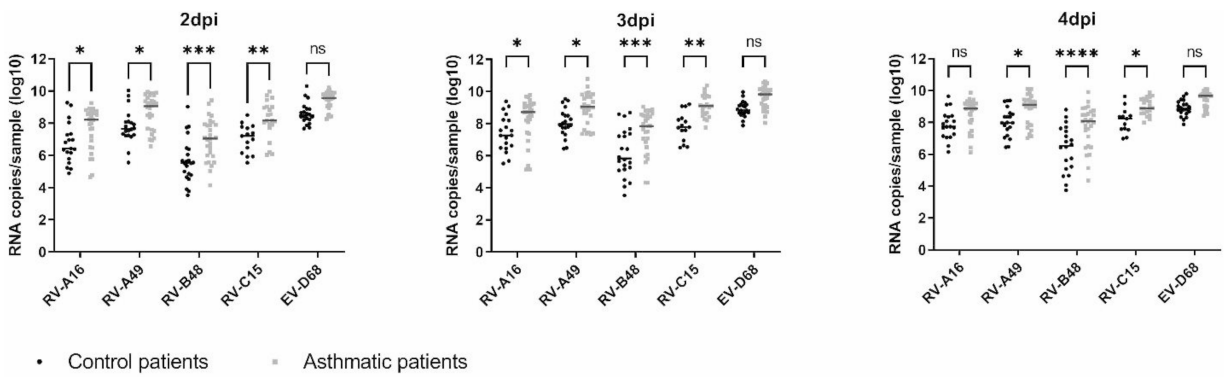

FIGURE 1
Virus production at the apical side of ALI culture of reconstituted HAE derived from non-asthmatic (control) or asthmatic patients represented as scatter plots with medians. Twelve control and 14 asthmatic donors were included (Supplementary Table S1). Statistically significant differences between HAE from asthmatic or control donors are indicated. ns: non-significant, *p<0.05, **p<0.01, ***p<0.001, and ****p<0.0001.

difference in basal expression levels of RV receptors in tissues from control or asthmatic patients speaks against their involvement as an initial trigger of the increased viral replication observed in tissues from asthmatic donors. Of note, *ICAM1* basal expression is lower than *LDLR* and *CDHR3* (1 to 2 logs) and *CDHR3* expression is higher than *LDLR* (Figure 2A).

In contrast, in epithelia infected for 4 days (Figures 2B–D), *LDLR* and *ICAM1* expression was induced by the infection and this induction was significantly stronger in asthmatic donors. Correlation analysis (Supplementary Table S2) further highlighted a significant positive correlation between *LDLR* and *ICAM1* expression and the replication of RV-A49 and RV-B48 in tissues derived from healthy donors and between *LDLR* expression and replication of RV-C15 in tissues derived from asthmatic donors. Conversely, infection induced the downregulation of *CDHR3* and more significantly in asthmatic donors (Figure 2D). Accordingly, a significant negative correlation was found between *CDHR3* level and the replication of RV-A16, RV-A49, RV-B48, and RV-C15 in tissues derived from asthmatic donors (Supplementary Table S2). Of note, changes in receptor expression levels induced by RV-B48 were smaller in both control tissues and tissues from asthmatic donors. These observations were confirmed at the protein level by western blot (Supplementary Figure S2). Again, these data and the correlation analyzes do not support a causative role of receptor expression levels in the observed increased replication in tissues derived from asthmatic donors. This is particularly relevant for CDHR3, for which a decreased expression in tissues from asthmatic donors correlated with increased RV-C15 replication. As variation in receptor expression levels follows replication levels, it seems a consequence rather than a cause of the high replication observed in tissues from asthmatic donors.

3.3. Antiviral response is more important in infected tissues from asthmatic donors

Type I and type III IFN-responses and induction of the interferon-stimulated gene 15 (*ISG15*) were compared by RT-sqPCR in control and tissues from asthmatic donors, 4 dpi (Figure 3).

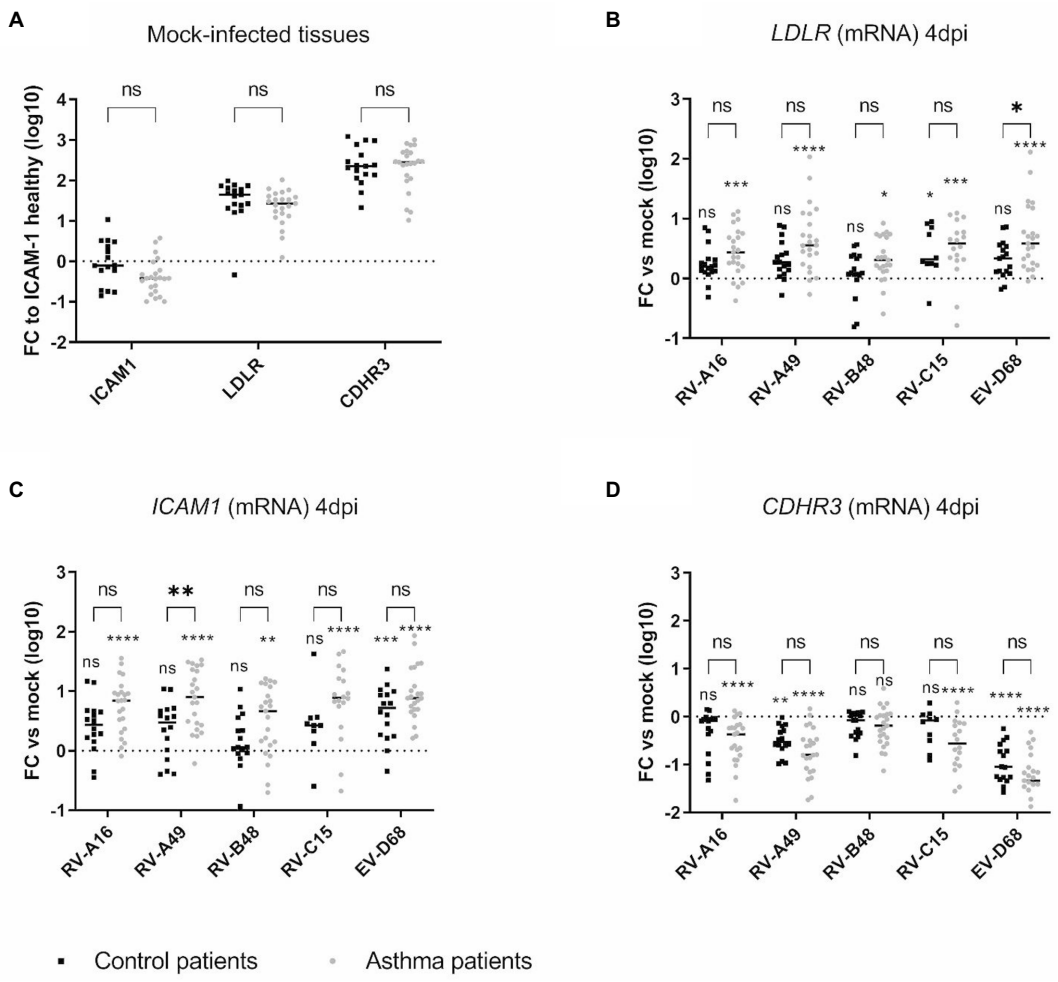

FIGURE 2
Expression of the different RV receptors in **(A)** mock-infected and in **(B–D)** infected tissues derived from asthmatic and control donors and measured by RT-sqPCR on total tissue lysates. In **(A)** the fold change (FC) is calculated relative to *ICAM1* expression in tissues derived from control donors. In **(B)**, **(C)**, and **(D)**, the fold change of *LDLR*, *ICAM1,* and *CDHR3* is calculated relative to expression in mock-infected tissues derived from donors within the same group (asthmatic or control). Eleven control and 12 asthmatic patients were included (Supplementary Table S1). The signs directly above each scatter plot indicate significance between mock-infected and infected tissues for each of the condition (asthma or control). The enlarged signs indicate significant differences between control and asthmatic donors. ns: non-significant, *p<0.05, **p<0.01, ***p<0.001, and ****p<0.0001.

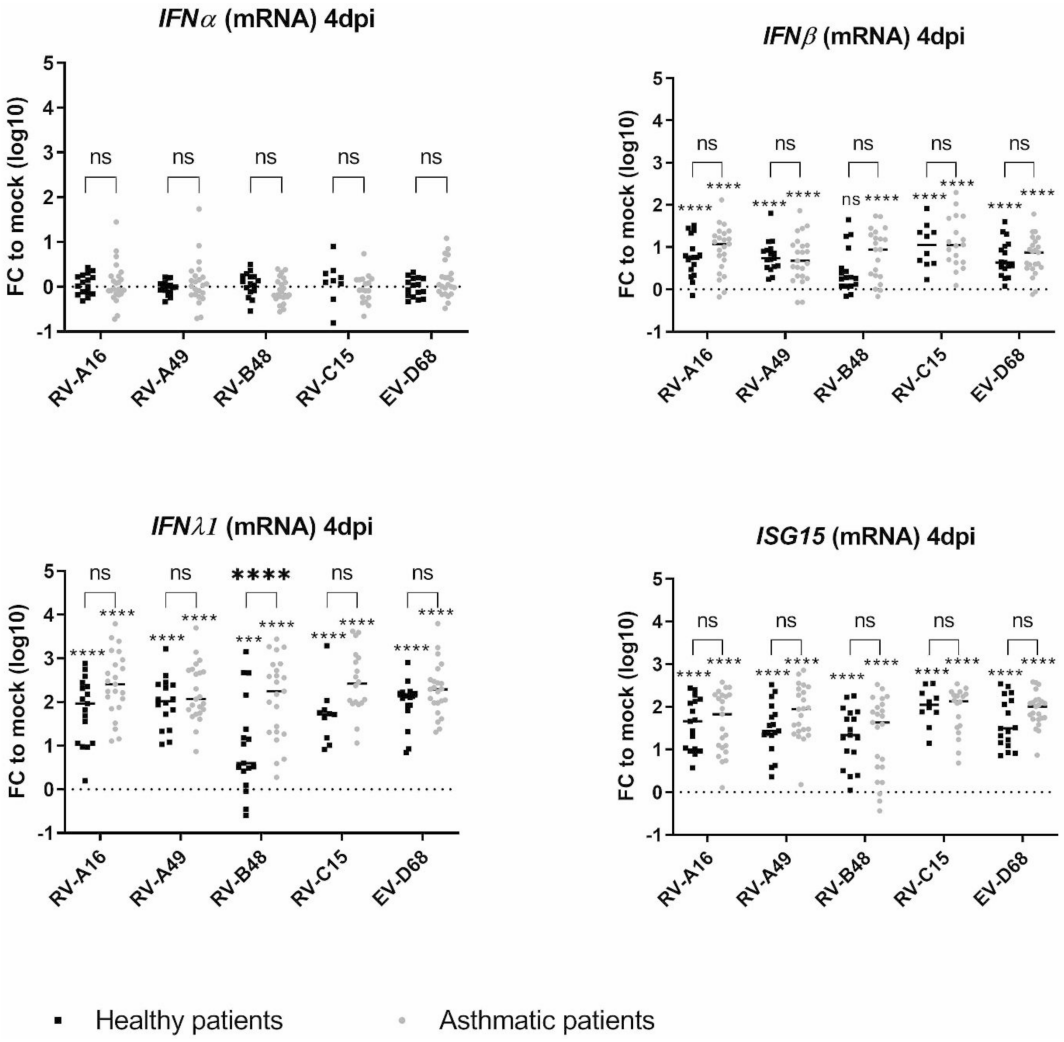

FIGURE 3
Expression of type I IFN, type III IFN, and ISG15 in infected tissues derived from asthmatic and non-asthmatic donors and measured by RT-sqPCR on total tissue lysates. The fold change (FC) is calculated relative to expression in mock-infected tissues derived from donors within the same group (asthmatic or control). Eleven control and 12 asthmatic patients were included (Supplementary Table S1). The signs directly above each scatter plot indicate significance between mock-infected and infected tissues for each of the condition (asthma or control). The enlarged signs indicate significant differences between control and asthmatic donors. ns: non-significant, *p<0.05, ***p<0.001, and ****p<0.0001.

While *IFNα* was almost not induced in both tissue types, in line with the low induction of this cytokine in infected respiratory tissues (Essaidi-Laziosi et al., 2018; Filipe et al., 2022), *IFNβ*, *IFNλ1* and *ISG15* were significantly induced with a significantly higher *IFNλ1* induction in tissues from asthmatic donors. This increase was confirmed in a subset of tissues (Supplementary Table S1) by IFNλ1/λ3-cytokine measurement in the basal medium collected from day 1 to 4 pi (Supplementary Figure S3). The increased antiviral effector production was striking for RV-B, probably due to the significantly higher viral production in tissues from asthmatic donors (Figure 1). Correlation analysis indeed highlighted a significant positive correlation between RV-A49 viral load and IFNλ induction in tissues from healthy donors and between RV-B48 viral load and both IFNλ and β induction in tissues from both healthy and asthmatic donors (Supplementary Table S2). In conclusion, we observed higher rather than lower IFN-induction in tissues from asthmatic donors and the level of induction seems to follow viral replication trend.

3.4. Transcriptomic analysis highlights structural differences in the response to infection in tissues from asthmatic or control patients

We performed a comparative transcriptomic analysis of tissues from control or asthmatic patients in the presence or absence of viral infection. We previously reported modifications of tissue metabolism and activation of innate immunity by RV-C15 and RV-B48 in control tissues (Essaidi-Laziosi et al., 2018). To compare the epithelial response of tissues derived from asthmatic donors, a larger transcriptomic analysis was carried out at 3dpi with the same viruses in tissues from control or asthmatic donors. RV-C15 induced more genes than RV-B48 in control tissues (9,320 versus 274 genes) (Figure 4A) as previously reported (Essaidi-Laziosi et al., 2018). Gene-induction by RV-B48 drastically increased in tissues from asthmatic donors (5,588 versus 271 genes), reflecting changes in replication levels. Differential gene expression was considerably

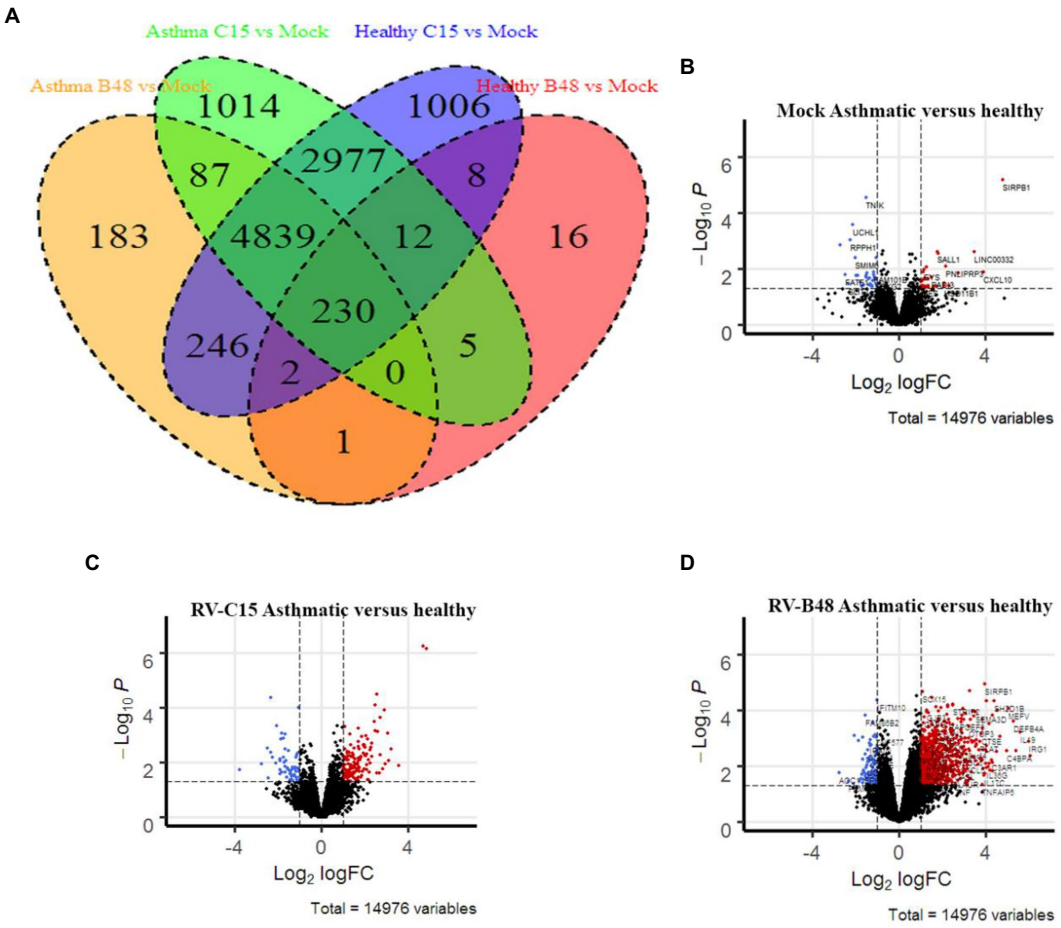

FIGURE 4
Differential gene expression in infected and mock-infected tissues derived from control versus asthmatic donors. **(A)** Venn diagram comparing the significant gene induction, relative to mock, in RV-B48 and RV-C15-infected tissues from control versus asthmatic donors. **(B–D)** Volcano plots summarizing the differential gene expression between control and asthmatic donors in **(B)** mock-infected, **(C)** RV-B48-infected, and **(D)** RV-C15-infected tissues. Red and blue dots correspond, respectively, to significantly upregulated and downregulated genes (p-value<0.05). Dotted vertical line indicates fold differences of 2, dotted horizontal lines indicate significance at a nominal p-value of 0.05.

higher in infected tissues compared to mock-infected tissues (Figures 4B–D).

Pathway enrichment analysis in tissues from controls versus asthmatic donors using Gene Ontology highlighted modified pathways. In non-infected tissues, enriched components were mostly related to envelope and membrane composition (Figure 5A). More focused comparison of genes involved in the differentiation and function of ciliated cells highlighted striking differences between asthmatic and control donors (Figure 5B). Similar pathways were differentially enriched after infection, particularly for RV-B. Again, the higher enrichment for RV-B is in line with the enhanced replication observed in asthmatic donors for this virus.

3.5. Tissues from asthmatic patients exhibit reduced MCC and increased mucus secretion

As most changes between asthmatic and controls (infected or not) were linked to tissue structure rather than induced tissue response, we compared the histology of tissues derived from healthy or asthmatic donors (Supplementary Figure S4A), as well as the tubulin expression and subcellular localization in infected or uninfected tissues (Supplementary Figure S4B). We did not observe macroscopic differences between the two groups. Since changes in transcriptomic profiles were already present in non-infected tissues (Figure 4; Essaidi-Laziosi et al., 2018), we then compared the MCC and mucus secretion in multiple non-infected tissues originating from a panel of distinct donors (Supplementary Table S1). As shown in Figure 6, tissues derived from asthmatic donors display a significantly decreased MCC and a significantly increased mucus secretion, confirmed by immunostaining of the muc5AC protein.

4. Discussion

In this study, we compared infections by RV-A major and minor group, RV-B, RV-C, and EV-D68, in HAE derived from asthmatic or control patients. First, we observed that RVs of all 3 species and, to some extent EV-D68, show increased replication in tissues from asthmatic patients and this increase is inversely associated with the replication of each virus in healthy tissues, with

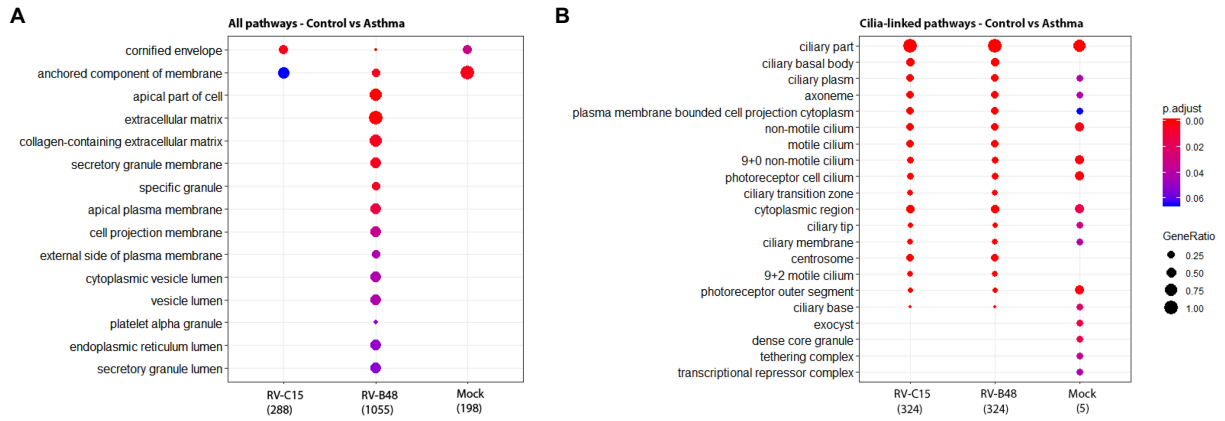

FIGURE 5
Enrichment of cellular pathways in infected and mock-infected tissues from control versus asthmatic donors. The top 15 of the most significantly enriched gene ontology cellular components analyzed from the total reads **(A)** and from reads of genes involved in the differentiation and function of ciliated cells **(B)** are shown, comparing epithelia originating from control versus asthmatic donors (Fold change >1, $p<0.05$) in mock, RV-B48 and RV-C15 infections.

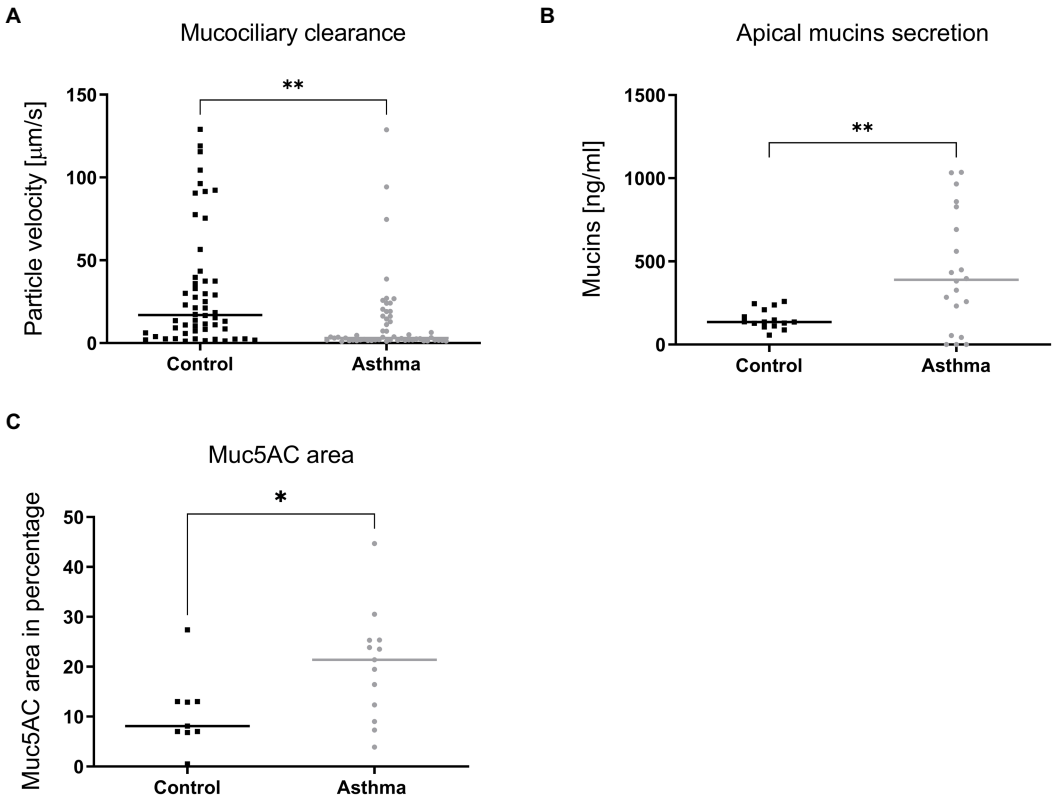

FIGURE 6
Mucociliary clearance **(A)**, mucus secretion **(B)** and expression of Muc5AC in immunostained tissue sections **(C)** compared in tissues derived from control or asthmatic donors. In **A**, 9 controls (54 inserts) and 7 asthmatic (55 inserts) donors were included in the comparison. In **B**, mucins were quantified from apical samples collected after 24h from tissues derived from 4 controls (15 inserts) and 5 asthmatic (20 inserts) donors. In **C**, tissues derived from 9 control and 9 asthmatic donors were processed. Statistically significant differences between HAE from asthmatic or control donors are indicated. *$p<0.05$; **$p<0.01$.

EV-D68 and RV-B48 showing the lowest and highest increase, respectively. The enhanced replication of RV-B48 in tissues from asthmatic donors was unexpected as this virus is less frequently associated with asthma exacerbation (Choi et al., 2021). However, RV-B replication and IFN-induction remained below the levels of the other viruses. In addition, the lower number of RV-B types (32 RV-B versus 80 RV-A and 57 RV-C) may also account for its lower detection in asthma exacerbations.

This overall effect on replication, independent of the species analyzed, made a causal association with viral receptor usage unlikely. Indeed, we observed no difference in basal receptor expression in the two groups of tissues. Nevertheless, after infection, ICAM1 and

LDLR, the major and minor group receptors, were significantly induced, and this induction was proportional to viral replication levels. ICAM1 and LDLR are induced by inflammation (Bianco et al., 2000; Zhang et al., 2016) explaining these results. However, correlation analyzes did not highlight a positive correlation between RV-A16, RV-B48, and RV-A49 viral loads and expression of their respective receptor ICAM1 or LDLR, in tissues derived from asthmatic donors. In contrast, CDHR3 expression was decreased and the decrease was inversely proportional to the replication level, with a significant negative correlation observed for all viruses (except EV-D68) in tissues derived from asthmatic donors, even for RV-C15 whose replication is increased in this group. Because CDHR3 is expressed on ciliated cells, the primary target of RVs and EV-D68, this decrease is likely related to disruption of ciliated cell metabolism and/or ciliated cell death. Overall, these data indicate that different baseline expression levels of receptors do not represent the initial trigger for increased replication in tissues derived from asthmatic donors. However, after the onset of infection, the higher expression of ICAM1 and LDLR could possibly favor multiplication of major and minor group RVs in tissues from asthmatic donors. The situation differs for RV-Cs, where decreased CDHR3 expression would instead limit viral spread.

Concerning CDHR3, we also assessed the impact of the rs6967330 SNP on viral replication. We identified, respectively, 5/12 and 6/14 tissues from control and asthmatic donors heterozygous for the asthma susceptibility allele plus one homozygous control. We did not observe any significant increase in RV-C replication in presence of the *CDHR3* susceptibility allele. Our data thus contradict previous studies performed in similar models, where increased RV-C binding and/or replication was observed (Basnet et al., 2019; Everman et al., 2019). This may be due to the differentiation stage of the tissues at the time of infection. Basnet and colleagues have shown that the difference of expression between the mutated and non-mutated allele is higher before 21 days of tissue differentiation (Basnet et al., 2019). Everman and colleagues (Everman et al., 2019) also highlighted a greater CDHR3 expression in differentiating airway epithelial cells. Both studies showed increased RV-C replication using in-house developed tissues less differentiated than the commercially available, fully differentiated tissues used in this study. Additional investigations are needed to assess the true impact of the *CHDR3* mutation on RV-C replication in fully differentiated HAE from asthmatic donors. Apart from its role as RV-C receptor, CDHR3 is involved in the differentiation of ciliated airway cells (Lutter and Ravanetti, 2019) and participates in the tissue barrier function (Basnet et al., 2019; Everman et al., 2019). Its involvement in asthma exacerbation may thus rely on several pleiotropic effects.

We next assessed whether a deficient IFN-response could account for the increased viral replication. As in our previous study conducted on HAE of control donors (Essaidi-Laziosi et al., 2018), we observed differential replication and IFN-induction between the studied strains, with RV-B48 inducing a weak IFN-response compared to the other viruses. We also confirmed that compared to IFNλ, IFNβ is weakly induced and IFNα almost not expressed from infected HAE. An observation confirmed by others using primary bronchial epithelial cells (Liew et al., 2022). We could not highlight a reduced IFN-response in tissues from asthmatic donors, in contrast, this induction turned to be higher at 4 dpi due to the increased viral replication. Our data on increased RV replication in asthmatic conditions are in line with many studies (Xatzipsalti et al., 2008; Jackson et al., 2014; Hansel et al., 2017; Dhariwal et al., 2021), while others do not observe increased replication (Kennedy et al., 2014; Heymann et al., 2020). Data on IFN-response remain also debated. It is widely accepted that asthma exacerbation after RV infection is in part related to a deficient IFN-response which, in turn, leads to T2-inflammation (Duerr et al., 2016). Nevertheless, many studies, particularly in adult populations, did not observe such a deficient IFN-response, or even found an increased response (Krammer et al., 2021; Yang et al., 2021; Jackson and Gern, 2022; Liew et al., 2022). These inconsistent observations may rely on the baseline level of asthma control and severity between studies, the population age, the model used, and/or the experimental settings. We are using fully differentiated commercially available HAE derived from nasal or bronchial biopsies of adult patients. Furthermore, this model lacks immune cells and as such, the complex interplay between infected epithelial cells and neighbor immune cells. It is thus not fully adapted to study innate response in its entirety. In addition, we measured IFN mRNA at 4 dpi and IL28/29 cytokine from 1 dpi. Some studies report a delayed IFN-response rather than a decreased one (Veerati et al., 2020). We cannot exclude that in our setting, antiviral response was delayed before 24 hpi, allowing increased replication which in turn resulted in higher IFN-induction. This hypothesis is supported by a recent experimental infection with RV-A16 highlighting strong IFN-response at 4 dpi in asthmatic patients (Farne et al., 2022). Nevertheless, if defective very shortly after infection, this IFN-response was very strong afterward and even stronger in asthma patients. At later time points, IFN-induction appears thus to be a consequence rather than a cause of the differences in viral replication between asthma and controls.

As neither receptor expression nor IFN-induction after 24 hpi could consistently account for the overall increased viral replication observed in tissues from asthmatic patients, we performed unbiased transcriptomic analysis of tissues, infected or not with RV-B48 and RV-C15. This analysis highlighted basic morphologic and physiologic differences between tissues derived from controls or asthmatic donors, even in absence of infection. These data were supported by diminished MCC in asthma-derived tissues. The critical role of MCC to limit viral infections is well established and patients presenting defective MCC (due to genetic or environmental causes) suffer from repeated infections (Adivitiya Kaushik et al., 2021). Altogether our observations suggest that the intrinsic defense mechanisms of the respiratory mucosae are affected in tissues derived from asthmatic patients, increasing permissiveness and susceptibility to RV or EV-D68 infections. Perturbation of the epithelial barrier function was observed previously in asthmatic patients (Xiao et al., 2011; Looi et al., 2018). Similarly, mucus hypersecretion was reported in asthmatic settings (Rogers and Barnes, 2006; Evans et al., 2009; Martinez-Rivera et al., 2018). Interestingly, this defective barrier function and perturbed mucus secretion are retained in this *ex vivo* reconstituted tissue culture model, derived after over 45 days from isolated cells taken out of the context of the asthmatic host. This strongly indicates an involvement of genomic imprinting mechanisms, as suggested in the scientific literature (Gruzieva et al., 2021).

To conclude, we could show increased replication of RV-A major and minor groups, RV-B, RV-C, and EV-D68 in HAE derived from asthmatic patients. Our data highlight that a global disruption of epithelial cell barrier function, rather than changes in receptor expression or a deficient IFN response, is likely a key factor in the increased permissiveness and susceptibility to RV or EV-D68 infections. All in all, this work provides novel insights into the mechanism underlying asthma exacerbations upon respiratory enterovirus infections.

Data availability statement

The data presented in the study are deposited in the NCBI website with the GEO accession number: GSE222129. Access: https://www.ncbi.nlm.nih.gov/geo/query/acc.cgi?acc=GSE222129.

Ethics statement

The studies involving human participants were reviewed and approved by commission cantonale d'éthique de la recherche CCER from Geneva. The patients/participants provided their written informed consent to participate in this study.

Author contributions

ME-L, LR, and CT contributed to conception and design of the study. ME-L, LR, BB, IP, and SoC performed the experimental work. ME-L, FP-R, and NH ran the bioinformatic part. LK, SH, and SaC contributed to tissue collection and/or development. ME-L and LR wrote the first draft of the manuscript. CT revised the manuscript. All authors contributed to the manuscript revision, and read and approved the submitted version.

Funding

The study was supported by the Swiss National Foundation (SNF) (Grant 310030_184777 to CT), the SNF Marie Heim-Vögtlin subsides (Grant PMPDP3-158269 and PMPDP3-158269 to ME-L), and the OrganoVIR (grant 812673) in the European Union's Horizon 2020 programme, and the Sandoz foundation (LR Salary).

Acknowledgments

We thank the iGE3 genomics platform of the University of Geneva, for HTS and transcriptome analysis and Jimmy Vernaz for technical help.

Conflict of interest

BB, SH and SaC are employed by Epithelix company.

The remaining authors declare that the research was conducted in the absence of any commercial or financial relationships that could be construed as a potential conflict of interest.

Publisher's note

All claims expressed in this article are solely those of the authors and do not necessarily represent those of their affiliated organizations, or those of the publisher, the editors and the reviewers. Any product that may be evaluated in this article, or claim that may be made by its manufacturer, is not guaranteed or endorsed by the publisher.

Supplementary material

The Supplementary material for this article can be found online at: https://www.frontiersin.org/articles/10.3389/fmicb.2023.1106945/full#supplementary-material

References

Adivitiya Kaushik, M. S., Chakraborty, S., Veleri, S., and Kateriya, S. (2021). Mucociliary respiratory epithelium integrity in molecular defense and susceptibility to pulmonary viral infections. *Biology (Basel)* 10:95. doi: 10.3390/biology10020095

Ambrosioni, J., Bridevaux, P. O., Wagner, G., Mamin, A., and Kaiser, L. (2014). Epidemiology of viral respiratory infections in a tertiary care Centre in the era of molecular diagnosis, Geneva, Switzerland, 2011–2012. *Clin. Microbiol. Infect.* 20, O578–O584. doi: 10.1111/1469-0691.12525

Baraldo, S., Contoli, M., Bazzan, E., Turato, G., Padovani, A., Marku, B., et al. (2012). Deficient antiviral immune responses in childhood: distinct roles of atopy and asthma. *J. Allergy Clin. Immunol.* 130, 1307–1314. doi: 10.1016/j.jaci.2012.08.005

Basnet, S., Bochkov, Y. A., Brockman-Schneider, R. A., Kuipers, I., Aesif, S. W., Jackson, D. J., et al. (2019). CDHR3 asthma-risk genotype affects susceptibility of airway epithelium to rhinovirus C infections. *Am. J. Respir. Cell Mol. Biol.* 61, 450–458. doi: 10.1165/rcmb.2018-0220OC

Bianco, A., Whiteman, S. C., Sethi, S. K., Allen, J. T., Knight, R. A., and Spiteri, M. A. (2000). Expression of intercellular adhesion molecule-1 (ICAM-1) in nasal epithelial cells of atopic subjects: a mechanism for increased rhinovirus infection? *Clin. Exp. Immunol.* 121, 339–345. doi: 10.1046/j.1365-2249.2000.01301.x

Bochkov, Y. A., and Gern, J. E. (2016). Rhinoviruses and their receptors: implications for allergic disease. *Curr. Allergy Asthma Rep.* 16:30. doi: 10.1007/s11882-016-0608-7

Bochkov, Y. A., Watters, K., Ashraf, S., Griggs, T. F., Devries, M. K., Jackson, D. J., et al. (2015). Cadherin-related family member 3, a childhood asthma susceptibility gene product, mediates rhinovirus C binding and replication. *Proc. Natl. Acad. Sci. U. S. A.* 112, 5485–5490. doi: 10.1073/pnas.1421178112

Bonnelykke, K., Coleman, A. T., Evans, M. D., Thorsen, J., Waage, J., Vissing, N. H., et al. (2018). Cadherin-related family member 3 genetics and rhinovirus C respiratory illnesses. *Am. J. Respir. Crit. Care Med.* 197, 589–594. doi: 10.1164/rccm.201705-1021OC

Bonnelykke, K., Sleiman, P., Nielsen, K., Kreiner-Moller, E., Mercader, J. M., Belgrave, D., et al. (2014). A genome-wide association study identifies CDHR3 as a susceptibility locus for early childhood asthma with severe exacerbations. *Nat. Genet.* 46, 51–55. doi: 10.1038/ng.2830

Choi, T., Devries, M., Bacharier, L. B., Busse, W., Camargo, C. A. Jr., Cohen, R., et al. (2021). Enhanced neutralizing antibody responses to rhinovirus C and age-dependent patterns of infection. *Am. J. Respir. Crit. Care Med.* 203, 822–830. doi: 10.1164/rccm.202010-3753OC

Contoli, M., Message, S. D., Laza-Stanca, V., Edwards, M. R., Wark, P. A., Bartlett, N. W., et al. (2006). Role of deficient type III interferon-lambda production in asthma exacerbations. *Nat. Med.* 12, 1023–1026. doi: 10.1038/nm1462

Corne, J. M., Marshall, C., Smith, S., Schreiber, J., Sanderson, G., Holgate, S. T., et al. (2002). Frequency, severity, and duration of rhinovirus infections in asthmatic and non-asthmatic individuals: a longitudinal cohort study. *Lancet* 359, 831–834. doi: 10.1016/S0140-6736(02)07953-9

Da Silva, J., Hilzendeger, C., Moermans, C., Schleich, F., Henket, M., Kebadze, T., et al. (2017). Raised interferon-beta, type 3 interferon and interferon-stimulated genes-evidence of innate immune activation in neutrophilic asthma. *Clin. Exp. Allergy* 47, 313–323. doi: 10.1111/cea.12809

Dhariwal, J., Cameron, A., Wong, E., Paulsen, M., Trujillo-Torralbo, M. B., Del Rosario, A., et al. (2021). Pulmonary innate lymphoid cell responses during rhinovirus-induced asthma exacerbations in vivo: a clinical trial. *Am. J. Respir. Crit. Care Med.* 204, 1259–1273. doi: 10.1164/rccm.202010-3754OC

Dobin, A., Davis, C. A., Schlesinger, F., Drenkow, J., Zaleski, C., Jha, S., et al. (2013). STAR: ultrafast universal RNA-seq aligner. *Bioinformatics* 29, 15–21. doi: 10.1093/bioinformatics/bts635

Dolganiuc, A., Kodys, K., Marshall, C., Saha, B., Zhang, S., Bala, S., et al. (2012). Type III interferons, IL-28 and IL-29, are increased in chronic HCV infection and induce myeloid dendritic cell-mediated FoxP3+ regulatory T cells. *PLoS One* 7:e44915. doi: 10.1371/journal.pone.0044915

Duerr, C. U., Mccarthy, C. D., Mindt, B. C., Rubio, M., Meli, A. P., Pothlichet, J., et al. (2016). Type I interferon restricts type 2 immunopathology through the regulation of group 2 innate lymphoid cells. *Nat. Immunol.* 17, 65–75. doi: 10.1038/ni.3308

Edwards, M. R., Regamey, N., Vareille, M., Kieninger, E., Gupta, A., Shoemark, A., et al. (2013). Impaired innate interferon induction in severe therapy resistant atopic asthmatic children. *Mucosal Immunol.* 6, 797–806. doi: 10.1038/mi.2012.118

Essaidi-Laziosi, M., Brito, F., Benaoudia, S., Royston, L., Cagno, V., Fernandes-Rocha, M., et al. (2018). Propagation of respiratory viruses in human airway epithelia reveals persistent virus-specific signatures. *J. Allergy Clin. Immunol.* 141, 2074–2084. doi: 10.1016/j.jaci.2017.07.018

Essaidi-Laziosi, M., Geiser, J., Huang, S., Constant, S., Kaiser, L., and Tapparel, C. (2020). Interferon-dependent and respiratory virus-specific interference in dual infections of airway epithelia. *Sci. Rep.* 10:10246. doi: 10.1038/s41598-020-66748-6

Essaidi-Laziosi, M., Shevtsova, A. S., and Roux, L. (2014). Minimal features of efficient incorporation of the hemagglutinin-neuraminidase protein into Sendai virus particles. *J. Virol.* 88, 303–313. doi: 10.1128/JVI.02041-13

Evans, C. M., Kim, K., Tuvim, M. J., and Dickey, B. F. (2009). Mucus hypersecretion in asthma: causes and effects. *Curr. Opin. Pulm. Med.* 15, 4–11. doi: 10.1097/MCP.0b013e32831da8d3

Everman, J. L., Sajuthi, S., Saef, B., Rios, C., Stoner, A. M., Numata, M., et al. (2019). Functional genomics of CDHR3 confirms its role in HRV-C infection and childhood asthma exacerbations. *J. Allergy Clin. Immunol.* 144, 962–971. doi: 10.1016/j.jaci.2019.01.052

Farne, H., Lin, L., Jackson, D. J., Rattray, M., Simpson, A., Custovic, A., et al. (2022). In vivo bronchial epithelial interferon responses are augmented in asthma on day 4 following experimental rhinovirus infection. *Thorax* 77, 929–932. doi: 10.1136/thoraxjnl-2021-217389

Filipe, I. C., Tee, H. K., Prados, J., Piuz, I., Constant, S., Huang, S., et al. (2022). Comparison of tissue tropism and host response to enteric and respiratory enteroviruses. *PLoS Pathog.* 18:e1010632. doi: 10.1371/journal.ppat.1010632

Gern, J. E. (2010). The ABCs of rhinoviruses, wheezing, and asthma. *J. Virol.* 84, 7418–7426. doi: 10.1128/JVI.02290-09

Greve, J. M., Davis, G., Meyer, A. M., Forte, C. P., Yost, S. C., Marlor, C. W., et al. (1989). The major human rhinovirus receptor is ICAM-1. *Cells* 56, 839–847. doi: 10.1016/0092-8674(89)90688-0

Gruzieva, O., Merid, S. K., Koppelman, G. H., and Melen, E. (2021). An update on the epigenetics of asthma. *Curr. Opin. Allergy Clin. Immunol.* 21, 175–181. doi: 10.1097/ACI.0000000000000723

Hansel, T. T., Tunstall, T., Trujillo-Torralbo, M. B., Shamji, B., Del-Rosario, A., Dhariwal, J., et al. (2017). A comprehensive evaluation of nasal and bronchial cytokines and chemokines following experimental rhinovirus infection in allergic asthma: increased interferons (IFN-gamma and IFN-lambda) and type 2 inflammation (IL-5 and IL-13). *EBioMedicine* 19, 128–138. doi: 10.1016/j.ebiom.2017.03.033

Hayashi, F., Hayashi, S., Matsuse, D., Yamasaki, R., Yonekura, K., and Kira, J. I. (2018). Hopkins syndrome following the first episode of bronchial asthma associated with enterovirus D68: a case report. *BMC Neurol.* 18:71. doi: 10.1186/s12883-018-1075-7

Heymann, P. W., Platts-Mills, T. A. E., Woodfolk, J. A., Borish, L., Murphy, D. D., Carper, H. T., et al. (2020). Understanding the asthmatic response to an experimental rhinovirus infection: exploring the effects of blocking IgE. *J. Allergy Clin. Immunol.* 146, 545–554. doi: 10.1016/j.jaci.2020.01.035

Hofer, F., Gruenberger, M., Kowalski, H., Machat, H., Huettinger, M., Kuechler, E., et al. (1994). Members of the low density lipoprotein receptor family mediate cell entry of a minor-group common cold virus. *Proc. Natl. Acad. Sci. U. S. A.* 91, 1839–1842. doi: 10.1073/pnas.91.5.1839

Iwane, M. K., Prill, M. M., Lu, X., Miller, E. K., Edwards, K. M., Hall, C. B., et al. (2011). Human rhinovirus species associated with hospitalizations for acute respiratory illness in young US children. *J. Infect. Dis.* 204, 1702–1710. doi: 10.1093/infdis/jir634

Jackson, D. J., and Gern, J. E. (2022). Rhinovirus infections and their roles in asthma: etiology and exacerbations. *J. Allergy Clin. Immunol. Pract.* 10, 673–681. doi: 10.1016/j.jaip.2022.01.006

Jackson, D. J., Makrinioti, H., Rana, B. M., Shamji, B. W., Trujillo-Torralbo, M. B., Footitt, J., et al. (2014). IL-33-dependent type 2 inflammation during rhinovirus-induced asthma exacerbations in vivo. *Am. J. Respir. Crit. Care Med.* 190, 1373–1382. doi: 10.1164/rccm.201406-1039OC

Jazaeri, S., Goldsmith, A. M., Jarman, C. R., Lee, J., Hershenson, M. B., and Lewis, T. C. (2021). Nasal interferon responses to community rhinovirus infections are similar in controls and children with asthma. *Ann. Allergy Asthma Immunol.* 126:e691, 690–695.e1. doi: 10.1016/j.anai.2021.01.023

Kanazawa, J., Masuko, H., Yatagai, Y., Sakamoto, T., Yamada, H., Kaneko, Y., et al. (2017). Genetic association of the functional CDHR3 genotype with early-onset adult asthma in Japanese populations. *Allergol. Int.* 66, 563–567. doi: 10.1016/j.alit.2017.02.012

Kennedy, J. L., Shaker, M., Mcmeen, V., Gern, J., Carper, H., Murphy, D., et al. (2014). Comparison of viral load in individuals with and without asthma during infections with rhinovirus. *Am. J. Respir. Crit. Care Med.* 189, 532–539. doi: 10.1164/rccm.201310-1767OC

Korematsu, S., Nagashima, K., Sato, Y., Nagao, M., Hasegawa, S., Nakamura, H., et al. (2018). "spike" in acute asthma exacerbations during enterovirus D68 epidemic in Japan: a nation-wide survey. *Allergol. Int.* 67, 55–60. doi: 10.1016/j.alit.2017.04.003

Krammer, S., Sicorschi Gutu, C., Grund, J. C., Chiriac, M. T., Zirlik, S., and Finotto, S. (2021). Regulation and function of interferon-lambda (IFNlambda) and its receptor in asthma. *Front. Immunol.* 12:731807. doi: 10.3389/fimmu.2021.731807

Lee, W. M., Lemanske, R. F. Jr., Evans, M. D., Vang, F., Pappas, T., Gangnon, R., et al. (2012). Human rhinovirus species and season of infection determine illness severity. *Am. J. Respir. Crit. Care Med.* 186, 886–891. doi: 10.1164/rccm.201202-0330OC

Liew, K. Y., Koh, S. K., Hooi, S. L., Ng, M. K. L., Chee, H. Y., Harith, H. H., et al. (2022). Rhinovirus-induced cytokine alterations with potential implications in asthma exacerbations: a systematic review and meta-analysis. *Front. Immunol.* 13:782936. doi: 10.3389/fimmu.2022.782936

Livak, K. J., and Schmittgen, T. D. (2001). Analysis of relative gene expression data using real-time quantitative PCR and the 2(-Delta Delta C(T)) method. *Methods* 25, 402–408. doi: 10.1006/meth.2001.1262

Looi, K., Buckley, A. G., Rigby, P. J., Garratt, L. W., Iosifidis, T., Zosky, G. R., et al. (2018). Effects of human rhinovirus on epithelial barrier integrity and function in children with asthma. *Clin. Exp. Allergy* 48, 513–524. doi: 10.1111/cea.13097

Lutter, R., and Ravanetti, L. (2019). Cadherin-related family member 3 (CDHR3) drives differentiation of ciliated bronchial epithelial cells and facilitates rhinovirus C infection, although with a little help. *J. Allergy Clin. Immunol.* 144, 926–927. doi: 10.1016/j.jaci.2019.07.021

Martinez-Rivera, C., Crespo, A., Pinedo-Sierra, C., Garcia-Rivero, J. L., Pallares-Sanmartin, A., Marina-Malanda, N., et al. (2018). Mucus hypersecretion in asthma is associated with rhinosinusitis, polyps and exacerbations. *Respir. Med.* 135, 22–28. doi: 10.1016/j.rmed.2017.12.013

Moss, R. B. (2016). Enterovirus 68 infection--association with asthma. *J. Allergy Clin. Immunol. Pract.* 4, 226–228. doi: 10.1016/j.jaip.2015.12.013

Robinson, M. D., Mccarthy, D. J., and Smyth, G. K. (2010). edgeR: a Bioconductor package for differential expression analysis of digital gene expression data. *Bioinformatics* 26, 139–140. doi: 10.1093/bioinformatics/btp616

Rogers, D. F., and Barnes, P. J. (2006). Treatment of airway mucus hypersecretion. *Ann. Med.* 38, 116–125. doi: 10.1080/07853890600585795

Royston, L., and Tapparel, C. (2016). Rhinoviruses and respiratory enteroviruses: not as simple as ABC. *Viruses* 8:16. doi: 10.3390/v8010016

Sopel, N., Pflaum, A., Kolle, J., and Finotto, S. (2017). The unresolved role of interferon-lambda in asthma Bronchiale. *Front. Immunol.* 8:989. doi: 10.3389/fimmu.2017.00989

Sykes, A., Macintyre, J., Edwards, M. R., Del Rosario, A., Haas, J., Gielen, V., et al. (2014). Rhinovirus-induced interferon production is not deficient in well controlled asthma. *Thorax* 69, 240–246. doi: 10.1136/thoraxjnl-2012-202909

Tapparel, C., Cordey, S., Junier, T., Farinelli, L., Van Belle, S., Soccal, P. M., et al. (2011). Rhinovirus genome variation during chronic upper and lower respiratory tract infections. *PLoS One* 6:e21163. doi: 10.1371/journal.pone.0021163

Veerati, P. C., Troy, N. M., Reid, A. T., Li, N. F., Nichol, K. S., Kaur, P., et al. (2020). Airway epithelial cell immunity is delayed during rhinovirus infection in asthma and COPD. *Front. Immunol.* 11:974. doi: 10.3389/fimmu.2020.00974

Xatzipsalti, M., Psarros, F., Konstantinou, G., Gaga, M., Gourgiotis, D., Saxoni-Papageorgiou, P., et al. (2008). Modulation of the epithelial inflammatory response to rhinovirus in an atopic environment. *Clin. Exp. Allergy* 38, 466–472. doi: 10.1111/j.1365-2222.2007.02906.x

Xiao, C., Puddicombe, S. M., Field, S., Haywood, J., Broughton-Head, V., Puxeddu, I., et al. (2011). Defective epithelial barrier function in asthma. *J. Allergy Clin. Immunol.* 128, 549–556.e12. doi: 10.1016/j.jaci.2011.05.038

Yang, Z., Mitlander, H., Vuorinen, T., and Finotto, S. (2021). Mechanism of rhinovirus immunity and asthma. *Front. Immunol.* 12:731846. doi: 10.3389/fimmu.2021.731846

Yu, G., Wang, L. G., Han, Y., and He, Q. Y. (2012). clusterProfiler: an R package for comparing biological themes among gene clusters. *OMICS* 16, 284–287. doi: 10.1089/omi.2011.0118

Zhang, Y., Ma, K. L., Ruan, X. Z., and Liu, B. C. (2016). Dysregulation of the low-density lipoprotein receptor pathway is involved in lipid disorder-mediated organ injury. *Int. J. Biol. Sci.* 12, 569–579. doi: 10.7150/ijbs.14027

Zhu, J., Message, S. D., Mallia, P., Kebadze, T., Contoli, M., Ward, C. K., et al. (2019). Bronchial mucosal IFN-alpha/beta and pattern recognition receptor expression in patients with experimental rhinovirus-induced asthma exacerbations. *J. Allergy Clin. Immunol.* 143:e114, 114–125.e4. doi: 10.1016/j.jaci.2018.04.003

frontiers | Frontiers in Microbiology

TYPE Mini Review
PUBLISHED 10 May 2023
DOI 10.3389/fmicb.2023.1190463

OPEN ACCESS

EDITED BY
Shijian Zhang,
Dana–Farber Cancer Institute, United States

REVIEWED BY
Lee Sherry,
University of Leeds, United Kingdom
Yu Zhou,
Dana–Farber Cancer Institute, United States

*CORRESPONDENCE
Amar Aganovic
amar.aganovic@uit.no

RECEIVED 20 March 2023
ACCEPTED 24 April 2023
PUBLISHED 10 May 2023

CITATION
Aganovic A (2023) pH-dependent endocytosis mechanisms for influenza A and SARS-coronavirus.
Front. Microbiol. 14:1190463.
doi: 10.3389/fmicb.2023.1190463

pH-dependent endocytosis mechanisms for influenza A and SARS-coronavirus

Amar Aganovic*

Faculty of Engineering Science and Technology, UiT The Arctic University of Norway, Tromsø, Norway

The ongoing SARS-CoV-2 pandemic and the influenza epidemics have revived the interest in understanding how these highly contagious enveloped viruses respond to alterations in the physicochemical properties of their microenvironment. By understanding the mechanisms and conditions by which viruses exploit the pH environment of the host cell during endocytosis, we can gain a better understanding of how they respond to pH-regulated anti-viral therapies but also pH-induced changes in extracellular environments. This review provides a detailed explanation of the pH-dependent viral structural changes preceding and initiating viral disassembly during endocytosis for influenza A (IAV) and SARS coronaviruses. Drawing upon extensive literature from the last few decades and latest research, I analyze and compare the circumstances in which IAV and SARS-coronavirus can undertake endocytotic pathways that are pH-dependent. While there are similarities in the pH-regulated patterns leading to fusion, the mechanisms and pH activation differ. In terms of fusion activity, the measured activation pH values for IAV, across all subtypes and species, vary between approximately 5.0 to 6.0, while SARS-coronavirus necessitates a lower pH of 6.0 or less. The main difference between the pH-dependent endocytic pathways is that the SARS-coronavirus, unlike IAV, require the presence of specific pH-sensitive enzymes (cathepsin L) during endosomal transport. Conversely, the conformational changes in the IAV virus under acidic conditions in endosomes occur due to the specific envelope glycoprotein residues and envelope protein ion channels (viroporins) getting protonated by H+ ions. Despite extensive research over several decades, comprehending the pH-triggered conformational alterations of viruses still poses a significant challenge. The precise mechanisms of protonation mechanisms of certain during endosomal transport for both viruses remain incompletely understood. In absence of evidence, further research is needed.

KEYWORDS

respiratory virus, influenza A, SARS-coronavirus, pH, endocytosis, enveloped virus

1. Introduction

During the first two decades of the 21st century, humanity has faced significant difficulties due to the emergence of highly pathogenic and contagious respiratory viruses, including severe acute respiratory syndrome coronavirus (SARS-CoV), Middle East respiratory syndrome coronavirus (MERS-CoV), IAV virus subtype H1N1, and the current

severe acute respiratory syndrome coronavirus 2 (SARS-CoV-2). The substantial levels of illness (Shi et al., 2017; James et al., 2018; Lopez-Leon et al., 2021), increased mortality (Zucs et al., 2005; Iuliano et al., 2018; Hansen et al., 2022; Msemburi et al., 2023), and significant socioeconomic consequences (Fendrick et al., 2003; Cutler and Summers, 2020) caused by these respiratory viruses have emphasized the need for effective measures to contain their spread. To mitigate the transmission of these viruses, both occupational and public health measures have been implemented, such as physical distancing, mask-wearing, disinfection, and the development of antiviral drugs, antibody-based therapies, and vaccines. In addition, since the recognition of airborne transmission as the main route of spread, engineering strategies have recommended the enhancement of indoor air quality through improved ventilation, air purifiers, and/or filtration of recirculated air (Sachs et al., 2022). Other approaches have also sought to take advantage of the sensitivity of enveloped viruses to environmental conditions, including temperature (Dabisch et al., 2020; Biryukov et al., 2021), UV levels (Dabisch et al., 2020; Biasin et al., 2021), and relative humidity (Dabisch et al., 2020). However, one environmental factor that has received limited attention during the pandemic is the potential impact of the pH value of the virus aerosol microenvironment (Luo et al., 2023).

Compared to the limited knowledge on the pH impact on viral survival in extracellular environments including aerosols and surfaces, inquiry into the impact of pH on respiratory viruses in intracellular environments began decades ago (Maeda et al., 1981). Both influenza and coronaviruses are known to be sensitive to changes in pH during the endocytosis process, which is a critical step in the infection cycle by which viruses enter host cells from the extracellular environment. For example, it is well-accepted that low pH induces viral disassembly and promotes the release of genetic material within the host cell (Stegmann et al., 1987). When the pH within the host cell becomes acidic (i.e., the concentration of hydrogen ions increases), the protein residues of the lipid membrane may become protonated, which eventually induces conformational changes in the envelope glycoproteins to a large extent, and to a lesser extent, in the viroporins (Caffrey and Lavie, 2021). This can cause the envelope to become more permeable, which may allow ions and other molecules to enter the virus and disrupt its structure. Additionally, changes in pH can also affect the electrostatic interactions between the viral proteins and the envelope, further destabilizing the virus (Shtykova et al., 2017). The COVID-19 pandemic has reignited interest in this topic, and recent studies have tried to elucidate the mechanisms involving pH-induced changes in the envelope disassembly of SARS-CoV-2 (Kreutzberger et al., 2022; Luo et al., 2023). In addition, the technological advancements in microscope technologies have enabled scientists to gain new insights into the mechanisms by which viruses are affected by changes in pH during endocytosis (Assaiya et al., 2021; Guaita et al., 2022).

In this review, I discuss developments in our understanding of the pH-induced endocytosis mechanisms in IAV and SARS-coronavirus. Drawing upon extensive literature from the last few decades and latest research, this mini-review provides a detailed explanation of the pH-dependent structural changes necessary for viral disassembly and fusion during endocytosis. Using this summary, I recognize the significant differences that result in pH-induced structural changes preceding the viral disassembly and initiating fusion with the host cell. The main aim of this review is to provide a better understanding of how the structural changes of two the highly contagious enveloped respiratory viruses differ in response to intracellular acidic environments.

2. Influenza A

Influenza is a negative-strand RNA virus with eight ribonucleoprotein particles (RNPs) contained within a lipid envelope derived from the host plasma membrane. The IAV viral envelope contains two major glycoproteins proteins, hemagglutinin (HA) and neuraminidase (NA), that project from the lipid membrane as spikes (Sriwilaijaroen and Suzuki, 2012). A third envelope protein is a homotetrameric protein 2 (AM2) consisting of an extracellular N-terminal segment, a transmembrane segment, and an intracellular C-terminal segment (Pielak and Chou, 2011). The lipid membrane envelope encapsulates the M1 protein, consisting of the N-terminal domain, middle domain, and C-terminal domain, which forms a rigid matrix layer under the lipid envelope and interacts with both the viral RNP particles and lipid envelope with the cytoplasmic tails of HA and NA (Lamb and Choppin, 1983; Bouvier and Palese, 2008; Dou et al., 2018).

2.1. IAV pH-regulated endocytic pathways: clathrin-mediated endocytosis

There are several types of viral entries to the cell, also known as endocytic pathways that can be utilized by influenza viruses, including predominantly clathrin-mediated and caveolin-mediated endocytosis (Lakadamyali et al., 2004; Brandenburg and Zhuang, 2007; de Vries et al., 2011). The pathways differ in the manner by which the virus particle attaches to the surface of the host cell. Caveolin-mediated endocytosis does not require sialic acid receptors for internalization of the virus, unlike clathrin-mediated endocytosis (Lakadamyali et al., 2004). The trafficking of clathrin-mediated endosomes relies on acidic pH, while the transport of caveolae containing vesicles to the destination is a neutral pH selection (Kiss and Botos, 2009). Therefore, pH-independent caveolin-mediated endocytosis is not considered in this paper. Before attaching to sialic acid, the HA glycoprotein in the viral membrane initially exists as a single polypeptide known as HA0, which must be cleaved by the host's trypsin and serine-like proteases (TMPRSS2) to form a complex consisting of three HA1 (positively charged) and three HA2 (negatively charged) polypeptide chains linked by two disulfide bonds (Chen et al., 1998). HA1, which is located distal to the virus membrane, is responsible for receptor binding. On the other hand, HA2, which is located proximal to the membrane, anchors HA in the envelope and contains the fusion peptide (Benton et al., 2020a). As shown on **Figure 1**, once the HA cleavage occurs, the receptor binding pocket at the top of the positively charged HA1 subunit becomes available for binding with negatively charged sialic-acid receptors (Mair et al., 2014a). After viral internalization, the incoming virus

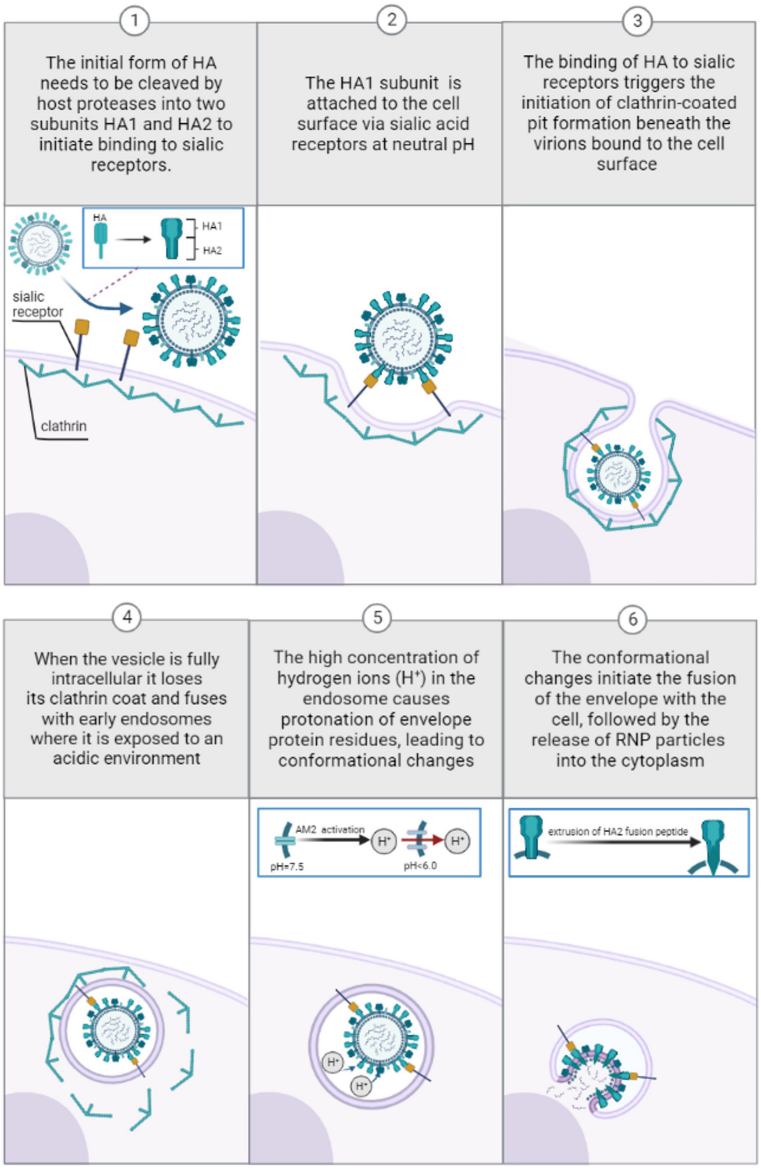

FIGURE 1
Pre-viral entry of Influenza virus and binding to sialic acid receptors during clathrin-mediated endocytosis at neutral pH (1–3). Viral entry and transport through endosomes during clathrin-mediated endocytosis: low pH-induced conformational changes (4–6).

is transported through early endosomes (pH range ~5.6–6.5) (Padilla-Parra et al., 2012), late endosomes (pH range ~5.0–5.5) (Wallabregue et al., 2016), and lysosomes (pH range between 4.6 and 5.0) (Luzio et al., 2007).

Eventually, the cleaved pre-fusion neutral pH HA (Staschke et al., 1998) is attached to the cell surface via sialic acid receptors. According to experimental observations (Carr et al., 1997), the cleaved extracellular HA protein is trapped in a metastable state at neutral pH before viral entry. At neutral pH, molecular modeling studies have demonstrated that there is a strong electrostatic attraction between the positively charged HA1 and negatively charged HA2 monomers, while there is a repulsive electrostatic force between three subunits of either HA1 or HA2 (Huang et al., 2002). Consequently, electrostatic repulsion between the three HA1 monomers and three HA2 monomers is offset by electrostatic attraction between the HA1 and HA2 domains, thereby preserving a metastable trimeric association of the monomers. The binding of HA1 to sialic residues on membrane cells triggers the initiation of clathrin-coated pit formation beneath the virions bound to the cell surface (Rust et al., 2004). These pits then bud from the membrane to form small intracellular clathrin-coated vesicles containing the virions and their bound receptors (Matlin et al., 1981; Lakadamyali et al., 2004). When the vesicle is fully intracellular it loses its clathrin coat and ultimately fuses with early endosomes where it is exposed to an acidic environment (pH range ~5.6–6.5) (Padilla-Parra et al., 2012). The high concentration of hydrogen ions (H+) in the endosome causes protonation of specific to envelope glycoprotein residues, leading to eventual conformational changes within the virus critical for later fusion with the host cell.

2.1.1. pH-induced hemagglutinin conformational changes

The pH dependence of the early stages of HA conformational change is regulated by the histidine residue HR184 of the HA1 and HA2 monomers (Mair et al., 2014b; Trost et al., 2019). The side chain of histidine is uncharged at physiological pH (~7.4) because it has a pKa of approximately 6. As the environmental pH decreases, the HA histidine residue with a pKa value greater than the environmental pH becomes protonated (Mair et al., 2014b; Trost et al., 2019). Protonation leads to a significant increase in positive net charge, inducing the repulsion of HA1 monomers (Huang et al., 2002) and the partial dissociation of HA1 globular domains (Zhou et al., 2014). Thus, protonation triggers the enlarging of the cleavage between HA1 and HA2 monomers. As a consequence, water can enter the central cavity, which in turn induces the structural transitions of the HA2 monomer/sequences (Kemble et al., 1992) which have originally been shielded from contact with water (Böttcher et al., 1999; Huang et al., 2002). Interaction with water induces extrusion of the HA-2 fusion peptide from its buried position in the HA trimer to the distal tip of the HA spike (Ruigrok et al., 1989), eventually triggering the disintegration of the viral membrane by forming a pore through which the genomic segments of the virus are released (Cross et al., 2009; Rice et al., 2022). An HA that is too acid stable may not be sufficiently sensitive to trigger fusion pH-dependent uncoating, meaning that acid stability could restrict a virus' ability to replicate in intracellular environments. Measured HA activation pH values across all subtypes and species range from ~5.0 to 6.0, trending higher in highly pathogenic H5N1 (Zaraket et al., 2013) and H7N9 strains (pH 5.6–6.0) (Chang et al., 2020) whereas seasonal human strains are more acid-stable (pH of fusion 5.0 to 5.6) (Galloway et al., 2013).

2.1.2. pH-induced AM2 conformational changes

The AM2 protein forms a pH-activated proton-selective channel (Sakaguchi et al., 1996; Cady et al., 2009) essential for the acidification of the virus interior, thereby facilitating the dissociation of the matrix protein M1 from the viral nucleoproteins—a step that precedes fusion-pore formation (Zebedee and Lamb, 1988; Ivanovic et al., 2012). As the pH of the endosome encapsulating the virus is lowered, the AM2 channel becomes activated, allowing a unidirectional proton across the membrane to equilibrate the pH of the virus interior with that of the acidic endosome (Kelly et al., 2003). Once activated, the M2 channel conducts 10 to 10,000 protons per second (Mould et al., 2000a; Lin and Schroeder, 2001). This pH-activated protonation is mediated by an interplay between four proton-selective histidine residues His-37 and the proton conductive four tryptophan 41 (Trp 41) residues, both located in a narrow aqueous pore of the transmembrane domain (TMD) (Wang et al., 1995; Venkataraman et al., 2005; Hu et al., 2006; Schnell and Chou, 2008). Two proton conduction mechanisms have been proposed: the "water wire model" and the "proton relay model" mechanism. According to the "water-wire model," the pore is essentially closed at neutral pH (pH = 7.5) as the Val 27 residue at the N terminal and the Trp 41 gate block water from freely entering into the pore, thus preventing proton diffusion across the membrane (Schnell and Chou, 2008). Lowering the pH protonates the imidazole rings of His-37, resulting in several imidazolium per channel, which repel each other and destabilize the transmembrane-helices packing. This conformational rearrangement breaks interactions between Trp 41 and Asp 44 residue and widens the pore, followed by a formation of a continuous hydrogen-bonded water network over which protons hop utilizing the Grotthuss mechanism (Chen et al., 2007). Carr–Purcell–Meiboom–Gill (CPMG) experiments have found that lowering the pH from 7.5 to 6.0, increases the frequency of Trp 41 gate opening by more than fourfold, while no significant frequency is changed when lowered to pH = 7.0 (Schnell and Chou, 2008). Under ideal conditions of the "water-wire model," the constricted N-terminal only allows protons to penetrate the aqueous pore through a hydrogen-bonded water network. This assumption is confirmed by many electrophysiological studies that show that the highly selective M2 channel is virtually impermeable to Na^+, K^+, or Cl^- ions regardless of external pH conditions (Chizhmakov et al., 1996, 2003; Mould et al., 2000b; Lin and Schroeder, 2001; Intharathep et al., 2008). Accordingly, the M2 protein only transports protons, and this permeation increases tenfold as the pH drops from below 8.5 until it reaches a saturation level close to pH = 4 (Chizhmakov et al., 1996). The selectivity, however, may not be absolute as the permeation of other ions through this channel has been suggested from earlier experiments (Pinto et al., 1992). It has been suggested that experimental artifacts from earlier studies are responsible for these differences (Chizhmakov et al., 1996).

On the other hand, the "proton-relay model" mechanism requires at least one non-protonated histidine at the gating region, with its two nitrogen atoms facing the extracellular side (Pinto et al., 1997; Chen et al., 2007). This model hypothesizes that one His-37 imidazole nitrogen atom is protonated by the entering hydronium ion before the other imidazole nitrogen releases its proton to the interior of the virus. Finally, the process is completed by flipping of imidazole rings, or tautomerization, to establish the original configuration to prepare for the next proton relay. The reliability of the model is uncertain as it appears that for a His residue to act as a proton relay two nitrogens from the same histidine residue must be exposed to water within the channel pore (Pinto et al., 1997). However, simulation studies have not revealed this specific conformation of His-37 (Phongphanphanee et al., 2010).

2.1.3. pH-induced neuraminidase conformational changes

Neuraminidase (NA)'s primary role is in the later stages of infection, where it aids in the detachment and spread of the virus to new cells by removing sialic acids from cellular receptors and newly synthesized HA and NA on nascent virions (Palese et al., 1974; Basak et al., 1985). This process prevents the virus from binding back to the dying host cell and enables the efficient release of RNA genomes (Palese et al., 1974). NA is most effective at a pH range of 5.5–6.0 (Mountford et al., 1982; Lentz et al., 1987; McKimm-Breschkin, 2000), although certain viruses have been found to maintain stable NA activity at a lower pH range of 4.0–5.0, resulting in enhanced replication kinetics (Takahashi and Suzuki, 2015).

2.1.4. pH-induced M1 conformational changes

The M1 protein binds both to the RNP complex and the lipid membrane. The M1–lipid binding is mediated through electrostatic interactions between the positively charged N-terminal domain residues (Arg76 and Arg78) and negatively charged cytoplasmic tails of HA and NA (Höfer et al., 2019), while the matrix

protein interacts with the viral RNP complex inside the virus via the C-terminal domain (Shtykova et al., 2017) but also the middle domain (Noton et al., 2007). It is hypothesized that the acidification in the endosome causes the M1 protein to undergo a conformational change which ultimately allows the disassembly of the RNP-M1-lipid membrane complex and RNP detachment from the membrane (Calder et al., 2010; Fontana et al., 2012). Research by cryo-electron tomography (ET) further showed that the intermolecular interactions in the M1 layer are affected when the virions were incubated at pH 5.0, and the matrix layer was no longer seen in the virions (Lee, 2010). Specifically, other cryo-ET studies have indicated that acidification affects the oligomerization state of the M1 protein; it has been demonstrated that intact M1 display multiple-ordered forms of oligomers at neutral pH 7.4 which are dissociated at pH 5.0 (Zhang et al., 2012). Not until recently has the first full structure of full-length M1 been observed; subtomogram observations showed it contains a five histidine residues cluster that may serve as the pH-sensitive disassembly switch (Peukes et al., 2020). Despite these findings, the precise mechanism of protonation of the M1 protein during endosomal transport remains poorly understood, and further research is needed (Selzer et al., 2020).

3. SARS-coronavirus

The positive-stranded RNA genome of SARS-coronavirus encodes three membrane proteins: the spike (S) glycoprotein, responsible for binding the cell-surface receptor to induce virus-host cell fusion (Huang et al., 2020); and the viral envelope proteins consisting of the membrane (M) glycoprotein and the envelope (E) protein. The S protein anchored in the viral membrane is a trimer with each protomer composed of S1 and S2 subunits non-covalently bound in the pre-fusion state (Örd et al., 2020).

3.1. pH-dependent infection routes: S protein conformational changes activated by cathepsin L during clathrin-mediated endocytosis

SARS-coronavirus entry into target cells starts with protease-induced preactivation of the S1/S2 cleavage (Peacock et al., 2021). The protease-activated cleavage is followed by S1 binding to the host cellular receptor angiotensin-converting enzyme 2 (ACE2) (Li et al., 2003). Successive ACE2 binding further weakens the protease-induced preactivation of the S1/S2 cleavage, followed by cleavage of the S2 unit to generate S2′ (Benton et al., 2020b). The S2′ fusion peptide is then liberated and eventually penetrated the host target cell, ultimately leading to the fusion of the viral and host cell membranes after which viral RNA is released into the cytoplasm, where it replicates (Walls et al., 2017; Benton et al., 2020b). The conformational changes in the S2 unit can be triggered by either the transmembrane serine protease TMPRSS2 (Tortorici et al., 2019) or lysosomal cysteine protease cathepsin L in the endosomal compartment following ACE2-mediated endocytosis (Hoffmann et al., 2020; Zhao et al., 2021). However, the timing and dynamics of these proteolytic cleavages differ for different coronavirus types. After protease-preactivation of the S1/S2 cleavage, SARS-CoV-2 can use mutually exclusive routes to penetrate cells: one fast TMPRSS2-mediated plasma membrane entry (10 min) and one slower (40–50 min) clathrin-mediated endocytosis where S2′ cleavage is performed by cathepsin L (Koch et al., 2021; Jackson et al., 2022). TMPRSS2 is active at the cell surface regardless of pH conditions (Koch et al., 2021; Jackson et al., 2022), unlike cathepsin L, which requires a low-pH environment typical of endolysosomes (Mohamed and Sloane, 2006; Koch et al., 2021; Jackson et al., 2022).

Thus, SARS-CoV-2 fusion is essentially independent of pH value as endosomal acid-dependent penetration through cathepsin L occurs only in cells devoid of TMPRSS2 (Koch et al., 2021) as shown in **Figure 2**. Although several studies support the view that TMPRSS2-dependent early entry route is more efficient and results in a more productive infection than the cathepsin L-activated mechanisms for some CoV strains (Shirato et al., 2017, 2018), other studies indicate that more recent Omicron SARS-CoV-2 variants favor the low-pH endosomal entry route (Meng et al., 2022). For fusion activity in SARS-CoV, cathepsin Ls have been shown to require reduced pH of at least 6.0 or lower, found in the endolysosomal compartment (Luzio et al., 2007; Padilla-Parra et al., 2012; Wallabregue et al., 2016). Human cathepsin L is very unstable (kinact = 0.15 s−1) at close to neutral conditions (pH = 7.4; 37°C) and the inactivation rates increase for at least one order of magnitude between pH 7.0 and 8.0 at 37°C [L109]. Interestingly, the cathepsin L activity is very temperature dependent: at pH = 7.4, a temperature rise from 5 to 37°C results in a thousand-fold increase in the inactivation rate (Turk et al., 1993). Bound to negatively charged surfaces, the cathepsin L activity also depends on the ionic composition of the exposed milieu (Dehrmann et al., 1995). Studies focusing on the composition of buffers have shown that different ionic solutions and ionic strengths have unique impacts on cathepsin L activity (Dehrmann et al., 1995, 1996). While in phosphate solutions the enzymatic activity occurs at a slightly acidic condition range of pH = 5.5–6.0 (Mason and Massey, 1992), the cathepsin L activity peaks at pH = 6.5 in acetate-MES2-Tris (AMT) buffers (Dehrmann et al., 1996) at constant molarity. In most enzyme-catalyzed reactions carried out in the laboratory the ionic strength is usually fairly high due largely to the high buffer concentrations needed to ensure constant pH. The higher the ionic strength, the greater the electrostatic interactions between ions in the solution, which can affect various chemical and physical properties of the solution (Kennedy, 1990). For instance, when increasing the ionic strength of a weak acid its optimum pH shifts to lower pH values at constant molarity, and the opposite trend is true for weak bases (Dennison, 2003). It has been observed that cathepsin L activity time is reduced with an increase in the ionic strength of phosphate buffer–a weak acid (Kennedy, 1990), implying increasing the ionic strength in weak acids may increase the optimum pH activity range for cathepsin L and vice versa. The effects of ionic strength on the activities of cathepsin Ls may be of key significance in establishing their true potential for extracellular activity processes such as anti-viral drug development (Turk et al., 1993; Dehrmann et al., 1995). While cathepsin L activity generally favors slightly acid conditions, in sodium citrate buffers cathepsin L is irreversibly inactivated at pH values lower than 4.0 (Turk et al., 1993), an acidic environment that can occur in intact cells where matured lysosomes may reach a pH as low as 3.8 (Berg et al., 1995; Van Dyke, 1995).

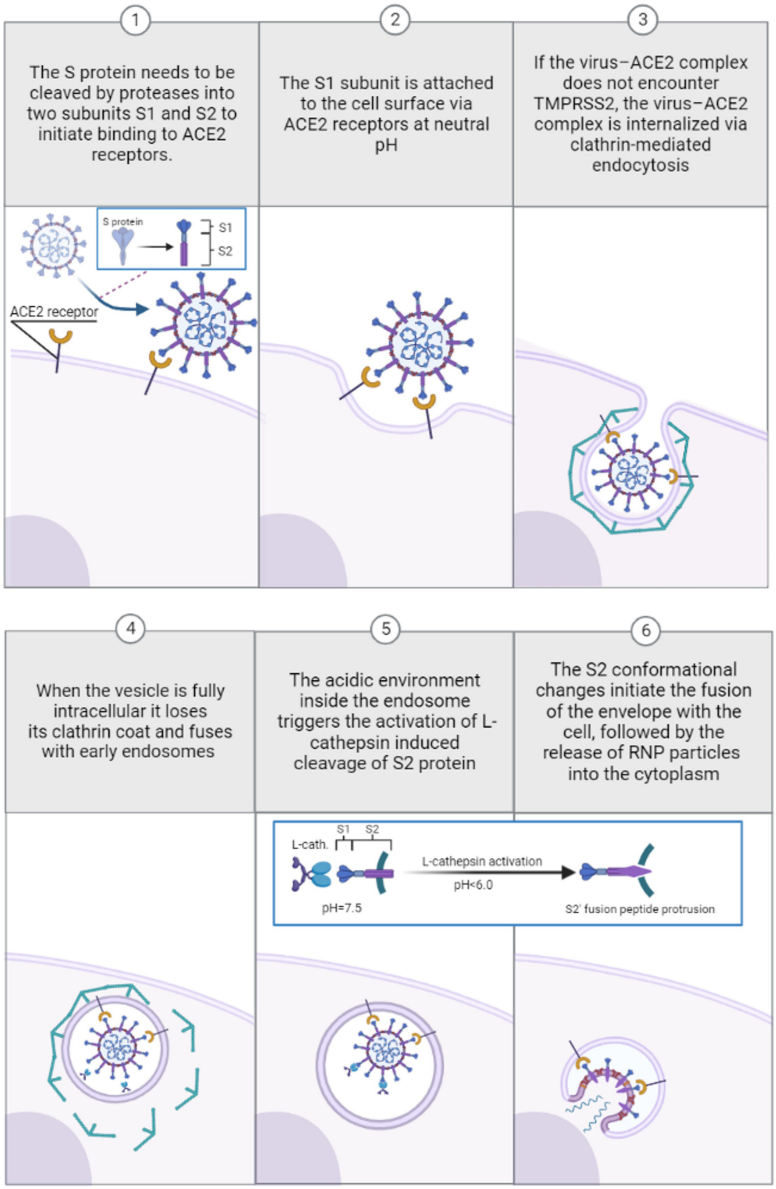

FIGURE 2
Pre-viral entry of SARS-coronavirus and binding to ACE-2 receptors during clathrin-mediated endocytosis in absence of TMPRSS2 (1–3). Viral entry and transport through endosomes during clathrin-mediated endocytosis: low pH-induced conformational changes induced by cathepsin L activation in acidified endosomes (4–6).

3.1.1. pH-induced M protein conformational changes

The M protein is the most abundant structural protein and contains three transmembrane helices, with a short amino-terminal ectodomain and a large carboxy-terminal endodomain (Kuo et al., 2007). The M protein defines the envelope shape and is directly involved in virus assembly, replication, and membrane budding (Hu et al., 2003; Neuman et al., 2011). Although the structure of M protein forms a dimer that is structurally related to the SARS-CoV-2 ion channel ORF3a (Ouzounis, 2020; Dolan et al., 2022), reported cryo-electron microscopy structures revealed that is unlikely that the so far known forms of M protein function as an ion channel because its transmembrane region is highly hydrophobic and has no apparent ion permeation pathway (Zhang et al., 2022). These findings do not rule out the possibility that the two currently recognized forms of the M protein, an elongated and a compact one (Neuman et al., 2011; Dolan et al., 2022), represent closed conformations, and that a different, unknown form is responsible for ion conduction. Although the function of coronavirus M appears to be analogous to that of the virus M1 protein of influenza A (Neuman et al., 2011), no similar pH-sensitive behavior has yet been observed.

3.1.2. pH-induced E protein conformational changes

The smallest of the major structural proteins, the multifunctional E protein acts on several aspects of the virus' life cycle, including virus assembly, budding and pathogenesis

(Schoeman and Fielding, 2019). The E protein is composed of a short hydrophilic N-terminal, followed by a large hydrophobic TMD, and ends with a long hydrophilic C-terminal domain, which compromises the majority of the protein Structurally, the TM domain of E forms a pH-sensitive pentameric ion channel (viroporin) on the ER/Golgi membrane, which is generally permeable to Ca2+, Na+, Mg2+ and K+ ions (Verdiá-Báguena et al., 2012; Nieto-Torres et al., 2015; Cabrera-Garcia et al., 2021; Xia et al., 2021), but also to H+ ions according to *in silico* studies and pH imaging (Cabrera-Garcia et al., 2021; Xia et al., 2021). In mammalian cells, the SARS-CoV-2 viroporin is activated at pH = 6.0 and 7.4, whereas at alkaline pH values of 8 and above the viroporin activity is reduced (Cabrera-Garcia et al., 2021; Xia et al., 2021). However, some inconsistencies between studies and tests have been noted. The varying ion channel characteristics of E proteins across different coronaviruses and even within different experimental settings have led to concerns that certain outcomes could be erroneous.

4. Discussion

In this review, I analyze and compare the conditions and mechanisms of pH-dependent endocytic pathways for IAV and SARS-coronavirus. While there are similarities in the pattern, there are notable differences in the mechanisms and incidence of pH-dependent endocytosis. Influenza viral entry primarily takes place via clathrin-mediated and caveolin-mediated endocytosis, but only the former is regulated by pH. After viral clathrin-mediated internalization, the incoming virion is transported through an acidic environment in early endosomes, late endosomes, and lysosomes. As the pH of the endosome encapsulating the virus is lowered, the virus structure undergoes several conformational changes. The lowered pH value induces the extrusion of the HA-2 fusion peptide from its buried position which forms a pore through which the genomic segments of the virus are released. In addition, the AM2 proton channel becomes activated, allowing a unidirectional proton across the membrane to equilibrate the pH of the virus interior with that of the acidic endosome. Lowered pH also induces conformational changes to the influenza NA and M1 protein, however, unlike HA and AM2 the precise mechanisms remain poorly understood, and further research is needed. Measured influenza activation pH values across all subtypes and species range from ∼5.0 to 6.0, trending higher in highly pathogenic H5N1 and H7N9 strains whereas seasonal human strains are more acid-stable (pH of fusion 5.0 to 5.6). Similar to IAV, SARS-CoV-2 can use mutually exclusive routes to penetrate cells: one fast pH-independent TMPRSS2-mediated plasma route, and one pH-dependent slow clathrin-mediated endocytosis via cathepsin L. The clathrin-mediated endocytosis through cathepsin L occurs only in cells devoid of TMPRSS2. Unlike TMPRSS2, which is active at the cell surface regardless of pH conditions, cathepsin L requires a low-pH environment typical of endolysosomes. Although several studies support the view that TMPRSS2-dependent early entry route is more efficient and results in a more productive infection than the cathepsin L-activated mechanisms for some SARS-coronavirus strains, recent studies indicate that Omicron SARS-CoV-2 variants favor the low-pH endosomal entry route. For fusion activity in SARS-coronavirus, cathepsin Ls have been shown to require reduced pH of at least 6.0 or lower. Although research has verified that the envelope E-protein serves as an ion channel when pH levels decrease, there have been certain inconsistencies observed between various studies and tests. Furthermore, unlike the influenza M1 protein, there has been no evidence of similar pH-sensitive behavior in the SARS-coronavirus M1 protein. However, studies also suggest that cathepsin L is irreversibly inactivated at pH values lower than 4.0, an acidic environment that may occur in matured lysosomes. The pH sensitivity of influenza A and SARS-CoV-2 viral glycoproteins is a potential target for therapeutic interventions and anti-viral drug treatments. So far, there is evidence suggesting that chloroquine, a weak base, inhibits the replication of those influenza A strains whose hemagglutinins require a low pH for their fusion activation (Di Trani et al., 2007). Chloroquine has shown potential in blocking the SARS-CoV-2 infection cycle by releasing basic side chains that raise the endosomal pH and inactivate cathepsin-L (Lan et al., 2022). However, the use of chloroquine for the treatment of COVID-19 triggered significant debate, especially since the drug is associated with side effects and exhibits only marginal efficacy (Chen et al., 2021; Kashour et al., 2021). With regard to alternative approaches for achieving endosomal deacidification, endosomal acidification inhibitors bafilomycin A1 and NH_4Cl were shown to exert antiviral effects against SARS-CoV-2 *in vitro* cell models and *in vivo* in hACE2 transgenic mice, and thus should be evaluated as potential COVID-19 treatments (Shang et al., 2021). In summary: while both influenza and coronavirus may pursue pH-regulated endocytic pathways, the influenza virus does not require the presence of specific pH-sensitive enzymes (cathepsin L) during endosomal transport to activate fusion with the host cell. The review also notes that the precise mechanism of protonation mechanisms of certain envelope glycoproteins during endosomal transport for both viruses remains incompletely understood, and further research is needed.

Author contributions

The author confirms being the sole contributor of this work and has approved it for publication.

Conflict of interest

The author declares that the research was conducted in the absence of any commercial or financial relationships that could be construed as a potential conflict of interest.

Publisher's note

References

Assaiya, A., Burada, A., Dhingra, S., and Kumar, J. (2021). An overview of the recent advances in cryo-electron microscopy for life sciences. *Emerg. Top. Life Sci.* 5, 151–168. doi: 10.1042/ETLS20200295

Basak, S., Tomana, M., and Compans, R. W. (1985). Sialic acid is incorporated into influenza hemagglutinin glycoproteins in the absence of viral neuraminidase. *Virus Res.* 2, 61–68. doi: 10.1016/0168-1702(85)90060-7

Benton, D., Gamblin, S., Rosenthal, P., and Skehel, J. (2020a). Structural transitions in influenza haemagglutinin at membrane fusion pH. *Nature* 583, 150–153. doi: 10.1038/s41586-020-2333-6

Benton, D. J., Wrobel, A., Xu, P., Roustan, C., Martin, S., Rosenthal, P., et al. (2020b). Receptor binding and priming of the spike protein of SARS-CoV-2 for membrane fusion. *Nature* 588, 327–330. doi: 10.1038/s41586-020-2772-0

Berg, T., Gjöen, T., and Bakke, O. (1995). Physiological functions of endosomal proteolysis. *Biochem. J.* 307:326. doi: 10.1042/bj3070313

Biasin, M., Bianco, A., Pareschi, G., Cavalleri, A., Cavatorta, C., Fenizia, C., et al. (2021). UV-C irradiation is highly effective in inactivating SARS-CoV-2 replication. *Sci. Rep.* 11:6260. doi: 10.1038/s41598-021-85425-w

Biryukov, J., Boydston, J., Dunning, R., Yeager, J., Wood, S., Ferris, A., et al. (2021). SARS-CoV-2 is rapidly inactivated at high temperature. *Environ. Chem. Lett.* 19, 1773–1777. doi: 10.1007/s10311-021-01187-x

Böttcher, C., Ludwig, K., Herrmann, A., Van Heel, M., and Stark, H. (1999). Structure of influenza haemagglutinin at neutral and at fusogenic pH by electron cryo-microscopy. *FEBS Lett.* 463, 255–259. doi: 10.1016/S0014-5793(99)01475-1

Bouvier, N. M., and Palese, P. (2008). The biology of influenza viruses. *Vaccine* 26(Suppl. 4), D49–D53. doi: 10.1016/j.vaccine.2008.07.039

Brandenburg, B., and Zhuang, X. (2007). Virus trafficking – learning from single-virus tracking. *Nat. Rev. Microbiol.* 5, 197–208. doi: 10.1038/nrmicro1615

Cabrera-Garcia, D., Bekdash, R., Abbott, G., Yazawa, M., and Harrison, N. (2021). The envelope protein of SARS-CoV-2 increases intra-Golgi pH and forms a cation channel that is regulated by pH. *J. Physiol.* 599, 2851–2868. doi: 10.1113/JP281037

Cady, S., Luo, W., Hu, F., and Hong, M. (2009). Structure and function of the influenza A M2 proton channel. *Biochemistry* 48, 7356–7364. doi: 10.1021/bi9008837

Caffrey, M., and Lavie, A. (2021). pH-Dependent mechanisms of influenza infection mediated by hemagglutinin. *Front. Mol. Biosci.* 8:777095. doi: 10.3389/fmolb.2021.777095

Calder, L., Wasilewski, S., Berriman, J., and Rosenthal, P. (2010). Structural organization of a filamentous influenza A virus. *Proc. Natl. Acad. Sci. U S A.* 107, 10685–10690. doi: 10.1073/pnas.1002123107

Carr, C., Chaudhry, C., and Kim, P. (1997). Influenza hemagglutinin is spring-loaded by a metastable native conformation. *Proc. Natl. Acad. Sci. U S A.* 94, 14306–14313. doi: 10.1073/pnas.94.26.14306

Chang, P., Sealy, J., Sadeyen, J., Bhat, S., Lukosaityte, D., Sun, Y., et al. (2020). Immune escape adaptive mutations in the H7N9 avian influenza hemagglutinin protein increase virus replication fitness and decrease pandemic potential. *J. Virol.* 94, e216–e220. doi: 10.1128/JVI.00216-20

Chen, H., Wu, Y., and Voth, G. (2007). Proton transport behavior through the influenza A M2 channel: insights from molecular simulation. *Biophys. J.* 93, 3470–3479. doi: 10.1529/biophysj.107.105742

Chen, J., Lee, K., Steinhauer, D., Stevens, D., Skehel, J., and Wiley, D. (1998). Structure of the hemagglutinin precursor cleavage site, a determinant of influenza pathogenicity and the origin of the labile conformation. *Cell* 95, 409–417. doi: 10.1016/S0092-8674(00)81771-7

Chen, Y., Li, M. X., Lu, G. D., Shen, H. M., and Zhou, J. (2021). Hydroxychloroquine/Chloroquine as therapeutics for COVID-19: truth under the Mystery. *Int. J. Biol. Sci.* 17, 1538–1546. doi: 10.7150/ijbs.59547

Chizhmakov, I., Geraghty, F., Ogden, D., Hayhurst, A., AntoniouM, and Hay, A. (1996). Selective proton permeability and pH regulation of the influenza virus M2 channel expressed in mouse erythroleukaemiacells. *J. Physiol.* 494, 329–336. doi: 10.1113/jphysiol.1996.sp021495

Chizhmakov, I., Ogden, D., Geraghty, F., Hayhurst, A., Skinner, A., Betakova, T., et al. (2003). Differences in conductance of M2 protonchannels of two influenza viruses at low and high pH. *J. Physiol.* 546, 427–438. doi: 10.1113/jphysiol.2002.028910

Cross, K., Langley, W., Russell, R., Skehel, J., and Steinhauer, D. (2009). Composition and functions of the influenza fusion peptide. *Protein Pept. Lett.* 16, 766–778. doi: 10.2174/092986609788681715

Cutler, D., and Summers, L. (2020). The COVID-19 pandemic and the $16 trillion virus. *JAMA* 324, 1495–1496. doi: 10.1001/jama.2020.19759

Dabisch, P., Schuit, M., Herzog, A., Beck, K., Wood, S., Krause, M., et al. (2020). The influence of temperature, humidity, and simulated sunlight on the infectivity of SARS-CoV-2 in aerosols. *Aerosol. Sci. Technol.* 55, 142–153. doi: 10.1080/02786826.2020.1829536

de Vries, E., Tscherne, D., Wienholts, M., Cobos-Jiménez, V., Scholte, F., García-Sastre, A., et al. (2011). Dissection of the influenza A virus endocytic routes reveals macropinocytosis as an alternative entry pathway. *PLoS Pathogens* 7:e1001329. doi: 10.1371/journal.ppat.1001329

Dehrmann, F., Coetzer, T., Pike, R., and Dennison, C. (1995). Mature cathepsin L is substantially active in the ionic milieu of the extracellular medium. *Arch. Biochem. Biophys.* 324, 93–98. doi: 10.1006/abbi.1995.9924

Dehrmann, F. M., Elliott, E., and Dennison, C. (1996). Reductive activation markedly increases the stability of cathepsins B and L to extracellular ionic conditions. *Biol. Chem. Hoppe-Seyler.* 377, 391–394. doi: 10.1515/bchm3.1996.377.6.391

Dennison, C. (2003). *A Guide to Protein Isolation*, 2nd Edn. Netherlands: Kluwer Academic Publishers. doi: 10.1007/978-94-017-0269-0

Di Trani, L., Savarino, A., Campitelli, L., Norelli, S., Puzelli, S., D'Ostilio, D., et al. (2007). Different pH requirements are associated with divergent inhibitory effects of chloroquine on human and avian influenza A viruses. *Virol. J.* 4:39. doi: 10.1186/1743-422X-4-39

Dolan, K., Dutta, M., Kern, D., Kotecha, A., Voth, G., and Brohawn, S. (2022). Structure of SARS-CoV-2 M protein in lipid nanodiscs. *eLife* 11:e81702. doi: 10.7554/eLife.81702

Dou, D., Revol, R., Östbye, H., Wang, H., and Daniels, R. (2018). Influenza A virus cell entry, replication, virion assembly and movement. *Front. Immunol.* 9:1581. doi: 10.3389/fimmu.2018.01581

Fendrick, A. M., Monto, A. S., Nightengale, B., and Sarnes, M. (2003). The economic burden of non-influenzarelated viral respiratory tract infection in the United States. *Arch. Intern. Med.* 163, 487–494. doi: 10.1001/archinte.163.4.487

Fontana, J., Cardone, G., Heymann, J., Winkler, D., and Steven, A. (2012). Structural changes in influenza virus at low pH characterized by cryo-electron tomography. *J. Virol.* 86, 2919–2929. doi: 10.1128/JVI.06698-11

Galloway, S., Reed, M., Russell, C., and Steinhauer, D. (2013). Influenza HA subtypes demonstrate divergent phenotypes for cleavage activation and pH of fusion: implications for host range and adaptation. *PLoS Pathog.* 9:e1003151. doi: 10.1371/journal.ppat.1003151

Guaita, M., Watters, S., and Loerch, S. (2022). Recent advances and current trends in cryo-electron microscopy. *Curr. Opin. Struct. Biol.* 77:102484. doi: 10.1016/j.sbi.2022.102484

Hansen, C., Chaves, S., Demont, C., and Viboud, C. (2022). Mortality associated with influenza and respiratory syncytial virus in the US, 1999-2018. *JAMA Network Open* 5:e220527. doi: 10.1001/jamanetworkopen.2022.0527

Höfer, C., Di Lella, S., Dahmani, I., Jungnick, N., Bordag, N., Bobone, S., et al. (2019). Structural determinants of the interaction between influenza A virus matrix protein M1 and lipid membranes. *Biochim Biophys. Acta Biomembr.* 1861, 1123–1134. doi: 10.1016/j.bbamem.2019.03.013

Hoffmann, M., Kleine-Weber, H., Schroeder, S., Krüger, N., Herrler, T., Erichsen, S., et al. (2020). SARS-CoV-2 cell entry depends on ACE2 and TMPRSS2 and is blocked by a clinically proven protease inhibitor. *Cell* 181, 271–280.e8. doi: 10.1016/j.cell.2020.02.052

Hu, J., Fu, R., Nishimura, K., Zhang, L., Zhou, H., Busath, D., et al. (2006). Histidines, heart of the hydrogen ion channel from influenza A virus: toward an understanding of conductance and proton selectivity. *Proc. Natl. Acad. Sci. U S A.* 103, 6865–6870. doi: 10.1073/pnas.0601944103

Hu, Y., Wen, J., Tang, L., Zhang, H., Zhang, X., Li, Y., et al. (2003). The M protein of SARS-CoV: basic structural and immunological properties. *Genom. Proteom. Bioinform.* 1, 118–130. doi: 10.1016/S1672-0229(03)01016-7

Huang, Q., Opitz, R., Knapp, E. W., and Herrmann, A. (2002). Protonation and stability of the globular domain of influenzavirus hemagglutinin. *Biophys. J.* 82, 1050–1058. doi: 10.1016/S0006-3495(02)75464-7

Huang, Y., Yang, C., Xu, X., Xu, W., and Liu, S. (2020). Structural and functional properties of SARS-CoV-2 spike protein: potential antivirus drug development for COVID-19. *Acta Pharmacol. Sin.* 41, 1141–1149. doi: 10.1038/s41401-020-0485-4

Intharathep, P., Laohpongspaisan, C., Rungrotmongkol, T., Loisruangsin, A., Malaisree, M., Decha, P., et al. (2008). How amantadine and rimantadine inhibit proton transport in the M2 protein channel. *J. Mol. Graph Model.* 27, 342–348. doi: 10.1016/j.jmgm.2008.06.002

Iuliano, A. D., Roguski, K., Chang, H., Muscatello, D., Palekar, R., Tempia, S., et al. (2018). Estimates of global seasonal influenza-associated respiratory mortality: a modelling study. *Lancet* 391, 1285–1300. doi: 10.1016/S0140-6736(17)33293-2

Ivanovic, T., Rozendaal, R., Floyd, D., Popovic, M., van Oijen, A., and Harrison, S. (2012). Kinetics of proton transport into influenza virions by the viral M2 channel. *PLoS One* 7:e31566. doi: 10.1371/journal.pone.0031566

Jackson, C., Farzan, M., Chen, B., and Choe, H. (2022). Mechanisms of SARS-CoV-2 entry into cells. *Nat. Rev. Mol. Cell Biol.* 23, 3–20. doi: 10.1038/s41580-021-00418-x

James, S. L., Abate, D., Abate, K., Abay, S., Abbafati, C., Abbasi, N., et al. (2018). Global, regional, and national incidence, prevalence, and years lived with disability for 354 diseases and injuries for 195 countries and territories, 1990–2017: a systematic analysis for the Global Burden of Disease Study 2017. *Lancet* 392, 1789–1858. doi: 10.1016/S0140-6736(18)32279-7

Kashour, Z., Riaz, M., Garbati, M., AlDosary, O., Tlayjeh, H., Gerberi, D., et al. (2021). Efficacy of chloroquine or hydroxychloroquine in COVID-19 patients: a systematic review and meta-analysis. *J. Antimicrob Chemother.* 76, 30–42. doi: 10.1093/jac/dkaa403

Kelly, M., Cook, J., Brown-Augsburger, P., Heinz, B., Smith, M., and Pinto, L. (2003). Demonstrating the intrinsic ion channel activity of virally encoded proteins. *FEBS Lett.* 552, 61–67. doi: 10.1016/S0014-5793(03)00851-2

Kemble, G., Bodian, D., Rosé, J., Wilson, I., and White, J. (1992). Intermonomer disulfide bonds impair the fusion activity of influenza virus hemagglutinin. *J. Virol.* 66, 4940–4950. doi: 10.1128/jvi.66.8.4940-4950.1992

Kennedy, C. D. (1990). Ionic strength and the dissociation of acids. *Biochem. Educ.* 18, 35–40. doi: 10.1016/0307-4412(90)90017-I

Kiss, A. L., and Botos, E. (2009). Endocytosis via caveolae: alternative pathway with distinct cellular compartments to avoid lysosomal degradation? *J. Cell. Mol. Med.* 13, 1228–1237. doi: 10.1111/j.1582-4934.2009.00754.x

Koch, J., Uckeley, Z., Doldan, P., Stanifer, M., Boulant, S., and Lozach, P. (2021). TMPRSS2 expression dictates the entry route used by SARS-CoV-2 to infect host cells. *EMBO J.* 40:e107821. doi: 10.15252/embj.2021107821

Kreutzberger, A., Sanyal, A., Saminathan, A., Bloyet, L., Stumpf, S., Liu, Z., et al. (2022). SARS-CoV-2 requires acidic pH to infect cells. *Proc. Natl. Acad. Sci. U S A.* 119:e2209514119. doi: 10.1073/pnas.2209514119

Kuo, L., Hurst, K., and Masters, P. (2007). Exceptional flexibility in the sequence requirements for coronavirus small envelope protein function. *J. Virol.* 81, 2249–2262. doi: 10.1128/JVI.01577-06

Lakadamyali, M., Rust, M., and Zhuang, X. (2004). Endocytosis of influenza viruses. *Microbes Infect.* 6, 929–936. doi: 10.1016/j.micinf.2004.05.002

Lamb, R. A., and Choppin, P. W. (1983). The structure and replication of influenza virus. *Annu. Rev. Biochem.* 52, 467–506. doi: 10.1146/annurev.bi.52.070183.002343

Lan, Y., He, W., Wang, G., Wang, Z., Chen, Y., Gao, F., et al. (2022). Potential antiviral strategy exploiting dependence of SARS-CoV-2 replication on lysosome-based pathway. *Int. J. Mol. Sci.* 23:6188. doi: 10.3390/ijms23116188

Lee, K. (2010). Architecture of a nascent viral fusion pore. *EMBO J.* 29, 1299–1311. doi: 10.1038/emboj.2010.13

Lentz, M. R., Webster, R. G., and Air, G. M. (1987). Site-directed mutation of the active site of influenza neuraminidase and implications for the catalytic mechanism. *Biochemistry* 26, 5351–5358. doi: 10.1021/bi00391a020

Li, W., Moore, M., Vasilieva, N., Sui, J., Wong, S., Berne, M., et al. (2003). Angiotensin-converting enzyme 2 is a functional receptor for the SARS coronavirus. *Nature* 426, 450–454. doi: 10.1038/nature02145

Lin, T. I., and Schroeder, C. (2001). Definitive assignment of proton selectivity and attoampere unitary current to the M2 ion channel protein of influenza A virus. *J. Virol.* 75:3647. doi: 10.1128/JVI.75.8.3647-3656.2001

Lopez-Leon, S., Wegman-Ostrosky, T., Perelman, C., Sepulveda, R., Rebolledo, P., Cuapio, A., et al. (2021). More than 50 long-term effects of COVID-19: a systematic review and meta-analysis. *Sci. Rep.* 11:16144. doi: 10.1038/s41598-021-95565-8

Luo, B., Schaub, A., Glas, I., Klein, L., David, S., Bluvshtein, N., et al. (2023). Expiratory aerosol pH: the overlooked driver of airborne virus inactivation. *Environ. Sci. Technol.* 57, 486–497. doi: 10.1021/acs.est.2c05777

Luzio, J., Pryor, P., and Bright, N. (2007). Lysosomes: fusion and function. *Nat. Rev. Mol. Cell Biol.* 8, 622–632. doi: 10.1038/nrm2217

Maeda, T., Kawasaki, K., and Ohnishi, S. (1981). Interaction of influenza virus hemagglutinin with target membrane lipids is a key step in virus-induced hemolysis and fusion at pH 5.2. *Proc. Natl. Acad. Sci. U S A.* 78, 4133–4137. doi: 10.1073/pnas.78.7.4133

Mair, C., Ludwig, K., Herrmann, A., and Sieben, C. (2014a). Receptor binding and pH stability - how influenza A virus hemagglutinin affects host-specific virus infection. *Biochim Biophys. Acta* 1838, 1153–1168. doi: 10.1016/j.bbamem.2013.10.004

Mair, C., Meyer, T., Schneider, K., Huang, Q., Veit, M., Herrmann, A., et al. (2014b). A histidine residue of the influenza virus hemagglutinin controls the pH dependence of the conformational change mediating membrane fusion. *J. Virol.* 88, 13189–13200. doi: 10.1128/JVI.01704-14

Mason, R. W., and Massey, S. D. (1992). Surface activation of pro-cathepsin L. *Biochem. Biophys. Res. Commun.* 189, 1659–1666. doi: 10.1016/0006-291X(92)90268-P

Matlin, K., Reggio, H., Helenius, A., and Simons, K. (1981). Infectious entry pathway of influenza virus in a canine kidney cell line. *J. Cell Biol.* 91(3 Pt 1), 601–613. doi: 10.1083/jcb.91.3.601

McKimm-Breschkin, J. L. (2000). Resistance of influenza viruses to neuraminidase inhibitors – a review. *Antivir. Res.* 47, 1–17. doi: 10.1016/S0166-3542(00)00103-0

Meng, B., Abdullahi, A., Ferreira, I., Goonawardane, N., Saito, A., Kimura, I., et al. (2022). Altered TMPRSS2 usage by SARS-CoV-2 Omicron impacts infectivity and fusogenicity. *Nature* 603, 706–714. doi: 10.1038/s41586-022-04474-x

Mohamed, M., and Sloane, B. (2006). Cysteine cathepsins: multifunctional enzymes in cancer. *Nat. Rev. Cancer* 6, 764–775. doi: 10.1038/nrc1949

Mould, J., Drury, J., Frings, S., Kaupp, U., Pekosz, A., and Pinto, L. (2000a). Permeation and activation of the M2ion channel ofinfluenza A virus. *J. Biol. Chem.* 275, 31038–31050. doi: 10.1074/jbc.M003663200

Mould, J. A., Li, H., Dudlak, C., Lear, J., Pekosz, A., Lamb, R., et al. (2000b). Mechanism for proton conduction of the M(2) ion channel of influenza A virus. *J. Biol. Chem.* 275, 8592–8599. doi: 10.1074/jbc.275.12.8592

Mountford, C. E., Grossman, G., Holmes, K. T., O'Sullivan, W. J., Hampson, A. W., Raison, R. L., et al. (1982). Effect of monoclonal anti-neuraminidase antibodies on the kinetic behavior of influenza virus neuraminidase. *Mol. Immunol.* 19, 811–816. doi: 10.1016/0161-5890(82)90007-4

Msemburi, W., Karlinsky, A., Knutson, V., Aleshin-Guendel, S., Chatterji, S., Wakefield, J., et al. (2023). The WHO estimates of excess mortality associated with the COVID-19 pandemic. *Nature* 613, 130–137. doi: 10.1038/s41586-022-05522-2

Neuman, B., Kiss, G., Kunding, A., Bhella, D., Baksh, M., Connelly, S., et al. (2011). A structural analysis of M protein in coronavirus assembly and morphology. *J. Struct. Biol.* 174, 11–22. doi: 10.1016/j.jsb.2010.11.021

Nieto-Torres, J. L., Verdiá-Báguena, C., Jimenez-Guardeño, J. M., Regla-Nava, J. A., Castaño-Rodriguez, C., Fernandez-Delgado, R., et al. (2015). Severe acute respiratory syndrome coronavirus E protein transports calcium ions and activates the NLRP3 inflammasome. *Virology* 485, 330–339. doi: 10.1016/j.virol.2015.08.010

Noton, S., Medcalf, E., Fisher, D., Mullin, A., Elton, D., Digard, P., et al. (2007). Identification of the domains of the influenza A virus M1 matrix protein required for NP binding, oligomerization and incorporation into virions. *J. General Virol.* 88(Pt 8), 2280–2290. doi: 10.1099/vir.0.82809-0

Örd, M., Faustova, I., and Loog, M. (2020). The sequence at Spike S1/S2 site enables cleavage by furin and phospho-regulation in SARS-CoV2 but not in SARS-CoV1 or MERS-CoV. *Sci. Rep.* 10:16944. doi: 10.1038/s41598-020-74101-0

Ouzounis, C. A. (2020). A recent origin of Orf3a from M protein across the coronavirus lineage arising by sharp divergence. *Comput. Struct. Biotechnol. J.* 18, 4093–4102. doi: 10.1016/j.csbj.2020.11.047

Padilla-Parra, S., Matos, P. M., Kondo, N., Marin, M., Santos, N., and Melikyan, G. B. (2012). Quantitative imaging of endosome acidification and single retrovirus fusion with distinct pool of early endosomes. *Proc. Natl. Acad. Sci. U S A.* 109, 17627–17632. doi: 10.1073/pnas.1211714109

Palese, P., Tobita, K., Ueda, M., and Compans, R. W. (1974). Characterization of temperature sensitive influenza virus mutants defective in neuraminidase. *Virology* 61, 397–410. doi: 10.1016/0042-6822(74)90276-1

Peacock, T. P., Goldhill, D. H., Zhou, J., Baillon, L., Frise, R., Swann, O., et al. (2021). The furin cleavage site in the SARS-CoV-2 spike protein is required for transmission in ferrets. *Nat. Microbiol.* 6, 899–909. doi: 10.1038/s41564-021-00908-w

Peukes, J., Xiong, X., Erlendsson, S., Qu, K., Wan, W., Calder, L., et al. (2020). The native structure of the assembled matrix protein 1 of influenza A virus. *Nature* 587, 495–498. doi: 10.1038/s41586-020-2696-8

Phongphanphanee, S., Rungrotmongkol, T., Yoshida, N., Hannongbua, S., and Hirata, F. (2010). Proton transport through the influenza A M2 channel: three-dimensional reference interaction site model study. *J. Am. Chem. Soc.* 132, 9782–9788. doi: 10.1021/ja1027293

Pielak, R. M., and Chou, J. J. (2011). Influenza M2 proton channels. *Biochimica Biophys. Acta* 1808, 522–529. doi: 10.1016/j.bbamem.2010.04.015

Pinto, L., Dieckmann, G., Gandhi, C., Papworth, C., Braman, J., Shaughnessy, M., et al. (1997). A functionally defined model for the M2 proton channel of influenza A virus suggests a mechanism for its ion selectivity. *Proc. Natl. Acad. Sci. U S A.* 94, 11301–11306. doi: 10.1073/pnas.94.21.11301

Pinto, L., Holsinger, L., and Lamb, R. (1992). Influenza virus M2 protein has ion channel activity. *Cell* 69, 517–528. doi: 10.1016/0092-8674(92)90452-I

Rice, A., Haldar, S., Wang, E., Blank, P., Akimov, S., Galimzyanov, T., et al. (2022). Planar aggregation of the influenza viral fusion peptide alters membrane structure and hydration, promoting poration. *Nat. Commun.* 13:7336. doi: 10.1038/s41467-022-34576-z

Ruigrok, R. W., Calder, L. J., and Wharton, S. A. (1989). Electron microscopy of the influenza virus submembranal structure. *Virology* 173, 311–316. doi: 10.1016/0042-6822(89)90248-1

Rust, M. J., Lakadamyali, M., Zhang, F., and Zhuang, X. (2004). Assembly of endocytic machinery around individual influenza viruses during viral entry. *Nat. Struct. Mol. Biol.* 11, 567–573. doi: 10.1038/nsmb769

Sachs, J., Karim, S., Aknin, L., Allen, J., Brosbøl, K., Colombo, F., et al. (2022). The Lancet Commission on lessons for the future from the COVID-19 pandemic. *Lancet* 400, 1224–1280. doi: 10.1016/S0140-6736(22)01585-9

Sakaguchi, T., Leser, G., and Lamb, R. (1996). The ion channel activity of the influenza virus M2 protein affects transport through the Golgi apparatus. *J. Cell Biol.* 133, 733–747. doi: 10.1083/jcb.133.4.733

Schnell, J., and Chou, J. (2008). Structure and mechanism of the M2 proton channel of influenza A virus. *Nature* 451, 591–595. doi: 10.1038/nature06531

Schoeman, D., and Fielding, B. (2019). Coronavirus envelope protein: current knowledge. *Virol. J.* 16:69. doi: 10.1186/s12985-019-1182-0

Selzer, L., Su, Z., Pintilie, G., Chiu, W., and Kirkegaard, K. (2020). Full-length three-dimensional structure of the influenza A virus M1 protein and its organization into a matrix layer. *PLoS Biol.* 18:e3000827. doi: 10.1371/journal.pbio.3000827

Shang, C., Zhuang, X., Zhang, H., Li, Y., Zhu, Y., Lu, J., et al. (2021). Inhibitors of endosomal acidification suppress SARS-CoV-2 replication and relieve viral pneumonia in hACE2 transgenic mice. *Virol. J.* 18:46. doi: 10.1186/s12985-021-01515-1

Shi, T., McAllister, D., O'Brien, K., Simoes, E., Madhi, S., Gessner, B., et al. (2017). Global, regional, and national disease burden estimates of acute lower respiratory infections due to respiratory syncytial virus in young children in 2015: a systematic review and modelling study. *Lancet* 390, 946–958. doi: 10.1016/S0140-6736(17)30938-8

Shirato, K., Kanou, K., Kawase, M., and Matsuyama, S. (2017). Clinical isolates of human coronavirus 229E bypass the endosome for cell entry. *J. Virol.* 91:JVI.01387-16. doi: 10.1128/JVI.01387-16

Shirato, K., Kawase, M., and Matsuyama, S. (2018). Wild-type human coronaviruses prefer cell-surface TMPRSS2 to endosomal cathepsins for cell entry. *Virology* 517, 9–15. doi: 10.1016/j.virol.2017.11.012

Shtykova, E. V., Dadinova, L. A., Fedorova, N. V., Golanikov, A., Bogacheva, E., Ksenofontov, A., et al. (2017). Influenza virus Matrix Protein M1 preserves its conformation with pH, changing multimerization state at the priming stage due to electrostatics. *Sci. Rep.* 7:16793. doi: 10.1038/s41598-017-16986-y

Sriwilaijaroen, N., and Suzuki, Y. (2012). Molecular basis of the structure and function of H1 hemagglutinin of influenza virus. *Proc. Japan Acad. Ser B Phys. Biol. Sci.* 88, 226–249. doi: 10.2183/pjab.88.226

Staschke, K., Hatch, S., Tang, J., Hornback, W., Munroe, J., Colacino, J., et al. (1998). Inhibition of influenza virus hemagglutinin-mediated membrane fusion by a compound related to podocarpic acid. *Virology* 248, 264–274. doi: 10.1006/viro.1998.9273

Stegmann, T., Booy, F., and Wilschut, J. (1987). Effects of low pH on influenza virus. Activation and inactivation of the membrane fusion capacity of the hemagglutinin. *J. Biol. Chem.* 262, 17744–17749. doi: 10.1016/S0021-9258(18)45442-7

Takahashi, T., and Suzuki, T. (2015). Low-pH stability of influenza A virus sialidase contributing to virus replication and pandemic. *Biol. Pharm. Bull.* 38, 817–826. doi: 10.1248/bpb.b15-00120

Tortorici, M., Walls, A., Lang, Y., Wang, C., Li, Z., Koerhuis, D., et al. (2019). Structural basis for human coronavirus attachment to sialic acid receptors. *Nat. Struct. Mol. Biol.* 26, 481–489. doi: 10.1038/s41594-019-0233-y

Trost, J., Wang, W., Liang, B., Galloway, S., Agbogu, E., Byrd-Leotis, L., et al. (2019). A conserved histidine in Group-1 influenza subtype hemagglutinin proteins is essential for membrane fusion activity. *Virology* 536, 78–90. doi: 10.1016/j.virol.2019.08.005

Turk, B., Dolenc, I., Turk, V., and Bieth, J. (1993). Kinetics of the pH-induced inactivation of human cathepsin L. *Biochemistry* 32, 375–380. doi: 10.1021/bi00052a046

Van Dyke, R. W. (1995). "Acidification of lysosomes and endosomes," in *Biology of the Lysosome, Subcellular Biochemistry*, eds J. B. Lloyd and R. W. Mason (New York, NY: Plenum Press), 331360. doi: 10.1007/978-1-4615-5833-0_10

Venkataraman, P., Lamb, R. A., and Pinto, L. H. (2005). Chemical rescue of histidine selectivity filter mutants of the M2 ion channel of influenza A virus. *J. Biol. Chem.* 280, 21463–21472. doi: 10.1074/jbc.M412406200

Verdiá-Báguena, C., Nieto-Torres, J. L., Alcaraz, A., DeDiego, M. L., Torres, J., Aguilella, V. M., et al. (2012). Coronavirus E protein forms ion channels with functionally and structurally-involved membrane lipids. *Virology* 432, 485–494. doi: 10.1016/j.virol.2012.07.005

Wallabregue, A., Moreau, D., Sherin, P., Moneva Lorente, P., Jarolímová, Z., Bakker, E., et al. (2016). Selective imaging of late endosomes with a pH-Sensitive diazaoxatriangulene fluorescent probe. *J. Am. Chem. Soc.* 138, 1752–1755. doi: 10.1021/jacs.5b09972

Walls, A. C., Tortorici, M., Snijder, J., Xiong, X., Bosch, B., Rey, F., et al. (2017). Tectonic conformational changes of a coronavirus spike glycoprotein promote membrane fusion. *Proc. Natl Acad. Sci. U S A.* 114, 11157–11162. doi: 10.1073/pnas.1708727114

Wang, C., Lamb, R., and Pinto, L. (1995). Activation of the M2 ion channel of influenza virus: a role for the transmembrane domain histidine residue. *Biophys. J.* 69, 1363–1371. doi: 10.1016/S0006-3495(95)80003-2

Xia, B., Shen, X., He, Y., Pan, X., Liu, F., Wang, Y., et al. (2021). SARS-CoV-2 envelope protein causes acute respiratory distress syndrome (ARDS)-like pathological damages and constitutes an antiviral target. *Cell Res.* 31, 847–860. doi: 10.1038/s41422-021-00519-4

Zaraket, H., Bridges, O., and Russell, C. (2013). The pH of activation of the hemagglutinin protein regulates H5N1 influenza virus replication and pathogenesis in mice. *J. Virol.* 87, 4826–4834. doi: 10.1128/JVI.03110-12

Zebedee, S., and Lamb, R. (1988). Influenza A virus M2 protein: monoclonal antibody restriction of virus growth and detection of M2 in virions. *J. Virol.* 62, 2762–2772. doi: 10.1128/jvi.62.8.2762-2772.1988

Zhang, K., Wang, Z., Liu, X., Yin, C., Basit, Z., Xia, B., et al. (2012). Dissection of influenza A virus M1 protein: pH-dependent oligomerization of N-terminal domain and dimerization of C-terminal domain. *PLoS One* 7:e37786. doi: 10.1371/journal.pone.0037786

Zhang, Z., Nomura, N., Muramoto, Y., Ekimoto, T., Uemura, T., Liu, K., et al. (2022). Structure of SARS-CoV-2 membrane protein essential for virus assembly. *Nat. Commun.* 13:4399. doi: 10.1038/s41467-022-32019-3

Zhao, M., Yang, W., Yang, F., Zhang, L., Huang, W., Hou, W., et al. (2021). Cathepsin L plays a key role in SARS-CoV-2 infection in humans and humanized mice and is a promising target for new drug development. *Sig. Transduct. Target Ther.* 6:134. doi: 10.1038/s41392-021-00558-8

Zhou, Y., Wu, C., and Huang, N. (2014). Exploring the early stages of the pH-induced conformational change of influenza hemagglutinin. *Proteins* 82, 2412–2428. doi: 10.1002/prot.24606

Zucs, P., Buchholz, U., Haas, W., and Uphoff, H. (2005). Influenza associated excess mortality in Germany, 1985-2001. *Emerg. Themes Epidemiol.* 2:6.

frontiers | Frontiers in Microbiology

TYPE Review
PUBLISHED 07 June 2023
DOI 10.3389/fmicb.2023.1213111

OPEN ACCESS

EDITED BY
Qiang Ding,
Tsinghua University, China

REVIEWED BY
Xin Yin,
Chinese Academy of Agricultural Sciences (CAAS), China
Zhen Luo,
Jinan University, China
Xiaohui Ju,
Tsinghua University, China

*CORRESPONDENCE
Yonggang Wang
✉ wangyg1982@jlu.edu.cn

†These authors have contributed equally to this work and share first authorship

RECEIVED 27 April 2023
ACCEPTED 18 May 2023
PUBLISHED 07 June 2023

CITATION
Zhao Y, Han X, Li C, Liu Y, Cheng J, Adhikari BK and Wang Y (2023) COVID-19 and the cardiovascular system: a study of pathophysiology and interpopulation variability. *Front. Microbiol.* 14:1213111. doi: 10.3389/fmicb.2023.1213111

COVID-19 and the cardiovascular system: a study of pathophysiology and interpopulation variability

Yifan Zhao[1†], Xiaorong Han[2†], Cheng Li[1], Yucheng Liu[3], Jiayu Cheng[1], Binay Kumar Adhikari[4] and Yonggang Wang[1*]

[1]Department of Cardiovascular Center, The First Hospital of Jilin University, Changchun, China, [2]Department of Special Care Center, Fuwai Hospital, National Clinical Research Center for Cardiovascular Diseases, National Center for Cardiovascular Diseases, Chinese Academy of Medical Science and Peking Union Medical College, Beijing, China, [3]Department of Family and Community Medicine, Feinberg School of Medicine, McGaw Medical Center of Northwestern University, Chicago, IL, United States, [4]Department of Cardiology, Nepal Armed Police Force Hospital, Kathmandu, Nepal

The severe acute respiratory syndrome coronavirus 2 (SARS-CoV-2) infection in humans can lead to various degrees of tissue and organ damage, of which cardiovascular system diseases are one of the main manifestations, such as myocarditis, myocardial infarction, and arrhythmia, which threaten the infected population worldwide. These diseases threaten the cardiovascular health of infected populations worldwide. Although the prevalence of coronavirus disease 2019 (COVID-19) has slightly improved with virus mutation and population vaccination, chronic infection, post-infection sequelae, and post-infection severe disease patients still exist, and it is still relevant to study the mechanisms linking COVID-19 to cardiovascular disease (CVD). This article introduces the pathophysiological mechanism of COVID-19-mediated cardiovascular disease and analyzes the mechanism and recent progress of the interaction between SARS-CoV-2 and the cardiovascular system from the roles of angiotensin-converting enzyme 2 (ACE2), cellular and molecular mechanisms, endothelial dysfunction, insulin resistance, iron homeostasis imbalance, and psychosocial factors, respectively. We also discussed the differences and mechanisms involved in cardiovascular system diseases combined with neocoronavirus infection in different populations and provided a theoretical basis for better disease prevention and management.

KEYWORDS

SARS-CoV-2, COVID-19, cardiovascular disease, metabolic syndrome, endothelium, ACE2

1. Introduction

The global pandemic of the new coronavirus poses a great challenge to health care systems. In addition to the direct physical damage, the economic and social stress caused by the rampant virus is affecting the psychological health of people around the world to varying degrees (Liu D. et al., 2021; Isath et al., 2023a). Different cardiovascular system (CVD) complications can occur after the severe acute respiratory syndrome coronavirus 2 (SARS-CoV-2) infection, including myocarditis (0.128%–0.15%; Fairweather et al., 2023; Keller et al., 2023), stress cardiomyopathy (0.1%–5.6%; Chung et al., 2021; Davis et al., 2023), pulmonary embolism (PE;

1.9%; Hobohm et al., 2023), heart failure (3%–33%; Chung et al., 2021), and myocardial infarction (0.9%–11%; Chung et al., 2021). In this general situation, SARS-CoV-2 combined with cardiac disease can lead to a worse clinical prognosis, and patients usually have a higher mortality rate. For example, patients with combined myocarditis have a higher mortality rate than those without myocarditis (24.3% vs. 18.9%; Keller et al., 2023), and patients with combined pulmonary embolism have a significantly higher mortality rate (28.7%) than patients with neocoronavirus without combined PE (17.7%; Hobohm et al., 2023). Currently, a large number of studies have taken the first step toward revealing the interaction between the coronavirus disease 2019 (COVID-19) and the cardiovascular system, but some of the specific mechanisms are still unclear. Also, due to individualized differences, different populations tolerate and respond differently to the disease (Liu F. et al., 2021; Tobler et al., 2022). In this review, we seek to explore how cardiac structure and function are affected in the context of COVID-19 and to discuss inter-population differences in COVID-19 comorbid cardiovascular disease for better risk stratification and precise management in the post-epidemic period.

2. Mechanism of interaction between SARS-CoV-2 and the cardiovascular system

2.1. ACE2

ACE2 is an important receptor for neocoronavirus invasion of human cells and is widely distributed in various organs of the body, such as the lung, heart, gastrointestinal tract, and kidney, and it has a high affinity for the viral protein receptor-binding domain (RBD). The binding of the two induces spatial folding and conformational changes in the RBD, promotes membrane fusion, and induces viral entry into cells through endocytosis (Chung et al., 2021). ACE2 is an extremely important and beneficial biomolecule for the cardiovascular system, which can promote the conversion of AngII to Ang1-7, reduce cardiac pathological remodeling, and exert cardiovascular protective effects (Kuriakose et al., 2021). When ACE2 binds and interacts with SARS-CoV-2 spike (S) protein, the structural domain of metalloprotease protein-17 (ADAM17) is activated and cleaves the extracellular region of ACE2, leading to an increase in soluble ACE2 (sACE2) in the plasma and a decrease in cell surface ACE2 expression. In turn, a decrease in ACE2 not only amplifies the deleterious effects of AngII but also further upregulates ADAM17 expression, creating a vicious cycle (Lambert et al., 2005; Zipeto et al., 2020; Liu F. et al., 2021; García-Escobar et al., 2022).

There is a correlation between the tropism and severity of viral infections and the expression of host cell receptors. Increased expression of plasma soluble ACE2 was found in patients with myocardial infarction, atrial fibrillation, valvular disease, and heart failure, reflecting a higher basal ACE2 expression and increased susceptibility in this population (García-Escobar et al., 2022; Silva et al., 2022). Therefore, patients with pre-existing cardiovascular disease may experience more severe complications and adverse events after infection with neocoronavirus. In an ACE2-deficient environment, SARS-CoV-2 entry into cells induces further downregulation of ACE2, amplifying the adverse effects of the ACE/AngII/AT1 axis and attenuating the beneficial effects of the ACE2/Ang1-7 (Angiotensin1-7) /mas axis, leading to cardiomyocyte fibrosis, endothelial damage, mediating inflammatory responses and vasoconstriction, and accelerating cardiovascular diseases such as hypertension and heart failure's further progression (Verdecchia et al., 2020; García-Escobar et al., 2021).

Hypertension, diabetes, and smoking, as risk factors for neocoronavirus infection, can increase ACE2 expression and promote viral entry into cells, leading to energy metabolism and dysfunction (Gao et al., 2021; Kato et al., 2022). This was confirmed by Kato et al., who used rat cardiomyocytes as a model for SARS-CoV-2 pseudovirus infection and found that stimulation by risk factors for cardiac disease can promote ACE2 expression and increase viral susceptibility. In addition, upregulation of ACE2 expression could be achieved by the SARS-CoV-2 S protein by promoting the formation of the TRPC3-NoX2 complex, which is an important target of viral infection and can lead to structural and functional damage of the heart, and the SARS-CoV-2 pseudovirus could promote the release of extracellular ATP through pannexin1 (Panx1), leading to increased reactive oxygen species production while promoting the formation of the TRPC3-NoX2 complex (Kato et al., 2022).

Among the isoforms of apolipoprotein E (APOE), APOE4 has been recognized as a risk factor for the cardiovascular system, which increases the risk of atherosclerosis by increasing LDL levels (Mahley, 2016; Marais, 2019). It has been found that APOE binding to ACE2 attenuates the interaction of ACE2 with viral stinger proteins, inhibits SARS-CoV-2 pseudovirus infection, and attenuates the inflammatory response (Zhang et al., 2022). However, the inhibitory effect of APOE4 was lower due to different conformational structures. In addition to this, patients carrying the APOEε4 gene have a higher susceptibility to SARS-CoV-2 and increased inflammatory factors in the serum (Zhang et al., 2022). Therefore, exploring the relationship between APOE and COVID-19 may provide new ideas to further investigate the interaction between SARS-CoV-2 and cardiovascular disease, which is expected to further accurately assess patient risk and guide treatment.

2.2. Cellular and molecular mechanisms

It has been more than 2 years since the prevalence of COVID-19, and with the changing trend of the disease epidemic, the focus of research has transitioned from the study of pathogenesis in the acute phase to the exploration of clinical symptoms that persist after recovery from infection. Long COVID refers to signs and symptoms that persist or develop after acute neocoronavirus infection, affect almost all organs of the body, and can lead to more than 200 different clinical manifestations (Gyöngyösi et al., 2023). Among them, cardiovascular disease is very common, often with a poor prognosis, and its cellular and molecular pathological mechanisms have been investigated by several research teams.

Neutrophils produce neutrophil extracellular traps (NETs), structures composed of granular and nuclear components that are involved in pathophysiological processes such as autoimmune and inflammatory responses, platelet activation, and the promotion of inflammatory storms and thrombotic disease (Lee et al., 2017; Cedervall, 2018). COVID-19 was found to trigger increased expression of NETs through multiple mechanisms, and NETs play an

important role in the transition from acute to chronic persistent neocoronavirus infection (Zuo et al., 2020; Gyöngyösi et al., 2023). In addition, Warnatsch et al. showed that cholesterol crystals in atherosclerosis promote the release of NETs, which activate macrophages to release cytokines and lead to the further development of atherosclerotic aseptic inflammation (Warnatsch et al., 2015). Therefore, the persistence of long COVID cardiovascular symptoms is closely associated with NETs, and targeted inhibition of NETs may be an effective therapeutic option to mitigate cardiac injury. In addition to this, epigenetic reprogramming of hematopoietic progenitor cells and cellular dysregulation may be involved in the clinical manifestations of the long COVID cardiovascular system, but the above mechanisms are only highly speculative, and the exact pathological process needs to be further clarified (Gyöngyösi et al., 2023).

Numerous researchers attention has recently turned to the role played by cellular senescence in long COVID. The invasion of SARS-CoV-2 into humans is found to increase the host cell's stress response and induce cellular senescence, which increases the pro-inflammatory, tissue-damaging senescence-associated secretory phenotype (SASP) via Toll-like receptor 3 (TLR3; Tripathi et al., 2021). SASP activates neutrophils to produce NETs, promotes platelet activation, and enhances the inflammatory response of the virus to the body. Meanwhile, SASP can expand cellular senescence through a paracrine pathway, which further leads to tissue and organ damage (Schmitt et al., 2023). Therefore, targeted inhibition of TLR3 or senescent cells is meaningful to mitigate the adverse clinical outcomes caused by COVID-19, and further exploration of this is warranted.

2.3. Endothelial cell dysfunction

Endothelial cells are very important for maintaining vasoconstriction and diastole, regulating the flow of cells, molecules, and fluids inside and outside the blood vessels, maintaining the balance of coagulation and fibrinolysis, and participating in immune inflammatory responses (Krüger-Genge et al., 2019). When endothelial cells become structurally and functionally impaired, it will promote the development of many cardiovascular diseases, such as atherosclerosis, coronary artery disease, and hypertension (Incalza et al., 2018). Numerous studies have shown that neocoronavirus infection can cause serious cardiovascular system complications and that patients with pre-existing cardiac disease have a higher incidence of adverse events and mortality after infection with neocoronavirus, with endothelial damage being an important part of the pathogenesis (Kang et al., 2020; Shi et al., 2020; Gu et al., 2021; Rossouw et al., 2022). Histological and pathological findings of patients who died from neointimal pneumonia suggested the presence of endothelial inflammation and degradation of endothelial cells in multiple organs throughout the body, and the presence of viral structures in endothelial cells was observed by electron microscopy (Fodor et al., 2021). Thus, the involvement of endothelial cells in the pathological development of the neocoronavirus was further confirmed.

The pathological mechanism of endothelial cell structure and dysfunction caused by SARS-CoV-2 is complex. First, the virus itself attacks and damages endothelial cells. Among the SRAS-CoV-2 proteins, S protein disrupts endothelial cell integrity, and nucleocapsid protein (NP) induces a pro-inflammatory cell phenotype that triggers the release of inflammatory factors and cytokines by binding to TLR2 in endothelial cells, triggering the NF-κB and MAPK signaling pathways (Qian et al., 2021). Both of these proteins drive viral-mediated endothelial injury. S proteins consist of S1 and S2 subunits that bind to glycosaminoglycans on vascular endothelial cells, enabling them to recognize and interact with ACE2 on the cell surface, thereby inducing viral infection of cells (Rossouw et al., 2022). Unlike cardiomyocytes, S protein-mediated viral entry into pulmonary vascular endothelial cells is followed by an upregulation of ACE2 expression and an accompanying decrease in endothelial NO synthase (eNOS) activity (Lei et al., 2021). eNOS reduction can lead to decreased NO synthesis and increased catabolism, resulting in endothelial injury (Cai and Harrison, 2000). In addition to structural damage, this experiment also demonstrated the presence of endothelial dysfunction: endothelium-dependent dilation was blocked in the pulmonary arteries of hamsters receiving a sham virus infection, whereas non-endothelium-dependent dilation was unaffected (Lei et al., 2021). An *in vitro* study showed that the endothelial permeability of brain microvascular endothelial cells in normal and diabetic mice treated with SARS-CoV-2 S protein increased in both groups, and the expression of vascular endothelial (VE)-cadherin, junctional adhesion molecule-A (JAM-A), connexin 43, and platelet endothelial cell adhesion molecule-1 (PECAM-1), which are essential for maintaining the structural integrity and normal function of the endothelium, was significantly reduced. This study demonstrated that SARS-CoV-2 can cause impaired endothelial structure and function and reduce vascular barrier function, providing strong theoretical support for the mechanism of virus-endothelial cell interaction (Raghavan et al., 2021). In addition to the above mechanisms, S proteins can activate the alternative pathway of complement (APC) to increase endothelial cytotoxicity and activate NLRP3 present in vascular endothelial cells, leading to endothelial cell dysfunction (Yu et al., 2020; Rossouw et al., 2022).

Studies have shown that in addition to direct viral damage to endothelial cells, SARS-CoV-2 can also indirectly damage endothelial cells through oxidative stress, which is a long-lasting pathological process (Fodor et al., 2021). SARS-CoV-2 can induce activation of NADPH-oxidase and promote superoxide (O_2^-) production, which leads to mitochondrial damage (Fodor et al., 2021). Montiel et al. found that after viral infection, damaged mitochondria can promote β-oxidation of fatty acids in vascular endothelial cells to increase oxidative stress (Montiel et al., 2022). In addition to this, oxidative stress can promote the oxidation of thiols in SARS-CoV-2 and SARS-CoV-2 proteins to disulfides, increasing viral binding to ACE2 and thus aggravating the infection (Hati and Bhattacharyya, 2020). Therefore, the reduction of oxidative stress is an essential component for the intervention and control of the recent and long-term complications of a neocoronavirus infection.

Under normal conditions, endothelial cells prevent thrombosis by inhibiting platelet aggregation and fibrin formation. Increased expression of adhesion molecules and platelet aggregation occur when severe infections lead to endothelial cell damage (Gavriilaki et al., 2020; Prasad et al., 2021; Rossouw et al., 2022). A new coronavirus infection can cause a greatly increased incidence of thrombotic events, such as pulmonary embolism and myocardial infarction, which are inextricably linked to endothelial cell dysfunction. It was found that some patients with neocoronavirus infection have different types of antibodies in their sera that activate endothelial cells to increase the

expression of surface adhesion molecules such as intercellular adhesion molecule-1, E-selectin, and vascular cell adhesion molecule-1, increasing the incidence of adverse thrombotic events (Shi et al., 2022). Meanwhile, Toll receptor 7 (TLR7) on the platelet surface during SARS-CoV-2 infection binds to the single-stranded RNA of SAR2-CoV-2, accelerating endothelial damage and leading to increased thrombotic susceptibility (Rossouw et al., 2022). Severe SAR2-CoV-2 can lead to endothelial cell injury, causing excessive platelet stress, and the interaction between the two disrupts the pre-existing homeostatic balance of the vasculature, thereby causing cardiovascular system disorders by mechanisms involving microvascular occlusion, cellular oxidative stress, and the release of pro-thrombotic/pro-coagulant factors (Rossouw et al., 2022). In addition to coagulation disorders, endothelial cell dysfunction can be secondary to inflammatory responses and increased vascular permeability, leading to the development of myocardial edema and myocarditis (Gavriilaki et al., 2020; Prasad et al., 2021; Rossouw et al., 2022).

2.4. Insulin resistance

Insulin resistance is closely associated with cardiovascular disease and can cause myocardial fibrosis and myocardial injury and even induce cardiac insufficiency through abnormal insulin metabolism, mitochondrial dysfunction, hyperglycemia, and glucose toxicity (Jia et al., 2018; Nakamura et al., 2022). Currently, several studies have demonstrated that COVID-19 can induce the development of insulin resistance, which increases the incidence of cardiovascular disease and more severe infectious complications. Shin et al. found that SARS-CoV-2 infection can mediate an impaired insulin/insulin-like growth factor signaling pathway through interferon regulatory factor 1 (IRF1), resulting in metabolic abnormalities and tissue damage such as insulin resistance, new-onset diabetes, etc., and IRF1 expression is higher in men, diabetic, and obese populations, a group that can develop a more severe outcome of SARS-CoV-2 infection (Shin et al., 2022). He et al. demonstrated that insulin resistance is due to SARS-CoV-2 upregulation of RE1 silencing transcription factor (REST) expression to regulate the metabolic factors myeloperoxidase (MPO), apelin, and myostatin gene expression, that such metabolic disorders are not improved by the disappearance of the virus *in vivo*, and that this pathology develops over time (He et al., 2021). The above study not only provides an important reference for exploring the mechanism of interaction between COVID-19 and metabolic disorders but also provides an important theoretical basis for risk stratification and the prognosis of infected patients.

2.5. Iron homeostasis imbalance

Several studies have recently demonstrated the involvement of iron metabolism in the development of COVID-19. Baier et al. demonstrated for the first time that SARS-CoV-2 infection can cause an imbalance in iron homeostasis and intracellular iron accumulation, leading to decreased iron storage capacity, which induces ROS production to cause increased oxidative stress and cellular damage in cardiomyocytes (Baier et al., 2022). The interaction between SARS-CoV-2 and iron metabolism disorders was also demonstrated by Han et al. SARS-CoV-2 induces ferroptosis in human sinoatrial node pacemaker cells, causing severe lipid peroxidation, which results in pacing dysfunction and bradycardia (Han et al., 2022). Reducing intracellular iron accumulation and improving the dysregulation of iron metabolism might be important in reducing myocardial injury and arrhythmogenesis, which need further exploration and research.

2.6. Psychosocial factors

COVID-19 has altered people's old lifestyles, impaired physical functioning, increased economic and social stress, and put the physical and mental health of people worldwide at great risk. A study of a global meta-analysis of anxiety, depression, and stress before and during the COVID-19 pandemic showed that the prevalence of each of these negative emotions increased during the pandemic (Daniali et al., 2023). In addition to this, the COVID-19 outbreak and epidemic and some of the measures taken to reduce the further spread of the disease led to unemployment, reduced income, a lack of physical activity, and social isolation, all of which are adverse effects that are risk factors for cardiovascular disease and increase the incidence and potential for worsening of the disease (Lau and McAlister, 2021). COVID-19, affective disorders, and cardiovascular disease do not exist independently but can coexist and interact with each other, increasing the risk of adverse outcomes (Bucciarelli et al., 2022). Older adults are a vulnerable population for cardiovascular disease and COVID-19 and are susceptible to the negative effects of stressful life events. Ward et al. showed a significant increase in depression and loneliness in the elderly population during the neocoronavirus epidemic (Ward et al., 2023), while Gerhards et al. similarly demonstrated that during the COVID-19 epidemic, patients with cardiovascular disease in the elderly population were significantly more likely to be depressed and lonely compared to depression and psychological burden in healthy individuals (Gerhards et al., 2023). Interestingly, it has been documented that the correlation between life isolation and cardiovascular disease was stronger in participants < 65 years of age compared to those >65 years of age (Holt-Lunstad et al., 2015; Gronewold et al., 2020). In general, the potential psychological disorders brought on by neocoronavirus infection cannot be ignored and can increase the risk of cardiovascular disease through a variety of physiological mechanisms in the body, despite the fact that there are varied results regarding the risk of cardiovascular disease at various ages under the influence of significant social events (Gronewold et al., 2021; Figure 1).

3. Differences and analysis of cardiovascular system diseases combined with COVID-19 in different populations

3.1. Gender

Gender differences are one of the key determinants of disease progression and outcome and have received increasing attention and research. Several studies have found that among patients infected with SARS-CoV-2, disease morbidity, severity, and mortality appear to be higher in men than in women (Chen et al., 2020; Marik et al., 2021;

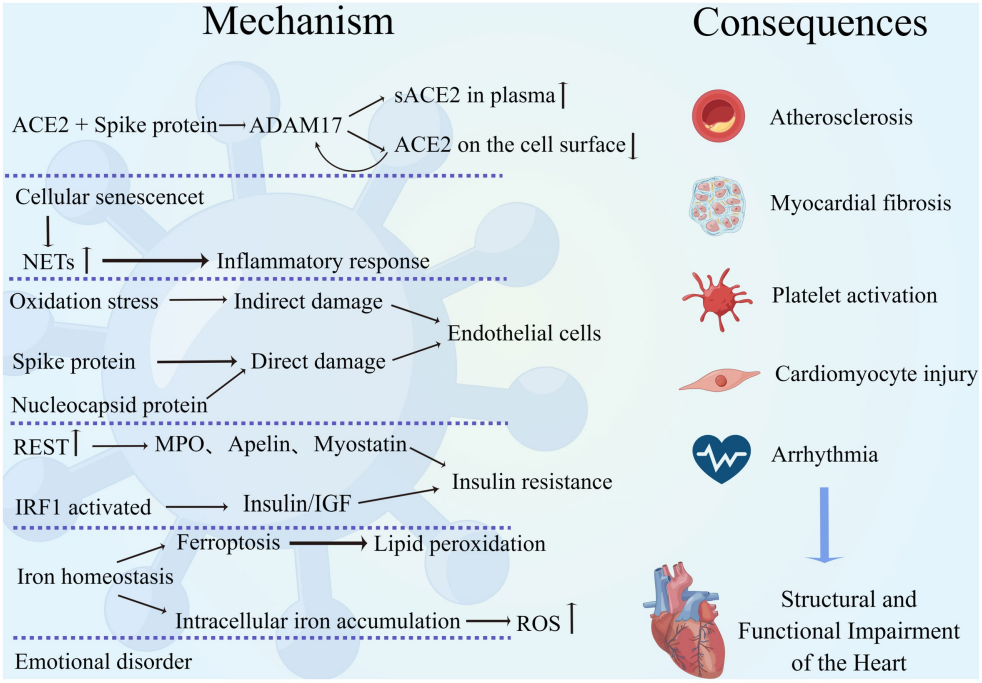

FIGURE 1
Mechanism of interaction between COVID-19 and the cardiovascular system. SARS-CoV-2 interacts with the cardiovascular system through multiple mechanisms, leading to a variety of adverse outcomes such as atherosclerosis, myocardial fibrosis, excessive platelet activation, cardiomyocyte injury, and arrhythmias, resulting in structural and functional damage to the heart. (By Figdraw).

Wehbe et al., 2021; Torres et al., 2023). Cardiovascular system disease is one of the common comorbidities and complications of neocoronavirus infection, and their interaction can increase the risk of death in patients (Wehbe et al., 2020; Woodruff et al., 2023). Recently, a series of explorations have been conducted regarding gender differences in cardiac disease combined with COVID-19. The prevalence of COVID-19 in combination with cardiovascular disease is higher in male patients worldwide (Gebhard et al., 2020). The increased mortality associated with acute myocardial infarction in COVID-19 patients is higher in men than in women (Yeo et al., 2023). Isath et al. found more men among patients with COVID-19 combined with heart failure by analyzing the baseline characteristics of patients admitted with heart failure in the United States (Isath et al., 2023b). The above studies suggest that men may have greater susceptibility to and more severe adverse clinical outcomes from neocoronavirus infections.

The reasons for this are the involvement of ACE2 and type II transmembrane serine protease (TMPRSS2) expression, sex hormones, and immune and inflammatory responses. ACE2 and TMPRSS2 are key factors in promoting SARS-CoV-2 entry into cells (Hoffmann et al., 2020), and it was found that plasma concentrations of ACE2 were higher in males, while TMPRSS2 is more expressed in males and regulated by androgens (Okwan-Duodu et al., 2021), which may lead to an increased initial viral load (Viveiros et al., 2022). When SARS-CoV-2 binds to ACE2, it activates metalloproteinase 17 (ADAM17), which induces ACE2 membrane shedding, exacerbates the accumulation of AngII, and diminishes the cardioprotective effects of ACE2 (Gheblawi et al., 2020). TLR7 recognizes single-stranded RNA and promotes interferon production, playing an important role in the immune response to new coronary infections. Females can express higher amounts of TLR7, thereby increasing resistance to viruses (Bienvenu et al., 2020; Wehbe et al., 2021). Sex hormone-dependent innate immunity leads to gender differences in the face of viral infections. Estradiol enhances the antiviral response by increasing the number of neutrophils and natural killer cells and decreasing pro-inflammatory cytokines, whereas androgens have immunosuppressive effects (Viveiros et al., 2021; Bechmann et al., 2022; Brandi, 2022). Recently, the first exploration regarding the effect of COVID-19 on patients with stress cardiomyopathy was conducted by Hajra et al. This study found that stress cardiomyopathy combined with COVID-19 was predominantly in men, and, interestingly, stress cardiomyopathy was more common in women (Hajra et al., 2023). It is worth noting that there are still flaws and controversies regarding the above mechanisms and studies. For example, it is too limited to consider only the ACE2 expression and ignore ACE2's own function. Differences in sex hormone levels in older patients may affect the observed sex differences. Both confounding factors and vaccination may affect the outcome of the studied patients.

Currently, the exploration of gender differences for COVID-19 combined with CVD is more based on physiological mechanisms. However, the impact of the new coronavirus on the psychological aspects of humans cannot be ignored. It has been found that the COVID-19 pandemic can lead to more stress in women from various aspects such as social, economic, work, and family, exacerbating the development of psychological disorders such as depression and anxiety and thus leading to an increased risk of CVD (Gulati and Kelly, 2020; Bucciarelli et al., 2022).

Gender differences in COVID-19 combined with CVD should be investigated further, not only in terms of physiological mechanisms but also to emphasize the importance of psychosocial factors in

disease development. Not only will this allow for better risk stratification for patients, but it will also allow for more refined and accurate treatment.

3.2. Age

Age is an important risk factor for increased mortality in patients with COVID-19, and older adults usually have a higher susceptibility as well as more severe clinical outcomes (Bonanad et al., 2020; Zhou et al., 2020; Torres et al., 2023). As previously mentioned, COVID-19 can increase the incidence of cardiovascular disease through endothelial damage, an immune inflammatory response, and coagulation abnormalities, and patients with underlying cardiac disease or the presence of cardiovascular disease risk factors are more likely to experience serious outcomes (Tian et al., 2020). Several studies have demonstrated that the risk of cardiovascular complications is greatly increased in the elderly population with a COVID-19 infection. Pellicori et al. found that some patients with COVID-19 can develop different types of cardiovascular complications during hospitalization and that the risk of CVD increases with age (Pellicori et al., 2021). Hajra et al. demonstrated that advanced age is a risk factor for stress cardiomyopathy and an independent predictor of mortality in patients with combined COVID-19 (Hajra et al., 2023). Hypertension is a common cardiovascular comorbidity in patients with COVID-19 (Harrison et al., 2021; Pellicori et al., 2021), and its pathogenesis is closely related to ACE2. ACE2 is both an important target of SARS-CoV-2 infected cells, and its elevated expression may be associated with an increased risk of infection while acting as a protective factor of the cardiovascular system to mitigate the deleterious effects of AngII. SARS-CoV-2-infected cells result in a further reduction of ACE2, while downregulation of ACE2 expression leads to more severe cardiac dysfunction. Thus, elderly people with down-regulated ACE2 expression have a more severe infection outcome (AlGhatrif et al., 2020). Older adults with cardiometabolic disease (CMD) have more severe adverse outcomes when infected with neocoronavirus, making social isolation particularly important for this high-risk population. However, DOVE et al. found that this population is more vulnerable to the negative psychological effects of social isolation, which can exacerbate the severity of cardiovascular disease, which requires us to weigh the pros and cons of each aspect in our clinical work and give targeted treatment and prevention recommendations (Dove et al., 2022).

Age is an uncontrollable risk factor for COVID-19 and cardiovascular disease, and exploring the link between age and disease pathogenesis will facilitate better risk stratification and management of patients. The physical and mental health of the elderly is highly vulnerable to disease itself and social factors; therefore, both "body" and "mind" should be the focus of our care and support for this population.

3.3. Metabolic syndrome

Metabolic syndrome (MetS) is a complex group of metabolic disorder syndromes, including obesity, dyslipidemia, hyperglycemia, and hypertension, which are closely associated with the development of cardiovascular diseases (Hamjane et al., 2020; Fahed et al., 2022). Epidemiology has shown that the prevalence of MetS has increased in all regions of the world, posing a huge health, economic, and medical burden and becoming an important health problem in modern society (Saklayen, 2018; Li et al., 2022). The pathogenesis of MetS is closely related to insulin resistance, chronic inflammation, mitochondrial dysfunction, and neurological activation, and interestingly, the above pathological processes are also involved in the development of cardiovascular disease and COVID-19 (Fahed et al., 2022; Dissanayake, 2023). A large body of evidence suggests that MetS leads to an increased risk of death and the development of serious complications in patients with COVID-19, often with a worse clinical outcome when combined with cardiovascular disease (Rico-Martín et al., 2021; Frere and tenOever, 2022).

Obesity, as a manifestation of the metabolic syndrome, can enhance SARS-CoV-2 susceptibility by increasing ACE2 expression. In addition, it was found that obese patients have elevated levels of n6-acetyl-l-lysine and p-cresol, which induce cytokine storm production and exacerbate the severity of COVID-19 (Jalaleddine et al., 2022). Protein lysine acetylation leads to impaired cardiac energy metabolism, and p-cresol enhances the risk of atherosclerosis and thrombosis in uremic patients (Jalaleddine et al., 2022). Increased blood glucose increases the risk of SARS-CoV-2 infection and the possibility of cardiovascular system disease through mechanisms such as the promotion of viral replication, platelet activation, and an excessive inflammatory response. Conversely, COVID-19 infection can cause disturbances in glucose regulation and induce serious complications (Aluganti Narasimhulu and Singla, 2022). Lipids are not only the structural basis of cells but also involved in several physiological or pathological activities in the body, which are essential for the development of the cardiovascular system and COVID-19. Lipid metabolism plays an important role in the processes of virus-cell fusion, endocytosis, replication, and cytokinesis, so statins are beneficial in reducing viral infections, while their plaque stabilizing effect reduces the probability of cardiovascular disease (Abu-Farha et al., 2020). Much controversy remains regarding the interaction between hypertension and COVID-19. Studies suggest that hypertension can occur in the acute phase of SARS-CoV-2 infection or as a sequela and has the potential to be a long-term predictor of COVID-19, but the evidence against the above view is not sufficient, and there are no studies to prove that pre-existing hypertension is an independent risk factor for increased mortality in COVID-19 (D'Elia et al., 2023; Matsumoto et al., 2023; Shibata et al., 2023). However, it is undeniable that hypertension, as a systemic disease, can lead to serious adverse clinical outcomes in patients with COVID-19, posing a significant threat to individual health and the global health care system (Abdalla et al., 2023; Figure 2).

4. Summary and outlook

The incidence of cardiovascular disease was significantly higher in the SARS-CoV-2 infection state, with significant differences across populations. COVID-19 patients with preexisting cardiovascular disease risk factors or cardiac disease had worse clinical outcomes. In addition to ACE2-mediated viral entry, endothelial dysfunction, iron homeostasis imbalance, and psychosocial factors involved in pathological development, severe electrolyte disturbances, respiratory failure, and impaired mitochondria can also lead to cardiac

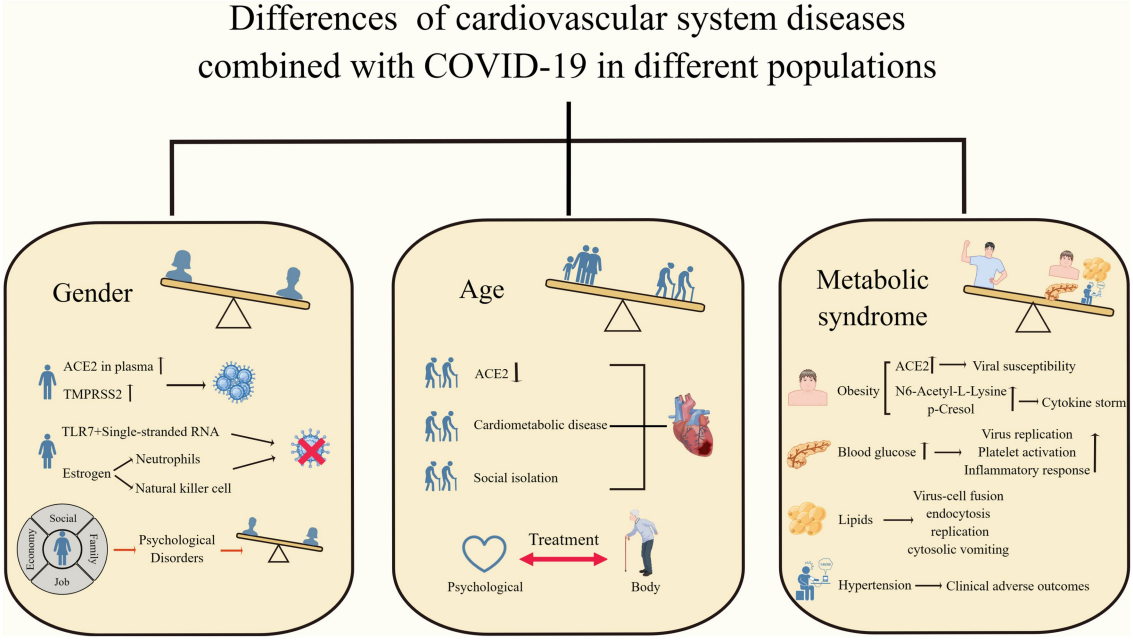

FIGURE 2
Differences in cardiovascular system diseases combined with COVID-19 in different populations. Men, older adults, and patients with metabolic syndrome have worse clinical outcomes when faced with COVID-19 combined with cardiovascular disease. (By Figdraw).

involvement (Wu et al., 2020; Adeghate et al., 2021; Chang et al., 2023). Take consideration of the spreading time of COVID-19 and the multiple variant strains, the long-term effects of SARS-CoV-2 on the heart are not yet known, and we still need to conduct long-term follow-up and a lot of research and exploration.

Author contributions

YZ and XH reviewed the literature and drafted this review. CL, YL, JC, and YW reviewed the literature, gave critical comments, and revised the manuscript. BA gave critical comments and revised the manuscript. All authors contributed to the article and approved the submitted version.

Funding

The study was supported by the National Natural Science Foundation of China (grant numbers: 82170362 to YW and 82000347 to CL). This study was also supported by Jilin Province Science and technology development plan project (grant numbers: 20230508061RC to YW and YDZJ202301ZYTS441 to CL), China Postdoctoral Science Foundation (2021M691209 to YW), and Jilin Medical and Health Talents Special (JLSWSRCZX2021-061 to YW).

Conflict of interest

The authors declare that the research was conducted in the absence of any commercial or financial relationships that could be construed as a potential conflict of interest.

Publisher's note

All claims expressed in this article are solely those of the authors and do not necessarily represent those of their affiliated organizations, or those of the publisher, the editors and the reviewers. Any product that may be evaluated in this article, or claim that may be made by its manufacturer, is not guaranteed or endorsed by the publisher.

References

Abdalla, M., El-Arabey, A. A., and Gai, Z. (2023). Hypertension is still a moving target in the context of COVID-19 and post-acute COVID-19 syndrome. *J. Med. Virol.* 95:e28128. doi: 10.1002/jmv.28128

Abu-Farha, M., Thanaraj, T. A., Qaddoumi, M. G., Hashem, A., Abubaker, J., and Al-Mulla, F. (2020). The Role of Lipid Metabolism in COVID-19 Virus Infection and as a Drug Target. *Int. J. Mol. Sci.* 21:3544. doi: 10.3390/ijms21103544

Adeghate, E. A., Eid, N., and Singh, J. (2021). Mechanisms of COVID-19-induced heart failure: a short review. *Heart Fail. Rev.* 26, 363–369. doi: 10.1007/s10741-020-10037-x

AlGhatrif, M., Cingolani, O., and Lakatta, E. G. (2020). The Dilemma of Coronavirus Disease 2019, Aging, and Cardiovascular Disease: Insights From Cardiovascular Aging Science. *JAMA Cardiol.* 5, 747–748. doi: 10.1001/jamacardio.2020.1329

Aluganti Narasimhulu, C., and Singla, D. K. (2022). Mechanisms of COVID-19 pathogenesis in diabetes. *Am. J. Physiol. Heart Circ. Physiol.* 323, H403–h420. doi: 10.1152/ajpheart.00204.2022

Baier, M. J., Wagner, S., Hupf, J., Evert, K., Evert, M., Sossalla, S., et al. (2022). Cardiac iron overload promotes cardiac injury in patients with severe COVID-19. *Infection* 50, 547–552. doi: 10.1007/s15010-021-01722-6

Bechmann, N., Barthel, A., Schedl, A., Herzig, S., Varga, Z., Gebhard, C., et al. (2022). Sexual dimorphism in COVID-19: potential clinical and public health implications. *Lancet Diabetes Endocrinol.* 10, 221–230. doi: 10.1016/s2213-8587(21)00346-6

Bienvenu, L. A., Noonan, J., Wang, X., and Peter, K. (2020). Higher mortality of COVID-19 in males: sex differences in immune response and cardiovascular comorbidities. *Cardiovasc. Res.* 116, 2197–2206. doi: 10.1093/cvr/cvaa284

Bonanad, C., García-Blas, S., Tarazona-Santabalbina, F., Sanchis, J., Bertomeu-González, V., Fácila, L., et al. (2020). The Effect of Age on Mortality in Patients With COVID-19: A Meta-Analysis With 611,583 Subjects. *J. Am. Med. Dir. Assoc.* 21, 915–918. doi: 10.1016/j.jamda.2020.05.045

Brandi, M. L. (2022). Are sex hormones promising candidates to explain sex disparities in the COVID-19 pandemic? *Rev. Endocr. Metab. Disord.* 23, 171–183. doi: 10.1007/s11154-021-09692-8

Bucciarelli, V., Nasi, M., Bianco, F., Seferovic, J., Ivkovic, V., Gallina, S., et al. (2022). Depression pandemic and cardiovascular risk in the COVID-19 era and long COVID syndrome: Gender makes a difference. *Trends Cardiovasc. Med.* 32, 12–17. doi: 10.1016/j.tcm.2021.09.009

Cai, H., and Harrison, D. G. (2000). Endothelial dysfunction in cardiovascular diseases: the role of oxidant stress. *Circ. Res.* 87, 840–844. doi: 10.1161/01.res.87.10.840

Cedervall, J. (2018). Hamidi A and Olsson A K: Platelets, NETs and cancer. *Thromb. Res.* 164, S148–s152. doi: 10.1016/j.thromres.2018.01.049

Chang, X., Ismail, N. I., Rahman, A., Xu, D., Chan, R. W. Y., Ong, S. G., et al. (2023). Long COVID-19 and the Heart: Is Cardiac Mitochondria the Missing Link? *Antioxid. Redox Signal.* 38, 599–618. doi: 10.1089/ars.2022.0126

Chen, T., Wu, D., Chen, H., Yan, W., Yang, D., Chen, G., et al. (2020). Clinical characteristics of 113 deceased patients with coronavirus disease 2019: retrospective study. *BMJ* 368:m1091. doi: 10.1136/bmj.m1091

Chung, M. K., Zidar, D. A., Bristow, M. R., Cameron, S. J., Chan, T., Harding, C. V., et al. (2021). COVID-19 and Cardiovascular Disease: From Bench to Bedside. *Circ. Res.* 128, 1214–1236. doi: 10.1161/circresaha.121.317997

Daniali, H., Martinussen, M., and Flaten, M. A. (2023). A global meta-analysis of depression, anxiety, and stress before and during COVID-19. *Health Psychol.* 42, 124–138. doi: 10.1037/hea0001259

Davis, M. G., Bobba, A., Majeed, H., Bilal, M. I., Nasrullah, A., Ratmeyer, G. M., et al. (2023). COVID-19 With Stress Cardiomyopathy Mortality and Outcomes Among Patients Hospitalized in the United States: A Propensity Matched Analysis Using the National Inpatient Sample Database. *Curr. Probl. Cardiol.* 48:101607. doi: 10.1016/j.cpcardiol.2023.101607

D'Elia, L., Giaquinto, A., Zarrella, A. F., Rendina, D., Iaccarino Idelson, P., Strazzullo, P., et al. (2023). Hypertension and mortality in SARS-COV-2 infection: A meta-analysis of observational studies after 2 years of pandemic. *Eur. J. Intern. Med.* 108, 28–36. doi: 10.1016/j.ejim.2022.11.018

Dissanayake, H. (2023). COVID-19 and metabolic syndrome. *Best Pract. Res. Clin. Endocrinol. Metab.* 101753:101753. doi: 10.1016/j.beem.2023.101753

Dove, A., Guo, J., Calderón-Larrañaga, A., Vetrano, D. L., Fratiglioni, L., and Xu, W. (2022). Association between social isolation and reduced mental well-being in Swedish older adults during the first wave of the COVID-19 pandemic: the role of cardiometabolic diseases. *Aging* 14, 2462–2474. doi: 10.18632/aging.203956

Fahed, G., Aoun, L., Bou Zerdan, M., Allam, S., Bou Zerdan, M., Bouferraa, Y., et al. (2022). Metabolic Syndrome: Updates on Pathophysiology and Management in 2021. *Int. J. Mol. Sci.* 23:786. doi: 10.3390/ijms23020786

Fairweather, D., Beetler, D. J., di Florio, D. N., Musigk, N., Heidecker, B., Cooper, L. T., et al. (2023). COVID-19, Myocarditis and Pericarditis. *Circ. Res.* 132, 1302–1319. doi: 10.1161/circresaha.123.321878

Fodor, A., Tiperciuc, B., Login, C., Orasan, O. H., Lazar, A. L., Buchman, C., et al. (2021). Endothelial Dysfunction, Inflammation, and Oxidative Stress in COVID-19-Mechanisms and Therapeutic Targets. *Oxid. Med. Cell. Longev.* 2021:8671713. doi: 10.1155/2021/8671713

Frere, J. J., and tenOever, B. R. (2022). Cardiometabolic syndrome—an emergent feature of Long COVID? *Nat. Rev. Immunol.* 22, 399–400. doi: 10.1038/s41577-022-00739-8

Gao, Y. D., Ding, M., Dong, X., Zhang, J. J., Kursat Azkur, A., Azkur, D., et al. (2021). Risk factors for severe and critically ill COVID-19 patients: A review. *Allergy* 76, 428–455. doi: 10.1111/all.14657

García-Escobar, A., Jiménez-Valero, S., Galeote, G., Jurado-Román, A., García-Rodríguez, J., and Moreno, R. (2021). The soluble catalytic ectodomain of ACE2 a biomarker of cardiac remodelling: new insights for heart failure and COVID19. *Heart Fail. Rev.* 26, 961–971. doi: 10.1007/s10741-020-10066-6

García-Escobar, A., Vera-Vera, S., Jurado-Román, A., Jiménez-Valero, S., Galeote, G., and Moreno, R. (2022). Calcium Signaling Pathway Is Involved in the Shedding of ACE2 Catalytic Ectodomain: New Insights for Clinical and Therapeutic Applications of ACE2 for COVID-19. *Biomol. Ther.* 12:76. doi: 10.3390/biom12010076

Gavriilaki, E., Anyfanti, P., Gavriilaki, M., Lazaridis, A., Douma, S., and Gkaliagkousi, E. (2020). Endothelial Dysfunction in COVID-19: Lessons Learned from Coronaviruses. *Curr. Hypertens. Rep.* 22:63. doi: 10.1007/s11906-020-01078-6

Gebhard, C., Regitz-Zagrosek, V., Neuhauser, H. K., Morgan, R., and Klein, S. L. (2020). Impact of sex and gender on COVID-19 outcomes in Europe. *Biol. Sex Differ.* 11:29. doi: 10.1186/s13293-020-00304-9

Gerhards, S. K., Luppa, M., Röhr, S., Pabst, A., Bauer, A., Frankhänel, T., et al. (2023). Depression and Anxiety in Old Age during the COVID-19 Pandemic: A Comparative Study of Individuals at Cardiovascular Risk and the General Population. *Int. J. Environ. Res. Public Health* 20:2975. doi: 10.3390/ijerph20042975

Gheblawi, M., Wang, K., Viveiros, A., Nguyen, Q., Zhong, J. C., Turner, A. J., et al. (2020). Angiotensin-Converting Enzyme 2: SARS-CoV-2 Receptor and Regulator of the Renin-Angiotensin System: Celebrating the 20th Anniversary of the Discovery of ACE2. *Circ. Res.* 126, 1456–1474. doi: 10.1161/circresaha.120.317015

Gronewold, J., Engels, M., van de Velde, S., Cudjoe, T. K. M., Duman, E. E., Jokisch, M., et al. (2021). Effects of Life Events and Social Isolation on Stroke and Coronary Heart Disease. *Stroke* 52, 735–747. doi: 10.1161/strokeaha.120.032070

Gronewold, J., Kropp, R., Lehmann, N., Schmidt, B., Weyers, S., Siegrist, J., et al. (2020). Association of social relationships with incident cardiovascular events and all-cause mortality. *Heart* 106, 1317–1323. doi: 10.1136/heartjnl-2019-316250

Gu, S. X., Tyagi, T., Jain, K., Gu, V. W., Lee, S. H., Hwa, J. M., et al. (2021). Thrombocytopathy and endotheliopathy: crucial contributors to COVID-19 thromboinflammation. *Nat. Rev. Cardiol.* 18, 194–209. doi: 10.1038/s41569-020-00469-1

Gulati, G., and Kelly, B. D. (2020). Domestic violence against women and the COVID-19 pandemic: What is the role of psychiatry? *Int. J. Law Psychiatry* 71:101594. doi: 10.1016/j.ijlp.2020.101594

Gyöngyösi, M., Alcaide, P., Asselbergs, F. W., Brundel, B., Camici, G. G., Martins, P. D. C., et al. (2023). Long COVID and the cardiovascular system-elucidating causes and cellular mechanisms in order to develop targeted diagnostic and therapeutic strategies: a joint Scientific Statement of the ESC Working Groups on Cellular Biology of the Heart and Myocardial and Pericardial Diseases. *Cardiovasc. Res.* 119, 336–356. doi: 10.1093/cvr/cvac115

Hajra, A., Malik, A., Bandyopadhyay, D., Goel, A., Isath, A., Gupta, R., et al. (2023). Impact of COVID-19 in patients hospitalized with stress cardiomyopathy: A nationwide analysis. *Prog. Cardiovasc. Dis.* 76, 25–30. doi: 10.1016/j.pcad.2022.12.002

Hamjane, N., Benyahya, F., Nourouti, N. G., Mechita, M. B., and Barakat, A. (2020). Cardiovascular diseases and metabolic abnormalities associated with obesity: What is the role of inflammatory responses? A systematic review. *Microvasc. Res.* 131:104023. doi: 10.1016/j.mvr.2020.104023

Han, Y., Zhu, J., Yang, L., Nilsson-Payant, B. E., Hurtado, R., Lacko, L. A., et al. (2022). SARS-CoV-2 Infection Induces Ferroptosis of Sinoatrial Node Pacemaker Cells. *Circ. Res.* 130, 963–977. doi: 10.1161/circresaha.121.320518

Harrison, S. L., Buckley, B. J. R., Rivera-Caravaca, J. M., Zhang, J., and Lip, G. Y. H. (2021). Cardiovascular risk factors, cardiovascular disease, and COVID-19: an umbrella review of systematic reviews. *Eur Heart J Qual Care Clin Outcomes* 7, 330–339. doi: 10.1093/ehjqcco/qcab029

Hati, S., and Bhattacharyya, S. (2020). Impact of Thiol-Disulfide Balance on the Binding of Covid-19 Spike Protein with Angiotensin-Converting Enzyme 2 Receptor. *ACS Omega* 5, 16292–16298. doi: 10.1021/acsomega.0c02125

He, X., Liu, C., Peng, J., Li, Z., Li, F., Wang, J., et al. (2021). COVID-19 induces new-onset insulin resistance and lipid metabolic dysregulation via regulation of secreted metabolic factors. *Signal Transduct. Target. Ther.* 6:427. doi: 10.1038/s41392-021-00822-x

Hobohm, L., Sagoschen, I., Barco, S., Farmakis, I. T., Fedeli, U., Koelmel, S., et al. (2023). COVID-19 infection and its impact on case fatality in patients with pulmonary embolism. *Eur. Respir. J.* 61:2200619. doi: 10.1183/13993003.00619-2022

Hoffmann, M., Kleine-Weber, H., Schroeder, S., Krüger, N., Herrler, T., Erichsen, S., et al. (2020). SARS-CoV-2 Cell Entry Depends on ACE2 and TMPRSS2 and Is Blocked by a Clinically Proven Protease Inhibitor. *Cells* 181, 271–280.e8. doi: 10.1016/j.cell.2020.02.052

Holt-Lunstad, J., Smith, T. B., Baker, M., Harris, T., and Stephenson, D. (2015). Loneliness and social isolation as risk factors for mortality: a meta-analytic review. *Perspect. Psychol. Sci.* 10, 227–237. doi: 10.1177/1745691614568352

Incalza, M. A., D'Oria, R., Natalicchio, A., Perrini, S., Laviola, L., and Giorgino, F. (2018). Oxidative stress and reactive oxygen species in endothelial dysfunction associated with cardiovascular and metabolic diseases. *Vascul. Pharmacol.* 100, 1–19. doi: 10.1016/j.vph.2017.05.005

Isath, A., Malik, A., Bandyopadhyay, D., Goel, A., Hajra, A., Dhand, A., et al. (2023b). COVID-19, Heart Failure Hospitalizations, and Outcomes: A Nationwide Analysis. *Curr. Probl. Cardiol.* 48:101541. doi: 10.1016/j.cpcardiol.2022.101541

Isath, A., Malik, A. H., Goel, A., Gupta, R., Shrivastav, R., and Bandyopadhyay, D. (2023a). Nationwide Analysis of the Outcomes and Mortality of Hospitalized COVID-19 Patients. *Curr. Probl. Cardiol.* 48:101440. doi: 10.1016/j.cpcardiol.2022.101440

Jalaleddine, N., Hachim, M., Al-Hroub, H., Saheb Sharif-Askari, N., Senok, A., Elmoselhi, A., et al. (2022). N6-Acetyl-L-Lysine and p-Cresol as Key Metabolites in the Pathogenesis of COVID-19 in Obese Patients. *Front. Immunol.* 13:827603. doi: 10.3389/fimmu.2022.827603

Jia, G., Whaley-Connell, A., and Sowers, J. R. (2018). Diabetic cardiomyopathy: a hyperglycaemia- and insulin-resistance-induced heart disease. *Diabetologia* 61, 21–28. doi: 10.1007/s00125-017-4390-4

Kang, Y., Chen, T., Mui, D., Ferrari, V., Jagasia, D., Scherrer-Crosbie, M., et al. (2020). Cardiovascular manifestations and treatment considerations in COVID-19. *Heart* 106, 1132–1141. doi: 10.1136/heartjnl-2020-317056

Kato, Y., Nishiyama, K., Man Lee, J., Ibuki, Y., Imai, Y., Noda, T., et al. (2022). TRPC3-Nox2 Protein Complex Formation Increases the Risk of SARS-CoV-2 Spike Protein-Induced Cardiomyocyte Dysfunction through ACE2 Upregulation. *Int. J. Mol. Sci.* 24:102. doi: 10.3390/ijms24010102

Keller, K., Sagoschen, I., Konstantinides, S., Gori, T., Münzel, T., and Hobohm, L. (2023). Incidence and risk factors of myocarditis in hospitalized patients with COVID-19. *J. Med. Virol.* 95:e28646. doi: 10.1002/jmv.28646

Krüger-Genge, A., Blocki, A., Franke, R. P., and Jung, F. (2019). Vascular Endothelial Cell Biology: An Update. *Int. J. Mol. Sci.* 20:4411. doi: 10.3390/ijms20184411

Kuriakose, J., Montezano, A. C., and Touyz, R. M. (2021). ACE2/Ang-(1-7)/Mas1 axis and the vascular system: vasoprotection to COVID-19-associated vascular disease. *Clin. Sci.* 135, 387–407. doi: 10.1042/CS20200480

Lambert, D. W., Yarski, M., Warner, F. J., Thornhill, P., Parkin, E. T., Smith, A. I., et al. (2005). Tumor necrosis factor-alpha convertase (ADAM17) mediates regulated ectodomain shedding of the severe-acute respiratory syndrome-coronavirus (SARS-CoV) receptor, angiotensin-converting enzyme-2 (ACE2). *J. Biol. Chem.* 280, 30113–30119. doi: 10.1074/jbc.M505111200

Lau, D., and McAlister, F. A. (2021). Implications of the COVID-19 Pandemic for Cardiovascular Disease and Risk-Factor Management. *Can. J. Cardiol.* 37, 722–732. doi: 10.1016/j.cjca.2020.11.001

Lee, K. H., Kronbichler, A., Park, D. D., Park, Y., Moon, H., Kim, H., et al. (2017). Neutrophil extracellular traps (NETs) in autoimmune diseases: A comprehensive review. *Autoimmun. Rev.* 16, 1160–1173. doi: 10.1016/j.autrev.2017.09.012

Lei, Y., Zhang, J., Schiavon, C. R., He, M., Chen, L., Shen, H., et al. (2021). SARS-CoV-2 Spike Protein Impairs Endothelial Function via Downregulation of ACE 2. *Circ. Res.* 128, 1323–1326. doi: 10.1161/circresaha.121.318902

Li, W., Qiu, X., Ma, H., and Geng, Q. (2022). Incidence and long-term specific mortality trends of metabolic syndrome in the United States. *Front. Endocrinol.* 13:1029736. doi: 10.3389/fendo.2022.1029736

Liu, D., Baumeister, R. F., and Zhou, Y. (2021). Mental health outcomes of coronavirus infection survivors: A rapid meta-analysis. *J. Psychiatr. Res.* 137, 542–553. doi: 10.1016/j.jpsychires.2020.10.015

Liu, F., Liu, F., and Wang, L. (2021). COVID-19 and cardiovascular diseases. *J. Mol. Cell Biol.* 13, 161–167. doi: 10.1093/jmcb/mjaa064

Mahley, R. W. (2016). Apolipoprotein E: from cardiovascular disease to neurodegenerative disorders. *J. Mol. Med.* 94, 739–746. doi: 10.1007/s00109-016-1427-y

Marais, A. D. (2019). Apolipoprotein E in lipoprotein metabolism, health and cardiovascular disease. *Pathology* 51, 165–176. doi: 10.1016/j.pathol.2018.11.002

Marik, P. E., DePerrior, S. E., Ahmad, Q., and Dodani, S. (2021). Gender-based disparities in COVID-19 patient outcomes. *J. Invest. Med.* 69, 814–818. doi: 10.1136/jim-2020-001641

Matsumoto, C., Shibata, S., Kishi, T., Morimoto, S., Mogi, M., Yamamoto, K., et al. (2023). Long COVID and hypertension-related disorders: a report from the Japanese Society of Hypertension Project Team on COVID-19. *Hypertens. Res.* 46, 601–619. doi: 10.1038/s41440-022-01145-2

Montiel, V., Lobysheva, I., Gérard, L., Vermeersch, M., Perez-Morga, D., Castelein, T., et al. (2022). Oxidative stress-induced endothelial dysfunction and decreased vascular nitric oxide in COVID-19 patients. *EBioMedicine* 77:103893. doi: 10.1016/j.ebiom.2022.103893

Nakamura, K., Miyoshi, T., Yoshida, M., Akagi, S., Saito, Y., Ejiri, K., et al. (2022). Pathophysiology and Treatment of Diabetic Cardiomyopathy and Heart Failure in Patients with Diabetes Mellitus. *Int. J. Mol. Sci.* 23:3587. doi: 10.3390/ijms23073587

Okwan-Duodu, D., Lim, E. C., You, S., and Engman, D. M. (2021). TMPRSS2 activity may mediate sex differences in COVID-19 severity. *Signal Transduct. Target. Ther.* 6:100. doi: 10.1038/s41392-021-00513-7

Pellicori, P., Doolub, G., Wong, C. M., Lee, K. S., Mangion, K., Ahmad, M., et al. (2021). COVID-19 and its cardiovascular effects: a systematic review of prevalence studies. *Cochrane Database Syst. Rev.* 3:CD013879. doi: 10.1002/14651858.Cd013879

Prasad, M., Leon, M., Lerman, L. O., and Lerman, A. (2021). Viral Endothelial Dysfunction: A Unifying Mechanism for COVID-19. *Mayo Clin. Proc.* 96, 3099–3108. doi: 10.1016/j.mayocp.2021.06.027

Qian, Y., Lei, T., Patel, P. S., Lee, C. H., Monaghan-Nichols, P., Xin, H. B., et al. (2021). Direct Activation of Endothelial Cells by SARS-CoV-2 Nucleocapsid Protein Is Blocked by Simvastatin. *J. Virol.* 95:e0139621. doi: 10.1128/jvi.01396-21

Raghavan, S., Kenchappa, D. B., and Leo, M. D. (2021). SARS-CoV-2 Spike Protein Induces Degradation of Junctional Proteins That Maintain Endothelial Barrier Integrity. *Front Cardiovasc Med* 8:687783. doi: 10.3389/fcvm.2021.687783

Rico-Martín, S., Calderón-García, J. F., Basilio-Fernández, B., Clavijo-Chamorro, M. Z., and Sánchez Muñoz-Torrero, J. F. (2021). Metabolic Syndrome and Its Components in Patients with COVID-19: Severe Acute Respiratory Syndrome (SARS) and Mortality. A Systematic Review and Meta-Analysis. *J Cardiovasc Dev Dis* 8:162. doi: 10.3390/jcdd8120162

Rossouw, T. M., Anderson, R., Manga, P., and Feldman, C. (2022). Emerging Role of Platelet-Endothelium Interactions in the Pathogenesis of Severe SARS-CoV-2 Infection-Associated Myocardial Injury. *Front. Immunol.* 13:776861. doi: 10.3389/fimmu.2022.776861

Saklayen, M. G. (2018). The Global Epidemic of the Metabolic Syndrome. *Curr. Hypertens. Rep.* 20:12. doi: 10.1007/s11906-018-0812-z

Schmitt, C. A., Tchkonia, T., Niedernhofer, L. J., Robbins, P. D., Kirkland, J. L., and Lee, S. (2023). COVID-19 and cellular senescence. *Nat. Rev. Immunol.* 23, 251–263. doi: 10.1038/s41577-022-00785-2

Shi, S., Qin, M., Shen, B., Cai, Y., Liu, T., Yang, F., et al. (2020). Association of Cardiac Injury With Mortality in Hospitalized Patients With COVID-19 in Wuhan, China. *JAMA Cardiol.* 5, 802–810. doi: 10.1001/jamacardio.2020.0950

Shi, H., Zuo, Y., Navaz, S., Harbaugh, A., Hoy, C. K., Gandhi, A. A., et al. (2022). Endothelial Cell-Activating Antibodies in COVID-19. *Arthritis Rheumatol.* 74, 1132–1138. doi: 10.1002/art.42094

Shibata, S., Kobayashi, K., Tanaka, M., Asayama, K., Yamamoto, E., Nakagami, H., et al. (2023). COVID-19 pandemic and hypertension: an updated report from the Japanese Society of Hypertension project team on COVID-19. *Hypertens. Res.* 46, 589–600. doi: 10.1038/s41440-022-01134-5

Shin, J., Toyoda, S., Nishitani, S., Onodera, T., Fukuda, S., Kita, S., et al. (2022). SARS-CoV-2 infection impairs the insulin/IGF signaling pathway in the lung, liver, adipose tissue, and pancreatic cells via IRF1. *Metabolism* 133:155236. doi: 10.1016/j.metabol.2022.155236

Silva, M. G., Corradi, G. R., Pérez Duhalde, J. I., Nuñez, M., Cela, E. M., Gonzales Maglio, D. H., et al. (2022). Plasmatic renin-angiotensin system in normotensive and hypertensive patients hospitalized with COVID-19. *Biomed. Pharmacother.* 152:113201. doi: 10.1016/j.biopha.2022.113201

Tian, W., Jiang, W., Yao, J., Nicholson, C. J., Li, R. H., Sigurslid, H. H., et al. (2020). Predictors of mortality in hospitalized COVID-19 patients: A systematic review and meta-analysis. *J. Med. Virol.* 92, 1875–1883. doi: 10.1002/jmv.26050

Tobler, D. L., Pruzansky, A. J., Naderi, S., Ambrosy, A. P., and Slade, J. J. (2022). Long-Term Cardiovascular Effects of COVID-19: Emerging Data Relevant to the Cardiovascular Clinician. *Curr. Atheroscler. Rep.* 24, 563–570. doi: 10.1007/s11883-022-01032-8

Torres, C., García, J., Meslé, F., Barbieri, M., Bonnet, F., Camarda, C. G., et al. (2023). Identifying age- and sex-specific COVID-19 mortality trends over time in six countries. *Int. J. Infect. Dis.* 128, 32–40. doi: 10.1016/j.ijid.2022.12.004

Tripathi, U., Nchioua, R., Prata, L., Zhu, Y., Gerdes, E. O. W., Giorgadze, N., et al. (2021). SARS-CoV-2 causes senescence in human cells and exacerbates the senescence-associated secretory phenotype through TLR-3. *Aging* 13, 21838–21854. doi: 10.18632/aging.203560

Verdecchia, P., Cavallini, C., Spanevello, A., and Angeli, F. (2020). The pivotal link between ACE2 deficiency and SARS-CoV-2 infection. *Eur. J. Intern. Med.* 76, 14–20. doi: 10.1016/j.ejim.2020.04.037

Viveiros, A., Gheblawi, M., Aujla, P. K., Sosnowski, D. K., Seubert, J. M., Kassiri, Z., et al. (2022). Sex- and age-specific regulation of ACE2: Insights into severe COVID-19 susceptibility. *J. Mol. Cell. Cardiol.* 164, 13–16. doi: 10.1016/j.yjmcc.2021.11.003

Viveiros, A., Rasmuson, J., Vu, J., Mulvagh, S. L., Yip, C. Y. Y., Norris, C. M., et al. (2021). Sex differences in COVID-19: candidate pathways, genetics of ACE2, and sex hormones. *Am. J. Physiol. Heart Circ. Physiol.* 320, H296–h304. doi: 10.1152/ajpheart.00755.2020

Ward, M., Briggs, R., McGarrigle, C. A., De Looze, C., O'Halloran, A. M., and Kenny, R. A. (2023). The bi-directional association between loneliness and depression among older adults from before to during the COVID-19 pandemic. *Int. J. Geriatr. Psychiatry* 38:e5856. doi: 10.1002/gps.5856

Warnatsch, A., Ioannou, M., Wang, Q., and Papayannopoulos, V. (2015). Inflammation: Neutrophil extracellular traps license macrophages for cytokine production in atherosclerosis. *Science* 349, 316–320. doi: 10.1126/science.aaa8064

Wehbe, Z., Hammoud, S., Soudani, N., Zaraket, H., El-Yazbi, A., and Eid, A. H. (2020). Molecular Insights Into SARS COV-2 Interaction With Cardiovascular Disease: Role of RAAS and MAPK Signaling. *Front. Pharmacol.* 11:836. doi: 10.3389/fphar.2020.00836

Wehbe, Z., Hammoud, S. H., Yassine, H. M., Fardoun, M., El-Yazbi, A. F., and Eid, A. H. (2021). Molecular and Biological Mechanisms Underlying Gender Differences in COVID-19 Severity and Mortality. *Front. Immunol.* 12:659339. doi: 10.3389/fimmu.2021.659339

Woodruff, R. C., Garg, S., George, M. G., Patel, K., Jackson, S. L., Loustalot, F., et al. (2023). Acute Cardiac Events During COVID-19-Associated Hospitalizations. *J. Am. Coll. Cardiol.* 81, 557–569. doi: 10.1016/j.jacc.2022.11.044

Wu, C. I., Postema, P. G., Arbelo, E., Behr, E. R., Bezzina, C. R., Napolitano, C., et al. (2020). SARS-CoV-2, COVID-19, and inherited arrhythmia syndromes. *Heart Rhythm* 17, 1456–1462. doi: 10.1016/j.hrthm.2020.03.024

Yeo, Y. H., Wang, M., He, X., Lv, F., Zhang, Y., Zu, J., et al. (2023). Excess risk for acute myocardial infarction mortality during the COVID-19 pandemic. *J. Med. Virol.* 95:e28187. doi: 10.1002/jmv.28187

Yu, J., Yuan, X., Chen, H., Chaturvedi, S., Braunstein, E. M., and Brodsky, R. A. (2020). Direct activation of the alternative complement pathway by SARS-CoV-2 spike proteins is blocked by factor D inhibition. *Blood* 136, 2080–2089. doi: 10.1182/blood.2020008248

Zhang, H., Shao, L., Lin, Z., Long, Q. X., Yuan, H., Cai, L., et al. (2022). APOE interacts with ACE2 inhibiting SARS-CoV-2 cellular entry and inflammation in COVID-19 patients. *Signal Transduct. Target. Ther.* 7:261. doi: 10.1038/s41392-022-01118-4

Zhou, F., Yu, T., Du, R., Fan, G., Liu, Y., Liu, Z., et al. (2020). Clinical course and risk factors for mortality of adult inpatients with COVID-19 in Wuhan, China: a retrospective cohort study. *Lancet* 395, 1054–1062. doi: 10.1016/s0140-6736(20)30566-3

Zipeto, D., Palmeira, J. D. F., Argañaraz, G. A., and Argañaraz, E. R. (2020). ACE2/ADAM17/TMPRSS2 Interplay May Be the Main Risk Factor for COVID-19. *Front. Immunol.* 11:576745. doi: 10.3389/fimmu.2020.576745

Zuo, Y., Yalavarthi, S., Shi, H., Gockman, K., Zuo, M., Madison, J. A., et al. (2020). Neutrophil extracellular traps in COVID-19. JCI. *Insight* 5:e138999. doi: 10.1172/jci.insight.138999

frontiers | Frontiers in Microbiology

TYPE Mini Review
PUBLISHED 21 June 2023
DOI 10.3389/fmicb.2023.1219846

OPEN ACCESS

EDITED BY
Wei Wei,
First Affiliated Hospital of Jilin University, China

REVIEWED BY
Ralph A. Tripp,
University System of Georgia, United States

*CORRESPONDENCE
Pedro A. Piedra
✉ ppiedra@bcm.edu

†These authors have contributed equally to this work and share first authorship

RECEIVED 09 May 2023
ACCEPTED 01 June 2023
PUBLISHED 21 June 2023

CITATION
Rezende W, Neal HE, Dutch RE and Piedra PA (2023) The RSV F p27 peptide: current knowledge, important questions. *Front. Microbiol.* 14:1219846. doi: 10.3389/fmicb.2023.1219846

The RSV F p27 peptide: current knowledge, important questions

Wanderson Rezende[1,2†], Hadley E. Neal[3†], Rebecca E. Dutch[3] and Pedro A. Piedra[1,4*]

[1]Department of Molecular Virology and Microbiology, Baylor College of Medicine, Houston, TX, United States, [2]Department of Pharmacology, Baylor College of Medicine, Houston, TX, United States, [3]Department of Molecular and Cellular Biochemistry, University of Kentucky, Lexington, KY, United States, [4]Department of Pediatrics, Baylor College of Medicine, Houston, TX, United States

Respiratory syncytial virus (RSV) remains a leading cause of hospitalizations and death for young children and adults over 65. The worldwide impact of RSV has prioritized the search for an RSV vaccine, with most targeting the critical fusion (F) protein. However, questions remain about the mechanism of RSV entry and RSV F triggering and fusion promotion. This review highlights these questions, specifically those surrounding a cleaved 27 amino acids long peptide within F, p27.

KEYWORDS

respiratory syncytial virus (RSV), p27, fusion protein (F), cleavage, F protein trimer

1. The RSV F protein: cleavage sites and the p27 peptide

Respiratory syncytial virus (RSV) remains a leading cause of hospitalizations and death for young children and adults over 65 (Rha et al., 2020; McLaughlin et al., 2022). RSV is an enveloped, single-stranded, negative-sense RNA virus belonging to the *Pneumoviridae* family (Amarasinghe et al., 2019). Similar to paramyxoviruses, pneumoviruses consist of a nucleocapsid protein complex (a nucleocapsid protein (N) encapsidating the genetic material, the polymerase (L) and polymerase co-factor, P (phosphoprotein)), a matrix (M) protein layer linking the nucleocapsid protein complex with the phospholipid envelope, and three transmembrane glycoproteins (King et al., 2012). The fusion protein (F) and attachment (G) glycoproteins promote membrane fusion and viral entry. Functional and structural studies suggest that the pneumovirus small hydrophobic (SH) protein forms pH-dependent viroporin that regulates membrane permeability, infectivity, and prevent host cell apoptosis (Fuentes et al., 2007; Gan et al., 2012; Masante et al., 2014).

RSV F is synthesized as an inactive precursor (F0) which undergoes cleavage by host cell proteases to yield two disulfide-linked subunits, F1 and F2 (Collins and Mottett, 1991; Day et al., 2006), which are fusion competent. Fusion active F is in a metastable "prefusion" state until a triggering event induces conformational changes, exposing the fusion peptide, which inserts into the target membrane, followed by formation of a six-helix bundle which is hypothesized to drive membrane fusion (Smith et al., 2009; King et al., 2012). This process is similar for all paramyxo- and pneumoviruses; however, RSV F has several differences that remain to be fully understood.

Collins et al. (1984) and Elango et al. (1985), respectively, first sequenced RSV F, showing it is 574 amino acids with a polybasic motif (KKRKRR136) corresponding to a furin consensus site. Unlike closely related paramyxovirus F proteins, the polybasic sequence is six amino acids long, leading Bolt et al. to suggest that other proteases could be involved in

cleavage (such as proprotein convertase 5 and 7; Basak et al., 2001) and activate RSV F (Bolt et al., 2000). However, it was not until 2001 that González-Reyes et al. (2001) and Zimmer et al. (2001a) independently demonstrated that RSV F is cleaved at two polybasic sites (RARR109 and KKRKRR136), generating two major subunits: the F2 subunit (20 kDa, AA 26 to 109), and F1 (50 kDa, AA 137 to 574), and releasing an internal peptide of 27 amino acids, termed p27 (AA 110–136) (Figure 1A). The fate of this fragment post-cleavage is still unknown.

Through site-directed mutagenesis of Bovine Respiratory Syncytial Virus (BRSV), Zimmer et al. (2002) determined that furin cleavage at site R109 impaired but did not abolish fusion activity *in vitro*, highlighting the importance of cleavage at site R136, which exposes the fusion peptide at the N-terminus of the F1 subunit. Rawling et al. (2011) generated chimeric mutations of Sendai virus (SeV) fusion to include one or both RSV furin recognition sites rather than the single cleavage site normally in SeV F. SeV F normally requires the HN attachment protein for fusion triggering, while. RSV F can promote fusion in cell culture without the G protein (Techaarpornkul et al., 2001). Interestingly, all SeV F/RSV cleavage site chimeric mutants formed syncytia without HN protein, suggesting that the ability of RSV F to fuse without the attachment protein is facilitated, at least in part, by the additional cleavage site.

There are two known RSV subtypes, A and B, classified as such by divergences in antigenic profile from the RSV/A Long strain (prototypic strain historically used for *in vitro* studies and vaccine development; McLellan et al., 2013c; Pandya et al., 2019). Hause et al. (2017) compared sequence variability of more than 1,000 RSV sequences of subtypes A and B to the RSV/A Long, showing that although the F protein is well-conserved across RSV genotypes, the p27 region of RSV/B strains exhibited significantly more non-synonymous amino acid changes than the RSV/A strains. However, entropy analysis – the measure of variability at each amino acid position – revealed that within the same subtype, several amino acid positions within the p27 sequence of RSV/As are more variable than in RSV/Bs.

As reported by Rajan et al. (2022), RSV infection in HEp-2 or A549 cells (commonly used for *in vitro* studies) have different viral growth kinetics and host response when infected with RSV/A or B. Additionally, the efficiency of p27 cleavage shows to be cell line dependent, as higher levels of mature F proteins retaining p27 are found on the surface of RSV-infected HEp-2 cells compared to A549 cells, independent of RSV subtypes (Rezende et al., 2023). On the other hand, cleavage of p27 is also subtype dependent, since F proteins from RSV/A were less efficiently cleaved (retaining more p27) than the F proteins expressed on the surface of cells infected with RSV/B (Rezende et al., 2023). Moreover, the authors showed that for both subtypes, the p27 cleavage efficiency declines over time (Rezende et al., 2023).

These studies highlight that despite a highly conserved F protein sequence among RSV subtypes and genotypes, the cleavage of p27 relies on host factors (e.g., enzyme turnover, vesicular transport,

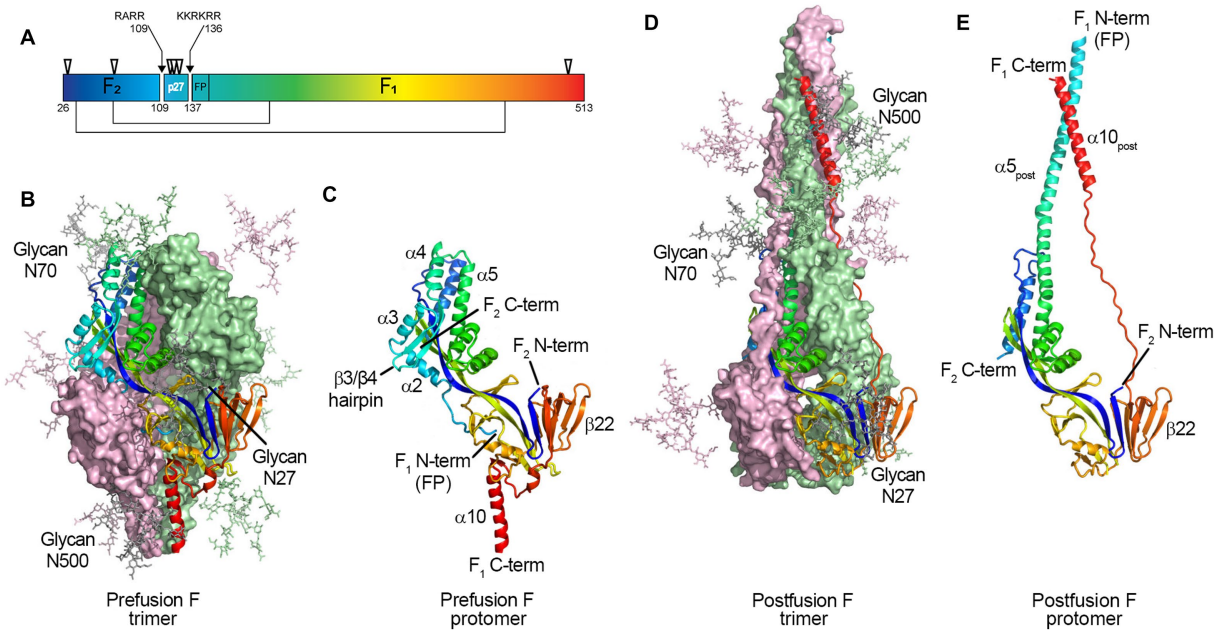

FIGURE 1
Structure of the RSV F protein on prefusion and postfusion conformations. **(A)** primary structure showing the disulfide bonds between F1 and F2 subunits (thin lines), N-glycosylation sites (▽), and the Fusion Peptide (FP) on F1 N-term; the p27 peptide is shown between cleavage sites R109 and R136 (arrows). F protein trimer on the **(B)** prefusion and **(D)** postfusion conformations with N-Glycans N27, N70, and N500 modeled as sticks. F1+F2 protomers on prefusion **(C)** and postfusion **(E)** conformations. The RSV F protein prefusion trimer **(B)** is formed by the interaction between three F1+F2 protomers **(C)**. In the process of viral entry, the prefusion trimer **(B)** undergoes structural rearrangement to a final postfusion conformation **(D)**. The FP (F_1 N-term), β3/β4 hairpin, and alpha-helices α2, α3, and α4 rearrange, fusing with α5 **(C)** to form an extended postfusion helix, $\alpha5_{post}$ **(E)**; the prefusion β22 parallel strand unravels so the α10 helix **(C)** can meet $\alpha5_{post}$, finalizing the postfusion conformation **(E)**. Although not shown in crystal structures, the p27 peptide remains at the F1 N-term when partially cleaved, capping the Fusion Peptide, which hinders the fusion efficiency. From McLellan et al. (2013b). Structure of RSV Fusion Glycoprotein Trimer Bound to a Prefusion-Specific Neutralizing Antibody. Science (80-) 340:1113–1117. Reprinted with permission from AAAS.

post-translational modifications, and innate immunity) rather than exclusively on enzymatic accessibility to cleavage sites.

2. Insights on the p27 glycosylation sites

Glycosylation is a crucial post-translational modification, as it impacts structure, function, stability, and translocation to the cell surface (Beyene et al., 2004; Vigerust and Shepherd, 2007; Ellgaard et al., 2016). RSV F has five N-linked glycosyolation sites which are well conserved among subtypes (N27, N70, N116, N126, and N500) (Zimmer et al., 2001b); with an additional N120 glycosylation site for some strains (Tan et al., 2012; Kimura et al., 2017). Two and for some strains three glycosylation sites are located within the p27 segment (N116, N120, and N126; Figure 1A).

Zimmer et al. (2001b) and Leemans et al. (2018) used systematic N – Q mutations to show that glycosylation in the p27 segment does not impact cleavage or transport of the F protein to the cell surface. Furthermore, F proteins containing the mutations N116Q or N126Q did not display molecular weight differences compared to wild-type. Therefore, Leemans et al. concluded that p27 was cleaved entirely off in a mature F protein. Both groups observed formation of larger syncytia in BSR T7/5 cells transfected with the mutant N116Q. Viral proteins can use glycosylation to shield antigenic sites, evading antibody recognition (Klink et al., 2006); however, Leemans et al. demonstrated that glycosylation of p27 at N116 and N126 did not significantly compromise binding of Palivizumab or other neutralizing antibodies targeting the prefusion conformation.

Leemans et al. (2019), incorporated the same mutations into recombinant viruses. During infection of HEp-2 cells, the molecular weight of the F proteins expressed by viruses encoding mutations N116Q or N126Q was comparable to F from wild-type virus. However, infection with mutant virus RSV F N116Q showed a decrease in syncytium formation compared to wild-type RSV. Although the presence of glycosylated p27 was not confirmed, changes in syncytium format *in vitro* and *in vivo* indicate that glycosylation of at least one site on p27 might have an important role in RSV biology.

3. The impact of p27 on RSV entry

RSV F on the cell surface is generally thought to be cleaved and fusogenically active (González-Reyes et al., 2001; Zimmer et al., 2001a). F0 could not be detected on the cell surface in an RSV infection model (Bolt et al., 2000). However, p27 was recently reported on the cell surface of infected cells, leading to the suggestion that uncleaved or partially cleaved F was on the cell surface (Lee et al., 2022). Krzyzaniak et al. (2013) also suggested that RSV F exists on the viral surface in a partially cleaved state (Figure 2). They detected peptides corresponding to the p27 region on purified RSV/A particles through Liquid Chromatography coupled with Mass Spectrometry (LC/MS) analysis. Western blot analysis of infected HeLa cells was consistent with cleavage at site R109 occurring before viral assembly, while cleavage at R136 occurred only after viral micropinocytosis upon viral entry (Krzyzaniak et al., 2013). However, contrary to the closely related human metapneumovirus (HMPV), RSV fusion is pH-independent, indicating that acidification of endosomes may not be required for cleavage of F, and consequently, for RSV entry (Srinivasakumar et al., 1991). The question of when both cleavage events occur has remained controversial, and additional work is needed to clarify the differing studies.

4. Insights on the impact of p27 on the F protein trimer

Fusion-competent RSV F is formed by non-covalent interactions between three disulfide-linked F1 and F2 protomers (Figures 1B–E) (McLellan et al., 2013c; Gilman et al., 2015; Krarup et al., 2015). Gilman et al. in 2015 characterized an RSV-neutralizing antibody, AM14, that recognizes cleaved, trimeric prefusion F (Gilman et al., 2015). AM14 binding was dependent on furin cleavage, either because of interference of p27 on AM14 binding through steric inhibition, or because F is unable to trimerize prior to cleavage. In the same year, a study by Krarup et al. determined that p27 destabilizes the protein trimer (Krarup et al., 2015). When incubating soluble F proteins in 0.1% SDS at room temperature, 50% of trimers without p27 were monomerized, while 97% of trimers containing p27 did (Krarup et al., 2015).

Gilman et al. evaluated stability of trimerized F using an antibody specific for soluble, prefusion F trimers (Gilman et al., 2019). The trimers of F1 + F2 heterodimers on the cell surface existed in dynamic equilibrium of associated-dissociated trimers, suggesting a "breathing" mechanism for the trimerization (Liu et al., 2008; Munro et al., 2014; Rutten et al., 2018).

5. The impact of p27 on F protein structure

The first evidence study of RSV F quaternary structure was in 2000 when Calder et al. used electron microscopy to show that F protein trimers from the RSV/A Long strain aggregated in rosette structures that were cone-like or lollipop-like rods (Calder et al., 2000). Morphological comparison between the RSV F protein and the parainfluenza 3 and 5 (PIV3 and PIV5) F protein structures indicated that cone-shaped trimers likely corresponded to a prefusion F (pre-triggered) while the lollipop-shaped trimers corresponded to a postfusion F (post-triggered) protein (Yin et al., 2005, 2006; Liljeroos et al., 2013).

Gozáles-Reyes et al. and Ruiz-Argüello et al. reported that complete enzymatic cleavage of F0 (release of p27) or partial cleavage at R136 alone (p27 remaining uncleaved from F2) led to the formation of rosettes and changes in morphology from cone to lollipop structures (González-Reyes et al., 2001; Ruiz-Argüello et al., 2002). However, Chaiwatpongsakorn et al., expressing F protein trimers from the RSV/A D53 strain, found cleavage of p27 was not the driving factor for morphological changes, but instead thermodynamic and physicochemical factors (e.g., temperature and low molarity) were the triggers (Chaiwatpongsakorn et al., 2011).

In 2011, McLellan et al. and Swanson et al. independently determined the crystal structure of the postfusion conformation of the F protein of RSV/A A2 strain. Both constructs truncated the

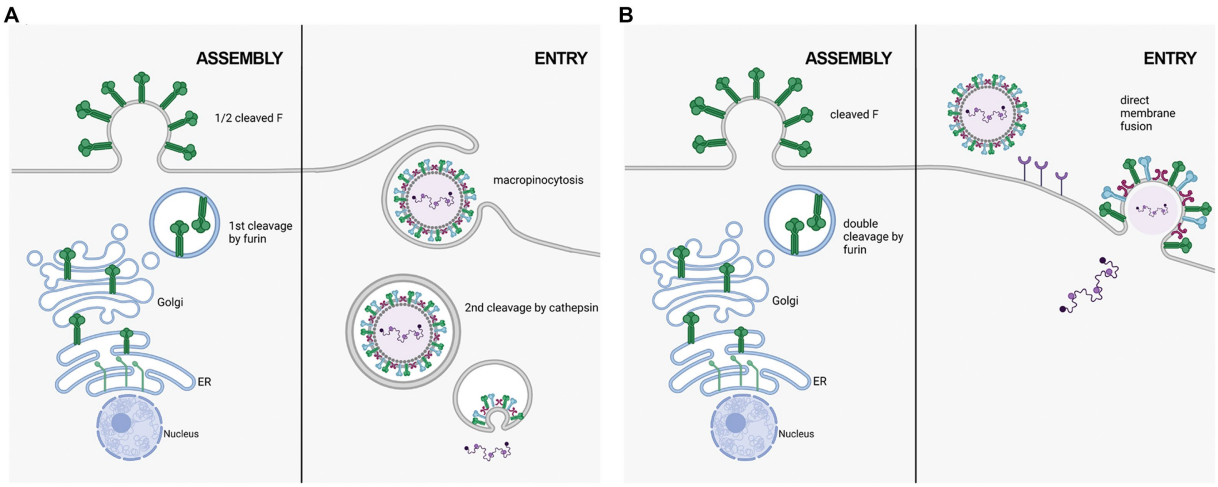

FIGURE 2
Two proposed mechanisms of RSV entry. **(A)** in the macropinocytosis method of entry, F is only cleaved at FCS1 in the trans golgi, expressing on the viral surface in a half-cleaved state. Newly synthesized virus enters host cells through macropinocytisis, allowing for FCS2 to be cleaved by cathepsin L in an endosome. This activates F, facilitating fusion with the endosomal membrane and releasing the viral genetic material into the host cell cytoplasm. **(B)** in the direct plasma membrane method of entry, F traffics through the secretory pathway to be cleaved at both FCS1 and FCS2 by furin, expressing on the viral surface in a fully cleaved state. Entry occurs through receptor binding, resulting in the fusion of the viral and host cell membranes facilitated by F.

initial portion of the fusion peptide to minimize aggregation, keeping the furin cleavage sites intact (McLellan et al., 2011; Swanson et al., 2011). Similar to parainfluenza viruses, the stalk portion of the postfusion F monomer is composed of two anti-parallel helices formed by the N- and C-terminus of the F1 subunit, juxtaposing the fusion peptide and transmembrane region. The stalk of the lollipop-shaped postfusion F is formed by a bundle of six alpha-helices, creating a thermodynamically stable structure. The absence of p27 on the postfusion structure was attributed to the complete cleavage of both furin sites during protein synthesis (Figure 1).

In 2012, Smith et al. reported the expression and purification of a near full-length F protein based on the RSV/A A2 strain (Smith et al., 2012), optimized by mutating the furin cleavage R136 (from KKRKRR136 to KKQKQQ136, cleaving F0 on R109 only) and deleting the first ten amino acids of the N-terminus of the F1 subunit. This construct generated antibodies targeting antigenic sites specific to pre- and postfusion RSV structures, including antibodies sharing the same antigenic site as Palivizumab.

McLellan et al. first published a partial structure of RSV F in the prefusion conformation in 2013 by co-crystalizing the prefusion-specific D25 antibody with a near wild-type F protein from the RSV/A A2 strain. The same group then published the structure of a prefusion construct without co-crystallizing monoclonal antibodies, named DS-Cav1 (McLellan et al., 2013a,b). The prefusion monomer structure is compact, made of two lobes (one proximal and one distal from the viral membrane) connected by two parallel beta-strands (one from F1 and one from F2) stabilized by several inter-monomer contacts. The membrane-proximal lobe from the neighboring monomer stabilizes the highly hydrophobic fusion peptide at the N-terminus of the F1 subunit. In 2015, a mutational analysis by Krarup et al. led to a model where p27 cleavage is needed to allow trimerization and fusion peptide burial in a hydrophobic cavity (Krarup et al., 2015).

The conformational change of RSV F trimers from prefusion to postfusion requires drastic rearrangements, which led Gilman et al. to study the dynamics of F in solution and on lipid membranes (Gilman et al., 2019). They observed that the prefusion trimer alternates between discrete open-and-closed states in a breathing-like motion similar to the HIV Env protein, and the same dynamics are observed on the surface of cells expressing the full-length RSV F protein. Moreover, on the surface of immortalized cell lines transfected with wild-type RSV F protein or F variants harboring a Foldon trimerization motif, the authors concluded that the F protein naturally exists in an equilibrium between monomer and trimer on cellular membranes.

To date, no structural determination method could characterize the most flexible regions of the F protein (the transmembrane domain, the cytoplasmic segment, and the p27 peptide region; Krueger et al., 2021). However, in 2021, Krueger et al., using small-angle neutron and small-angle X-ray scattering techniques (SANS and SAXS, respectively), determined the quaternary structure of prefusogenic F formulated on Polysorbate 80 nanoparticles and modeled the positioning of such regions within the trimeric structure (Krueger et al., 2021). When formulated on nanoparticles, trimeric prefusogenic F was recognized by monoclonal antibodies specific to either pre- or postfusion arrangements. Most importantly, prefusogenic F retains a partially cleaved p27, indicating that the flexibility of p27 did not destabilize the F protein trimeric arrangement. Moreover, RSV-infected cells displaying F protein trimers with partially cleaved protomers shows higher levels of surface F protein on prefusion conformation (Rezende et al., 2023); F protein trimers with detectable p27 are more thermally stable than those comprised of completely cleaved F proteins protomers (Rezende et al., 2023), although more studies are needed to evaluate the impact of p27 on RSV infectivity and replication cycle.

According to Krueger et al., in the prefusogenic structure, the p27 on the N-terminus of the F1 subunit would be solvent exposed, supporting Krarup's observation that fusion peptide+p27 would not fit in the cavity formed within the prefusion structure (Krarup et al., 2015). On the other hand, the partially cleaved RSV F proteins can form trimers without the assistance of a Foldon trimerization motif (Krueger et al., 2021).

6. Humoral and mucosal immune response to p27 during natural infection

In 2016, Fuentes et al. published the first report demonstrating an immune response to p27 upon natural RSV infection (Fuentes et al., 2016). Looking at sera from five infants before and after their first RSV infection, the authors identified new antigenic sites using whole-genome-phage display libraries (GFPDL) encoding peptides covering the length of F. One new antigenic site mapped to p27. The authors then synthesized peptides covering the p27 region and surveyed serum samples from a cohort of children (<2 years old), adolescents (10–14 years old), and adults (30–45 years old) using Surface Plasmon Resonance (SPR). Although p27-binding antibodies were identified in all age groups, reactivity was higher in children than adolescents and lowest in adults. The authors suggested the immune response to p27 came from an uncleaved F0 precursor, present in immature virions and dying infected cells. Based on the work from Tapia et al., the immune pressure caused by the high mutation rate in the p27 region may be the driver for a high antibody response to p27 (Tapia et al., 2014).

Humoral and mucosal immunity to p27 was found in RSV infected hematopoietic cell transplant (HCT) recipients (Fuentes et al., 2019). Fuentes et al. again used GFPDL and SPR to examine blood serum and nasal washes of 11 HCT patients infected with RSV/A who stopped shedding the virus in less than 14 days (early recovery) or over 14 days (late recovery). Both groups developed antibodies recognizing p27. However, early-recovered patients generated mucosal antibodies with higher binding to p27 than late-recovered patients.

Leemans et al. evaluated the immune response to recombinant F proteins lacking glycosylation on N116 or N126. BALB/c mice immunized with plasmids encoding F N116Q generated an enhanced neutralizing antibody response compared to the control (Leemans et al., 2018). Immunization of BALB/c mice with a recombinant infectious RSV harboring the N116Q mutation (Leemans et al., 2019) generated higher neutralizing antibody titers compared to the wild-type RSV F virus.

Ye et al. quantified the amount of IgG, IgA, and p27-like antibodies (P27LA, natural antibodies capable of competing with a monoclonal anti-p27) in serum and nasal washes of 33 HCT patients during (acute) and post (convalescent) RSV infection (Ye et al., 2020). Anti-p27 IgG and IgA concentrations in both serum and nasal wash samples were about 1,000-fold lower than other F-specific sites (Ye et al., 2018, 2019). P27LA also showed a 1,000-fold lower concentration level than the correlate of immunity PCA (Palivizumab Competitive Antibody; Ye et al., 2018, 2019). Anti-p27 antibodies did not appear to improve the overall neutralizing antibody activity against RSV. However, a reduction in antibody concentration in nasal wash samples from convalescent HCT patients suggests that mucosal anti-p27 antibodies bind to either released viruses or virus-infected epithelial cells, aiding in controlling respiratory tract infection.

In 2019, Patel et al. demonstrated that prefusogenic F protein formulated in nanoparticles is recognized by pre-F specific monoclonal antibodies (antigenic sites Ø and VIII – also called V) and by monoclonal antibodies targeting antigenic sites shared between pre-F and post-F conformations (sites II and IV; Patel et al., 2019). The prefusogenic F protein also elicited significant levels of functional neutralizing antibodies and competitive antibodies to antigenic sites Ø, VIII, II, IV, and p27 in a challenge cotton rat model, preventing viral replication in the lungs with no significant histopathology. The prefusogenic nanoparticle formulation was further developed into a vaccine candidate for maternal immunization, eliciting a strong, broad antibody response and neutralizing antibody activity. It was the first RSV vaccine candidate targeting protection of newborns by vaccinating pregnant individuals during late gestation showing efficient antibody transplacental transfer [reviewed elsewhere (Blunck et al., 2021)].

Blunck et al. (2022) reported the kinetics of immunity to p27 in healthy adults under age 65, naturally infected with RSV/A or RSV/B during the 2018–2019 RSV season. The cohort of 19 subjects was divided into uninfected, acutely infected, and recently infected individuals based on levels of neutralizing antibody titers. As observed in HCT patients, all subjects presented detectable anti-p27 IgG and IgA levels. Throughout the study, uninfected individuals maintained constant levels of serum IgG anti-p27, while acutely infected and recently infected individuals experienced an increase and decrease in anti-p27 antibodies, respectively. However, p27 was not an immunodominant epitope in this cohort of healthy adults.

7. p27 *in vitro* and *in vivo*: first evidence of p27 detection on the surface of infected cells and histopathology sections

To better understand the protective antigenic sites within F, Lee et al. (2022) chemically synthesized peptides spanning the entire F protein. BALB/c mice were vaccinated with these peptides and challenged intranasally with RSV/A A2 strain. At 5 days post-challenge, mice immunized with the p27 region had significantly lower lung viral titers and pathology scores compared to mock-vaccinated mice (Lee et al., 2022), suggesting that p27 may elicit a protective immune response; however, the protective effect is unlikely due to neutralizing antibody activity. The authors instead speculate that p27 may induce antibody-dependent cell cytotoxicity (ADCC) and T cell-mediated effector functions.

Additionally, lung tissues immunostained with anti-F-p27 antisera showed p27 surface expression post-infection. A549 cells infected with RSV/A A2 showed comparable surface staining, confirming p27 surface expression *in vitro* (Lee et al., 2022). The authors attribute this to the expression of F0 on the surface of infected cells, consistent with the results seen in 2013 by Krzyzaniak et al. (2013). However, other studies have determined that F0 is inefficient in reaching or unable to reach the cell surface (Collins and Mottett, 1991; Bolt et al., 2000; Sugrue et al., 2001). A mechanistic understanding of how p27 is expressed on the cell surface has yet to be uncovered.

8. Gaps in knowledge and future directions

Important work in electron microscopy, crystallography, and structure modeling over the past 20 years has increased our understanding of the RSV F protein structure; however, the biological roles and fate of p27 remain elusive.

Cleavage of p27 is not a requirement for cellular transport, as the F protein can exist in a heterogenous population of uncleaved, partially cleaved, and fully cleaved F proteins on the cell surface (San-Juan-Vergara et al., 2012; Krzyzaniak et al., 2013; Lee et al., 2022). However, it is unknown if the fully cleaved p27 is secreted as free peptide or if it has an intracellular role that improves viral fitness. In addition, although the F protein sequence is well-conserved between RSV subtypes and genotypes, the p27 region is variable (Hause et al., 2017); therefore, future studies that address such sequence differences may shed light on F protein structure, entry mechanism, and infectivity (Fuentes et al., 2016).

It is unclear if complete cleavage of the F protein is required for trimerization of F1 + F2 heterodimers, although it is accepted that a partially cleaved p27 within the F protein cavity would disrupt the trimerization (Krarup et al., 2015). On the other hand, the "breathing" motion of the F protein trimer and models of prefusogenic F trimer indicate that the RSV F protein could trimerize while harboring a partially cleaved p27 (Gilman et al., 2019).

While immunological data showed that p27 elicits serum antibody responses in RSV-infected individuals of all ages, the lackluster neutralizing activity of anti-p27 IgG antibodies raises the possibility that protection might come from ADCC or other cell-mediated immune mechanisms, and this deserves further investigation (Blunck et al., 2022). Likewise, the role of mucosal anti-p27 IgA antibodies in viral clearance requires additional studies. Lastly, the humoral and mucosal immune responses to p27 might be potentially powerful biomarkers of RSV infection.

Author contributions

WR and HN participated in the writing and preparation of the manuscript. RD and PP reviewed and approved it for publication. All authors contributed to the article and approved the submitted version.

Funding

Discretionary funds: PP. The authors also acknowledge supplemental funding provided by Baylor Research Advocates for Student Scientists (BRASS) to WR.

Conflict of interest

The authors declare that the research was conducted in the absence of any commercial or financial relationships that could be construed as a potential conflict of interest.

Publisher's note

References

Amarasinghe, G. K., Ayllón, M. A., Bào, Y., Basler, C. F., Bavari, S., Blasdell, K. R., et al. (2019). Taxonomy of the order Mononegavirales: update 2019. *Arch. Virol.* 164, 1967–1980. doi: 10.1007/s00705-019-04247-4

Basak, A., Zhong, M., Munzer, J. S., Chrétien, M., and Seidah, N. G. (2001). Implication of the proprotein convertases furin, PC5 and PC7 in the cleavage of surface glycoproteins of Hong Kong, Ebola and respiratory syncytial viruses: a comparative analysis with fluorogenic peptides. *Biochem. J.* 353, 537–545. doi: 10.1042/0264-6021:3530537

Beyene, A., Basu, A., Meyer, K., and Ray, R. (2004). Influence of N-linked glycans on intracellular transport of hepatitis C virus E1 chimeric glycoprotein and its role in pseudotype virus infectivity. *Virology* 324, 273–285. doi: 10.1016/j.virol.2004.03.039

Blunck, B. N., Aideyan, L., Ye, X., Avadhanula, V., Ferlic-Stark, L., Zechiedrich, L., et al. (2022). Antibody responses of healthy adults to the p27 peptide of respiratory syncytial virus fusion protein. *Vaccine* 40, 536–543. doi: 10.1016/j.vaccine.2021.11.087

Blunck, B. N., Rezende, W., and Piedra, P. A. (2021). Profile of respiratory syncytial virus prefusogenic fusion protein nanoparticle vaccine. *Expert Rev. Vaccines* 20, 351–364. doi: 10.1080/14760584.2021.1903877

Bolt, G., Pedersen, L. Ø., and Birkeslund, H. H. (2000). Cleavage of the respiratory syncytial virus fusion protein is required for its surface expression: role of furin. *Virus Res.* 68, 25–33. doi: 10.1016/S0168-1702(00)00149-0

Calder, L. J., González-Reyes, L., García-Barreno, B., Wharton, S. A., Skehel, J. J., Wiley, D. C., et al. (2000). Electron microscopy of the human respiratory syncytial virus fusion protein and complexes that it forms with monoclonal antibodies. *Virology* 271, 122–131. doi: 10.1006/viro.2000.0279

Chaiwatpongsakorn, S., Epand, R. F., Collins, P. L., Epand, R. M., and Peeples, M. E. (2011). Soluble respiratory syncytial virus fusion protein in the fully cleaved, Pretriggered state is triggered by exposure to low-molarity buffer. *J. Virol.* 85, 3968–3977. doi: 10.1128/JVI.01813-10

Collins, P. L., Huang, Y. T., and Wertz, G. W. (1984). Nucleotide sequence of the gene encoding the fusion (F) glycoprotein of human respiratory syncytial virus. *Proc. Natl. Acad. Sci. U. S. A.* 81, 7683–7687. doi: 10.1073/pnas.81.24.7683

Collins, P. L., and Mottett, G. (1991). Post-translational processing and oligomerization of the fusion glycoprotein of human respiratory syncytial virus. *J. Gen. Virol.* 72, 3095–3101. doi: 10.1099/0022-1317-72-12-3095

Day, N. D., Branigan, P. J., Liu, C., Gutshall, L. L., Luo, J., Melero, J. A., et al. (2006). Contribution of cysteine residues in the extracellular domain of the F protein of human respiratory syncytial virus to its function. *Virol. J.* 3, 1–11. doi: 10.1186/1743-422X-3-34

Elango, N., Satake, M., Coligan, J. E., Norrby, E., Camargo, E., and Venkatesan, S. (1985). Nucleic acids research Respiratory syncytial virus fusion glycoprotein: Nucleotide sequence of mRNA, identification of cleavage activation site and amino acid sequence of N-terminus of F1 subunit. *Nucleic. Acids Res.* 13, 1559–1574. doi: 10.1093/nar/13.5.1559

Ellgaard, L., McCaul, N., Chatsisvili, A., and Braakman, I. (2016). Co- and post-translational protein folding in the ER. *Traffic* 17, 615–638. doi: 10.1111/tra.12392

Fuentes, S., Coyle, E. M., Beeler, J., Golding, H., and Khurana, S. (2016). Antigenic fingerprinting following primary RSV infection in young children identifies novel antigenic sites and reveals unlinked evolution of human antibody repertoires to fusion and attachment glycoproteins. *PLoS Pathog.* 12, 1–24. doi: 10.1371/journal.ppat.1005554

Fuentes, S., Hahn, M., Chilcote, K., Chemaly, R. F., Shah, D. P., Ye, X., et al. (2019). Antigenic fingerprinting of respiratory syncytial virus (RSV)-A–infected hematopoietic cell transplant recipients reveals importance of mucosal anti–RSV G antibodies in control of RSV infection in humans. *J. Infect. Dis.* 221, 636–646. doi: 10.1093/infdis/jiz608

Fuentes, S., Tran, K. C., Luthra, P., Teng, M. N., and He, B. (2007). Function of the respiratory syncytial virus small hydrophobic protein. *J. Virol.* 81, 8361–8366. doi: 10.1128/JVI.02717-06

Gan, S.-W., Tan, E., Lin, X., Yu, D., Wang, J., Ming-Yeong Tan, G., et al. (2012). The small hydrophobic protein of the human respiratory syncytial virus forms Pentameric ion channels. *J. Biol. Chem.* 287, 24671–24689. doi: 10.1074/jbc.M111.332791

Gilman, M. S. A., Furmanova-Hollenstein, P., Pascual, G., van 't Wout, A. B., Langedijk, J. P. M., and McLellan, J. S. (2019). Transient opening of trimeric prefusion RSV F proteins. *Nat. Commun.* 10:2105. doi: 10.1038/s41467-019-09807-5

Gilman, M. S. A., Moin, S. M., Mas, V., Chen, M., Patel, N. K., Kramer, K., et al. (2015). Characterization of a Prefusion-specific antibody that recognizes a quaternary, cleavage-dependent epitope on the RSV fusion glycoprotein. *PLoS Pathog* 11:e1005035. doi: 10.1371/journal.ppat.1005035

González-Reyes, L., Begoñ, A., Ruiz-Argü Ello, M., García-Barreno, B., Calder, L., Ló Pez, J. A., et al. (2001). Cleavage of the human respiratory syncytial virus fusion protein at two distinct sites is required for activation of membrane fusion. *Proc. Natl. Acad. Sci. U S A* 98, 9859–9864. doi: 10.1073/pnas.151098198

Hause, A. M., Henke, D. M., Avadhanula, V., Shaw, C. A., Tapia, L. I., and Piedra, P. A. (2017). Sequence variability of the respiratory syncytial virus (RSV) fusion gene among contemporary and historical genotypes of RSV/a and RSV/B. *PLoS One* 12:e0175792. doi: 10.1371/journal.pone.0175792

Kimura, H., Nagasawa, K., Kimura, R., Tsukagoshi, H., Matsushima, Y., Fujita, K., et al. (2017). Molecular evolution of the fusion protein (F) gene in human respiratory syncytial virus subgroup B. *Infect. Genet. Evol.* 52, 1–9. doi: 10.1016/j.meegid.2017.04.015

King, A., Adams, M., Carstens, E., and Lefkowitz, E. (2012). Part II-the negative sense single stranded RNA viruses virus taxonomy: Ninth Report of the International Committee on Taxonomy of Viruses Family Paramyxoviridae.

Klink, H. A., Brady, R. P., Topliff, C. L., Eskridge, K. M., Srikumaran, S., and Kelling, C. L. (2006). Influence of bovine respiratory syncytial virus F glycoprotein N-linked glycans on in vitro expression and on antibody responses in BALB/c mice. *Vaccine* 24, 3388–3395. doi: 10.1016/j.vaccine.2005.12.067

Krarup, A., Truan, D., Furmanova-Hollenstein, P., Bogaert, L., Bouchier, P., Bisschop, I. J. M., et al. (2015). A highly stable prefusion RSV F vaccine derived from structural analysis of the fusion mechanism. *Nat. Commun.* 6:8143. doi: 10.1038/ncomms9143

Krueger, S., Curtis, J. E., Scott, D. R., Grishaev, A., Glenn, G., Smith, G., et al. (2021). Structural characterization and Modeling of a respiratory syncytial virus fusion glycoprotein nanoparticle vaccine in solution. *Mol. Pharm.* 18, 359–376. doi: 10.1021/acs.molpharmaceut.0c00986

Krzyzaniak, M. A., Zumstein, M. T., Gerez, J. A., Picotti, P., and Helenius, A. (2013). Host cell entry of respiratory syncytial virus involves macropinocytosis followed by proteolytic activation of the F protein. *PLoS Pathog.* 9:e1003309. doi: 10.1371/journal.ppat.1003309

Lee, J., Lee, Y., Klenow, L., Coyle, E. M., Tang, J., Ravichandran, S., et al. (2022). Protective antigenic sites identified in respiratory syncytial virus fusion protein reveals importance of p27 domain. *EMBO Mol. Med.* 14, 1–14. doi: 10.15252/emmm.202013847

Leemans, A., Boeren, M., Van der Gucht, W., Martinet, W., Caljon, G., Maes, L., et al. (2019). Characterization of the role of N-glycosylation sites in the respiratory syncytial virus fusion protein in virus replication, syncytium formation and antigenicity. *Virus Res.* 266, 58–68. doi: 10.1016/j.virusres.2019.04.006

Leemans, A., Boeren, M., Van der Gucht, W., Pintelon, I., Roose, K., Schepens, B., et al. (2018). Removal of the N-glycosylation sequon at position N116 located in p27 of the respiratory syncytial virus fusion protein elicits enhanced antibody responses after DNA immunization. *Viruses* 10:426. doi: 10.3390/v10080426

Liljeroos, L., Krzyzaniak, M. A., Helenius, A., and Butcher, S. J. (2013). Architecture of respiratory syncytial virus revealed by electron cryotomography. *Proc. Natl. Acad. Sci.* 110, 11133–11138. doi: 10.1073/pnas.1309070110

Liu, J., Bartesaghi, A., Borgnia, M. J., Sapiro, G., and Subramaniam, S. (2008). Molecular architecture of native HIV-1 gp120 trimers. *Nature* 455, 109–113. doi: 10.1038/nature07159

Masante, C., El Najjar, F., Chang, A., Jones, A., Moncman, C. L., and Dutch, R. E. (2014). The human Metapneumovirus small hydrophobic protein has properties consistent with those of a Viroporin and can modulate viral Fusogenic activity. *J. Virol.* 88, 6423–6433. doi: 10.1128/JVI.02848-13

McLaughlin, J. M., Khan, F., Schmitt, H. J., Agosti, Y., Jodar, L., Simoes, E. A. F., et al. (2022). Respiratory syncytial virus-associated hospitalization rates among US infants: a systematic review and meta-analysis. *J. Infect. Dis.* 225, 1100–1111. doi: 10.1093/infdis/jiaa752

McLellan, J. S., Chen, M., Joyce, M. G., Sastry, M., Stewart-Jones, G. B. E., Yang, Y., et al. (2013a). Structure-based design of a fusion glycoprotein vaccine for respiratory syncytial virus. *Science* 342, 592–598. doi: 10.1126/science.1243283

McLellan, J. S., Chen, M., Leung, S., Graepel, K. W., Du, X., Yang, Y., et al. (2013b). Structure of RSV fusion glycoprotein trimer bound to a prefusion-specific neutralizing antibody. *Science* 340, 1113–1117. doi: 10.1126/science.1234914

McLellan, J. S., Ray, W. C., and Peeples, M. E. (2013c). Structure and Function of Respiratory Syncytial Virus Surface Glycoproteins. *Curr. Top. Microbiol. Immunol.* 83–104. doi: 10.1007/978-3-642-38919-1_4

McLellan, J. S., Yang, Y., Graham, B. S., and Kwong, P. D. (2011). Structure of respiratory syncytial virus fusion glycoprotein in the Postfusion conformation reveals preservation of neutralizing epitopes. *J. Virol.* 85, 7788–7796. doi: 10.1128/JVI.00555-11

Munro, J. B., Gorman, J., Ma, X., Zhou, Z., Arthos, J., Burton, D. R., et al. (2014). Conformational dynamics of single HIV-1 envelope trimers on the surface of native virions. *Science* 346, 759–763. doi: 10.1126/science.1254426

Pandya, M., Callahan, S., Savchenko, K., and Stobart, C. (2019). A contemporary view of respiratory syncytial virus (RSV) biology and strain-specific differences. *Pathogens* 8:67. doi: 10.3390/pathogens8020067

Patel, N., Massare, M. J., Tian, J. H., Guebre-Xabier, M., Lu, H., Zhou, H., et al. (2019). Respiratory syncytial virus prefusogenic fusion (F) protein nanoparticle vaccine: structure, antigenic profile, immunogenicity, and protection. *Vaccine* 37, 6112–6124. doi: 10.1016/j.vaccine.2019.07.089

Rajan, A., Piedra, F.-A., Aideyan, L., McBride, T., Robertson, M., Johnson, H. L., et al. (2022). Multiple respiratory syncytial virus (RSV) strains infecting HEp-2 and A549 cells reveal cell line-dependent differences in resistance to RSV infection. *J. Virol.* 96:e0190421. doi: 10.1128/jvi.01904-21

Rawling, J., Cano, O., Garcin, D., Kolakofsky, D., and Melero, J. A. (2011). Recombinant Sendai viruses expressing fusion proteins with two Furin cleavage sites mimic the syncytial and receptor-independent infection properties of respiratory syncytial virus. *J. Virol.* 85, 2771–2780. doi: 10.1128/JVI.02065-10

Rezende, W., Ye, X., Angelo, L. S., Carisey, A. F., Avadhanula, V., and Piedra, P. A. (2023). The efficiency of p27 cleavage during in vitro respiratory syncytial virus (RSV) infection is cell line and RSV subtype dependent. *J. Virol.* 97:e0025423. doi: 10.1128/jvi.00254-23

Rha, B., Curns, A. T., Lively, J. Y., Campbell, A. P., Englund, J. A., Boom, J. A., et al. (2020). Respiratory syncytial virus-associated hospitalizations among young children: 2015–2016. *Pediatrics* 146:e20193611. doi: 10.1542/peds.2019-3611

Ruiz-Argüello, M. B., González-Reyes, L., Calder, L. J., Palomo, C., Martín, D., Saíz, M. J., et al. (2002). Effect of proteolytic processing at two distinct sites on shape and aggregation of an anchorless fusion protein of human respiratory syncytial virus and fate of the intervening segment. *Virology* 298, 317–326. doi: 10.1006/viro.2002.1497

Rutten, L., Lai, Y. T., Blokland, S., Truan, D., Bisschop, I. J. M., Strokappe, N. M., et al. (2018). A universal approach to optimize the folding and stability of Prefusion-closed HIV-1 envelope trimers. *Cell Rep.* 23, 584–595. doi: 10.1016/j.celrep.2018.03.061

San-Juan-Vergara, H., Sampayo-Escobar, V., Reyes, N., Cha, B., Pacheco-Lugo, L., Wong, T., et al. (2012). Cholesterol-rich microdomains as docking platforms for respiratory syncytial virus in Normal human bronchial epithelial cells. *J. Virol.* 86, 1832–1843. doi: 10.1128/JVI.06274-11

Smith, E. C., Popa, A., Chang, A., Masante, C., and Dutch, R. E. (2009). Viral entry mechanisms: the increasing diversity of paramyxovirus entry. *FEBS J.* 276, 7217–7227. doi: 10.1111/j.1742-4658.2009.07401.x

Smith, G., Raghunandan, R., Wu, Y., Liu, Y., Massare, M., Nathan, M., et al. (2012). Respiratory syncytial virus fusion glycoprotein expressed in insect cells form protein nanoparticles that induce protective immunity in cotton rats. *PLoS One* 7:e50852. doi: 10.1371/journal.pone.0050852

Srinivasakumar, N., Ogra, P. L., and Flanagan', T. D. (1991). Characteristics of fusion of respiratory syncytial virus with HEp-2 cells as measured by R18 fluorescence Dequenching assay. *J. Virol.* 65, 4063–4069. doi: 10.1128/jvi.65.8.4063-4069.1991

Sugrue, R. J., Brown, C., Brown, G., Aitken, J., and McL Rixon, H. W. (2001). Furin cleavage of the respiratory syncytial virus fusion protein is not a requirement for its transport to the surface of virus-infected cells. *J. Gen. Virol.* 82, 1375–1386. doi: 10.1099/0022-1317-82-6-1375

Swanson, K. A., Settembre, E. C., Shaw, C. A., Dey, A. K., Rappuoli, R., Mandl, C. W., et al. (2011). Structural basis for immunization with postfusion respiratory syncytial virus fusion F glycoprotein (RSV F) to elicit high neutralizing antibody titers. *Proc. Natl. Acad. Sci.* 108, 9619–9624. doi: 10.1073/pnas.1106536108

Tan, L., Lemey, P., Houspie, L., Viveen, M. C., and Jansen, N. J. G. (2012). Genetic variability among complete human respiratory syncytial virus subgroup a genomes: bridging molecular evolutionary dynamics and epidemiology. *PLoS One* 7:51439. doi: 10.1371/journal.pone.0051439

Tapia, L. I., Shaw, C. A., Aideyan, L. O., Jewell, A. M., Dawson, B. C., Haq, T. R., et al. (2014). Gene sequence variability of the three surface proteins of human respiratory syncytial virus (HRSV) in Texas. *PLoS One* 9:e90786. doi: 10.1371/journal.pone.0090786

Techaarpornkul, S., Barretto, N., and Peeples, M. E. (2001). Functional analysis of recombinant respiratory syncytial virus deletion mutants lacking the small hydrophobic and/or attachment glycoprotein gene. *J. Virol.* 75, 6825–6834. doi: 10.1128/JVI.75.15.6825-6834.2001

Vigerust, D. J., and Shepherd, V. L. (2007). Virus glycosylation: role in virulence and immune interactions. *Trends Microbiol.* 15, 211–218. doi: 10.1016/j.tim.2007.03.003

Ye, X., de Rezende, W. C., Iwuchukwu, O. P., Avadhanula, V., Ferlic-Stark, L. L., Patel, K. D., et al. (2020). Antibody response to the furin cleavable twenty-seven amino acid peptide (P27) of the fusion protein in respiratory syncytial virus (RSV) infected adult hematopoietic cell transplant (HCT) recipients. *Vaccines (Basel)* 8:192. doi: 10.3390/vaccines8020192

Ye, X., Iwuchukwu, O. P., Avadhanula, V., Aideyan, L. O., McBride, T. J., Ferlic-Stark, L. L., et al. (2018). Comparison of Palivizumab-like antibody binding to different conformations of the RSV F protein in RSV-infected adult hematopoietic cell transplant recipients. *J. Infect. Dis.* 217, 1247–1256. doi: 10.1093/infdis/jiy026

Ye, X., Iwuchukwu, O. P., Avadhanula, V., Aideyan, L. O., McBride, T. J., Ferlic-Stark, L. L., et al. (2019). Antigenic site-specific competitive antibody responses to the fusion protein of respiratory syncytial virus were associated with viral clearance in hematopoietic cell transplantation adults. *Front. Immunol.* 10:706. doi: 10.3389/fimmu.2019.00706

Yin, H.-S., Paterson, R. G., Wen, X., Lamb, R. A., and Jardetzky, T. S. (2005). Structure of the uncleaved ectodomain of the paramyxovirus (hPIV3) fusion protein. *PNAS* 102, 9288–9293. doi: 10.1073/pnas.0503989102

Yin, H. S., Wen, X., Paterson, R. G., Lamb, R. A., and Jardetzky, T. S. (2006). Structure of the parainfluenza virus 5 F protein in its metastable, prefusion conformation. *Nat. Cell Biol.* 439, 38–44. doi: 10.1038/nature04322

Zimmer, G., Budz, L., and Herrler, G. (2001a). Proteolytic activation of respiratory syncytial virus fusion protein. *J. Biol. Chem.* 276, 31642–31650. doi: 10.1074/jbc.M102633200

Zimmer, G., Conzelmann, K.-K., and Herrler, G. (2002). Cleavage at the Furin consensus sequence RAR/KR 109 and presence of the intervening peptide of the respiratory syncytial virus fusion protein are dispensable for svirus replication in cell culture. *J. Virol.* 76, 9218–9224. doi: 10.1128/JVI.76.18.9218-9224.2002

Zimmer, G., Trotz, I., and Herrler, G. (2001b). N-Glycans of F protein differentially affect fusion activity of human respiratory syncytial virus. *J. Virol.* 75, 4744–4751. doi: 10.1128/JVI.75.10.4744-4751.2001

frontiers | Frontiers in Microbiology

TYPE Original Research
PUBLISHED 22 June 2023
DOI 10.3389/fmicb.2023.1196451

OPEN ACCESS

EDITED BY
Shijian Zhang,
Dana–Farber Cancer Institute, United States

REVIEWED BY
Hao Hu,
Washington University in St. Louis, United States
Jing Yang,
Tongji University, China

*CORRESPONDENCE
Boyan Jiao
✉ j198319831983@126.com

†These authors have contributed equally to this work

RECEIVED 29 March 2023
ACCEPTED 02 May 2023
PUBLISHED 22 June 2023

CITATION
Li L, Liu T, Wang Q, Ding Y, Jiang Y, Wu Z, Wang X, Dou H, Jia Y and Jiao B (2023) Genetic characterization and whole-genome sequencing-based genetic analysis of influenza virus in Jining City during 2021–2022. *Front. Microbiol.* 14:1196451. doi: 10.3389/fmicb.2023.1196451

Genetic characterization and whole-genome sequencing-based genetic analysis of influenza virus in Jining City during 2021–2022

Libo Li[1†], Tiantian Liu[1†], Qingchuan Wang[2], Yi Ding[1], Yajuan Jiang[1], Zengding Wu[3], Xiaoyu Wang[1], Huixin Dou[1], Yongjian Jia[1] and Boyan Jiao[1*]

[1]Department of Laboratory, Jining Center for Disease Control and Prevention, Jining, China, [2]Department of Medicine, Jining Municipal Government Hospital, Jining, China, [3]Department of AI and Bioinformatics, Nanjing Chengshi BioTech (TheraRNA) Co., Ltd., Nanjing, China

Background: The influenza virus poses a significant threat to global public health due to its high mutation rate. Continuous surveillance, development of new vaccines, and public health measures are crucial in managing and mitigating the impact of influenza outbreaks.

Methods: Nasal swabs were collected from individuals with influenza-like symptoms in Jining City during 2021-2022. Reverse transcription-quantitative polymerase chain reaction (RT-qPCR) was used to detect influenza A viruses, followed by isolation using MDCK cells. Additionally, nucleic acid detection was performed to identify influenza A H1N1, seasonal H3N2, B/Victoria, and B/Yamagata strains. Whole-genome sequencing was conducted on 24 influenza virus strains, and subsequent analyses included characterization, phylogenetic construction, mutation analysis, and assessment of nucleotide diversity.

Results: A total of 1,543 throat swab samples were collected. The study revealed the dominance of the B/Victoria influenza virus in Jining during 2021-2022. Whole-genome sequencing showed co-prevalence of B/Victoria influenza viruses in the branches of Victoria clade 1A.3a.1 and Victoria clade 1A.3a.2, with a higher incidence observed in winter and spring. Comparative analysis demonstrated lower similarity in the HA, MP, and PB2 gene segments of the 24 sequenced influenza virus strains compared to the Northern Hemisphere vaccine strain B/Washington/02/2019. Mutations were identified in all antigenic epitopes of the HA protein at R133G, N150K, and N197D, and the 17-sequence antigenic epitopes exhibited more than 4 amino acid variation sites, resulting in antigenic drift. Moreover, one sequence had a D197N mutation in the NA protein, while seven sequences had a K338R mutation in the PA protein.

Conclusion: This study highlights the predominant presence of B/Victoria influenza strain in Jining from 2021 to 2022. The analysis also identified amino acid site variations in the antigenic epitopes, contributing to antigenic drift.

KEYWORDS

influenza virus, whole-genome sequencing, mutation, genome characterization, Jining City

1. Introduction

The influenza virus is a common pathogen in the human respiratory tract, causing approximately 290,000 to 650,000 deaths each year. It is considered one of the major public health problems worldwide (Chavez and Hai, 2021; Tyrrell et al., 2021). Influenza virus is a single positive-stranded RNA virus, which is further divided into four types: type A, type B, type C, and type D

based on the antigenicity of nucleoprotein and matrix protein (Carascal et al., 2022). Influenza A and B viruses are the primary cause of illness in humans. Influenza A viruses are divided into subtypes based on the antigenicity of hemagglutinin (HA) and neuraminidase (NA). HA is divided into 18 subtypes, while NA is divided into 11 subtypes (Duraes-Carvalho and Salemi, 2018). In contrast, the influenza B virus has only one subtype, which is further divided into two lineages: Victoria lineage and Yamagata lineage based on the antigenic characteristics and HA sequence of influenza B (Hay et al., 2001; Toure et al., 2022).

Both influenza A and B viruses are composed of eight segments of the gene, including haemagglutinin (HA), neuraminidase (NA), matrix protein (MP), nucleoprotein (NP), nonstructural (NS), polymerase acidic (PA), polymerase basic 1 (PB1), and polymerase basic 2 (PB2) genes. These gene segments between different types can undergo genetic recombination (Zhu et al., 2013; Liang et al., 2022). Among these segments, the HA protein of influenza virus is a major surface antigen prone to mutation, which can cause antigenic changes that help the virus evade host immunity and cause influenza outbreaks (Liu et al., 2018; Wu and Wilson, 2020). Currently, the seasonal influenza virus pathogens that infect humans are mainly influenza A H1N1 influenza virus, seasonal influenza A H3N2 subtype virus, B Victoria series influenza virus, and B Yamagata series influenza virus (Wu and Wilson, 2020). These four influenza viruses alternate in prevalence during different years (Liu et al., 2022).

The influenza virus can cause fever, cough, sore throat, pneumonia, and even death, and the general population is susceptible. Vaccination is an effective method to prevent influenza. However, the influenza virus is prone to mutation, undergoes antigenic drift, and produces immune escape. Both NA and PA inhibitors are specific drugs for treating influenza; however, with the continuous use of drugs, the virus may develop drug-resistant mutations, which reduces the therapeutic effectiveness of the drugs.

Influenza is highly prevalent during the winter and spring months in northern China, and monitoring typically occurs from April to March of the following year (Liu et al., 2022). Jining, being one of the most densely populated cities in northern China, the threat of seasonal flu outbreaks in this region should not be underestimated. In this study, we analyzed the epidemic patterns and genome-wide characteristics of the influenza virus monitored in Jining City from 2021 to 2022. Our goal was to gain insight into the epidemic characteristics of the influenza virus and the evolutionary trends of circulating strains in order to improve outbreak prevention strategies.

2. Materials and methods

2.1. Specimens collection

According to the requirements of the National Influenza Center of China, between 1 April 2021 and 31 March 2022, throat swab specimens for influenza-like illness (ILI) (body temperature ≥ 38°C, with either cough or sore throat) were collected at Jining First People's Hospital and Rencheng District Maternal and Child Health Planning Service Center. A minimum of 10 samples were collected each week from April 2021 to September 2021, and a minimum of 20 samples were collected each week from October 2021 to March 2022, resulting in a total of 1,543 samples. The collected specimens were immediately stored at 2–8°C and transferred to the Influenza Surveillance Network Laboratory of Jining Center for Disease Control and Prevention within 24 h for testing.

2.2. Laboratory testing

A volume of 200 μl throat swab sample was taken, and the automatic nucleic acid extraction instrument (GeneRotex 96) of Xi'an Tianlong Technology Co., Ltd. and the virus nucleic acid extraction reagent (T138) of Xi'an Tianlong Technology Co., Ltd. for nucleic acid extraction were used. Also, Guangzhou Daan Biotechnology Co., Ltd. Type A H1N1 (DS0042), Seasonal H3N2 (DS0091), B/Victoria series (D0970), and B/Yamagata series (D0960) influenza virus nucleic acid detection kit (PCR-fluorescent probe method) were used for nucleic acid detection.

2.3. Influenza virus culture

Madin–Darby canine kidney (MDCK) cells were cultured in DMEM (GIBCO 11995–065) medium with 10% FBS (GIBCO 16000–044) at 37°C. After the cells reached 90% confluence, the culture medium was discarded and washed with 5-ml PBS for three times. Then, 1 ml of a throat swab sample with positive influenza virus was inoculated; incubated at 35°C for 1 h; discarded the throat swab sample; added 5 mL of DMEM (containing 2 μg/mL TPCK-trypsin, 100 U/ml penicillin, and 100 μg/ml chain tetracycline), and incubated at 35°C. After 3–4 days, the cells were frozen–thawed three times, and 1% red blood cells were used to measure the HA titer of influenza virus strains. Twenty-four influenza virus strains with virus titer ≥1:8 was isolated, and the strain numbers were as follows: B/shandongrencheng/11484, 11,485, 11,486, 11,487, 11,488, 11,494, 11,495, 11,499, 11,504, 11,506/2021; B/shandongrencheng/1115, 1,122, 1,125, 1,126, 1,127, 1,128, 1,169, 1,176, 1,210, 1,211, 1,252, 1,291, 1,354, 1,356/2022. Sampling dates for the 24 strains were 5 November 2021 (5 strains), 5 December 2021 (5 strains), 6 January 2022 (6 strains), 5 February 2022 (5 strains), and 3 March 2022 (3 strains). Of the 24 strains, 16 strains were isolated from the male patients and 8 strains were isolated from the female patients. Age distribution was as follows: 1 patient aged 0–5 years, 8 patients aged 6–15 years, 6 patients aged 16–25 years, 8 patients aged 26–60 years, and 1 patient aged above 61 years.

2.4. Whole-genome sequencing

Influenza virus gene capture using Beijing Micro Future's ULSENTM® Ultra-Sensitive Influenza Virus Whole-Genome Capture Kit. Reaction system: DEPC-treated ddH_2O, 12 μl; B whole-genome amplification mix, 25 μl; BWGP-Mix, 4 μl; EF Enzyme 1 μl; and virus culture cell line nucleic acid, 8 μl. Reaction conditions: 45°C, 60 min; 55°C, 30 min; 94°C, 2 min; 94°C, 20 s; 40°C, 30 s; 68°C, 3 min 30 s; 5 cycles; 94°C, 20 s; 58°C, 30 s; 68°C, 3 min 30 s; 40 cycles; and 68°C, 10 min. After purifying the product with AMPure XP (BECKMAN A63880), the library was amplified with Nextera® XT Library Prep Kit (Illumina 15032352) and sequenced with Illumina NextSeq2000 sequencer and NextSeqTM 2000 P3 Reagent Cartridge 300 cycles (Illumina 20045959) sequencing reagent.

2.5. Genome assembly and analysis

Whole genome of the influenza virus on sequenced data was assembled using the QIAGEN CLC Genomics Workbench 21

software. Download 2021–2022 Northern Hemisphere BV influenza virus vaccine representative strain B/Washington/02/2019 (EPI_ISL_341131), 2021–2022 global BV influenza virus sequence, and BV early isolate sequence from the GISAID database. Using the Kimura two-parameter model of the Neighbor-joining method of the MEGA 7.0.14 software to construct the evolutionary tree of eight gene segments of the influenza virus. Nucleotide and amino acid homology analysis was performed using MegAlign of the DNASTAR 7.0.1 software; the amino acid sequence alignment was performed using the align of the MEGA 7.0.14 software to analyze the amino acid difference sites; and analysis of protein *N*-glycosylation sites was carried out using the NetNGlyc 1.0 Server software. The data presented in the study are deposited in the e Global Initiative on Sharing All Influenza Data (GISAID)[1] repository, accession number list in Supplementary Table S1.

3. Results

3.1. Positive rate of BV influenza virus

From April 2021 to March 2022, 1,543 specimens from patients with influenza-like illness (ILI) were tested, of which 380 (24.63%) were positive for BV influenza virus. No cases of influenza A H1N1, seasonal H3N2, and BY influenza viruses were detected. The BV influenza viruses were not detected from April 2022 to September 2022, but began to be detected in ILI in late October 2022. The highest positive rate of influenza viruses in ILI was observed in December 2022 and January 2022. The favorable rates of BV influenza viruses in different months were statistically significant ($\chi^2 = 409.002$, $p < 0.001$). The favorable rates of BV influenza virus in males and females were 22.67 and 26.69%, respectively ($\chi^2 = 3.382$, $p = 0.07$). The positive rates of BV influenza virus in different age groups were 8.15% for 0–5 years; 32.22% for 6–15 years; 26.91% for 16–25 years, 33.98% for 26–60 years, and 9.46% for those above 60 years, respectively ($\chi^2 = 103.411$, $p < 0.001$) (Table 1). In summary, the study found a high prevalence of BV influenza virus in ILI cases in Jining City from October 2021 to March 2022, with the highest positive rate observed in December 2021 and January 2022. The virus showed significant differences in favorable rates across different age groups and months.

3.2. Nucleotide diversity of B/Victoria influenza viruses

This study successfully sequenced 24 whole genomes of B/Victoria influenza viruses. The nucleotide similarity of 8 gene fragments in the sequences of 24 strains ranged from 98.3 to 100%. Compared with the WHO-recommended BV influenza virus vaccine strain B/Washington/02/2019 for the Northern Hemisphere 2021–2022, the nucleotide similarity of the 8 gene segments varied from 98.2 to 99.7%. The amino acid similarity of the encoded protein was the lowest at 97.2% and was the highest at 100% (Table 2).

Additionally, the evolutionary distances of HA, NA, MP, NP, NS, PA, PB1, and PB2 genes in the 24 sequences were 0.0076, 0.0078, 0.0069, 0.0056, 0.0045, 0.0052, 0.0048, and 0.0065, respectively, when compared with B/Washington/02/2019. The evolutionary distances of HA, NA, MP, NP, NS, PA, PB1, and PB2 genes were 0.0129, 0.0093, 0.0159, 0.0063, 0.0090, 0.0078, 0.0048, and 0.0159, respectively (Table 2). Overall, this study provides valuable insights into the genetic characteristics and evolutionary distances of B/Victoria influenza viruses, which can help inform the development and selection of appropriate vaccine strains.

3.3. Analysis of genetic variation and evolution of B/Victoria influenza viruses

In this study, the genetic evolution of B/Victoria influenza viruses in Jining was analyzed using the sequences of their eight segments. A phylogenetic tree was constructed using the eight-segment sequences from 24 B/Victoria strains, including the global BV influenza virus (2021–2022), influenza vaccine strains recommended by WHO, and early BV isolates. The results revealed that the eight segments of the seven sequences were all closely related and located in the same evolutionary clade. Notably, the HA genes of these sequences all belonged to the Victoria clade 1A.3a.1. The remaining strains were found in a separate evolutionary clade, with their HA genes belonging to the Victoria clade 1A.3a.2 (Figure 1). Overall, the phylogenetic analysis of the eight-segment sequences of B/Victoria influenza viruses in Jining revealed two distinct evolutionary clades, with the HA genes of the sequences belonging to either the Victoria clade 1A.3a.1 or the Victoria clade 1A.3a.2.

3.4. Amino acid variant analysis

Compared with B/Washington/02/2019, the HA, NA, and PA genes showed the highest number of amino acid variation sites. HA is crucial for the antigenic variation of the influenza virus, and its heavy chain region contains both antigenic determinants and receptor binding sites (Liu et al., 2018). These include the 120-loop (116–137 aa), 150-loop (141–150 aa), 160-loop (160–172 aa), and 190-helix (193–202 aa) for antigenic epitopes, as well as the 140-loop (136–143 aa), 190-helix (193–202 aa), and 240-loop (237–242 aa) for the HA receptor binding site (Wang et al., 2007; Liu et al., 2018). Table 3 shows that out of the 24 HA protein sequences, 20 variations were found, with 9 occurring in epitopes, including 5 in the 120-loop, 2 in the 150-loop, 1 in the 160-loop, and 1 in the 190-helix. Additionally, there were three mutations in the HA receptor binding site, with 1 in the 190-helix and 2 in the 240-loop.

The active catalytic site of NA protein is composed of 19 amino acids, including R116, E117, D149, R150, R154, W177, S178, D197, I221, R223, E226, H273, E275, E276, R292, N294, R374, Y409, and E428 (Chen et al., 2019). Among the 24 sequences, 20 sites of NA protein were mutated, and one of the sequences had the D197N mutation in the catalytic site of NA. The NA inhibitors are the primary antiviral drugs used to treat influenza. However, mutations such as E105K, P139S, G140R, D197N, and H273Y in BV influenza viruses can cause resistance to NA inhibitors (Farrukee et al., 2015, 2018). In this study, it was observed that one sequence had a D197N drug resistance mutation.

Nucleoprotein is a crucial structural protein that makes up the nucleocapsid of the influenza virus. It contains specific amino acid

1 www.gisaid.org

TABLE 1 The positive rate of nucleic acid testing and composition characteristics of BV influenza in Jining between 2021–2022.

Variables	Testing	Influenza A (H1N1), Influenza A (H3N2), Influenza B (Yamagata)		Influenza B (Victoria)	
	Specimens number	Positives number	Positive rate (%)	Positives number	Positive rate (%)
Month					
April–September 2021	309	0	0	0	0
October 2021	171	0	0	3	1.75
November 2021	204	0	0	41	20.10
December 2021	232	0	0	129	56.60
January 2022	242	0	0	133	54.96
February 2022	180	0	0	49	27.22
March 2022	205	0	0	25	12.20
Gender					
Male	790	0	0	179	22.67
Female	753	0	0	201	26.69
Age (in years)					
0–5	405	0	0	33	8.15
6–15	329	0	0	106	32.22
16–25	223	0	0	60	26.91
26–60	512	0	0	174	33.98
≥61	74	0	0	7	9.46
Total	1543	0	0	380	24.63

TABLE 2 Similarity analysis of the whole genome of BV influenza virus in Jining.

Gene	Protein	Sequence similarity between 24 strains (%)		Similarity compared to B/Washington/02/2019(%)	
		Nucleotides	Amino acid	Nucleotides	Amino acid
HA	HA	98.3–100	98.2–100	98.3–99.0	97.9–98.8
NA	NA	98.6–100	97.6–100	98.8–99.3	98.7–99.4
MP	M1	98.7–100	99.2–100	98.2–98.7	98.8–99.6
	M2		96.3–100		97.2–99.1
NP	NP	98.8–100	99.1–100	99.1–99.6	99.1–100
NS	NS1	99.0–100	97.5–100	98.8–99.2	98.2–99.6
	NEP		99.2–100		97.5–98.4
PA	PA	98.6–100	98.3–100	98.7–99.4	98.6–99.7
PB1	PB1	98.8–100	98.8–100	99.2–99.7	99.2–99.7
PB2	PB2	98.8–100	98.8–100	98.2–98.6	99.1–99.9

sites that are important for its nuclear import and export, including K44, R45, and F209, and the 125–149 aa region of the RNA-binding domain of NP (Ng et al., 2012; Sherry et al., 2014). In the 24 sequences analyzed, nine amino acid sites in NP proteins were found to be mutated, with the E128D mutation appearing in the RNA binding domain of 7 sequences.

M1 is a crucial matrix protein that forms the structure of the influenza virus. It contains a nuclear localization signal (NLS), nuclear export signal (NES), and phosphorylation modification sites, which play a role in promoting the nuclear export of influenza virus ribonucleoprotein (vRNP). In the influenza B virus, the NLS is located at amino acids 76–94, while the NES is located at amino acids 3–14 and 124–133. The key phosphorylation sites are T80 and S84 (Cao et al., 2014). The present study found that none of the 24 sequences analyzed showed mutations in the NLS, NES, T80, and S84.

NS1 and NEP are nonstructural proteins of influenza; NS1 has diverse biological functions, including binding to host mRNA, inhibiting interferon, and interacting with many host proteins (Nogales et al., 2018). It consists of two functional domains, an N-terminal RNA-binding domain (RBD, 1–90 aa) and a C-terminal effector domain (ED, 120–261 aa), which are connected by a short interdomain linker region (LR, 91–119 aa) (Jumat et al., 2016). Among the 24 sequences analyzed, 14 amino acid site variations were observed

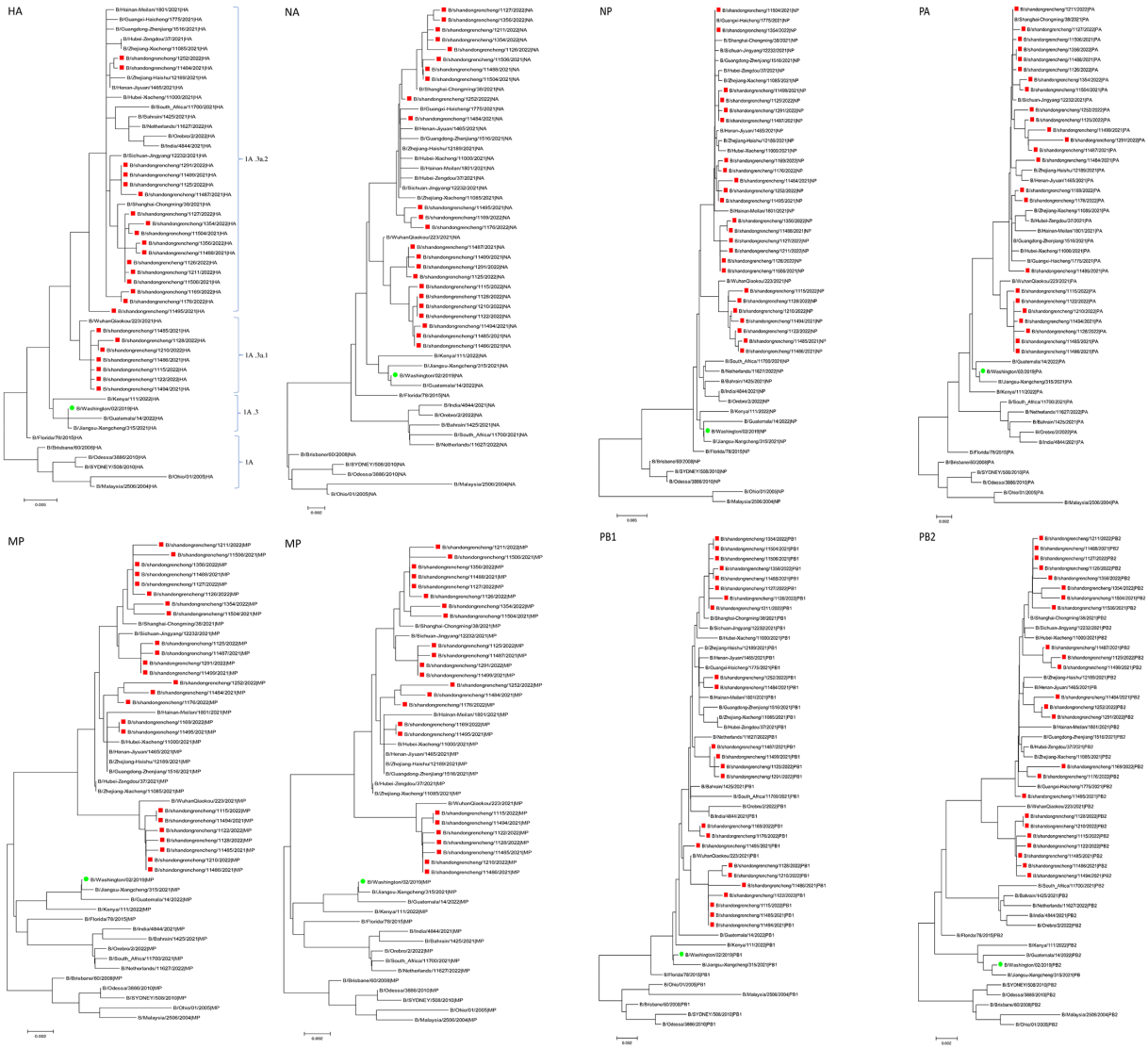

FIGURE 1
The phylogenetic analysis of influenza viruses circulating in Jining during 2021–2022 (red) compared with the Northern Hemisphere vaccine strain B/Washington/02/2019 (green). HA, hemagglutinin. NA, neuraminidase.

in NS1, with 1 variation found in the RBD, 4in the linker region, and 9 in the effector domain. On the contrary, NEP is a nuclear export protein that facilitates the nuclear export of viral RNP. Its nuclear export signal (NES) is located at 11–23 aa of NEP (Paragas et al., 2001). In the 24 sequences, three amino acids were identified in NEP, but none of them were found in the NES sites.

Polymerase acidic inhibitors are currently important specific drugs for treating influenza B, and their sites of action are T20, F24, M34, N37, and I38. None of the 24 strains examined in this study had mutations at these sites (Takashita, 2021). However, the K338R mutation in PA was present in 7 out of 24 sequences and is known to enhance the replication ability of influenza (Bae et al., 2018). The PB1 gene can also undergo mutations that enhance replication ability (Binh et al., 2013), such as D27V/N and N44Q; however, none of the 24 sequences had mutations in these sites. PB2 binds to the cap structure through Q325, W359, and Y434 alleles (Kim et al., 2018), and none of the 24 sequences had mutations in these sites either.

In this study, multiple amino acid variations were observed in the PA, HA, NA, NP, and NS1 proteins of the influenza B virus, with some mutations potentially affecting drug resistance and viral replication. In contrast, the M1 and NEP proteins showed no mutations in the analyzed sequences.

3.5. Glycosylation site analysis

Glycosylation of the HA and NA of influenza virus is a crucial mechanism for immune evasion and persistent viral infection (Kim et al., 2018). One HA sequence has an N59K mutation that eliminates a glycosylation site in N59. The N197D variant in all 24 sequences results in the loss of the glycosylation site at N197. An S109F mutation in NS1 of 11 sequences also leads to losing a glycosylation site at N107. Finally, one PB2 sequence has a D473N mutation, creating a new glycosylation site at N473 (Table 3). Overall, the mutations N59K in HA, N197D in

TABLE 3 Analysis of amino acid variation sites of B/Victoria influenza viruses in Jining City during 2021–2022.

Virus strain	HA																					NA																							M1					
	58	59	117	122	127	129	133	144	150	169	184	197	203	217	220	238	241	279	411	559	12	35	45	51	53	59	73	128	148	193	197	219	233	303	336	343	371	390	399	453	15	42	46	89	136	245
B/Washington/02/2019	L	N	V	H	A	D	R	P	N	A	G	N	K	A	V	G	P	R	Q	V	F	D	I	P	D	N	L	K	G	V	D	N	G	V	P	K	K	D	V	G	T	A	I	T	G	K
B/shandongrencheng/11484/2021	L	N	V	Q	T	D	G	L	K	A	E	D	R	A	V	G	P	K	Q	V	F	D	I	P	N	S	L	K	G	V	D	N	E	V	P	K	K	D	V	G	I	A	I	R	G	K
B/shandongrencheng/11485/2021	L	N	V	H	A	D	G	P	K	A	E	D	K	A	M	G	Q	K	Q	V	F	G	I	Q	D	N	L	K	G	V	D	N	G	I	P	E	K	D	V	R	I	A	I	R	G	R
B/shandongrencheng/11486/2021	L	N	V	H	A	D	G	P	K	A	E	D	K	A	M	G	Q	K	Q	I	F	G	I	Q	D	N	L	K	G	V	D	N	G	I	P	E	K	D	V	R	I	A	I	R	G	K
B/shandongrencheng/11487/2021	H	K	V	Q	T	D	G	L	K	A	E	D	R	A	V	G	P	K	Q	V	F	D	I	P	D	N	L	K	G	V	D	N	G	I	P	E	K	E	V	G	I	A	V	R	G	K
B/shandongrencheng/11488/2021	L	N	I	Q	T	D	G	L	K	T	E	D	R	A	V	G	P	K	Q	V	F	D	I	P	N	S	L	K	G	V	D	N	E	V	P	E	K	D	V	G	I	A	I	R	G	K
B/shandongrencheng/11494/2021	L	N	V	H	A	D	G	P	K	A	E	D	K	A	M	G	Q	K	Q	V	F	G	I	Q	D	N	L	K	G	V	D	N	G	I	P	E	K	D	A	R	I	A	I	R	G	K
B/shandongrencheng/11495/2021	L	N	V	Q	T	D	G	P	K	A	E	D	K	A	V	G	Q	K	Q	V	F	D	I	P	N	S	F	K	G	V	D	N	E	I	P	K	N	D	V	G	I	A	I	T	G	K
B/shandongrencheng/11499/2021	L	N	V	Q	T	D	G	L	K	A	E	D	R	A	V	G	P	K	Q	V	F	D	I	P	D	N	L	K	G	V	D	N	G	I	P	E	K	E	V	G	I	A	I	R	G	K
B/shandongrencheng/11504/2021	L	N	V	Q	T	D	G	L	K	T	E	D	R	A	V	G	P	K	Q	V	F	D	I	P	N	S	L	K	G	V	D	N	E	V	P	E	K	D	V	G	I	A	I	R	G	K
B/shandongrencheng/11506/2021	L	N	V	Q	T	D	G	L	K	T	E	D	R	A	V	G	P	K	Q	V	F	D	I	P	N	S	L	R	G	V	D	N	E	V	P	E	K	D	V	G	I	A	I	R	G	K
B/shandongrencheng/1115/2022	L	N	V	H	A	D	G	P	K	A	E	D	K	A	M	G	Q	K	Q	V	F	G	I	Q	D	N	L	K	G	V	D	N	G	I	P	E	K	D	V	G	I	A	I	R	G	K
B/shandongrencheng/1122/2022	L	N	V	H	A	D	G	P	K	A	E	D	K	V	M	G	Q	K	Q	V	F	G	I	Q	D	N	L	K	G	V	D	N	G	I	P	E	K	D	V	R	I	A	I	R	G	K
B/shandongrencheng/1125/2022	L	N	V	Q	T	D	G	L	K	A	E	D	R	A	V	G	P	K	Q	V	F	D	I	P	D	N	L	K	G	V	D	N	G	I	P	E	K	E	V	G	I	A	I	R	G	K
B/shandongrencheng/1126/2022	L	N	V	Q	T	D	G	L	K	T	E	D	R	A	V	G	P	K	Q	V	F	D	M	P	N	S	L	K	R	V	D	N	E	V	P	E	K	D	V	G	I	A	I	R	G	K
B/shandongrencheng/1127/2022	L	N	V	Q	T	D	G	L	K	T	E	D	R	A	V	G	P	K	Q	V	F	D	I	P	N	S	L	K	G	V	N	N	E	V	P	E	K	D	V	G	I	A	I	R	G	K
B/shandongrencheng/1128/2022	L	N	V	H	A	D	G	P	K	A	E	D	K	A	M	G	Q	K	Q	V	F	G	I	Q	D	N	L	K	G	V	D	N	G	I	P	E	K	D	V	R	I	V	I	R	G	K

(Continued)

10.3389/fmicb.2023.1196451

TABLE 3 (Continued)

Virus strain	HA																					NA																						M1					
	58	59	117	122	127	129	133	144	150	169	184	197	203	217	220	238	241	279	411	559		12	35	45	51	53	59	73	128	148	193	197	219	233	303	336	343	371	390	399	453		15	42	46	89	136	245
B/shandongrencheng/1169/2022	L	N	V	Q	T	D	G	L	K	A	E	D	R	A	V	G	P	K	Q	V		F	D	I	P	N	N	L	K	G	V	D	N	E	V	P	K	N	D	V	G		I	A	I	T	G	K
B/shandongrencheng/1176/2022	L	N	V	Q	T	D	G	L	K	A	E	D	R	A	V	G	P	K	Q	V		F	D	I	P	N	S	L	K	G	V	D	S	E	V	P	K	N	D	V	G		I	A	I	R	G	K
B/shandongrencheng/1210/2022	L	N	V	H	A	D	G	P	K	A	E	D	K	A	M	G	Q	K	Q	V		F	G	I	Q	D	N	L	K	G	V	D	N	G	I	P	E	K	D	V	R		I	A	I	R	G	K
B/shandongrencheng/1211/2022	L	N	V	Q	T	D	G	L	K	T	E	D	R	A	V	G	P	K	Q	V		V	D	I	P	N	S	L	K	G	V	D	N	E	V	P	E	K	D	V	G		I	A	I	R	G	K
B/shandongrencheng/1252/2022	L	N	V	Q	T	D	G	L	K	A	E	D	R	A	V	G	P	K	Q	V		F	D	I	P	N	S	L	K	G	V	D	N	E	V	P	Q	K	D	V	G		I	A	I	R	E	K
B/shandongrencheng/1291/2022	L	N	V	Q	T	D	G	L	K	A	E	D	R	A	V	G	P	K	Q	V		F	D	I	P	D	N	L	K	G	V	D	N	G	I	P	E	K	E	V	G		I	A	I	R	G	K
B/shandongrencheng/1354/2022	L	N	V	Q	T	N	G	L	K	T	E	D	R	A	V	G	P	K	K	V		F	D	I	P	N	S	L	K	G	I	D	N	E	V	P	E	K	D	V	G		I	A	I	T	G	K
B/shandongrencheng/1356/2022	L	N	V	Q	T	D	G	L	K	T	E	D	R	A	V	E	P	K	Q	V		F	D	I	P	N	S	L	K	G	V	D	N	E	V	T	E	K	D	V	G		I	A	I	R	G	K

Virus strain	M2						NP									NS1																NEP			PA															
	14	24	70	73	79	88	37	51	78	113	120	128	183	379	512	3	105	106	109	116	122	126	132	138	198	203	205	212	224	3	26	88	36	112	119	121	195	196	214	230	252	338	352	387	399	400	432
B/Washington/02/2019	I	T	M	V	E	E	T	P	S	A	A	E	K	K	T	N	C	M	S	K	Y	P	D	E	P	S	S	A	V	N	S	M	F	D	I	V	D	V	I	I	V	K	A	C	V	A	E
B/shandongrencheng/11484/2021	I	A	M	V	E	E	T	L	S	A	A	E	K	E	T	D	C	V	S	K	C	P	N	E	P	S	S	A	V	D	Y	V	F	D	I	V	D	V	I	I	A	K	A	Y	V	A	E
B/shandongrencheng/11485/2021	I	A	M	V	E	E	I	P	C	A	A	D	K	E	N	N	C	V	F	K	C	P	N	E	P	S	S	A	V	N	Y	V	F	D	I	V	D	V	I	I	A	R	A	C	V	A	E
B/shandongrencheng/11486/2021	I	A	M	V	E	E	I	P	S	A	A	D	K	E	N	N	C	V	F	K	C	P	N	E	P	S	S	A	V	N	Y	V	F	D	I	V	D	V	I	I	A	R	A	C	V	A	E
B/shandongrencheng/11487/2021	I	A	I	V	E	E	T	P	S	A	A	E	K	K	T	N	C	V	F	K	C	S	N	E	P	S	S	A	V	N	Y	V	F	D	I	V	D	V	I	I	A	K	A	Y	V	A	E
B/shandongrencheng/11488/2021	I	A	I	V	E	E	T	P	S	A	A	E	K	K	T	N	C	V	S	K	C	P	N	E	P	S	S	A	V	N	Y	V	F	D	I	V	D	V	I	I	A	K	A	Y	V	A	E
B/shandongrencheng/11494/2021	I	A	M	L	E	E	I	P	S	A	A	D	R	E	T	N	C	V	F	K	C	P	N	E	P	S	S	A	I	N	Y	V	F	D	I	V	D	V	I	I	A	R	A	C	V	A	E
B/shandongrencheng/11495/2021	I	A	M	V	E	E	T	P	S	A	A	E	K	E	T	N	C	V	S	E	C	P	N	E	S	S	S	A	V	N	Y	V	F	D	L	V	D	V	I	I	A	K	A	Y	V	A	E

(Continued)

10.3389/fmicb.2023.1196451

TABLE 3 (Continued)

Virus strain	M2						NP									NS1														NEP			PA														
	14	24	70	73	79	88	37	51	78	113	120	128	183	379	512	3	105	106	109	116	122	126	132	138	198	203	205	212	224	3	26	88	36	112	119	121	195	196	214	230	252	338	352	387	399	400	432
B/shandongrencheng/11499/2021	I	A	I	V	E	E	T	P	S	A	A	E	K	K	T	N	R	V	F	K	C	S	N	D	P	S	S	A	V	N	Y	V	F	D	L	V	G	F	I	I	A	K	A	Y	M	A	E
B/shandongrencheng/11504/2021	I	A	I	V	K	E	T	P	S	A	A	E	K	K	T	N	C	V	S	K	C	P	N	E	P	S	S	A	V	N	Y	V	F	D	I	V	D	V	I	I	A	K	T	Y	V	P	E
B/shandongrencheng/11506/2021	I	A	I	V	E	E	T	P	S	A	A	E	K	K	T	N	C	V	S	K	C	P	N	E	P	S	L	A	V	N	Y	V	F	N	I	V	D	V	I	I	A	K	A	Y	V	A	E
B/shandongrencheng/1115/2022	I	A	M	L	E	E	I	P	S	A	A	D	K	K	T	N	C	V	F	K	C	P	N	E	P	S	S	A	V	N	Y	V	F	D	I	V	D	V	I	I	A	R	A	C	V	A	E
B/shandongrencheng/1122/2022	I	A	M	V	E	E	I	P	S	A	A	D	K	K	N	N	C	V	F	K	C	P	N	E	P	S	S	A	V	N	Y	V	F	D	I	V	D	V	I	I	A	R	A	C	V	A	E
B/shandongrencheng/1125/2022	I	A	I	V	E	E	T	P	S	A	A	E	K	K	T	N	C	V	F	K	C	S	N	E	P	S	S	A	V	N	Y	V	F	D	I	V	D	V	I	I	A	K	A	Y	V	A	E
B/shandongrencheng/1126/2022	I	A	I	V	E	E	T	P	S	A	A	E	K	K	T	N	C	V	S	K	C	P	N	E	P	S	S	A	V	N	Y	V	F	D	I	V	D	V	I	I	A	K	A	Y	V	A	E
B/shandongrencheng/1127/2022	I	A	I	V	E	E	T	P	S	A	A	E	K	K	T	N	C	V	S	K	C	P	N	E	P	S	S	A	V	N	Y	V	F	D	I	V	D	V	I	I	A	K	A	Y	V	A	E
B/shandongrencheng/1128/2022	I	A	M	V	E	E	I	P	S	T	A	D	K	K	T	N	C	V	F	K	C	P	N	E	P	S	S	A	V	N	Y	V	F	D	I	V	D	V	I	I	A	R	A	C	V	A	E
B/shandongrencheng/1169/2022	I	A	M	V	E	E	T	P	S	A	A	E	K	K	T	N	C	V	S	K	C	P	N	E	S	S	S	A	V	N	Y	V	F	D	I	V	D	V	I	I	A	K	A	Y	V	A	E
B/shandongrencheng/1176/2022	I	A	M	L	E	E	T	P	S	A	A	E	K	E	T	N	C	V	S	K	C	P	N	E	S	S	S	V	V	N	Y	V	Y	D	I	V	D	V	I	I	A	K	A	Y	V	A	E
B/shandongrencheng/1210/2022	I	A	M	V	E	E	I	P	S	A	A	D	K	E	T	N	C	V	F	K	C	P	N	E	P	S	S	A	V	N	Y	V	F	D	I	I	D	V	I	I	A	R	A	C	V	A	K
B/shandongrencheng/1211/2022	I	A	I	V	E	E	T	P	S	A	A	E	K	K	T	N	C	V	S	K	C	P	N	E	P	S	S	A	V	N	Y	V	F	D	I	V	D	V	I	I	A	K	A	Y	V	A	E
B/shandongrencheng/1252/2022	T	A	M	L	E	E	T	P	S	A	T	E	K	E	T	D	C	V	S	K	C	P	N	E	P	Y	S	A	V	D	Y	V	F	D	I	V	D	V	V	L	A	K	A	Y	V	A	E
B/shandongrencheng/1291/2022	I	A	I	V	E	E	T	P	S	A	A	E	K	K	T	N	C	V	F	K	C	S	N	E	P	S	S	A	V	N	Y	V	F	D	I	V	D	V	I	I	A	K	A	Y	V	A	E
B/shandongrencheng/1354/2022	I	A	I	V	E	D	T	P	S	A	A	E	K	K	T	N	C	V	S	K	C	P	N	E	P	S	S	A	V	N	Y	V	F	D	I	V	D	V	I	I	A	K	T	Y	V	A	E
B/shandongrencheng/1356/2022	I	A	I	V	E	E	T	P	S	A	A	E	K	K	T	N	C	V	S	K	C	P	N	E	P	S	S	A	V	N	Y	V	F	D	I	V	D	V	I	I	A	K	A	Y	V	A	E

(Continued)

TABLE 3 (Continued)

Virus strain	PA													PB1															PB2																		
	502	504	508	520	522	523	524	528	559	575	670	717	720	48	51	60	184	386	436	454	459	476	566	576	652	686	687	744	14	56	77	109	156	168	181	199	258	268	272	276	313	393	401	468	473	484	590
B/Washington/02/2019	K	Q	R	E	S	S	T	V	V	R	D	L	V	E	N	V	V	R	L	N	M	M	K	K	K	Q	C	A	R	S	I	D	M	I	T	M	S	I	S	S	I	K	I	S	D	N	A
B/shandongrencheng/11484/2021	K	Q	R	E	S	S	T	V	A	G	D	L	V	E	N	V	V	K	I	D	M	M	K	K	K	Q	C	A	R	N	I	N	M	I	T	I	S	I	S	S	T	K	I	S	D	A	A
B/shandongrencheng/11485/2021	K	Q	R	E	S	S	T	V	V	R	D	L	V	D	S	V	V	R	L	D	M	M	K	K	K	Q	C	A	R	N	I	D	M	I	T	I	S	I	S	S	I	K	V	S	D	N	A
B/shandongrencheng/11486/2021	K	Q	R	E	S	S	T	V	V	R	D	L	V	D	S	V	V	R	L	D	M	M	R	K	K	H	D	A	R	N	I	D	M	I	T	I	S	I	S	S	I	K	V	S	D	N	A
B/shandongrencheng/11487/2021	K	Q	R	E	S	S	T	A	V	R	D	L	V	E	N	V	V	R	I	D	M	M	K	K	R	Q	C	T	R	N	I	N	M	I	T	I	S	I	S	S	T	K	I	L	D	N	A
B/shandongrencheng/11488/2021	K	Q	R	E	S	S	T	V	V	R	D	L	V	E	N	V	V	R	I	D	M	M	K	K	K	Q	C	A	K	N	I	N	M	I	T	I	S	I	S	S	I	K	I	S	D	N	A
B/shandongrencheng/11494/2021	K	Q	R	E	S	S	T	V	V	R	D	L	V	D	S	V	V	R	L	D	M	M	K	K	K	Q	C	A	R	N	I	D	M	I	T	I	S	I	S	S	I	E	V	S	D	N	A
B/shandongrencheng/11495/2021	K	Q	R	E	S	S	T	V	A	R	D	L	E	E	N	I	V	R	L	D	M	M	K	K	K	Q	C	A	R	N	I	D	M	I	T	I	S	I	S	S	I	K	I	S	D	N	A
B/shandongrencheng/11499/2021	K	Q	R	E	S	S	T	A	V	R	D	L	V	E	N	V	V	R	I	D	M	K	K	K	R	Q	C	T	R	N	I	N	M	I	T	I	S	I	S	S	T	K	I	L	D	A	A
B/shandongrencheng/11504/2021	K	Q	R	E	S	S	T	V	V	R	D	L	V	E	N	V	V	R	I	D	I	M	K	K	K	Q	C	A	K	N	I	N	V	I	T	I	S	I	S	S	I	K	I	S	D	N	T
B/shandongrencheng/11506/2021	K	Q	R	E	S	S	T	V	V	R	D	L	V	E	N	V	V	R	I	D	M	M	K	K	K	Q	C	A	K	N	I	N	M	K	T	I	S	I	S	S	I	K	I	S	D	N	A
B/shandongrencheng/1115/2022	K	Q	R	E	S	S	T	V	V	R	D	F	V	D	S	V	V	R	L	D	M	M	K	K	K	Q	C	A	R	N	I	D	M	I	T	I	S	I	S	S	I	K	V	S	D	N	A
B/shandongrencheng/1122/2022	K	Q	R	E	S	S	T	V	V	R	D	L	V	D	S	V	V	R	L	D	M	M	K	K	K	Q	C	A	R	N	I	D	M	I	T	I	S	I	S	S	I	K	V	S	N	N	A
B/shandongrencheng/1125/2022	K	Q	R	E	S	S	T	V	V	R	D	L	V	E	N	V	V	R	I	D	M	K	K	K	R	Q	C	T	R	N	I	N	M	I	T	I	S	I	S	S	T	K	I	L	D	A	A
B/shandongrencheng/1126/2022	K	Q	R	E	S	S	T	V	V	R	D	L	V	E	N	V	V	R	I	D	M	M	K	K	K	Q	C	A	K	N	I	N	M	I	T	I	S	I	S	S	I	K	I	S	D	N	A
B/shandongrencheng/1127/2022	K	Q	R	E	S	S	T	V	V	R	D	L	V	E	N	V	V	R	L	D	M	M	K	K	K	Q	C	A	K	N	I	N	M	I	T	I	S	I	S	S	I	K	I	S	D	N	A
B/shandongrencheng/1128/2022	K	Q	R	E	S	S	T	V	V	R	E	L	V	D	S	V	V	R	L	D	M	M	K	K	K	Q	C	A	R	N	I	D	M	I	T	I	S	I	S	S	I	K	V	S	D	A	A
B/shandongrencheng/1169/2022	K	Q	R	E	S	S	T	V	V	R	D	L	V	E	N	I	V	R	L	D	M	M	K	K	K	Q	C	A	R	N	M	N	M	I	T	I	T	K	A	T	I	K	I	S	D	N	A

(Continued)

10.3389/fmicb.2023.1196451

TABLE 3 (Continued)

Virus strain	PA												
	502	504	508	520	522	523	524	528	559	575	670	717	720
B/shandongrencheng/1176/2022	K	Q	R	E	S	S	T	V	V	R	D	L	V
B/shandongrencheng/1210/2022	K	Q	R	E	S	S	T	V	V	R	D	L	V
B/shandongrencheng/1211/2022	K	Q	R	E	S	S	T	V	V	R	D	L	V
B/shandongrencheng/1252/2022	K	Q	R	E	S	S	T	V	V	R	D	L	V
B/shandongrencheng/1291/2022	E	R	G	G	G	G	A	A	V	R	D	L	V
B/shandongrencheng/1354/2022	K	Q	R	E	S	S	T	V	V	R	D	L	V
B/shandongrencheng/1356/2022	K	Q	R	E	S	S	T	V	V	R	D	L	V

Virus strain	PB1														
	48	51	60	184	386	436	454	459	476	566	576	652	686	687	744
B/shandongrencheng/1176/2022	E	N	I	I	R	L	D	M	M	K	K	K	Q	C	A
B/shandongrencheng/1210/2022	D	S	V	V	R	L	D	M	M	K	K	K	Q	C	A
B/shandongrencheng/1211/2022	E	N	V	V	R	I	D	M	M	K	K	K	Q	C	A
B/shandongrencheng/1252/2022	E	N	V	V	R	I	D	M	M	K	R	K	Q	C	A
B/shandongrencheng/1291/2022	E	N	V	V	R	I	D	M	K	K	K	R	Q	C	T
B/shandongrencheng/1354/2022	E	N	V	V	R	I	D	M	M	K	K	K	Q	C	A
B/shandongrencheng/1356/2022	E	N	V	V	R	I	D	M	M	K	K	K	Q	C	A

Virus strain	PB2																		
	14	56	77	109	156	168	181	199	258	268	272	276	313	393	401	468	473	484	590
B/shandongrencheng/1176/2022	R	N	I	N	M	I	T	I	S	I	S	S	T	K	I	S	D	N	A
B/shandongrencheng/1210/2022	R	N	I	D	M	I	T	I	S	I	S	S	I	K	V	S	D	A	A
B/shandongrencheng/1211/2022	K	N	I	N	M	I	T	I	S	I	S	S	I	K	I	S	D	N	A
B/shandongrencheng/1252/2022	R	N	I	N	M	I	T	I	S	I	S	S	I	K	I	S	D	N	A
B/shandongrencheng/1291/2022	R	N	I	N	M	I	T	I	S	I	S	S	T	K	I	S	D	N	A
B/shandongrencheng/1354/2022	K	N	I	N	M	I	T	I	S	I	S	S	I	K	I	S	D	A	T
B/shandongrencheng/1356/2022	K	N	I	N	M	I	T	I	S	I	S	S	I	K	I	S	D	N	A

both HA and NA, S109F in NS1, and D473N in PB2 alter glycosylation sites, potentially affecting immune evasion and persistent viral infection.

4. Discussion

Over the past two decades, studies on viruses have been extensively carried out due to their association with both acute self-limiting and long-term chronic diseases in humans, including the influenza virus responsible for the common "flu" (Li et al., 2016; Chen X. et al., 2017; Chen Y. et al., 2017; Jiao et al., 2017; Shi et al., 2017; Duan et al., 2018; Yuan et al., 2023). Many pathogens cause influenza-like illnesses, the most important of which is the influenza virus (Clementi et al., 2021). Influenza virus infection can cause severe disease burden, causing fever, cough, headache, pneumonia, and even death, resulting in a severe disease burden (Feng et al., 2020; Castillo-Rodriguez et al., 2022). The WHO influenza established a global surveillance network and recommends annual influenza vaccine strains for the northern and southern hemispheres. China is one of the most crucial member countries for influenza surveillance and has established a surveillance network covering all prefecture-level cities (Liu et al., 2022). Jining City is an ordinary medium-sized prefecture-level city in northern China, with a total area of 11,000 km^2 and a population of 8.358 million. It has a warm temperate monsoon climate with four distinct seasons. Jining City has built an influenza surveillance network laboratory. According to the epidemic characteristics of influenza with high incidence in winter and spring, about 1,500 influenza-like case specimens from two sentinel hospitals are monitored for influenza from April to March of the following year.

From April 2021 to March 2022, Jining City's influenza surveillance network laboratory reported a 24.63% positive rate of influenza virus among influenza-like illnesses, with BV influenza virus being the primary prevalent subtype during the winter and spring seasons in northern China (Feng et al., 2020; Liu et al., 2022). The highest positive rate was observed in December and January, followed by November and February, while the lowest positive rate was observed from April to September. Additionally, the percentage distributions by age category showed slightly higher rates in the 6–60 year groups and lower rates in the 0–5 year groups and above 65 year groups as shown in Table 1.

Compared to the vaccine strain B/Washington/02/2019, the HA and PB2 gene segments of the Jining strain exhibit the lowest similarity and the highest gene evolution distance. Although both strains belong to the Victoria clade 1A branch on the evolutionary tree (162–164 aa missing in HA); they are located in different clades. Jining has two epidemic strains the Victoria clade 1A.3a.1 and Victoria clade 1A.3a.2, which are cocirculating. In the 2019–2020 influenza season, BV lineage influenza viruses in Jining City were mainly located in the Victoria clade 1A.3 branch, indicating that the BV lineage influenza viruses in Jining City have evolved from the Victoria clade 1A.3 branch to the Victoria clade 1A.3a.1 and Victoria clade 1A.3a.2 evolutionary branches. In addition, on the phylogenetic tree, the isolated strains worldwide are also mainly distributed in the Victoria clade 1A.3a.1 and Victoria clade 1A.3a.2 evolutionary branches. However, a small number of strains in the 2021–2022 season were located in the Victoria clade 1A.3 branch, indicating that the global circulation of BV lineage influenza viruses in the 2021–2022 season is a polymorphic epidemic with multiple units coexisting, mainly in the Victoria clade 1A.3a.1 and Victoria clade 1A.3a.2 evolutionary branches.

Variant strains with different amino acids on hemagglutinin (HA) continue to emerge due to the high mutation rate of influenza viruses. When there are more than four amino acid variations in the HA antigenic determinants, and the variations are distributed on at least two antigenic determinants, antigenic drift occurs, forming a new influenza variant (Liu et al., 2018). Out of the 24 sequences analyzed, the HA epitope of 7 sequences located in the Victoria clade 1A.3a.1 only had 3 amino acid changes. In contrast, the HA epitope of 17 sequences found in the Victoria clade 1A.3a.2 clusters had 5–8 amino acid site variations distributed across 3 or 4 antigenic determinants. These variations may change the antigenicity of the influenza virus, lead to the formation of new variants, and possibly affect the protective effect of vaccine strains. The receptor binding sites of HA have 2–3 amino acid mutations, which may impact the binding of HA and receptors. The N197D variant found in all 24 sequences is not only located in the antigenic epitope of HA but also in the receptor binding site. However, the mutation of N197, an important glycosylation site in the B/Victoria virus, resulted in the loss of the N197 glycosylation site in these 24 sequences. This loss, in turn, affects the changes in HA antigenicity and promotes the reproduction of the influenza virus in embryonated eggs (Nakagawa et al., 2004; Saito et al., 2004). Currently, NA, PA, PB1, and PB2 inhibitors are all specific drugs used for the treatment of influenza A virus. However, only NA and PA inhibitors are specific drugs for the treatment of influenza B infection (Takashita, 2021). The function of NA is to cleave the glycosidic bonds between the HA and the influenza receptor, allowing the virus to be released from the host cell surface. The NA inhibitors can specifically bind to the active site of the NA enzyme, inhibit the activity of the NA enzyme, and inhibit the release of the virus. PA is a component of the polymerase of the influenza virus, and PA inhibitors can inhibit the endonuclease activity of the viral polymerase, thereby inhibiting the replication of the influenza virus. However, with the continuous mutation of the influenza virus genes, especially when the active site or adjacent amino acid sites of NA and PA undergo mutations, it may reduce the binding of the inhibitor to NA and PA, and reduce the virus's sensitivity to the inhibitor, resulting in drug-resistant mutants that make the treatment of influenza more challenging (Takashita, 2021). The D197N mutation may result in resistance to NA inhibitors, indicating the possible emergence of NA inhibitor-resistant variants in B/Victoria influenza viruses in Jining City. Studies have shown that the N197D mutation can affect the antigenic properties of the HA protein, potentially allowing the virus to evade recognition by the host immune system. This is because the glycosylation site can act as a shield to mask the virus from antibodies produced by the host. Additionally, the mutation may alter the shape of the HA protein, making it more difficult for antibodies to bind and neutralize the virus (Tsai and Tsai, 2019). This demonstrates that PA and NA inhibitors can still be used to treat influenza, but there is a need to strengthen the monitoring of drug-resistant mutations.

PA, PB1, and PB2 are the three subunits that make up the RNA polymerase of influenza virus (Wandzik et al., 2021). Among them, K338 of PA is located in the polymerase's core position. The K338R mutation in PA has been shown to enhance the activity of B/Victoria influenza virus RNA polymerase, thereby increasing its pathogenicity (Bae et al., 2018). In this study, it was found that none of the 17 sequences in the Victoria clade 1A.3a.2 had the K338R mutation, while all 7 sequences in the Victoria clade 1A.3a.1 had the K338R mutation in their PA subunit.

This study analyzed the influenza epidemic and gene evolution variation in Jining City from 2021 to 2022, showing that the B/Victoria

influenza virus's antigenic epitopes have partially mutated and formed new variants. These new variants are poorly matched with the WHO-recommended northern hemisphere vaccine strains, which should be adjusted accordingly. Furthermore, the 24 nucleic acid and protein sequences in Jining have undergone some variation, displaying differences in variation sites, homology, evolutionary characteristics, and genetic distances. This suggests that the B/Victoria strain of influenza virus is still evolving and mutating; thus, influenza surveillance needs further strengthening.

Data availability statement

The datasets presented in this study can be found in online repositories. The names of the repository/repositories and accession number(s) can be found in the article/Supplementary material.

Ethics statement

The studies involving human participants were reviewed and approved by Ethics Committee at Jining Center for Disease Control and Prevention. Written informed consent to participate in this study was provided by the participants' legal guardian/next of kin.

Author contributions

LL, TL, and BJ conceived and designed the experiments. LL performed the experiments and analyzed the data. LL, QW, YD, TL, YaJ, ZW, XW, HD, YoJ, and BJ interpreted the data. LL, QW, and BJ wrote the manuscript. All authors contributed to the article and approved the submitted version.

Funding

This study was supported by Science and Technology Development Funds for Shandong Medical and Health (202112060725) and Key Research and Development Funds for Jining Medical and Health (2021018).

Conflict of interest

ZW was employed by Nanjing Chengshi BioTech (TheraRNA) Co., Ltd.

The remaining authors declare that the research was conducted in the absence of any commercial or financial relationships that could be construed as a potential conflict of interest.

Publisher's note

Supplementary material

The Supplementary material for this article can be found online at: https://www.frontiersin.org/articles/10.3389/fmicb.2023.1196451/full#supplementary-material

References

Bae, J. Y., Lee, I., Kim, J. I., Park, S., Yoo, K., Park, M., et al. (2018). A single amino acid in the polymerase acidic protein determines the pathogenicity of influenza B viruses. *J. Virol.* 92:e00259-18. doi: 10.1128/JVI.00259-18

Binh, N. T., Wakai, C., Kawaguchi, A., and Nagata, K. (2013). The N-terminal region of influenza virus polymerase PB1 adjacent to the PA binding site is involved in replication but not transcription of the viral genome. *Front. Microbiol.* 4:398. doi: 10.3389/fmicb.2013.00398

Cao, S., Jiang, J., Li, J., Li, Y., Yang, L., Wang, S., et al. (2014). Characterization of the nucleocytoplasmic shuttle of the matrix protein of influenza B virus. *J. Virol.* 88, 7464–7473. doi: 10.1128/JVI.00794-14

Carascal, M. B., Pavon, R. D. N., and Rivera, W. L. (2022). Recent Progress in recombinant influenza vaccine development toward Heterosubtypic immune response. *Front. Immunol.* 13:878943. doi: 10.3389/fimmu.2022.878943

Castillo-Rodriguez, L., Malo-Sanchez, D., Diaz-Jimenez, D., Garcia-Velasquezet, I., Pulido, P., Castaneda-Orjuela, C., et al. (2022). Economic costs of severe seasonal influenza in Colombia, 2017-2019: a multi-center analysis. *PLoS One* 17:e0270086. doi: 10.1371/journal.pone.0270086

Chavez, J., and Hai, R. (2021). Effects of cigarette smoking on influenza virus/host interplay. *Pathogens* 10:1636. doi: 10.3390/pathogens10121636

Chen, Y., Jiao, B., Yao, M., Shi, X., Zheng, Z., Li, S., et al. (2017). ISG12a inhibits HCV replication and potentiates the anti-HCV activity of IFN-alpha through activation of the Jak/STAT signaling pathway independent of autophagy and apoptosis. *Virus Res.* 227, 231–239. doi: 10.1016/j.virusres.2016.10.013

Chen, F., Liu, T., Xu, J., Huang, Y., Liu, S., and Yang, J. (2019). Key amino acid residues of neuraminidase involved in influenza a virus entry. *Pathogens Disease* 77:ftz063. doi: 10.1093/femspd/ftz063

Chen, X., Ye, H., Li, S., Jiao, B., Wu, J., Zeng, P., et al. (2017). Severe fever with thrombocytopenia syndrome virus inhibits exogenous type I IFN signaling pathway through its NSs invitro. *PLoS One* 12:e0172744. doi: 10.1371/journal.pone.0172744

Clementi, N., Ghosh, S., De Santis, M., Castelli, M., Criscuolo, E., Zanoni, I., et al. (2021). Viral respiratory pathogens and lung injury. *Clin. Microbiol. Rev.* 34:e00103-20. doi: 10.1128/CMR.00103-20

Duan, X., Li, S., Holmes, J. A., Tu, Z., Li, Y., Cai, D., et al. (2018). MicroRNA 130a regulates both hepatitis C virus and hepatitis B virus replication through a central metabolic pathway. *J. Virol.* 92:e02009-17. doi: 10.1128/JVI.02009-17

Duraes-Carvalho, R., and Salemi, M. (2018). In-depth phylodynamics, evolutionary analysis and in silico predictions of universal epitopes of influenza a subtypes and influenza B viruses. *Mol. Phylogenet. Evol.* 121, 174–182. doi: 10.1016/j.ympev.2018.01.008

Farrukee, R., Leang, S. K., Butler, J., Lee, R. T. C., Maurer-Stroh, S., Tilmanis, D., et al. (2015). Influenza viruses with B/Yamagata- and B/Victoria-like neuraminidases are differentially affected by mutations that alter antiviral susceptibility. *J. Antimicrob. Chemother.* 70, 2004–2012. doi: 10.1093/jac/dkv065

Farrukee, R., Zarebski, A. E., McCaw, J. M., Bloom, J. D., Reading, P. C., and Hurt, A. C. (2018). Characterization of influenza B virus variants with reduced neuraminidase inhibitor susceptibility. *Antimicrob. Agents Chemother.* 62:e01081-18. doi: 10.1128/AAC.01081-18

Feng, L., Feng, S., Chen, T., Yang, J., Lau, Y. C., Peng, Z., et al. (2020). Burden of influenza-associated outpatient influenza-like illness consultations in China, 2006-2015: a population-based study. *Influenza Other Respir. Viruses* 14, 162–172. doi: 10.1111/irv.12711

Hay, A. J., Gregory, V., Douglas, A. R., and Lin, Y. P. (2001). The evolution of human influenza viruses. *Philos. Trans. R. Soc. Lond. Ser. B Biol. Sci.* 356, 1861–1870. doi: 10.1098/rstb.2001.0999

Jiao, B., Shi, X., Chen, Y., Ye, H., Yao, M., Hong, W., et al. (2017). Insulin receptor substrate-4 interacts with ubiquitin-specific protease 18 to activate the Jak/STAT signaling pathway. *Oncotarget* 8, 105923–105935. doi: 10.18632/oncotarget.22510

Jumat, M. R., Wong, P., Lee, R. T. C., Maurer-Stroh, S., Tan, B. H., and Sugrue, R. J. (2016). Molecular and biochemical characterization of the NS1 protein of non-cultured influenza B virus strains circulating in Singapore. *Microbial Genomics* 2:e000082. doi: 10.1099/mgen.0.000082

Kim, P., Jang, Y. H., Kwon, S. B., Lee, C., Han, G., and Seong, B. (2018). Glycosylation of hemagglutinin and neuraminidase of influenza a virus as signature for ecological spillover and adaptation among influenza reservoirs. *Viruses* 10:183. doi: 10.3390/v10040183

Li, Y., Li, S., Duan, X., Chen, Y., Jiao, B., Ye, H., et al. (2016). Interferon-stimulated gene 15 conjugation stimulates hepatitis B virus production independent of type I interferon signaling pathway in vitro. *Mediat. Inflamm.* 2016, 1–9. doi: 10.1155/2016/7417648

Liang, J., Li, Q., Cai, L., Yuan, Q., Chen, L., Lin, Q., et al. (2022). Adaptation of two wild bird-origin H3N8 avian influenza viruses to mammalian hosts. *Viruses* 1097:14. doi: 10.3390/v14051097

Liu, S. T. H., Behzadi, M. A., Sun, W., Freyn, A. W., Liu, W. C., Broecker, F., et al. (2018). Antigenic sites in influenza H1 hemagglutinin display species-specific immunodominance. *J. Clin. Invest.* 128, 4992–4996. doi: 10.1172/JCI122895

Liu, T., Wang, P., Meng, F., Ding, G., Wu, J., Song, S., et al. (2022). Incidence, circulation, and spatiotemporal analysis of seasonal influenza in Shandong, China, 2008-2019: a retrospective study. *Influenza Other Respir. Viruses* 16, 594–603. doi: 10.1111/irv.12959

Nakagawa, N., Kubota, R., Maeda, A., and Okuno, Y. (2004). Influenza B virus victoria group with a new glycosylation site was epidemic in Japan in the 2002-2003 season. *J. Clin. Microbiol.* 42, 3295–3297. doi: 10.1128/JCM.42.7.3295-3297.2004

Ng, A. K., Lam, M. K., Zhang, H., Liu, J., Au, S. W., Chan, P. K., et al. (2012). Structural basis for RNA binding and homo-oligomer formation by influenza B virus nucleoprotein. *J. Virol.* 86, 6758–6767. doi: 10.1128/JVI.00073-12

Nogales, A., Martinez-Sobrido, L., Topham, D. J., and DeDiego, M. (2018). Modulation of innate immune responses by the influenza a NS1 and PA-X proteins. *Viruses* 10:708. doi: 10.3390/v10120708

Paragas, J., Talon, J., O'Neill, R. E., Anderson, D. K., García-Sastre, A., and Palese, P. (2001). Influenza B and C virus NEP (NS2) proteins possess nuclear export activities. *J. Virol.* 75, 7375–7383. doi: 10.1128/JVI.75.16.7375-7383.2001

Saito, T., Nakaya, Y., Suzuki, T., Ito, R., Saito, T., Saito, H., et al. (2004). Antigenic alteration of influenza B virus associated with loss of a glycosylation site due to host-cell adaptation. *J. Med. Virol.* 74, 336–343. doi: 10.1002/jmv.20178

Sherry, L., Smith, M., Davidson, S., and Jackson, D. (2014). The N terminus of the influenza B virus nucleoprotein is essential for virus viability, nuclear localization, and optimal transcription and replication of the viral genome. *J. Virol.* 88, 12326–12338. doi: 10.1128/JVI.01542-14

Shi, X., Jiao, B., Chen, Y., Li, S., and Chen, L. (2017). MxA is a positive regulator of type I IFN signaling in HCV infection. *J. Med. Virol.* 89, 2173–2180. doi: 10.1002/jmv.24867

Takashita, E. (2021). Influenza polymerase inhibitors: mechanisms of action and resistance. *Cold Spring Harb. Perspect. Med.* 11:11. doi: 10.1101/cshperspect.a038687

Toure, C. T., Fall, A., Andriamandimby, S. F., Jallow, M. M., Goudiaby, D., Kiori, D., et al. (2022). Epidemiology and molecular analyses of influenza B viruses in Senegal from 2010 to 2019. *Viruses* 14:1063. doi: 10.3390/v14051063

Tsai, C. P., and Tsai, H. J. (2019). Influenza B viruses in pigs, Taiwan. *Influenza Other Respir. Viruses* 13, 91–105. doi: 10.1111/irv.12588

Tyrrell, C. S., Allen, J. L. Y., and Gkrania-Klotsas, E. (2021). Influenza: epidemiology and hospital management. *Medicine* 49, 797–804. doi: 10.1016/j.mpmed.2021.09.015

Wandzik, J. M., Kouba, T., and Cusack, S. (2021). Structure and function of influenza polymerase. *Cold Spring Harb. Perspect. Med.* 11:11. doi: 10.1101/cshperspect.a038372

Wang, Q., Tian, X., Chen, X., and Ma, J. (2007). Structural basis for receptor specificity of influenza B virus hemagglutinin. *Proc. Natl. Acad. Sci. U. S. A.* 104, 16874–16879. doi: 10.1073/pnas.0708363104

Wu, N. C., and Wilson, I. A. (2020). Structural biology of influenza hemagglutinin: an amaranthine adventure. *Viruses* 12:1053. doi: 10.3390/v12091053

Yuan, Y., Jiao, B., Qu, L., Yang, D., and Liu, R. (2023). The development of COVID-19 treatment. *Front. Immunol.* 14:1125246. doi: 10.3389/fimmu.2023.1125246

Zhu, G., Wang, R., Xuan, F., Daszak, P., Anthony, S. J., Zhang, S., et al. (2013). Characterization of recombinant H9N2 influenza viruses isolated from wild ducks in China. *Vet. Microbiol.* 166, 327–336. doi: 10.1016/j.vetmic.2013.05.013

frontiers | Frontiers in Microbiology

TYPE Original Research
PUBLISHED 22 June 2023
DOI 10.3389/fmicb.2023.1186510

OPEN ACCESS

EDITED BY
Wei Wei,
First Affiliated Hospital of Jilin University, China

REVIEWED BY
Milan Surjit,
Translational Health Science and Technology Institute (THSTI), India
Yan Li,
First Affiliated Hospital of Jilin University, China

*CORRESPONDENCE
Santanu Bose
✉ santanu.bose@wsu.edu

†These authors have contributed equally to this work and share first authorship

‡These authors have contributed equally to this work and share senior authorship

‡PRESENT ADDRESS
Swechha M. Pokharel,
Department of Microbiology,
Perelman School of Medicine,
University of Pennsylvania,
Philadelphia,
PA, United States

RECEIVED 14 March 2023
ACCEPTED 08 June 2023
PUBLISHED 22 June 2023

CITATION
Pokharel SM, Mohanty I, Mariasoosai C, Miura TA, Maddison LA, Natesan S and Bose S (2023) Human beta defensin-3 mediated activation of β-catenin during human respiratory syncytial virus infection: interaction of HBD3 with LDL receptor-related protein 5. *Front. Microbiol.* 14:1186510. doi: 10.3389/fmicb.2023.1186510

Human beta defensin-3 mediated activation of β-catenin during human respiratory syncytial virus infection: interaction of HBD3 with LDL receptor-related protein 5

Swechha M. Pokharel[1†§], Indira Mohanty[1†], Charles Mariasoosai[2], Tanya A. Miura[3], Lisette A. Maddison[4], Senthil Natesan[2‡] and Santanu Bose[1*‡]

[1]Department of Veterinary Microbiology and Pathology, College of Veterinary Medicine, Washington State University, Pullman, WA, United States, [2]College of Pharmacy and Pharmaceutical Sciences, Washington State University, Spokane, WA, United States, [3]Department of Biological Sciences, University of Idaho, Moscow, ID, United States, [4]Center for Reproductive Biology, College of Veterinary Medicine, Washington State University, Pullman, WA, United States

Respiratory Syncytial Virus (RSV) is a non-segmented negative-sense RNA virus belonging to the paramyxovirus family. RSV infects the respiratory tract to cause pneumonia and bronchiolitis in infants, elderly, and immunocompromised patients. Effective clinical therapeutic options and vaccines to combat RSV infection are still lacking. Therefore, to develop effective therapeutic interventions, it is imperative to understand virus-host interactions during RSV infection. Cytoplasmic stabilization of β-catenin protein results in activation of canonical Wingless (Wnt)/β-catenin signaling pathway that culminates in transcriptional activation of various genes regulated by T-cell factor/lymphoid enhancer factor (TCF/LEF) transcription factors. This pathway is involved in various biological and physiological functions. Our study shows RSV infection of human lung epithelial A549 cells triggering β-catenin protein stabilization and induction of β-catenin mediated transcriptional activity. Functionally, the activated β-catenin pathway promoted a pro-inflammatory response during RSV infection of lung epithelial cells. Studies with β-catenin inhibitors and A549 cells lacking optimal β-catenin activity demonstrated a significant loss of pro-inflammatory chemokine interleukin-8 (IL-8) release from RSV-infected cells. Mechanistically, our studies revealed a role of extracellular human beta defensin-3 (HBD3) in interacting with cell surface Wnt receptor LDL receptor-related protein-5 (LRP5) to activate the non-canonical Wnt independent β-catenin pathway during RSV infection. We showed gene expression and release of HBD3 from RSV-infected cells and silencing of HBD3 expression resulted in reduced stabilization of β-catenin protein during RSV infection. Furthermore, we observed the binding of extracellular HBD3 with cell surface localized LRP5 protein, and our *in silico* and protein–protein interaction studies have highlighted a direct interaction of HBD3 with LRP5. Thus, our studies have identified the β-catenin pathway as a key regulator of pro-inflammatory response during RSV infection of human lung epithelial cells. This pathway was induced during RSV infection via a non-canonical Wnt-independent mechanism involving paracrine/autocrine action of extracellular HBD3 activating cell surface Wnt receptor complex by directly interacting with the LRP5 receptor.

KEYWORDS

respiratory syncytial virus, human beta defensin-3, pro-inflammatory response, LDL receptor-related protein-5, β-catenin

Introduction

Respiratory Syncytial Virus (RSV) is a respiratory RNA virus causing pneumonia and bronchiolitis in infants, the elderly, and immunocompromised patients (Falsey et al., 2005; Nair et al., 2010; Griffiths et al., 2017). It is estimated that RSV infection is responsible for 30 million lower respiratory tract infections annually, primarily among children, which results in 3 million RSV infection-related hospitalizations and 200,000 death (Nair et al., 2010). Although prophylactic monoclonal antibodies (e.g., palivizumab; Romero, 2003) and antiviral agents such as ribavirin show variable clinical outcomes (Diseases, 1993), effective clinical therapeutic options to combat RSV infection are still lacking. Additionally, the RSV vaccine is currently unavailable (Hurwitz, 2011; Graham and Anderson, 2013), RSV-associated diseases like pneumonia and bronchiolitis manifest due to exaggerated inflammation in the airway (Imai et al., 2008; Murawski et al., 2009; Ruuskanen et al., 2011; Foronjy et al., 2016; Russell et al., 2017). Therefore, to develop effective therapeutic and prophylactic interventions, it is imperative to understand virus-host mechanisms during RSV infection.

Human lung epithelial cells play an important role in RSV infection since these cells are the major target of RSV during the early phases of respiratory tract infection (Kong et al., 2004; Kota et al., 2008; Hosakote et al., 2009; Chang et al., 2012; Shirato et al., 2012; Mgbemena et al., 2013; Hillyer et al., 2018; Corsello et al., 2022; Rajan et al., 2022). Productive infection of human lung epithelial cells by RSV results in the production of infectious progeny virion particles (Kong et al., 2004; Kota et al., 2008; Chang et al., 2012; Shirato et al., 2012; Mgbemena et al., 2013; Hillyer et al., 2018; Rajan et al., 2022). Although macrophages are the primary pro-inflammatory response generator during RSV infection, lung epithelial cells are the first innate immune responders in the airway since these cells are infected during the early phase of infection. Therefore, it is important to understand the virus-host mechanisms in human lung epithelial cells following RSV infection.

Canonical Wingless (Wnt)/β-catenin pathway is a well-established signaling cascade regulating the expression of Wnt target genes involved in various biological and physiological functions (Clevers, 2006; Zhan et al., 2017; Ren et al., 2021; Rim et al., 2022). Wnt is a soluble secreted extracellular protein that interacts with the cell surface Frizzled (Fzd) and LDL receptor-related proteins (LRP5 and LRP6) receptor complex to activate downstream events that prevent degradation of β-catenin protein in the cytoplasm. Stabilization of β-catenin protein results in its activation and subsequent translocation to the nucleus to act as a transcriptional activator of Wnt-responsive genes by associating with T-cell factor/lymphoid enhancer factor (TCF/LEF) transcription factors. Although many viruses, including respiratory viruses like influenza A virus, activate β-catenin via the Wnt pathway (More et al., 2018), to date, it is unknown whether RSV induces β-catenin activation and the role of any such activation in regulating host response during RSV infection.

Our study has demonstrated β-catenin activation by RSV in infected human lung epithelial A549 cells. Furthermore, we show β-catenin mediated transcriptional activity promoting pro-inflammatory response in RSV-infected A549 cells. Interestingly, in contrast to canonical Wnt ligand-dependent β-catenin pathway activation by extracellular Wnt ligands, we have uncovered a yet unknown non-canonical Wnt ligand-independent β-catenin pathway activation during RSV infection. We show extracellular human beta defensin-3 (HBD3) released from RSV-infected cells stabilizing β-catenin protein in infected cells. Furthermore, HBD3 interacted with Wnt receptor LRP5 to stabilize β-catenin protein for its activation of the β-catenin pathway in RSV-infected cells. Thus, in our current study, we have identified extracellular HBD3 as an "alarmin" molecule stimulating Wnt-independent β-catenin pathway in RSV-infected cells for triggering a pro-inflammatory response.

Results

Respiratory syncytial virus stabilizes β-catenin protein to activate β-catenin mediated transcriptional activation

Wnt/ β-catenin canonical pathway is activated following the activation of the Fzd/LRP receptor complex by extracellular Wnt ligand (Clevers, 2006; Zhan et al., 2017; Ren et al., 2021; Rim et al., 2022). This event prevents the degradation of β-catenin protein. Accumulation of β-catenin due to its stabilization results in its translocation to the nucleus. In the nucleus, β-catenin interacts with TCF/LEF transcription factors to transactivate Wnt-responsive genes. So far, it is still unknown whether RSV activates the β-catenin pathway. Therefore, we investigated whether RSV stabilizes β-catenin protein leading to activation of TCF/LEF transcription factor-driven transactivation of Wnt-target genes.

First, we investigated whether RSV infection triggers β-catenin protein stabilization since this event results in β-catenin-mediated transcriptional activation of Wnt-responsive genes. To evaluate the status of β-catenin protein, we infected human lung epithelial A549 cells with RSV. At various post-infection time-periods, the level of β-catenin protein was assessed by western blotting with anti-β-catenin antibody. RSV infection triggered β-catenin protein stabilization since enhanced levels of β-catenin protein were detected in RSV infected cells (Figures 1A,B).

We next examined whether the accumulation of β-catenin protein in RSV-infected cells resulted in the activation of TCF/LEF transcription factors. For these studies, we transfected A549 cells with TOP-Flash luciferase reporter plasmid. TOP-Flash luciferase reporter contains a promoter for binding (and activation) of activated TCF/LEF transcriptional factors upstream of the luciferase gene (Lin et al., 2016; Lee et al., 2022). Therefore, TOP-Flash luciferase reporter is widely used to study transcriptional activation by β-catenin. A549 cells transfected with TOP-Flash reporter were infected with RSV, followed by luciferase assay analysis of the cell lysate. In accordance with enhanced accumulation of β-catenin protein (Figures 1A,B), RSV

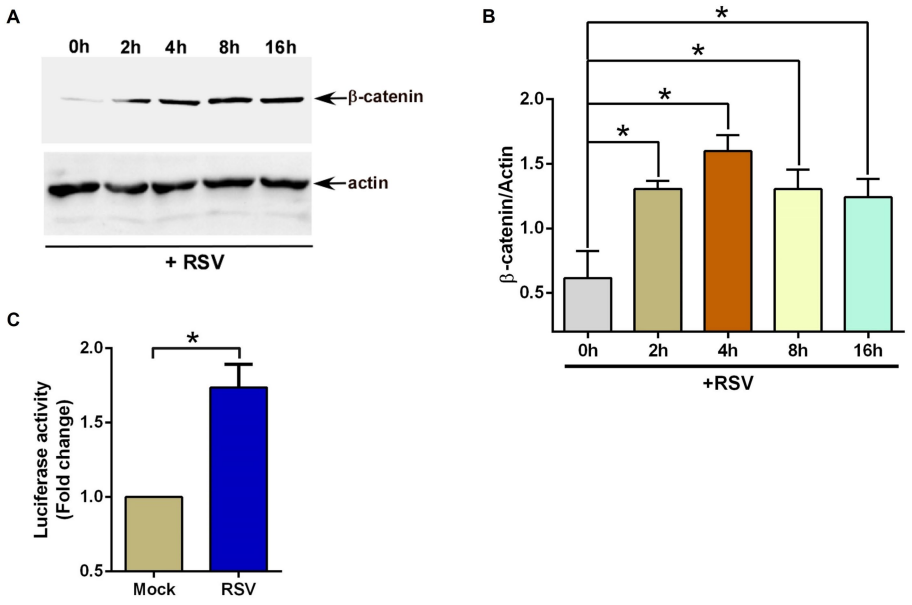

FIGURE 1
RSV induces β-catenin during infection of lung epithelial cells. **(A)** Human lung epithelial A549 cells were infected with RSV (MOI=1) for 0–16h. β-catenin and actin levels were determined in cell lysates by western blotting using corresponding antibodies. **(B)** Densitometry analysis of β-catenin protein levels relative to actin protein (β-catenin/Actin) in RSV-infected A549 cells. **(C)** TOP-Flash luciferase assay of A549 cells co-transfected with firefly-luciferase-TOP-Flash and renilla-luciferase plasmids. Co-transfected cells were infected with RSV (MOI=1) for 16h. A dual luciferase reagent was utilized to determine firefly and renilla luciferase activity. The relative TOP-Flash luciferase activity was calculated based on the mean value of firefly/renilla luciferase activity. The value is represented as a fold change in TOP-Flash activity in RSV-infected cells compared to mock infected cells. The densitometric values represent the mean±SEM from three independent studies (*$p \leq 0.05$). Luciferase assay represents mean±SEM from three independent experiments performed in triplicates [*$p \leq 0.05$ (n=24; technical replicates)].

also activated β-catenin-dependent transcriptional activity since RSV infection resulted in luciferase gene expression via TCF/LEF transcription factor-dependent promoter activity (Figure 1C). These results suggested RSV mediated enhanced stability and accumulation of β-catenin protein and subsequent activation of β-catenin mediated transcriptional activity in infected lung epithelial cells.

β-Catenin activity is required for an optimal pro-inflammatory response during RSV infection

Compared to macrophages, human lung epithelial cells like A549 cells do not robustly produce pro-inflammatory cytokines like TNF, IL-6, and IL-1β. Instead, RSV-infected A549 cells trigger efficient production of pro-inflammatory chemokine IL-8 (in humans, IL-8 is encoded by the *CXCL8* gene; Fiedler et al., 1995; Thomas et al., 2000; Rudd et al., 2005). IL-8 is a major neutrophil chemoattractant (Baggiolini et al., 1989; Bazzoni et al., 1991), and neutrophils are implicated in the development of exaggerated RSV-associated lung disease in children and infants (Everard et al., 1994; McNamara et al., 2003; Emboriadou et al., 2007; Sebina and Phipps, 2020). High levels of IL-8 have been detected in infants with severe RSV-associated bronchiolitis (Biswas et al., 1995). Furthermore, IL-8 serves as a biomarker for RSV-associated lung disease severity (Bont et al., 1999). Therefore, we evaluated the pro-inflammatory response in RSV-infected human lung epithelial A549 cells by analyzing the production of IL-8 following the blocking of β-catenin activity by two widely used β-catenin inhibitors, iCRT3, and iCRT14 (Gonsalves et al., 2011; Trujano-Camacho et al., 2021). These inhibitors block β-catenin-mediated transcriptional activity by inhibiting the interaction of β-catenin with TCF/LEF transcription factors.

To assess the role of β-catenin activity, A549 cells were treated with either DMSO (vehicle control) or β-catenin inhibitors (iCRT3 and iCRT14) during RSV infection. Medium supernatant was collected from infected cells to analyze IL-8 production by ELISA. β-catenin activity is essential for an optimal pro-inflammatory response during RSV infection, since significant loss of IL-8 production was observed in cells treated with β-catenin inhibitors (Figures 2A,B). Approximately 50% loss of pro-inflammatory response in RSV-infected cells was noted following β-catenin activity inhibition (Figures 2A,B). To confirm that diminished pro-inflammatory response is not due to reduced RSV infection, we used recombinant RSV expressing mKate2 protein (mKate2-RSV; Bedient et al., 2020). Treatment of cells with β-catenin inhibitors did not alter RSV replication/infection as deduced by western blot analysis of cell lysate with anti-RFP antibody, which detects mKate2 protein (Figures 2C–F). These results demonstrated an important role of β-catenin activity in supporting optimal pro-inflammatory response during RSV infection of human lung epithelial A549 cells.

β-Catenin expression is required for an optimal pro-inflammatory response during RSV infection

Since blocking β-catenin activity resulted in dampened pro-inflammatory response during RSV infection (Figures 2A,B),

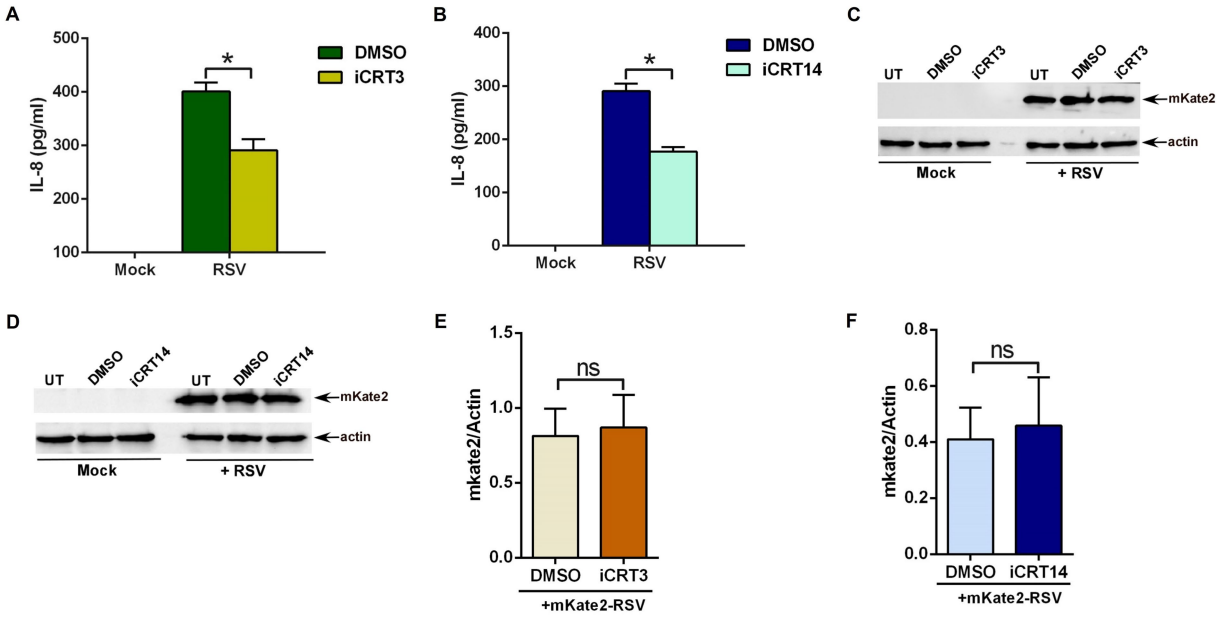

FIGURE 2
β-catenin activity is required for an optimal pro-inflammatory response during RSV infection. **(A)** Human lung epithelial A549 cells were infected with RSV (MOI=3) in the presence of either DMSO (vehicle control) or β-catenin inhibitor iCRT3 (25μM). Medium supernatant collected from these cells was analyzed for IL-8 production by ELISA. **(B)** A549 cells were infected with RSV (MOI=3) in the presence of either DMSO (vehicle control) or β-catenin inhibitor iCRT14 (25μM). Medium supernatant collected from these cells was analyzed for IL-8 production by ELISA. **(C)** A549 cells were infected with recombinant RSV expressing mKate2 protein (RSV-mKate2; MOI=1) in the presence of either DMSO (vehicle control) or β-catenin inhibitor iCRT3 (25μM). Cell lysate collected from these cells was subjected to western blotting with an anti-RFP antibody to detect the mKate2 protein. **(D)** A549 cells were infected with RSV-mKate2 (MOI=1) in the presence of either DMSO (vehicle control) or β-catenin inhibitor iCRT14 (25μM). Cell lysate collected from these cells was subjected to western blotting with an anti-RFP antibody to detect the mKate2 protein. **(E,F)** Densitometry analysis of mKate2 protein levels relative to actin protein (mKate2/Actin) in RSV-mKate2 infected A549 cells treated with either DMSO or β-catenin inhibitors (iCRT3 and iCRT14). ELISA data are shown as Mean±SEM [*$p \leq 0.05$ (n=22; technical replicates; three independent experiments)]. The densitometric values represent the mean±SEM from three independent studies (*$p \leq 0.05$). ns; non-significant.

we further validated these results by using CRISPR-Cas9 genome-editing (Ran et al., 2013; Hsu et al., 2014; Musunuru, 2017; Hillary and Ceasar, 2022; Wang et al., 2022; Zhu, 2022) to obtain stable A549 cells lacking optimal β-catenin activity. We decided to generate a truncated version of β-catenin since previous studies have highlighted the existence of a compensatory mechanism in case of complete loss of β-catenin protein in cells (Liu et al., 2022). Several homologs exist for the Wnt/β-catenin pathway, which gives rise to redundancy to fall back on an alternative cellular pathway (Liu et al., 2022). To avoid this complication, we obtained a cell line with truncated β-catenin protein rather than generating β-catenin null cells.

The typical strategy for employing CRISPR/Cas9 to disrupt a gene has been to target near the 5′ end and isolate a mutation that should lead to a frameshift and premature termination codon and no protein would be expected (Hsu et al., 2014). Instead of such a null cell line, we isolated a clone harboring a 425 bp deletion which removes part of intron 2 extending into exon 3 (Supplementary Figure S1). Western blot analysis showed full-length (FL) 92 kDa β-catenin protein in wild-type (FL-catenin A549cells) control cells expressing control or scrambled guide-RNA (gRNA; Figure 3A). In contrast, a truncated 82 kDa β-catenin protein was detected in A549 cells with the CRISPR induced deletion (Δ-catenin A549 cells; Figure 3A). The truncated β-catenin protein observed on the western blot is the likely result of the 425 bp deletion, with splicing expected from exon 2 to exon 4 (Supplementary Figure S1). This would result in a CTNNB1 (CTNNB1 gene encodes β-catenin protein) isoform of approximately 10 kDa less than the wild-type and lacking the 77 amino acids encoded by exon 3.

To validate the loss of β-catenin activity in Δ-catenin cells, we transfected FL-catenin and Δ-catenin cells with TOP-Flash luciferase reporter plasmid. Transfected cells were then treated with lithium chloride (LiCl), a potent inducer of β-catenin-mediated transcriptional activity (Clément-Lacroix et al., 2005; Lin et al., 2016; Lee et al., 2022). Luciferase assay revealed robust induction of β-catenin mediated transcriptional activity in FL-catenin cells (Figure 3B). In contrast, significant loss of such activity (reduction by 50%) was noted in LiCl treated Δ-catenin cells (Figure 3B). This result demonstrated dampened β-catenin dependent transcriptional activity in Δ-catenin cells.

Next, we investigated whether β-catenin activity is required for a pro-inflammatory response during RSV infection. For these studies, we infected FL-catenin and Δ-catenin cells with RSV. As expected, RSV triggered a pro-inflammatory response in FL-catenin cells since high levels of IL-8 was produced from infected FL-catenin cells (Figure 3C). In contrast, drastic loss (reduction by 75%) of IL-8 production was observed in RSV infected Δ-catenin cells (Figure 3C). These results demonstrated a key requirement of β-catenin activity for a pro-inflammatory response during RSV infection of lung epithelial cells.

Human beta-defensin 3 stabilizes β-catenin protein to activate the β-catenin-mediated transcriptional activation

To identify non-canonical extracellular ligands for activation of the β-catenin pathway via a Wnt-independent mechanism, we focused

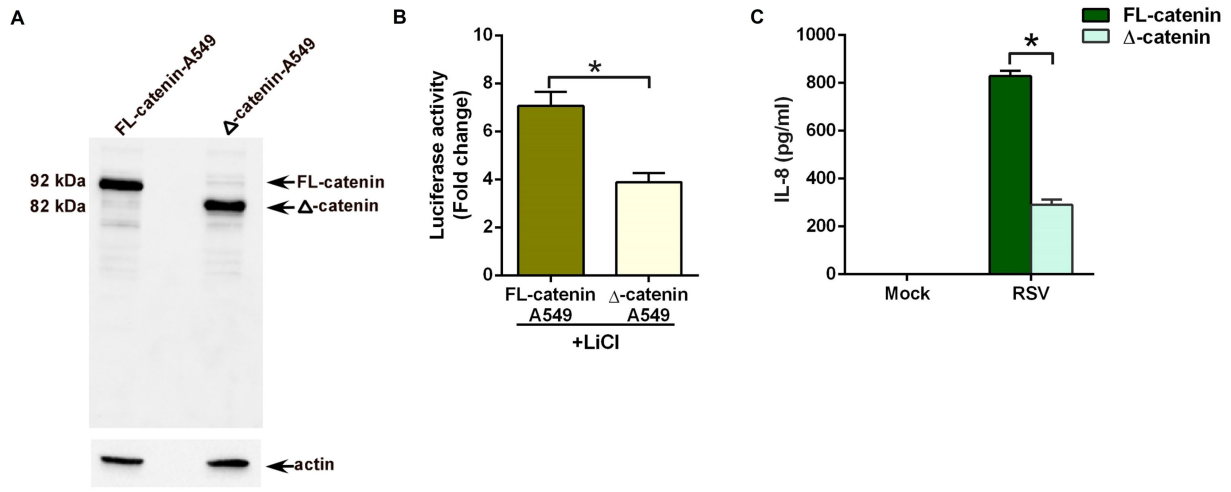

FIGURE 3
Reduced pro-inflammatory response during RSV infection of lung epithelial cells lacking full-length β-catenin protein. **(A)** CRISPR-Cas9 technology was used to generate stable human lung epithelial A549 cells lacking full-length β-catenin protein. Cell lysates from A549 cells expressing full-length 92kDa β-catenin protein (FL-catenin-A549 cells) and A549 cells expressing truncated 82kDa β-catenin protein (Δ-catenin-A549 cells) were subjected to western blotting with β-catenin antibody. **(B)** TOP-Flash luciferase assay of A549 cells expressing either FL-catenin or Δ-catenin were co-transfected with firefly-luciferase-TOP-Flash and renilla-luciferase plasmids. Co-transfected cells were treated with Lithium Chloride (LiCl; 25mM) for 24h. A dual luciferase reagent was utilized to determine firefly and renilla luciferase activity. The relative TOP-Flash luciferase activity was calculated based on the mean value of firefly/renilla luciferase activity. The value is represented as a fold change in TOP-Flash activity in LiCl-treated cells compared to vehicle (water) treated cells. **(C)** A549 cells expressing either FL-catenin or Δ-catenin were infected with RSV (MOI=3). Medium supernatant collected from these cells was analyzed for IL-8 production by ELISA. Luciferase assay represents mean±SEM from two independent experiments performed in triplicates [*$p \leq 0.05$ (n=16; technical replicates)]. ELISA data are shown as Mean±SEM [*$p \leq 0.05$ (n=24; technical replicates; three independent experiments)].

our attention on human beta-defensins or HBDs. HBDs (primarily HBD1-3) are cationic anti-microbial peptides derived from mucosal epithelial cells (Fruitwala et al., 2019; Xu and Lu, 2020). HBDs are released to the extracellular milieu upon infection, and they constitute an important innate defense factor against invading pathogens, including viruses. We have previously shown that single-stranded non-segmented RNA viruses like RSV (Kota et al., 2008) and VSV (vesicular stomatitis virus; Basu et al., 2010) triggers the release of HBD2 and HBD3, respectively, in the extracellular milieu and these HBDs block viral cellular entry. More importantly, one study reported β-catenin activation by HBD3 in human non-epithelial dental cells (human periodontal ligament cells; Zhou et al., 2018). Based on these previous studies, we next investigated whether extracellular HBD3 is capable of modulating β-catenin protein stability and β-catenin-associated transcriptional activity in lung epithelial cells.

We first evaluated the ability of purified HBD3 to activate the β-catenin pathway by stabilizing cytoplasmic β-catenin protein. For these studies, we treated A549 cells with purified HBD3 (10 μg/ml) for 16 h. Previous studies showed that treating A549 cells with more than 20 μg/ml of purified HBD3 protein triggers cytotoxicity (Su et al., 2018). Therefore, we used 10 μg/ml of HBD3 protein to ensure cell viability. Treated cells were subjected to western blot analysis with anti-β-catenin antibody. HBD3 treatment led to enhanced β-catenin protein levels due to its stabilization (Figures 4A,B). Next, we investigated whether purified HBD3 triggers β-catenin-dependent transcriptional activity in A549 cells. A549 cells transfected with TOP-Flash luciferase reporter plasmid were treated with purified HBD3 for 16 h. Subsequent luciferase assay with cell lysates revealed activation of β-catenin-mediated transcriptional activity by HBD3 (Figure 4C). Thus, we have identified HBD3 as an extracellular ligand involved in Wnt ligand-independent β-catenin activation in lung epithelial cells.

HBD3 is induced/released during RSV infection of human lung epithelial cells

Similar to RSV-infected cells (Figure 1), HBD3 also activated β-catenin-mediated transcriptional activity (Figure 4). Therefore, we next investigated the possibility of RSV inducing HBD3 expression and its release from infected cells to stabilize β-catenin protein via autocrine/paracrine action. To examine HBD3 expression during RSV infection, we assessed HBD3 mRNA levels in A549 cells during RSV infection. Although HBD3 is expressed at basal levels in uninfected cells, RSV infection induced HBD3 expression, since PCR analysis revealed enhanced levels of HBD3 transcripts in RSV-infected A549 cells compared to mock-infected cells (Figures 5A,B). The enhanced expression also resulted in HBD3 release into the extracellular milieu following RSV infection as determined by performing ELISA analysis with medium supernatant obtained from RSV-infected A549 cells (Figure 5C). These results demonstrated RSV-mediated induction of HBD3 expression for its release from infected lung epithelial cells.

HBD3 is involved in β-catenin protein stabilization during RSV infection

Next, we investigated whether HBD3 plays any role in modulating β-catenin protein stability during RSV infection. We focused on

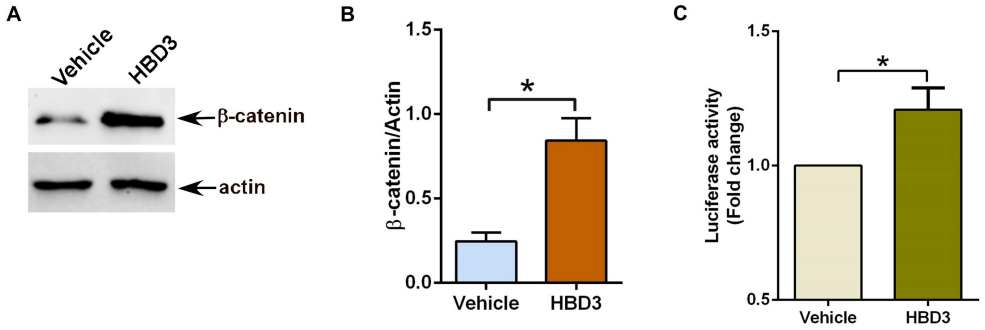

FIGURE 4
Human defensin-3 induces β-catenin activity in lung epithelial cells. **(A)** Human lung epithelial A549 cells were treated with either vehicle (0.1% BSA in PBS) or purified human defensin-3 (HBD3) protein (10μg/ml) for 16h. β-catenin and actin levels were determined in cell lysates by western blotting using corresponding antibodies. **(B)** Densitometry analysis of β-catenin protein levels relative to actin protein (β-catenin/Actin) in the vehicle and HBD3-treated A549 cells. **(C)** TOP-Flash luciferase assay of A549 cells co-transfected with firefly-luciferase-TOP-Flash and renilla-luciferase plasmids. Co-transfected cells were treated with either vehicle (0.1% BSA in PBS) or HBD3 for 16h. A dual luciferase reagent was utilized to determine firefly and renilla luciferase activity. The relative TOP-Flash luciferase activity was calculated based on the mean value of firefly/renilla luciferase activity. The value is represented as a fold change in TOP-Flash activity in HBD3-treated cells compared to vehicle-treated cells. The densitometric values represent the mean±SEM from three independent studies (*$p \leq 0.05$). Luciferase assay represents mean±SEM from two independent experiments performed in triplicates [*$p \leq 0.05$ ($n=6$; technical replicates)].

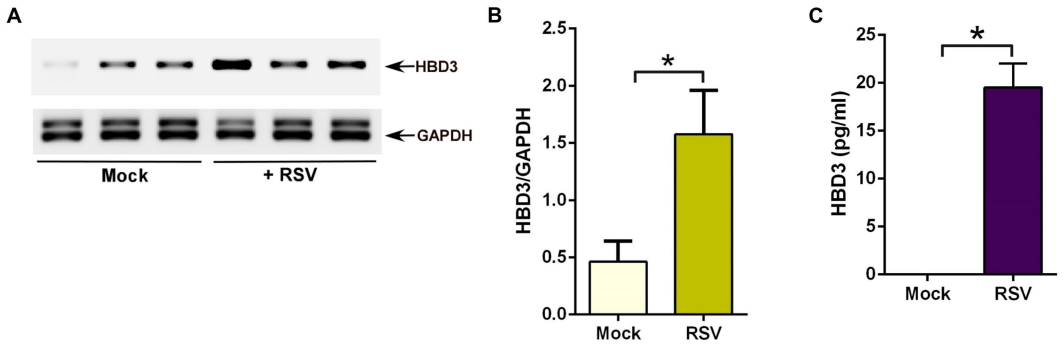

FIGURE 5
RSV induces HBD3 expression and release from lung epithelial cells. **(A)** Human lung epithelial A549 cells were infected with RSV (MOI=1) for 16h. RNA isolated from these cells was subjected to RT-PCR to analyze the expression of HBD3 and GAPDH (loading control). The PCR from three independent experiments (each lane corresponds to each independent experiment) are shown in the mock-infected and RSV-infected panels. **(B)** Densitometry analysis of HBD3 mRNA levels relative to GAPDH mRNA (HBD3/GAPDH) in mock vs. RSV-infected (16 post-infection) A549 cells. **(C)** Medium supernatant collected from RSV-infected (MOI=1; 16h post-infection) A549 cells were analyzed for HBD3 release by ELISA. The densitometric values represent the mean±SEM from three independent studies (*$p \leq 0.05$). ELISA data are shown as Mean±SEM [*$p \leq 0.05$ ($n=18$; technical replicates; three independent experiments)].

β-catenin protein stability since stabilization of β-catenin protein results in activation of β-catenin mediated transcriptional activity, including expression/production of pro-inflammatory mediator IL-8. For these studies, we silenced HBD3 expression in A549 cells by siRNA. Efficient silencing was evident from western blot analysis showing reduced HBD3 protein levels in cells transfected with HBD3-specific siRNA compared to cells transfected with control scrambled siRNA (Figures 6A,B). HBD3 silenced cells were subsequently infected with RSV to evaluate β-catenin protein status during infection. As expected, RSV infection resulted in enhanced β-catenin protein levels due to its stabilization during infection of control siRNA transfected cells (Figure 6C). Interestingly, such stabilization of β-catenin protein was lacking in RSV infected cells silenced for HBD3 expression (Figures 6C,D). These results demonstrated the role of HBD3 in stabilizing β-catenin protein during RSV infection. Thus, HBD3 acts as a non-Wnt ligand to stabilize β-catenin protein for triggering β-catenin-mediated transcriptional activity in RSV-infected lung epithelial cells.

Interaction of HBD3 with LRP5

We have identified HBD3 as a ligand involved in β-catenin activation during RSV infection. Therefore, we next investigated the mechanism by which HBD3 may confer its β-catenin activation function. Nineteen different Wnt ligands engage with cell surface receptor complexes comprising of 10 different frizzled receptors (Fzd) and LRP5/6 to activate β-catenin by triggering its stabilization (Clevers, 2006; Zhan et al., 2017; Ren et al., 2021; Rim et al., 2022). In the absence of Wnt signaling, β-catenin associates with the dissociation complex (Axin, GSK-3, APC, CK1) to undergo ubiquitin-proteasome mediated degradation. However, binding of Wnt ligands to the Fzd/

10.3389/fmicb.2023.1186510

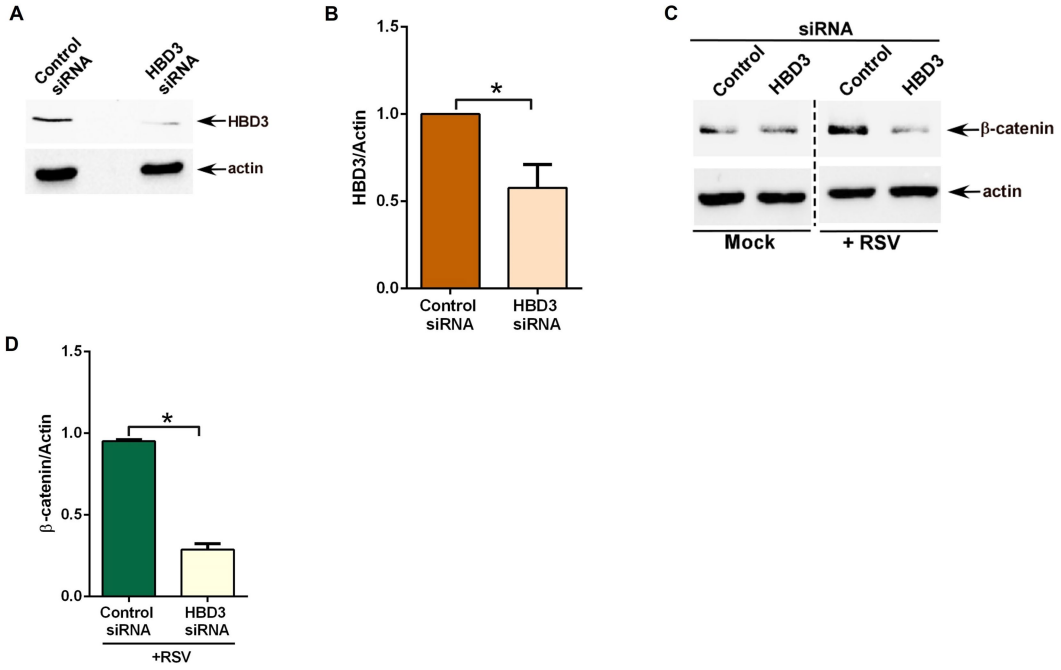

FIGURE 6
HBD3 promotes β-catenin protein stabilization during RSV infection of lung epithelial cells. **(A)** Human lung epithelial A549 cells were transfected with either control scrambled siRNA or siRNA specific for HBD3. HBD3 and actin levels were determined in cell lysates of siRNA-transfected cells by western blotting using corresponding antibodies. **(B)** Densitometry analysis of HBD3 protein levels relative to actin protein (HBD3/Actin) in control siRNA and HBD3 siRNA transfected A549 cells. **(C)** Control siRNA and HBD3 siRNA transfected cells were infected with RSV (MOI=1) for 16h. β-catenin and actin levels were determined in cell lysates by western blotting using corresponding antibodies. **(D)** Densitometry analysis of β-catenin protein levels relative to actin protein (β-catenin/Actin) in RSV-infected A549 cells transfected with either control siRNA or HBD3 siRNA. The densitometric values represent the mean±SEM from three independent studies (*$p \leq 0.05$).

LRP receptor complex transduces a signal to disrupt the dissociation complex, and as a result, β-catenin protein is stabilized due to loss of its degradation via the proteasome. Subsequently, β-catenin is targeted to the nucleus for transactivation of Wnt-responsive genes.

To identify whether HBD3 can interact with Wnt receptors, we first evaluated the plausible interaction of HBD3 with LRP5. We chose LRP5 since, unlike human Fzd receptors, which consist of 10 structurally related proteins, Wnt can trigger signaling by interacting with LRP5 in complex with one of the Fzd receptors. We initially examined the possible interaction of extracellular HBD3 with cell surface localized LRP5 by using purified biotinylated-HBD3 protein (biot-HBD3). The interaction of extracellular HBD3 with cell surface localized LRP5 was studied by incubating chilled (to prevent internalization of biot-HBD3 added extracellularly) A549 cells over-expressing FLAG-tagged LRP5 protein with biot-HBD3. After incubation, cell lysate precipitated with avidin-agarose, was subjected to western blotting with anti-FLAG antibody to detect FLAG-LRP5. HBD3 interacted with cell surface LRP5, since immune-blotting of avidin-precipitated lysate with anti-FLAG antibody detected FLAG-LRP5 protein (Figure 7A). In contrast, such interaction was not noted in control cells expressing empty FLAG plasmid (Figure 7A).

Since we observed the interaction of HBD3 with cell surface LRP5, we next evaluated whether this interaction constitutes direct binding between two proteins. This study was important since well-established Wnt ligands directly interact with LRP5 protein. LRP5 protein is a large 180 kDa protein comprising several distinct extracellular domains, including four β-propeller domains (P1, P2, P3, P4), four EGF-like domains (E1, E2, E3, E4), and three LDLR type A domains (Figure 7B). Four β-propeller domains (P1, P2, P3, P4) and four EGF-like domains (E1, E2, E3, E4) are tandemly located next to each other and are designated as PE1, PE2, PE3, and PE4 domains (Figure 7B). Wnt1, Wnt2, Wnt2b, Wnt6, Wnt8a, Wnt9a, Wnt9b, Wnt10b interacts with PE1and PE2 domain of LRP5, whereas Wnt3, Wnt3a binds to the P3 domain of LRP5 to activate β-catenin signaling. We first examined whether HBD3 interacts with the PE3 extracellular domain of LRP5. For these studies, we used truncated recombinant purified LRP5 protein (aa769–aa1016, 28 kDa) encompassing majority of the PE3 (major portion of P3 and full portion of E3) domain and partial segment of the PE4 (only the N-terminal portion of P4) domain of LRP5 protein (Figure 7B). For cell-free *in vitro* interaction assay, we incubated purified non-biotinylated HBD3 (control) and biotinylated-HBD3 proteins with avidin-agarose. Subsequently, avidin-agarose beads were incubated with recombinant purified truncated LRP5 protein. Following incubation, the bound proteins were subjected to western blotting with an anti-LRP5 antibody. Our studies revealed direct interaction of HBD3 with LRP5 since we detected the HBD3-LRP5 complex bound to the agarose beads (Figure 7C). Interestingly, HBD3 interacted with the same region of LRP5 protein involved in binding to the Wnt and Wnt3a ligand. Thus, our studies have identified HBD3 as a new ligand for the LRP5 receptor involved in β-catenin activation. We also show that the PE3 domain of LRP5 is involved in interaction with HBD3.

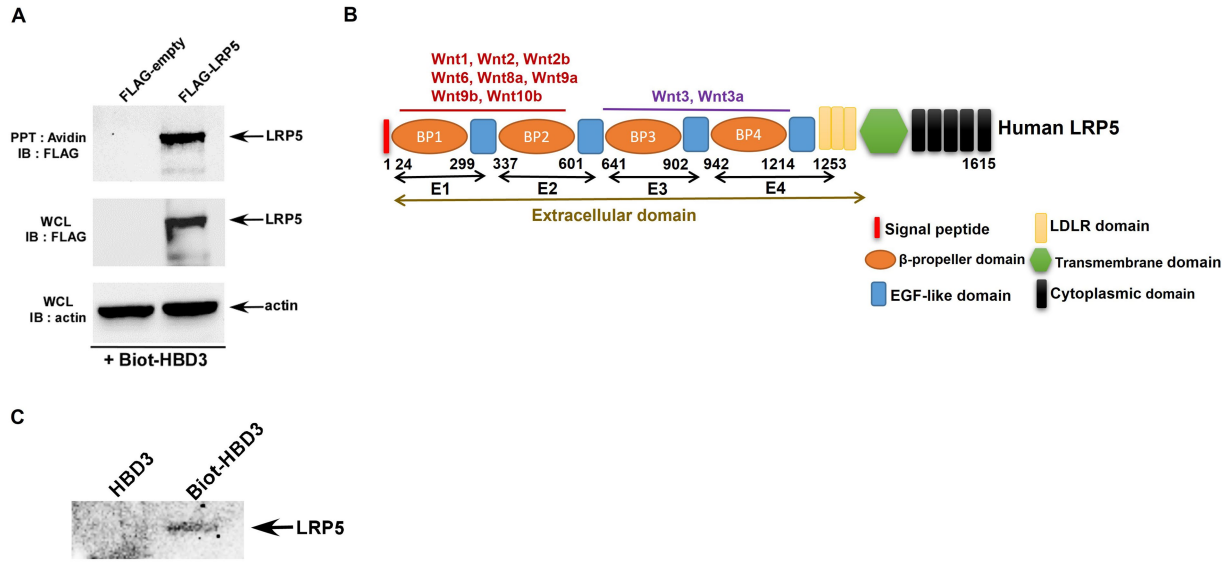

FIGURE 7
Interaction of HBD3 with LRP5. **(A)** Human lung epithelial A549 cells were transfected with either empty FLAG plasmid (FLAG-empty) or plasmid encoding FLAG-tagged LRP5 protein (FLAG-LRP5). Chilled FLAG-empty and FLAG-LRP5 A549 cells were incubated with biotinylated purified HBD3 protein (Biotin-HBD3) at 4°C for 4h. Following incubation, cell lysates were precipitated (PPT) with avidin-agarose and subsequently immuno-blotted (IB) with FLAG antibody to detect LRP5. Whole-cell lysates (WCL) were also blotted with FLAG and actin antibodies. **(B)** A schematic showing the domain structure of the LRP5 protein. **(C)** Biot-HBD3 and non-biotinylated HBD3 (control) were precipitated (PPT) with avidin-agarose. The avidin-agarose was then incubated with purified truncated LRP5 protein comprising of the E3 and E4 domains of the extracellular domain of LRP5. Following incubation, the agarose-avidin-bound protein was subjected to immunoblotting with the LRP5 antibody. The immune blots are representative of three independent experiments with similar results.

In silico studies of HBD3-LRP5 interaction

Since HBD3 directly interacted with LRP5, we next performed a series of *in silico* modeling studies to obtain detailed information about the LRP5-HBD3 interaction.

Modeling the binary (LRP5-HBD3) and ternary (LRP5-HBD3-FZD) complexes

Wnt ligands interact promiscuously with 10 FZD receptors and two LRPs (LRP5 and LRP6), and each Wnt ligand has the potential to activate several pairs of LRP and FZD receptors (Janda et al., 2012; Dijksterhuis et al., 2015). Previous studies have revealed that the Wnt ligands are likely sandwiched between the LRP5 and FZD8 receptors to form the LRP5-Wnt-FZD8 heterotrimer interaction complex (Hirai et al., 2019). As our study reveals that HBD3 activates the β -catenin pathway through interactions with LRP5, we hypothesize that HBD3 acts like a Wnt ligand in a manner similar to other known Wnt ligands. Therefore, we used the LRP5-Wnt-FZD8 ternary interaction model as a template to generate the plausible binary (LRP5-HBD3) and ternary (LRP5-HBD3-FZD8) complexes. To generate such a model, initially, HBD3 was docked to LRP5, and the resulting LRP5-HBD3 complex was subsequently docked to the FZD8 receptor.

Docking of LRP5 and HBD3

LRP5 belongs to a single-pass transmembrane family of proteins. The extracellular portion of LRP5 consists of four β-propeller domains (P1, P2, P3, P4) connected by epidermal growth factor (EGF)-like domains (E1, E2, E3, E4), and three LDLR (low-density lipoprotein receptor) type A (LA) domains preceding the transmembrane helix (Figure 7B; Supplementary Figures S2A,B; Matoba et al., 2017). Each pair of the four β-propeller and EGF-like domains are designated as PE1, PE2, PE3, and PE4 (Figure 7B). As the LRP5 structure is unavailable, LRP6, the nearest homolog with ~70% sequence identity, was used as a template for homology modeling of the PE3-PE4 domains of LRP5. Earlier studies indicate that Wnt and other ligands of LRP5 bind at the PE3 domain of LRP5 (Ahn et al., 2011; Bourhis et al., 2011; Cheng et al., 2011; Zebisch et al., 2016; Hirai et al., 2019). Therefore, the residues from the LRP5-PE3 domain namely, A667, V694, E721, T737, N762, W780, R805, D824, H847, W863, V889, and M890 were chosen as the interaction site for docking of HBD3 (Supplementary Figure S2C; Cheng et al., 2011). Since there were no sequence similarities between HBD3 and other known LRP5 interacting proteins, all residues of HBD3 were considered for docking. As a novel binding partner of LRP5, the docking of HBD3 without predefined residues was expected to predict the potential binding interface between LRP5 and HBD3 in an unbiased manner. The optimal binding conformation of HBD3 with LRP5 with a HADDOCK score of −146.2 showed several non-bonded interactions at the interface. HBD3 residues such as Y5, P19, G20, I24, G23, T27, R31, Y32, and R36 formed prominent interactions with the LRP5 PE3 domain residues R652, E676, S695, Y719, W780, R805, D824, H847, H974 and G1007 to form a stable complex. The resultant HBD3-LRP5 complex was then used for subsequent docking to the FZD8 receptor (Figure 8A).

Docking of FZD8 to the LRP5-HBD3 complex

FZD8 receptors are class F G protein-coupled receptors (GPCRs) and are known to activate the canonical β-catenin pathway (Wright et al., 2019). FZD8 receptors form heterodimeric signaling complexes

with LPR5/6 through their conserved extracellular cysteine-rich domain (Tsutsumi et al., 2020). The FZD8-Wnt complex's crystal structures show that Wnt interacts with FZD8 at two locations to form the complex (Supplementary Figure S3A). Therefore, the LPR5-HBD3 complex was docked independently at the two known sites of the FZD8 receptor, namely site-1 and site-2. Site-1 comprised of residues, such as E68, Q71, F72, Y92, F127, P130, D131, and R132 and site-2 comprised of residues, such as I46, Y48, F86, I95, L97, D99, Y100, K102, L104, L147, M149, D150, and N152 (Supplementary Figures S3B,C). The HBD3 residues, except those interacting with LRP5, were chosen as the potential FZD8-interacting site. Among the two sites of the FZD8 receptor, site 2 exhibited a higher binding affinity towards the LRP5-HBD3 complex. The binding energy, calculated as docking score, of the FZD8 with LRP5-HBD3 complex at site 2 (−95.7) was observed to be higher than that of site 1 (−85.3). In this high-affinity binding mode, FZD8 formed interactions with both HBD3 and the LRP5 receptor. Most notably, in this binding mode, HBD3 was seen sandwiched between FZD8 and LRP5, reminiscent of the LRP5-Wnt-FZD8 complex (Figures 8A,B). Several residues from site 2 of FZD8, including I46, G47, E77, P82, D83, F86, E98, D99, Y125, and Y151, formed non-bonded contacts with the residues of HBD3 (C40, V42, K48, R58, R60, and R65) and LRP5 (K953, R997, and H1197), respectively (Figures 8C–G).

MD simulations of the binary and ternary complexes

To examine the stability of the interactions among the LRP5-HBD3 and LRP5-FZD8-HBD3 complexes, we performed MD simulations of the complexes, each for 500 ns. Overall, the binary and ternary complexes were observed to be stable throughout the simulation time. During the first 50–100 ns of the simulations, the complexes underwent notable conformational changes (reflected by the RMSD value of ~5 Å), finetuning interactions between the interfaces, and then stabilized through the rest of the simulation time (Supplementary Figure S4).

H-bonds at the interfaces

To evaluate the critical H-bonds involved in formation and stabilization of the complexes, all three interface hydrogen bond interactions (LRP5-HBD3, HBD3-FZD, and FZD8-LRP5) were analyzed (Figures 8A,B). Several H-bonds were observed among the interacting proteins. However, only a set of H-bonds were found stable for most of the simulation time and are discussed here (boxes in Figure 8C). Interestingly, there were many H-bonds observed in the LRP5-HBD3 interface, of which the most stable ones formed around 100 ns into the simulation. The N-terminal residues M1 and H4 of HBD3 were found to interact with sidechain carboxylic oxygens of E714 and backbone amide nitrogen of H974 of LRP5, respectively (Figure 8D). During the simulation, M1 and H4 of HBD3 moved closer to E714 and H974 of LRP5 and formed H-bonds. Similarly, the sidechain amino group of K675 forms H-bonds with backbone carbonyl oxygens of L13 and L15 of HBD3 (Figure 8E). These H-bonds with were found to be consistent after 200 ns of the simulation (Figure 9A).

In the case of the HBD3-FZD8 interaction interface, K30 of HBD3 formed H-bonds with sidechain ε nitrogen of H124 (Figure 8F). Similarly, the C40 backbone amide nitrogen of HBD3 interacted with the backbone carbonyl oxygen of G20 of FZD8. All these H-bonds were observed to be flexible during the initial 80 ns but gradually stabilized for the rest of the simulation time (Figure 9A). In the FZD8-LRP5 interaction interface, two lysine residues, K697 and K953, from PE3 and PE4 β-propeller domains of LPR5, were interacting with E50 of FZD8. The sidechain amino group of K697 from the PE3 β-propeller domain of LRP5 forms an H-bond with the backbone carbonyl oxygen of E50 of FZD8. A salt bridge interaction between the sidechain amino group of K953 (PE4 β-propeller of LRP5) and the carboxyl group of E50 (FZD8) was found to be stable at the FZD8-LRP5 interaction interface (Figure 8G). The FZD8 receptor interacts and forms stable H-bonds with both HBD3 and LRP5 receptors. A comparison of the H-bonds between FZD8-HBD3 and FZD8-LRP5 showed that the

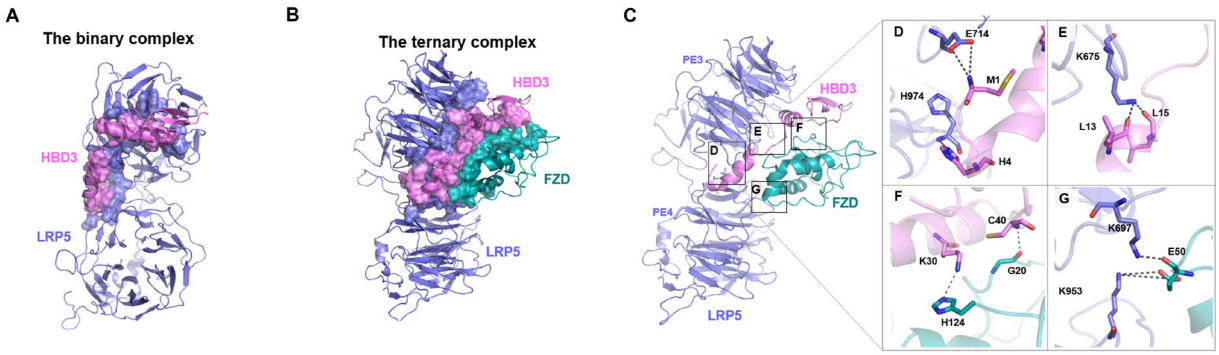

FIGURE 8
The plausible binding modes and critical interactions of the binary (LRP5-HBD3) and ternary (LRP5-HBD3-FZD8) complexes. **(A,B)** Protein–protein docking and molecular dynamics simulations revealed potential binding modes of the LRP5-HBD3 and LRP5-HBD3-FZD8 interaction complexes, respectively. The residues involved in the formation of the complex are shown in surface representation, and LPR5, HBD3, and FZD8 are colored in steel blue, light pink, and teal, respectively. HBD3 binds between the β-propeller domain-3 of LPR5 and the cysteine-rich domain of the FZD8 receptor. FZD8 receptor interacts with HBD3 as well as with the LRP5 receptor residues. **(C)** Stable H-bond interactions observed during the MD simulations of the complex are highlighted in boxes. **(D)** The sidechain carboxylic group of E714 of LRP5 interacts with the backbone amide nitrogen of M1 of HBD3, and the backbone amide nitrogen of H974 of LRP5 interacts with side chain ε nitrogen of H4 of HBD3. **(E)** The sidechain amino group of K675 of LRP5 interacts with backbone carbonyl oxygens of L13 and L15 of HBD3. **(F)** The sidechain amino group of K30 of HBD3 interacts with the ε nitrogen of FZD8 H124. Similarly, the backbone amide nitrogen of C40 of HBD3 forms an H-bond with the backbone carbonyl oxygen of FZD8 G20. **(G)** The sidechain terminal amino group of K953 of LRP5 forms a salt bridge with the sidechain carboxyl group of E50. Similarly, the sidechain amino group of K697 of LRP5 formed an H-bond with the backbone carbonyl oxygen of E50 of the FZD8 receptor.

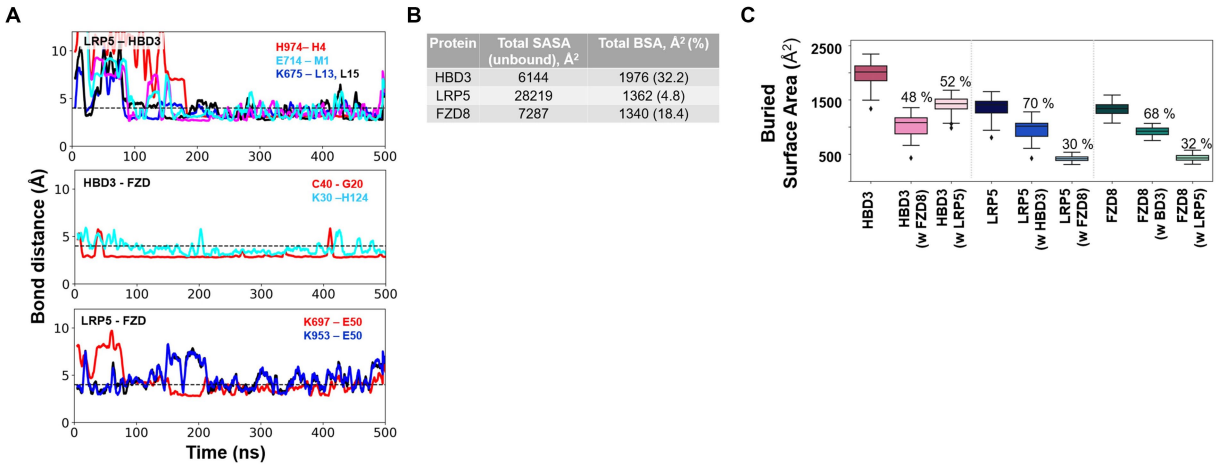

FIGURE 9
Critical H-bond interactions and the extent of protein–protein interactions as measured by the buried solvent-accessible surface area (SASA) of individual proteins upon complex formation. **(A)** Multiple stable H-bond interactions were observed in the LRP5-HBD3-FZD8 ternary complex. H-bond interactions between LRP5-HBD3, HBD3-FZD8, and LRP5-FZD8 are shown. **(B)** Total solvent-accessible surface area (SASA) of the three proteins in their unbound states and the amount of SASA lost due to complex formation, called buried surface area (BSA) and %, are given. **(C)** The total BSA and the fraction of the buried surface area for each interacting partner of HBD3, LRP5, and FZD8 receptors were calculated from the MD simulation. The BSA of HBD3 shows that HBD3 shares its interaction surface approximately equally with LRP5 and FZD8 receptors. On the other hand, LRP5 and FZD receptors share a larger fraction of interaction surface with HBD3. The fraction of interaction surface for LRP5 and FZD8 receptors was relatively smaller in comparison to their total SASA.

polar contacts are becoming stronger after the initial fine-tuning of the interaction surfaces (Figure 9A). Overall, the variation and flexibility in interactions illustrate the adaptability of the interaction surfaces between the receptors.

Hydrophobic interactions quantified as percent contact occupancy

To evaluate the critical interactions involved in stabilizing the complex, residue contacts at all three interfaces of complexes (LRP5-HBD3, HBD3-FZD8, and FZD8-LRP5) were analyzed. We applied a distance-based cutoff (4 Å) to evaluate all non-bonded interactions involved in the interacting surfaces. As several residue interactions were observed among the interacting proteins, only interactions that were observed in more than 80% of the simulation time were discussed here. From the contact analysis of the LRP5-HBD3 interface, the residues G673, K675, E676, H711, E714, F715, W780, R805, H847, F849, W863, F888, M890, P972, L973, H974, G975 and P1010 of LRP5 were observed to be in contact with the HBD3 residues, including M1, R2, H4, Y5, L13, I24, I25, L28, Y31, Y32 and V35. The N-terminal residue M1 of HBD3 forms contact with the PE3 β-propeller domain in the cleft formed in between the PE3 and PE4 β-propeller domains. In addition, the α helix in HBD3, formed by residues 24–36, mainly interacted at the surface of the PE3 domain (Figure 8A; Supplementary Figure S5).

HBD3 was sandwiched between LRP5 and FZD8. HBD3 residues, such as F8, L11, F12, L15, P17, V18, K30, R34, G37, R39, and C40, formed contacts with the FZD8 receptor residues, including G18, G20, Y21, Q22, I51, Q52, C53, S54, P55, P93, L94, Q97, and Y98. Interestingly, HBD3 appears to engage in a significantly greater number of contacts with FDZ8 than with LPR5 (Figure 8C; Supplementary Figure S6). In our molecular docking studies, the interaction of the FZD8 receptor with LRP5 was unexpected and different from the previously described LRP5-Wnt-FZD8 interaction model. Interestingly, in addition to the interactions with HBD3, the FZD8 receptor also had contact with the LRP5 receptor residues throughout the simulation period. Specifically, the residues of FZD8, W46, P47, E50, Q52 and Y98 were in contact with the S695 and K697 of the PE3 β-propeller domain and K953, S954, R977, A1196 and H1197 of the PE4 β-propeller domain of LRP5 (Figure 8G; Supplementary Figure S7).

The extent of protein–protein interactions was quantified as the buried solvent-accessible surface area upon complex formation.

We performed the solvent-accessible surface area calculation (SASA) to estimate the extent to which the proteins' surfaces were buried (buried surface area, BSA) during the formation of LPR5-HBD3 and LPR5-HBD3-FZD3 complexes. The SASA values represent the average calculated through the entire 500 ns MD simulations. The fraction of BSA for each protein is significantly different, ranging from 5 to 30% (Figure 9B). The PE3-PE4 domains of LPR5 are much larger than HBD3 and the CRD domain of FZD8. Only ~4.8% of the LPR5 PE3-PE4 domain's surface was buried in the complex formation, of which ~70% of the surface was engaged in interactions with HBD3 and ~30% of the surface was involved in interactions with FZD8 (Figure 9C). Similarly, ~32.17% of the surface of HBD3 was buried in the complex, of which ~52% of the surface involved in the interactions with LPR5 and ~48% with FZD8 receptor, which indicates that HBD3 shares the interaction surface almost equally with LRP5 and FZD8 receptors (Figure 9C). In the case of FZD8 receptor CRD, ~18.39% of the surface was buried in the complex, of which ~68% of the surface was engaged in the interactions with HBD3 and ~32% with LRP5 (Figure 9C). In addition, we have calculated the polar and non-polar fractions of the total SASA, which revealed that the ternary complex is stabilized mostly by non-polar interactions (Supplementary Figure S8). From the comparison of the BSA of the LPR5, HBD3, and FZD8, it was clear that HBD3 is sandwiched between LRP5 and FZD8 receptors and interacts through distinct

surfaces. Moreover, both LRP5 and FZD receptors share larger fractions of their interaction surfaces with HBD3, indicating stable and favorable interactions.

Discussion

There is an urgent need to develop antiviral therapeutics and vaccines for Respiratory Syncytial Virus (RSV) since it is a leading cause of mortality and morbidity among infants, the elderly, and immunocompromised patients (Diseases, 1993; Falsey et al., 2005; Nair et al., 2010; Hurwitz, 2011; Graham and Anderson, 2013; Griffiths et al., 2017; Romero et al., 2017). To achieve this goal, it is critical to understand RSV-host interactions and mechanisms that trigger the pro-inflammatory response. Pro-inflammatory response plays a critical role in developing severe airway inflammatory diseases such as pneumonia and bronchiolitis during RSV infection (Imai et al., 2008; Murawski et al., 2009; Ruuskanen et al., 2011; Foronjy et al., 2016; Russell et al., 2017). Additionally, inflammatory response constitutes a key cellular immune mechanism dictating vaccine efficacy. In the current study, we have identified a yet unknown pro-inflammatory pathway utilized by the host during RSV infection. We show the essential role of β-catenin dependent signaling pathway in positively regulating pro-inflammatory response in RSV-infected human lung epithelial cells.

The canonical Wnt/β-catenin pathway is a key signal transduction pathway involved in a wide spectrum of biological mechanisms (Clevers, 2006; Zhan et al., 2017; Ren et al., 2021; Rim et al., 2022), including regulating immunity (Ma and Hottiger, 2016). One specific mechanism comprises of expressing pro-inflammatory genes that culminate in inflammation. β-catenin signaling pathway promoted expression and production of pro-inflammatory cytokines/chemokines from macrophages (Zhao et al., 2015; Huang et al., 2018). Towards that end, the β-catenin signaling pathway also contributed to lung inflammation during sepsis (Sharma et al., 2017). Compared to macrophages, the role of β-catenin in epithelial cells during pro-inflammatory response is very limited. Only one study reported the involvement of β-catenin in stimulating pro-inflammatory cytokines in LPS-treated bronchial epithelial cells (Jang et al., 2014). Studies focusing on the role of β-catenin during infection with RNA respiratory viruses are limited. A study showed Wnt/β-catenin signaling pathway regulating influenza A virus (IAV is an orthomyxovirus) replication in epithelial cells (More et al., 2018). Additionally, we have previously demonstrated the trans-activation of the human parainfluenza virus type 3 gene by β-catenin (Bose and Banerjee, 2003). However, the role of β-catenin as a pro-inflammatory mediator during infection with RNA respiratory viruses is limited. Especially, it was unknown whether pneumoviruses like RSV trigger β-catenin activation and the role of such activation during virus-host interaction. In the current study, we demonstrated β-catenin activation by RSV and further showed the role of β-catenin in positively regulating pro-inflammatory response by virtue of inducing the production of key pro-inflammatory chemokine IL-8. In contrast to earlier studies with IAV, β-catenin signaling had no role in RSV replication/infection, but it was involved in the production of pro-inflammatory mediator IL-8.

Lung injury during RSV infection is associated with an influx of inflammatory immune cells into the airway (Imai et al., 2008; Murawski et al., 2009; Ruuskanen et al., 2011; Foronjy et al., 2016; Russell et al., 2017). Neutrophils constitute one of the infiltrating inflammatory cell types contributing to exaggerated lung inflammation and injury during RSV infection (Everard et al., 1994; McNamara et al., 2003; Emboriadou et al., 2007; Sebina and Phipps, 2020). Neutrophil recruitment to the RSV-infected lower respiratory tract is mediated by chemokine IL-8 released from lung epithelial cells and monocytes (Baggiolini et al., 1989; Bazzoni et al., 1991; Biswas et al., 1995; Bont et al., 1999). IL-8 (encoded by the CXCL8 gene in humans) is a chemokine with a C-X-C motif that acts as a potent chemoattractant for neutrophils (Baggiolini et al., 1989; Bazzoni et al., 1991). High levels of IL-8 in respiratory secretions have been detected in RSV-infected infants with severe respiratory disease (Biswas et al., 1995). IL-8 also serves as a biomarker defining lung disease severity in RSV-infected infants (Bont et al., 1999). IL-8 is the major chemokine secreted by RSV-infected lung epithelial cells, including human lung epithelial A549 cells (Fiedler et al., 1995; Thomas et al., 2000; Rudd et al., 2005). Interestingly, in A549 cells, IL-8 constitutes the only pro-inflammatory mediator detected at appreciable levels compared to other pro-inflammatory factors like TNF, IL-6, and IL-1β. IL-8 production during RSV infection is triggered by two transcription factors, NF-kB and NF-IL6 (Jamaluddin et al., 1996; Mastronarde et al., 1996). Interestingly, a study with human hepatocytes has identified the IL-8 gene as a direct target of β-catenin and TCF4 transcription factors (Lévy et al., 2002). A consensus TCF/LEF site was detected in the IL-8 promoter, and that site was essential for the transactivation of the IL-8 gene by β-catenin in association with the p300 co-activator (Lévy et al., 2002). Moreover, the β-catenin pathway was involved in positively regulating the expression and release of IL-8 from macrophages (Masckauchan, 2005) and endothelial cells (Jang et al., 2014) following allergic reactions and angiogenesis, respectively. However, the role of β-catenin, if any, in IL-8 production during virus infection has not been investigated yet. Our current study has highlighted the involvement of β-catenin signaling in triggering IL-8 production during RSV infection. Based on the critical role of IL-8 in conferring exaggerated airway inflammation during RSV infection (Baggiolini et al., 1989; Bazzoni et al., 1991; Everard et al., 1994; Biswas et al., 1995; Bont et al., 1999; McNamara et al., 2003; Emboriadou et al., 2007; Sebina and Phipps, 2020), our results have unfolded a new virus-host mechanism required for the efficient production of potent chemotactic factors like IL-8.

In addition to unfolding the β-catenin pathway as an IL-8 inducer during RSV infection, we have also identified a new mechanism triggering β-catenin activation during viral infection. We have identified human beta-defensin 3 (HBD3) as an extracellular ligand involved in activation β-catenin by virtue of interacting with the well-established Wnt receptor LRP5 which is part of the β-catenin activating Fzd-LRP5/6 receptor complex. Defensins are anti-microbial cationic peptides regulating pathogen burden, immunity, and host defense (Fruitwala et al., 2019; Xu and Lu, 2020). Apart from the anti-microbial property, we and others have demonstrated the additional role of defensins in controlling virus infection. Specifically, beta-defensins are involved in counteracting virus infection by various mechanisms. We have previously identified HBD2 and HBD3 as key epithelial cell-derived beta-defensins involved in controlling RSV and VSV (Vesicular Stomatitis Virus is a non-segmented negative-sense RNA virus like RSV) infections by blocking viral cellular entry (Kota et al., 2008; Basu et al., 2010). However, the role of beta-defensins

during cellular signaling of RSV-infected cells has not been reported previously. Particularly, it was unknown whether beta-defensins can modulate pro-inflammatory response in RSV-infected cells. Based on a previous study showing β-catenin activation by HBD3 in human non-epithelial dental cells (human periodontal ligament cells; Zhou et al., 2018), we investigated whether HBD3 can act as a non-canonical ligand (i.e., compared to canonical Wnt ligand) for β-catenin activation in RSV infected lung epithelial cells. Our study demonstrated that HBD3 released from RSV-infected cells is involved in activating β-catenin during RSV infection. Furthermore, our interaction studies showed direct interaction of HBD3 with LRP5, a receptor that is part of the multi-protein receptor complex (Fzd-LRP5/6) involved in Wnt-mediated β-catenin activation.

HBD3 interacts with at least three cell surface receptors, melanocortin receptors, CCR6, and CD98 (Semple et al., 2010; Colavita et al., 2015; Shelley et al., 2020). However, none of these receptors are involved in immune signaling. Our study has identified LRP5 as a new HBD3 receptor involved in pro-inflammatory signaling. Moreover, we show that HBD3-LRP5 interaction may drive activation of the β-catenin pathway leading to a pro-inflammatory response due to the production of potent neutrophilic chemokine IL-8. HBD3 interacted with cell surface localized LRP5, and such interaction was mediated via direct protein–protein interaction. The extracellular domain of LRP5 is comprised of – (a) four β-propeller domains, (b) four EGF-like domains, and (c) one LDLR type A domain (Clevers, 2006; Zhan et al., 2017; Ren et al., 2021; Rim et al., 2022; Figure 7B). The four β-propeller and four EGF-like domains are localized tandemly and designated as PE1, PE2, PE3, and PE4. During canonical Wnt/β-catenin signaling, the canonical ligand Wnt binds to these domains to activate β-catenin signaling. To date, 10 Wnt ligands exist, and previous studies have shown that Wnt3a is involved in β-catenin activation in IAV-infected lung epithelial cells (More et al., 2018). Wnt3a binds to the PE3 domain of the LRP5 protein. Interestingly, purified HBD3 is also bound to the PE3 domain of LRP5 protein, as deduced from our *in vitro* interaction studies with purified HBD3 and truncated LRP5 proteins. Our in-silico studies also provided a structural basis for the interactions between LRP5 and HBD3. Importantly, we obtained the potential binding orientations and critical residues at the interacting surfaces of the proteins using protein–protein docking. Subsequently, we evaluated the stability of the complex using 0.5 μs long MD simulations (Figure 8). Our simulations revealed that HBD3 interacts with LRP5 at its PE3 propeller domain, similar to other Wnt ligands reported before. The polar H-bond and nonpolar hydrophobic interactions between the two protein surfaces were assessed qualitatively by monitoring the H-bond distances and contact occupancy (%), respectively. Multiple H-bonds were observed between the LRP5-HBD3 interface. Similarly, the contact occupancy provides the fraction of the simulation time during which residues from the two proteins are within 4 Å distance (Figure 9; Supplementary Figure S5), indicating van der Waal and hydrophobic interactions. Both parameters indicate stable and lasting interactions between the proteins, involving the burial of greater than 30% of the solvent-accessible surface area of HBD3.

Earlier studies have shown that the Wnt ligands act at the cell surface by forming a heterotrimeric ternary complex with LRP5 and frizzled receptors such as FZD8 (Hirai et al., 2019). We modeled such a ternary complex of HBD3 with LRP5 and FZD8 in which HBD3 was sandwiched between the two other proteins (Figure 10). The extracellular cysteine-rich domain of FZD8 was successfully docked to the HBD3 surface distal to its LRP5-binding interface. Surprisingly, the 0.5 μs-long MD simulations of this ternary complex revealed unexpected interactions of FZD8 with both HBD3 and the upper region of the PE4 domain of LRP5. These interactions were quite stable and lasted for the entire simulation time. Similar to the binary LRP5-HBD3 complex, both polar H-bond distances and contact occupancy (%) indicated the stability of the residue interactions of the ternary complex. Based on the observations, we propose this ternary model of LRP5-HBD3-FZD8 as potential mechanism through which HBD3 produces a proinflammatory response via the β-catenin pathway (Figure 10).

In summary, our studies have identified the HBD3/β-catenin signaling pathway as a new non-canonical β-catenin activating pathway involved in triggering a pro-inflammatory response in RSV-infected lung epithelial cells. We envision that the HBD3/β-catenin network acts both via paracrine and autocrine loop to amplify the inflammatory response in non-infected and infected cells, respectively.

Materials and methods

Cell culture and viruses

Human lung epithelial cells (A549) were purchased from American Type Culture Collection (ATCC). Cells were cultured in complete Dulbecco's modified Eagle medium (DMEM; Gibco) containing 10%

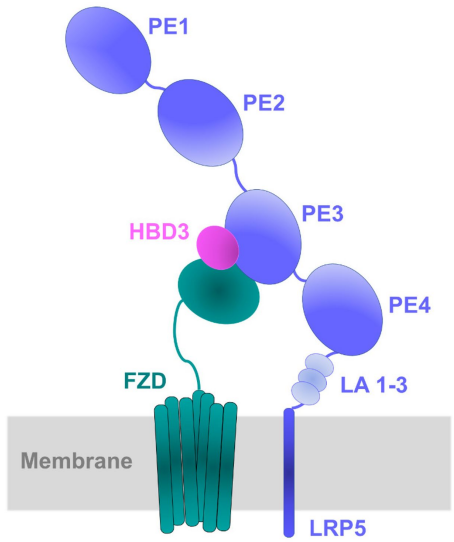

FIGURE 10
Schematic diagram of the proposed model for LRP5-HBD3-FZD8 ternary complex. Protein–protein docking, and MD simulations predicted the potential interactions of HBD3 with LRP5 and FZD8. HBD3 appears to be sandwiched between LRP5 and FZD8. Specifically, HBD3 binds mostly to the PE3 propeller domain of LRP5 protein.

fetal bovine serum (FBS), 100 IU/ml penicillin, and 100ug/ml streptomycin unless otherwise stated (Kota et al., 2008; Chang et al., 2012; Mgbemena et al., 2012, 2013). Human respiratory syncytial virus (RSV A2 strain) was purified as described previously (Kota et al., 2008; Chang et al., 2012; Mgbemena et al., 2013). Recombinant human RSV expressing mKate2 protein (mKate2-RSV) was propagated from pSynk-A2 as described previously (Hotard et al., 2012; Meng et al., 2014; Bedient et al., 2020). pSynk-A2 and helper plasmids were provided by Dr. Martin Moore (Emory University) and BSRT7/5 cells were provided by Dr. Ursula Buchholz (National Institutes of Health).

Cell treatment and virus infection

Cells were infected with RSV and mKate2-RSV at the multiplicity of infection (MOI) of 1 or 3. Virus adsorption was performed for 1.5 h (at 37°C) in OPTI-MEM medium (Gibco). Following adsorption, cells were washed with Dulbecco's phosphate-buffered saline (DPBS; Gibco) and infection was continued in the presence or absence of a complete medium. In some experiments, cells were pre-treated with either vehicle (DMSO) or Wnt/β-catenin pathway inhibitors (iCRT3 or iCRT14; 25uM; Sigma) and infected with RSV in the absence and presence of these inhibitors. For human beta-defensins 3 (HBD3) treatment studies, A549 cells were treated with 10ug/ml of purified HBD3 (Peprotech) or vehicle (PBS with 0.1% BSA). Cells were also treated with either lithium chloride (LiCl; Sigma) or vehicle (water) for 24 h. A549 cells were transfected with either empty-FLAG plasmid or FLAG-tagged LRP5 (FLAG-LRP5; 200 ng/ml) by using Lipofectamine 2000 (Life Technologies).

Generation of A549 cells expressing truncated β-catenin protein

A549 cells expressing either full-length β-catenin protein (FL-catenin) or truncated β-catenin protein (Δ-catenin) were generated by Synthego Corporation using CRISPR-Cas9 technology with the sgRNA sequence of GAGTGGTAAAGGCAATCCTG located in exon 3. Individual clones were isolated by limiting dilution from the cell pool provided by Synthego. To identify those that would likely have diminished activity without being a null, the mutation(s) carried by each clone was determined by PCR amplification of the region surrounding the sgRNA target site using F primer 5′ATCCCCCTGCTTTCCTCTCT3′ and R primer 5′ACATAGCAGCTCGTACCCTC3′. Clones that carried deletions were sequenced to determine the mutation.

Luciferase assay

Cells (A549, FL-catenin, and Δ-catenin cells) were co-transfected with M50 Super 8× TOP-Flash firefly luciferase reporter plasmid (Addgene) and a plasmid encoding Renilla luciferase for 16 h. Transfected cells were either infected with RSV or treated with purified HBD3 protein. Luciferase plasmid-transfected FL-catenin and Δ-catenin cells were also treated with LiCl. Following infection/treatment, the Dual-Luciferase® reporter assay system (Promega) was used for luciferase analysis. Luciferase activity was determined using a microplate luminometer (Promega).

siRNA transfection

Scrambled control siRNA and HBD3 siRNA were purchased from Santa Cruz Biotechnology. A549 cells were transfected with these siRNAs (60 pmol) by using Lipofectamine 2000 (Life Technologies). HBD3 silencing was confirmed by western blotting with an HBD3 antibody.

ELISA

Human IL-8 ELISA kit was purchased from Invitrogen. HBD3 ELISA kit was obtained from MyBioSource. IL-8 and HBD3 levels in the medium supernatant were determined following the manufacturer's instructions. ELISA values of the experimental group (i.e., RSV-infected cells or cells infected with RSV in the presence of iCRT3 or iCRT14) represent values obtained following subtraction of background signal from the control group (i.e., mock cells or cells infected with RSV in the presence of control vehicle).

Western blot

A549 cells were lysed using 1%-Triton X-100 (pH 7.4), EDTA-free protease inhibitor cocktail (Roche Diagnostics) in PBS. Cell lysates were subjected to SDS-PAGE and separated proteins were transferred onto 0.2 μm nitrocellulose membrane (GE Health care) and blotted with specific antibodies. β-catenin and FLAG antibodies were purchased from Sigma-Aldrich. LRP5 antibody was obtained from Cell signaling. β-actin antibody was purchased from Bethyl Laboratories. HBD3-8A antibody was deposited to the DSHB by Starner, T. (DSHB Hybridoma Product hBD-3-8A). An anti-RFP antibody was purchased from Invitrogen. Western blots were quantified using ChemiDoc™ XRS + software Image Lab 5.1 (BioRad).

RNA isolation and reverse transcriptase-PCR (RT-PCR)

Total RNA was extracted using TRIzol reagent (Life Technologies) following supplier's instructions. Isolated RNA was treated with RNase-free DNase I (Thermoscientific) and cDNA was synthesized using a High-Capacity cDNA Reverse Transcription Kit (Applied Biosystems). RT-PCR was performed using 2X Taq Red master mix (Apex) in a final reaction of 25 μl. The amplification cycle was as follows: an initial denaturing step (95°C for 3 min) was followed by 34 cycles of denaturing (95°C for 30 s), annealing (55.7°C for 30 s–), and extending (72°C for 1 min), followed by 5 min at 72°C for elongation. Following amplification, the PCR products were analyzed on 2% agarose gels and bands were visualized by ChemiDoc XRS (BioRad). The PCR product bands were quantified using ChemiDoc™ XRS + software Image Lab 5.1 (BioRad). Housekeeping gene glyceraldehyde-3-phosphate dehydrogenase (GAPDH) was used as a loading control. The primers used to detect the indicated genes are listed below:

Human GAPDH forward, (5′ GATCATCAGCAATGCCTCCT-3′) and human GAPDH reverse, (5′ TGTGGTCATGAGTCCTTCCA-3′).

Human HBD3 forward, (5′ TCCAGGTCATGGAGGAATCAT-3′) and human HBD3 reverse, (5′ CGAGCACTTGCCGATCTGT-3′).

Interaction of biotinylated HBD3 protein with LRP5 protein

The EZ-link® TFPA-PEG3-Biotin kit (Thermo Fisher Scientific, Massachusetts, USA) was used to biotinylate purified HBD3 protein (Peprotech). Biotinylation was performed in the dark as per the manufacturer's instructions. For cell surface interaction studies, A549 cells were transfected with either an empty-FLAG vector or LRP5-FLAG for 16 h. After 16 h, cells were cooled to 4°C for 2 h, and the chilled cells were subsequently incubated with biotinylated-HBD3 for 4 h at 4°C. Cells were lysed with PBS containing 1% TritonX-100 and protease inhibitors. Cell lysates were incubated with NeutrAvidin-agarose beads (Thermo Fisher Scientific) for 16 h at 4°C. After washing the agarose beads with wash buffer (10 mM Tris–HCL with protease inhibitor), the proteins bound to avidin–agarose beads were subjected to western blotting with anti-FLAG antibody. For cell-free interaction studies, we biotinylated purified HBD3 protein and purchased purified truncated LRP5 protein with Fc tag (purchased from antibodies online.com). The purified truncated LRP5 protein consisted of E3 and E4 regions (aa769–aa1016) of the LRP5 extracellular domain. For the interaction studies, biotinylated-HBD3 and non-biotinylated HBD3 (control) were incubated (16 h at 4°C) with avidin–agarose beads. Following washing, the agarose beads were further incubated (16 h at 4°C) with purified truncated LRP5 protein. Washed beads were boiled with SDS sample buffer, followed by SDS-PAGE and western blotting with LRP5 antibody.

Statistical analysis

All data were analyzed using GraphPad Prism software (6.0). For ELISA and luciferase assay, a significance test was carried out using Student's *t*-test. Western blot densitometric values were quantified by using ChemiDoc™ XRS + software Image Lab 5.1 (BioRad), and Student's *t*-test was utilized to determine significance.

Modeling of LRP5-HBD3-FZD complex structure

Structures

To examine the potential interactions of HBD3 with LRP5 and Frizzled-8 receptor (FZD8), we assembled the binary (HBD3-LRP5), and ternary (HBD3-LRP5-FZD8) complexes using protein–protein docking of the three proteins. Multiple experimental structures are available for FZD8, whereas the structures for LRP5 and HBD3 are yet to be resolved. For FZD8, we used the X-ray crystal structure of the protein in complex with a surrogate Wnt agonist (PDB ID: 5UN5, resolution of 2.99 Å; Janda et al., 2017). The structure of LRP5 was modeled using the X-ray crystal structure of its closest homolog, LRP6 (PDB ID: 4DG6, resolution 2.9 Å), using modeler v10.3 (Webb and Sali, 2016). From the generated model structures, the structure with the least energy refinement score was considered the best model (Shen and Sali, 2006). Similarly, for HBD3, only a partial NMR structure is available in the PDB database. Hence the full-length model from the AlphaFold database is used (https://alphafold.ebi.ac.uk/entry/P81534; Varadi et al., 2022). The quality of the generated models (LRP5 homology model and HBD3 Alpha fold model) was further validated by the Ramachandran plot using the SAVES server (https://saves.mbi.ucla.edu/; Bowie et al., 1991; Lüthy et al., 1992; Colovos and Yeates, 1993; Pontius et al., 1996). The details are provided as Supplementary Figures S9, S10. Finally, the modeled structures were further geometry-optimized to remove any bad contacts and energy-minimized using MOE v2015 and used for subsequent protein–protein docking and MD simulations (Ccgi, 2016).

Protein–protein docking

For modeling the binary and ternary complexes of LRP5, FZD8, and HBD3, sequential protein–protein docking simulations were carried out in two steps – (1) docking of HBD3 with LPR5, and (2) docking of the LRP5-HBD3 complex with FZD8. For docking of HBD3 with LRP5, the following residues of the PE3 (β propeller) domain of LRP5 (A667, V694, E721, T737, N762, W780, R805, D824, H847, W863, V889, and M890) were selected as the potential interaction site (Supplementary Figures S2C). For HBD3, all residues were selected to generate all possible binding conformations of HBD3 with LPR5. Furthermore, to generate a ternary FZD8-LRP5-HBD3 complex, the LRP5-HBD3 complex obtained from the previous step was docked to FZD8, using the residues of HBD3 that do not interact with LRP5, as the potential interaction site. In the case of FZD8, two possible binding interfaces were selected and docked individually. All the protein–protein docking simulations were performed using the HADDOCK v2.4 server (https://bianca.science.uu.nl/haddock2.4; Honorato et al., 2021). For each protein–protein docking simulation, at most 30,000 possible binding orientations were generated, amongst which 2000 poses were considered for post-docking minimization, and finally, 1,000 poses were filtered and used for scoring and clustering. Apart from these, other docking parameters were kept at their default values in HADDOCK. Among the resulting clusters with multiple docking poses, a cluster with plausible binding orientations and interactions and the lowest binding energies was considered for subsequent MD simulations.

MD simulations

To examine the stability, binding modes, and residue interactions of the binary and ternary complexes, we performed unbiased MD simulations using GROMACS v2021 (Abraham et al., 2015). The input files for the MD simulations were generated using the Input Generator-Solution Builder module of CHARMM-GUI (Lee et al., 2016) with CHARMM36 forcefield (Huang and MacKerell Jr, 2013). The system was solvated using TIP3P (Jorgensen et al., 1983) water molecules in a cubic box such that the distance between any atom of the protein complex and the box edge was at least 10 Å. Subsequently, the system was neutralized (net charge = 0), and the salt concentration was brought to 0.15 M by adding 182 Na^+ and 174 Cl^- ions. The simulations were performed under periodic boundary conditions and with the Particle Mesh Ewald (PME) method for calculating the long-range electrostatic interactions (Darden et al., 1993). The van der Waals interactions were smoothly switched off at 12 A°. Further, the solvated system was minimized (1,000 steps) to remove any steric clashes in the system. Following the minimization step, equilibration and production runs were performed with an integration time step of

2 fs, and all the bond lengths involving hydrogen atoms were fixed using the SHAKE algorithm (Andersen, 1983). The system was equilibrated using an NPT ensemble at 1 atm pressure and 310 K temperature with constraints, the production simulations were carried out for 500 ns without any constraints, and the trajectory was saved for every 10 picoseconds.

Data availability statement

The original contributions presented in the study are included in the article/Supplementary material, further inquiries can be directed to the corresponding author.

Author contributions

SP, IM, CM, and LM performed the experiments. SP, IM, CM, LM, TM, SN, and SB contributed to the experimental design, data analysis and interpretation, preparation of figures and tables, and preparation of the manuscript. All authors contributed to the article and approved the submitted version.

Funding

This research was supported by grants from the National Institutes of Health R01AI083387 (SB) and R01GM137022 (SN).

Acknowledgments

The authors thank Martin Moore and Ursula Buchholz for providing reagents.

Conflict of interest

The authors declare that the research was conducted in the absence of any commercial or financial relationships that could be construed as a potential conflict of interest.

Publisher's note

Supplementary material

The Supplementary material for this article can be found online at: https://www.frontiersin.org/articles/10.3389/fmicb.2023.1186510/full#supplementary-material

References

Abraham, M. J., Murtola, T., Schulz, R., Páll, S., Smith, J. C., Hess, B., et al. (2015). GROMACS: high performance molecular simulations through multi-level parallelism from laptops to supercomputers. *SoftwareX* 1-2, 19–25. doi: 10.1016/j.softx.2015.06.001

Ahn, V. E., Chu, M. L.-H., Choi, H.-J., Tran, D., Abo, A., and Weis, W. I. (2011). Structural basis of Wnt signaling inhibition by Dickkopf binding to LRP5/6. *Dev. Cell* 21, 862–873. doi: 10.1016/j.devcel.2011.09.003

Andersen, H. C. (1983). Rattle: A "velocity" version of the shake algorithm for molecular dynamics calculations. *J. Comput. Phys.* 52, 24–34. doi: 10.1016/0021-9991(83)90014-1

Baggiolini, M., Walz, A., and Kunkel, S. L. (1989). Neutrophil-activating peptide-1/interleukin 8, a novel cytokine that activates neutrophils. *J. Clin. Invest.* 84, 1045–1049. doi: 10.1172/JCI114265

Basu, M., Kota, S., Banerjee, A. K., and Bose, S. (2010). Role of human beta defensin 3 during type I interferon mediated antiviral response against vesicular stomatitis virus. *Int. J. Interf. Cytokine Mediat. Res.* 2, 23–32. doi: 10.2147/IJICMR.S6799

Bazzoni, F., Cassatella, M. A., Rossi, F., Ceska, M., Dewald, B., and Baggiolini, M. (1991). Phagocytosing neutrophils produce and release high amounts of the neutrophil-activating peptide 1/interleukin 8. *J. Exp. Med.* 173, 771–774. doi: 10.1084/jem.173.3.771

Bedient, L., Pokharel, S. M., Chiok, K. R., Mohanty, I., Beach, S. S., Miura, T. A., et al. (2020). Lytic cell death mechanisms in human respiratory syncytial virus-infected macrophages: roles of pyroptosis and necroptosis. *Viruses* 12:932. doi: 10.3390/v12090932

Biswas, S., Friedland, J. S., Remick, D. G., Davies, E. G., and Sharland, M. (1995). Elevated plasma interleukin 8 in respiratory syncytial virus bronchiolitis. *Pediatr. Infect. Dis. J.* 14:919. doi: 10.1097/00006454-199510000-00027

Bont, L., Heijnen, C. J., Kavelaars, A., van Aalderen, W. M. C., Brus, F., Draaisma, J. T., et al. (1999). Peripheral blood cytokine responses and disease severity in respiratory syncytial virus bronchiolitis. *Eur. Respir. J.* 14, 144–149. doi: 10.1034/j.1399-3003.1999.14a24.x

Bose, S., and Banerjee, A. (2003). β-Catenin associates with human parainfluenza virus type 3 ribonucleoprotein complex and activates transcription of viral genome RNA in vitro. *Gene Expr. J. Liver Res.* 11, 241–249. doi: 10.3727/000000003783992252

Bourhis, E., Wang, W., Tam, C., Hwang, J., Zhang, Y., Spittler, D., et al. (2011). Wnt antagonists bind through a short peptide to the first β-propeller domain of LRP5/6. *Structure* 19, 1433–1442. doi: 10.1016/j.str.2011.07.005

Bowie, J. U., Lüthy, R., and Eisenberg, D. (1991). A method to identify protein sequences that fold into a known three-dimensional structure. *Science* 253, 164–170. doi: 10.1126/science.1853201

Ccgi, M. (2016). Molecular operating environment (MOE), 2013.08. Chem. Comput. Gr. Inc., Montr. 354.

Chang, T.-H., Segovia, J., Sabbah, A., Mgbemena, V., and Bose, S. (2012). Cholesterol-rich lipid rafts are required for release of infectious human respiratory syncytial virus particles. *Virology* 422, 205–213. doi: 10.1016/j.virol.2011.10.029

Cheng, Z., Biechele, T., Wei, Z., Morrone, S., Moon, R. T., Wang, L., et al. (2011). Crystal structures of the extracellular domain of LRP6 and its complex with DKK1. *Nat. Struct. Mol. Biol.* 18, 1204–1210. doi: 10.1038/nsmb.2139

Clément-Lacroix, P., Ai, M., Morvan, F., Roman-Roman, S., Vayssière, B., Belleville, C., et al. (2005). Lrp5-independent activation of Wnt signaling by lithium chloride increases bone formation and bone mass in mice. *Proc. Natl. Acad. Sci.* 102, 17406–17411. doi: 10.1073/pnas.0505259102

Clevers, H. (2006). Wnt/β-catenin signaling in development and disease. *Cells* 127, 469–480. doi: 10.1016/j.cell.2006.10.018

Colavita, I., Nigro, E., Sarnataro, D., Scudiero, O., Granata, V., Daniele, A., et al. (2015). Membrane protein 4F2/CD98 is a cell surface receptor involved in the internalization and trafficking of human β-Defensin 3 in epithelial cells. *Chem. Biol.* 22, 217–228. doi: 10.1016/j.chembiol.2014.11.020

Colovos, C., and Yeates, T. O. (1993). Verification of protein structures: patterns of nonbonded atomic interactions. *Protein Sci.* 2, 1511–1519. doi: 10.1002/pro.5560020916

Corsello, T., Qu, Y., Ivanciuc, T., Garofalo, R. P., and Casola, A. (2022). Antiviral activity of extracellular vesicles derived from respiratory syncytial virus-infected airway epithelial cells. *Front. Immunol.* 13:13. doi: 10.3389/fimmu.2022.886701

Darden, T., York, D., and Pedersen, L. (1993). Particle mesh Ewald: an N· log (N) method for Ewald sums in large systems. *J. Chem. Phys.* 98, 10089–10092. doi: 10.1063/1.464397

Dijksterhuis, J. P., Baljinnyam, B., Stanger, K., Sercan, H. O., Ji, Y., Andres, O., et al. (2015). Systematic mapping of WNT-FZD protein interactions reveals functional selectivity by distinct WNT-FZD pairs. *J. Biol. Chem.* 290, 6789–6798. doi: 10.1074/jbc.M114.612648

Diseases, C. (1993). Use of ribavirin in the treatment of respiratory syncytial virus infection. *Pediatrics* 92, 501–504. doi: 10.1542/peds.92.3.501

Emboriadou, M., Hatzistilianou, M., Magnisali, C., Sakelaropoulou, A., Exintari, M., Conti, P., et al. (2007). Human neutrophil elastase in RSV bronchiolitis. *Ann. Clin. Lab. Sci.* 37, 79–84.

Everard, M. L., Swarbrick, A., Wrightham, M., McIntyre, J., Dunkley, C., James, P. D., et al. (1994). Analysis of cells obtained by bronchial lavage of infants with respiratory syncytial virus infection. *Arch. Dis. Child.* 71, 428–432. doi: 10.1136/adc.71.5.428

Falsey, A. R., Hennessey, P. A., Formica, M. A., Cox, C., and Walsh, E. E. (2005). Respiratory syncytial virus infection in elderly and high-risk adults. *N. Engl. J. Med.* 352, 1749–1759. doi: 10.1056/Nejmoa043951

Fiedler, M. A., Wernke-Dollries, K., and Stark, J. M. (1995). Respiratory syncytial virus increases IL-8 gene expression and protein release in A549 cells. *Am. J. Physiol. Cell. Mol. Physiol.* 269, L865–L872. doi: 10.1152/ajplung.1995.269.6.L865

Foronjy, R. F., Ochieng, P. O., Salathe, M. A., Dabo, A. J., Eden, E., Baumlin, N., et al. (2016). Protein tyrosine phosphatase 1B negatively regulates S100A9-mediated lung damage during respiratory syncytial virus exacerbations. *Mucosal Immunol.* 9, 1317–1329. doi: 10.1038/mi.2015.138

Fruitwala, S., El-Naccache, D. W., and Chang, T. L. (2019). Multifaceted immune functions of human defensins and underlying mechanisms. *Seminars Cell Dev. Biol.* 88, 163–172. doi: 10.1016/j.semcdb.2018.02.023

Gonsalves, F. C., Klein, K., Carson, B. B., Katz, S., Ekas, L. A., Evans, S., et al. (2011). An RNAi-based chemical genetic screen identifies three small-molecule inhibitors of the Wnt/wingless signaling pathway. *Proc. Natl. Acad. Sci.* 108, 5954–5963. doi: 10.1073/pnas.1017496108

Graham, B. S., and Anderson, L. J. (2013). Challenges and opportunities for respiratory syncytial virus vaccines. *Challenges Oppor. Respir. Syncytial Virus Vaccines* 372, 391–404. doi: 10.1007/978-3-642-38919-1_20

Griffiths, C., Drews, S. J., and Marchant, D. J. (2017). Respiratory syncytial virus: infection, detection, and new options for prevention and treatment. *Clin. Microbiol. Rev.* 30, 277–319. doi: 10.1128/CMR.00010-16

Hillary, V. E., and Ceasar, S. A. (2022). A review on the mechanism and applications of CRISPR/Cas9/Cas12/Cas13/Cas14 proteins utilized for genome engineering. *Mol. Biotechnol.* 65, 1–15. doi: 10.1007/s12033-022-00567-0

Hillyer, P., Shepard, R., Uehling, M., Krenz, M., Sheikh, F., Thayer, K. R., et al. (2018). Differential responses by human respiratory epithelial cell lines to respiratory syncytial virus reflect distinct patterns of infection control. *J. Virol.* 92, e02202–e02217. doi: 10.1128/JVI.02202-17

Hirai, H., Matoba, K., Mihara, E., Arimori, T., and Takagi, J. (2019). Crystal structure of a mammalian Wnt–frizzled complex. *Nat. Struct. Mol. Biol.* 26, 372–379. doi: 10.1038/s41594-019-0216-z

Honorato, R. V., Koukos, P. I., Jiménez-García, B., Tsaregorodtsev, A., Verlato, M., Giachetti, A., et al. (2021). Structural biology in the clouds: the WeNMR-EOSC ecosystem. *Front. Mol. Biosci.* 8:729513. doi: 10.3389/fmolb.2021.729513

Hosakote, Y. M., Liu, T., Castro, S. M., Garofalo, R. P., and Casola, A. (2009). Respiratory syncytial virus induces oxidative stress by modulating antioxidant enzymes. *Am. J. Respir. Cell Mol. Biol.* 41, 348–357. doi: 10.1165/rcmb.2008-0330OC

Hotard, A. L., Shaikh, F. Y., Lee, S., Yan, D., Teng, M. N., Plemper, R. K., et al. (2012). A stabilized respiratory syncytial virus reverse genetics system amenable to recombination-mediated mutagenesis. *Virology* 434, 129–136. doi: 10.1016/j.virol.2012.09.022

Hsu, P. D., Lander, E. S., and Zhang, F. (2014). Development and applications of CRISPR-Cas9 for genome engineering. *Cells* 157, 1262–1278. doi: 10.1016/j.cell.2014.05.010

Huang, J., and MacKerell, A. D. Jr. (2013). CHARMM36 all-atom additive protein force field: validation based on comparison to NMR data. *J. Comput. Chem.* 34, 2135–2145. doi: 10.1002/jcc.23354

Huang, L., Xiang, M., Ye, P., Zhou, W., and Chen, M. (2018). Beta-catenin promotes macrophage-mediated acute inflammatory response after myocardial infarction. *Immunol. Cell Biol.* 96, 100–113. doi: 10.1111/imcb.1019

Hurwitz, J. L. (2011). Respiratory syncytial virus vaccine development. *Expert Rev. Vaccines* 10, 1415–1433. doi: 10.1586/erv.11.120

Imai, Y., Kuba, K., Neely, G. G., Yaghubian-Malhami, R., Perkmann, T., van Loo, G., et al. (2008). Identification of oxidative stress and toll-like receptor 4 signaling as a key pathway of acute lung injury. *Cells* 133, 235–249. doi: 10.1016/j.cell.2008.02.043

Jamaluddin, M., Garofalo, R., Ogra, P. L., and Brasier, A. R. (1996). Inducible translational regulation of the NF-IL6 transcription factor by respiratory syncytial virus infection in pulmonary epithelial cells. *J. Virol.* 70, 1554–1563. doi: 10.1128/jvi.70.3.1554-1563.1996

Janda, C. Y., Dang, L. T., You, C., Chang, J., de Lau, W., Zhong, Z. A., et al. (2017). Surrogate Wnt agonists that phenocopy canonical Wnt and β-catenin signalling. *Nature* 545, 234–237. doi: 10.1038/nature22306

Janda, C. Y., Waghray, D., Levin, A. M., Thomas, C., and Garcia, K. C. (2012). Structural basis of Wnt recognition by frizzled. *Science* 337, 59–64. doi: 10.1126/science.1222879

Jang, J., Ha, J.-H., Chung, S.-I., and Yoon, Y. (2014). β-Catenin regulates NF-κB activity and inflammatory cytokine expression in bronchial epithelial cells treated with lipopolysaccharide. *Int. J. Mol. Med.* 34, 632–638. doi: 10.3892/ijmm.2014.1807

Jorgensen, W. L., Chandrasekhar, J., Madura, J. D., Impey, R. W., and Klein, M. L. (1983). Comparison of simple potential functions for simulating liquid water. *J. Chem. Phys.* 79, 926–935. doi: 10.1063/1.445869

Kong, X., San Juan, H., Behera, A., Peeples, M. E., Wu, J., Lockey, R. F., et al. (2004). ERK-1/2 activity is required for efficient RSV infection. *FEBS Lett.* 559, 33–38. doi: 10.1016/S0014-5793(04)00002-X

Kota, S., Sabbah, A., Harnack, R., Xiang, Y., Meng, X., and Bose, S. (2008). Role of human β-defensin-2 during tumor necrosis factor-α/NF-κB-mediated innate antiviral response against human respiratory syncytial virus. *J. Biol. Chem.* 283, 22417–22429. doi: 10.1074/jbc.M710415200

Lee, J., Cheng, X., Swails, J. M., Yeom, M. S., Eastman, P. K., Lemkul, J. A., et al. (2016). CHARMM-GUI input generator for NAMD, GROMACS, AMBER, OpenMM, and CHARMM/OpenMM simulations using the CHARMM36 additive force field. *J. Chem. Theory Comput.* 12, 405–413. doi: 10.1021/acs.jctc.5b00935

Lee, M. G., Oh, H., Park, J. W., You, J. S., and Han, J.-W. (2022). Nuclear S6K1 enhances oncogenic Wnt signaling by inducing Wnt/β-catenin transcriptional complex formation. *Int. J. Mol. Sci.* 23:16143. doi: 10.3390/ijms232416143

Lévy, L., Neuveut, C., Renard, C.-A., Charneau, P., Branchereau, S., Gauthier, F., et al. (2002). Transcriptional activation of interleukin-8 by β-catenin-Tcf4. *J. Biol. Chem.* 277, 42386–42393. doi: 10.1074/jbc.M207418200

Lin, Y., Ohkawara, B., Ito, M., Misawa, N., Miyamoto, K., Takegami, Y., et al. (2016). Molecular hydrogen suppresses activated Wnt/β-catenin signaling. *Sci. Rep.* 6, 1–14. doi: 10.1038/srep31986

Liu, J., Xiao, Q., Xiao, J., Niu, C., Li, Y., Zhang, X., et al. (2022). Wnt/β-catenin signalling: function, biological mechanisms, and therapeutic opportunities. *Signal Transduct. Target. Ther.* 7:3. doi: 10.1038/s41392-021-00762-6

Lüthy, R., Bowie, J. U., and Eisenberg, D. (1992). Assessment of protein models with three-dimensional profiles. *Nature* 356, 83–85. doi: 10.1038/356083a0

Ma, B., and Hottiger, M. O. (2016). Crosstalk between Wnt/β-catenin and NF-κB signaling pathway during inflammation. *Front. Immunol.* 7:378. doi: 10.3389/fimmu.2016.00378

Masckauchan, T. N. (2005). Shawber CJ, Funahashi Y, Li CM, Kitajewski J. Wnt/beta-catenin signal. induces proliferation, Surviv. Interleukin-8 hum. *Endothel. Cells Angiogenes.* 8, 43–51. doi: 10.1007/s10456-005-5612-9

Mastronarde, J. G., He, R., Monick, M. M., Mukaida, N., Matsushima, K., and Hunninghake, G. W. (1996). Induction of interleukin (IL)-8 gene expression by respiratory syncytial virus involves activation of nuclear factor (NF)-κB and NF-IL-6. *J. Infect. Dis.* 174, 262–267. doi: 10.1093/infdis/174.2.262

Matoba, K., Mihara, E., Tamura-Kawakami, K., Miyazaki, N., Maeda, S., Hirai, H., et al. (2017). Conformational freedom of the LRP6 ectodomain is regulated by N-glycosylation and the binding of the Wnt antagonist Dkk1. *Cell Rep.* 18, 32–40. doi: 10.1016/j.celrep.2016.12.017

McNamara, P. S., Ritson, P., Selby, A., Hart, C. A., and Smyth, R. L. (2003). Bronchoalveolar lavage cellularity in infants with severe respiratory syncytial virus bronchiolitis. *Arch. Dis. Child.* 88, 922–926. doi: 10.1136/adc.88.10.922

Meng, J., Lee, S., Hotard, A. L., and Moore, M. L. (2014). Refining the balance of attenuation and immunogenicity of respiratory syncytial virus by targeted codon deoptimization of virulence genes. *MBio* 5, e01704–e01714. doi: 10.1128/mBio.01704-14

Mgbemena, V., Segovia, J., Chang, T.-H., and Bose, S. (2013). KLF6 and iNOS regulates apoptosis during respiratory syncytial virus infection. *Cell. Immunol.* 283, 1–7. doi: 10.1016/j.cellimm.2013.06.002

Mgbemena, V., Segovia, J. A., Chang, T.-H., Tsai, S.-Y., Cole, G. T., Hung, C.-Y., et al. (2012). Transactivation of inducible nitric oxide synthase gene by Kruppel-like factor 6 regulates apoptosis during influenza A virus infection. *J. Immunol.* 189, 606–615. doi: 10.4049/jimmunol.1102742

More, S., Yang, X., Zhu, Z., Bamunuarachchi, G., Guo, Y., Huang, C., et al. (2018). Regulation of influenza virus replication by Wnt/β-catenin signaling. *PLoS One* 13:e0191010. doi: 10.1371/journal.pone.0191010

Murawski, M. R., Bowen, G. N., Cerny, A. M., Anderson, L. J., Haynes, L. M., Tripp, R. A., et al. (2009). Respiratory syncytial virus activates innate immunity through toll-like receptor 2. *J. Virol.* 83, 1492–1500. doi: 10.1128/JVI.00671-08

Musunuru, K. (2017). The hope and hype of CRISPR-Cas9 genome editing: a review. *JAMA Cardiol.* 2, 914–919. doi: 10.1001/jamacardio.2017.1713

Nair, H., Nokes, D. J., Gessner, B. D., Dherani, M., Madhi, S. A., Singleton, R. J., et al. (2010). Global burden of acute lower respiratory infections due to respiratory syncytial virus in young children: a systematic review and meta-analysis. *Lancet* 375, 1545–1555. doi: 10.1016/S0140-6736(10)60206-1

Pontius, J., Richelle, J., and Wodak, S. J. (1996). Deviations from standard atomic volumes as a quality measure for protein crystal structures. *J. Mol. Biol.* 264, 121–136. doi: 10.1006/jmbi.1996.0628

Rajan, A., Piedra, F.-A., Aideyan, L., McBride, T., Robertson, M., Johnson, H. L., et al. (2022). Multiple respiratory syncytial virus (RSV) strains infecting HEp-2 and A549 cells reveal cell line-dependent differences in resistance to RSV infection. *J. Virol.* 96, e01904–e01921. doi: 10.1128/jvi.01904-21

Ran, F. A., Hsu, P. D., Wright, J., Agarwala, V., Scott, D. A., and Zhang, F. (2013). Genome engineering using the CRISPR-Cas9 system. *Nat. Protoc.* 8, 2281–2308. doi: 10.1038/nprot.2013.143

Ren, Q., Chen, J., and Liu, Y. (2021). LRP5 and LRP6 in Wnt signaling: similarity and divergence. *Front. Cell Dev. Biol.* 9:670960. doi: 10.3389/fcell.2021.670960

Rim, E. Y., Clevers, H., and Nusse, R. (2022). The Wnt pathway: from signaling mechanisms to synthetic modulators. *Annu. Rev. Biochem.* 91, 571–598. doi: 10.1146/annurev-biochem-040320-103615

Romero, J. R. (2003). Palivizumab prophylaxis of respiratory syncytial virus disease from 1998 to 2002: results from four years of palivizumab usage. *Pediatr. Infect. Dis. J.* 22, S46–S54. doi: 10.1097/01.inf.0000053885.34703.84

Romero, C. A., Remor, A., Latini, A., De Paul, A. L., Torres, A. I., and Mukdsi, J. H. (2017). Uric acid activates NRLP3 inflammasome in an in-vivo model of epithelial to mesenchymal transition in the kidney. *J. Mol. Histol.* 48, 209–218. doi: 10.1007/s10735-017-9720-9

Rudd, B. D., Burstein, E., Duckett, C. S., Li, X., and Lukacs, N. W. (2005). Differential role for TLR3 in respiratory syncytial virus-induced chemokine expression. *J. Virol.* 79, 3350–3357. doi: 10.1128/JVI.79.6.3350-3357.2005

Russell, C. D., Unger, S. A., Walton, M., and Schwarze, J. (2017). The human immune response to respiratory syncytial virus infection. *Clin. Microbiol. Rev.* 30, 481–502. doi: 10.1128/CMR.00090-16

Ruuskanen, O., Lahti, E., Jennings, L. C., and Murdoch, D. R. (2011). Viral pneumonia. *Lancet* 377, 1264–1275. doi: 10.1016/S0140-6736(10)61459-6

Sebina, I., and Phipps, S. (2020). The contribution of neutrophils to the pathogenesis of RSV bronchiolitis. *Viruses* 12:808. doi: 10.3390/v12080808

Semple, F., Webb, S., Li, H., Patel, H. B., Perretti, M., Jackson, I. J., et al. (2010). Human β-defensin 3 has immunosuppressive activity in vitro and in vivo. *Eur. J. Immunol.* 40, 1073–1078. doi: 10.1002/eji.200940041

Sharma, A., Yang, W.-L., Ochani, M., and Wang, P. (2017). Mitigation of sepsis-induced inflammatory responses and organ injury through targeting Wnt/β-catenin signaling. *Sci. Rep.* 7:9235. doi: 10.1038/s41598-017-08711-6

Shelley, J. R., Davidson, D. J., and Dorin, J. R. (2020). The dichotomous responses driven by β-defensins. *Front. Immunol.* 11:1176. doi: 10.3389/fimmu.2020.01176

Shen, M., and Sali, A. (2006). Statistical potential for assessment and prediction of protein structures. *Protein Sci.* 15, 2507–2524. doi: 10.1110/ps.062416606

Shirato, K., Ujike, M., Kawase, M., and Matsuyama, S. (2012). Increased replication of respiratory syncytial virus in the presence of cytokeratin 8 and 18. *J. Med. Virol.* 84, 365–370. doi: 10.1002/jmv.23196

Su, F., Chen, X., Liu, X., Liu, G., and Zhang, Y. (2018). Expression of recombinant HBD3 protein that reduces mycobacterial infection capacity. *AMB Express* 8, 1–9. doi: 10.1186/s13568-018-0573-8

Thomas, L. H., Wickremasinghe, M. I. Y., Sharland, M., and Friedland, J. S. (2000). Synergistic upregulation of interleukin-8 secretion from pulmonary epithelial cells by direct and monocyte-dependent effects of respiratory syncytial virus infection. *J. Virol.* 74, 8425–8433. doi: 10.1128/JVI.74.18.8425-8433.2000

Trujano-Camacho, S., Cantú-de León, D., Delgado-Waldo, I., Coronel-Hernández, J., Millan-Catalan, O., Hernández-Sotelo, D., et al. (2021). Inhibition of Wnt-β-catenin signaling by ICRT14 drug depends of post-transcriptional regulation by HOTAIR in human cervical cancer HeLa cells. *Front. Oncol.* 11:729228. doi: 10.3389/fonc.2021.729228

Tsutsumi, N., Mukherjee, S., Waghray, D., Janda, C. Y., Jude, K. M., Miao, Y., et al. (2020). Structure of human Frizzled5 by fiducial-assisted cryo-EM supports a heterodimeric mechanism of canonical Wnt signaling. *elife* 9:e58464. doi: 10.7554/eLife.58464

Varadi, M., Anyango, S., Deshpande, M., Nair, S., Natassia, C., Yordanova, G., et al. (2022). AlphaFold protein structure database: massively expanding the structural coverage of protein-sequence space with high-accuracy models. *Nucleic Acids Res.* 50, D439–D444. doi: 10.1093/nar/gkab1061

Wang, S.-W., Gao, C., Zheng, Y.-M., Yi, L., Lu, J.-C., Huang, X.-Y., et al. (2022). Current applications and future perspective of CRISPR/Cas9 gene editing in cancer. *Mol. Cancer* 21, 1–27. doi: 10.1186/s12943-022-01518-8

Webb, B., and Sali, A. (2016). Comparative protein structure modeling using MODELLER. *Curr. Protoc. Bioinformatics* 54, 5–6. doi: 10.1002/cpbi.3

Wright, S. C., Kozielewicz, P., Kowalski-Jahn, M., Petersen, J., Bowin, C.-F., Slodkowicz, G., et al. (2019). A conserved molecular switch in class F receptors regulates receptor activation and pathway selection. *Nat. Commun.* 10:667. doi: 10.1038/s41467-019-08630-2

Xu, D., and Lu, W. (2020). Defensins: a double-edged sword in host immunity. *Front. Immunol.* 11:764. doi: 10.3389/fimmu.2020.00764

Zebisch, M., Jackson, V. A., Zhao, Y., and Jones, E. Y. (2016). Structure of the dual-mode Wnt regulator Kremen1 and insight into ternary complex formation with LRP6 and Dickkopf. *Structure* 24, 1599–1605. doi: 10.1016/j.str.2016.06.020

Zhan, T., Rindtorff, N., and Boutros, M. (2017). Wnt signaling in cancer. *Oncogene* 36, 1461–1473. doi: 10.1038/onc.2016.304

Zhao, W., Sun, Z., Wang, S., Li, Z., and Zheng, L. (2015). Wnt1 participates in inflammation induced by lipopolysaccharide through upregulating scavenger receptor A and NF-kB. *Inflammation* 38, 1700–1706. doi: 10.1007/s10753-015-0147-8

Zhou, J., Zhang, Y., Li, L., Fu, H., Yang, W., and Yan, F. (2018). Human β-defensin 3-combined gold nanoparticles for enhancement of osteogenic differentiation of human periodontal ligament cells in inflammatory microenvironments. *Int. J. Nanomedicine* 13, 555–567. doi: 10.2147/IJN.S150897

Zhu, Y. (2022). Advances in CRISPR/Cas9. *Biomed. Res. Int.* 2022, 1–13. doi: 10.1155/2022/9978571

frontiers | Frontiers in Microbiology

TYPE Review
PUBLISHED 27 June 2023
DOI 10.3389/fmicb.2023.1169547

OPEN ACCESS

EDITED BY
Anna Kramvis,
University of the Witwatersrand, South Africa

REVIEWED BY
Jacques Fantini,
Aix Marseille Université, France
Gustaf E. Rydell,
University of Gothenburg, Sweden

*CORRESPONDENCE
Matthias Ballauff
matthias.ballauff@fu-berlin.de
Andreas Herrmann
a.herrmann2@fu-berlin.de

†These authors have contributed equally to this work and share last authorship

RECEIVED 19 February 2023
ACCEPTED 08 June 2023
PUBLISHED 27 June 2023

CITATION
Lauster D, Osterrieder K, Haag R, Ballauff M and Herrmann A (2023) Respiratory viruses interacting with cells: the importance of electrostatics.
Front. Microbiol. 14:1169547.
doi: 10.3389/fmicb.2023.1169547

Respiratory viruses interacting with cells: the importance of electrostatics

Daniel Lauster[1], Klaus Osterrieder[2], Rainer Haag[3], Matthias Ballauff[3]*† and Andreas Herrmann[3]*†

[1]Institut für Pharmazie, Biopharmazeutika, Freie Universität Berlin, Berlin, Germany, [2]Institut für Virologie, Freie Universität Berlin, Berlin, Germany, [3]Institut für Chemie und Biochemie, SupraFAB, Freie Universität Berlin, Berlin, Germany

The COVID-19 pandemic has rekindled interest in the molecular mechanisms involved in the early steps of infection of cells by viruses. Compared to SARS-CoV-1 which only caused a relatively small albeit deadly outbreak, SARS-CoV-2 has led to fulminant spread and a full-scale pandemic characterized by efficient virus transmission worldwide within a very short time. Moreover, the mutations the virus acquired over the many months of virus transmission, particularly those seen in the Omicron variant, have turned out to result in an even more transmissible virus. Here, we focus on the early events of virus infection of cells. We review evidence that the first decisive step in this process is the electrostatic interaction of the spike protein with heparan sulfate chains present on the surface of target cells: Patches of cationic amino acids located on the surface of the spike protein can interact intimately with the negatively charged heparan sulfate chains, which results in the binding of the virion to the cell surface. In a second step, the specific interaction of the receptor binding domain (RBD) within the spike with the angiotensin-converting enzyme 2 (ACE2) receptor leads to the uptake of bound virions into the cell. We show that these events can be expressed as a semi-quantitative model by calculating the surface potential of different spike proteins using the Adaptive Poison-Boltzmann-Solver (APBS). This software allows visualization of the positive surface potential caused by the cationic patches, which increased markedly from the original Wuhan strain of SARS-CoV-2 to the Omicron variant. The surface potential thus enhanced leads to a much stronger binding of the Omicron variant as compared to the original wild-type virus. At the same time, data taken from the literature demonstrate that the interaction of the RBD of the spike protein with the ACE2 receptor remains constant within the limits of error. Finally, we briefly digress to other viruses and show the usefulness of these electrostatic processes and calculations for cell-virus interactions more generally.

KEYWORDS

SARS-CoV-2, variants, electrostatic interaction, spike protein, surface charge

1. Introduction

Electrostatic interaction of proteins with highly charged natural polyelectrolytes such as DNA is a long-standing problem of biophysics (Record et al., 1976, 1978) and is known to play a major role in many biological processes (Achazi et al., 2021). Glycosaminoglycans (GAGs) present a class of important natural polyelectrolytes that can interact with a great variety of

proteins in a well-defined manner (Toledo et al., 2021; Ricard-Blum and Perez, 2022; Vallet et al., 2022). In particular, highly charged GAGs such as heparan sulfate (HS) play a central role in the organization of the extracellular matrix (Karamanos et al., 2021, 2022). Here, heparan sulfate proteoglycans (HSPG) consist of transmembrane, glycosyl-phosphatidyl-inositol-anchored, or secreted proteins onto which the highly negatively charged HS chains are attached (Condomitti and de Wit, 2018). HSPG can bind many different proteins including extracellular matrix proteins, growth factors, morphogens, cytokines and chemokines (Karamanos et al., 2021). Moreover, HSPG act as attachment factors for a number of viruses and bacteria (Chang et al., 2011; Cagno et al., 2019). Interacting with HSPG increases the concentration of virions on the cell surface, thus enhancing their chances for binding their cognate receptor(s) for cell entry. The length and pattern of sulfation are tissue- and cell type-specific (Marques et al., 2021), and, therefore, likely play an important role in pathogen tropism (Lee et al., 2022).

With the advent of the pandemic caused by severe acute respiratory syndrome coronavirus-2 (SARS-CoV-2), virus entry into cells has become a pressing and much-studied topic. The viral homotrimeric spike (S) glycoprotein mediates binding and subsequent steps of the early phase of host cell infection. Recent work has clearly demonstrated that the interaction of SARS-CoV-2 spike with HSPG on the surface of the target cell is the first and critical step in the infection process (Clausen et al., 2020; Kim et al., 2020; Liu et al., 2021; Nie et al., 2021; Kearns et al., 2022). In Figure 1, we show this process schematically: A patch of positive charge on the spike protein interacts closely with the highly negative charges of the HS chains of the HSPG. In a second step, the virion can find and interact with its specific host cell receptor for cell entry. Typically, angiotensin-converting enzyme 2 (ACE2) serves as a cellular receptor, but other cell surface molecules such as neuropilin-1 (Daly et al., 2020) and integrin (Liu J. et al., 2022) have also been shown to serve in that role. Hence, the strong electrostatic interaction of a highly charged GAG with the envelope proteins of SARS-CoV-2 is central for this critical first step of infection. This fact is supported by the observation that highly-charged synthetic polyelectrolytes (Nie et al., 2021) or heparin (Mycroft-West et al., 2020) can inhibit virus infection by competing with HSPG (Hoffmann et al., 2022). The electrostatic interaction between virus and HS may become even more important when considering the mutations of the S protein and the much higher infectivity of SARS-CoV-2 variants. As revealed by molecular modeling (Jawad et al., 2022; Nie et al., 2022; Pascarella et al., 2022; Fantini et al., 2023a) when compared with the authentic Wuhan-type spike, the positive patch on the surface is enlarged in its counterparts of the Delta and the Omicron variants, which suggests a much stronger binding of the virion to HSPG (see below). This finding underscores the central role of electrostatic interaction for virus infection in the early phase of binding to host cells (Cagno et al., 2019).

Studies on the interaction of the SARS-CoV-2 virion with HSPG have renewed the general interest in complex formations of GAGs with proteins. It has been posited that the positive patches on the surface of proteins can be rationalized in terms of the Cardin-Weintraub sequences (Cardin and Weintraub, 1989; Cardin et al., 1991; Rudd et al., 2017), where two or three basic amino

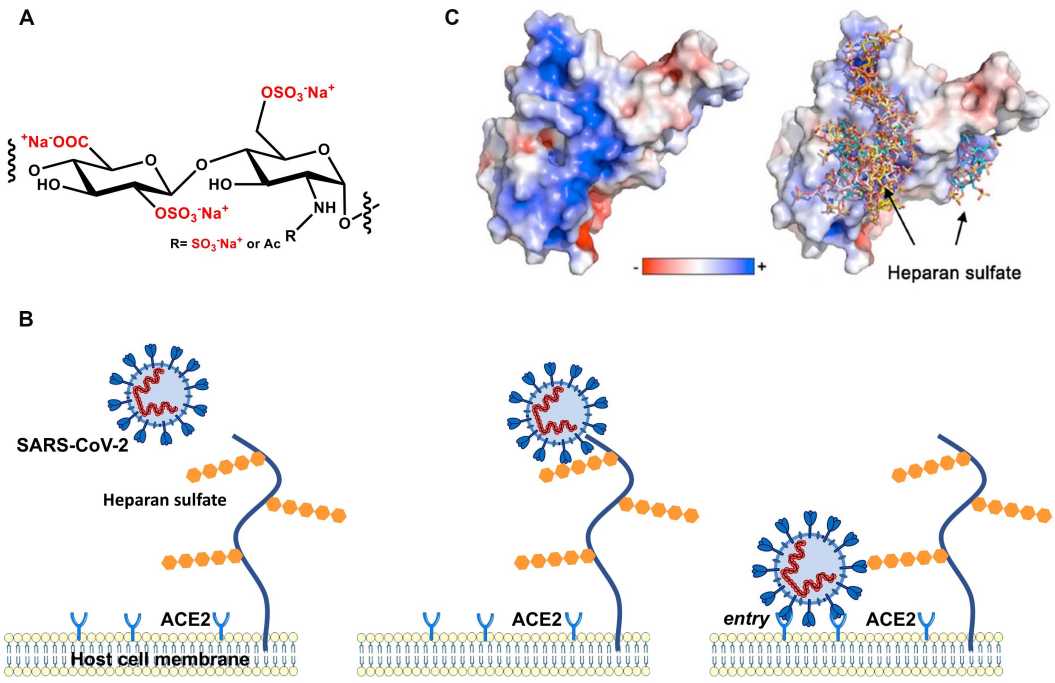

FIGURE 1
Early stages of cellular infection by SARS-CoV-2. **(A)** Repeating unit of heparan sulfate. **(B)** In the first step, S interacts closely with heparan sulfate attached to HSPG by strong electrostatic interactions. In a second step, interaction of S with the ACE2 receptor initiates uptake of the virion into the cell by endocytosis and, ultimately, S-mediated fusion of the virus envelope with endosomal membranes. **(C)** The electrostatic potential map of the receptor binding domain (RBD) of the wild-type (Wuhan) spike glycoprotein is represented. Positively charged amino acids located on the surface of the S homotrimer interact strongly with the highly negatively charged heparan sulfate moieties of the HSPG.

acids are grouped together with hydrophobic amino acids. Recently, Kim et al. have traced back the enhanced binding of the SARS-CoV-2 virion to HSPG compared to SARS-CoV-1 to additional Cardin-Weintraub sequences on its spike protein (Kim et al., 2020). Moreover, Liu et al. have found that the binding of well-defined HS oligomers to the receptor binding domain (RBD) depends on their length and sequence. Specifically, a minimum length of 6 repeating HS units was found to be necessary for binding (Liu et al., 2021).

As mentioned above, the general theory of the interaction of polyelectrolytes with proteins has been worked out many years ago (Record et al., 1978), and has since been applied to many natural and synthetic polyelectrolytes (Xu et al., 2019; Achazi et al., 2021). The theory is based on Manning's prediction of counterion condensation (Manning, 1969) of polyelectrolyte chains: A part of the counterions of a highly negatively charged polyelectrolyte will be firmly immobilized or condensed on the chain. Interaction with a patch of positive charge on a protein will liberate a corresponding number of these condensed counterions. The counterion release will then increase the entropy of the system, providing a strong driving force for complex formation of the polyelectrolyte and the protein. Since the condensed counterions are firmly bound to the polyelectrolyte, they will act much in a way of a chemically-bound species during complex formation. Hence, their activity enters directly in the mass action law and the free energy of binding scales logarithmically with the salt concentration in the system (Record et al., 1978). Strong interaction of a polyelectrolyte with a protein has thus two ingredients: (i) a patch of positive amino acids of sufficient size, that is, of typically 3 to 4 cationic amino acids grouped in a Cardin-Weintraub sequence, and (ii) a highly-charged polyelectrolyte chain at which counterion condensation takes place.

This model has met with gratifying success when applied to the binding of DNA to various proteins (Lohman and Mascotti, 1992; Mascotti and Lohman, 1993; Bergqvist et al., 2001, 2003; Achazi et al., 2021) or to the interaction of synthetic polyelectrolytes with proteins (Xu et al., 2019). Also, the interaction of heparin with various proteins can be rationalized in terms of this model (Olson et al., 1991; Thompson et al., 1994; Mascotti and Lohman, 1995; Hileman et al., 1998; Friedrich et al., 2001; Capila and Linhardt, 2002; Schedin-Weiss et al., 2002a,b, 2004; Jairajpuri et al., 2003; Seyrek and Dubin, 2010; Walkowiak et al., 2020; Malicka et al., 2022). Taken together, all the cited studies demonstrate clearly that the counterion release model provides a valid and fully quantitative description of complex formation between polyelectrolytes and proteins.

Here, we review and discuss recent findings on virus attachment to HSPG and cell surfaces and compare our results with the counterion release model of complex formation between highly charged polyelectrolytes and proteins. Special emphasis is put on the results obtained with SARS-CoV-2. We show that the results provide a firm basis for discussing the role of electrostatic interaction for virus infection in general. The paper is organized as follows: Section "Electrostatic interaction of proteins with polyelectrolytes" contains a brief survey of the modeling of electrostatic interaction. In section "Electrostatics in virus infection", the model will be used for a comparison with experimental results obtained with SARS-CoV-2 and related viruses. The extension of these ideas to less-well studied viruses is given in section "Human Respiratory Syncytial Virus and human Metapneumovirus", and a brief conclusion will wrap up the discussion.

2. Electrostatic interaction of proteins with polyelectrolytes

2.1. Proteins interact with polyelectrolytes by counterion release even at high ionic strength

As already discussed in previous expositions of the subject, the main driving force for the binding of highly charged polyelectrolytes to proteins is the release of counterions. Figure 2 shows this process in a schematic fashion: A fraction of the counterions is condensed onto the polyelectrolyte. The criterion for counterion condensation is the charge parameter(Manning, 1969) $\xi = \lambda_b/l$, where l is the distance of the charges along the chain. λ_b is the Bjerrum-length, the distance between two elementary charges at which electrostatic interaction is in the order of the thermal energy k_BT. λ_b is 0.7 nm in water at 25°C. If $\xi > 1$, a fraction $1-1/\xi$ of the counterions will be condensed, that is, it will be strongly correlated to the macroion ["Manning condensation" (Manning, 1969)]. As an important consequence, condensed counterions will not contribute to the osmotic pressure of the system. Heparin is among the natural polyelectrolytes with the highest charge and characterized by a charge parameter $\xi = 2.84$ (Minsky et al., 2013; Walkowiak et al., 2020). If such a highly charged polyelectrolyte forms a complex with a protein, a patch of positively charged amino acids on the surface of the protein becomes a multivalent counterion of the polyelectrolyte, thus releasing a corresponding number of counterions. The increase of entropy effected by this counterion release is a major driving force for complex formation. Counterion condensation can also be characterized by the surface concentration c_{ci}, which can be estimated from the number of condensed ions per unit length and a diameter of the cylinder in which the ions are confined (see Figure 2; Manning, 1978; Xu et al., 2017, 2018, 2019). Estimates of this concentration are in the order of 1 M for typical, highly charged polyelectrolytes such as DNA or heparin (Xu et al., 2019). This concentration is much higher than the physiological salt concentration of 0.15 M and a release of condensed ions to the bulk phase will therefore result in a considerable gain of free energy of nearly 2 k_BT per ion.

The positive patch on the protein must have a certain size of 2 or 3 cationic amino acids to act in this way. This fact is the background for the finding that Cardin-Weintraub sequences (Cardin and Weintraub, 1989; Cardin et al., 1991) in which cationic amino acids B are grouped together with hydrophobic moieties X as "XBBXBX" and "XBBBXXBX" sequences/motifs. Rudd et al. (2017) have reanalyzed these GAG-binding sites for a large number of systems and concluded that sequences act only through their presence on the protein surface, exactly as shown in Figure 2.

These considerations can be put into a quantitative frame as discussed recently (Xu et al., 2019; Achazi et al., 2021; Walkowiak and Ballauff, 2021; Malicka et al., 2022): the free energy of binding $\Delta G_b(T, c_s)$ follows from the binding constant K_b through

$$\Delta G_b(T, c_s) = -\mathrm{RT} \ln K_b \quad (1)$$

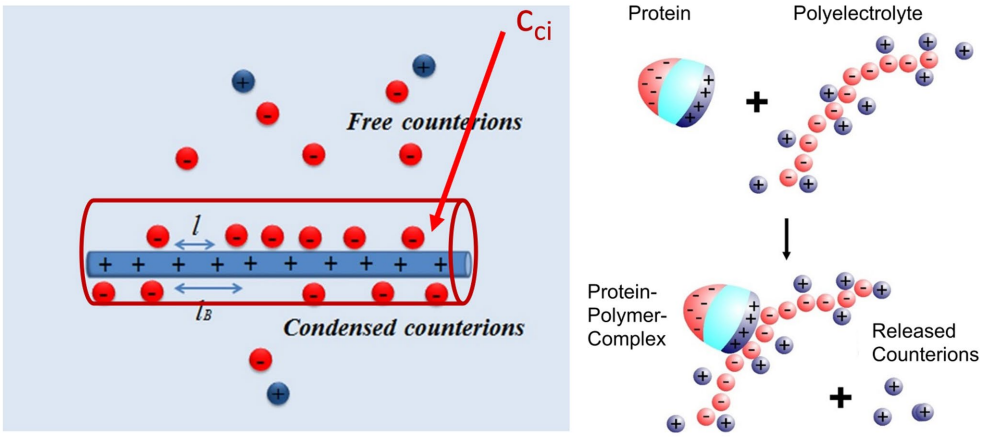

FIGURE 2
Counterion release as main driving force for complex formation between a polyelectrolyte and a protein (Achazi et al., 2021). Left-hand side: A part of the counterions of the highly charged macroion is condensed, that is, highly correlated to the macroion and does not contribute to the measured osmotic pressure. This enrichment of ions near the macroion can be characterized by a surface concentration c_{ci} which for heparin is of the order of 1M (Walkowiak and Ballauff, 2021; Malicka et al., 2022). Right-hand side: Complex formation of a protein with such a macroion is due to the close interaction of a patch of positive charge on the surface of the protein with the polyelectrolyte. The positive patch becomes a multivalent counterion of the macroion thus releasing a concomitant number of monovalent counterions into the bulk solution. The free energy of binding hence consists of an entropic term due to this effect and a term due to interaction at direct contact [*cf.* the discussion of eq. (2) below].

which characterizes the equilibrium between the components and the complex of the polyelectrolyte with the protein. The condensed counterions liberated during complex formation will act in this equilibrium as a chemical component, and the free energy of binding will thus scale with ln c_s where c_s is the salt concentration in the system (Record et al., 1978). The free energy derived from this model is given in eq. (2) (Achazi et al., 2021).

$$\Delta G_b\left(T,c_s\right) = \mathrm{RT}\Delta n_{ci}\ln c_s - \mathrm{RT}\frac{2}{55.6}\Delta w c_s + \Delta G_{res} \qquad (2)$$

The first term is due to the effect of counterion release as described above scaling with the logarithm of the salt concentration in the solution. The term Δn_{ci} is the number of released counterions. The second term addresses the change of hydration during complex formation. Here Δw is the net contribution to the free energy of binding. In many cases studied so far, this term is small and can be disregarded in a first approximation. Finally, the third term ΔG_{res} is the free energy resulting from the interaction at direct contact, mainly by salt bridges and hydrogen bonding (Xu and Ballauff, 2019; Walkowiak and Ballauff, 2021). We note that any distinct pattern of the arrangement of charged groups of polyelectrolytes is not considered by this theoretical approach (see also below "Effects of finite length of the polyelectrolyte: Heparin/HS must exceed a certain length to bind to proteins").

Eq. (2) has been applied repeatedly to the analysis of heparin interacting with different proteins [*cf.* the discussion in Achazi et al. (2021)]. In all cases studied so far, it was found that $\Delta w = 0$; it follows that plots of ln K_b against ln c_s are strictly linear. Extrapolation to a salt concentration of 1 M was used to obtain ΔG_{res}, whereas the number of released counterions Δn_{ci} was found to be typically around 3. A more recent analysis of the binding of lysozyme to heparin corroborated the main conclusions of earlier work (Malicka et al., 2022). The second term in eq. (2) describing the effect of hydration was analyzed in detail. It was found that hydration as embodied in Δw hardly contribute to the measured free energy of binding ΔG_b for salt ions located approximately in the middle of the Hofmeister series (Malicka et al., 2022). Hence, for a first approximation of the binding constant, it suffices to take into account only the first and the third term of eq. (2).

2.2. Effects of finite length of the polyelectrolyte: heparin/HS must exceed a certain length to bind to proteins

The above theoretical model of counterion condensation assumes a rodlike polyelectrolyte of infinite length. If the macroion has a finite length, however, the fraction of condensed counterions decreases and vanishes at a critical length. This problem has been considered first for DNA by Record et al. (1978) who showed that the extent of counterion on a polyelectrolyte must be corrected by a term that scales with 1/*N*, where *N* is the degree of polymerization. Netz (2003) and Kim and Netz (2015) reconsidered the problem for a rod-like polyelectrolyte modeled as a cylinder of finite radius. The average degree of counterion condensation was given in an analytical expression for salt-free solutions, while Manning developed an expression that describes effects at the termini of rod-like polyelectrolytes (Manning, 2008). Minsky et al. (2013) demonstrated the effect of finite length in a careful study of the electrophoretic mobility of heparin oligomers at low ionic strength. By measuring the effective charge of oligomers of different average chain lengths, the authors could show that the average number of condensed counterions increases with increasing chain lengths.

One can conclude from the studies that counterion condensation is greatly diminished for short macroions and that counterion release is no longer effective for the binding of polyelectrolytes to proteins. This fact results in a much weaker interaction of heparin oligomers with various proteins. Thus, Hernaiz and colleagues found the

dissociation constant K_D of a complex between a synthetic peptide form the human amyloid peptide P with heparin increases by one order of magnitude when going from the polymer heparin to the tetrasaccharide (Hernaiz et al., 2002). Similar findings have since been reported by other groups (Zhang et al., 2015; Nguyen and Rabenstein, 2016; Kohling et al., 2019). Recently, Liu et al. demonstrated this effect in a carefully study assessing the interaction of GAGs of various structures and lengths with the RDB of SARS-CoV-2 (Liu et al., 2021). They have used a library of well-defined HS oligosaccharides to determine the conditions that must be met for a HS oligosaccharide to bind to the S proteins of wt SARS-CoV-2. They found that the binding of HS depends on both the length and the pattern of the arrangement of the sulfate groups. In addition to a minimum length equal to that of hexamers, at least 8 sulfate groups were required for significant binding. Octasaccharides with 9 or 12 sulfate groups showed much stronger binding. Polymers composed of trisulfated repeating units displayed the highest affinity implicating that a high charge density favors binding. These conditions for binding HS were found for both the RBD and the S protein of wt SARS-CoV-2, with the affinity for the S protein being about an order of magnitude higher. The latter was attributed to a further HS binding site at the furin-cleavage site in addition to a binding site at the RBD (Liu et al., 2021).

An important observation by Liu et al. was that a removal of only one sulfate from a hexasaccharide (see comparison of structure 90 or 91 of Liu et al.) caused a significant reduction in HS affinity to the full length S protein and – but to a lower extent – to the isolated RBD. The authors concluded that this result points to specific interactions of sulfates with the protein which would be in line with the HS sulfate code hypothesis. The latter suggests that specific HS epitopes on the cell surface may allow to recruit specific HS-binding proteins (Xu and Esko, 2014). However, Liu et al. did not preclude that electrostatic interactions are of relevance for HS binding to the S protein.

Nie et al. (2021) also found, using linear polyglycerol sulfates (LPGS), that short-chain LPGS with a low number of sulfate groups (6 repeating units) had no inhibitory effect on the infection of Vero E6 cells by wt SARS-CoV-2, but long-chain LPGS with 20 repeating units caused a strong inhibition of infection. Increasing the degree of sulfation led to a greater reduction of infected cells, confirming that a high charge density given by sulfate groups promotes the inhibitory effect of LPGS. An independent support of this conclusion was provided by Hao et al. using a heparan sulfate microarray. They have shown for both the full-length S protein and the RBD of SARS-CoV-2 that the stepwise addition of 6-O-sulfate groups gradually enhanced binding. At this stage of investigation, the authors concluded that the number of sulfate groups is relevant for binding, but not the length of the HS (Hao et al., 2021). These findings are in accord with the theory of electrostatic interaction as described above: Counterion condensation is the necessary condition for electrostatic interaction of sufficient strength and only operative for chains exceeding a minimum chain length. However, so far, the theory does not consider specific arrangements of the ligands for binding (Xu and Esko, 2014). Further studies are warranted if and how such specific arrangements can be integrated into theoretical considerations.

3. Electrostatics in virus infection

The role of virion binding to HSPG as the first step of infection has been the subject of a careful review by Cagno et al. (2019). The authors showed that this first interaction is clearly the decisive step for the efficiency of infection of many viruses. Here, we will analyze in detail the relevance of opposite charges for the initial interaction between virus and target cell focusing on coronaviruses.

3.1. Wildtype SARS-CoV-2

As all coronaviruses, SARS-CoV-2 uses its homotrimeric envelope spike glycoprotein (S) to attach to the host cell. The wild-type (Wuhan) S features 1,273 amino acid residues in total, and 1,208 of them form the ectodomain. Each monomer consists of two subunits, S1 and S2 which are a result of proteolytic cleavage. S2 contains the hydrophobic transmembrane domain anchoring the protein to the envelope. Cleavage of S into the two subunits is performed by host cell enzymes that include furin and TMPRSS2 at distinct sites, and the process is essential for the subsequent conformational change of the protein that exposes the hydrophobic peptides triggering fusion (Hoffmann et al., 2020). Taking advantage of the knowledge of SARS-CoV-1 which caused a small-scale pandemic in 2002/2003, ACE2 was quickly identified as a specific receptor for SARS-CoV-2 (Hoffmann et al., 2020). S1 binds to ACE2 with a specific receptor-binding motive (RBM) localized in the RBD, which covers residues 333 to 527 (residue numbers given correspond to the original Wuhan S sequence).

However, it is not the interaction of the spike protein with ACE2 which is decisive for initial binding but the electrostatic interaction of the spike protein with the HSPG. Evidence for the electrostatic nature of the first step of virus binding to cell surfaces also comes from inhibition studies (Mycroft-West et al., 2020; Nie et al., 2021; Tree et al., 2021; Guimond et al., 2022). Highly charged polyelectrolytes such as heparin or the synthetic linear polyglycerol sulfate (Nie et al., 2021) tightly interact with the RBD electrostatically so that binding of the virion to HSPG is no longer possible. MD simulations provided additional support for this interaction directly and revealed that the more flexible linear polyglycerol sulfates could bind more tightly to the RBD exceeding the entropic costs by far, ultimately leading to a stronger inhibition (Nie et al., 2021).

To gain detailed insight into the interaction between S and anionic ligands based on opposite charges, the analysis of the surface potential of the protein and the possible identification of potential binding sites is extremely helpful. Here, we demonstrate this fact by calculating and visualizing the surface potential of the ectodomain or selected motifs of S using the software "Adaptive Poison-Boltzmann-Solver" (APBS; Jurrus et al., 2018). This program allows us to calculate numerically the surface potential of a given protein and visualize the result.

In Figure 3 (left), the distribution of positively charged amino acids in the top region and the surface potential of the ectodomain of the S protein of the original Wuhan (wt) SARS-CoV-2 are shown. It is obvious that the most distal part of the ectodomain, i.e., the top region, is characterized by a positive surface potential, while the stem region is characterized by domains with a neutral or even negative potential. Thus, the top region provides a potential target for negatively charged ligands.

Figure 4A (left) shows the surface potential map of the RBD for the wild type (Nie et al., 2021). Here, a channel of positive charge is seen on the surface of the RBD into which the strongly negative HS

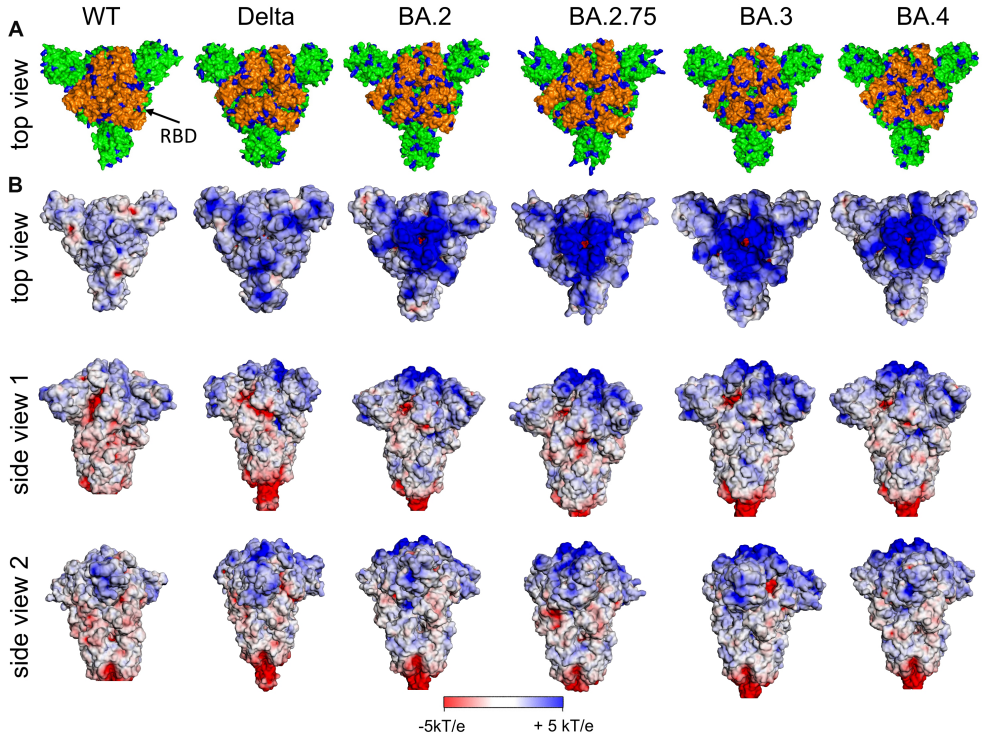

FIGURE 3
(A) Distribution of positively charged amino acids Arg and Lys (blue) in the top domain [RBD orange (arrow)] and **(B)** surface potential of the (Wuhan, wt) SARS-CoV-2S ectodomain and various variants of concern (VoC) in the closed state of RBDs at pH 7.0 [pdb: 7QUS (wt); 7SBK (Delta); 7XIX (BA.2); 7YQU (BA.2.75); 7XIY (BA.3); 7XNS (BA.4)]. Note, in the interest of stability the furin cleavage site in the stem region has been removed for the various spike proteins as usually done for 3D structure determination and other experimental setups.

chain fits well. The SARS-CoV-2 RBD of the Wuhan strain with the positively charged amino acids (Figure 3A, left) contributes significantly to the positive potential of the distal region of the S ectodomain and is shown from various perspectives in Figure 4. Apart from the RBD binding site for ACE2 (top view), the positive surface potential of the segments shown in the side views is of specific interest. In particular, the extended stretch of a positive surface potential (Figure 4 left, wt, red arrow in "side view 1") has been implicated as binding site for heparan sulfate by molecular modeling (Clausen et al., 2020; Nie et al., 2022). The analysis of the structure of S has revealed a well-defined RBD binding site for HS (Clausen et al., 2020; Liu et al., 2021). Since S comes as a trimer, three binding sites for the HS chains are leading to a multivalent interaction with remarkable strength. Clausen et al. (2020) stabilized the "open" or "closed" RBD conformation by site-directed mutagenesis of S and found a comparable binding affinity of both states for HS (Clausen et al., 2020). It has been also shown that binding of HS to the RBD does not only support the transition of the RBD to the "open spike" conformation required for binding to ACE2, but also stabilizes this conformation (Clausen et al., 2020; Yin et al., 2022). Using cryo-EM, Clausen et al. found that a sulfated heparin-derived icosasaccharide fragment caused a significant increase in the total amount of bound ACE2 to the S-trimer of wt SARS-CoV-2, due to the increased proportion of S-trimers carrying one or two ACE2 and a concomitant decrease in unbound S-trimers. As Liu et al. (2021) has provided evidence that the binding affinity of ACE2 to the RBD is only marginally reduced in the presence of an RBD binding octasaccharide we surmise that HSPG could increase the probability of ACE2 binding to the RBD of the S protein by favoring the open conformation rather than enhancing the affinity of ACE2 to the RBD *per se*. Based on the observation that the affinity of ACE2 to the RBD is about 15 to 20 fold higher than that to the S protein (Wrapp et al., 2020) and on their own observations, Shang et al. (2020) suggested that the dynamics between open and closed conformation and a preference for the latter could explain the difference of ACE2 affinity between RBD and the S protein. Thus, enhancing just the fraction of S proteins being in the open conformation could already lead an increase of the amount of bound ACE2 without affecting the affinity of ACE2 to the RBD.

Based on studies of the role of specific N-linked glycans of S in supporting the conversion in the open conformation of the RBD and its stabilization, Kearns et al. (2022) have hypothesized in their review that HS can support or even replace the action of the specific cellular receptor (Puray-Chavez et al., 2021). For the S protomer, 22 N-linked glycosylation sites were predicted. Experimentally, it could be shown that at least 17 of them are glycosylated (Casalino et al., 2020; Walls et al., 2020; Watanabe et al., 2020). As with the spike proteins of other viruses, the extensive glycosylation of the protein surface masks the antigenic sites and thus provides a protective shield against the immune system which is supported by the high flexibility of the glycan structures. A subsequent study has shown both experimentally and by molecular modeling simulations that certain

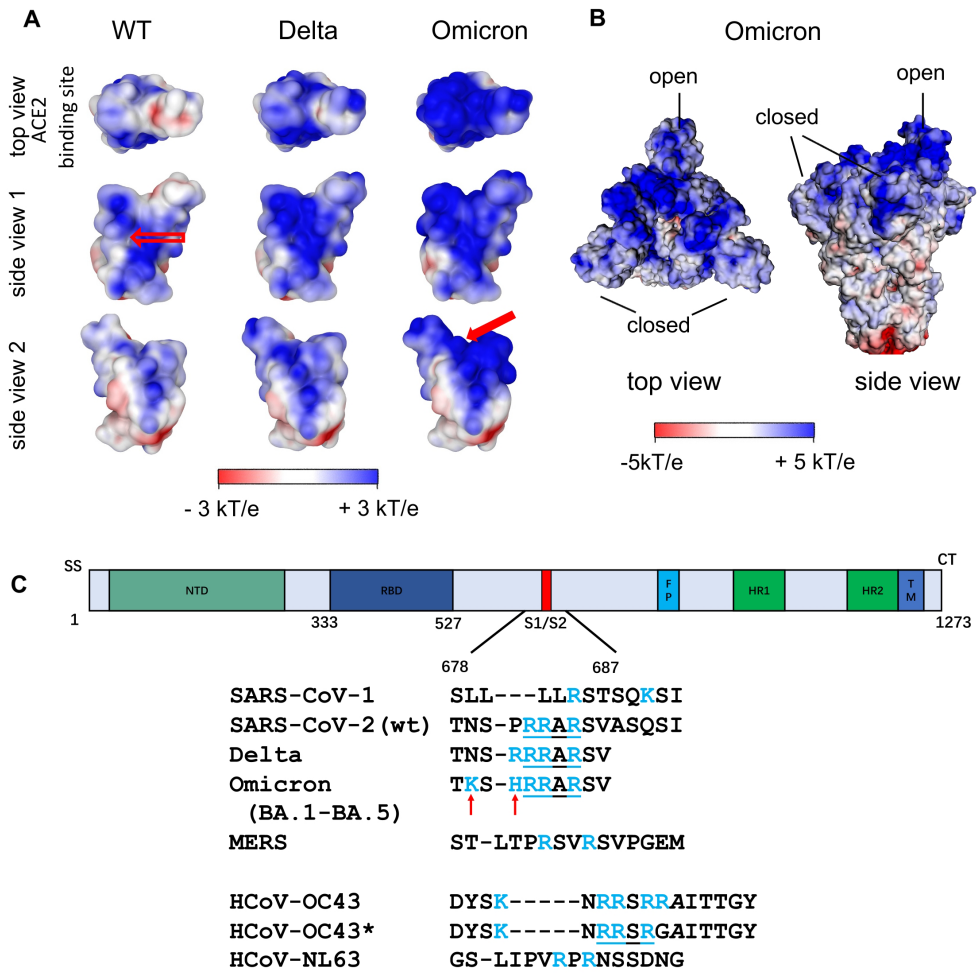

FIGURE 4
(A) Surface potential map of the RBD of the Wuhan (wt), the Delta and the Omicron variant at pH 7.0 (Nie et al., 2022). The top view corresponds to the top view of S with the open conformation of the RBD, i.e., the view of the ACE2 binding site. The stretch of positively charged amino acids in the Wuhan RBD (see empty arrow in "side view 1") has been proposed as heparan sulfate binding site. A second binding site of similar affinity was found for Omicron variants (see filled red arrow in "side view 2"; Nie et al., 2022). **(B)** Surface potential of the ectodomain of the trimeric S of the Omicron variant (B.1.1.529) with two RBDs being in the closed state and one RBD in the open state (pdb 7TGW). **(C)** Additional Cardin-Weintraub sites at the furin cleavage site of S Wuhan (wt) SARS-CoV-2S and SARS-CoV-2 VOCs. For comparison, the corresponding sequences of SARS-CoV-1, MERS and of the endemic coronaviruses HCoV-NL63 and HCoV-OC43/HCoV-OC43* are shown. In contrast to HCoV-OC43, HCoV-OC43* has undergone multiple passages in cultured cells (de Haan et al., 2008).

N-glycans–specifically the one linked to position N343–can facilitate the opening of the RBD and thus its binding to ACE2 (Sztain et al., 2021). Another molecular modeling study had concluded that an open conformation of the RBD can be stabilized by the glycans linked to N165 and N234 (Casalino et al., 2020). The N165 glycan stabilizes the up conformation by moving under the RBD when it has taken the up conformation (Harbison et al., 2022). The fact that the RBD binding site of HS significantly overlaps with the RBD binding site for N165 led Kearns et al. (2022) to hypothesize that HS can take over the function of the N165 glycan and thus promote the binding of RBD to ACE2. Puray-Chavez et al. (2021) has found that a lung adenocarcinoma cell line which did not express ACE2 can be infected by SARS-CoV-2 in the presence of HS. However, other cellular receptors such as neutrophilin-1 and integrin have been shown to mediate cell entry (Daly et al., 2020; Liu J. et al., 2022).

Additional strong support for the importance of electrostatic interaction comes from a comparison of SARS-CoV-1 and SARS-CoV-2. Kim et al. have called attention to a second cationic binding location at the furin cleavage site when comparing SARS-CoV-1 with SARS-CoV-2 S (Figure 4C; Kim et al., 2020). The new binding site which is preserved in the Delta and all currently dominating Omicron variants (BA.1-BA.5, XBB.1.5, XBB.1.16) features a sequence of amino acids that follows the classical Cardin-Weintraub scheme (alternating hydrophobic (X) and positively (B) charged amino acids as XBBXBX or XBBBXXBX; Cardin and Weintraub, 1989; Cardin et al., 1991), and presents an additional binding site for HS [*cf.* the discussion of this point by Liu et al. (2021)]. This new site should lead to a much stronger binding of SARS-CoV-2 S to HS when compared to that of SARS-CoV-1. Indeed, Kim et al. found that K_D for the binding of the SARS-CoV-1 monomer to heparin is 0.5 μM, whereas the $K_D = 40$ pM for the interaction in the case of SARS-CoV-2 S (Kim et al., 2020). This more than 10,000-fold increase of the binding strength can only be explained by the transition from a complex with a single binding

site to a complex in which two HS chains are bound to S. A rough estimate can be done from previous work on the basis of eq. (2): ΔG_{res} was found to be 20 kJ/mol or 7.9 k_BT for the interaction of lysozyme with heparin where Δn_{ci} is 3 (Malicka et al., 2022). Similar values can be assumed for the interaction of the RBD with HS: Here, the patch on the surface is large enough so that 3 cationic amino acids can interact with HS. As discussed above, Δw can be set to zero in good approximation. Then, using eq. (2), we can estimate for a salt concentration of 0.15 M that $\Delta G_b \cong 7.9 + 5.7 = 13.6$ k_BT, which would result in a $K_D \cong 1$ µM. For SARS-CoV-1, which does not have this additional binding site at the furin cleavage site discussed above, Kim et al. found a value of $K_D = 0.51$ µM, which is in the same order of magnitude (Kim et al., 2020). A second binding site appears at the furin cleavage site as shown for the wild type and the SARS-CoV-2 VOCs (see Figure 4). Now, the HS chains have two patches on the S monomer to which they can bind simultaneously. This means that the free energies of two binding sites increase dramatically, and the K_D is predicted to be of the order of 1 pM whereas Kim et al. find a value of 40 pM from their surface plasmon resonance (SPR) experiments. Apart from the large variation of the K_D measured by SPR between independent studies (see below), given the various stringent assumptions in this simple calculation of Kim et al. there is at least semi-quantitative agreement. Evidently, the enormous increase of the binding strength of S to heparin from SARS-CoV-1 to SARS-CoV-2 is in full accord with an additional binding site of HSPG to the S trimer (Figures 3, 4).

3.2. Higher cationic S surface charge of SARS-CoV-2 VoCs

Perhaps the most convincing evidence for the central role of electrostatics for the infection with SARS-CoV-2 comes from studies of its mutants. Several VoCs have turned out to be 2- to about 5-fold more infectious than the original Wuhan virus. This increased infectivity is caused by mutations primarily in the S ectodomain, which enhance binding affinity and/or support more efficient fusion with the target membrane (Cao et al., 2022a; Syed et al., 2022; Sun et al., 2023). These variants of increased fitness and/or resistance to vaccine protection/immune responses have displaced the original Wuhan virus, and then one VoC was replaced, sometimes in a matter of weeks, by the next more transmissible variant. The dominant VoCs in 2022 are Omicron strains, especially strains BA.4. and BA.5. The subvariants BA.2.75.2 and the Omicron BA.5 descendant BQ.1.1 are expected to become predominant in Western countries in the winter season 2022/2023 (Planas et al., 2022), while the Omicron variant XBB originated by recombination of two BA.2 descendants has become dominant in South and Southeast Asian countries (Tamura et al., 2022) and began to spread strongly in the U.S. in January 2023. These various Omicron species have more than 60 mutations with respect to the Wuhan virus, more than half of them in the ectodomain of the S monomer.

An important change along the successively evolving VoCs was the increase of positively charged amino acids in the S ectodomain, especially in the top region as shown in Figure 4 including the RBD (Figure 3A, orange). The additional positive amino acids on the surface led to an increased positive surface potential both in the closed and in the open state of the RBD (Figure 4B). The increase of positive charges is seen when analyzing subsequent variants leading to four more positive amino acids for the Delta variant and up to a total of nine more for the Omicron variants (Barroso da Silva et al., 2022; Nie et al., 2022; Pascarella et al., 2022; Fantini et al., 2023a,b). A second binding site for heparan sulfate in the RBD of Omicron variants is directly obvious from Figure 4A indicated by the filled red arrow in side view 2 (Nie et al., 2022). We hypothesize, that the marked increase of positive charges leads to a much stronger binding of HS to the S of Omicron variants.

It is important to note that the interaction of ACE2 with the RBD is of similar strength for the different mutants (Han et al., 2022). A comparison performed by Han et al. recently revealed that the dissociation constant K_D of the ACE2-S complex varies between 5 nM for the Alpha and 31 nM for the Omicron variant, whereas $K_D = 24.6$ nM is found for the original Wuhan virus (Han et al., 2022). An overview of K_D values of the interaction between ACE2 and the isolated RBD or the RBD of the complete ectodomain of the S-glycoprotein for different SARS-CoV-2 VoCs is shown in Figure 5. Only K_D values measured by SPR are shown here, as this method has been most commonly used to characterize the affinity between ACE2 and the RBD. Preliminary data shows that the affinity of the recent variant XBB.1.5 is in the same order of the various Omicron variants (Yue et al., 2023). The K_D values are distributed over a wider range and the data are afflicted by a rather large experimental error. No clear trend of decreasing K_D values for the Omicron variants is evident within the present limits of error. Moreover, the free energy of the interaction between ACE2 and the RBD in units of k_BT is given by the natural logarithm of K_D, and differences between K_D values as seen in Figure 5 will exert only a small influence on the complex

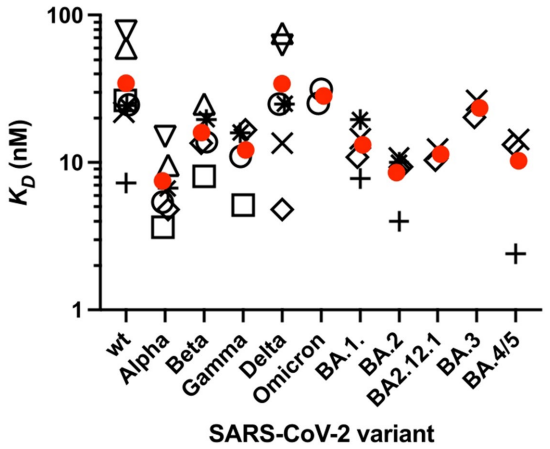

FIGURE 5
Affinity K_D of the RBD of the spike protein of SARS-CoV-2 variants to ACE2 measured by SPR. K_D was measured at 25°C or RT. Values are taken from several studies (open circle). Only studies that performed measurements on at least three SASR-CoV-2 variants were selected. Furthermore, only variants for which at least two, but typically three or more independent measurements were available are presented. Circles correspond to the isolated RBD, K_D values of the RBD [open square (Han et al., 2021); open circles (Han et al., 2022); open triangle up (Cameroni et al., 2022); open triangle down (McCallum et al., 2021); plus sign (Nutalai et al., 2022; Tuekprakhon et al., 2022); (Dejnirattisai et al., 2022); × (Cao et al., 2022b); open rhombus (Cao et al., 2022a); star (Li et al., 2022)]. Average K_D values are taken from each study. Mean values of these K_D values are shown (red circles).

formation between ACE2 and the RBD. Hence, the stability of the ACE2-S complex is comparable for all variants and cannot be responsible for their much higher infectivity as compared to the original strain.

The present analysis suggests that inhibitors designed to prevent binding to the host cell and thus virus infection should also consider negative charged entities that target the top domain of the S protein of SARS-CoV-2 VoCs and block its docking onto the HSPG. Indeed, a recent *in vivo* study showed the potential of a negatively charged polyacrylic acid-gelatin hydrogel that prevent SARS-CoV2 virus infections in monkeys (Mei et al., 2023). Chonira et al. have shown that a trimeric DARPin (Designed Ankyrin Repeat Protein) fused to a T4 fold-on bound strongly to the top domain of the S protein of SARS-CoV-2 variants (Chonira et al., 2023). The surface of DARPin is essentially of a negative potential as confirmed by an APBS analysis (not shown). The authors found that trimeric DARPin binds best to the Omicron variants (IC_{50}: Wuhan–1834 pM; Delta (B.1.617.2)–183 pM; Omicron (B.1.1.529) – 7.3 pM). While specific residues of the RBM and DARPins are engaged, we deduce that electrostatic interactions are also involved in binding and are even more pronounced in the top domain of the Omicron variants due to the additional positively charged amino acids (Figures 3, 4).

3.3. SARS-CoV-1, MERS-CoV, and endemic human coronaviruses

Despite their homologous S proteins, human coronaviruses recognize different specific cellular receptors. Similar to the case of SARS-CoV-2, ACE2 serves as the host cell receptor for SARS-CoV-1 (Li et al., 2003), while the cognate receptor of MERS-CoV is dipeptidyl-aminopeptidase 4 (DPP4; Raj et al., 2013). Specific cellular receptors also vary among the endemic human coronaviruses HCoV-NL63, HCoV-OC43 and HCoV-229E. While HCoV-NL63 also utilizes ACE2 (Milewska et al., 2014), HCoV-OC43 specifically binds to acetyl neuraminic acid, while HCoV-229E uses aminopeptidase N for cell entry (Yeager et al., 1992). Neither the S protein of MERS-CoV nor those of HCoV-OC43, HCoV-NL63 and HCoV-229E contains a Cardin-Weintraub sequence (see www.uniprot.org entries K9N5Q8, A0A140E065, Q6Q1S2, P15432, respectively). Binding of monomeric S of SARS-CoV-1 but also of MERS-CoV to heparin was demonstrated by SPR, albeit binding is with much lower affinity in comparison to that of SARS-CoV-2 (Kim et al., 2020). However, MERS-CoV was shown to also employ sialic acid as a co-receptor along with its main receptor DPP4 (Li et al., 2017).

Recently, an inhibitory effect of lactoferrin on the infection of cell cultures by HCoV-OC43, HCoV-NL63, and HCoV-229E viruses was found. From the binding of lactoferrin to HS on the cell surface, it was concluded indirectly that HS may also serve as a co-receptor for these viruses (Hu et al., 2021). However, laboratory strains may have gained affinity to heparan sulfate due to mutations in the course of serial passages. For example, the potential furin cleavage site of the S protein of HCoV-OC43 -NRRSRRA- changed to a Cardin-Weintraub-motif -NRRSRGA- in the laboratory strain HCoV-OC43* (Figure 4C; de Haan et al., 2008). But direct evidence that HS acts as co-receptor of HCoV-OC43 and HCoV-229E on permissive host cells is missing. Milewska et al. (2014) have shown for HCoV-NL63 that ACE2 is required for cell entry but HSPG serve as a primary attachment molecule (Milewska et al., 2014). In a subsequent study it was found that the M membrane protein present in the HCoV-NL63 envelope but not S binds to HS (Naskalska et al., 2019). The 3D structure of this protein is unknown.

We have calculated the surface potential of the S protein of SARS-CoV-1, MERS-CoV, HCoV-NL63, HCoV-OC43 and HCoV-229E (Figure 6) as described above. The top domain of the S protein of SARS-CoV-1 was comparable to that of the Wuhan SARS-CoV-2 rationalizing the observation that SARS-CoV-1 employs HS as a co-receptor (Lang et al., 2011). In contrast to the S protein of SARS-CoV-2, we could not identify domains of remarkable positive surface potential in the top domain or the stem region of S of MERS-CoV, HCoV-NL63, or HCoV-OC43. This finding is in accord with the fact that no Cardin-Weintraub sequences are found in the spike protein of these viruses (see above). Since HCoV-OC43 and MERS-CoV use the abundant neuraminic acid as a receptor and co-receptor (see above), respectively, we assume that naturally occurring variants of these viruses had no selective pressure or advantage to adapt to HS as a coreceptor. Based on the positive surface potential of the top domain of the HCoV-229E S protein, this could be a potential binding site for HS. However, up to now there is no evidence for this in the literature.

4. Human respiratory syncytial virus and human metapneumovirus

The relevance of a positive surface potential of the spike protein hemagglutinin of influenza A virus for interaction with the negatively charged host cell receptor sialic acid (Fantini et al., 2023b) and changes of the surface potential of hemagglutinin associated with the evolution and spreading of avian influenza A virus clades (Righetto and Filippini, 2020) have been discussed recently. Influenza A viruses (IAVs) use specific sialic acid residues (Sia) of the host cell glycocalyx as receptors. Thus, human pathogenic IAVs preferentially bind to α2,6-linked sialic acids, whereas avian IAVs preferentially bind to α2,3-linked sialic acids. The specificity might be less dichotomous that assumed before (Childs et al., 2009; Xu et al., 2012; Liu M. et al., 2022). For example, Liu M. et al. (2022) have concluded from studies on the binding behavior of an avian IAV that the binding specificity to sialic acids might be less dichotomous than previously assumed. Using a Sia-deficient HEK293 cell line, they systematically modified the composition of 2,3 and 2,6 sialoglycans on the cell surface by cotransfection with specific sialyltransferases. At the same time, they used sialoglycoproteins secreted by these cells to study binding of the virus by bilayer interferometry. The authors were able to show that binding and entry of the avian virus was significantly promoted by the human 2,6 Sia receptor when the avian 2,3 Sia receptor was only present to a small extent. Byrd-Leotis et al. (2019) found by binding to an N-glycan array that a range of avian, swine and human IAVs bind also to phosphorylated, nonsialylated N-glycans. Previous studies indicated the importance of the IAV hemagglutinin (HA) surface potential for virus binding to sialic acid residues on the host cell surface. Righetto and Filippini (2020) investigated the surface potential of the sialic acid binding domain of low pathogenic H5 IAV strains circulating and spreading among wild birds that could become

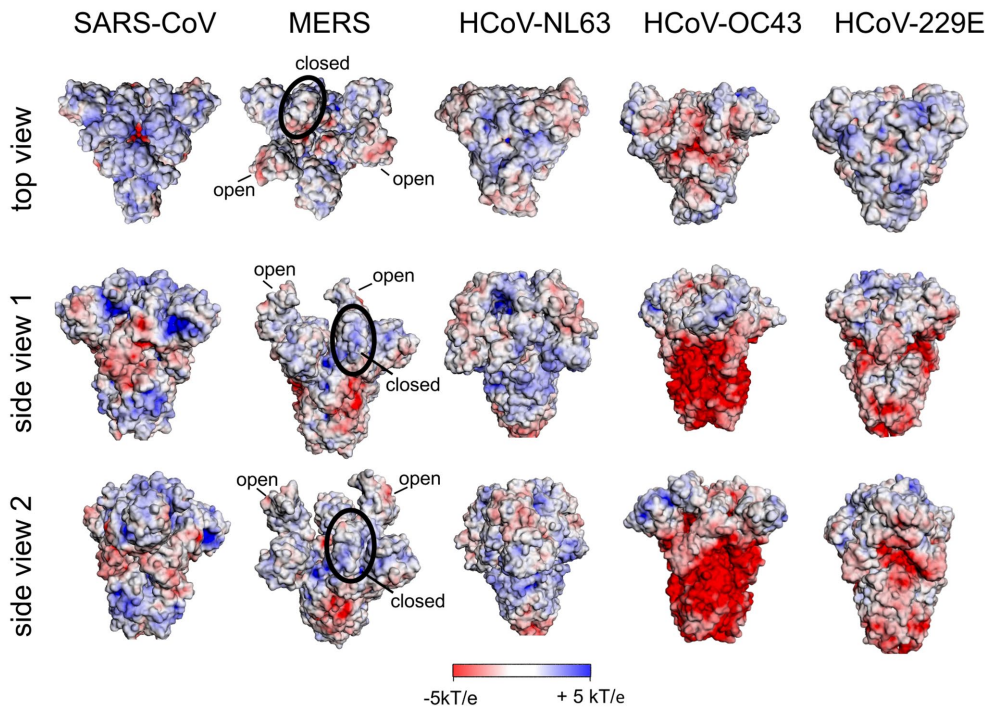

FIGURE 6
Surface potential of the ectodomain of the S protein of human coronaviruses. All structures are in the closed state of RBD except for MERS-CoV S. For the latter, two RBDs are in the open and one RBD in the closed state. A 3D structure with RBDs all in the closed state of RBD is not available [pdb: 5×58 (SARS-CoV); 5X5C (MERS-CoV); 5SZS (HCoV-NL63); 6OHW (pdb only available for HCoV-OC43*); 7CYC (HCoV-229E)].

highly pathogenic strains to poultry birds through genome variation. They found fingerprints of the binding domain surface potential specific for highly and low pathogenic H5 strains. In their review, Fantini et al. (2023a) pointed out that HA of IAV strains share the same arrangement of the cationic and aromatic residues as a canonical binding domain for sialic acids of negatively charged gangliosides (Suzuki, 1994), which is also used by other viruses such as Sendai virus (Markwell et al., 1981) and SV40 (Campanero-Rhodes et al., 2007) viruses [for more details see Fantini et al. (2023a) and references therein]. By analyzing the surface potential of the HA of the avian H5 IAV strain, Fantini et al. (2023a) hypothesized that the high positive surface potential of the HA tip of the ferret-transmissible H5 strain could allow the virus to infect multiple animal species and also become transmissible to humans. However, to our opinion, a more detailed analyses is still necessary to unravel the interplay between the stereo specific binding of HA to sialic acid residues of the host cell surface and the surface potential of the HA ectodomain for strain specific binding to host cells, and how a perturbation of this interaction is prevented by an interaction with HS.

Human respiratory syncytial virus (hRSV) and human metapneumovirus (hMPV) are important pathogens and cause infections in all age groups but predominantly affect infants. They preferentially infect the lower respiratory tract, mostly ciliated airway epithelial cells and type I alveolar pneumocytes (Schildgen et al., 2011; Battles and McLellan, 2019). Both viruses are members of the Pneumovirinae subfamily of the Paramyxoviridae family, and they are genetically closely related (Schildgen et al., 2011; Battles and McLellan, 2019). Two proteins are important for the early phases of virus infection are exposed on their envelope: the attachment protein (G) and the homotrimeric fusion protein (F). The F protein recognizes host cell-specific receptors and, after endocytic uptake of viruses, triggers the fusion of the viral envelope with the endosomal membrane of the host cell.

For both viruses it has been shown that the G protein binds to HS present in GAGs on the host cell surface (Chang et al., 2012; Klimyte et al., 2016) similar to the binding mechanism discussed above, namely, through a stretch of positively charged amino acids of a heparin-binding domain in the G protein. This domain is located between two mucin-like motifs as shown for hRSV (Krusat and Streckert, 1997; Feldman et al., 1999; Escribano-Romero et al., 2004). For both viruses, the G protein was found to be dispensable for virus replication *in vitro*, while the F protein is essential (Karron et al., 1997; Chang et al., 2012; Klimyte et al., 2016). It was shown that the F protein also mediates the initial binding of both viruses to the host cell through an interaction with cellular HS (Feldman et al., 2000; Chang et al., 2012). Based on the observations that both the G and F proteins of both viruses bind to HS, an analysis of the surface potential of the ectodomains of these proteins is of interest. However, this analysis is not possible for the G proteins because their ectodomains are disordered (Leyrat et al., 2014). One may hypothesize, however, that a flexible ectodomain enables an efficient interaction of positively charged amino acids with high content of negatively charged sialic acid and sulfate groups of mucus (Leal et al., 2017).

In contrast, the 3D structures of the ectodomains of the F proteins of both hRSV and hMPV are available. In Figure 7, we show the surface potential and the distribution of exposed and positively

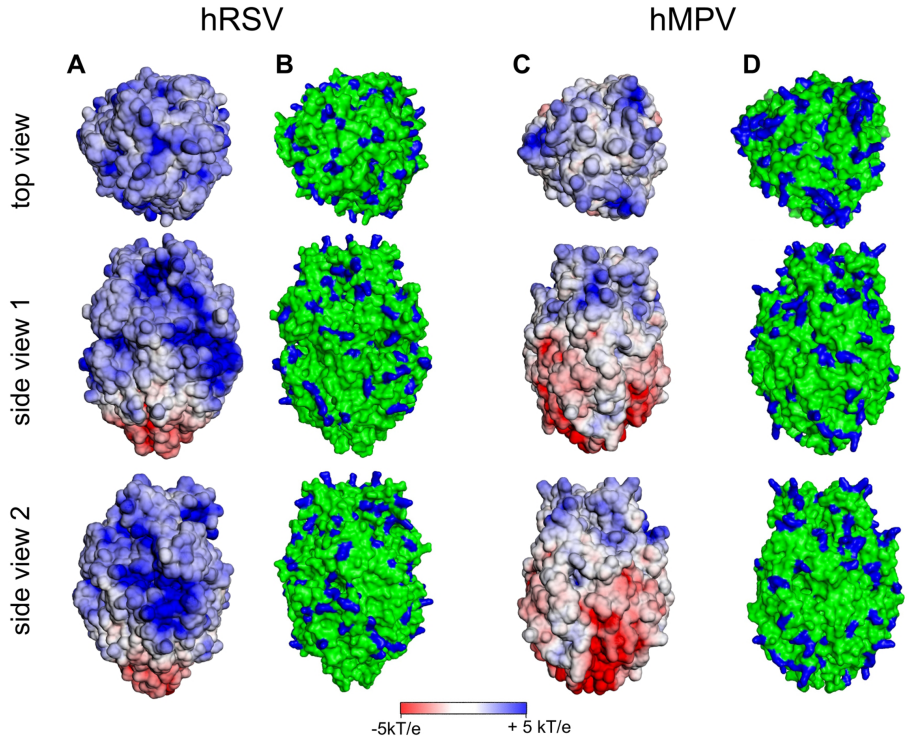

FIGURE 7
Surface potential **(A,C)** and surface distribution of positively charged amino acids Arg and Lys [blue; **(B,D)**] of human respiratory syncytial virus (hRSV; pdb 5UDE) and human metapneumovirus (hMPV; pdb 5WB0).

charged amino acids. As is obvious, both ectodomains are characterized by a pronounced positive surface potential that is more pronounced in the case of hRSV. Thus, binding to HS of the F proteins of either virus can be rationalized by the exposure of positively charged amino acids in the F ectodomains, which give rise to a positive surface potential as shown in Figure 7. Evidently, the analysis of the surface potential gives a more intuitive insight into the localization of positively charged patches than the surface distribution of positively charged amino acids. In consequence, this analysis strongly suggests for hRSV and hMPV a binding of the virion to the HSPG of the host cell as discussed above for SARS-CoV-2. The initial binding is mediated by interaction of G and F with HS. Subsequently, the F proteins recognize and interact with specific host cell receptors [for a review (Battles and McLellan, 2019)].

5. Conclusion

This survey has explored the relationship between positive surface charge patches on viral surface proteins with host cell binding. For SARS-CoV-2 this connection has clearly been shown: the first step of viral infection is the strong interaction of the positively charged patches on the surface of the spike protein with the negatively charged heparan sulfate chains on the cell surface. In a second step, cell entry is mediated by specific interaction with surface receptors such as ACE2. Surface potential maps generated by the Poisson-Boltzmann solver (APBS) were shown to provide a convenient tool to rationalize the interaction of the ectodomain of the virus with HS. A comparison with results for a number of different viruses underscored the validity of this approach. Hence, from our analysis and from data in literature, we may discern

(i) Viruses that need the interaction with HS for cell entry: SARS-CoV-2, Human respiratory syncytial virus (hRSV) and human metapneumovirus (hMPV)
(ii) Viruses that do not need this interaction: MERS, HCoV-NL63, and HCoV-OC43

The present analysis did not consider a possible change of the interaction by glycosylation of the spike proteins. This modification may affect the interaction considerably. However, the present survey suggests that glycosylation may alter the magnitude of binding constant but will not change the main conclusion presented here.

Author contributions

DL, KO, RH, MB, and AH are contributed to conception. MB and AH design the study and performed the theory and the calculations, respectively. DL, MB, and AH wrote the first draft of the manuscript. All authors contributed to manuscript revision, read, and approved the submitted version.

Funding

This work was funded by the Deutsche Forschungsgemeinschaft within the GRK 2662 "Charging into the Future" (DFG, German Research Foundation) Project ID 434130070 and the CRC 1449 "Dynamic Hydrogels at Biointerfaces" (DFG, German Research Foundation) Project ID 431232613 – SFB 1449.

Acknowledgments

The authors would like to thank Benedikt Kaufer (Institut für Virologie, Freie Universität Berlin) and Roland Netz (Institut für Physik, Freie Universität Berlin) for their critical review of the manuscript.

Conflict of interest

The authors declare that the research was conducted in the absence of any commercial or financial relationships that could be construed as a potential conflict of interest.

Publisher's note

All claims expressed in this article are solely those of the authors and do not necessarily represent those of their affiliated organizations, or those of the publisher, the editors and the reviewers. Any product that may be evaluated in this article, or claim that may be made by its manufacturer, is not guaranteed or endorsed by the publisher.

References

Achazi, K., Haag, R., Ballauff, M., Dernedde, J., Kizhakkedathu, J. N., Maysinger, D., et al. (2021). Understanding the interaction of polyelectrolyte architectures with proteins and Biosystems. *Angew. Chem. Int. Ed. Engl.* 60, 3882–3904. doi: 10.1002/anie.202006457

Barroso da Silva, F. L., Giron, C. C., and Laaksonen, A. (2022). Electrostatic features for the receptor binding domain of SARS-COV-2 wildtype and its variants. Compass to the severity of the future variants with the charge-rule. *J. Phys. Chem. B* 126, 6835–6852. doi: 10.1021/acs.jpcb.2c04225

Battles, M. B., and McLellan, J. S. (2019). Respiratory syncytial virus entry and how to block it. *Nat. Rev. Microbiol.* 17, 233–245. doi: 10.1038/s41579-019-0149-x

Bergqvist, S., O'Brien, R., and Ladbury, J. E. (2001). Site-specific cation binding mediates TATA binding protein-DNA interaction from a hyperthermophilic archaeon. *Biochemistry* 40, 2419–2425. doi: 10.1021/bi002488m

Bergqvist, S., Williams, M. A., O'Brien, R., and Ladbury, J. E. (2003). Halophilic adaptation of protein-DNA interactions. *Biochem. Soc. Trans.* 31, 677–680. doi: 10.1042/Bst0310677

Byrd-Leotis, L., Jia, N., Dutta, S., Trost, J. F., Gao, C., Cummings, S. F., et al. (2019). Influenza binds phosphorylated glycans from human lung. Science. *Advances* 5:eaav2554. doi: 10.1126/sciadv.aav2554

Cagno, V., Tseligka, E. D., Jones, S. T., and Tapparel, C. (2019). Heparan sulfate proteoglycans and viral attachment: true receptors or adaptation bias? *Viruses* 11:596. doi: 10.3390/v11070596

Cameroni, E., Bowen, J. E., Rosen, L. E., Saliba, C., Zepeda, S. K., Culap, K., et al. (2022). Broadly neutralizing antibodies overcome SARS-CoV-2 omicron antigenic shift. *Nature* 602, 664–670. doi: 10.1038/s41586-021-04386-2

Campanero-Rhodes, M. A., Smith, A., Chai, W., Sonnino, S., Mauri, L., Childs, R. A., et al. (2007). N-glycolyl GM1 ganglioside as a receptor for simian virus 40. *J. Virol.* 81, 12846–12858. doi: 10.1128/jvi.01311-07

Cao, Y., Song, W., Wang, L., Liu, P., Yue, C., Jian, F., et al. (2022a). Characterization of the enhanced infectivity and antibody evasion of omicron BA.2.75. *Cell Host Microbe* 30, 1527–1539.e5. doi: 10.1016/j.chom.2022.09.018

Cao, Y., Yisimayi, A., Jian, F., Song, W., Xiao, T., Wang, L., et al. (2022b). BA.2.12.1, BA.4 and BA.5 escape antibodies elicited by omicron infection. *Nature*. 608, 593–602. doi: 10.1038/s41586-022-04980-y

Capila, I., and Linhardt, R. J. (2002). Heparin–protein interactions. *Angew. Chem. Int. Ed.* 41, 390–412. doi: 10.1002/1521-3773(20020201)41:3<390::Aid-anie390>3.0.Co;2-b

Cardin, A. D., Demeter, D. A., Weintraub, H. J. R., and Jackson, R. L. (1991). Molecular design and modeling of protein heparin interactions. *Methods Enzymol.* 203, 556–583. doi: 10.1016/0076-6879(91)03030-K

Cardin, A. D., and Weintraub, H. J. R. (1989). Molecular modeling of protein-glycosaminoglycan interactions. *Arteriosclerosis* 9, 21–32. doi: 10.1161/01.Atv.9.1.21

Casalino, L., Gaieb, Z., Goldsmith, J. A., Hjorth, C. K., Dommer, A. C., Harbison, A. M., et al. (2020). Beyond shielding: the roles of Glycans in the SARS-CoV-2 spike protein. *ACS Cent. Sci.* 6, 1722–1734. doi: 10.1021/acscentsci.0c01056

Chang, A., Masante, C., Buchholz, U. J., and Dutch, R. E. (2012). Human Metapneumovirus (HMPV) binding and infection are mediated by interactions between the HMPV fusion protein and Heparan sulfate. *J. Virol.* 86, 3230–3243. doi: 10.1128/JVI.06706-11

Chang, Y. C., Wang, Z. P., Flax, L. A., Xu, D., Esko, J. D., Nizet, V., et al. (2011). Glycosaminoglycan binding facilitates entry of a bacterial pathogen into central nervous systems. *PLoS Pathog.* 7:e1002082. doi: 10.1371/journal.ppat.1002082

Childs, R. A., Palma, A. S., Wharton, S., Matrosovich, T., Liu, Y., Chai, W., et al. (2009). Receptor-binding specificity of pandemic influenza a (H1N1) 2009 virus determined by carbohydrate microarray. *Nat. Biotechnol.* 27, 797–799. doi: 10.1038/nbt0909-797

Chonira, V., Kwon, Y. D., Gorman, J., Case, J. B., Ke, Z. Q., Simeon, R., et al. (2023). A potent and broad neutralization of SARS-CoV-2 variants of concern by DARPins. *Nat. Chem. Biol.* 19, 284–291. doi: 10.1038/s41589-022-01193-2

Clausen, T. M., Sandoval, D. R., Spliid, C. B., Pihl, J., Perrett, H. R., Painter, C. D., et al. (2020). SARS-CoV-2 infection depends on cellular Heparan sulfate and ACE2. *Cells* 183:1043-+. doi: 10.1016/j.cell.2020.09.033

Condomitti, G., and de Wit, J. (2018). Heparan sulfate proteoglycans as emerging players in synaptic specificity. *Front. Mol. Neurosci.* 11. doi: 10.3389/fnmol.2018.00014

Daly, J. L., Simonetti, B., Klein, K., Chen, K. E., Williamson, M. K., Anton-Plagaro, C., et al. (2020). Neuropilin-1 is a host factor for SARS-CoV-2 infection. *Science* 370:861-+. doi: 10.1126/science.abd3072

de Haan, C. A. M., Haijema, B. J., Schellen, P., Schreur, P. W., te Lintelo, E., Vennema, H., et al. (2008). Cleavage of group 1 coronavirus spike proteins: how Furin cleavage is traded off against Heparan sulfate binding upon cell culture adaptation. *J. Virol.* 82, 6078–6083. doi: 10.1128/JVI.00074-08

Dejnirattisai, W., Huo, J., Zhou, D., Zahradník, J., Supasa, P., Liu, C., et al. (2022). SARS-CoV-2 omicron-B.1.1.529 leads to widespread escape from neutralizing antibody responses. *Cells* 185, 467–484.e15. doi: 10.1016/j.cell.2021.12.046

Escribano-Romero, E., Rawling, J., García-Barreno, B., and Melero, J. A. (2004). The soluble form of human respiratory syncytial virus attachment protein differs from the membrane-bound form in its oligomeric state but is still capable of binding to cell surface proteoglycans. *J. Virol.* 78, 3524–3532. doi: 10.1128/JVI.78.7.3524-3532.2004

Fantini, J., Azzaz, F., Chahinian, H., and Yahi, N. (2023a). Electrostatic surface potential as a key parameter in virus transmission and evolution: how to manage future virus pandemics in the post-COVID-19 era. *Viruses* 15:284. doi: 10.3390/v15020284

Fantini, J., Chahinian, H., and Yahi, N. (2023b). Convergent evolution dynamics of SARS-CoV-2 and HIV surface envelope glycoproteins driven by host cell surface receptors and lipid rafts: lessons for the future. *Int. J. Mol. Sci.* 24:1923. doi: 10.3390/ijms24031923

Feldman, S. A., Audet, S., and Beeler, J. A. (2000). The fusion glycoprotein of human respiratory syncytial virus facilitates virus attachment and infectivity via an interaction with cellular Heparan sulfate. *J. Virol.* 74, 6442–6447. doi: 10.1128/JVI.74.14.6442-6447.2000

Feldman, S. A., Hendry, R. M., and Beeler, J. A. (1999). Identification of a linear heparin binding domain for human respiratory syncytial virus attachment glycoprotein G. *J. Virol.* 73, 6610–6617. doi: 10.1128/JVI.73.8.6610-6617.1999

Friedrich, U., Blom, A. M., Dahlback, B., and Villoutreix, B. O. (2001). Structural and energetic characteristics of the heparin-binding site in antithrombotic protein C. *J. Biol. Chem.* 276, 24122–24128. doi: 10.1074/jbc.M011567200

Guimond, S. E., Mycroft-West, C. J., Gandhi, N. S., Tree, J. A., Le, T. T., Spalluto, C. M., et al. (2022). Synthetic Heparan sulfate mimetic Pixatimod (PG545) potently inhibits SARS-CoV-2 by disrupting the spike-ACE2 interaction. *Acs Cent. Sci.* 8, 527–545. doi: 10.1021/acscentsci.1c01293

Han, P. C., Li, L. J., Liu, S., Wang, Q. S., Zhang, D., Xu, Z. P., et al. (2022). Receptor binding and complex structures of human ACE2 to spike RBD from omicron and delta SARS-CoV-2. *Cells* 185:630-+. doi: 10.1016/j.cell.2022.01.001

Han, P., Su, C., Zhang, Y., Bai, C., Zheng, A., Qiao, C., et al. (2021). Molecular insights into receptor binding of recent emerging SARS-CoV-2 variants. *Nat. Commun.* 12:6103. doi: 10.1038/s41467-021-26401-w

Hao, W., Ma, B., Li, Z., Wang, X., Gao, X., Li, Y., et al. (2021). Binding of the SARS-CoV-2 spike protein to glycans. *Sci. Bull.* 66, 1205–1214. doi: 10.1016/j.scib.2021.01.010

Harbison, A. M., Fogarty, C. A., Phung, T. K., Satheesan, A., Schulz, B. L., and Fadda, E. (2022). Fine-tuning the spike: role of the nature and topology of the glycan shield in the structure and dynamics of the SARS-CoV-2 S. *Chem. Sci.* 13, 386–395. doi: 10.1039/D1SC04832E

Hernaiz, M. J., LeBrun, L. A., Wu, Y., Sen, J. W., Linhardt, R. J., and Heegaard, N. H. H. (2002). Characterization of heparin binding by a peptide from amyloid P component using capillary electrophoresis, surface plasmon resonance and isothermal titration calorimetry. *Eur. J. Biochem.* 269, 2860–2867. doi: 10.1046/j.1432-1033.2002.02964.x

Hileman, R. E., Jennings, R. N., and Linhardt, R. J. (1998). Thermodynamic analysis of the heparin interaction with a basic cyclic peptide using isothermal titration calorimetry. *Biochemistry* 37, 15231–15237. doi: 10.1021/bi980212x

Hoffmann, M., Kleine-Weber, H., Schroeder, S., Krüger, N., Herrler, T., Erichsen, S., et al. (2020). SARS-CoV-2 cell entry depends on ACE2 and TMPRSS2 and is blocked by a clinically proven protease inhibitor. *Cells* 181, 271–280.e8. doi: 10.1016/j.cell.2020.02.052

Hoffmann, M., Snyder, N. L., and Hartmann, L. (2022). Polymers inspired by heparin and Heparan sulfate for viral targeting. *Macromolecules* 55, 7957–7973. doi: 10.1021/acs.macromol.2c00675

Hu, Y., Meng, X., Zhang, F., Xiang, Y., and Wang, J. (2021). The in vitro antiviral activity of lactoferrin against common human coronaviruses and SARS-CoV-2 is mediated by targeting the heparan sulfate co-receptor. *Emerg. Microb. Infect.* 10, 317–330. doi: 10.1080/22221751.2021.1888660

Jairajpuri, M. A., Lu, A. Q., Desai, U., Olson, S. T., Bjork, I., and Bock, S. C. (2003). Antithrombin III phenylalanines 122 and 121 contribute to its high affinity for heparin and its conformational activation. *J. Biol. Chem.* 278, 15941–15950. doi: 10.1074/jbc.M212319200

Jawad, B., Adhikari, P., Podgornik, R., and Ching, W.-Y. (2022). Binding interactions between receptor-binding domain of spike protein and human angiotensin converting enzyme-2 in omicron variant. *J. Phys. Chem. Lett.* 13, 3915–3921. doi: 10.1021/acs.jpclett.2c00423

Jurrus, E., Engel, D., Star, K., Monson, K., Brandi, J., Felberg, L. E., et al. (2018). Improvements to the APBS biomolecular solvation software suite. *Protein Sci.* 27, 112–128. doi: 10.1002/pro.3280

Karamanos, N., Ricard-Blum, S., and Kletsas, D. (2022). Extracellular matrix: the dynamic structural and functional network in health and disease. *IUBMB Life* 74:926. doi: 10.1002/iub.2672

Karamanos, N. K., Theocharis, A. D., Piperigkou, Z., Manou, D., Passi, A., Skandalis, S. S., et al. (2021). A guide to the composition and functions of the extracellular matrix. *FEBS J.* 288, 6850–6912. doi: 10.1111/febs.15776

Karron, R. A., Buonagurio, D. A., Georgiu, A. F., Whitehead, S. S., Adamus, J. E., Clements-Mann, M. L., et al. (1997). Respiratory syncytial virus (RSV) SH and G proteins are not essential for viral replication in vitro: clinical evaluation and molecular characterization of a cold-passaged, attenuated RSV subgroup B mutant. *Proc. Natl. Acad. Sci. U. S. A.* 94, 13961–13966. doi: 10.1073/pnas.94.25.13961

Kearns, F. L., Sandoval, D. R., Casalino, L., Clausen, T. M., Rosenfeld, M. A., Spliid, C. B., et al. (2022). Spike-heparan sulfate interactions in SARS-CoV-2 infection. *Curr. Opin. Struct. Biol.* 76. doi: 10.1016/j.sbi.2022.102439

Kim, S. Y., Jin, W. H., Sood, A., Montgomery, D. W., Grant, O. C., Fuster, M. M., et al. (2020). Characterization of heparin and severe acute respiratory syndrome-related coronavirus 2 (SARS-CoV-2) spike glycoprotein binding interactions. *Antivir. Res.* 181:104873. doi: 10.1016/j.antiviral.2020.104873

Kim, W. K., and Netz, R. R. (2015). Barrier-induced dielectric counterion relaxation at super-low frequencies in salt-free polyelectrolyte solutions. *Euro. Phys. J. E* 38:120. doi: 10.1140/epje/i2015-15120-6

Klimyte, E. M., Smith, S. E., Oreste, P., Lembo, D., and Dutch, R. E. (2016). Inhibition of human Metapneumovirus binding to Heparan sulfate blocks infection in human lung cells and airway tissues. *J. Virol.* 90, 9237–9250. doi: 10.1128/JVI.01362-16

Kohling, S., Blaszkiewicz, J., Ruiz-Gomez, G., Fernandez-Bachiller, M. I., Lemmnitzer, K., Panitz, N., et al. (2019). Syntheses of defined sulfated oligohyaluronans reveal structural effects, diversity and thermodynamics of GAG-protein binding. *Chem. Sci.* 10, 866–878. doi: 10.1039/C8SC03649G

Krusat, T., and Streckert, H. J. (1997). Heparin-dependent attachment of respiratory syncytial virus (RSV) to host cells. *Arch. Virol.* 142, 1247–1254. doi: 10.1007/s007050050156

Lang, J., Yang, N., Deng, J., Liu, K., Yang, P., Zhang, G., et al. (2011). Inhibition of SARS pseudovirus cell entry by lactoferrin binding to heparan sulfate proteoglycans. *PLoS One* 6:e23710. doi: 10.1371/journal.pone.0023710

Leal, J., Smyth, H. D. C., and Ghosh, D. (2017). Physicochemical properties of mucus and their impact on transmucosal drug delivery. *Int. J. Pharm.* 532, 555–572. doi: 10.1016/j.ijpharm.2017.09.018

Lee, S., Inzerillo, S., Lee, G. Y., Bosire, E. M., Mahato, S. K., and Song, J. (2022). Glycan-mediated molecular interactions in bacterial pathogenesis. *Trends Microbiol.* 30, 254–267. doi: 10.1016/j.tim.2021.06.011

Leyrat, C., Paesen, G. C., Charleston, J., Renner, M., and Grimes, J. M. (2014). Structural insights into the human metapneumovirus glycoprotein ectodomain. *J. Virol.* 88, 11611–11616. doi: 10.1128/jvi.01726-14

Li, W., Hulswit, R. J. G., Widjaja, I., Raj, V. S., McBride, R., Peng, W., et al. (2017). Identification of sialic acid-binding function for the Middle East respiratory syndrome coronavirus spike glycoprotein. *Proc. Natl. Acad. Sci.* 114, E8508–E8517. doi: 10.1073/pnas.1712592114

Li, L., Liao, H., Meng, Y., Li, W., Han, P., Liu, K., et al. (2022). Structural basis of human ACE2 higher binding affinity to currently circulating omicron SARS-CoV-2 sub-variants BA.2 and BA.1.1. *Cells* 185, 2952–2960.e2910. doi: 10.1016/j.cell.2022.06.023

Li, W., Moore, M. J., Vasilieva, N., Sui, J., Wong, S. K., Berne, M. A., et al. (2003). Angiotensin-converting enzyme 2 is a functional receptor for the SARS coronavirus. *Nature* 426, 450–454. doi: 10.1038/nature02145

Liu, L., Chopra, P., Li, X. R., Bouwman, K. M., Tompkins, S. M., Wolfert, M. A., et al. (2021). Heparan sulfate proteoglycans as attachment factor for SARSCoV-2. *Acs Cent. Sci.* 7, 1009–1018. doi: 10.1021/acscentsci.1c00010

Liu, M., Huang, L. Z. X., Smits, A. A., Büll, C., Narimatsu, Y., van Kuppeveld, F. J. M., et al. (2022). Human-type sialic acid receptors contribute to avian influenza a virus binding and entry by hetero-multivalent interactions. *Nat. Commun.* 13:4054. doi: 10.1038/s41467-022-31840-0

Liu, J., Lu, F., Chen, Y., Plow, E., and Qin, J. (2022). Integrin mediates cell entry of the SARS-CoV-2 virus independent of cellular receptor ACE2. *J. Biol. Chem.* 298:101710. doi: 10.1016/j.jbc.2022.101710

Lohman, T. M., and Mascotti, D. P. (1992). Thermodynamics of ligand nucleic-acid interactions. *Methods Enzymol.* 212, 400–424.

Malicka, W., Haag, R., and Ballauff, M. (2022). Interaction of heparin with proteins: hydration effects. *J. Phys. Chem. B* 126, 6250–6260. doi: 10.1021/acs.jpcb.2c04928

Manning, G. S. (1969). Limiting Laws and Counterion condensation in polyelectrolyte solutions I. colligative properties. *J. Chem. Phys.* 51:924. doi: 10.1063/1.1672157

Manning, G. S. (1978). The molecular theory of polyelectrolyte solutions with applications to the electrostatic properties of polynucleotides. *Q. Rev. Biophys.* 11, 179–246.

Manning, G. S. (2008). Approximate solutions to some problems in polyelectrolyte theory involving nonuniform charge distributions. *Macromolecules* 41, 6217–6227. doi: 10.1021/ma800628v

Markwell, M. A., Svennerholm, L., and Paulson, J. C. (1981). Specific gangliosides function as host cell receptors for Sendai virus. *Proc. Natl. Acad. Sci. U. S. A.* 78, 5406–5410. doi: 10.1073/pnas.78.9.5406

Marques, C., Reis, C. A., Vivès, R. R., and Magalhães, A. (2021). Heparan sulfate biosynthesis and sulfation profiles as modulators of cancer signalling and progression. *Front. Oncol.* 11. doi: 10.3389/fonc.2021.778752

Mascotti, D. P., and Lohman, T. M. (1993). Thermodynamics of single-stranded RNA and DNA interactions with Oligolysines containing tryptophan–effects of base composition. *Biochemistry* 32, 10568–10579. doi: 10.1021/bi00091a006

Mascotti, D. P., and Lohman, T. M. (1995). Thermodynamics of charged oligopeptide-heparin interactions. *Biochemistry* 34, 2908–2915.

McCallum, M., Walls, A. C., Sprouse, K. R., Bowen, J. E., Rosen, L. E., Dang, H. V., et al. (2021). Molecular basis of immune evasion by the Delta and kappa SARS-CoV-2 variants. *Science* 374, 1621–1626. doi: 10.1126/science.abl8506

Mei, X., Li, J., Wang, Z., Zhu, D., Huang, K., Hu, S., et al. (2023). An inhaled bioadhesive hydrogel to shield non-human primates from SARS-CoV-2 infection. *Nat. Mater.* doi: 10.1038/s41563-023-01475-7

Milewska, A., Zarebski, M., Nowak, P., Stozek, K., Potempa, J., and Pyrc, K. (2014). Human coronavirus NL63 utilizes Heparan sulfate proteoglycans for attachment to target cells. *J. Virol.* 88, 13221–13230. doi: 10.1128/JVI.02078-14

Minsky, B. B., Atmuri, A., Kaltashov, I. A., and Dubin, P. L. (2013). Counterion condensation on heparin oligomers. *Biomacromolecules* 14, 1113–1121. doi: 10.1021/bm400006g

Mycroft-West, C. J., Su, D. H., Pagani, I., Rudd, T. R., Elli, S., Gandhi, N. S., et al. (2020). Heparin inhibits cellular invasion by SARS-CoV-2: structural dependence of the interaction of the spike S1 receptor-binding domain with heparin. *Thromb. Haemost.* 120, 1700–1715. doi: 10.1055/s-0040-1721319

Naskalska, A., Dabrowska, A., Szczepanski, A., Milewska, A., Jasik, K. P., and Pyrc, K. (2019). Membrane protein of human coronavirus NL63 is responsible for interaction with the adhesion receptor. *J. Virol.* 93, e00355–e00319. doi: 10.1128/jvi.00355-19

Netz, R. R. (2003). Polyelectrolytes in electric fields. *J. Phys. Chem. B* 107, 8208–8217. doi: 10.1021/jp022618w

Nguyen, K., and Rabenstein, D. L. (2016). Interaction of the heparin-binding consensus sequence of β-amyloid peptides with heparin and heparin-derived oligosaccharides. *J. Phys. Chem. B* 120, 2187–2197. doi: 10.1021/acs.jpcb.5b12235

Nie, C. A. X., Pouyan, P., Lauster, D., Trimpert, J., Kerkhoff, Y., Szekeres, G. P., et al. (2021). Polysulfates block SARS-CoV-2 uptake through electrostatic interactions**. *Angewandte Chemie-International Edition* 60, 15870–15878. doi: 10.1002/anie.202102717

Nie, C., Sahoo, A. K., Netz, R. R., Herrmann, A., Ballauff, M., and Haag, R. (2022). Charge matters: mutations in omicron variant favor binding to cells. *Chembiochem* 23:e202100681. doi: 10.1002/cbic.202100681

Nutalai, R., Zhou, D., Tuekprakhon, A., Ginn, H. M., Supasa, P., Liu, C., et al. (2022). Potent cross-reactive antibodies following omicron breakthrough in vaccinees. *Cells* 185, 2116–2131.e2118. doi: 10.1016/j.cell.2022.05.014

Olson, S. T., Halvorson, H., and Björk, I. (1991). Quantitative characterization of the thrombin-heparin interaction. Discrimination between specific and nonspecific binding models. *J. Biol. Chem.* 266, 6342–6352. doi: 10.1016/S0021-9258(18)38124-9

Pascarella, S., Ciccozzi, M., Bianchi, M., Benvenuto, D., Cauda, R., and Cassone, A. (2022). The electrostatic potential of the Omicron variant spike is higher than in Delta and Delta-plus variants: A hint to higher transmissibility? *J. Med. Virol.* 94, 1277–1280. doi: 10.1002/jmv.27528

Planas, D., Bruel, T., Staropoli, I., Guivel-Benhassine, F., Porrot, F., Maes, P., et al. (2022). Resistance of omicron subvariants BA.2.75.2, BA.4.6 and BQ.1.1 to neutralizing antibodies. *bioRxiv* 2022:516888. doi: 10.1101/2022.11.17.516888

Puray-Chavez, M., LaPak, K. M., Schrank, T. P., Elliott, J. L., Bhatt, D. P., Agajanian, M. J., et al. (2021). Systematic analysis of SARS-CoV-2 infection of an ACE2-negative human airway cell. *Cell Rep.* 36:109364. doi: 10.1016/j.celrep.2021.109364

Raj, V. S., Mou, H., Smits, S. L., Dekkers, D. H., Müller, M. A., Dijkman, R., et al. (2013). Dipeptidyl peptidase 4 is a functional receptor for the emerging human coronavirus-EMC. *Nature* 495, 251–254. doi: 10.1038/nature12005

Record, M. T., Anderson, C. F., and Lohman, T. M. (1978). Thermodynamic analysis of ion effects on the binding and conformational equilibria of proteins and nucleic acids: the roles of ion association or release, screening, and ion effects on water activity. *Q. Rev. Biophys.* 11, 103–178. doi: 10.1017/S003358350000202X

Record, M. T., Lohman, T. M., and Haseth, P. L. D. (1976). Ion effects on protein - nucleic-acid interactions. *Biophys. J.* 16:A14.

Ricard-Blum, S., and Perez, S. (2022). Glycosaminoglycan interaction networks and databases. *Curr. Opin. Struct. Biol.* 74:102355. doi: 10.1016/j.sbi.2022.102355

Righetto, I., and Filippini, F. (2020). Normal modes analysis and surface electrostatics of haemagglutinin proteins as fingerprints for high pathogenic type a influenza viruses. *BMC Bioinform.* 21:354. doi: 10.1186/s12859-020-03563-w

Rudd, T. R., Preston, M. D., and Yates, E. A. (2017). The nature of the conserved basic amino acid sequences found among 437 heparin binding proteins determined by network analysis. *Mol. BioSyst.* 13, 852–865. doi: 10.1039/C6mb00857g

Schedin-Weiss, S., Arocas, V., Bock, S. C., Olson, S. T., and Bjork, I. (2002a). Specificity of the basic side chains of Lys114, Lys125, and Arg129 of antithrombin in heparin binding. *Biochemistry* 41, 12369–12376. doi: 10.1021/bi020406j

Schedin-Weiss, S., Desai, U. R., Bock, S. C., Gettins, P. G. W., Olson, S. T., and Bjork, I. (2002b). Importance of lysine 125 for heparin binding and activation of antithrombin. *Biochemistry* 41, 4779–4788. doi: 10.1021/bi012163l

Schedin-Weiss, S., Desai, U. R., Bock, S. C., Olson, S. T., and Bjork, I. (2004). Roles of N-terminal region residues Lys11, Arg13, and Arg24 of antithrombin in heparin recognition and in promotion and stabilization of the heparin-induced conformational change. *Biochemistry* 43, 675–683. doi: 10.1021/bi030173b

Schildgen, V., Hoogen, B. V. D., Fouchier, R., Tripp, R. A., Alvarez, R., Manoha, C., et al. (2011). Human Metapneumovirus: lessons learned over the first decade. *Clin. Microbiol. Rev.* 24, 734–754. doi: 10.1128/CMR.00015-11

Seyrek, E., and Dubin, P. (2010). Glycosaminoglycans as polyelectrolytes. *Adv. Colloid Interf. Sci.* 158, 119–129. doi: 10.1016/j.cis.2010.03.001

Shang, J., Wan, Y., Luo, C., Ye, G., Geng, Q., Auerbach, A., et al. (2020). Cell entry mechanisms of SARS-CoV-2. *Proc. Natl. Acad. Sci.* 117, 11727–11734. doi: 10.1073/pnas.2003138117

Sun, X., Klingbeil, O., Lu, B., Wu, C., Ballon, C., Ouyang, M., et al. (2023). BRD8 maintains glioblastoma by epigenetic reprogramming of the p53 network. *Nature* 613, 195–202. doi: 10.1038/s41586-022-05551-x

Suzuki, Y. (1994). Gangliosides as influenza virus receptors. Variation of influenza viruses and their recognition of the receptor sialo-sugar chains. *Prog. Lipid Res.* 33, 429–457. doi: 10.1016/0163-7827(94)90026-4

Syed, A. M., Ciling, A., Taha, T. Y., Chen, I. P., Khalid, M. M., Sreekumar, B., et al. (2022). Omicron mutations enhance infectivity and reduce antibody neutralization of SARS-CoV-2 virus-like particles. *Proc. Natl. Acad. Sci. U S A* 119:e2200592119. doi: 10.1073/pnas.2200592119

Sztain, T., Ahn, S.-H., Bogetti, A. T., Casalino, L., Goldsmith, J. A., Seitz, E., et al. (2021). A glycan gate controls opening of the SARS-CoV-2 spike protein. *Nat. Chem.* 13, 963–968. doi: 10.1038/s41557-021-00758-3

Tamura, T., Ito, J., Uriu, K., Zahradnik, J., Kida, I., Nasser, H., et al. (2022). Virological characteristics of the SARS-CoV-2 XBB variant derived from recombination of two omicron subvariants. *bioRxiv* 2022:521986. doi: 10.1101/2022.12.27.521986

Thompson, L. D., Pantoliano, M. W., and Springer, B. A. (1994). Energetic characterization of the basic fibroblast growth factor-heparin interaction: identification of the heparin binding domain. *Biochemistry* 33, 3831–3840.

Toledo, A. G., Sorrentino, J. T., Sandoval, D. R., Malmstrom, J., Lewis, N. E., and Esko, J. D. (2021). A systems view of the Heparan sulfate Interactome. *J. Histochem. Cytochem.* 69, 105–119. doi: 10.1369/0022155420988661

Tree, J. A., Turnbull, J. E., Buttigieg, K. R., Elmore, M. J., Coombes, N., Hogwood, J., et al. (2021). Unfractionated heparin inhibits live wild type SARS-CoV-2 cell infectivity at therapeutically relevant concentrations. *Br. J. Pharmacol.* 178, 626–635. doi: 10.1111/bph.15304

Tuekprakhon, A., Nutalai, R., Dijokaite-Guraliuc, A., Zhou, D., Ginn, H. M., Selvaraj, M., et al. (2022). Antibody escape of SARS-CoV-2 omicron BA.4 and BA.5 from vaccine and BA.1 serum. *Cells* 185, 2422–2433.e13. doi: 10.1016/j.cell.2022.06.005

Vallet, S. D., Berthollier, C., and Ricard-Blum, S. (2022). The glycosaminoglycan interactome 2.0. American journal of physiology-cell. *Physiology* 322, C1271–C1278. doi: 10.1152/ajpcell.00095.2022

Walkowiak, J. J., and Ballauff, M. (2021). Interaction of polyelectrolytes with proteins: quantifying the role of water. *Adv. Sci.* 8:2100661. doi: 10.1002/advs.202100661

Walkowiak, J. J., Ballauff, M., Zimmermann, R., Freudenberg, U., and Werner, C. (2020). Thermodynamic analysis of the interaction of heparin with lysozyme. *Biomacromolecules* 21, 4615–4625. doi: 10.1021/acs.biomac.0c00780

Walls, A. C., Park, Y.-J., Tortorici, M. A., Wall, A., McGuire, A. T., and Veesler, D. (2020). Structure, function, and antigenicity of the SARS-CoV-2 spike glycoprotein. *Cells* 181, 281–292.e286. doi: 10.1016/j.cell.2020.02.058

Watanabe, Y., Allen, J. D., Wrapp, D., McLellan, J. S., and Crispin, M. (2020). Site-specific glycan analysis of the SARS-CoV-2 spike. *Science* 369, 330–333. doi: 10.1126/science.abb9983

Wrapp, D., Wang, N., Corbett, K. S., Goldsmith, J. A., Hsieh, C.-L., Abiona, O., et al. (2020). Cryo-EM structure of the 2019-nCoV spike in the prefusion conformation. *Science* 367, 1260–1263. doi: 10.1126/science.abb2507

Xu, X., Angioletti-Uberti, S., Lu, Y., Dzubiella, J., and Ballauff, M. (2019). Interaction of proteins with polyelectrolytes: comparison of theory to experiment. *Langmuir* 35, 5373–5391. doi: 10.1021/acs.langmuir.8b01802

Xu, X., and Ballauff, M. (2019). Interaction of lysozyme with a dendritic polyelectrolyte: quantitative analysis of the free energy of binding and comparison to molecular dynamics simulations. *J. Phys. Chem. B* 123, 8222–8231. doi: 10.1021/acs.jpcb.9b07448

Xu, D., and Esko, J. D. (2014). Demystifying heparan sulfate-protein interactions. *Annu. Rev. Biochem.* 83, 129–157. doi: 10.1146/annurev-biochem-060713-035314

Xu, R., McBride, R., Nycholat, C. M., Paulson, J. C., and Wilson, I. A. (2012). Structural characterization of the hemagglutinin receptor specificity from the 2009 H1N1 influenza pandemic. *J. Virol.* 86, 982–990. doi: 10.1128/jvi.06322-11

Xu, X., Ran, Q., Dey, P., Nikam, R., Haag, R., Ballauff, M., et al. (2018). Counterion-release entropy governs the inhibition of serum proteins by polyelectrolyte drugs. *Biomacromolecules* 19, 409–416. doi: 10.1021/acs.biomac.7b01499

Xu, X., Ran, Q. D., Haag, R., Ballauff, M., and Dzubiella, J. (2017). Charged dendrimers revisited: effective charge and surface potential of dendritic polyglycerol sulfate. *Macromolecules* 50, 4759–4769. doi: 10.1021/acs.macromol.7b00742

Yeager, C. L., Ashmun, R. A., Williams, R. K., Cardellichio, C. B., Shapiro, L. H., Look, A. T., et al. (1992). Human aminopeptidase N is a receptor for human coronavirus 229E. *Nature* 357, 420–422. doi: 10.1038/357420a0

Yin, W. C., Xu, Y. W., Xu, P. Y., Cao, X. D., Wu, C. R., Gu, C. Y., et al. (2022). Structures of the omicron spike trimer with ACE2 and an anti-omicron antibody. *Science* 375:1048. doi: 10.1126/science.abn8863

Yue, C., Song, W., Wang, L., Jian, F., Chen, X., Gao, F., et al. (2023). Enhanced transmissibility of XBB.1.5 is contributed by both strong ACE2 binding and antibody evasion. *bioRxiv* 2023:522427. doi: 10.1101/2023.01.03.522427

Zhang, F. M., Zhang, J. H., and Linhardt, R. J. (2015). Interactions between nattokinase and heparin/GAGs. *Glycoconj. J.* 32, 695–702. doi: 10.1007/s10719-015-9620-8

frontiers | Frontiers in Microbiology

TYPE Original Research
PUBLISHED 20 July 2023
DOI 10.3389/fmicb.2023.1227485

OPEN ACCESS

EDITED BY
Shijian Zhang,
Dana–Farber Cancer Institute, United States

REVIEWED BY
Hao Hu,
Washington University in St. Louis, United States
Anan Jongkaewwattana,
National Center for Genetic Engineering and Biotechnology (BIOTEC), Thailand

*CORRESPONDENCE
Ding Xiang Liu
✉ dxliu0001@scau.edu.cn

RECEIVED 23 May 2023
ACCEPTED 06 July 2023
PUBLISHED 20 July 2023

CITATION
Wei Y, Dai G, Huang M, Wen L, Chen RA and Liu DX (2023) Construction of an infectious cloning system of porcine reproductive and respiratory syndrome virus and identification of glycoprotein 5 as a potential determinant of virulence and pathogenicity.
Front. Microbiol. 14:1227485.
doi: 10.3389/fmicb.2023.1227485

Construction of an infectious cloning system of porcine reproductive and respiratory syndrome virus and identification of glycoprotein 5 as a potential determinant of virulence and pathogenicity

Yuqing Wei[1,2], Guo Dai[1], Mei Huang[3], Lianghai Wen[3], Rui Ai Chen[2] and Ding Xiang Liu[1,2]*

[1]Guangdong Province Key Laboratory Microbial Signals and Disease Control, Integrative Microbiology Research Centre, South China Agricultural University, Guangzhou, Guangdong, China, [2]Zhaoqing Branch Center of Guangdong Laboratory for Lingnan Modern Agricultural Science and Technology, Zhaoqing, Guangdong, China, [3]Zhaoqing Institute of Biotechnology Co., Ltd., Zhaoqing, Guangdong, China

Porcine reproductive and respiratory syndrome virus (PRRSV) infection of pigs causes a variety of clinical manifestations, depending on the pathogenicity and virulence of the specific strain. Identification and characterization of potential determinant(s) for the pathogenicity and virulence of these strains would be an essential step to precisely design and develop effective anti-PRRSV intervention. In this study, we report the construction of an infectious clone system based on PRRSV vaccine strain SP by homologous recombination technique, and the rescue of a chimeric rSP-HUB2 strain by replacing the GP5 and M protein-coding region from SP strain with the corresponding region from a highly pathogenic strain PRRSV-HUB2. The two recombinant viruses were shown to be genetically stable and share similar growth kinetics, with rSP-HUB2 exhibiting apparent growth and fitness advantages. Compared to in cells infected with PRRSV-rSP, infection of cells with rSP-HUB2 showed significantly more inhibition of the induction of type I interferon (IFN-β) and interferon stimulator gene 56 (ISG56), and significantly more promotion of the induction of proinflammatory cytokines IL-6, IL-8, ISG15 and ISG20. Further overexpression, deletion and mutagenesis studies demonstrated that amino acid residue F16 in the N-terminal region of the GP5 protein from HUB2 was a determinant for the phenotypic difference between the two recombinant viruses. This study provides evidence that GP5 may function as a potential determinant for the pathogenicity and virulence of highly pathogenic PRRSV.

KEYWORDS

porcine reproductive and respiratory syndrome virus, infectious clone, GP5, cytokines, pathogenicity and virulence

Introduction

Porcine reproductive and respiratory syndrome (PRRS) is a highly infectious disease of pigs characterized as 'blue-ear' pig disease (Terpstra et al., 1991; Shabir et al., 2016). The etiologic agent, porcine reproductive and respiratory syndrome virus (PRRSV), is an enveloped and positive-stranded RNA virus (Snijder et al., 2013). Its genomic RNA (gRNA) is approximately 15 kb in length and encodes 11 known open reading frames (ORFs). Two large ORFs, 1a and 1b, code for the nonstructural replicase proteins (nsps) that play essential roles in the viral replication cycle, including rearrangement of host membranes to establish viral replication complexes (RC), replication of gRNA and transcription of subgenomic RNAs (sgRNAs) for the efficient expression of viral proteins (Pasternak et al., 2001; Yuan et al., 2004). ORF2a, ORF2b, ORF3-7 and the recently discovered ORF5a encode structural proteins GP2, E, GP3, GP4, GP5, matrix protein (M), nucleocapsid protein (N) and GP5a, respectively, constituting the structural protein components of PRRSV virions. As small envelope proteins and secondary structural proteins, GP2, GP3 and GP4 interact to form heterotrimers, and together with E proteins, assist viral infectivity, bind to cell receptors, and effectively induce neutralizing antibody production and cellular immune response (Tian et al., 2017). N protein interacts with viral RNA to form nucleocapsid and participate in virion assembly. GP5a protein, a newly discovered novel structural protein in arteritis, is a non-glycosylated membrane protein and is also essential for viral activity (Veit et al., 2014), but its function needs further study.

GP5 is a highly glycosylated capsule protein of about 25 kDa, with the highest degree of variation in PRRSV. It consists of a cleavable signal peptide at the N-terminal, an extracellular domain containing multiple N-glycoylation sites, three putative hydrophobic transmembrane domains, and a long hydrophilic cytoplasmic tail region (Veit et al., 2014). GP5 is a key protein in the assembly of viral particles and is involved in the pathogenesis of viruses. It is also a key target protein of neutralizing antibodies and can induce both cellular and humoral immune responses (Veit et al., 2014). M is a non-glycoylated protein of about 18–19 kDa and is one of the most conserved structural proteins of PRRSV. It consists of a short extracellular domain (15–17 aa), three putative hydrophobic transmembrane domains, and a long hydrophilic cytoplasmic tail region (Veit et al., 2014). The transport of GP5 and M from the ER to the Golgi apparatus requires heterodimerization of M with GP5, suggesting that only properly assembled GP5/M complexes can pass through the quality control system of the ER. At the same time, GP5/M heterodimers are also integrated into the virions and play an important role in the adsorption, assembly and budding processes, and essential for the formation of infectious virions.

An atypical PRRSV strain causing high mortality and abortion storms was emerged in the late 1990s initially in the United States, and subsequently in other areas (Mengeling et al., 1998). Since June 2006, the epidemic of "high fever," caused by PRRSV variants, has caused great losses to the pig industry (Tian et al., 2007). Due to their high pathogenicity and virulence, these variants are also known as highly pathogenic PRRSV (HP-PRRSV; Xiao et al., 2008). Efforts were made to dissect the viral elements attributed to the high pathogenicity and virulence of these variants. Sequence comparison showed that many HP-PRRSV strains had a discontinuous deletion of several amino acids in nsp2, a multifunctional protein involved in viral replication and antiviral innate immune response (Allende et al., 2000; Kwon et al., 2008; Zhou et al., 2009; Faaberg et al., 2010; Morgan et al., 2013). A highly pathogenic PRRSV strain, HUB2, isolated from a pig farm in Hubei province also showed amino acid deletion in nsp2. So far, however, the association of nsp2 and other viral proteins from HP-PRRSV strains with their highly pathogenic phenotypes remains to be firmly established (Tong et al., 2007).

Regulation of the induction of antiviral and proinflammatory/inflammatory cytokines and chemokines is an important mechanism controlling the pathogenicity of many viruses. Indeed, secretion of several important cytokines (interleukin (IL)-8, IL-1β, interferon (IFN)-γ) is correlated with virus level, accounting for approximately 84% of the variations observed (Lunney et al., 2010). PRRSV infection induces the production of a variety of cytokines and inflammatory factors, including IL-1 and tumor necrosis factor-α (TNFα; Shen et al., 2000). PRRSV infection was reported to suppress host immune response by regulating IL-10 expression, resulting in increased mRNA levels of IL-1β, IFNα, IL-10, IL-12, TNFα and IFNγ during the first week of infection (Suradhat et al., 2003; Weesendorp et al., 2014). On the other hand, the quantity of innate cytokines secreted in PRRSV-infected pigs is significantly lower than with other viral infections (van Reeth et al., 1999). PRRSV mainly inhibited the secretion of type 1 IFNs (mainly IFN-a and IFN-β) by macrophages, and further inhibited the expression of antiviral factors induced by type 1 IFNs. It also stimulates Th1 cell-mediated immune responses that promote IFN-γ expression by PBMC at 4–8 weeks after PRRSV infection (Meier et al., 2003).

We have previously reported the complete nucleotide sequence of PRRSV-SP, a vaccine strain with low pathogenicity (Shen et al., 2000). In this study, a recombinant PRRSV-SP, PRRSV-rSP, was initially rescued from the full-length cDNA clone of PRRSV-SP. By replacing ORF5 and ORF6, coding for GP5 and M proteins, respectively, with the corresponding regions from the highly pathogenic strain PRRSV-HUB2, a chimeric recombinant virus, rSP-HUB2 was subsequently rescued. The two recombinant viruses were found to be genetically stable and share similar growth kinetics, with rSP-HUB2 showing apparent growth and fitness advantages. Interestingly, the two viruses induced differential expression of a number of antiviral and proinflammatory cytokines and chemokines. Further overexpression, deletion and mutagenesis studies demonstrated that amino acid residue F16 in the N-terminal region of the GP5 protein from HUB2 was a determinant for the phenotypic difference between the two recombinant viruses. This study provides evidence suggesting that GP5 may function as a potential determinant for the pathogenicity and virulence of HP-PRRSV.

Materials and methods

Virus, cell line, antibodies and reagents

PRRSV vaccine strain SP GenBank: (AF184212.1) was originally obtained from the Schering-Plough Animal Health Company and sequences for the GP5 and M from the highly pathogenic strain HUB2 were synthesized based on GenBank: EF112446.1.

PAM cells were prepared from 35-day-old normal weaned piglets (with PRSSV and anti-PRRSV antibodies testing negative) by removing the whole lungs and injecting 50 ~ 100 mL sterilized PBS

into the lungs from the trachea. After gently patting the surface of the lungs and gently rubbing repeatedly for 2–3 min, the lavage solution was recovered, filtered and centrifuged. The precipitated cells were re-suspended in RPMI 1640 nutrient medium with 10% FBS and cultured at 37°C, 5% CO_2. Marc-145 cell line was purchased from the American Type Culture Collection (ATCC10031), and IPAM cells (HTX2097) was purchased from Otwo Biotech (ShenZhen) Inc.

PRRSV positive serum was provided by Huanong (Zhaoqing) Biological Industry Technology Research Institute, China; HRP conjugated Goat anti-pig IgG was purchased from (Earthox); TIANprep Mini Plasmid Kit, FastKing RT Kit (with gDNase) and SuperReal PreMix Plus (SYBR Green) were purchased from Tiangen Biochemical Science and Technology; Gel Extraction Kit from OMEGA; Reverse Transcriptase M-MLV(RNase H-), 5×Reverse Transcriptase M-MLV Buffer, RNase Inhibitor and Random primers from TaKaRa; DMEM, FBS, pancreatin, penicillin and streptomycin from Gibco; restriction enzymes and high concentration T4 DNA Ligase from NEB; TransZol, 2×EasyPfu PCR SuperMix(−dye), 2×EasyTaq® PCR SuperMix(+dye), pEASY®-Basic Seamless Cloning and Assembly Kit from TransGen Biotech; mMESSAGE mMACHINE™ T7 Transcription Kit from Ambion; AEC(IHC) chromogenic working solution from Thermo.

Plasmids construction

The full-length cDNA clone of pBR322-PRRSV-SP was constructed by inserting the PRRSV-SP full-length cDNA into pBR322 under the control of the T7 promoter, followed by the T7 terminator and HDV sequence to ensure an accurate and productive mRNA synthesis. To distinguish the recombinant virus from WT virus, a T to A mutation at nucleotide position 3,448 was purposely introduced without altering the original amino acid sequence but eliminated a BsmBI site at the position. To construct pBR322-PRRSV-SP/HUB2, one fragment containing GP5 and M genes from HUB2 strain and three DNA fragments covering other regions of PRRSV-SP were joined by homologous recombination with the pEASY®-Basic Seamless Cloning and Assembly Kit.

Plasmids XJ40-GP5(SP), XJ40-M(SP), XJ40-GP5(HUB2) and XJ40-M(HUB2) were constructed by cloning the viral sequences into pXJ40 with the homologous recombination technique. Plasmid XJ40-GP5(HUB2/SP) was constructed by replacing the N-terminal 60 amino acids of GP5 protein from SP strain with the equivalent region from HUB2 strain; pXJ40-GP5(HUB2/SP)-M1, pXJ40-GP5(HUB2/SP)-M2 and pXJ40-GP5(HUB2/SP)-M3 were constructed by introducing F16 to S, Y24 to C and NNN33-35 to YSS mutations, respectively, with the homologous recombination technique.

The templates and primers used for construction of these plasmids were listed in Table 1.

Rescue of recombinant PRRSVs

The full-length plasmid BR322-PRRSV-SP and BR322-PRRSV-SP/HUB2 were linearized with NotI, purified with phenol/chloroform/isoamyl alcohol (25,24, 1), and used for *in vitro* transcription in 20 μL standard reaction volume according to the manufacturer's instruction. These transcripts were transfected into Marc-145 cells by electroporation. After incubating for 4–5 days until cytopathic lesions appeared, cells were harvested by freeze–thaw method and centrifuged at 5,000 rpm for 10 min at 4°C. The supernatants were harvested as the P0 virus stocks and stored at −80°C for future usage.

Validation of the rescued PRRSV-rSP and rSP-HUB2 by immunocytochemistry, Weston blot and sequencing

Each 100 μL of 10-time diluted recombinant virus from the viral stocks was inoculated into 96-well plates of MARC-145 monolayer cells. After adsorption at 37°C for 1 h, the medium was replaced with fresh DMEM containing 2% FBS. After incubation for 48 h, cells were washed twice with phosphate buffer and permeabilized with pre-cooled methanol at – 20°C for 30 min, incubated with anti-PRRSV serum and HRP conjugated goat anti-pig IgG with standard method.

Marc-145 cells were infected with the recombinant virus for 48–72 h and harvested. Cells were lysed with 150 μL of RIPA Buffer containing 1 mM PMSF, and analyzed by Western blot with anti-PPRSV serum and HRP conjugated goat anti-pig IgG. The protein expression was visualized with an Azure Biosystems C600 imaging system.

For sequencing confirmation, P0 virus stocks were passaged in MARC145 cells for 5–20 generations, and total RNAs were extracted for RT-PCR amplification and sequencing.

Characterization of the recombinant virus

Plaque assay, TCID50 and one-step growth curves were generally performed with standard methods in Marc-145 cells. Briefly, TCID50 was determined calculation with the Reed-Muench method by immunocytochemistry; for determining the one-step growth curves of PRRSV-rSP and rSP-HUB2, cells were infected with each virus at the multiplicity of infection (MOI) of 0.1, harvested at 0, 12, 24, 36, 48, 60, and 72 h post-infection (hpi), and TCID50 for each sample was determined. The average titers were calculated from triplicates.

RT-qPCR determination of viral and cellular RNAs

Total RNAs from virus-infected or transfected cells were extracted by the Trizol method and used as templates for the RT reaction with the FastKing gDNA dispelling RT superMix system (Tiangen). In a 20 μL standard reaction, 2 μg of template RNA was mixed with 4 μL of 5× Fastking-RT SuperMix (including FastKing RT enzyme, RNase inhibitor, random primers, oligo-dT primer, dNTP mixture and reaction buffer), supplemented with RNase-free water. The reaction was performed at 42°C for 15 min and 95°C for 3 min, and cDNA products were diluted 20-fold for qPCR analysis following the instructions for Super Real PreMix Plus (SYBR Green; Tiangen). In a 20 μL standard reaction, 8.4 μL of diluted cDNA, 10 μL of 2×SuperReal PreMix, 0.4 μL of 50×ROX reference dye, 0.6 μL of 10 μM forward primer (F) and 0.6 μL of 10 μM reverse primer (R) were added. The reaction procedure was set as follows: enzyme activation at 50°C for

TABLE 1 Templates and primers for plasmids construction.

Plasmid	Template	Primer (5′–3′)
pXJ40-GP5(SP)	pBR322-PRRSV-SP	Fwd: ACGCGGATCCATGTTGGGGAAATGCTTGACC Rev.: ACCGCTCGAGCTAGGGACGACCCCATTGTTC
pXJ40-M(SP)		
pXJ40-GP5(HUB2)	pBR322-PRRSV-SP/HUB2	Fwd: GATGATAAGTCCGGATCCATGTTGGGGAAGTGCTGAC Rev.: CTAGAGACGACCCCATTGTTCC
pXJ40-M(HUB2)		
pXJ40-GP5(HUB2/SP)	pXJ40-GP5(SP) pXJ40-GP5(HUB2)	Fwd: GATGATAAGTCCGGATCCATGTTGGGGAAGTGCTTGAC Rev.: CTAGAGACGACCCCATTGTTCC
pXJ40-GP5(HUB2/SP)-M1	pXJ40-GP5(HUB2/SP)	Fwd: CGATTGCTTTCTTTGTGGTGTATC Rev.: CCTGTTTTTGCTCACCCAGAAA Fwd: GGTGAGCAAAAACAGGAAGGCAA Rev.: CCACAAAGAAAGCAATCGCGAGCAAC
pXJ40-GP5(HUB2/SP)-M2		Fwd: ATCGTGCCGTTCTGTCTTGCTG Rev.: CCTGTTTTTGCTCACCCAGAAA Fwd: GGTGAGCAAAAACAGGAAGGCAA Rev.: ACAGAACGGCACGATACACCAC
pXJ40-GP5(HUB2/SP)-M3		Fwd: CTCGTCAACGCCAGCTACAGCAGCAGCTCTCATATTCAG Rev.: CCTGTTTTTGCTCACCCAGAAA Fwd: GGTGAGCAAAAACAGGAAGGCAA Rev.: GTAGCTGGCGTTGACGAGCAC

2 min, pre-denaturation at 95°C for 3 min, denaturation at 95°C for 3 s, annealing and extension at 60°C for 15 s (40 cycles). The melting curve was analyzed at 95°C for 15 s and 60°C for 60 s, and the results were presented as cyclic threshold (CT) values. The $2^{-\triangle\triangle CT}$ method was used to calculate the data and analyze the gene expression level with GAPDH as the reference gene.

Statistical analysis

The one-way ANOVA method was used to analyze the significant difference between the indicated sample and the respective control sample. Significance levels were presented by the value of p (ns, non-significant; $^{*}p < 0.05$; $^{**}p < 0.01$; $^{****}p < 0.0001$).

Result

Recovery of PRRSV-rSP vaccine strain and chimeric rSP-HUB2 strain from full-length cDNA clones

To recover a recombinant virus from the SP vaccine strain of PRRSV, the full-length cDNA was cloned into a pBR322-based plasmid flanked by the T7 promoter and T7 terminator sequences, generating pBR322-PRRSV-rSP (Figure 1A). Transfection of Marc145 cells with full-length *in vitro* transcripts from pBR322-PRRSV-rSP resulted in the rescue of the recombinant virus PRRSV-rSP. To recover a chimeric virus with GP5 and M genes replaced by equivalent sequences from a highly pathogenic strain, PRRSV-HUB2, pBR322-rSP-HUB2(GP5M) was constructed (Figure 1A). Transfection of Marc145 cells with the full-length *in vitro* transcripts from this construct led to the rescue of recombinant virus rSP-HUB2. In both cases, obvious pathogenic changes were observed in Marc145 cells from 36 h post-transfection (Figure 1B). The successful rescue of these two recombinant viruses was further confirmed by sequence verification, showing a point mutation (T3448A) and HUB2 strain-specific sequences in rSP-HUB2, and wild type SP sequence in PRRSV-rSP (Figure 1C). It was also noted that cytopathic changes usually appeared a few hours earlier in cells transfected with rSP-HUB2 transcripts than did in cells transfected with PRRSV-rSP transcripts.

Characterization of the growth properties and stability of PRRSV-rSP and rSP-HUB2

The growth properties of PRRSV-rSP and rSP-HUB2 in Marc145 cells were first characterized by immunocytochemistry and plaque assay. Similar shapes and sizes of the infection foci appeared in cells infected with the two viruses (Figure 2A), but slightly smaller plaques and higher viral titers were observed in rSP-HUB2-infected cells (Figure 2B). Further determination of the growth curves by TCID50 also revealed similar growth kinetics of the two recombinant viruses (Figure 2C). Once again, rSP-HUB2 reached a moderately higher (0.5 log) peak titer at 48 hpi, compared with the peak titer of PRRSV-rSP at the same time point post-infection (Figure 2C). Determination of viral protein expression by Western blot confirmed that earlier and moderately, but significantly higher accumulation of M protein was detected in cells infected with rSP-HUB2, compared with that in cells infected with PRRSV-rSP (Figure 2D). Certain inconsistencies between viral titers and the protein levels at various time points post-infection in these and several other repeated experiments were noted (Figures 2C,D). These inconsistencies might be caused by the relatively low sensitivity and experimental variations of the TCID50 assay.

The genetic stability of the two viruses was determined by nucleotide sequencing after passage in Marc145 cells for 22 passages, confirming that no additional nucleotide mutations occurred in the

10.3389/fmicb.2023.1227485

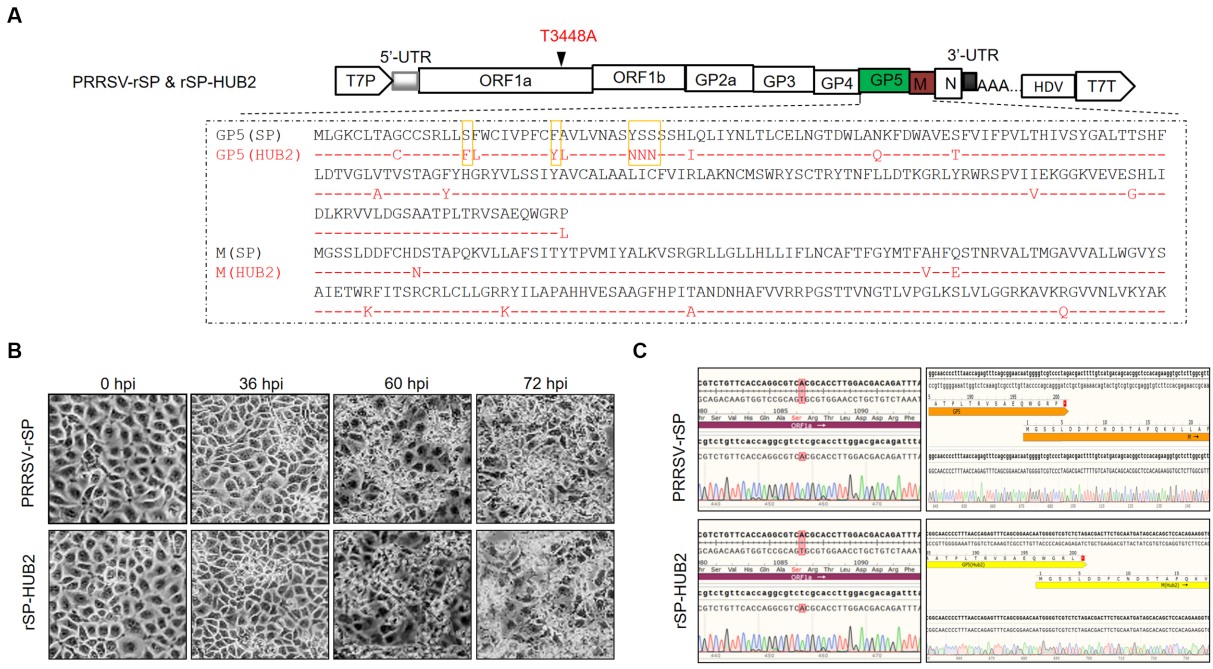

FIGURE 1
Rescue of recombinant PRRSV-rSP strain and chimeric rSP-HUB2 strain. **(A)** Diagram showing the genomic organization of PRRSV-rSP and rSP-HUB2. Illustrated include the positions of the T7 promoter, 5′-untranslated region (5′-UTR), different ORFs and protein-coding regions, the T3448A mutation, 3′-UTR, hepatitis delta virus sequence and the T7-terminator. The sequence comparison of GP5 and M proteins between the two recombinant viruses and the five boxed amino acids in GP5 used for mutagenesis in this study are also indicated. **(B)** Cytopathic effects of Marc145 cells transfected with the full-length *in vitro* transcribed PRRSV-rSP and rSP-HUB2 RNAs in time course experiments. The *in vitro* transcribed RNAs were electroporated into Marc145 cells and phase images were taken at 0, 24, 36, 48, 60 and 72 h post-electroporation, respectively. **(C)** Sequence validation of PRRSV-rSP and rSP-HUB2. The regions covering the T3448A mutation and the junction between GP5 and M were sequenced and shown.

two recombinant viruses during these passages. Taken together, these results indicate that replacement of GP5 and M in PRRSV-rSP with the equivalent sequences from the highly pathogenic HUB2 strain may render a growth advantage to the vaccine strain in Marc145 cells.

Differential induction of several innate immune and inflammatory genes in Marc145, IPAM and PAM cells infected with PRRSV-rSP and rSP-HUB2

To determine if the differences in the growth kinetics between the two recombinant viruses were dictated by their differential ability to induce cellular innate immune and inflammatory responses, Marc-145 and PMA cells were infected with 0.1 MOI of PRRSV-rSP and rSP-HUB2, and harvested at 0, 4, 12, 24, 36, 48, 60 and 72 hpi, respectively, for total RNA extraction and real-time qPCR analysis. The results demonstrated that the expression levels of IL-6, IL-8, IFN-β, ISG15, ISG20 and ISG56 were indeed differentially upregulated. As shown in Figure 3A, significantly higher induction levels of IL-6, IL-8, ISG15 and ISG20, respectively, were detected in rSP-HUB2-infected cells at 36 and 72 hpi, compared to the induction levels of these factors in cells infected with PRRSV-rSP at the same time points. On the contrary, the induction levels of IFN-β and ISG56 were more dramatically reduced in cells infected with rSP-HUB2 at 36 and 72 hpi, compared to their levels in cells infected with PRRSV-rSP at the same time points (Figure 3A). A similar differential induction pattern of these genes was also observed in these cells infected with the two recombinant viruses at other time points (Supplementary Figure 1). Consistently, the viral genomic RNA (gRNA) level of rSP-HUB2 was significantly higher than PRRSV-rSP (Figure 3A).

Western blot analysis of Marc-145 cells infected with the two recombinant viruses confirmed that earlier and generally higher accumulation of M protein was detected in cells infected with rSP-HUB2, compared with that in cells infected with PRRSV-rSP (Figure 3B). Taken together, these results confirm the differential induction of innate immune and proinflammatory responses by the two recombinant viruses, and prompted the subsequent studies to determine the roles played by the replacement region in chimeric rSP-HUB2 in the induction of these cytokines and chemokines.

Identification of GP5 protein from the highly pathogenic HUB2 strain as a main determinant responsible for the differential induction of innate immune and inflammatory responses

In order to identify the viral component(s) responsible for the differential induction of the innate immune and inflammatory genes, overexpression of M and GP5 proteins from PRRSV-rSP and rSP-HUB2, respectively, was carried out. The induction of the expression of these innate immune and inflammatory response-related genes was stimulated by Poly(I:C) instead of PRRSV infection to avoid the effects rendered by the viral proteins produced during

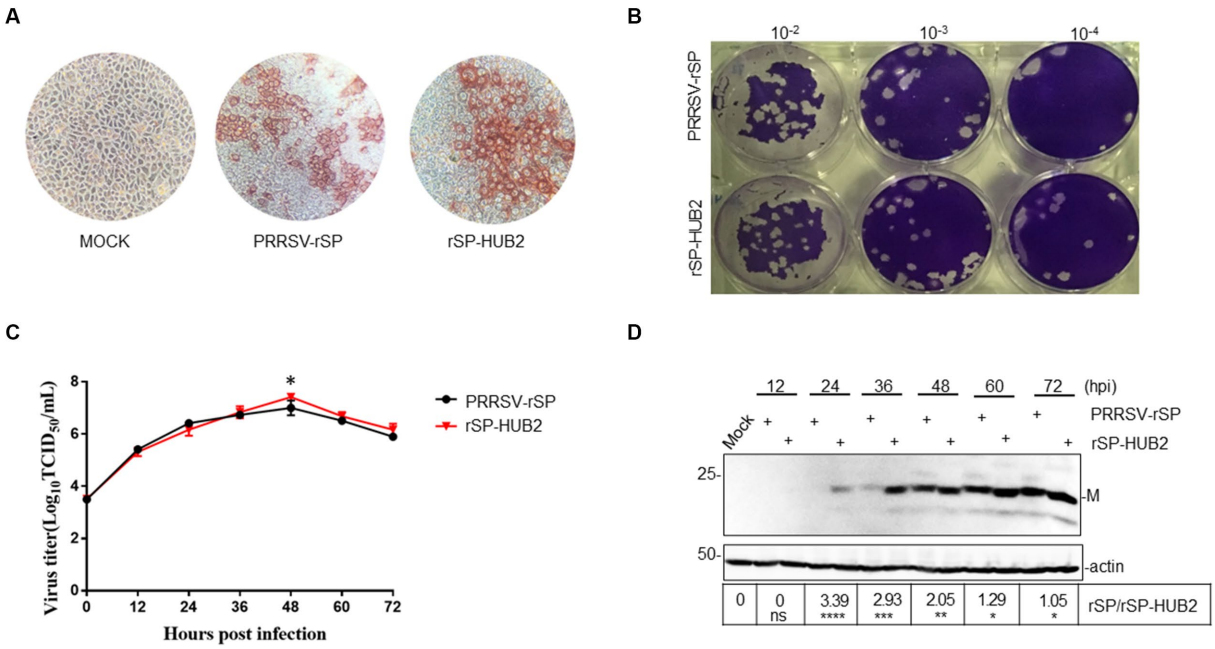

FIGURE 2
Characterization of the growth properties of PRRSV-rSP and rSP-HUB2. **(A)** Immunocytochemical examination of cells infected with PRRSV-rSP and rSP-HUB2. The recovered viruses were passaged in Marc-145 cells for 5 passages, harvested and 10-serially diluted. 100 μL each well of the diluted viruses were added to 96-well plates of Marc-145 cells with 90% confluency, cultured for 72 h, stained by immunocytochemistry and examined by light microscopy (20 ×). **(B)** Plaque assay. 200 μL each well of the 10-serially diluted viruses were added to Marc-145 cells in six-well plates. After incubation for 2 h, 2.5 mL of DMEM media mixed with low-melted-agarose were added to each well, continued incubation for 2–3 days, and visualized by staining with crystal violet. **(C)** Growth kinetics. Monolayers of Marc-145 cells were infected with PRRSV-rSP and rSP-HUB2, respectively, at an MOI of 0.1, and harvested at different time points post-infection. The titers of each virus were determined by TCID50 and plotted. *$p < 0.05$. **(D)** Western blot analysis of viral M protein in Marc-145 cells infected with PRRSV-rSP and rSP-HUB2. Marc-145 cells were infected with PRRSV-SP and rSP-HUB2, respectively, at an MOI of 0.1. Protein samples were resolved by SDS-PAGE and analyzed Western blot using a specific polyclonal antibody against M protein. Beta-actin was used as the loading control. Numbers on the left indicate protein sizes in kilodalton.

viral replication. Marc145 cells were co-transfected with pXJ40-FLAG-M(HUB2), pXJ40-FLAG-M(SP), pXJ40-FLAG-GP5(HUB2), pXJ40-FLAG-GP5(SP) or the empty vector pXJ40-FLAG, respectively with Poly(I:C; Figure 4A). The mRNA levels of IL-6, IL-8, IFN-β, ISG15, ISG20 and ISG56 at 12, 24, 36 and 48 h post-transfection were determined by RT-qPCR. Analysis of the M and GP5 protein levels by Western blot showed the expression of these proteins at very similar levels (Figure 4B). Overexpression of M protein from the two viruses did not render significant differential effects on the induction of these genes (Figure 4C). In cells overexpressing GP5 protein from both SP and HUB2 strains, however, differential expression of these cytokines and chemokines was observed. As shown in Figure 4C, overexpression of GP5(HUB2) induced significantly lower expression levels of IFN-β and ISG56, but significantly higher expression levels of IL-6, IL-8, ISG-15 and ISG-20, respectively, compared to the expression levels of these factors in cells transfected with GP5 from PRRSV-rSP at 36 h post-transfection. A similar pattern of differential induction of these genes in cells overexpressing the two GP5 proteins was also observed at other time points (Supplementary Figure 2). These results demonstrate that the GP5 protein from the highly pathogenic HUB2 strain may be the main determinant for the differential induction of these genes.

To further confirm and to locate the functional motif in GP5 responsible for this differential induction, the amino acid sequences of the two GP5 genes were compared, revealing that the major sequence differences were in the N-terminal first 60-amino-acid-region between the two GP5 proteins (Figure 1A). Accordingly, the first 60 amino acids in GP5(SP) were replaced with the equivalent region from GP5(HUB2), generating an expression plasmid pXJ40-FLAG-GP5(HUB2/SP) expressing the chimeric GP5 protein GP5(HUB2/SP; Figure 4A). Transfection of Marc145 cells with pXJ40-FLAG-GP5(HUB2/SP), pXJ40-FLAG-GP5(SP), pXJ40-FLAG-GP5(HUB2) and pXJ40-FLAG, respectively, in the presence of Poly(I:C) demonstrated that expression of the chimeric GP5 (GP5(HUB2/SP)) and GP5(HUB2) produced a similar enhancement effect on the induction of IL-6, IL-8, ISG15 and ISG20 and a similar suppressive effect on the expression of IFN-β and ISG56 (Figures 4B,C; Supplementary Figure 2). These results indicate that the sequence differences in the first 60 amino acids between GP5(SP) and GP5(HUB2) may play an essential role in the differential induction of these genes.

Identification of amino acid residues in GP5 protein critical for the differential induction of innate immune and proinflammatory responses

Comparison of the first 60 amino acid sequences between the two proteins showed differences at 10 amino acid positions between GP5(HUB2) and GP5(SP; Figure 1A). Five amino acids (F16S, Y24C, N33Y, N34S, and N35S) with significant changes in the amino acid properties were mutated back to the equivalent sequences in GP5(SP)

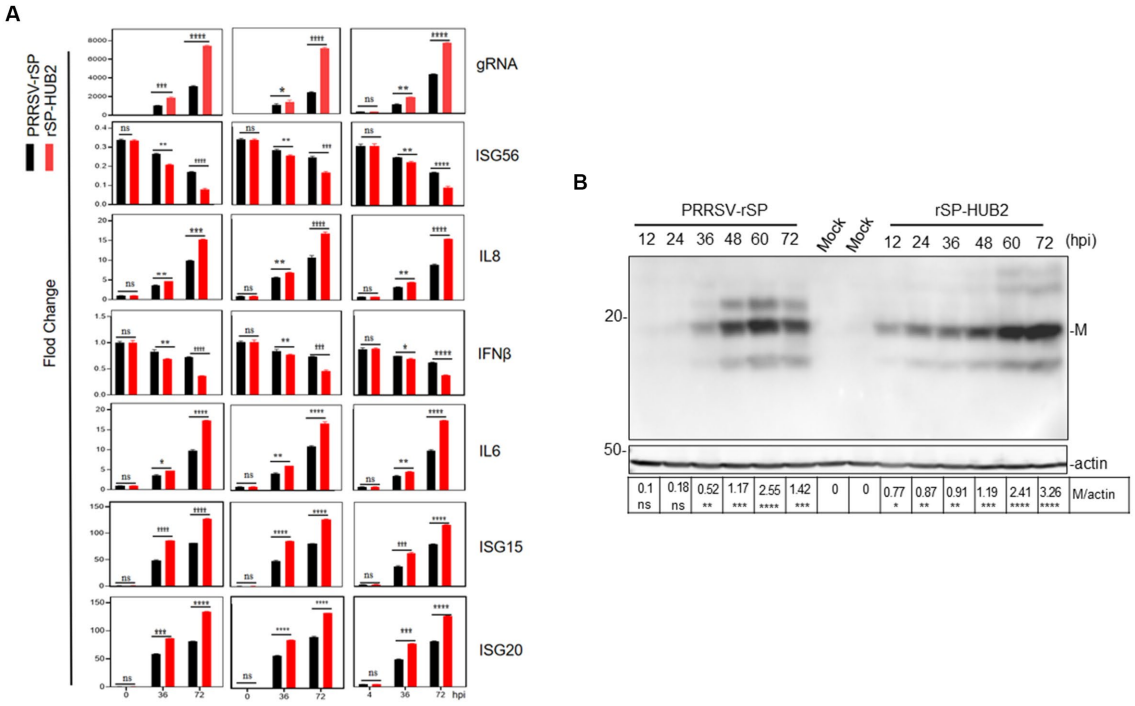

FIGURE 3
Differential induction of cytokines in Marc-145 and PAM cells infected with PRRSV-rSP and rSP-HUB2, as well as in IPAM cells transfected with the two viral RNAs, respectively. **(A)** RT-qPCR analysis of viral gRNA and mRNA levels of IL6, IL8, ISG15, ISG20, IFN-β and ISG56 in Marc-145, PAM and IPAM cells infected with PRRSV-rSP and rSP-HUB2, respectively. Cells were separately infected with PRRSV-rSP and rSP-HUB2 at an MOI of 1, harvested at 0, 36 and 72 hpi, respectively. Total RNAs were extracted and the levels of viral gRNA and above cytokines/chemokines were determined by RT-qPCR.*$p < 0.05$; **$p < 0.001$; ***$p < 0.0001$; ****$p < 0.00001$. **(B)** Western blot analysis of viral M protein. Cells were infected as described in **(A)** and viral M protein was analyzed by Western blot.

individually or with three amino acids together (Figures 1A, 5A). Two single-point (F16S and Y24C) and one triple-point (N33Y, N34S and N35S) mutations were introduced into the GP5(HUB2/SP) sequence, generating pXJ40-FLAG-GP5(HUB2/SP)-M1 (contains the F16S mutation), pXJ40-FLAG-GP5(HUB2/SP)-M2(Y24C mutation) and pXJ40-FLAG-GP5(HUB2/SP)-M3 (N33Y, N34S and N35S mutations; Figure 5A). Very similar expression efficiencies of these mutant proteins were detected in both Marc-145 and IPAM cells transfected with these constructs (Figure 5B).

Transfection of Marc145 and IPAM cells with pXJ40-flagGP5(HUB2/SP)-M3 in the presence of Poly(I:C) showed a similarly differential induction pattern of IL-6, IL-8, ISG15, ISG20, IFN-β and ISG56 as in cells overexpressing GP5(HUB2) and GP5(HUB2/SP), respectively, at 36 h post-transfection (Figure 5C), ruling out the potential involvement of these three residues in the differential induction of these genes (Figure 5C). Transfection of Marc145 and IPAM cells with pXJ40-flagGP5(HUB2/SP)-M1 in the presence of Poly(I:C) showed a similar induction pattern of IL-6, IL-8, ISG15 and ISG20 as in cells overexpressing GP5(SP), but the induction pattern of IFN-β and ISG56 was more similar to that in cells transfected with GP5(HUB2) and GP5(HUB2/SP), respectively, at 36 h post-transfection (Figure 5C). Very similar induction patterns of these genes were also observed in both Marc145 and IPAM cells overexpressing the two mutant constructs at other time points post-transfection (Supplementary Figure 3). These results suggest that amino acid residue Y16 might be involved in the differential induction of these pathogenic factors, but not in the induction of the two IFN genes. For some unknown reasons, however, the expression of flagGP5(HUB2/SP)-M2 in both Marc145 and IPAM cells induced an identical induction profile as in cells transfected with the vector control (Figure 5C; Supplementary Figure 3). Taken together, these results demonstrate that the F16-containing motif would be responsible for the differential induction of these proinflammatory genes by the two GP5 proteins.

The growth and fitness advantage of rSP-HUB2

The growth and fitness advantages of rSP-HUB2 over PRRSV-rSP were then tested by a competition assay in Marc-145 cells in the presence or absence of the type I IFN activation. Cells were treated with or without Poly(I:C), and infected with an MOI of approximately 0.1 of PRRSV-rSP and rSP-HUB2 mixture at the ratio of 9:1, and continuously passaged for 6 passages. Total RNAs were extracted from each passage, the GP5-M regions were amplified by RT-PCR, and the PCR products were sequenced to determine the relative abundances of the GP5M region from the two viruses, by comparing and calculating the average peaks between F16 and S16, Y24 and C24, and N33 and Y33. In the absence of type I IFN activation, the relative abundance of rSP-HUB2 clones were increased from 10 to 90% after 6 passages (Figure 6A). In the presence of Poly (I:C), the relative abundance of rSP-HUB2 clones were also increased, but at a slower pace (Figure 6B). It rose from 10% at passage 1 to 60% at passage 6

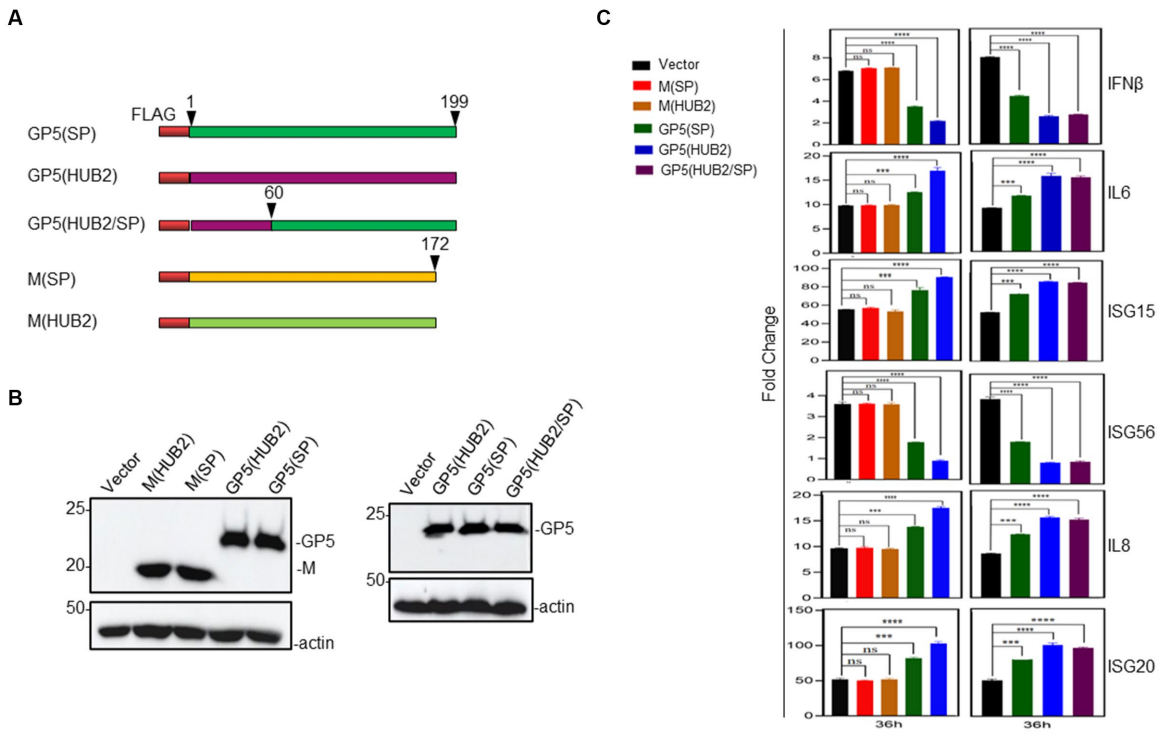

FIGURE 4
Effects of overexpression of GP5 and M proteins on Poly(I:C)-induced expression of IL-6, IL-8, ISG15, ISG20, IFN-β and ISG56 in MARC-145 cells. **(A)** Diagram showing three GP5 and two M constructs used in the overexpression experiments. The regions of GP5 and M from two different viruses were shown in different colors. **(B)** Western blot analysis of the expression of M and GP5 proteins in transfected cells. Marc-145 cells were transfected pXJ40-FLAG-M(HUB2), pXJ40-FLAG-M(SP), pXJ40-FLAG-GP5(HUB2), pXJ40-FLAG-GP5(SP) and empty vector pXJ40-FLAG, respectively, together with Poly(I:C), and harvested at 48 h post-transfection. Protein samples were resolved by SDS-PAGE and analyzed by Western blot using an anti-FLAG antibody. Beta-actin was used as the loading control. Numbers on the left indicate protein sizes in kilodalton. **(C)** RT-qPCR analysis of mRNA levels of IL-6, IL-8, ISG15, ISG20, IFN-β and ISG56 in transfected Marc-145 cells. Cells were transfected as described in **(B)** and harvested at 36 h points post-transfection. Total RNAs were extracted and mRNA levels of above cytokines/chemokines were determined by RT-qPCR.*$p < 0.05$; **$p < 0.001$; ***$p < 0.0001$; ****$p < 0.00001$.

(Figure 6B). These results confirm that replacement of the GP5-M region in rSP-HUB2 indeed renders advantages in growth, fitness and evasion of type I IFN action to the recombinant virus, unraveling an important potential virulence determinant in this region.

Discussion

The pathogenicity and virulence of different PRRSV strains vary dramatically, but the main virulence determinant(s) is yet to be firmly identified and characterized. In this study, a recombinant virus, rSP-HUB2, was rescued by replacing GP5 and M genes in vaccine strain PRRSV-rSP with equivalent sequences from a highly pathogenic strain HUB2, using a reverse genetics approach. The rescued rSP-HUB2 exhibited growth and fitness advantages in cultured cells and induced differential expression of a number of innate immune and proinflammatory genes. These include a significantly higher induction of IL-6, IL-8, ISG15 and ISG20, and a significantly more suppression of IFN-β and ISG56 induction, compared with its parental strain PRRSV-rSP. Further studies by overexpression, deletion and mutagenesis revealed that F16 at the N-terminal first 60 amino acids of GP5 may play an important regulatory role in the differential induction of these cytokines and chemokines. This region may be a potential virulence factor of a highly pathogenic PRRSV.

Infection of pigs by virulent and highly virulent PRRSV strains may cause increased mortality, abortion-storms or a severe interstitial pneumonia accompanied by a strong inflammatory response and severe suppurative bronchopneumonia (Rossow, 1998; Blaha, 2000; Rosell et al., 2000). Several viral factors, including the ability to get entry into target cells, viral replication rate, damage to host cells and induction of cell death or specific immune response, may determine the pathogenicity and virulence of a specific strain. Since the re-emergence of virulent strains, numerous studies have been carried out to define the virulence determinant(s). The presence of discontinuous 30 amino acid deletions in nsp2-coding region in both virulent PRRSV-1 and virulent PRRSV-2 strains was reported in many studies and was considered as genetic markers for virulent strains (Li et al., 2007; Zhou et al., 2008; do et al., 2016; Canelli et al., 2017). However, as these mutations were also found in some low virulent strains, their biological significance remains to be determined (Zhou et al., 2014). Deletion of specific nsp2 epitopes may play a role in modulating host immunity and viral infectivity (Chen et al., 2010), which was supported by a more recent study showing the loss of infectivity of a mutant JXwn06 strain (with a mutation in nsp2), due to changes in the cell tropism (Song et al., 2019). Furthermore, ORF1b region, specifically nsp9 and nsp10, contributes to the fatal *in vivo* and *in vitro* virulence of JXwn06 strain, with residues 586 and 592 of nsp9 being highlighted as critical sites regulating the replication of this virulent PRRSV-2 strain (Xu et al., 2018). In this line, other studies

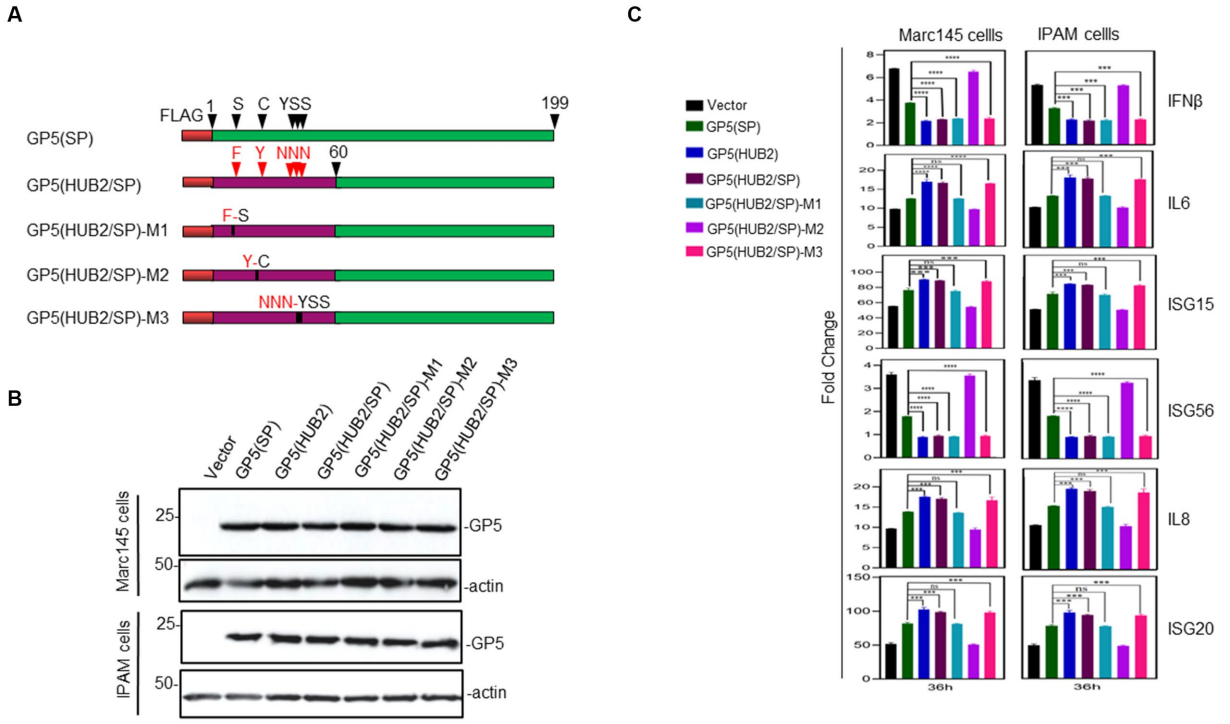

FIGURE 5
Effects of GP5-HUB2F16S/SP, GP5-HUB2Y24C/SP and GP5-HUB2NNN33–35YSS/SP on IL-6, IL-8, ISG15, ISG20, IFN-β and ISG56 expressions triggered by poly(I:C) in Marc-145 and IPAM cells. **(A)** Diagram showing five wild type and mutant GP5 constructs used in the overexpression experiments. The regions of GP5 from two different viruses and point mutations introduced were illustrated. **(B)** Western blot analysis of the expression of M and GP5 proteins in transfected cells. Marc-145 and IPAM cells were transfected pXJ40-FLAG-GP5-HUB2F16S/SP, pXJ40-FLAG-GP5-HUB2Y24C/SP, pXJ40-FLAG-GP5-HUB2NNN33–35YSS/SP, pXJ40-FLAG-GP5-HUB2, pXJ40-FLAG-GP5(HUB2/SP), pXJ40-FLAG-GP5-SP and empty vector pXJ40-FLAG, respectively, together with Poly(I:C), and harvested at 48 h post-transfection. Protein samples were resolved by SDS-PAGE and analyzed by Western blot using an anti-FLAG antibody. Beta-actin was used as the loading control. Numbers on the left indicate protein sizes in kilodalton. **(C)** RT-qPCR analysis of mRNA levels of IL-6, IL-8, ISG15, ISG20, IFN-β and ISG56 in transfected Marc-145 and IPAM cells. Cells were transfected as described in **(B)** and harvested at 36 h post-transfection. Total RNAs were extracted and mRNA levels of above cytokines/chemokines were determined by RT-qPCR. *$p < 0.05$; **$p < 0.001$; ***$p < 0.0001$; ****$p < 0.00001$.

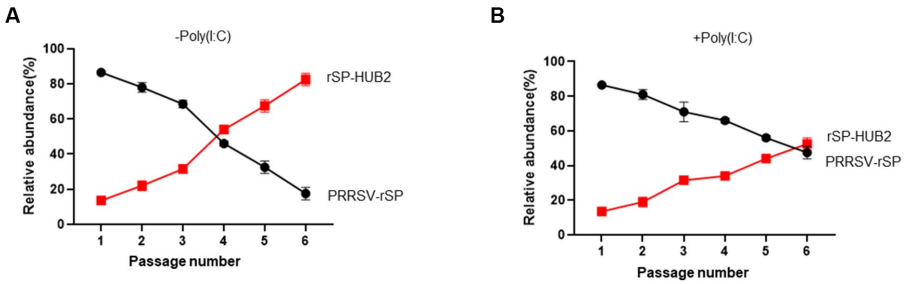

FIGURE 6
The growth and fitness advantages of rSP-HUB2 **(A)** Competition assays between rSP-HUB2 and PRRSV-rSP in the absence of type I IFN activation. Marc-145 cells were infected with PRRSV-rSP and rSP-HUB2 mixture at the ratio of 9:1 and continuously passaged for 6 passages. The relative abundance of each virus was determined by sequencing the GP5-M regions. **(B)** Competition assays between rSP-HUB2 and PRRSV-rSP in the presence of type I IFN activation. Marc-145 cells were transfected with Poly(I:C) and infected with PRRSV-rSP and rSP-HUB2 mixture at the ratio of 9:1 4 h post-transfection. After repeating the transfection/infection for 6 passages, the relative abundance of each virus was determined by sequencing the GP5-M regions.

recently identified a role of amino acids 519–544 in nsp9 in the pathogenicity and replication efficiency of the virulent HuN4 PRRSV-2 strain (Zhao et al., 2018). These results were largely in agreement with a previous study using a virulent PRRSV infectious clone (FL12) from the virulent NVSL 97–7,895 PRRSV-2 strain, pointing out that multiple genes, including nsp3-8 and ORF5 regions as the main virulence determinants together with nsp1-3, nsp10-12 (ORF1b) and ORF2, are associated with PRRSV virulence (Kwon et al., 2008). This hypothesis would be also supported by the finding of mutations and deletions in ORF5 as possible viral genetic determinants for virulence in some

virulent Asian PRRSV-2 strains, such as HuN4 (Ko Ko et al., 2019). Our observations presented in this study add more supportive evidence that ORF5-encoded GP5 functions as a critical virulence determinant.

The most variable region of PRRSV structural proteins is GP5 protein, and the homology varies greatly between strains of different subtypes. For example, the homology between the American and European strains is generally at the range from only 51 to 55% (Key et al., 2001). Neutralizing activity of PRRSV has been shown to correlate with the level of antibodies against GP5, both *in vivo* and *in vitro* (Wissink et al., 2003; Plagemann, 2004). Currently, several sites in GP5 have been demonstrated to be associated with antibody production, including three B cell epitopes, one conserved non-immunoneutralizing epitope and two CD4+T cell epitopes reported in this protein (de Lima et al., 2006; Vashisht et al., 2008). Neutralization antibody epitopes were also identified in GP4 and M proteins (Díaz et al., 2005). As most PRRSV GP5 protein contains three or more aspartate-linked glycosylation sites (Mardassi et al., 1995), oligosaccharides may also play a key role in the production of infectious PRRSV virus (Ansari et al., 2006). These aspartate glycosylation sites were also found to be adjacent to neutralizing epitopes, suggesting that they may interfere with the binding of antibody to neutralizing epitopes (Jiang et al., 2007). Glycosylation of GP5 inhibits the production of neutralizing antibodies (Ansari et al., 2006). Neutralizing antibodies appeared to be able to completely neutralize homologous viruses of sows and their piglets (Osorio et al., 2002), but unable to neutralize heterogenous virus isolates (Bautista and Molitor, 1999; Kwang et al., 1999; Ostrowski et al., 2002). In these cases, antibody response only provides weak protection, and long-term low levels of antibodies will lead to antibody-dependent enhancement effect, causing greater harm to the animal (Ostrowski et al., 2002). In this study, NNN33-35 residues in GP5 from the highly pathogenic HUB2 strain may create a putative N-linked glycosylation site. However, as overexpression of both wild type and chimeric GP5 proteins carrying these three amino acids did not show migration shift on SDS-PAGE gel, it is unclear if this site would be indeed modified by glycosylation in virus-infected cells.

Innate immunity is the front line in antiviral immune responses and bridges adaptive immunity against viral infections (Wu and Hur, 2015), PRRSV engages several strategies to evade the porcine innate immune responses. A previous study showed that PRRSV infection inhibited IFN-β production primarily by interfering with the MAVS activation in the RIG-I signaling pathway (Luo et al., 2008). PRRSV nsp4, the 3C-like protease (3CLSP), cleaves MAVS at Glu268 and the endoribonuclease activity of nsp11 degrades MAVS and RIG-I mRNA, inhibiting type I IFN signaling (Dong et al., 2015; Sun et al., 2016). PRRSV infection in swine also causes severe interstitial pneumonia (Morgan et al., 2016), indicating that the inflammatory response plays an important role in infection and pathogenesis of PRRSV (van REETH et al., 1999). Previous studies showed that the expressions of IL-1β, IL-8 and TNF-α were significantly elevated in virulent PRRSV-infected swine (Thanawongnuwech et al., 2004). Similarly, HP-PRRSV generates high levels of inflammatory cytokines including IL-1, IL-6 and TNF-α in peripheral blood (Li et al., 2017), indicating that HP-PRRSV may aggravate inflammation and damage tissues and organs. In addition, in pregnant gilts that were challenged on 85 days of gestation and euthanized 21 days post-infection, expression of cytokine genes was significantly upregulated in the thymus and spleen of the fetuses (Alex Pasternak et al., 2020). PRRSV also upregulates cytokine in PAMs and microglia (Qiao et al., 2011; Chen et al., 2014).

PRRSV N and nsp2 proteins have been reported as activators activating NF-kB during infection, whereas nsp1α, 1β, 2, 4 and 11 are known as suppressors (Lee and Kleiboeker, 2005). The contradictory roles of PRRSV proteins in NF-κB regulation further complicates the pathogenesis of this virus. Suppression of NF-κB may lead to the suppression of type I IFN response and activation of NF-κB may result in the production of proinflammatory cytokines. PRRSV infection of PAM cells activates the NLRP3 inflammasomes, inducing IL-1β production dependent on the TLR4/MyD88/NF-κB signaling pathway, and viral RNA can be sensed by cytosolic RNA sensor DDX19A (Bi et al., 2014; Li et al., 2015). PRRSV E protein was able to increase IL-1β release from LPS-primed PAM cells, while nsp11 may inhibit the secretion of IL-1β (Zhang et al., 2013). The endoribonuclease activity of nsp11 is essential for inhibition of IL-1β production (Wang et al., 2015)and NLRP3 inflammasome in microglia (Chen et al., 2018). PRRSV infection also induces IL-10 expression *in vivo* and *in vitro* (Suradhat et al., 2003; Singleton et al., 2018), and this induction depends on the NF-κB activation and p38 MAPK signaling (Hou et al., 2012). By screening PRRSV structural and nonstructural proteins, GP5 was identified as an IL-10 inducer, and its overexpression induced the phosphorylation of p38 (Hou et al., 2012; Song et al., 2013). In this study, we demonstrate that the regulatory effects of PRRSV-rSP and rSP-HUB2 on inflammatory factors are closely related to GP5. Infection of cells with the original HUB2 isolate would lend more supports to this conclusion, but, unfortunately, was constrained by the unavailability of this viral isolate. As the two recombinant viruses share the same SP backbone with differences in the GP5/M region only, the phenotypic differences observed in this study would be attributable to this region.

In summary, we report the construction of infectious clone systems for PRRSV-rSP vaccine strain and a chimeric strain rSP-HUB2. The two viruses are genetically stable, with the chimeric strain exhibiting growth and fitness advantages. Infection of cells with the two recombinant viruses showed differential regulation of the induction of a number of innate immune and proinflammatory genes in infected cells, which was partially attributable to amino acid residue F16 in GP5(HUB2). Further studies would be required to unravel other mechanisms underlying the growth and fitness advantage of this chimeric virus, in addition to its ability to differentially induce the expression of these innate immune and proinflammatory genes. Overall, this study has identified a potential PRRSV virulence determinant and would be instrumental in studying the pathogenicity of PRRSV and in precise modification of virulent strains for developing live attenuated vaccines against PRRSV infection.

Data availability statement

The datasets presented in this study can be found in online repositories. The names of the repository/repositories and accession number(s) can be found in the article/Supplementary material.

Ethics statement

Ethical review and approval was not required for the animal study because PAM cells used in this study were a gift from Zhaoqing Da Huanong Biopharmaceutical Co., Ltd., and were prepared from pigs in the Experimental Animal Center of Xinxing Dahua Agricultural, Poultry and Egg Co., Ltd., Yunfu, China, approved number SCXK (Guangdong) 2018-0019.

Author contributions

MH, RC, and DL contributed to conception and design of the study. YW, GD, and LW performed the experiments. YW and GD organized the database. YW, GD, and DL performed the statistical analysis. YW wrote the manuscript draft and DL did critical revision. All authors contributed to the article and approved the submitted version.

Funding

This work was partially supported by National Natural Science Foundation of China grants (31972660 and 32170152) and Zhaoqing Xijiang Innovative Team Foundation of China (grant number P20211154-0202).

Conflict of interest

MH and LW were employed by the company Zhaoqing Institute of Biotechnology Co., Ltd.

The remaining authors declare that the research was conducted in the absence of any commercial or financial relationships that could be construed as a potential conflict of interest.

Publisher's note

All claims expressed in this article are solely those of the authors and do not necessarily represent those of their affiliated organizations, or those of the publisher, the editors and the reviewers. Any product that may be evaluated in this article, or claim that may be made by its manufacturer, is not guaranteed or endorsed by the publisher.

Supplementary material

The Supplementary material for this article can be found online at: https://www.frontiersin.org/articles/10.3389/fmicb.2023.1227485/full#supplementary-material

References

Alex Pasternak, J., MacPhee, D. J., and Harding, J. (2020). Fetal cytokine response to porcine reproductive and respiratory syndrome virus-2 infection. *Cytokine* 126:154883. doi: 10.1016/j.cyto.2019.154883

Allende, R., Kutish, G. F., Laegreid, W., Lu, Z., Lewis, T. L., Rock, D. L., et al. (2000). Mutations in the genome of porcine reproductive and respiratory syndrome virus responsible for the attenuation phenotype. *Arch. Virol.* 145, 1149–1161. doi: 10.1007/s007050070115

Ansari, I. H., Kwon, B., Osorio, F. A., and Pattnaik, A. K. (2006). Influence of N-linked glycosylation of porcine reproductive and respiratory syndrome virus GP5 on virus infectivity, antigenicity, and ability to induce neutralizing antibodies. *J. Virol.* 80, 3994–4004. doi: 10.1128/JVI.80.8.3994-4004.2006

Bautista, E. M., and Molitor, T. W. (1999). IFNγ inhibits porcine reproductive and respiratory syndrome virus replication in macrophages. *Arch. Virol.* 144, 1191–1200. doi: 10.1007/s007050050578

Bi, J., Song, S., Fang, L., Wang, D., Jing, H., Gao, L., et al. (2014). Porcine reproductive and respiratory syndrome virus induces IL-1beta production depending on TLR4/MyD88 pathway and NLRP3 inflammasome in primary porcine alveolar macrophages. *Mediat. Inflamm.* 2014:403515. doi: 10.1155/2014/403515

Blaha, T. (2000). The "colorful" epidemiology of PRRS. *Vet. Res.* 31, 77–83. doi: 10.1051/vetres:2000109

Canelli, E., Catella, A., Borghetti, P., Ferrari, L., Ogno, G., de Angelis, E., et al. (2017). Phenotypic characterization of a highly pathogenic Italian porcine reproductive and respiratory syndrome virus (PRRSV) type 1 subtype 1 isolate in experimentally infected pigs. *Vet. Microbiol.* 210, 124–133. doi: 10.1016/j.vetmic.2017.09.002

Chen, X. X., Guo, Z., Jin, Q., Qiao, S., Li, R., Li, X., et al. (2018). Porcine reproductive and respiratory syndrome virus induces interleukin-1β through MyD88/ERK/AP-1 and NLRP3 inflammasome in microglia. *Vet. Microbiol.* 227, 82–89. doi: 10.1016/j.vetmic.2018.10.030

Chen, X. X., Quan, R., Guo, X. K., Gao, L., Shi, J., and Feng, W. H. (2014). Up-regulation of pro-inflammatory factors by HP-PRRSV infection in microglia: implications for HP-PRRSV neuropathogenesis. *Vet. Microbiol.* 170, 48–57. doi: 10.1016/j.vetmic.2014.01.031

Chen, Z., Zhou, X., Lunney, J. K., Lawson, S., Sun, Z., Brown, E., et al. (2010). Immunodominant epitopes in nsp2 of porcine reproductive and respiratory syndrome virus are dispensable for replication, but play an important role in modulation of the host immune response. *J. Gen. Virol.* 91, 1047–1057. doi: 10.1099/vir.0.016212-0

de Lima, M., Pattnaik, A. K., Flores, E. F., and Osorio, F. A. (2006). Serologic marker candidates identified among B-cell linear epitopes of Nsp2 and structural proteins of a north American strain of porcine reproductive and respiratory syndrome virus. *Virology* 353, 410–421. doi: 10.1016/j.virol.2006.05.036

Díaz, I., Darwich, L., Pappaterra, G., Pujols, J., and Mateu, E. (2005). Immune responses of pigs after experimental infection with a European strain of porcine reproductive and respiratory syndrome virus. *J. Gen. Virol.* 86, 1943–1951. doi: 10.1099/vir.0.80959-0

do, D. T., Park, C., Choi, K., Jeong, J., Nguyen, T. T., le, D. T. H., et al. (2016). Nucleotide sequence analysis of Vietnamese highly pathogenic porcine reproductive and respiratory syndrome virus from 2013 to 2014 based on the NSP2 and ORF5 coding regions. *Arch. Virol.* 161, 669–675. doi: 10.1007/s00705-015-2699-1

Dong, J., Xu, S., Wang, J., Luo, R., Wang, D., Xiao, S., et al. (2015). Porcine reproductive and respiratory syndrome virus 3C protease cleaves the mitochondrial antiviral signalling complex to antagonize IFN-β expression. *J. Gen. Virol.* 96, 3049–3058. doi: 10.1099/jgv.0.000257

Faaberg, K. S., Kehrli, M. E. Jr., Lager, K. M., Guo, B., and Han, J. (2010). In vivo growth of porcine reproductive and respiratory syndrome virus engineered nsp2 deletion mutants. *Virus Res.* 154, 77–85. doi: 10.1016/j.virusres.2010.07.024

Hou, J., Wang, L., Quan, R., Fu, Y., Zhang, H., and Feng, W. H. (2012). Induction of interleukin-10 is dependent on p38 mitogen-activated protein kinase pathway in macrophages infected with porcine reproductive and respiratory syndrome virus. *Virol. J.* 9:165. doi: 10.1186/1743-422X-9-165

Jiang, W., Jiang, P., Wang, X., Li, Y., Wang, X., and du, Y. (2007). Influence of porcine reproductive and respiratory syndrome virus GP5 glycoprotein N-linked glycans on immune responses in mice. *Virus Genes* 35, 663–671. doi: 10.1007/s11262-007-0131-y

Key, K. F., Haqshenas, G., Guenette, D. K., Swenson, S. L., Toth, T. E., and Meng, X. J. (2001). Genetic variation and phylogenetic analyses of the ORF5 gene of acute porcine reproductive and respiratory syndrome virus isolates. *Vet. Microbiol.* 83, 249–263. doi: 10.1016/S0378-1135(01)00427-8

Ko Ko, Y., Pamonsinlapatham, P., Myint, A., Latt, A. Z., Aye, K., Rungpragayphan, S., et al. (2019). Sequence and phylogenetic analyses ofNsp2-HVII,ORF5, andORF7 coding regions of highly pathogenic porcine reproductive and respiratory syndrome virus from Myanmar. *Transbound. Emerg. Dis.* 66, 1073–1076. doi: 10.1111/tbed.13118

Kwang, J., Yang, S., Osorio, F. A., Christian, S., Wheeler, J. G., Lager, K. M., et al. (1999). Characterization of antibody response to porcine reproductive and respiratory syndrome virus ORF5 product following infection and evaluation of its diagnostic use in pigs. *J. Vet. Diagn. Investig.* 11, 391–395. doi: 10.1177/104063879901100501

Kwon, B., Ansari, I. H., Pattnaik, A. K., and Osorio, F. A. (2008). Identification of virulence determinants of porcine reproductive and respiratory syndrome virus through construction of chimeric clones. *Virology* 380, 371–378. doi: 10.1016/j.virol.2008.07.030

Lee, S. M., and Kleiboeker, S. B. (2005). Porcine arterivirus activates the NF-κB pathway through IκB degradation. *Virology* 342, 47–59. doi: 10.1016/j.virol.2005.07.034

Li, J., Hu, L., Liu, Y., Huang, L., Mu, Y., Cai, X., et al. (2015). DDX19A senses viral RNA and mediates NLRP3-dependent Inflammasome activation. *J. Immunol.* 195, 5732–5749. doi: 10.4049/jimmunol.1501606

Li, Y., Wang, X., Bo, K., Wang, X., Tang, B., Yang, B., et al. (2007). Emergence of a highly pathogenic porcine reproductive and respiratory syndrome virus in the mid-eastern region of China. *Vet. J.* 174, 577–584. doi: 10.1016/j.tvjl.2007.07.032

Li, J., Wang, S., Li, C., Wang, C., Liu, Y., Wang, G., et al. (2017). Secondary *Haemophilus parasuis* infection enhances highly pathogenic porcine reproductive and respiratory syndrome virus (HP-PRRSV) infection-mediated inflammatory responses. *Vet. Microbiol.* 204, 35–42. doi: 10.1016/j.vetmic.2017.03.035

Lunney, J. K., Fritz, E. R., Reecy, J. M., Kuhar, D., Prucnal, E., Molina, R., et al. (2010). Interleukin-8, interleukin-1β, and interferon-γ levels are linked to PRRS virus clearance. *Viral Immunol.* 23, 127–134. doi: 10.1089/vim.2009.0087

Luo, R., Xiao, S., Jiang, Y., Jin, H., Wang, D., Liu, M., et al. (2008). Porcine reproductive and respiratory syndrome virus (PRRSV) suppresses interferon-β production by interfering with the RIG-I signaling pathway. *Mol. Immunol.* 45, 2839–2846. doi: 10.1016/j.molimm.2008.01.028

Mardassi, H., Mounir, S., and Dea, S. (1995). Molecular analysis of the ORFs 3 to 7 of porcine reproductive and respiratory syndrome virus, Québec reference strain. *Arch. Virol.* 140, 1405–1418. doi: 10.1007/BF01322667

Meier, W. A., Galeota, J., Osorio, F. A., Husmann, R. J., Schnitzlein, W. M., and Zuckermann, F. A. (2003). Gradual development of the interferon-gamma response of swine to porcine reproductive and respiratory syndrome virus infection or vaccination. *Virology* 309, 18–31. doi: 10.1016/S0042-6822(03)00009-6

Mengeling, W. L., Lager, K. M., and Vorwald, A. C. (1998). Clinical consequences of exposing pregnant gilts to strains of porcine reproductive and respiratory syndrome (PRRS) virus isolated from field cases of "atypical" PRRS. *Am. J. Vet. Res.* 59, 1540–1544.

Morgan, S. B., Frossard, J. P., Pallares, F. J., Gough, J., Stadejek, T., Graham, S. P., et al. (2016). Pathology and virus distribution in the lung and lymphoid tissues of pigs experimentally inoculated with three distinct type 1 PRRS virus isolates of varying pathogenicity. *Transbound. Emerg. Dis.* 63, 285–295. doi: 10.1111/tbed.12272

Morgan, S. B., Graham, S. P., Salguero, F. J., Sánchez Cordón, P. J., Mokhtar, H., Rebel, J. M. J., et al. (2013). Increased pathogenicity of European porcine reproductive and respiratory syndrome virus is associated with enhanced adaptive responses and viral clearance. *Vet. Microbiol.* 163, 13–22. doi: 10.1016/j.vetmic.2012.11.024

Osorio, F. A., Galeota, J. A., Nelson, E., Brodersen, B., Doster, A., Wills, R., et al. (2002). Passive transfer of virus-specific antibodies confers protection against reproductive failure induced by a virulent strain of porcine reproductive and respiratory syndrome virus and establishes sterilizing immunity. *Virology* 302, 9–20. doi: 10.1006/viro.2002.1612

Ostrowski, M., Galeota, J. A., Jar, A. M., Platt, K. B., Osorio, F. A., and Lopez, O. J. (2002). Identification of neutralizing and nonneutralizing epitopes in the porcine reproductive and respiratory syndrome virus GP5 ectodomain. *J. Virol.* 76, 4241–4250. doi: 10.1128/JVI.76.9.4241-4250.2002

Pasternak, A. O., van den Born, E., Spaan, W. J., and Snijder, E. J. (2001). Sequence requirements for RNA strand transfer during nidovirus discontinuous subgenomic RNA synthesis. *EMBO J.* 20, 7220–7228. doi: 10.1093/emboj/20.24.7220

Plagemann, P. G. (2004). GP5 ectodomain epitope of porcine reproductive and respiratory syndrome virus, strain Lelystad virus. *Virus Res.* 102, 225–230. doi: 10.1016/j.virusres.2004.01.031

Qiao, S., Feng, L., Bao, D., Guo, J., Wan, B., Xiao, Z., et al. (2011). Porcine reproductive and respiratory syndrome virus and bacterial endotoxin act in synergy to amplify the inflammatory response of infected macrophages. *Vet. Microbiol.* 149, 213–220. doi: 10.1016/j.vetmic.2010.11.006

Rosell, C., Segalés, J., Ramos-Vara, J. A., Folch, J. M., Rodriguez-Arrioja, G. M., Duran, C. O., et al. (2000). Identification of porcine circovirus in tissues of pigs with porcine dermatitis and nephropathy syndrome. *Vet. Rec.* 146, 40–43. doi: 10.1136/vr.146.2.40

Rossow, K. D. (1998). Porcine reproductive and respiratory syndrome. *Vet. Pathol.* 35, 1–20. doi: 10.1177/030098589803500101

Shabir, N., Khatun, A., Nazki, S., Kim, B., Choi, E. J., Sun, D., et al. (2016). Evaluation of the cross-protective efficacy of a chimeric porcine reproductive and respiratory syndrome virus constructed based on two field strains. *Viruses* 8:240. doi: 10.3390/v8080240

Shen, S., Kwang, J., Liu, W., and Liu, D. X. (2000). Determination of the complete nucleotide sequence of a vaccine strain of porcine reproductive and respiratory syndrome virus and identification of the Nsp2 gene with a unique insertion. *Arch. Virol.* 145, 871–883. doi: 10.1007/s007050050680

Singleton, H., Graham, S. P., Frossard, J. P., Bodman-Smith, K. B., and Steinbach, F. (2018). Infection of monocytes with European porcine reproductive and respiratory syndrome virus (PRRSV-1) strain Lena is significantly enhanced by dexamethasone and IL-10. *Virology* 517, 199–207. doi: 10.1016/j.virol.2018.02.017

Snijder, E. J., Kikkert, M., and Fang, Y. (2013). Arterivirus molecular biology and pathogenesis. *J. Gen. Virol.* 94, 2141–2163. doi: 10.1099/vir.0.056341-0

Song, S., Bi, J., Wang, D., Fang, L., Zhang, L., Li, F., et al. (2013). Porcine reproductive and respiratory syndrome virus infection activates IL-10 production through NF-κB and p38 MAPK pathways in porcine alveolar macrophages. *Dev. Comp. Immunol.* 39, 265–272. doi: 10.1016/j.dci.2012.10.001

Song, J., Gao, P., Kong, C., Zhou, L., Ge, X., Guo, X., et al. (2019). The nsp2 hypervariable region of porcine reproductive and respiratory syndrome virus strain JXwn06 is associated with viral cellular tropism to primary porcine alveolar macrophages. *J. Virol.* 93:e01436-19. doi: 10.1128/JVI.01436-19

Sun, Y., Ke, H., Han, M., Chen, N., Fang, W., and Yoo, D. (2016). Nonstructural protein 11 of porcine reproductive and respiratory syndrome virus suppresses both MAVS and RIG-I expression as one of the mechanisms to antagonize type I interferon production. *PLoS One* 11:e0168314. doi: 10.1371/journal.pone.0168314

Suradhat, S., Thanawongnuwech, R., and Poovorawan, Y. (2003). Upregulation of IL-10 gene expression in porcine peripheral blood mononuclear cells by porcine reproductive and respiratory syndrome virus. *J. Gen. Virol.* 84, 453–459. doi: 10.1099/vir.0.18698-0

Terpstra, C., Wensvoort, G., and Pol, J. M. (1991). Experimental reproduction of porcine epidemic abortion and respiratory syndrome (mystery swine disease) by infection with Lelystad virus: Koch's postulates fulfilled. *Vet. Q.* 13, 131–136.

Thanawongnuwech, R., Thacker, B., Halbur, P., and Thacker, E. L. (2004). Increased production of proinflammatory cytokines following infection with porcine reproductive and respiratory syndrome virus and *Mycoplasma hyopneumoniae*. *Clin. Diagn. Lab. Immunol.* 11, 901–908. doi: 10.1128/CDLI.11.5.901-908.2004

Tian, D., Cao, D., Lynn Heffron, C., Yugo, D. M., Rogers, A. J., Overend, C., et al. (2017). Enhancing heterologous protection in pigs vaccinated with chimeric porcine reproductive and respiratory syndrome virus containing the full-length sequences of shuffled structural genes of multiple heterologous strains. *Vaccine* 35, 2427–2434. doi: 10.1016/j.vaccine.2017.03.046

Tian, K., Yu, X., Zhao, T., Feng, Y., Cao, Z., Wang, C., et al. (2007). Emergence of fatal PRRSV variants: unparalleled outbreaks of atypical PRRS in China and molecular dissection of the unique hallmark. *PLoS One* 2:e526. doi: 10.1371/journal.pone.0000526

Tong, G. Z., Zhou, Y. J., Hao, X. F., Tian, Z. J., An, T. Q., and Qiu, H. J. (2007). Highly pathogenic porcine reproductive and respiratory syndrome, China. *Emerg. Infect. Dis.* 13, 1434–1436. doi: 10.3201/eid1309.070399

van Reeth, K., Labarque, G., Nauwynck, H., and Pensaert, M. (1999). Differential production of proinflammatory cytokines in the pig lung during different respiratory virus infections: correlations with pathogenicity. *Res. Vet. Sci.* 67, 47–52. doi: 10.1053/rvsc.1998.0277

Vashisht, K., Goldberg, T. L., Husmann, R. J., Schnitzlein, W., and Zuckermann, F. A. (2008). Identification of immunodominant T-cell epitopes present in glycoprotein 5 of the north American genotype of porcine reproductive and respiratory syndrome virus. *Vaccine* 26, 4747–4753. doi: 10.1016/j.vaccine.2008.06.047

Veit, M., Matczuk, A. K., Sinhadri, B. C., Krause, E., and Thaa, B. (2014). Membrane proteins of arterivirus particles: structure, topology, processing and function. *Virus Res.* 194, 16–36. doi: 10.1016/j.virusres.2014.09.010

Wang, C., Shi, X., Zhang, X., Wang, A., Wang, L., Chen, J., et al. (2015). The endoribonuclease activity essential for the nonstructural protein 11 of porcine reproductive and respiratory syndrome virus to inhibit NLRP3 Inflammasome-mediated IL-1β induction. *DNA Cell Biol.* 34, 728–735. doi: 10.1089/dna.2015.2929

Weesendorp, E., Rebel, J. M. J., Popma-de Graaf, D. J., Fijten, H. P. D., and Stockhofe-Zurwieden, N. (2014). Lung pathogenicity of European genotype 3 strain porcine reproductive and respiratory syndrome virus (PRRSV) differs from that of subtype 1 strains. *Vet. Microbiol.* 174, 127–138. doi: 10.1016/j.vetmic.2014.09.010

Wissink, E., van Wijk, H. A. R., Kroese, M. V., Weiland, E., Meulenberg, J. J. M., Rottier, P. J. M., et al. (2003). The major envelope protein, GP5, of a European porcine reproductive and respiratory syndrome virus contains a neutralization epitope in its N-terminal ectodomain. *J. Gen. Virol.* 84, 1535–1543. doi: 10.1099/vir.0.18957-0

Wu, B., and Hur, S. (2015). How RIG-I like receptors activate MAVS. *Curr. Opin. Virol.* 12, 91–98. doi: 10.1016/j.coviro.2015.04.004

Xiao, X. L., Wu, H., Yu, Y. G., Cheng, B. Z., Yang, X. Q., Chen, G., et al. (2008). Rapid detection of a highly virulent Chinese-type isolate of porcine reproductive and respiratory syndrome virus by real-time reverse transcriptase PCR. *J. Virol. Methods* 149, 49–55. doi: 10.1016/j.jviromet.2008.01.009

Xu, L., Zhou, L., Sun, W., Zhang, P., Ge, X., Guo, X., et al. (2018). Nonstructural protein 9 residues 586 and 592 are critical sites in determining the replication efficiency and fatal virulence of the Chinese highly pathogenic porcine reproductive and respiratory syndrome virus. *Virology* 517, 135–147. doi: 10.1016/j.virol.2018.01.018

Yuan, S., Murtaugh, M. P., Schumann, F. A., Mickelson, D., and Faaberg, K. S. (2004). Characterization of heteroclite subgenomic RNAs associated with PRRSV infection. *Virus Res.* 105, 75–87. doi: 10.1016/j.virusres.2004.04.015

Zhang, K., Hou, Q., Zhong, Z., Li, X., Chen, H., Li, W., et al. (2013). Porcine reproductive and respiratory syndrome virus activates inflammasomes of porcine alveolar macrophages via its small envelope protein E. *Virology* 442, 156–162. doi: 10.1016/j.virol.2013.04.007

Zhao, K., Gao, J. C., Xiong, J. Y., Guo, J. C., Yang, Y. B., Jiang, C. G., et al. (2018). Two residues in NSP9 contribute to the enhanced replication and pathogenicity of highly pathogenic porcine reproductive and respiratory syndrome virus. *J. Virol.* 92:e02209-17. doi: 10.1128/JVI.02209-17

Zhou, L., Chen, S., Zhang, J., Zeng, J., Guo, X., Ge, X., et al. (2009). Molecular variation analysis of porcine reproductive and respiratory syndrome virus in China. *Virus Res.* 145, 97–105. doi: 10.1016/j.virusres.2009.06.014

Zhou, Y. J., Hao, X. F., Tian, Z. J., Tong, G. Z., Yoo, D., An, T. Q., et al. (2008). Highly virulent porcine reproductive and respiratory syndrome virus emerged in China. *Transbound. Emerg. Dis.* 55, 152–164. doi: 10.1111/j.1865-1682.2008.01020.x

Zhou, L., Yang, X., Tian, Y., Yin, S., Geng, G., Ge, X., et al. (2014). Genetic diversity analysis of genotype 2 porcine reproductive and respiratory syndrome viruses emerging in recent years in China. *Biomed. Res. Int.* 2014:748068. doi: 10.1155/2014/748068

frontiers | Frontiers in Microbiology

TYPE Review
PUBLISHED 14 August 2023
DOI 10.3389/fmicb.2023.1232453

OPEN ACCESS

EDITED BY
Wei Wei,
First Affiliated Hospital of Jilin University, China

REVIEWED BY
Wajihul Hasan Khan,
All India Institute of Medical Sciences, India
Parismita Kalita,
Washington University in St. Louis,
United States

*CORRESPONDENCE
Kebin Zheng
✉ zhengkebinzkb@163.com
Zhiwei Sun
✉ zwsun@ccmu.edu.cn
Yuhao Zhang
✉ zyhazzy@163.com

†These authors have contributed equally to this work and share first authorship

RECEIVED 31 May 2023
ACCEPTED 25 July 2023
PUBLISHED 14 August 2023

CITATION
Zeng Z, Geng X, Wen X, Chen Y, Zhu Y, Dong Z, Hao L, Wang T, Yang J, Zhang R, Zheng K, Sun Z and Zhang Y (2023) Novel receptor, mutation, vaccine, and establishment of coping mode for SARS-CoV-2: current status and future. *Front. Microbiol.* 14:1232453. doi: 10.3389/fmicb.2023.1232453

Novel receptor, mutation, vaccine, and establishment of coping mode for SARS-CoV-2: current status and future

Zhaomu Zeng[1,2,3†], Xiuchao Geng[4†], Xichao Wen[3†], Yueyue Chen[5], Yixi Zhu[6], Zishu Dong[7], Liangchao Hao[8], Tingting Wang[3], Jifeng Yang[3], Ruobing Zhang[3], Kebin Zheng[3*], Zhiwei Sun[5*] and Yuhao Zhang[9*]

[1]Department of Neurosurgery, Jiangxi Provincial People's Hospital, The First Affiliated Hospital of Nanchang Medical College, Nanchang, China, [2]Department of Neurosurgery, Xiangya Hospital Jiangxi Hospital of Central South University, National Regional Medical Center for Nervous System Diseases, Nanchang, China, [3]Department of Neurosurgery, Affiliated Hospital of Hebei University, Baoding, China, [4]Department of Nursing, School of Medicine, Taizhou University, Taizhou, China, [5]Department of Toxicology and Sanitary Chemistry, School of Public Health, Capital Medical University, Beijing, China, [6]Department of Pharmacy, The Second Affiliated Hospital of Nanchang University, Nanchang, China, [7]Department of Zoology, Advanced Research Institute, Jiangxi University of Chinese Medicine, Nanchang, China, [8]Department of Plastic Surgery, Shaoxing People's Hospital, Shaoxing, China, [9]Cancer Center, Department of Neurosurgery, Zhejiang Provincial People's Hospital (Affiliated People's Hospital), Hangzhou Medical College, Hangzhou, China

Since the outbreak of severe acute respiratory syndrome coronavirus 2 (SARS-CoV-2) and its resultant pneumonia in December 2019, the cumulative number of infected people worldwide has exceeded 670 million, with over 6.8 million deaths. Despite the marketing of multiple series of vaccines and the implementation of strict prevention and control measures in many countries, the spread and prevalence of SARS-CoV-2 have not been completely and effectively controlled. The latest research shows that in addition to angiotensin converting enzyme II (ACE2), dozens of protein molecules, including AXL, can act as host receptors for SARS-CoV-2 infecting human cells, and virus mutation and immune evasion never seem to stop. To sum up, this review summarizes and organizes the latest relevant literature, comprehensively reviews the genome characteristics of SARS-CoV-2 as well as receptor-based pathogenesis (including ACE2 and other new receptors), mutation and immune evasion, vaccine development and other aspects, and proposes a series of prevention and treatment opinions. It is expected to provide a theoretical basis for an in-depth understanding of the pathogenic mechanism of SARS-CoV-2 along with a research basis and new ideas for the diagnosis and classification, of COVID-19-related disease and for drug and vaccine research and development.

KEYWORDS

Omicron variant, entry receptors, attachment factors, COVID-19 vaccines, heterologous booster immunization, small molecule antiviral drugs

1. Introduction

Since the outbreak of coronavirus disease 2019 (COVID-19) at the end of 2019, it has rapidly spread to almost all countries and regions in the world and become a major global public health threat (Thakur and Ratho, 2022). SARS-CoV-2 has been evolving and mutating continuously, resulting in more than 1,000 variant strains worldwide (Cosar et al., 2022). Because the mutation of the virus is a decisive factor in future trends of the COVID-19 pandemic, the emergence of mutant strains has aroused widespread concern in society. To strengthen the monitoring and tracking of SARS-CoV-2 variants, the World Health Organization (WHO) classified them into variants of concern (VOCs) and variants of interest (VOIs) according to their transmissibility and pathogenicity. Among them, VOCs are the variant strains with the greatest impact on the global pandemic, including Alpha, Beta, Gamma, Delta, and Omicron (Chen K. et al., 2022; Salehi-Vaziri et al., 2022; **Table 1**). To date, although the pathogenicity of Omicron variants seems to be gradually decreasing, their virus transmission and susceptibility are gradually increasing. Especially for children, elderly individuals or patients with underlying diseases, SARS-CoV-2 infection is still a major health threat (Mistry et al., 2021; Pellegrino et al., 2022). According to the real-time statistics of Johns Hopkins University in the United States, the number of confirmed cases of COVID-19 in the world has exceeded 670 million, and unfortunately, over 6.8 million people have died (Johns Hopkins University, 2022). It is very important to understand the virological characteristics of SARS-CoV-2 variants for the prevention and control of the COVID-19 pandemic.

Governments and scientists have made many efforts to prevent, control and treat COVID-19 and have found some suitable control methods including mRNA vaccines (Naseri et al., 2022). Previous studies have shown that angiotensin-converting enzyme II (ACE2) is the main membrane receptor for SARS-CoV-2 entry into host cells (Pandey et al., 2021). However, with further follow-up study, dozens of newly discovered protein receptors have been found to mediate or assist SARS-CoV-2 in invading human cells (Ge et al., 2021; Wang J. et al., 2021), indicating SARS-CoV-2 may have many complex pathogenic mechanisms and providing new research directions for finding or developing effective antiviral drugs. In addition, with the continuous observed mutation and immune evasion of viruses, the research and development of related vaccines is also facing great challenges (Jafari et al., 2022; Pellegrino et al., 2022).

In this paper, we comprehensively reviewed the genomic characteristics, pathogenesis and latest research on SARS-CoV-2 attacking human cells through multiple receptors other than ACE2. This article comprehensively introduces the genomic characteristics of SARS-CoV-2, as well as the latest research progress on human cell infection based on ACE2 and various other receptor pathways. In addition, we summarize the virus mutations (especially the Omicron variant) and vaccine development and finally propose some new perspectives on responding to the SARS-CoV-2 pandemic. We hope this review can provide a literature basis for a better understanding of the molecular characteristics and pathogenic mechanism of SARS-CoV-2 and lay a theoretical foundation for precise diagnosis, specific drug development, and vaccine development of related diseases caused by SARS-CoV-2 infection.

2. Genomic organization of SARS-CoV-2

Severe acute respiratory syndrome coronavirus 2 is a single- and positive-strand RNA virus with an envelope. As a highly pathogenic coronavirus, it belongs to Betacoronavirus (Kadam et al., 2021). The genome sequence of SARS-CoV-2 (approximately 29.9 kb in size) has approximately 80 and 50% homology to those of SARS-CoV and MERS-CoV, respectively (Arya et al., 2021). Two-thirds of the genome contains 15 open reading frames (ORFs), which encode 16 non-structural proteins (Nsp1-16) to form replicase-transcriptase complexes (Rahnavard et al., 2021). Studies have shown that Nsp1 can hinder ribosome binding to host mRNA and inhibit protein synthesis in host cells, Nsp2 can promote virus replication by inhibiting the autophagy defense mechanism of host cells and destroying mitochondrial function, and Nsp3 can cleave the N-terminus of the polyprotein to produce independent functional Nsp1 and Nsp2 and reduce the antiviral ability of host cells by changing the protein balance. Nsp4 uses the plasma membrane of the endoplasmic reticulum to mediate the formation of vesicle structures, Nsp5 participates in the cleavage of other Nsps after synthesis, Nsp6 interacts with Nsp3 and Nsp4 to promote the formation of virus replication organelles with double-membrane vesicle structures, Nsp7 and Nsp8 form hexadecameric complexes and act as primer enzymes allowing Nsp12 to stabilize viral RNA, Nsp10 can activate the 2′-O-methyltransferase activity of Nsp16, and Nsp12 is a catalytic subunit with RNA-dependent RNA polymerase activity that can catalyze viral RNA synthesis and assist in viral RNA replication in combination with Nsp7 and Nsp8. Nsp13 can untangle the entangled viral RNA strand and facilitate subsequent viral RNA replication. Nsp14 has a 3′–5′ exonuclease domain, which can enhance the proofreading ability during viral RNA replication. Nsp15 can remove viral RNA fragments to minimize the antiviral defense response of host cells. Nsp16 is a 2′-O-ribose methyltransferase that methylates the 5′ cap of viral RNA and inhibits its degradation by cells (Yadav et al., 2021; Yang and Rao, 2021; Yoshimoto, 2021; Bai et al., 2022). The remaining third of the genome encodes nine accessory proteins (ORF3a, ORF3b, ORF6, ORF7a, ORF7b, ORF8, ORF9b, ORF9c, and ORF10) and four structural proteins [spike (S) protein, envelope (E) protein, membrane (M) protein and nucleocapsid (N) protein] (Rahnavard et al., 2021). Accessory proteins are not necessary for virus replication (Gao X. et al., 2021), but they regulate innate immunity and promote viral infection. The S protein is the most important surface protein of SARS-CoV-2 and is closely related to its transmission ability. The N protein is abundant in SARS-CoV-2, is a highly immunogenic protein and participates in genome replication and cell signaling pathway regulation (Arya et al., 2021; **Figure 1**).

The S protein plays an important role in the virus subtype and vaccine response and is responsible for the entry of SARS-CoV-2 into host cells (Seyran et al., 2021). The S protein is mainly composed of the S1 and S2 functional subunits. The S1 subunit

TABLE 1 Basic overview and main characteristics of five VOCs.

WHO lable	Pango lineage	First detected in the country/Detection date	Status	Spike protein substitutions	Attributes
Alpha	B.1.1.7	United Kingdom/ September-2020	VOC:18-December-2020	H69del/V70del/Y144del/N501Y/A570D/ D614G/P681H/T716I/S982A/D1118H	Attack the immune system, with enhanced transmission and increased virulence
Beta	B.1.351	South Africa/ May-2020	VOC:18-December-2020	L18F/D80A/D215G/L242del/A243del/ L244de/R246I/K417N/E484K/N501Y/ D614G/A701V	It is highly contagious and can avoid vaccines and immune cell tracking, but the transmission power is weak
Gamma	P.1	Brazil/ November-2020	VOC:11-January-2021	L18F/T20N/P26S/D138Y/R190S/K417T/ E484K/N501Y/D614G/H655Y/T1027I/ V1176F	Damage immunity and enhance transmission
Delta	B.1.617.2	India/ October-2020	VOI: 4-April-2021 VOC:11-May-2021	T19R/G142D/E156del/F157del/R158G/ L452R/T478K/D614G/P681R/D950N	The transmission speed is fast, the viral load is high, and the infection ability is extremely strong
Omicron	B.1.1.529	India/ October-2020	VUM:24-November-2021 VOC:26-November-2021	A67V/H69del/V70del/T95I/G142D/ V143del/Y144del/Y145del/N211del/ L212I/ins214EPE/G339D/S371L/S373P/ S375F/K417N/N440K/G446S/S477N/ T478K/E484A/Q493R/G496S/Q498R/ N501Y/Y505H/T547K/D614G/H655Y/ N679K/P681H/N764K/D796Y/N856K/ Q954H/N969K/L981F	Strong transmissibility and immune evasion ability, less virulence

is composed of the N-terminal domain (NTD) and receptor-binding domain (RBD), and its function is to recognize receptor proteins of host cells. The S2 subunit mainly consists of a fusion peptide, heptapeptide repeat sequence 1 and central helix, which are responsible for assisting the membrane fusion process between the virus and host cells (Seyran et al., 2021). Therefore, it is very important to understand the receptor recognition mechanism of SARS-CoV-2, which determines its infectivity, host range and pathogenesis.

3. SARS-CoV-2 infection mediated by ACE2

After the structural characteristics of the SARS-CoV-2 membrane fusion protein were determined, ACE2 was identified as its main binding receptor. Hoffmann et al. further found that the S protein of SARS-CoV-2 is the key to viral invasion into cells. In contrast to other coronaviruses (CoVs), the S protein of SARS-CoV-2 has a site composed of multiple arginine residues at the junction of the S1 and S2 subunits, which can be recognized and cleaved by Furin (Xia et al., 2020). In fact, the S protein is cut by Furin in the Golgi apparatus of the host during biosynthesis, which is the premise of SARS-CoV-2 infecting host cells (Walls et al., 2020). Usually, mature S protein exists in a metastable prefusion conformation. To bind to the receptor, the RBD in the S1 subunit undergoes a hinged conformational motion between two states of "up" and "down". When the RBD is in the "up" state, it can bind to the receptor ACE2; in the "down" state, it cannot (Yan et al., 2020). The three-dimensional structure of the S protein is observed by cryo-electron microscopy. Only one RBD is in the "up" conformation, and the other two are in the "down" conformation without binding activity. The binding of one RBD in the "up" conformation with ACE2 leads to the other two RBDs adopting unstable "up" conformations (Wrapp et al., 2020), which further destroys the stability of the prefusion trimer and promotes the transformation of the S protein from a metastable prefusion conformation to a stable fusion conformation.

Studies have confirmed that SARS-CoV-2 mainly infects host cells through membrane fusion and endosomal fusion. When the RBD successfully recognizes and binds ACE2, it causes the S1 subunit to detach and the S2 subunit to adopt a highly stable postfusion conformation, thus performing its membrane fusion function. If enough cell surface protease transmembrane serine protease 2 (TMPRSS2) can be induced to cleave the S2′ site, FP in the exposed S2 subunit is inserted into the host cell membrane at the same time. Then, heptad repeat 1 (HR1) and HR2 gradually approach, narrowing the distance between the virus outer membrane and host cell membrane. Finally, HR1 and HR2 are induced to form an 6-helix bundle structure in an alternating reverse parallel arrangement so that the virus envelope fuses directly with the cell membrane and releases genetic material. In contrast, if the RBD is not recognized and cleaved by TMPRSS2 on the cell surface after binding with ACE2, the SARS-CoV-2-ACE2 complex enters the cell through the reticulin-mediated endocytosis pathway, and the S2′ site is cleaved by Cathepsin

10.3389/fmicb.2023.1232453

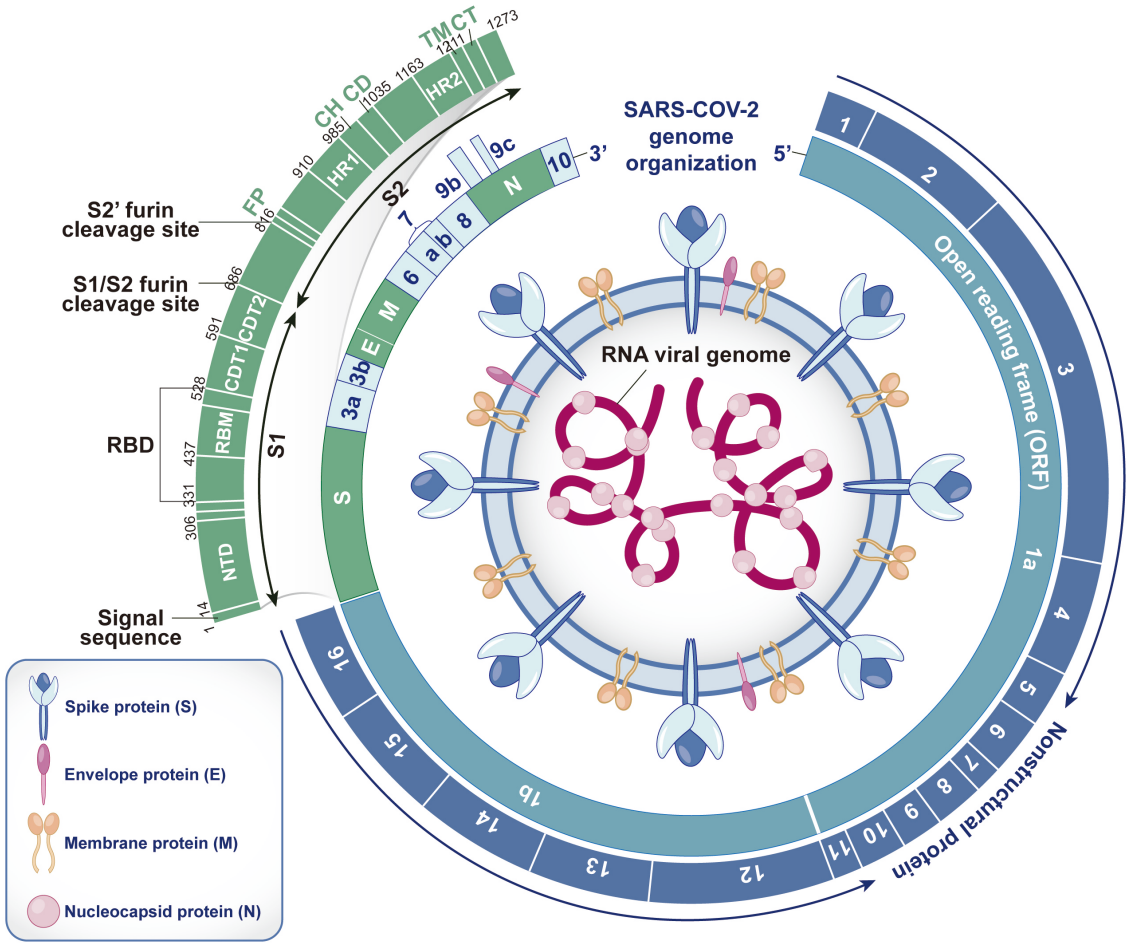

FIGURE 1
Structure, RNA genome and encoding protein of SARS-CoV-2. SARS-CoV-2 contains spike (S) protein, envelope (E) protein, membrane (M) protein and nucleocapsid (N) protein. The S, E, and M proteins are embedded in the bilayer phospholipid envelope, and the RNA genome is located in the center, wrapped by N protein. The RNA genome of SARS-CoV-2 consists of 15 open reading frames (ORFs), which can encode 16 non-structural proteins (Nsp1-16), 4 structural proteins (S, E, M, and N) and 9 auxiliary proteins (ORF3a, ORF3b, ORF6, ORF7a, ORF7b, ORF8, ORF9b, ORF9c, and ORF10). As the most important surface protein of SARS CoV-2, S protein is mainly composed of S1 and S2 functional subunits and plays a key role in the process of virus invasion and replication. (S1, receptor-binding subunit; S2, membrane fusion subunit; NTD, N-terminal domain; RBM, receptor binding motif; RBD, receptor binding domain; CDT1&CDT2, C-terminal domain; FP, furin peptide; HR1&HR2, heptad repeats; CH, central helix; CD, connector domain; TM, transmembrane domain; CT, cytoplasmic tail).

(Cat) B/L in the endosome. Then, the virus envelope fuses with the endosome membrane, and the virus RNA genome is released into the cytoplasm (Frolova et al., 2022; Jackson et al., 2022). In summary, after the S protein binds to the receptor, the effectiveness of proteases such as TMPRRS2, Cat B/L and Furin on target cells largely determines how the virus enters host cells. In the absence of TMPRSS2 expression, Cat B/L is very important for SARS-CoV-2 infection mediated by the S protein. In addition, because SARS-CoV-2 has a unique Furin cleavage site and the proteolytic activation of Cat B/L depends on endosome acidification, while the entry pathway mediated by TMPRSS2 is not affected by pH, SARS-CoV-2 utilizes the TMPRSS2-dependent membrane fusion pathway to infect human cells (Ou et al., 2021; **Figure 2**).

To sum up, SARS-CoV-2 infection mediated by ACE2 is a multimolecular interaction process, and the complexity of this process means that inhibitors developed for a single target do not necessarily have reliable curative effects in clinical treatment and cannot be further popularized. Therefore, it is necessary to further clarify the role of other receptors and proteases of SARS-CoV-2 in of viral infection and to find more virus-host interaction mechanisms specific to SARS-CoV-2 to clarify why the virus has strong infection and transmission ability. This is not only helpful to fully understand the biological characteristics of the virus but also provides a basis for the treatment of COVID-19 and accelerates research on rapid diagnosis and targeted drugs.

4. SARS-CoV-2 infection mediated by other receptors

For the overall concept of SARS-CoV-2 receptors on cell membranes, the prerequisite is whether the relevant receptors can directly interact with S proteins and undergo conformational changes. However, some viruses rely not only on receptors and suitable host cells but also cell surface molecules that may help

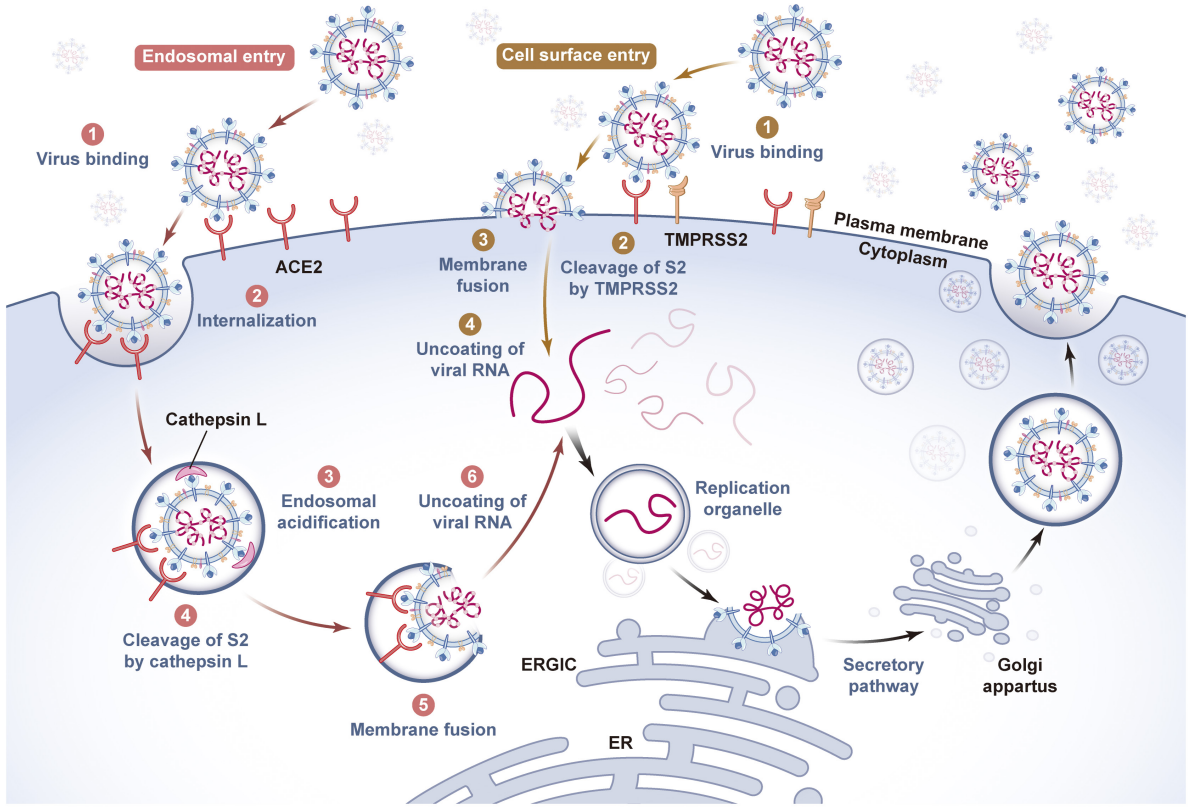

FIGURE 2
Invasion and release mechanism of SARS-CoV-2 based on ACE2 receptor. The host cells infected by SARS-CoV-2 mainly include virus adsorption, invasion, genetic material release, genome replication and transcription, assembly, budding and other processes. As a key protein for SARS-CoV-2 to recognize host cells, spike protein has a strong binding force with the cell membrane surface receptor ACE2. There are two fusion pathways for SARS-CoV-2 to invade host cells, one is viral envelope-endosome membrane fusion pathway mediated by endocytosis, and the other is viral envelope-cell membrane fusion pathway. When the viral genome is released into the cytoplasm of the host cells, it will induce the endoplasmic reticulum to form a replication organelle with a double membrane structure, complete genome RNA replication and structural protein synthesis, and assemble and generate new viral particles at the endoplasmic reticulum of the host cells, which will be transported by golgi to the host cell membrane and released to the outside of the cell by exocytosis. The whole process is critical to the survival and pathogenicity of SARS-CoV-2, and requires the participation of host cell proteases such as Furin, TMPRSS2 and Cathepsin L. (ACE2, angiotensin-converting enzyme II; TMPRSS2, transmembrane serine protease 2; ER, endoplasmic reticulum; ERGIC, endoplasmic reticulum- golgi intermediate compartment).

viruses locate and enter host cells but do not play a decisive role in the infection process and are therefore called attachment factors (coreceptors) (Evans and Liu, 2020). Therefore, virus receptors can be roughly divided into two categories: entry receptors and attachment factors (Mercer et al., 2020). As early as the beginning of the epidemic, researchers found that in the process of SARS-CoV-2 infection, the entry of virus into host cells does not depend on the binding of a single receptor with the S protein but requires the participation of multiple transmembrane proteins in target cells, which also play an important role in the process of virus transmission and can enhance the attachment and invasion ability of SARS-CoV-2 to host cells (Qi et al., 2020). At present, ACE2 is still recognized as the main entry receptor of SARS-CoV-2-infected host cells. However, the expression distribution of ACE2 in human tissues is relatively limited. In virus-positive tissues such as the brain, heart, liver and even lung, ACE2 is expressed in only a small number of cells, and the expression level is low (Scialo et al., 2020), which obviously cannot fully explain the multiorgan tropism of SARS-CoV-2. Therefore, researchers speculate that other receptors may help SARS-CoV-2 enter host cells and have been exploring in this direction. Here, we list a series of important viral receptors and outline their roles in SARS-CoV-2 infection, hoping to further reveal the pathogenesis of SARS-CoV-2 and show the potential value of these protein receptors in the treatment of COVID-19.

4.1. Entry receptors

4.1.1. AXL

Although it has been confirmed that ACE2 is the main receptor for SARS-CoV-2 entering human cells, studies have shown that ACE2 is only expressed in the kidney and digestive system, and its overall expression in human lungs and trachea is low. Therefore, there may be other receptors that promote SARS-CoV-2 entry into respiratory system cells. Wang S. et al. (2021) confirmed this hypothesis, and SARS-CoV-2 can invade the respiratory system by using the tyrosine-protein kinase receptor UFO (AXL) protein in host cells. They found that AXL is highly expressed

in H1299 and BEAS-2B cells and can directly combine with the NTD of the virus S protein, enter host cells by the reticulin-mediated endocytosis pathway, and colocalize in early endosomes. Moreover, the experimental results also show that there is no cross-inhibition function between ACE2 and AXL. ACE2 knockout has no effect on SARS-CoV-2 infection of H1299 cells, while AXL knockout significantly weakens the viral infection of host cells. It is clear that AXL is a new receptor of SARS-CoV-2 and can independently mediate viral infection of the human respiratory system without relying on ACE2. In addition, in HEK293T cells with both ACE2 and AXL knockout, overexpression of AXL alone can significantly promote viral infection, while the addition of soluble recombinant AXL protein or recombinant NTD protein can inhibit AXL-mediated viral infection, which further confirms that AXL-mediated SARS-CoV-2 infection cannot depend on ACE2. In a word, AXL is a novel entry receptor of SARS-CoV-2 that can significantly promote viral invasion and reproduction and plays an important role in SARS-CoV-2 infection of the human respiratory system. Moreover, AXL can also be used as a potential target for future COVID-19 targeted therapy.

4.1.2. TfR

In a breakthrough in SARS-CoV-2 research, transferrin receptor (TfR) has been proven to be another receptor that affects the entry of SARS-CoV-2 into the host. Researchers found that the expression of TfR in the lung tissue and trachea of SARS-CoV-2-infected monkeys and humanized ACE2 (hACE2) mice increased significantly (Tang et al., 2020). There is a direct interaction between TfR and SARS-CoV-2, and the colocalization signal can be observed in the membrane and cytoplasm of Vero-E6 cells infected by SARS-CoV-2, which indicates that TfR is a membrane receptor of SARS-CoV-2. More importantly, the colocalization signals of TfR, ACE2 and S proteins were also detected on the membrane of infected cells, but only the TfR-S protein complex was observed in the cytoplasm. In other words, TfR can transport SARS-CoV-2 from the cell membrane to the cytoplasm independently of ACE2. Similarly, in Vero E6 and A549 cells with ACE2 knockout, overexpression of TfR can significantly promote viral infection, while knocking down TfR can inhibit viral infection, which once again indicates that TfR can mediate SARS-CoV-2 entry into host cells independently of ACE2. In addition, adding antibodies or polypeptides designed based on the TfR amino acid sequence showed good protective effects *in vitro* and *in vivo*, which could effectively prevent pathological lung injury caused by SARS-CoV-2 infection. These results indicate that TfR is the entry receptor of SARS-CoV-2 infection, and its discovery will further expand our understanding of the SARS-CoV-2 infection mechanism and provide new clues for exploring the therapeutic targets of COVID-19.

4.1.3. ASGR1 and KREMEN1

Systematic analysis of the host cell receptor lineage of SARS-CoV-2 and the search for unknown functional receptors are of great importance for further exploring the complexity of SARS-CoV-2 in tropism and clinical manifestations. Accordingly, Gu et al. (2022) established a genome-wide secretory omics interaction screening system and screened the receptors or ligands of target proteins under physiological conditions. The results turned out that asialoglycoprotein receptor 1 (ASGR1) and kringle containing transmembrane protein 1 (KREMEN1) could interact with multiple domains of the SARS-CoV-2 S protein. ASGR1 can bind to the RBD and NTD, and KREMEN1 can bind to the RBD, NTD and S2 subunits. Further *in vitro* infection experiments confirmed that overexpression of ASGR1 and KREMEN1 can promote SARS-CoV-2 pseudoviral infection in ACE2 knockout cells, indicating that ASGR1 and KREMEN1 can act as entry receptors in ACE2-independent cell lines and directly mediate SARS-CoV-2 infection independent of ACE2. The difference is that they have no effect on SARS-CoV and MERS-CoV infection, and there is no binding site between ASGR1 and the S protein of the virus, which indicates that ASGR1 and KREMEN1 are specific receptors of SARS-CoV-2. In addition, ACE2, ASGR1 and KREMEN1, which can mediate SARS-CoV-2 invasion, are collectively called ASK entry receptors, and different ACE2/ASGR1/KREMEN1 receptor combinations are used to mediate SARS-CoV-2 entry into different types of cells. The results showed that the ASK receptors together constitute the molecular basis of SARS-CoV-2 cell and tissue tropism. Moreover, the correlation between ASK receptor expression and virus susceptibility is obviously stronger than that of any single entry receptor at both the cellular and tissue levels. Moreover, SARS-CoV-2 can invade different types of cells by using different receptors, among which ASGR1 plays a role in liver cell lines, KREMEN1 plays a role in lung cell lines, and ACE2 plays a wide role in both lung and liver cell lines. In addition, the researchers also developed blocking monoclonal antibodies against ASGR1 and KREMEN1. The research findings suggested that these antibodies could significantly inhibit SARS-CoV-2 infection in human lung organs. More importantly, compared with any single targeting antibody, a "cocktail antibody" targeting ASK receptors can significantly inhibit SARS-CoV-2 infection of lung organs. In conclusion, ASGR1 and KREMEN1, as entry receptors of SARS-CoV-2, play an important role in SARS-CoV-2 infection independent of that of ACE2. This study provides important information and clues for explaining and deeply understanding the tropism and pathogenesis of SARS-CoV-2 and provides new targets and treatment strategies for drug research and development against COVID-19.

4.1.4. Integrin

One of the main pathological symptoms of many severe COVID-19 patients is platelet abnormalities, such as thrombocytopenia, microvascular thrombosis, and abnormal coagulation function. Kuhn et al. (2023) conducted in-depth exploration of the reasons. Their research confirmed that Integrin is the most abundant receptor protein on the surface of platelets (does not express ACE2 receptor). Among them, Integrins α5β1 and αvβ3, as the entry receptors of SARS-CoV-2, can directly recognize and bind to the RGD ligand motif (arginine-glycine-aspartic protein sequence) in the RBD domain of the S protein and do not depend on ACE2-mediated viral infection of platelet cells. In addition, the interaction between the S protein and Integrin αvβ3 can trigger the remodeling of Actin in cells and induce the formation of filamentous pseudopodia on the cell surface. These processes further activate platelets, ultimately leading to extensive microthrombosis and poor prognosis. Similarly, the infection of T cells by SARS-CoV-2 and related immune responses are closely related to the prognosis of COVID-19. Severe patients

often exhibit symptoms such as T-cell overactivation, apoptosis, and lymphocyte reduction in the clinic. However, there is almost no expression of ACE2 and other known SARS-CoV-2 receptors on T cells, and how SARS-CoV-2 infects T cells and triggers their functional abnormalities has always been a focus of attention in the field of coronavirus research. The work of Huang et al. (2023) further clarified this problem, and their research results showed that lymphocyte Integrin α4β1, α4β7, α5β1, and αLβ2, as newly identified receptors for SARS-CoV-2, can directly recognize the three binding motifs in the S protein RBD and mediate viral entry into T cells. After integrin activation, the binding ability of RBD to these Integrins is significantly enhanced, which can significantly promote SARS-CoV-2 infection of T cells. In addition, the combination of RBD and Integrin further triggered the phosphorylation of Src and Akt proteins in T cells and upregulated the membrane expression level of the activation molecule CD25, as well as the inflammatory factors interleukin-2, interferon-γ and tumor necrosis factor-α at the transcriptional level, in turn inhibiting T-cell proliferation. In a word, SARS-CoV-2, under the direct effect of lymphocyte Integrin, enters T cells to regulate the T-cell immune response and inhibit cell proliferation, which is one of the important reasons for the high-level inflammatory environment and lymphocyte reduction in the body. As an entry receptor for SARS-CoV-2 on T cells, lymphocyte Integrin may be a potential therapeutic target in COVID-19 treatment.

4.2. Attachment factors

4.2.1. NRP1

Daly et al. (2020) from Bristol University confirmed that SARS-CoV-2 can bind to a cell surface protein called neuropilin-1 (NRP1). This attachment factor is widely expressed in lung cells and olfactory cells and has the highest expression level in endothelial cells. It was further found that in HEK293T cells with almost no endogenous expression of ACE2 and NRP1, overexpression of NRP1 did not affect the infection degree of SARS-CoV-2 pseudovirus, but coexpression of NRP1, ACE2 and TMPRSS2 significantly promoted viral entry and infection. Similarly, in Caco-2 cells with endogenous expression of ACE2, the overexpression of NRP1 significantly increased the degree of pseudoviral infection. These results suggest that NRP1 can promote the key linkage between the SARS-CoV-2 S protein and ACE2 receptor and the infectivity of SARS-CoV-2 in the presence of the ACE2 entry receptor. In addition, immunoprecipitation and other techniques showed that NRP1 could directly bind to the RRAR amino acid sequence on the S1 subunit of the virus. In contrast, SARS-CoV-2 infection can be significantly inhibited by blocking this interaction with RNA interference technology, monoclonal antibodies and selective inhibitors. Cantuti-Castelvetri et al. (2020) also found that SARS-CoV-2 infected NRP1-expressing cells in the nasal cavity in the pathological analysis of olfactory epithelium obtained from autopsies of deceased COVID-19 patients. Importantly, SARS-CoV-2 infection was also detected in oligodendrocyte transcription factor 2 (OLIG2)-positive cells, which are mainly expressed by olfactory neuron progenitor cells, which can reconstruct axons of the nose and brain when we lose our sense of smell (caused by SARS-CoV-2 infection), so the above reconstruction pathway may be used by SARS-CoV-2 to invade the nervous system. These results provide a new perspective for the treatment of COVID-19, and blocking the binding of SARS-CoV-2 to ACE2 and NRP1 will become a valuable treatment strategy.

Bone marrow macrophages (BMMs) are the main source of osteoclasts, as they can differentiate into osteoclasts by cell fusion. In a recent study (Gao et al., 2022), Liu et al. (2022) found that SARS-CoV-2 can efficiently infect BMMs through viral infection experiments in mice and primary BMMs, leading to bone system damage. Further mechanistic studies showed that the expression of ACE2 in BMMs was very low, while the expression of another receptor, NRP1, was positively correlated with SARS-CoV-2 infection. Moreover, TMPRSS2 was minimally expressed in BMMS, but Cat B/L was highly expressed, with a close relationship to NRP1 expression, suggesting that SARS-CoV-2 probably entered BMMS through the Cat B/L-mediated endosomal pathway. Notably, contrary to previous research reports, SARS-CoV-2 infection of BMMs only depends on the NRP1 receptor, without the participation of ACE2. In addition, SARS-CoV-2 infection of BMMS can significantly inhibit their differentiation into osteoclasts, resulting in abnormal bone resorption and destroyed bone homeostasis. Overall, this study provides the first important evidence for SARS-CoV-2 infection mediated by NRP1 in BMMs for the first time and establishes a potential relationship between osteoclast differentiation disorder and skeletal system metabolism disorder in COVID-19 patients.

4.2.2. CD147

CD147, also known as Basigin or EMMPRIN, belongs to the immunoglobulin superfamily. Early as in the study of SARS-CoV and other viruses (Faghihi, 2020), CD147 was proven to promote viral invasion of host cells, and CD147-antagonistic peptide-9 was shown to exert a significant inhibitory effect on SARS-CoV infection. Subsequently, researchers used CD147 as a candidate target and conducted a series of studies on the spread of SARS-CoV-2. In the research of Wang Z. et al. (2020), it was found that CD147, as an attachment factor, can help SARS-CoV-2 enter host cells through endocytosis. In this study, antiviral detection was carried out *in vitro*. The above research indicated that adding meplazumab (humanized anti-CD147 antibody) could significantly inhibit SARS-CoV-2 infection of host cells and significantly promoted the rehabilitation of infected patients. Afterward, the researchers verified the binding between CD147 and the S protein, and the results of immunoelectron microscopy showed that the two proteins were colocalized in Vero E6 cells infected by SARS-CoV-2. Overall, CD147, as a coreceptor, is a newly identified way for SARS-CoV-2 to infect host cells and provides an important target for the development of specific antiviral drugs. In addition, patients with severe and critical COVID-19 are often likely to have pulmonary fibrosis. Another study by the team showed that CD147 was involved in SARS-CoV-2-induced pulmonary fibrosis in addition to mediating SARS-CoV-2 into the host and initiating the COVID-19 cytokine storm (Wu et al., 2022). CD147 has been identified as the key regulatory factor of SARS-CoV-2- and bleomycin-induced fibroblast activation. Knockdown of CD147 can directly inhibit TGF-β-stimulated lung fibroblast activation and thus reduce susceptibility to bleomycin-induced pulmonary fibrosis. In contrast, the application of meplazumab can significantly inhibit the accumulation of activated fibroblasts and

the production of extracellular matrix proteins, thus alleviating the further development of pulmonary fibrosis caused by SARS-CoV-2. In a word, the above studies indicate that CD147 can promote SARS-CoV-2-induced progressive pulmonary fibrosis and provide a theoretical and experimental basis for formulating treatment strategies for fibrosis symptoms.

4.2.3. KIM1

Autopsy and virological studies found many virus inclusion bodies and particles in the kidneys of COVID-19 patients (Wysocki et al., 2020), which indicated that SARS-CoV-2 had renal tissue tropism, and the kidney was another organ susceptible to SARS-CoV-2 in addition to the lung. However, ACE2 inhibitors did not significantly improve the prognosis of COVID-19 patients, and the expression level of ACE2 in the kidney decreased significantly after viral infection, which suggested that there may be other receptors of SARS-CoV-2 in the kidney. In view of the above conjecture, Yang et al. (2021) proposed that kidney injection molecule-1 (KIM1) is an attachment factor of SARS-CoV-2, which can mediate the invasion of the virus into the kidney. Studies have confirmed that KIM1, which is significantly upregulated during kidney injury, can bind with the RBD of SARS-CoV-2, enabling the virus to better attach to the cell membrane and enter cells through reticulin-mediated endocytosis. Moreover, the viral RBD can bind to KIM1 and ACE2 through different binding pockets, suggesting that these two receptors may exert a synergistic effect to mediate SARS-CoV-2 infection. In addition, based on the interaction sequence between KIM1 and SARS-CoV-2, the team designed two polypeptides to block viral infection, among which AP2, a polypeptide consisting of 14 amino acids, can significantly reduce the aggregation of SARS-CoV-2 on the cell surface. Importantly, the team also proposed the theory of "malignant circulation" for SARS-CoV-2 invasion of the kidney; that is, in the early stage of SARS-CoV-2 invasion of the kidney, it mainly binds ACE2 (the expression level is higher than that of KIM1 in the physiological state), and after virus-induced acute kidney injury, the expression level of KIM1 is upregulated, thus promoting secondary viral infection mediated by KIM1 and ACE2, aggravating kidney injury and further upregulating KIM1. In conclusion, the expression level of KIM1 is upregulated only after kidney injury, which indicates that it is relevant and specific to renal function. At the same time, KIM1 was identified as a new target for SARS-CoV-2 to invade cells, providing an important theoretical basis for the development of polypeptide drugs, small molecule drugs and antibody drugs based on this target to treat COVID-19.

4.2.4. SR-B1

Scavenger receptor class B type I (SR-B1), as the core of the lipid delivery system, has been widely recognized in hepatocytes, ovarian cells and testicular interstitial cells. It can mediate the selective absorption of cholesterol esters and play an important role in the metabolism of high-density lipoprotein (HDL) and the "reverse transport" of cholesterol (Powers and Sahoo, 2022). A research result from several cooperative teams confirmed that the S1 subunit of SARS-CoV-2 has specific affinity for HDL, and SR-B1 acts as the cell surface receptor of HDL, making HDL a "bridge" between the virus S protein and SR-B1 receptor (Wei et al., 2020). Therefore, in host cells expressing ACE2, the increase in HDL can significantly promote the adhesion and invasion of SARS-CoV-2 to the cell surface. In contrast, HDL-enhanced SARS-CoV-2 infection can be directly inhibited when cultured cells are treated with a monoclonal antibody (blocking the HDL binding site on the S1 subunit) or SR-B1 antagonist *in vitro*. In addition, to further explore the relationship between SR-B1 and SARS-CoV-2 infectivity, SR-B1 overexpression and knockdown were shown to increase and decrease virus RNA levels in host cells, respectively. In addition, immunohistochemical analysis showed that SR-B1 and ACE2 could be coexpressed on the cell surface of many susceptible tissues (such as lung, retina, kidney, small intestine, colon, etc.), suggesting that SR-B1 may be a coreceptor of ACE2 and enhance the infectivity of SARS-CoV-2 in various susceptible organs and tissues. In general, this study reveals for the first time that SR-B1 is an attachment factor of SARS-CoV-2, which not only clarifies the relationship between SARS-CoV-2 and lipid metabolism but also helps to improve people's understanding of the pathogenesis of SARS-CoV-2 and provides a theoretical basis for screening and developing new antiviral drugs.

4.2.5. HSPG

Heparan sulfate (HS) is a kind of linear polysaccharide with electronegativity. It connects with the core protein *in vivo* to form a heparan sulfate proteoglycan (HSPG) structure, which exists in the cell membrane and extracellular matrix of mammalian tissue. Infection usually begins with the virus attaching to the glycan on the cell surface. Therefore, to further understand the binding of spike protein and sugar molecules, Tang et al. (2020) used glycan microarray and surface plasmon resonance techniques to test the binding differences of S proteins, subunits and domains of SARS-CoV-2 (Hao et al., 2021), SARS-CoV and MERS-CoV to different HS. The research results show that the S protein of these three human coronaviruses can bind to HS, and the position and degree of sulfation of HS are the key factors affecting its binding. The more glucosamine 6-O-sulfate groups and the higher the sulfation degree, the more easily viral protein binds to HS. The main reason for this is that the expression levels of sulfate transferases vary in different tissues or cells of the same tissue at different stages, resulting in diversity in the structure and function of HS linked by the same core protein. HSPG exhibits different sulfation patterns in different tissues, developmental stages, and pathological states, and this binding specificity may contribute to the tropism of SARS-CoV-2 for human cells. In contrast, the chain length and monosaccharide composition of HS have little effect on binding. Overall, HSPG binding is the molecular basis mediating viral attachment to host cells. Similarly, in the research of Clausen et al. (2020), HSPG was confirmed to exist on the surface of lung cells, and SARS-CoV-2 can adhere to host cells with low affinity in advance by combining with HSPG, thus increasing the virus concentration on the surface of the cell membrane. Moreover, the combination of the two can also induce structural changes in the S protein, forming an "open" conformation, further enhancing the interaction between RBD and ACE2 and initiating the viral infection program. Importantly, SARS-CoV-2 entering lung cells must bind HSPG and ACE2 located on the cell surface at the same time. In addition, removing HSPG with an enzyme or using heparin (competitive binding S protein) can prevent SARS-CoV-2 from binding to HSPG on the cell surface, hinder the adsorption of virus to host cells, and thus inhibit viral infection. To sum

up, HSPG is a necessary coreceptor in the process of SARS-CoV-2 infection that can help the virus gradually form aggregates on the cell surface. Moreover, HSPG can enhance the openness of RBD and promote its interaction with receptors, thereby triggering the fusion pathway between virus and cell membrane. Therefore, it is very important to a deep understanding of the pathogenic mechanism of SARS-CoV-2 in human cells for the prevention and treatment of COVID-19.

4.2.6. MYH9

Severe acute respiratory syndrome coronavirus 2 is highly contagious because the virus can infect host cells in many ways. To further explore the specific mechanism by which SARS-CoV-2 infects human lung tissue cells, Chen et al. (2021) jointly identified the receptor protein myosin heavy chain 9 (MYH9) interacting with the virus S protein and confirmed that the binding of the two proteins was realized by the direct binding of the C-terminal domain of MYH9 (named PRA) to the NTD of the S2 subunit and S1 subunit of SARS-CoV-2. In addition, researchers have found that knocking out the MYH9 gene in the wild-type human lung cancer cell lines A549 and Calu-3 by CRISPR/Cas9 technology can significantly inhibit SARS-CoV-2 infection. In contrast, overexpression of MYH9 or PRA enhanced viral infection in wild-type A549 and H1299 cells. Notably, endosome or myosin inhibitors can effectively block SARS-CoV-2 from entering lung cells, but TMPRSS2 and Cat B/L inhibitors are ineffective, which indicates that MYH9 promotes the endocytosis of SARS-CoV-2 and bypasses the TMPRSS2 and Cat B/L pathways. Equally importantly, overexpression of MYH9 did not enhance SARS-CoV-2 pseudoviral infection in ACE2 knockout A549 cells but only enhanced viral infection in wild-type A549 cells. Therefore, the presence of ACE2 is necessary for the entry of SARS-CoV-2 mediated by MYH9. MYH9 can act as a coreceptor for SARS-CoV-2 to enter the host and enhance viral infection by promoting the endocytosis of SARS-CoV-2 dependent on ACE2, but this process does not require the participation of TMPRSS2 and the CatB/L pathway. Overall, MYH9 plays a key role in SARS-CoV-2 infection in cells with low expression of ACE2 (lung tissue cells), and it may be another important potential target for future clinical intervention strategies.

4.2.7. C-type lectins and TTYH2

Excessive lung immune inflammation caused by SARS-CoV-2 entering the human body is considered the main driving factor aggravating COVID-19. Therefore, clarifying the immune pathogenesis caused by SARS-CoV-2 is the key to adopting correct intervention strategies for disease treatment. As previously reported (Liao et al., 2020), researchers detected the existence of viral RNA in immune cells (especially myeloid cells) isolated from alveolar lavage fluid of COVID-19 patients. However, the expression level of the ACE2 receptor molecule in immune cells is very low, which suggests that there may be other receptor molecules mediating the interaction between SARS-CoV-2 and immune cells. In response to this question, Xie et al. cooperated to provide a new explanation (Lu et al., 2021). Researchers have identified six myeloid cell membrane proteins that bind to the virus S protein, which can be used as attachment factors of SARS-CoV-2. Among them, c-type lectins (DC-SIGN, L-SIGN, LSECtin, ASGR1 and CLEC10A) mainly bind to the non-RBD (NTD or CTD) domain of the S protein, while tweety family member 2 (TTYH2), similar to ACE2, mainly binds to the RBD domain of the S protein. However, further virus verification experiments found that the interaction between SARS-CoV-2 and these surface receptors could not affect viral infection and replication but could cause myeloid cells to produce large amounts of proinflammatory cytokines (IL1B, IL8, CXCL10, CCL2, etc.) and upregulate the expression of inflammation-related genes (EGR1, THBD, C4A, and SOCS3). Moreover, RNA sequencing analysis of single cells in alveolar lavage fluid of COVID-19 patients showed that these inflammatory factors were not only closely related to the severity of symptoms but also positively related to the expression of receptors on the surface of myeloid cells. In addition, the researchers designed a bispecific nanoantibody (aiming at two blocking modes of myeloid cell receptor and ACE2 receptor), which can not only effectively prevent SARS-CoV-2 infection mediated by ACE2 but also block the excessive inflammatory reaction caused by SARS-CoV-2 through myeloid cell receptor. In total, this study reported for the first time that the interaction between SARS-CoV-2 and immune cell surface receptors can lead to excessive inflammatory reactions and proposed using bispecific nanoantibodies to block the viral infection pathway and immune overactivation at the same time as a potential treatment strategy for severe COVID-19 patients.

4.2.8. GRP78

Glucose regulated protein 78 (GRP78) is a molecular chaperone protein that usually exists in the endoplasmic reticulum of cells. However, new research suggests that GRP78 is also localized on the cell surface, serving as an attachment factor for SARS-CoV-2. On the target cell surface, it can promote the viral endocytosis by directly interacting with the S protein and endogenous ACE2 receptor (Shin et al., 2022). Notably, the soluble form of GRP78 can exist in the systemic circulation, especially in COVID-19 patients, and its protein expression level significantly increases with increasing severity of SARS-CoV-2 infection. Moreover, soluble GRP78 can form complexes with viral particles in the body circulation or plasma membrane, thus enhancing the stability of the virus and further promoting the adhesion and invasion of SARS-CoV-2 to the host cell surface. Moreover, GRP78 plays a key role as on exogenous viral protein. It can act as the host virus chaperone of SARS-CoV-2 proteins (such as S, E, N, NSPs, and ORFs) and participate in processes such as the folding, assembly and degradation of viral proteins through its own chaperone function (Nassar et al., 2021). In addition, the continuous mutation of the virus and its own adaptability have always been key issues that urgently need to be addressed in anti-SARS-CoV-2 treatment. To further explore whether targeting GRP78 can treat COVID-19, researchers tested a new small molecule drug HA15 (GRP78 inhibitor) on infected lung cells (Ha et al., 2022). The results indicate that this drug can specifically bind to GRP78 and inhibit its activity, effectively reducing the number and size of SARS-CoV-2 plaques produced in infected cells. The researchers also carried out similar studies in animal models infected with SARS-CoV-2. The results showed that HA15 significantly reduced the viral load in the lungs, and the safe dose had no harmful effect on normal cells. Surprisingly, the original purpose of this drug development is to combat cancer. This targeted inhibitor will build a bridge between

cancer treatment and COVID-19 treatment. It may be possible to treat different diseases together.

4.2.9. DPP4

Dipeptidyl peptidase-4 (DPP4) is a serine protease that exists on the cell surface in the form of dimer. It is widely distributed in human tissues and functions as a multifunctional protein. DPP4 is expressed in the respiratory tract, kidneys, liver, small intestine, and central nervous system. In addition, it is widely expressed on the surface of activated immune cells, including CD4 + T cells, CD8 + T cells, B cells, NK cells, dendritic cells and macrophages. It can regulate the production of cytokines, chemokines and peptide hormones, thus participating in various immune or inflammatory reactions. A bioinformatics study based on the protein crystal structure revealed that DPP4 can serve as a cell surface binding target for the virus S protein RBD (Li et al., 2020) and enhance SARS-CoV-2 infection of otherwise non-susceptible cells by promoting ACE2 receptor-dependent endocytosis, and mutation of E484 and its adjacent residues is an important factor in this binding ability. Notably, camostat mesylate (serine protease inhibitor) has been proven to be effective in inhibiting SARS-CoV-2 infection. Since DPP4 is a serine protease, DPP4 inhibitors may also be developed as therapeutic drugs targeting COVID-19. In addition, another study related to DPP4 inhibitors found that diabetes patients are more likely to be infected with SARS-CoV-2 and develop severe cases of COVID-19; moreover, SARS-CoV-2 can change the expression of DPP4 in diabetes patients through interaction with insulin, leptin and interleukin-6 (IL-6) and trigger uncontrolled glucose metabolism disorder and inflammation, thereby increasing the mortality of COVID-19 (Rakhmat et al., 2021). Due to the important role of DPP4 in glucose metabolism, the application of DPP4 inhibitors can help reduce the severity of the disease through this pathway, preventing lung inflammation and reducing lung injury. In general, the potential use of DPP4 as a binding target (coreceptor) for SARS-CoV-2 may provide new insights into the pathogenesis of the virus and help develop monitoring and treatment strategies to address the challenges of COVID-19.

4.2.10. Other coreceptors

In addition to the attachment factors mentioned above, the following coreceptors have been confirmed to play key roles in SARS-CoV-2 infection. The susceptibility of cells to viruses may be closely related to interaction with these receptor proteins, which can ensure the triggering of SARS-CoV-2 attachment and invasion of the host at appropriate locations. For example, T-cell immunoglobulin and mucin domain 1 (TIM-1) and TIM-4, as important phosphatidylserine (PS) receptors in the TIM and TAM families, can directly interact with PS on the outer leaflet of SARS-CoV-2, enhancing viral infection by promoting ACE2-dependent SARS-CoV-2 endocytosis fusion (Bohan et al., 2021). A disintegrin and metalloprotease 17 (ADAM17), as one of the coreceptors for SARS-CoV-2 entering the host, is mainly triggered by the virus S protein to cleave ACE2, further leading to extracellular detachment of ACE2 and enhancing host protease activity, promoting virus cytoplasmic fusion (Jocher et al., 2022). Similarly, the attachment factor B^0AT1 (SLC6A19) can enhance the stability of ACE2 and assemble it into a high-quality and stable heterodimer structure, and the ACE2-B^0AT1 complex can simultaneously bind two S proteins, significantly promoting SARS-CoV-2 recognition and infection of host cells (Yan et al., 2020). In addition, the S protein can directly bind to the pattern recognition receptor toll-like receptor 4 (TLR4) to enhance viral attachment on the surface of host cells, increase the virus concentration on the membrane surface, activate the downstream signal of TLR4 and upregulate the related inflammatory factors IL-1B and IL-6, thus inducing the body's antibacterial-like natural immune response (Zhao et al., 2021). In contrast, there are also some receptors on the host cell that inhibit viral entry. Previous research results have shown that interferon-induced transmembrane protein 3 (IFITM3) is a protein that can prevent SARS-CoV-2 from passing through the cell membrane. Its main mechanism is to prevent the fusion of the viral envelope and cell plasma membrane by regulating the fluidity of the host cell membrane, thus preventing viral invasion (Xu et al., 2022). Lymphocyte antigen-6E (LY6E) is a glycosyl phosphatidylinositol-anchored cell surface receptor that also plays a role in body defense. It inhibits SARS-CoV-2-induced cell infection by interfering with S protein-mediated membrane fusion and cytoskeleton rearrangement (Rajah et al., 2022). The ezrin protein receptor is encoded by the EZR gene, which can inhibit viral infection of the host by reducing the expression of key receptors (ACE2 and TLR) related to SARS-CoV-2. Ezrin peptide has also been proven to be particularly effective in inhibiting viral pneumonia and is a key way to prevent and treat severe COVID-19 (Gadanec et al., 2021). These reports provide new insights into the interaction between SARS-CoV-2 and the host. Further research on this aspect can help us better understand the host tropism and pathogenicity of SARS-CoV-2 and provide a theoretical basis and potential targets for the prevention and treatment of COVID-19.

5. SARS-CoV-2 is mutating

5.1. Alpha

The Alpha variant, numbered B.1.1.7, was first identified in the UK in September 2020 and began spreading rapidly in mid-December (Schuit et al., 2021). In addition to the mutation D614G in the S protein, in the RBD of the S protein of the Alpha mutant, asparagine at position 501 was replaced by tyrosine (N501Y), which increased the affinity between the RBD and ACE2. This resulted in the Alpha variant being able to infect cells with lower ACE2 levels than nasal and bronchial epithelial cells. Although the loss of amino acid 144 on the NTD of the S protein did not cause significant structural rearrangement, it led to drug resistance to most anti-NTD monoclonal antibodies (Domingo and de Benito, 2021; Mohammad et al., 2021). Therefore, compared with the original strain, the main feature of the Alpha variant strain is its ability to combat the immune system, which enhances not only transmissibility but also virulence and can lead to breakthrough of the existing natural immunity of humans and to secondary infection (Peters et al., 2021).

5.2. Beta

The Beta variant, numbered B.1.351, was first discovered in South Africa in May 2020 and soon became the most

widespread variant strain in South Africa (Bhattarai et al., 2021). In addition to the N501Y mutation in the S protein, lysine at amino acid position 417 in the RBD is replaced by asparagine (K417N), and glutamate at amino acid position 484 is replaced by lysine (E484K). Among them, the N501Y mutation enhances receptor recognition, and the additional K417N and E484K mutations facilitate immune evasion, which promotes resistance to neutralization by therapeutic monoclonal antibodies against the RBD. In addition, the replacement of leucine at position 18 with phenylalanine (L18F) and the loss of amino acids at positions 242, 244, and 243 causes rearrangement of the NTD epitope, which significantly reduces the antiviral efficacy of monoclonal antibodies against the NTD (Sutton et al., 2022; Yadav et al., 2022). Therefore, the main features of the Beta variant strain are vaccination-induced immunity escape, elevated transmissibility, and evasion of immune cell recognition, thus reducing the protection afforded by COVID-19 vaccines (Bhattarai et al., 2021; Liang et al., 2022).

5.3. Gamma

The Gamma variant, numbered P.1, was first discovered in Brazil in November 2020, and it is the most important SARS-CoV-2 strain in South America (Loconsole et al., 2021). Compared with the sequence of the Beta mutant, in the S protein RBD of the Gamma mutant, lysine at position 417 is replaced with threonine (K417T), while the E484K and N501Y mutations are retained. In addition, there is an L18F mutation in the NTD, and threonine at position 20 is replaced by asparagine (T20N), proline at position 26 is replaced by serine (P26S), etc., (Raman et al., 2021; Yépez et al., 2022). Therefore, for the ACE2 receptor, the Gamma variant has a binding affinity similar to that of the Beta variant, and mutation at these sites significantly reduces the neutralizing efficacy of monoclonal antibodies against the RBD and NTD. The main characteristic of the Gamma variant is that it can evade immunity and transmit more readily. Its transmissibility is twice that of the original strain, and some people can still undergo reinfection after recovering from infection by the Gamma strain (Brinkkemper et al., 2021).

5.4. Delta

The Delta variant, numbered B.1.617.2, was first discovered in India in October 2020, and it spread globally, causing major outbreaks in India, Britain and other countries (Bhattacharya et al., 2022). The Delta mutant also carried the D614G mutation. In addition, in the S protein RBD, leucine at position 452 is replaced by arginine (L452R), threonine at position 478 is replaced by lysine (T478K), threonine at position 19 is replaced by arginine (T19R), glycine at position 142 is replaced by aspartic acid (G142D), the amino acids at positions 156 and 157 are missing, etc. Among them, the L452R mutation is closely related to the increased infectivity of the delta variant and reduction of neutralization by convalescent plasma and specific monoclonal antibodies (Wilhelm et al., 2021; Dhawan et al., 2022). Therefore, the main characteristics of the Delta variant are fast transmission speed, high viral load and strong adaptability to the body. Statistical analysis shows that Delta has the strongest infection ability among all variant strains at present, and its infection rate is twice that of the Alpha strain and 1,260 times that of the original strain (Yi et al., 2022). Even more worrisome is that the condition of patients infected with the Delta variant progresses rapidly, and the average time to the severe stage is only 5 days (Zhan et al., 2022).

5.5. Omicron

The Omicron variant, numbered B.1.1.529, was first discovered in South Africa in November 2021, becoming the fifth VOC, and it has gradually replaced Delta and become prevalent worldwide (Rana et al., 2022). The Omicron variant contains more than 50 mutations, including 37 mutation sites on the S protein alone, representing the most frequent mutation in the S protein among variants at present (Bazargan et al., 2022). Importantly, the Omicron variant incorporates the other four key mutation sites of the S protein of other VOCs, and there are 15 amino acid mutation sites in the RBD region, including K417N, T478K, and N501Y, among which E484A and Q493R are unique to Omicron. Among these mutations, the K417N, N501Y, Q493R, and Y505H mutations can enhance the binding ability of the virus to ACE2 and thus increase its infectivity. Mutations such as S477N, T478K, and E484A may enhance the immune evasion ability of viruses, thus avoiding the surveillance of the immune system (Khandia et al., 2022; Tian et al., 2022). Furin, a highly specific endonuclease, can enhance the pathogenicity of viruses. There are three mutations (H655Y, N679K, and P681H) near the furin cleavage site of the Omicron variant, which may enhance the cleavage of the S protein and its fusion with host cells and further promote the replication and transmission of the virus (Bansal and Kumar, 2022). In addition, the R203K/G204R mutation in the N protein is closely related to an increase in viral RNA expression and viral load, which may enhance viral virulence (Singhal, 2022). Therefore, the main features of the Omicron variant strain are its strong transmissibility and immune evasion ability. Omicron is called a supervariant strain, and the number of cases due to Omicron is rising much faster than that of previous SARS-CoV-2 outbreaks. Fortunately, it has less virulence and causes low mortality, and some infected people have no symptoms (Trunfio et al., 2022).

In the early stages of the Omicron epidemic, three subtypes emerged, namely, BA.1-3, with BA.2 having the strongest epidemic intensity (Tiecco et al., 2022). Compared with the previous subtypes, Omicron subtype BA.4 and BA.5 have stronger cell fusion ability in alveolar epithelial cells, so with the accelerated spread of BA.4/5 in many countries, the world set off the seventh wave of the epidemic surge (Tallei et al., 2022). XBB is a recombinant strain of Omicron BA.2.10.1 and BA.2.75, with stronger transmission and immune escape ability than the early prevalent Omicron variant (Vogel, 2023). It is currently the dominant epidemic strain in multiple countries worldwide. XBB.1.5 was first found in the United States in October 2022 and has been marked as the most infectious SARS-CoV-2 subtype variant thus far, with at least 26 subbranches (XBB.1.5.1~XBB.1.5.10) (Channabasappa et al., 2023). According to the data released by the US Centers for Disease Control and Prevention (CDC) website, during the week of March 12-18, 2023, cases of XBB.1.5 accounted for 90.2% of the total

TABLE 2 Comparison of 11 COVID-19 vaccines included in the WHO emergency use list.

Types of vaccines	Representative vaccines	Fundamental	Advantages	Disadvantages
Inactivated virus vaccine	BBIBP-CorV/ Coronavac/ Covaxin	The virus is cultured *in vitro* and inactivated by physicochemical methods. The inactivated virus only retains immunogenicity and causes specific immune response as antigen	Mature technology, easy preparation and large-scale production. The inactivated virus does not replicate in the host and is not contagious	The immunogenicity is insufficient and adjuvant needs to be added. The immune effect period is short and multiple injections are needed. Weak ability to cope with virus mutation
mRNA vaccine	BNT162b2/ mRNA-1273	The mRNA expressing S protein is introduced into the body through a specific delivery system, and the S protein is expressed in the body and induced to produce specific immune response	Short research and development cycle, low production cost, and timely response to the outbreak of mutant strains. No virus component, no risk of infection	Poor stability and high requirements for storage and transportation conditions. There is virulence risk. Large-scale production process needs to be optimized
Viral vector vaccine	Vaxzevria/ Covishield/ Ad26.COV2.S/ Ad5-nCoV	The S protein gene is inserted into the modified adenovirus genome which is harmless to the body, and then inject it into the human body to stimulate the body to produce specific immune response	No adjuvant is needed, and the adverse reactions are small. The number of vaccinations is less, which can induce immune response faster and is suitable for large-scale population vaccination	The body may have pre-existing immunity to adenovirus vector, which will reduce the immune effect of vaccine
Subunit vaccine	Covovax/ Nuvaxovid	The S protein or its protein fragment is prepared directly *in vitro* by genetic engineering recombination method, and then inject it into vivo to induce specific immune response	High safety and good stability. Easy storage and transportation	The immunogenicity is weak, and additional adjuvants are needed to enhance it

number of cases of COVID-19, and the virus strain developed from a low-frequency epidemic to an absolute advantage epidemic strain in less than 3 months (Center for Disease Control and Prevention [CDC], 2023). XBB.1.9 was first detected in Indonesia in September 2022 and currently has three sub branches (XBB.1.9.1 to 1.9.3) (Velavan et al., 2023). Notably, although there has been an increase in cases of XBB.1.9 worldwide recently and its transmission potential is higher than that of XBB.1.5, individuals who have been infected with XBB.1.5 will not be infected with XBB.1.9 again in the short term, which greatly suppresses its spread (World Health Organization [WHO], 2022b). Recently, a new strain FU.1 (XBB.1.16.1.1) with stronger infectivity has emerged in multiple regions worldwide. Experts have warned that the danger of FU.1 is very high, with 50% higher infectivity than the current epidemic strain, and it has only just begun to spread globally (Herald Sun, 2023). In short, although the COVID-19 epidemic no longer constitutes a "public health emergency of international concern," it is still a serious infectious disease, and we need to consider it a serious threat to human health.

6. Effectiveness of the COVID-19 vaccines against the Omicron variants

At present, COVID-19 continues to spread in many places worldwide, and vaccination is one of the most effective strategies for pandemic prevention. According to the data released by the WHO on March 30th, 2023, there are 183 vaccines in clinical trials and 199 vaccines in preclinical trials (World Health Organization [WHO], 2023). These vaccines mainly include subunit vaccines (32%), inactivated vaccines (12%) and attenuated live vaccines (1%), as well as emerging mRNA vaccines (24%), viral vector vaccines (14%), DNA vaccines (9%), and virus-like particle vaccines (4%) (Li G. et al., 2022), among which 11 vaccines are included in the Global Emergency Use List (EUL) (**Table 2**). However, SARS-CoV-2 variants appear frequently, and whether the existing COVID-19 vaccines can effectively slow the spread of the current pandemic variants has become a global issue of general concern to the public. Here, we focus on the latest research progress of these 11 vaccines from the perspective of the technical route, working mechanisms, advantages and disadvantages of the vaccines and neutralization efficacy against Omicron pandemic strains, hoping to further improve the rationale and accuracy of COVID-19 prevention and control measures (**Figure 3**).

6.1. Inactivated virus vaccines

Inactivated vaccine technology is recognized as a mature classic technology worldwide. In its preparation, the virus strain should be first isolated, amplified and cultured in susceptible cells and then inactivated, purified and adsorbed by an adjuvant so that the original virus strain loses pathogenicity and retains antigenicity. Subsequently, helper T cells can be activated by antigen-presenting cells, and then B cells can be induced to produce humoral immunity (Wang Z. et al., 2020). Although inactivated virus particles can no longer infect, they contain the complete structural proteins of the virus, which can simultaneously induce the production of polyclonal antibodies against various SARS-CoV-2 antigens (such as the S protein and N protein). However, due to the complexity of virus culture and inactivation procedures, the development and production of inactivated vaccines requires more

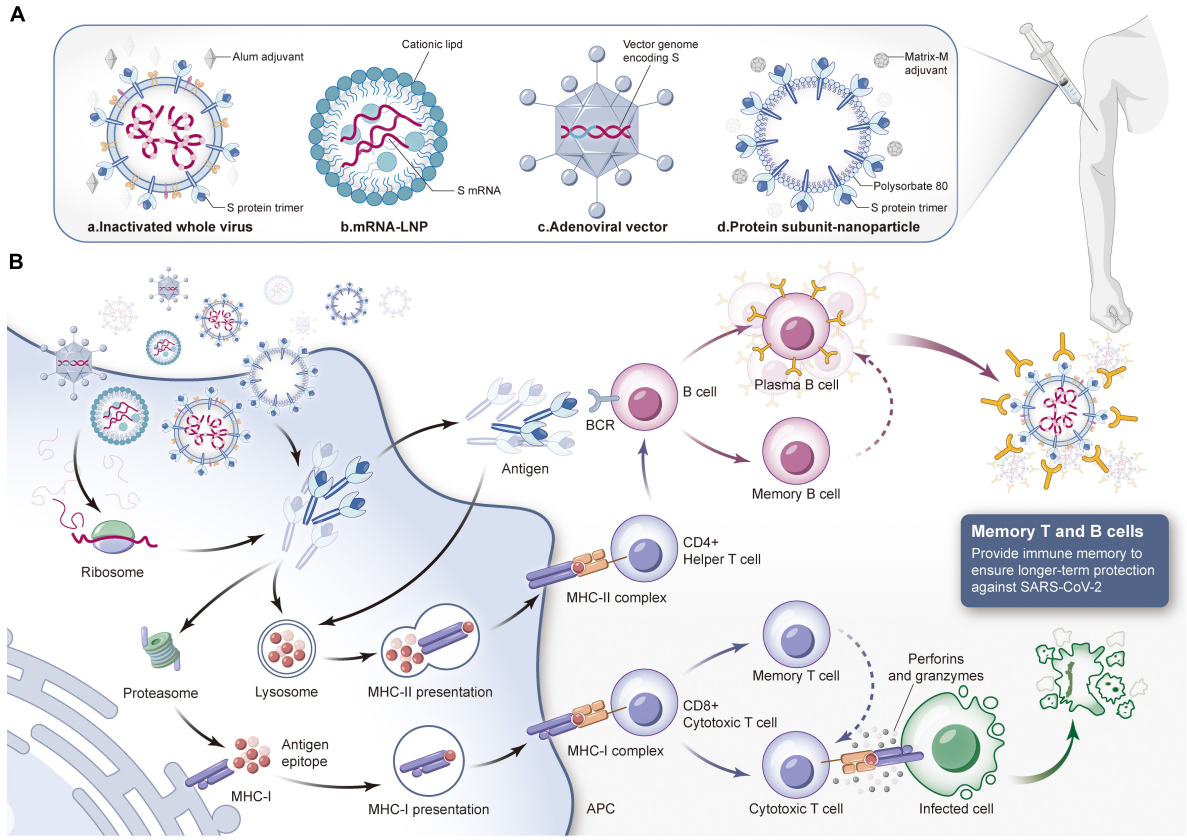

FIGURE 3
Composition of different types of COVID-19 vaccines and the mechanism of protective immune response induced by them. **(A)** Different types of COVID-19 vaccines. a. Inactivated virus vaccine: Use physical and chemical methods to inactivate SARS-CoV-2 and add specific adjuvants. The inactivated virus injected into the body has no pathogenicity but only retains immunogenicity. b. mRNA vaccine: Lipid nanoparticles are used as delivery carriers to introduce mRNA expressing spike (S) protein into the body to produce neutralization reaction. c. Virus vector vaccine: Integrate S protein gene into adenovirus genome to construct recombinant adenovirus vaccine, and then inject it into muscle. d. Protein subunit vaccine: The S protein or its subunit fragment prepared *in vitro* is mixed with a specific adjuvant and injected into the human body to induce the immune response of the body. Then stimulate the immune system to produce specific immune response against SARS-CoV-2. **(B)** The human immune system will produce immune response against the invading vaccine components. When COVID-19 vaccine is injected into the body, it can be internalized by antigen presenting cells, and S protein or its subunit fragments can be transmitted or synthesized in the cytoplasm. If the target antigen is decomposed into small fragments by the proteasome complex, MHC-I molecules can present the antigen fragments to the cell surface to facilitate the recognition of $CD8^+$cytotoxic T cells. Activated cytotoxic T cells kill infected cells by secreting lymphokines such as perforin and granzyme. If the target antigen secreted is reabsorbed by cells, it will be degraded by lysosomes and presented to $CD4^+$helper T cells through MHC-II molecules on the cell surface. B cells will be activated by the stimulation of antigen, proliferate and differentiate into plasma cells, secrete specific antibodies, and the antibodies can combine with SARS-CoV-2 to make them lose their infectivity. At the same time, they will guide macrophages to phagocytosis and eliminate pathogens. In addition, both memory T cells and memory B cells have the ability to recognize specific antigens. If they encounter the same target antigen invasion again in the future, they can be quickly activated to kill the invading pathogens. (LNP, lipid nanoparticle; APC, antigen-presenting cell; MHC, major histocompatibility complex; BCR, B cell receptor).

time (Khoshnood et al., 2022). Moreover, the immune protection duration is relatively short, and two or even multiple invasive injections are required (Khoshnood et al., 2022).

According to the up-to-date information from the WHO, three inactivated vaccines have been granted emergency use authorization, including BBIBP-CorV produced by the Beijing Institute of Biological Products Co., Ltd. and CoronaVac produced by Beijing Kexing Biological Products Co., Ltd. Covaxin was developed by Bharat Biotech (World Health Organization [WHO], 2022a). BBIBP-CorV is the first COVID-19 vaccine listed by the WHO for emergency use in China. In the early stage of the widespread pandemic of the Omicron variant, Professor Zhang Wenhong and Professor Wang Pengfei of Fudan University jointly evaluated the immune evasion ability of the Omicron variant after two doses of BBIBP-CorV and the third booster vaccination. Studies showed that the antibody titer level of the subjects vaccinated with two inactivated vaccines against the Omicron strain decreased by at least 5.3-fold compared with that against the original strain. However, after the third booster injection, the antibody titer increased significantly, and the antibody-positive rate reached at least 75% (Ai et al., 2022). CoronaVac is the most widely administered COVID-19 vaccine in the world. The latest study comprehensively analyzed the immune response induced by the third booster dose of the CoronaVac injection. The strong immune memory could be quickly recalled by the third injection, and the neutralizing activity of serum against the original strain, Delta variant strain and Omicron variant strain increased by 4.08-fold, 5.0-fold, and 3.6-fold, respectively. Subsequently,

Chen R. et al. (2022) also dynamically monitored specific cellular immunity against SARS-CoV-2. It was found that the RBD protein-specific B cells and memory B cells for the original strain induced by the third injection could also cross-recognize the RBD of Delta and Omicron variants. Regarding Covaxin, the WHO recently issued a statement that it would suspend the procurement and supply of Covaxin due to manufacturing practice defects found during inspection and suggested that countries receiving this vaccine "take appropriate actions" (Thiagarajan, 2022).

6.2. mRNA vaccines

As a powerful tool against the COVID-19 pandemic, mRNA vaccines have been widely studied. These vaccines can introduce mRNA expressing antigen targets into the body through a specific delivery system, and then the proteins are translated and expressed, whereupon they effectively stimulate the body to produce specific immune responses (a dual humoral immunity and T-cell immunity mechanism) to achieve efficient immune protection (Fang et al., 2022). The mRNA vaccine uses the gene sequence of SARS-CoV-2, containing viral component and carrying no risk of infection. In addition, mRNA vaccines have short research and development cycles, simple production processes and easy mass production, which can improve the global vaccination rate. More importantly, for the constantly mutating SARS-CoV-2, once a new variant sequence is determined, researchers can develop a new vaccine to deal with the mutant strain in the shortest time by modifying the mRNA sequence of the target. However, mRNA molecules have a short half-life and poor stability and are extremely sensitive to high temperature, which makes vaccine storage and transportation difficult (Jin et al., 2021; Szabó et al., 2022).

Since the emergence of COVID-19, the medical prospects of mRNA vaccines have been fully proven. At present, mRNA vaccines included in the EUL by the WHO include BNT162b2, which was jointly developed by Pfizer/BioNTech, and mRNA-1273, which was produced by Moderna (World Health Organization [WHO], 2022a). Both vaccines were developed with the design strategy of wrapping mRNA encoding the SARS-CoV-2 S spike protein with lipid nanoparticles (LNPs) (Noori et al., 2022), and vaccinees are afforded good protection. A study led by Professor Lu Ligong found that among people who have been vaccinated with two doses of an inactivated virus vaccine, those who choose BNT162b2 for the booster injection will effectively produce more neutralizing antibodies against Omicron (Li G. et al., 2022). Similarly, Muecksch et al.'s (2022) research shows that compared with people who received only 2 shots of an mRNA vaccine, those who received a third shot of mRNA-1273 exhibit enhanced ability of the body to produce broad-spectrum neutralizing antibodies, and more than 50% can neutralize Omicron variants. In addition, as reported Moderna Company, the first mRNA vaccine, mRNA-1273.214 specifically targeting Omicron will be launched soon, covering 32 mutations of the S protein and exhibiting an excellent neutralizing effect on Omicron (BA.4/5). Compared with that before mRNA-1273 booster vaccination, the neutralizing antibody level increased by 8-fold, and the geometric mean titer (GMT) of antibodies increased from 432 to 3,070 1 month after mRNA-1273.214 booster vaccination (Chalkias et al., 2022).

6.3. Viral vector vaccines

Viral vector vaccines use improved and safe viruses (such as adenovirus, HIV, etc.) as vectors to deliver genes encoding viral protective antigens to host cells (Deng S. et al., 2022), thus activating the human body to produce specific neutralizing antibodies and develop immune protection. There are two kinds of viral vector vaccines. One is non-replicative; the virus retains its complete structure and infectivity, but its self-replication function is lost. It needs the help of specific transformed cells or helper viruses to stimulate the human body to produce effective immunity. The other is the replication type, which can also replicate and produce more vector viruses to complete a new round of infection, express more specific antigens, and then trigger a stronger immune response (Jacob-Dolan and Barouch, 2022). The viral vector vaccines approved for SARS-CoV-2 protection are all recombinant vaccines based on adenovirus as the delivery vector and S protein as the target. Its advantage lies in the high transgenic efficiency of the adenovirus vector, which can transduce different types of human tissues and cells, and the vaccine can be inoculated with only one injection, with an average of 14 days to achieve immune protection. Therefore, it is time-saving, convenient, efficient and suitable for rapid large-scale vaccination of populations (Chen L. et al., 2022). However, because adenovirus vectors are generally susceptible, most humans have antibodies to neutralize adenovirus, which leads to the immune system attacking viral vectors, thus reducing the effectiveness of the vaccines (McCann et al., 2022).

Globally, four kinds of adenovirus vaccines have been authorized by the WHO for emergency use. These vaccines are Vaxzevria and Covishield, which were jointly developed by Oxford University/AstraZeneca, Ad26.COV2.S developed by Johnson & Johnson and Ad5-nCoV produced by Consino Biological AG (World Health Organization [WHO], 2022a). Research results have proven that although the preventive effect of the vaccine decreased compared with that against the original strain, individuals initially immunized with 2 doses of Vaxzevria still retained neutralizing activity against Omicron. After the third-dose booster injection, the titer of neutralizing antibody against Omicron increased significantly (Hastert et al., 2022). During the fourth COVID-19 wave in South Africa triggered by the Omicron strain, Gray Glenda's team conducted mass spectrometry analysis on serum samples from critically ill patients who were vaccinated with 2 doses of Ad26.COV2. The research findings suggested that Ad26.COV2.S booster injection could effectively prevent hospitalization with severe COVID-19, and the effective rate was 55% 14 days after inoculation, 74% 14–28 days after inoculation, and 72% 1–2 months after inoculation. The curative effect of critically ill COVID-19 patients admitted to the ICU is also very significant. The effective rate was 82% 1-2 months after vaccination (Gray et al., 2022). The researchers randomly divided 904 subjects who had been vaccinated with 2 doses of inactivated vaccine 6 months

prior into 3 groups, namely, the 1-dose Ad5-nCoV heterologous boosted group, 1-dose ZF2001 heterologous boosted group and 1-dose CoronaVac homologous boosted group. The data showed that 14 days after booster vaccination, the neutralizing antibody GMT against the Omicron strain of the Ad5-nCoV group was 261 and that of the ZF2001 group and the CoronaVac group was 86 and 54, respectively. In addition, the positive rate of IFN-γ production in the Ad5-nCoV heterologous boosted group was 68.8%, and the cellular immune response intensity was significantly better than that in the other two groups (Sapkota et al., 2022). Therefore, Ad5-nCoV was selected as the booster injection for heterologous boosting, which is the best choice for protective immune effects at present.

6.4. Subunit vaccines

A protein subunit vaccine is a new vaccine that can induce immune protection based on the recombination of the protective antigen gene of the virus with a plasmid or viral vector and introducing it into a recipient cell expression system, inducing the production of specific antigen proteins and purifying them (Golob et al., 2021). Subunit vaccines usually employ the S protein or RBD protein of SARS-CoV-2 as candidate vaccine antigens to eliminate epitopes with poor immune effects. This approach can not only improve the utilization efficiency of antigen epitopes but also avoid the production of unrelated antibodies and reduce the side effects of vaccines (Mekonnen et al., 2022). On the other hand, because such a vaccine needs only the recombination and expression of effective antigen fragments *in vitro* without any live virus, vaccine production can be conducted in an ordinary biosafety laboratory, which significantly reduces the production cost, and the storage and transportation of the vaccine are more convenient, enabling large-scale production capacity (Díaz-Dinamarca et al., 2022; Heidary et al., 2022). However, because this kind of vaccine includes only a part of the virus structure, its immunogenicity is relatively low, so it is necessary to add appropriate adjuvants to enhance the immune effect of the vaccine.

With the ongoing development of vaccines against COVID-19, subunit vaccines have become the largest category of vaccine research and development. NVX-CoV2373 (Covovax and Nuvaxvid) is a protein subunit vaccine jointly developed by Novavax/Serum Institute of India and was listed by the WHO for emergency use on December 17 and 21, 2021, respectively (World Health Organization [WHO], 2022a). Early in the Omicron outbreak, Novavax released raw data on the cross-reaction of NVX-CoV2373 for Omicron. The results showed that NVX-CoV2373 produced an extensive cross-reactive immune response to Omicron and other SARS-CoV-2 variants. Compared with that after the initial immunization with two doses of NVX-CoV2373, the body produced a stronger immune response after the third-dose booster injection, and the anti-S protein IgG antibody and ACE2-binding inhibitory antibody levels increased by 9.3 times and 19.9 times, respectively (Tarke et al., 2022). In addition, recent data have shown that NVX-CoV2373 can produce an effective immune response to many Omicron subtypes, including BA.5, which has the strongest immune evasion ability (Zeng et al., 2022). Overall, NVX-CoV2373 plays an important role in fighting against the new SARS-CoV-2 variants.

6.5. Other types of vaccines

In addition to the abovementioned COVID-19 vaccines, other types of vaccines have been developed, tested and approved for use. For example, the working mechanism of DNA vaccines belonging to the third-generation technical approach is to introduce DNA fragments encoding antigen proteins into host cells, which then continuously express natural antigens *in vivo* to induce the human body to produce a sustained and effective immune response (Wang X. et al., 2022). Compared with mRNA vaccines, DNA vaccines have higher stability and are easier to produce and store, but they may also integrate DNA into the host chromosome to cause mutations and induce autoimmune diseases (Hadj Hassine, 2022). At present, only ZyCoV-D developed by Zydus Cadila has been authorized for emergency use and approved for vaccination for people over 12 years old. It is not only the first DNA COVID-19 vaccine officially approved for marketing but also the first DNA vaccine applied to humans in the world (Khobragade et al., 2022). In fact, more than a dozen DNA COVID-19 vaccines are undergoing clinical trials, and INO-4800, which was jointly developed by Inovio and Aidi Weixin, has made the fastest progress and attracted the most attention (Kraynyak et al., 2022). Virus-like particles (VLP) vaccines is a kind of nano particles formed by self-assembly of one or more structural proteins of a virus. It has similar spatial structure and composition with natural virus particles, and can effectively induce immune protective response in human body. Because they do not contain viral genetic material, VLP vaccines are not infectious and have relatively high safety. However, their immunogenicity is insufficient. Similar to subunit vaccines, they need adjuvants and multiple immunizations to enhance the immune effect, and their preparation is complex and difficult (Tariq et al., 2021). CoviFenz (VLPs based on plants), a COVID-19 vaccine jointly developed by GSK/Medicago, has been officially approved by the Canadian Ministry of Health for marketing. This vaccine is the first approved plant-derived COVID-19 vaccine (Hemmati et al., 2022).

Attenuated vaccines consist of pathogen variants with weakened or no virulence obtained by attenuating pathogens by specific methods before inoculating them into the human body to induce an immune response (Okamura and Ebina, 2021). In contrast to inactivated virus vaccines, an attenuated vaccine retains the replication ability and immunogenicity of the original strain, so its immune effect is stronger, and its action time is longer. However, there may be potential pathogenic risks in immunocompromised people vaccinated with attenuated vaccines. More importantly, because the attenuation and screening of pathogens in the early stage takes a large amount of time, it is very difficult to complete the research and development of products in a short time, which indicates that attenuated vaccines will not be the first choice for managing outbreaks (Chen, 2022). To date, only two candidate vaccines, COVI-VAC and MV-014-212, have been approved for clinical trials (Wang S. et al., 2021; Tioni et al., 2022). Moreover, some COVID-19 vaccines (synthetic peptide vaccines and circular RNA vaccines) are in an accelerated process of research and development (Qu et al., 2022), with the hope that they can produce remarkable protective effects in the clinic.

7. Establish a mode to cope with the COVID-19 epidemic

To date, the COVID-19 epidemic has gone from the original virus strain to fifth generation VOCs. Obvious changes have taken place in the genomics, biology and epidemiology of Omicron. The extremely strong transmission and immune evasion ability is accompanied by a decline in the pathogenicity of the virus itself. Combined with the population immune barrier established by previous infection and vaccination, compared with the previous variant strains, the related epidemic shows the characteristics of strong transmission and a low severity rate and mortality rate (Trunfio et al., 2022), which opens a new stage of the COVID-19 epidemic. At the same time, faced with a series of problems, such as Omicron's influence on epidemic prevention policy, livelihoods and social and economic operations, human cognition and response to the COVID-19 epidemic will also enter a new stage. How can humans coexist with viruses at the lowest cost? How can epidemic prevention strategies be optimized to account for epidemic control, livelihood and the economy? These are common problems faced by all countries in the world. Accordingly, we believe that the ultimate control mode of COVID-19 will be the application of COVID-19 vaccines and COVID-19-specific drugs for prevention and treatment to jointly enhance the ability of human beings to cope with the COVID-19 epidemic. In addition, strengthening the monitoring of mutant strains by means of science and technology and adopting appropriate and effective public health protection strategies are also important links to control the spread of the epidemic. In short, we must be soberly aware that relaxing the prevention and control of the epidemic does not mean letting go of the epidemic; we coexist with SARS-CoV-2 but not allow it to spread freely. Because Omicron is still evolving, no one knows the future epidemic trend and the impact of dominant variants on human beings and society.

7.1. Effective promotion of vaccination and innovation

New variants of SARS-CoV-2 frequently appear all over the world, and the Omicron variant shows stronger transmissibility and immune evasion ability than previous strains, which directly leads to a certain degree of decline in the protective efficacy of the early developed vaccines (Zhou et al., 2022). Fortunately, even so, Omicron variants are still within the protection scope of these vaccines, and the protection rate of the vaccines is still higher than the established standard of the WHO (a protection rate of vaccines over 50%) (Fernandes et al., 2022). Many studies have proven that vaccination can reduce the transmission risk of the Omicron variant in the population and effectively reduce the incidence of severe illness and mortality after infection (Fernandes et al., 2022; Guo et al., 2022). Therefore, actively promoting vaccination among social groups and establishing an effective immune barrier are currently the most important means to control the COVID-19 pandemic. However, we must also admit that the current vaccines cannot completely prevent Omicron infection, and we still need to further innovate and develop specific vaccines, expecting the emergence of new vaccines based on Omicron variants that can provide stronger and more lasting protective efficacy.

7.2. Promotion of heterologous booster immunization

In the context of the more "cunning" Omicron variant, vaccination against COVID-19 remains one of the most effective pandemic prevention measures. Studies have shown that the level of neutralizing antibodies in people who have completed basic immunization will obviously decrease over time. To better prevent infection caused by the Omicron variant globally, timely booster immunization can rapidly improve the neutralizing antibody level and immune protection ability of recipients, thus producing a better protective effect on the body (Meng et al., 2022). At present, according to whether the technical routes of the booster vaccine and basic immunization vaccine are consistent, booster immunization can be divided into two methods, namely, homologous booster immunization and heterologous booster immunization. Among them, the preventive effect of the latter is more prominent (Deng J. et al., 2022). A clinical study by Al Kaabi showed that people who had received two doses of BBIBP-CorV inactivated vaccine could produce a strong immune response against the Omicron variant after receiving one dose of NVSI-06-07 protein subunit vaccine by heterologous boosting, and their antibody level was 19.5 times that before boosting. Compared with that of subjects who received homologous boosting with the BBIBP-CorV inactivated vaccine, the neutralizing antibody GMT increased by 7.7 times (Al Kaabi et al., 2022). In addition, ARCoVaX is a new COVID-19 mRNA vaccine jointly developed by Aibo Biology, Academy of Military Medical Sciences and Watson Biological. The results of clinical trials showed that when ARCoVaX booster injection was sequentially inoculated after basic immunization with two inactivated vaccines, it induced a strong neutralizing antibody reaction to Delta and Omicron variants, and the neutralizing reaction remained at a high level until 90 days after inoculation. In addition, compared with homologous vaccination with an inactivated vaccine, heterologous vaccination with ARCoVaX can induce a stronger humoral immune response, which can effectively prevent virus escape and severe illness (Liu et al., 2022). On the whole, clinical research on heterologous booster immunization provides a new idea for vaccination strategies for COVID-19 and provides a more accurate basis for strengthening the optimization of immunization strategies.

At present, many countries and regions worldwide have adopted or recommended heterologous immunization as a booster vaccination strategy for COVID-19 vaccines, especially adenovirus vector vaccines, which can effectively strengthen the protection provided by other vaccines and reduce the incidence of severe diseases (Lv et al., 2022). There are two main advantages of heterologous booster immunization: first, different vaccines can complement each other and increase the neutralizing antibody level of recipients; second, everyone's constitution is different, which may result in side effects for a certain type of vaccine. Vaccination via different technical routes can circumvent this situation (Nguyen et al., 2022). All in all, heterologous booster immunization is expected to improve the intensity, breadth and persistence of

the immune response through the combination of vaccines with different mechanisms, provide more comprehensive and powerful immune protection for the body, and further reduce the risk of breakthrough infection caused by the Omicron strain.

7.3. Accelerating the research and development of small molecule antiviral drugs

Antiviral drugs are the first choice to treat SARS-CoV-2 infection. Only by completely eliminating SARS-CoV-2 can COVID-19 be cured. Macromolecular antibody drugs can neutralize viruses directly, but they are easily degraded in the digestive tract, so they cannot be taken orally. Most of them are injected and mainly used for inpatients, and there are some problems, such as high research and development costs and difficulty dealing with virus variation (Huang et al., 2022). In contrast, the development of small molecule chemical drugs is of great importance in the environment of repeated global epidemics. The preparation process of small molecule chemical drugs is simple and mature, which can quickly realize mass production to meet the surge in the number of infected people caused by the Omicron outbreak (Sargsyan et al., 2023). Moreover, such drugs are stable, and most of them are taken orally, which not only greatly improves the compliance of patients but also facilitates administration to the vast numbers of outpatient and home patients, reducing the strain on medical resources and ensuring timely treatment of critically ill patients (Hemmati et al., 2022). The whole process of viral infection can be divided into adsorption, invasion, shelling, replication, assembly and release (Biskupek et al., 2022), so interfering with viral invasion and replication processes is an effective direction for antiviral drug action. At present, oral small molecule antiviral drugs used clinically can be divided into two categories according to their targets: one category is ACE2 inhibitors and membrane fusion inhibitors that target the S protein to hinder viral invasion, while the other is RNA polymerase inhibitors and 3C-like protease (3CLpro) inhibitors that target RNA polymerase and 3CLpro to prevent virus replication (Kralj et al., 2021). From the perspective of drug marketing speed, it is difficult to develop ACE2 inhibitors and membrane fusion inhibitors. More importantly, the mutation of SARS-CoV-2 mainly occurs on the S protein, while RNA polymerase and 3CLpro are highly conserved in SARS-CoV-2 and thus undergo less mutation. Therefore, inhibitors of these two enzymes will have lower off-target effects and will remain effective for all variant strains (Chen R. et al., 2022), making them an important focus of future research and development of anti-SARS-CoV-2 drugs.

At present, dozens of small molecule antiviral drugs for treating COVID-19 are being intensively developed worldwide, almost all of which are RNA polymerase and 3CLpro inhibitors. Some of these drugs have made remarkable progress in research and have obtained marketing licenses or emergency use authorization in many countries. For example, Molnupiravir represents a new generation of RNA polymerase inhibitors developed by Merck. As the world's first oral small molecule drug, it is mainly used for the treatment of severe and mild and moderate adult patients with high hospitalization risk. It was first launched in the UK in November 2021 (Flisiak et al., 2022). One study included 775 adults with mild to moderate COVID-19 as subjects, including patients with basic diseases such as obesity, diabetes or heart disease with higher risk. Oral administration of Molnupiravir (400 mg) for 5 days significantly reduced the hospitalization rate and mortality. The hospitalization rate of the treatment group was 7.3% (no deaths), while that of the control group was 14.1% (8 deaths) (Czarnecka et al., 2022). Similarly, Paxlovid, developed by Pfizer, is one of the most effective oral drugs at present, and was approved by the FDA to be marketed in the United States in December 2021 for patients with severe risk and non-hospitalized mild to moderate COVID-19 pneumonia. Paxlovid is a combination package that consists of two drugs: nematvir inhibits the 3CLpro of SARS-CoV-2, and ritonavir inhibits the Cytochrome P450 3A4 (CYP3A4) enzyme of the human body, preventing nematvir from being metabolized by the human body and maintaining its blood concentration for a long time (Marzolini et al., 2022). The results of clinical trials showed that when Paxlovid was taken within 3 days of symptoms, the hospitalization rate was only 0.8%, and there were no deaths. In the placebo group, the hospitalization rate was 7%, and the mortality rate reached 1.8% (Kueh, 2022). In total, it is very important to develop broad-spectrum, convenient and low-cost specific drugs for the effective prevention and control of the COVID-19 epidemic. With the development and marketing of oral small-molecule antiviral drugs and the comprehensive vaccination of vaccines, mankind will eventually win the war without gunpowder, and the impact of the COVID-19 epidemic on world production and life will eventually be eliminated.

7.4. Strengthening the monitoring of mutant strains

Recently, the China CDC reported the opinion that the Omicron variant will not be the last variant (Chinese Center for Disease Control and Prevention, 2022). Therefore, the monitoring of new variants and the possible impacts of transmission, pathogenicity and immune evasion are the focus of current pandemic prevention and control. Real-time fluorescence quantitative PCR nucleic acid detection has high specificity and sensitivity and has become the "gold standard" for diagnosing SARS-CoV-2 infection (Wang H. et al., 2022). However, because SARS-CoV-2 is an RNA virus, variation in the target sequence develops easily, and too low a viral content in the sample to be detected due to weakening of the virus shedding ability and even some inappropriate operations (including sample collection, transportation, storage and processing, etc.) may lead to negative results in qRT-PCR detection (Rai et al., 2021). In fact, there have been patients worldwide who have been tested more than ten times before having a positive result (MacKenzie et al., 2022). Therefore, no one can guarantee that there will be no mutant strain in the future that can avoid the existing nucleic acid detection, and such a variant may be hidden in a remote part of the world.

High-throughput next-generation sequencing (NGS) is a powerful tool to analyze the genetic relationship between viral

evolution and disease, track the epidemic situation, develop new therapies and develop vaccines. This technology can obtain the genome sequence information of unknown viruses for the first time, making it possible not only to effectively monitor the mutation of SARS-CoV-2 but also to identify, trace and analyze the virus epidemiology (de Mello Malta et al., 2021), which is of great significance for cutting off transmission route and tracking the transmission situation. In addition, the successful acquisition of the complete sequence of the mutant strain provides the basis for the subsequent establishment of a rapid detection method. For patients with negative nucleic acid detection and highly suspect clinical phenotypes, NGS technology can also be used for further confirmation (Quer et al., 2022). On the other hand, although NGS has obvious advantages of high throughput, high sensitivity and high accuracy, its detection cost is high, the detection process is cumbersome, and professionals are required to analyze sequencing results, which is not suitable for rapid and mass screening and diagnosis, so it is difficult to be widely used (Quer et al., 2022). In summary, SARS-CoV-2 mutations are still uncertain. All countries should enhance their ability to monitor and sequence mutant strains as much as possible and share complete genome sequence data with international public platforms to help each other cope with the evolving COVID-19 epidemic.

7.5. Improve self-immunity and adhere to public health protection measures

"It takes a good blacksmith to make steel" (a metaphor indicating that you need your own strength to do anything) is a familiar traditional Chinese saying. People of all ages are generally susceptible to SARS-CoV-2 because it is a novel pathogen, especially elderly individuals with underlying diseases (diabetes, cardiovascular and cerebrovascular diseases, malignant tumors, etc.) that readily cause complications and critical illness after infection and account for the vast majority of deaths (Gao Y. et al., 2021; Laza et al., 2022). This suggests that there may be a close relationship between immunity and symptoms or manifestations of SARS CoV-2 infection and whether it will develop into severe disease. Therefore, we should scientifically strengthen our physical fitness and enhance our own immunity to resist the invasion of viruses into the our body.

Regarding the current situation and trend of global pandemic development, it can be assumed that SARS-CoV-2 variants will persist. From the perspective of viral transmission, viral replication and mutation complement each other. Effectively controlling the number of infected people in society can directly reduce the chances of viral replication and mutation (Chekol Abebe et al., 2022). Therefore, compliance with public health protection measures is key to controlling the spread of the pandemic, especially in areas where SARS-CoV-2 is spreading intensely. In other words, even after vaccination, we cannot relax our vigilance, and we still need to take preventive measures such as mask wearing, frequent ventilation, frequent disinfection, safe social distancing and reducing unnecessary gatherings.

8. Conclusion

Although the transmission capacity of SARS-CoV-2 has not abated, and at present, the transmission coefficient (Rt) of the new Omicron variant XBB.1.5 has exceeded 1.6, making it spread rapidly in the United States and other countries (Vogel, 2023), it is encouraging that the pathogenicity of the virus is gradually decreasing. In particular, the current mainstream Omicron mutants account for more than 95% of patients with mild or even asymptomatic infections (Rajpal et al., 2022). For SARS-CoV-2 to survive in the long term, variants will continuously reduce their virulence as they search for new hosts. During the "self-evolution" process, although some "radicals" (sudden increases in virulence) are inevitable, the vast majority of viruses will gradually extend the host incubation period and weaken pathogenicity through mutations to better adapt to survival. From this perspective, SARS-CoV-2 is "intelligent."

To sum up, this article comprehensively reviews the genome characteristics of SARS-CoV-2, the pathogenesis of multiple membrane receptors including the classical route of ACE2-mediated viral infection, viral mutation, vaccine development, and the "new model" for COVID-19 epidemic. However, because the virus has the characteristics of mutation and immune escape, potential new developments in pathogenesis, membrane receptor types, and potential vaccines and treatment targets may not have been discovered in a timely manner. In addition, some traditional antiviral drugs, including azvudine, have been clinically proven to be effective in blocking the replication of SARS-CoV-2, which means that some drugs used for other diseases may also play an effective antiviral role in COVID-19 infection. These are the limitations of the content of this article. Therefore, we need to analyze and explore the mutation laws and immune escape mechanisms of SARS-CoV-2 from the perspective of viral mutation, which will lay an important genetic foundation for the research and development of specific antiviral drugs and vaccines. In addition, actively integrating traditional antiviral drug and accelerating clinical trials of drug safety will play an important role in quickly finding more mature COVID-19-specific drugs.

In 2023, the COVID-19 pandemic in most countries and regions in the world, including China, is showing a tendency to stabilize, which is the result of the joint efforts of medical staff and people worldwide. However, SARS-CoV-2 has not completely disappeared, so timely monitoring of mutant strains will become particularly important. Notably, even if you are infected with SARS-CoV-2, you do not have to be afraid if you respond rationally. The most important thing is that the public should refrain from discrimination against positively infected people, eliminate prejudice as much as possible, and not let positively infected people bear the consequences of "social death."

Author contributions

ZZ, XG, and XW were the major contributors to the writing and revision of the manuscript. YC, YXZ, ZD, and LH collected the related references and participated in discussions. TW, JY, and RZ made substantial contributions to the conception or design of the work. KZ, ZS, and YHZ approved the final version of the

manuscript. All authors contributed to the article and approved the submitted version.

Funding

The present study was financially supported by grants from the National Natural Science Foundation of China (nos: 81930091 and 21805197); the Post-graduate's Innovation Fund Project of Hebei Province (no: CXZZBS2022015); the Government-funded Clinical Medicine Outstanding Talent Training Project (no: 360017); the Medical Science Foundation of Hebei University (no: 2020A11); the Seed Foundation of Zhejiang Provincial People's Hospital (no: ZRY2022J003); and the China Postdoctoral Science Foundation (no: 2023M733164).

Acknowledgments

We would like to express our heartfelt gratitude to all the medical workers, the volunteers and the public for their efforts in fighting the COVID-19 pandemic. In addition, we special thank Dr. Shiting Qin (Shanghai Glossop Biotechnology Co., Ltd.) for figure formatting.

Conflict of interest

The authors declare that the research was conducted in the absence of any commercial or financial relationships that could be construed as a potential conflict of interest.

Publisher's note

All claims expressed in this article are solely those of the authors and do not necessarily represent those of their affiliated organizations, or those of the publisher, the editors and the reviewers. Any product that may be evaluated in this article, or claim that may be made by its manufacturer, is not guaranteed or endorsed by the publisher.

References

Ai, J., Wang, X., He, X., Zhao, X., Zhang, Y., Jiang, Y., et al. (2022). Antibody evasion of SARS-CoV-2 Omicron BA.1, BA.1.1, BA.2, and BA.3 sub-lineages. *Cell Host Microbe* 30, 1077–1083.e4. doi: 10.1016/j.chom.2022.05.001

Al Kaabi, N., Yang, Y., Zhang, J., Xu, K., Liang, Y., Kang, Y., et al. (2022). Immunogenicity and safety of NVSI-06-07 as a heterologous booster after priming with BBIBP-CorV: A phase 2 trial. *Signal Transduct. Target Ther.* 7:172. doi: 10.1038/s41392-022-00984-2

Arya, R., Kumari, S., Pandey, B., Mistry, H., Bihani, S., Das, A., et al. (2021). Structural insights into SARS-CoV-2 proteins. *J. Mol. Biol.* 433:166725. doi: 10.1016/j.jmb.2020.11.024

Bai, C., Zhong, Q., and Gao, G. (2022). Overview of Sars-CoV-2 genome-encoded proteins. *Sci. China Life Sci.* 65, 280–294. doi: 10.1007/s11427-021-1964-4

Bansal, K., and Kumar, S. (2022). Mutational cascade of SARS-CoV-2 leading to evolution and emergence of omicron variant. *Virus Res.* 315:198765. doi: 10.1016/j.virusres.2022.198765

Bazargan, M., Elahi, R., and Esmaeilzadeh, A. (2022). Omicron: Virology, immunopathogenesis, and laboratory diagnosis. *J. Gene Med.* 24:e3435. doi: 10.1002/jgm.3435

Bhattacharya, M., Chatterjee, S., Sharma, A., Lee, S., and Chakraborty, C. (2022). Delta variant (B.1.617.2) of SARS-CoV-2: Current understanding of infection, transmission, immune escape, and mutational landscape. *Folia Microbiol.* 68, 17–28. doi: 10.1007/s12223-022-01001-3

Bhattarai, N., Baral, P., Gerstman, B., and Chapagain, P. (2021). Structural and dynamical differences in the spike protein RBD in the SARS-CoV-2 variants B.1.1.7 and B.1.351. *J. Phys. Chem. B* 125, 7101–7107. doi: 10.1021/acs.jpcb.1c01626

Biskupek, I., Sieradzan, A., Czaplewski, C., Liwo, A., Lesner, A., and Giełdoń, A. (2022). Theoretical investigation of the coronavirus SARS-CoV-2 (COVID-19) infection mechanism and selectivity. *Molecules* 27:2080. doi: 10.3390/molecules27072080

Bohan, D., Van Ert, H., Ruggio, N., Rogers, K., Badreddine, M., Aguilar Briseño, J., et al. (2021). Phosphatidylserine receptors enhance SARS-CoV-2 infection. *PLoS Pathog.* 17:e1009743. doi: 10.1371/journal.ppat.1009743

Brinkkemper, M., Brouwer, P., Maisonnasse, P., Grobben, M., Caniels, T., Poniman, M., et al. (2021). A third SARS-CoV-2 spike vaccination improves neutralization of variants-of-concern. *NPJ Vaccines* 6:146. doi: 10.1038/s41541-021-00411-7

Cantuti-Castelvetri, L., Ojha, R., Pedro, L., Djannatian, M., Franz, J., Kuivanen, S., et al. (2020). Neuropilin-1 facilitates SARS-CoV-2 cell entry and infectivity. *Science* 370, 856–860. doi: 10.1126/science.abd2985

Center for Disease Control and Prevention [CDC] (2023). *Nowcast estimates in United States for 3/12/2023-3/18/2023*. Available online at: https://covid.cdc.gov/covid-data-tracker/#variant- proportions (accessed June 25, 2023).

Chalkias, S., Harper, C., Vrbicky, K., Walsh, S., Essink, B., Brosz, A., et al. (2022). A bivalent omicron-containing booster vaccine against Covid-19. *N. Engl. J. Med.* 387, 1279–1291. doi: 10.1056/NEJMoa2208343

Channabasappa, N., Niranjan, A., and Emran, T. B. (2023). SARS-CoV-2 variant omicron XBB.1.5:challenges and prospects-correspondence. *Int. J. Surg.* 109, 1054–1055. doi: 10.1097/JS9.0000000000000276

Chekol Abebe, E., Tiruneh, G., Behaile, T., Asmamaw Dejenie, T., Mengie Ayele, T., Tadele Admasu, F., et al. (2022). Mutational pattern, impacts and potential preventive strategies of omicron SARS-CoV-2 variant infection. *Infect. Drug Resist.* 15, 1871–1887. doi: 10.2147/idr.S360103

Chen, J. (2022). Should the world collaborate imminently to develop neglected live-attenuated vaccines for COVID-19? *J. Med. Virol.* 94, 82–87. doi: 10.1002/jmv.27335

Chen, J., Fan, J., Chen, Z., Zhang, M., Peng, H., Liu, J., et al. (2021). Nonmuscle myosin heavy chain IIA facilitates SARS-CoV-2 infection in human pulmonary cells. *Proc. Natl. Acad. Sci. U.S.A.* 118:e2111011118. doi: 10.1073/pnas.2111011118

Chen, K., Tsung-Ning Huang, D., and Huang, L. (2022). SARS-CoV-2 variants - evolution, spike protein, and vaccines. *Biomed. J.* 45, 573–579. doi: 10.1016/j.bj.2022.04.006

Chen, L., Cai, X., Zhao, T., Han, B., Xie, M., Cui, J., et al. (2022). Safety of global SARS-CoV-2 vaccines, a meta-analysis. *Vaccines* 10:596. doi: 10.3390/vaccines10040596

Chen, R., Gao, Y., Liu, H., Li, H., Chen, W., and Ma, J. (2022). Advances in research on 3C-like protease (3CLpro) inhibitors against SARS-CoV-2 since 2020. *RSC Med. Chem.* 14, 9–21. doi: 10.1039/d2md00344a

Chen, Y., Chen, L., Yin, S., Tao, Y., Zhu, L., Tong, X., et al. (2022). The third dose of coronvac vaccination induces broad and potent adaptive immune responses that recognize SARS-CoV-2 delta and omicron variants. *Emerg. Microbes Infect.* 11, 1524–1536. doi: 10.1080/22221751.2022.2081614

Chinese Center for Disease Control and Prevention (2022). *Prevention and control of COVID-19*. Available online at: https://www.chinacdc.cn/yw_9324/ (accessed June 20, 2022).

Clausen, T., Sandoval, D., Spliid, C., Pihl, J., Perrett, H., Painter, C., et al. (2020). SARS-CoV-2 infection depends on cellular heparan sulfate and ACE2. *Cell* 183, 1043–1057. doi: 10.1016/j.cell.2020.09.033

Cosar, B., Karagulleoglu, Z., Unal, S., Ince, A., Uncuoglu, D., Tuncer, G., et al. (2022). SARS-CoV-2 mutations and their viral variants. *Cytokine Growth Factor Rev.* 63, 10–22. doi: 10.1016/j.cytogfr.2021.06.001

Czarnecka, K., Czarnecka, P., Tronina, O., and Durlik, M. (2022). Molnupiravir outpatient treatment for adults with COVID-19 in a real-world setting-a single center experience. *J. Clin. Med.* 11:6464. doi: 10.3390/jcm11216464

Daly, J., Simonetti, B., Klein, K., Chen, K., Williamson, M., Antón-Plágaro, C., et al. (2020). Neuropilin-1 is a host factor for SARS-CoV-2 infection. *Science* 370, 861–865. doi: 10.1126/science.abd3072

de Mello Malta, F., Amgarten, D., Val, F., Cervato, M., de Azevedo, B., de Souza Basqueira, M., et al. (2021). Mass molecular testing for COVID19 using NGS-based technology and a highly scalable workflow. *Sci. Rep.* 11:7122. doi: 10.1038/s41598-021-86498-3

Deng, J., Ma, Y., Liu, Q., Du, M., Liu, M., and Liu, J. (2022). Comparison of the effectiveness and safety of heterologous booster doses with homologous booster doses for SARS-CoV-2 vaccines: A systematic review and meta-analysis. *Int. J. Environ. Res. Public Health* 19:10752. doi: 10.3390/ijerph191710752

Deng, S., Liang, H., Chen, P., Li, Y., Li, Z., Fan, S., et al. (2022). Viral vector vaccine development and application during the Covid-19 pandemic. *Microorganisms* 10:1450. doi: 10.3390/microorganisms10071450

Dhawan, M., Sharma, A., Priyanka, Thakur, N., Rajkhowa, T., and Choudhary, O. (2022). Delta Variant (B.1.617.2) of SARS-CoV-2: Mutations, impact, challenges and possible solutions. *Hum. Vaccin. Immunother.* 18:2068883. doi: 10.1080/21645515.2022.2068883

Díaz-Dinamarca, D., Salazar, M., Castillo, B., Manubens, A., Vasquez, A., Salazar, F., et al. (2022). Protein-based adjuvants for vaccines as immunomodulators of the innate and adaptive immune response: Current knowledge, challenges, and future opportunities. *Pharmaceutics* 14:1671. doi: 10.3390/pharmaceutics14081671

Domingo, P., and de Benito, N. (2021). Alpha variant SARS-CoV-2 infection: How it all starts. *EBioMedicine* 74:103703. doi: 10.1016/j.ebiom.2021.103703

Evans, J., and Liu, S. (2020). Multifaceted roles of TIM-family proteins in virus-host interactions. *Trends Microbiol.* 28, 224–235. doi: 10.1016/j.tim.2019.10.004

Faghihi, H. (2020). CD147 as an alternative binding site for the spike protein on the surface of SARS-CoV-2. *Eur. Rev. Med. Pharmacol. Sci.* 24, 11992–11994. doi: 10.26355/eurrev_202012_23985

Fang, E., Liu, X., Li, M., Zhang, Z., Song, L., Zhu, B., et al. (2022). Advances in COVID-19 mRNA vaccine development. *Signal Transduct. Target Ther.* 7:94. doi: 10.1038/s41392-022-00950-y

Fernandes, Q., Inchakalody, V., Merhi, M., Mestiri, S., Taib, N., Moustafa Abo El-Ella, D., et al. (2022). Emerging COVID-19 variants and their impact on SARS-CoV-2 diagnosis, therapeutics and vaccines. *Ann. Med.* 54, 524–540. doi: 10.1080/07853890.2022.2031274

Flisiak, R., Zarębska-Michaluk, D., Rogalska, M., Kryńska, J., Kowalska, J., Dutkiewicz, E., et al. (2022). Correction: Real-world experience with molnupiravir during the period of SARS-CoV-2 Omicron variant dominance. *Pharmacol. Rep.* 74:1328. doi: 10.1007/s43440-022-00419-3

Frolova, E., Palchevska, O., Lukash, T., Dominguez, F., Britt, W., and Frolov, I. (2022). Acquisition of furin cleavage site and further SARS-CoV-2 evolution change the mechanisms of viral entry, infection spread, and cell signaling. *J. Virol.* 96:e0075322. doi: 10.1128/jvi.00753-22

Gadanec, L., McSweeney, K., Qaradakhi, T., Ali, B., Zulli, A., and Apostolopoulos, V. (2021). Can SARS-CoV-2 virus use multiple receptors to enter host cells? *Int. J. Mol. Sci.* 22:992. doi: 10.3390/ijms22030992

Gao, J., Mei, H., Sun, J., Li, H., Huang, Y., Tang, Y., et al. (2022). Neuropilin-1-mediated SARS-CoV-2 infection in bone marrow-derived macrophages inhibits osteoclast differentiation. *Adv. Biol.* 6:2200007. doi: 10.1002/adbi.202200007

Gao, X., Zhu, K., Qin, B., Olieric, V., Wang, M., and Cui, S. (2021). Crystal structure of SARS-CoV-2 Orf9b in complex with human TOM70 suggests unusual virus-host interactions. *Nat. Commun.* 12:2843. doi: 10.1038/s41467-021-23118-8

Gao, Y., Ding, M., Dong, X., Zhang, J., Kursat Azkur, A., Azkur, D., et al. (2021). Risk factors for severe and critically ill COVID-19 patients: A review. *Allergy* 76, 428–455. doi: 10.1111/all.14657

Ge, J., Zhang, S., Zhang, L., and Wang, X. (2021). Structural basis of severe acute respiratory syndrome coronavirus 2 infection. *Curr. Opin. HIV AIDS* 16, 74–81. doi: 10.1097/coh.0000000000000658

Golob, J., Lugogo, N., Lauring, A., and Lok, A. (2021). SARS-CoV-2 vaccines: A triumph of science and collaboration. *JCI Insight* 6:e149187. doi: 10.1172/jci.insight.149187

Gray, G., Collie, S., Goga, A., Garrett, N., Champion, J., Seocharan, I., et al. (2022). Effectiveness of Ad26.Cov2.S and Bnt162b2 vaccines against omicron variant in South Africa. *N. Engl. J. Med.* 386, 2243–2245. doi: 10.1056/NEJMc2202061

Gu, Y., Cao, J., Zhang, X., Gao, H., Wang, Y., Wang, J., et al. (2022). Receptome profiling identifies Kremen1 and ASGR1 as alternative functional receptors of SARS-CoV-2. *Cell Res.* 32, 24–37. doi: 10.1038/s41422-021-00595-6

Guo, Y., Han, J., Zhang, Y., He, J., Yu, W., Zhang, X., et al. (2022). SARS-CoV-2 omicron variant: Epidemiological features, biological characteristics, and clinical significance. *Front. Immunol.* 13:877101. doi: 10.3389/fimmu.2022.877101

Ha, D., Huang, B., Wang, H., Rangel, D., Krieken, R., Liu, Z., et al. (2022). Targeting GRP78 suppresses oncogenic KRAS protein expression and reduces viability of cancer cells bearing various KRAS mutations. *Neoplasia* 33:100837. doi: 10.1016/j.neo.2022.100837

Hadj Hassine, I. (2022). COVID-19 vaccines and variants of concern: A review. *Rev. Med. Virol.* 32:e2313. doi: 10.1002/rmv.2313

Hao, W., Ma, B., Li, Z., Wang, X., Gao, X., Li, Y., et al. (2021). Binding of the SARS-CoV-2 spike protein to glycans. *Sci. Bull.* 66, 1205–1214. doi: 10.1016/j.scib.2021.01.010

Hastert, F., Hein, S., von Rhein, C., Benz, N., Husria, Y., Oberle, D., et al. (2022). The SARS-CoV-2 variant omicron is able to escape vaccine-induced humoral immune responses, but is counteracted by booster vaccination. *Vaccines* 10:794. doi: 10.3390/vaccines10050794

Heidary, M., Kaviar, V., Shirani, M., Ghanavati, R., Motahar, M., Sholeh, M., et al. (2022). A comprehensive review of the protein subunit vaccines against COVID-19. *Front. Microbiol.* 13:927306. doi: 10.3389/fmicb.2022.927306

Hemmati, F., Hemmati-Dinarvand, M., Karimzade, M., Rutkowska, D., Eskandari, M., Khanizadeh, S., et al. (2022). Plant-derived VLP: A worthy platform to produce vaccine against SARS-CoV-2. *Biotechnol. Lett.* 44, 45–57. doi: 10.1007/s10529-021-03211-0

Herald Sun (2023). *Victoria's COVID wave is slowing but mutant substrain FU.1 in China, India likely on the way*. Available online at: http://www.heraldsun.com.au/ (accessed June 28, 2023).

Huang, M., Pan, X., Wang, X., Ren, Q., Tong, B., Dong, X., et al. (2023). Lymphocyte integrins mediate entry and dysregulation of T cells by SARS-CoV-2. *Signal Transduct. Target Ther.* 8:84. doi: 10.1038/s41392-023-01348-0

Huang, Q., Han, X., and Yan, J. (2022). Structure-based neutralizing mechanisms for SARS- CoV-2 antibodies. *Emerg. Microbes Infect.* 11, 2412–2422. doi: 10.1080/22221751.2022.2125348

Jackson, C., Farzan, M., Chen, B., and Choe, H. (2022). Mechanisms of SARS-CoV-2 entry into cells. *Nat. Rev. Mol. Cell Biol.* 23, 3–20. doi: 10.1038/s41580-021-00418-x

Jacob-Dolan, C., and Barouch, D. (2022). COVID-19 vaccines: Adenoviral vectors. *Annu. Rev. Med.* 73, 41–54. doi: 10.1146/annurev-med-012621-102252

Jafari, A., Danesh Pouya, F., Niknam, Z., Abdollahpour-Alitappeh, M., Rezaei-Tavirani, M., and Rasmi, Y. (2022). Current advances and challenges in COVID-19 vaccine development: From conventional vaccines to next-generation vaccine platforms. *Mol. Biol. Rep.* 49, 4943–4957. doi: 10.1007/s11033-022-07132-7

Jin, Y., Hou, C., Li, Y., Zheng, K., and Wang, C. (2021). Mrna vaccine: How to meet the challenge of SARS-CoV-2. *Front. Immunol.* 12:821538. doi: 10.3389/fimmu.2021.821538

Jocher, G., Grass, V., Tschirner, S., Riepler, L., Breimann, S., Kaya, T., et al. (2022). ADAM10 and ADAM17 promote SARS-CoV-2 cell entry and spike protein-mediated lung cell fusion. *EMBO Rep.* 23:e54305. doi: 10.15252/embr.202154305

Johns Hopkins University (2022). *Coronavirus COVID-19 dashboard*. Available online at: https://coronavirus.jhu.edu/map.html (accessed September 15, 2022).

Kadam, S., Sukhramani, G., Bishnoi, P., Pable, A., and Barvkar, V. (2021). SARS-CoV-2, the pandemic coronavirus: Molecular and structural insights. *J. Basic Microbiol.* 61, 180–202. doi: 10.1002/jobm.202000537

Khandia, R., Singhal, S., Alqahtani, T., Kamal, M., El-Shall, N., Nainu, F., et al. (2022). Emergence of SARS-CoV-2 omicron (B.1.1.529) variant, salient features, high global health concerns and strategies to counter it amid ongoing COVID-19 pandemic. *Environ. Res.* 209:112816. doi: 10.1016/j.envres.2022.112816

Khobragade, A., Bhate, S., Ramaiah, V., Deshpande, S., Giri, K., Phophle, H., et al. (2022). Efficacy, safety, and immunogenicity of the DNA SARS-CoV-2 vaccine (Zycov-D): The interim efficacy results of a phase 3, randomised, double-blind, placebo-controlled study in India. *Lancet* 399, 1313–1321. doi: 10.1016/s0140-6736(22)00151-9

Khoshnood, S., Arshadi, M., Akrami, S., Koupaei, M., Ghahramanpour, H., Shariati, A., et al. (2022). An overview on inactivated and live-attenuated SARS-CoV-2 vaccines. *J. Clin. Lab. Anal.* 36:e24418. doi: 10.1002/jcla.24418

Kralj, S., Jukič, M., and Bren, U. (2021). Commercial SARS-CoV-2 targeted, protease inhibitor focused and protein-protein interaction inhibitor focused molecular libraries for virtual screening and drug design. *Int. J. Mol. Sci.* 23:393. doi: 10.3390/ijms23010393

Kraynyak, K., Blackwood, E., Agnes, J., Tebas, P., Giffear, M., Amante, D., et al. (2022). SARS-CoV-2 DNA vaccine INO-4800 induces durable immune responses capable of being boosted in a phase 1 open-label trial. *J. Infect Dis.* 225, 1923–1932. doi: 10.1093/infdis/jiac016

Kueh, B. (2022). Rehospitalization, emergency visits after paxlovid treatment are rare. *JAMA* 328:323. doi: 10.1001/jama.2022.11942

Kuhn, C., Basnet, N., Bodakuntla, S., Alvarez-Brecht, P., Nichols, S., Martinez-Sanchez, A., et al. (2023). Direct Cryo-ET observation of platelet deformation induced by SARS-CoV-2 spike protein. *Nat. Commun.* 14:620. doi: 10.1038/s41467-023-36279-5

Laza, R., Dragomir, C., Musta, V., Lazureanu, V., Nicolescu, N., Marinescu, A., et al. (2022). Analysis of deaths and favorable developments of patients with SARS-CoV-2 hospitalized in the largest hospital for infectious diseases and pneumo-phthisiology in the West of the Country. *Int. J. Gen. Med.* 15, 3417–3431. doi: 10.2147/ijgm.S359483

Li, G., Zhou, Z., Du, P., Zhan, M., Li, N., Xiong, X., et al. (2022). Heterologous mRNA vaccine booster increases neutralization of SARS-CoV-2 omicron BA.2 variant. *Signal Transduct. Target Ther.* 7:243. doi: 10.1038/s41392-022-01062-3

Li, M., Wang, H., Tian, L., Pang, Z., Yang, Q., Huang, T., et al. (2022). COVID-19 vaccine development: Milestones, lessons and prospects. *Signal Transduct. Target Ther.* 7:146. doi: 10.1038/s41392-022-00996-y

Li, Y., Zhang, Z., Yang, L., Lian, X., Xie, Y., Li, S., et al. (2020). The MERS-CoV receptor DPP4 as a candidate binding target of the SARS-CoV-2 spike. *iScience* 23:101160. doi: 10.1016/j.isci.2020.101160

Liang, H., Wu, Y., Yau, V., Yin, H., Lowe, S., Bentley, R., et al. (2022). SARS-CoV-2 variants, current vaccines and therapeutic implications for COVID-19. *Vaccines* 10:1538. doi: 10.3390/vaccines10091538

Liao, M., Liu, Y., Yuan, J., Wen, Y., Xu, G., Zhao, J., et al. (2020). Single-cell landscape of bronchoalveolar immune cells in patients with COVID-19. *Nat. Med.* 26, 842–844. doi: 10.1038/s41591-020-0901-9

Liu, X., Li, Y., Wang, Z., Cao, S., Huang, W., Yuan, L., et al. (2022). Safety and superior immunogenicity of heterologous boosting with an rbd-based SARS-CoV-2 mRNA vaccine in Chinese adults. *Cell Res.* 32, 777–780. doi: 10.1038/s41422-022-00681-3

Loconsole, D., Sallustio, A., Centrone, F., Casulli, D., Ferrara, M., Sanguedolce, A., et al. (2021). An autochthonous outbreak of the SARS-CoV-2 P.1 variant of concern in Southern Italy, April 2021. *Trop. Med. Infect. Dis.* 6:151. doi: 10.3390/tropicalmed6030151

Lu, Q., Liu, J., Zhao, S., Castro, M., Laurent-Rolle, M., and Dong, J. (2021). SARS-CoV-2 exacerbates proinflammatory responses in myeloid cells through C-type lectin receptors and tweety family member 2. *Immunity* 54, 1304–1319. doi: 10.1016/j.immuni.2021.05.006

Lv, J., Wu, H., Xu, J., and Liu, J. (2022). Immunogenicity and safety of heterologous versus homologous prime-boost schedules with an adenoviral vectored and mRNA COVID-19 vaccine: A systematic review. *Infect. Dis. Poverty* 11:53. doi: 10.1186/s40249-022-00977-x

MacKenzie, E., Hareza, D., Collison, M., Czapar, A., Kraft, A., Waxse, B., et al. (2022). Clinical characteristics of hospitalized patients with false-negative severe acute respiratory coronavirus virus 2 (SARS-CoV-2) test results. *Infect. Control Hosp. Epidemiol.* 43, 467–473. doi: 10.1017/ice.2021.146

Marzolini, C., Kuritzkes, D., Marra, F., Boyle, A., Gibbons, S., Flexner, C., et al. (2022). Recommendations for the management of drug-drug interactions between the COVID-19 antiviral nirmatrelvir/ritonavir (paxlovid) and comedications. *Clin. Pharmacol. Ther.* 112, 1191–1200. doi: 10.1002/cpt.2646

McCann, N., O'Connor, D., Lambe, T., and Pollard, A. (2022). Viral vector vaccines. *Curr. Opin. Immunol.* 77:102210. doi: 10.1016/j.coi.2022.102210

Mekonnen, D., Mengist, H., and Jin, T. (2022). SARS-CoV-2 subunit vaccine adjuvants and their signaling pathways. *Expert Rev. Vaccines* 21, 69–81. doi: 10.1080/14760584.2021.1991794

Meng, H., Mao, J., and Ye, Q. (2022). Strategies and safety considerations of booster vaccination in COVID-19. *Bosn J. Basic Med. Sci.* 22, 366–373. doi: 10.17305/bjbms.2021.7082

Mercer, J., Lee, J., Saphire, E., and Freeman, S. (2020). SnapShot: Enveloped virus entry. *Cell* 182, 786–786. doi: 10.1016/j.cell.2020.06.033

Mistry, P., Barmania, F., Mellet, J., Peta, K., Strydom, A., Viljoen, I., et al. (2021). SARS-CoV-2 variants, vaccines, and host immunity. *Front. Immunol.* 12:809244. doi: 10.3389/fimmu.2021.809244

Mohammad, A., Abubaker, J., and Al-Mulla, F. (2021). Structural modelling of SARS-CoV-2 alpha variant (B.1.1.7) suggests enhanced furin binding and infectivity. *Virus Res.* 303:198522. doi: 10.1016/j.virusres.2021.198522

Muecksch, F., Wang, Z., Cho, A., Gaebler, C., Ben Tanfous, T., DaSilva, J., et al. (2022). Increased memory B cell potency and breadth after a SARS-CoV-2 mRNA boost. *Nature* 607, 128–134. doi: 10.1038/s41586-022-04778-y

Naseri, K., Aliashrafzadeh, H., Otadi, M., Ebrahimzadeh, F., Badfar, H., and Alipourfard, I. (2022). Human responses in public health emergencies for infectious disease control: An overview of controlled topologies for biomedical applications. *Contrast Media Mol. Imaging* 2022:6324462. doi: 10.1155/2022/6324462

Nassar, A., Ibrahim, I., Amin, F., Magdy, M., Elgharib, A., Azzam, E., et al. (2021). A review of human coronaviruses' receptors: The host-cell targets for the crown bearing viruses. *Molecules* 26:6455. doi: 10.3390/molecules26216455

Nguyen, T., Quach, T., Tran, T., Phuoc, H., Nguyen, H., Vo, T., et al. (2022). Reactogenicity and immunogenicity of heterologous prime-boost immunization with COVID-19 vaccine. *Biomed. Pharmacother.* 147:112650. doi: 10.1016/j.biopha.2022.112650

Noori, M., Nejadghaderi, S., Arshi, S., Carson-Chahhoud, K., Ansarin, K., Kolahi, A., et al. (2022). Potency of BNT162B2 and mRNA-1273 vaccine-induced neutralizing antibodies against severe acute respiratory syndrome-CoV-2 variants of concern: A systematic review of *in Vitro* studies. *Rev. Med. Virol.* 32:e2277. doi: 10.1002/rmv.2277

Okamura, S., and Ebina, H. (2021). Could live attenuated vaccines better control COVID-19? *Vaccine* 39, 5719–5726. doi: 10.1016/j.vaccine.2021.08.018

Ou, T., Mou, H., Zhang, L., Ojha, A., Choe, H., and Farzan, M. (2021). Hydroxychloroquine-mediated inhibition of SARS-CoV-2 entry is attenuated by TMPRSS2. *PLoS Pathog.* 17:e1009212. doi: 10.1371/journal.ppat.1009212

Pandey, M., Ozberk, V., Eskandari, S., Shalash, A., Joyce, M., Saffran, H., et al. (2021). Antibodies to neutralising epitopes synergistically block the interaction of the receptor-binding domain of SARS-CoV-2 to ACE 2. *Clin. Transl. Immunol.* 10:e1260. doi: 10.1002/cti2.1260

Pellegrino, R., Chiappini, E., Licari, A., Galli, L., and Marseglia, G. (2022). Prevalence and clinical presentation of long COVID in children: A systematic review. *Eur. J. Pediatr.* 181, 3995–4009. doi: 10.1007/s00431-022-04600-x

Peters, M., Bastidas, O., Kokron, D., and Henze, C. (2021). Transformations, lineage comparisons, and analysis of down-to-up protomer states of variants of the SARS-CoV-2 prefusion spike protein, including the UK variant B.1.1.7. *Microbiol. Spectr.* 9:e0003021. doi: 10.1128/Spectrum.00030-21

Powers, H., and Sahoo, D. (2022). SR-B1's next top model: Structural perspectives on the functions of the HDL receptor. *Curr. Atheroscler. Rep.* 24, 277–288. doi: 10.1007/s11883-022-01001-1

Qi, F., Qian, S., Zhang, S., and Zhang, Z. (2020). Single cell RNA sequencing of 13 human tissues identify cell types and receptors of human coronaviruses. *Biochem. Biophys. Res. Commun.* 526, 135–140. doi: 10.1016/j.bbrc.2020.03.044

Qu, L., Yi, Z., Shen, Y., Lin, L., Chen, F., Xu, Y., et al. (2022). Circular RNA vaccines against SARS-CoV-2 and emerging variants. *Cell* 185, 1728–1744.e16. doi: 10.1016/j.cell.2022.03.044

Quer, J., Colomer-Castell, S., Campos, C., Andrés, C., Piñana, M., Cortese, M., et al. (2022). Next-generation sequencing for confronting virus pandemics. *Viruses* 14:600. doi: 10.3390/v14030600

Rahnavard, A., Dawson, T., Clement, R., Stearrett, N., Pérez-Losada, M., and Crandall, K. (2021). Epidemiological associations with genomic variation in SARS-CoV-2. *Sci. Rep.* 11:23023. doi: 10.1038/s41598-021-02548-w

Rai, P., Kumar, B., Deekshit, V., Karunasagar, I., and Karunasagar, I. (2021). Detection technologies and recent developments in the diagnosis of COVID-19 infection. *Appl. Microbiol. Biotechnol.* 105, 441–455. doi: 10.1007/s00253-020-11061-5

Rajah, M., Bernier, A., Buchrieser, J., and Schwartz, O. (2022). The mechanism and consequences of SARS-CoV-2 spike-mediated fusion and syncytia formation. *J. Mol. Biol.* 434:167280. doi: 10.1016/j.jmb.2021.167280

Rajpal, V., Sharma, S., Kumar, A., Chand, S., Joshi, L., Chandra, A., et al. (2022). "Is Omicron mild"? Testing this narrative with the mutational landscape of its three lineages and response to existing vaccines and therapeutic antibodies. *J. Med. Virol.* 94, 3521–3539. doi: 10.1002/jmv.27749

Rakhmat, I., Kusmala, Y., Handayani, D., Juliastuti, H., Nawangsih, E., Wibowo, A., et al. (2021). Dipeptidyl peptidase-4 (DPP-4) inhibitor and mortality in coronavirus disease 2019 (COVID-19)-A systematic review, meta-analysis, and meta-regression. *Diabetes Metab. Syndr.* 15, 777–782. doi: 10.1016/j.dsx.2021.03.027

Raman, R., Patel, K., and Ranjan, K. (2021). COVID-19: Unmasking emerging SARS-CoV-2 variants, vaccines and therapeutic strategies. *Biomolecules* 11:993. doi: 10.3390/biom11070993

Rana, R., Kant, R., Huirem, R., Bohra, D., and Ganguly, N. (2022). Omicron variant: Current insights and future directions. *Microbiol. Res.* 265:127204. doi: 10.1016/j.micres.2022.127204

Salehi-Vaziri, M., Fazlalipour, M., Seyed Khorrami, S., Azadmanesh, K., Pouriayevali, M., Jalali, T., et al. (2022). The ins and outs of SARS-CoV-2 variants of concern (VOCs). *Arch. Virol.* 167, 327–344. doi: 10.1007/s00705-022-05365-2

Sapkota, B., Saud, B., Shrestha, R., Al-Fahad, D., Sah, R., Shrestha, S., et al. (2022). Heterologous prime-boost strategies for COVID-19 vaccines. *J. Travel Med.* 29:taab191. doi: 10.1093/jtm/taab191

Sargsyan, K., Mazmanian, K., and Lim, C. (2023). A strategy for evaluating potential antiviral resistance to small molecule drugs and application to SARS-CoV-2. *Sci. Rep.* 13:502. doi: 10.1038/s41598-023-27649-6

Schuit, M., Biryukov, J., Beck, K., Yolitz, J., Bohannon, J., Weaver, W., et al. (2021). The stability of an isolate of the SARS-CoV-2 B.1.1.7 lineage in aerosols is similar to 3 earlier isolates. *J. Infect. Dis.* 224, 1641–1648. doi: 10.1093/infdis/jiab171

Scialo, F., Daniele, A., Amato, F., Pastore, L., Matera, M., Cazzola, M., et al. (2020). ACE2: The major cell entry receptor for SARS-CoV-2. *Lung* 198, 867–877. doi: 10.1007/s00408-020-00408-4

Seyran, M., Takayama, K., Uversky, V., Lundstrom, K., Palù, G., Sherchan, S., et al. (2021). The structural basis of accelerated host cell entry by SARS-CoV-2†. *FEBS J.* 288, 5010–5020. doi: 10.1111/febs.15651

Shin, J., Toyoda, S., Fukuhara, A., and Shimomura, I. (2022). GRP78, a novel host factor for SARS-CoV-2: The emerging roles in COVID-19 related to metabolic risk factors. *Biomedicines* 10:1995. doi: 10.3390/biomedicines10081995

Singhal, T. (2022). The emergence of omicron: Challenging times are here again! *Indian J. Pediatr.* 89, 490–496. doi: 10.1007/s12098-022-04077-4

Sutton, M., Radniecki, T., Kaya, D., Alegre, D., Geniza, M., Girard, A., et al. (2022). Detection of SARS-CoV-2 B.1.351 (Beta) variant through wastewater surveillance

before case detection in a community, Oregon, USA. *Emerg. Infect. Dis.* 28, 1101–1109. doi: 10.3201/eid2806.211821

Szabó, G., Mahiny, A., and Vlatkovic, I. (2022). COVID-19 mRNA vaccines: Platforms and current developments. *Mol. Ther.* 30, 1850–1868. doi: 10.1016/j.ymthe.2022.02.016

Tallei, T., Alhumaid, S., AlMusa, Z., Fatimawali, Kusumawaty, D., Alynbiawi, A., et al. (2022). Update on the omicron sub-variants BA.4 and BA.5. *Rev. Med. Virol.* doi: 10.1002/rmv.2391 [Epub ahead of print].

Tang, X., Yang, M., Duan, Z., Liao, Z., Liu, L., Cheng, R., et al. (2020). Transferrin receptor is another receptor for SARS-CoV-2 entry. *bioRxiv* [Preprint]. doi: 10.1101/2020.10.23.350348

Tariq, H., Batool, S., Asif, S., Ali, M., and Abbasi, B. (2021). Virus-like particles: Revolutionary platforms for developing vaccines against emerging infectious diseases. *Front. Microbiol.* 12:790121. doi: 10.3389/fmicb.2021.790121

Tarke, A., Coelho, C., Zhang, Z., Dan, J., Yu, E., Methot, N., et al. (2022). SARS-CoV-2 vaccination induces immunological T cell memory able to cross-recognize variants from alpha to omicron. *Cell* 185, 847–859.e11. doi: 10.1016/j.cell.2022.01.015

Thakur, V., and Ratho, R. (2022). Omicron (B.1.1.529): A new SARS-CoV-2 variant of concern mounting worldwide fear. *J. Med. Virol.* 94, 1821–1824. doi: 10.1002/jmv.27541

Thiagarajan, K. (2022). Covid-19: WHO suspends supplies of India's covaxin through UN agencies. *BMJ* 377:o902. doi: 10.1136/bmj.o902

Tian, D., Sun, Y., Xu, H., and Ye, Q. (2022). The emergence and epidemic characteristics of the highly mutated SARS-CoV-2 omicron variant. *J. Med. Virol.* 94, 2376–2383. doi: 10.1002/jmv.27643

Tiecco, G., Storti, S., Arsuffi, S., Degli Antoni, M., Focà, E., Castelli, F., et al. (2022). Omicron Ba.2 lineage, the "stealth" variant: Is it truly a silent epidemic? A literature review. *Int. J. Mol. Sci.* 23:7315. doi: 10.3390/ijms23137315

Tioni, M., Jordan, R., Pena, A., Garg, A., Wu, D., Phan, S., et al. (2022). Mucosal administration of a live attenuated recombinant COVID-19 vaccine protects nonhuman primates from SARS-CoV-2. *NPJ Vaccines* 7:85. doi: 10.1038/s41541-022-00509-6

Trunfio, M., Portesani, F., Vicinanza, S., Nespoli, P., Traverso, F., Cortese, G., et al. (2022). Real-Life evidence of lower lung virulence in COVID-19 inpatients infected with SARS-CoV-2 omicron variant compared to wild-type and delta SARS-CoV-2 pneumonia. *Lung* 200, 573–577. doi: 10.1007/s00408-022-00566-7

Velavan, T., Ntoumi, F., Kremsner, P., Lee, S., and Meyer, C. (2023). Emergence and geographic dominance of omicron subvariants XBB/XBB.1.5 and BF.7-the public health challenges. *Int. J. Infect. Dis.* 128, 307–309. doi: 10.1016/j.ijid.2023.01.024

Vogel, L. (2023). What to know about omicron XBB.1.5. *CMAJ* 195, E127–E128. doi: 10.1503/cmaj.1096034

Walls, A., Park, Y., AleTortorici, M., Wall, A., McGuire, A., and Veesler, D. (2020). Structure, function, and antigenicity of the SARS-CoV-2 spike glycoprotein. *Cell* 181, 281–292. doi: 10.1016/j.cell.2020.02.058

Wang, H., Xiang, Y., Hu, R., Ji, R., and Wang, Y. (2022). Research progress in laboratory detection of SARS-CoV-2. *Ir. J. Med. Sci.* 191, 509–517. doi: 10.1007/s11845-021-02604-4

Wang, J., Yang, G., Wang, X., Wen, Z., Shuai, L., Luo, J., et al. (2021). SARS-CoV-2 uses metabotropic glutamate receptor subtype 2 as an internalization factor to infect cells. *Cell Discov.* 7:119. doi: 10.1038/s41421-021-00357-z

Wang, K., Chen, W., Zhou, Y., Lian, J., Zhang, Z., Du, P., et al. (2020). SARS-CoV-2 invades host cells via a novel route: CD147-spike protein. *bioRxiv* [Preprint]. doi: 10.1101/2020.03.14.988345

Wang, S., Qiu, Z., Hou, Y., Deng, X., Xu, W., Zheng, T., et al. (2021). AXL is a candidate receptor for SARS-CoV-2 that promotes infection of pulmonary and bronchial epithelial cells. *Cell Res.* 31, 126–140. doi: 10.1038/s41422-020-00460-y

Wang, X., Rcheulishvili, N., Cai, J., Liu, C., Xie, F., Hu, X., et al. (2022). Development of DNA vaccine candidate against SARS-CoV-2. *Viruses* 14:1049. doi: 10.3390/v14051049

Wang, Y., Yang, C., Song, Y., Coleman, J., Stawowczyk, M., Tafrova, J., et al. (2021). Scalable live-attenuated SARS-CoV-2 vaccine candidate demonstrates preclinical safety and efficacy. *Proc. Natl. Acad. Sci. U.S.A.* 118:e2102775118. doi: 10.1073/pnas.2102775118

Wang, Z., Zhang, H., Lu, J., Xu, K., Peng, C., Guo, J., et al. (2020). Low toxicity and high immunogenicity of an inactivated vaccine candidate against COVID-19 in different animal models. *Emerg. Microbes Infect.* 9, 2606–2618. doi: 10.1080/22221751.2020.1852059

Wei, C., Wan, L., Yan, Q., Wang, X., Zhang, J., Yang, X., et al. (2020). HDL-scavenger receptor B type 1 facilitates SARS-CoV-2 entry. *Nat. Metab.* 2, 1391–1400. doi: 10.1038/s42255-020-00324-0

Wilhelm, A., Toptan, T., Pallas, C., Wolf, T., Goetsch, U., Gottschalk, R., et al. (2021). Antibody-mediated neutralization of authentic SARS-CoV-2 B.1.617 variants harboring L452r and T478k/E484q. *Viruses* 13:1693. doi: 10.3390/v13091693

World Health Organization [WHO] (2022b). *Tracking SARS-CoV-2 variants*. Available online at: https://www.who.int/activities/tracking-SARS-CoV-2-variants (accessed June 25, 2023).

World Health Organization [WHO] (2022a). *COVID-19 vaccines with WHO emergency use listing*. Available online at: https://extranet.who.int/pqweb/vaccines/vaccinescovid-19-vaccine-eul-issued (accessed May 19, 2022).

World Health Organization [WHO] (2023). *The COVID-19 vaccine tracker and landscape compiles detailed information of each COVID-19 vaccine candidate in development by closely monitoring their progress through the pipeline*. Available online at: https://www.who.int/publications/m/item/draft-landscape-of-covid-19-candidate-vaccines (accessed June 28, 2023).

Wrapp, D., Wang, N., Corbett, K., Goldsmith, J., Hsieh, C., Abiona, O., et al. (2020). Cryo-EM structure of the 2019-nCoV spike in the prefusion conformation. *Science* 367, 1260–1263. doi: 10.1126/science.abb2507

Wu, J., Chen, L., Qin, C., Huo, F., Liang, X., Yang, X., et al. (2022). CD147 contributes to SARS-CoV-2-induced pulmonary fibrosis. *Nature* 7:382. doi: 10.1038/s41392-022-01230-5

Wysocki, J., Lores, E., Ye, M., Soler, M., and Batlle, D. (2020). Kidney and lung ACE2 expression after an ACE inhibitor or an Ang II receptor blocker: Implications for COVID-19. *J. Am. Soc. Nephrol.* 31, 1941–1943. doi: 10.1681/ASN.2020050667

Xia, S., Lan, Q., Su, S., Wang, X., Xu, W., Liu, Z., et al. (2020). The role of furin cleavage site in SARS-CoV-2 spike protein-mediated membrane fusion in the presence or absence of trypsin. *Signal Transduct. Target Ther.* 5:92. doi: 10.1038/s41392-020-0184-0

Xu, F., Wang, G., Zhao, F., Huang, Y., Fan, Z., Mei, S., et al. (2022). IFITM3 inhibits SARS-CoV-2 infection and is associated with COVID-19 susceptibility. *Viruses* 14:2553. doi: 10.3390/v14112553

Yadav, P., Sarkale, P., Razdan, A., Gupta, N., Nyayanit, D., Sahay, R., et al. (2022). Isolation and characterization of SARS-CoV-2 beta variant from UAE travelers. *J. Infect. Public Health* 15, 182–186. doi: 10.1016/j.jiph.2021.12.011

Yadav, R., Chaudhary, J., Jain, N., Chaudhary, P., Khanra, S., Dhamija, P., et al. (2021). Role of structural and non-structural proteins and therapeutic targets of SARS-CoV-2 for COVID-19. *Cells* 10:821. doi: 10.3390/cells10040821

Yan, R., Zhang, Y., Li, Y., Xia, L., Guo, Y., and Zhou, Q. (2020). Structural basis for the recognition of SARS-CoV-2 by full-length human ACE2. *Science* 367, 1444–1448. doi: 10.1126/science.abb2762

Yang, C., Zhang, Y., Zeng, X., Chen, H., Chen, Y., Yang, D., et al. (2021). Kidney injury molecule-1 is a potential receptor for SARS-CoV-2. *J. Mol. Cell. Biol.* 13, 185–196. doi: 10.1093/jmcb/mjab003

Yang, H., and Rao, Z. (2021). Structural biology of SARS-CoV-2 and implications for therapeutic development. *Nat. Rev. Microbiol.* 19, 685–700. doi: 10.1038/s41579-021-00630-8

Yépez, Y., Marcano-Ruiz, M., Bezerra, R., Fam, B., Ximenez, J., Silva, W. Jr., et al. (2022). Evolutionary history of the SARS-CoV-2 gamma variant of concern (P.1): A perfect storm. *Genet. Mol. Biol.* 45:e20210309. doi: 10.1590/1678-4685-gmb-2021-0309

Yi, S., Kim, J., Choe, Y., Hong, S., Choi, S., Ahn, S., et al. (2022). SARS-CoV-2 delta variant breakthrough infection and onward secondary transmission in household. *J. Korean Med. Sci.* 37:e12. doi: 10.3346/jkms.2022.37.e12

Yoshimoto, F. (2021). A biochemical perspective of the nonstructural proteins (NSPs) and the spike protein of SARS CoV-2. *Protein J.* 40, 260–295. doi: 10.1007/s10930-021-09967-8

Zeng, B., Gao, L., Zhou, Q., Yu, K., and Sun, F. (2022). Effectiveness of COVID-19 vaccines against SARS-CoV-2 variants of concern: A systematic review and meta-analysis. *BMC Med.* 20:200. doi: 10.1186/s12916-022-02397-y

Zhan, Y., Yin, H., and Yin, J. Y. (2022). B.1.617.2 (Delta) variant of SARS-CoV-2: Features, transmission and potential strategies. *Int. J. Biol. Sci.* 18, 1844–1851. doi: 10.7150/ijbs.66881

Zhao, Y., Kuang, M., Li, J., Zhu, L., Jia, Z., Guo, X., et al. (2021). SARS-CoV-2 spike protein interacts with and activates TLR4. *Cell Res.* 31:825. doi: 10.1038/s41422-021-00501-0

Zhou, H., Møhlenberg, M., Thakor, J., Tuli, H., Wang, P., Assaraf, Y., et al. (2022). Sensitivity to vaccines, therapeutic antibodies, and viral entry inhibitors and advances to counter the SARS-CoV-2 omicron variant. *Clin. Microbiol. Rev.* 35:e0001422. doi: 10.1128/cmr.00014-22

frontiers | Frontiers in Microbiology

TYPE Mini Review
PUBLISHED 21 August 2023
DOI 10.3389/fmicb.2023.1251705

OPEN ACCESS

EDITED BY
Qiang Ding,
Tsinghua University, China

REVIEWED BY
Sourish Ghosh,
Indian Institute of Chemical Biology (CSIR), India

*CORRESPONDENCE
Wen-Chi Su
✉ t23514@mail.cmuh.org.tw

RECEIVED 11 July 2023
ACCEPTED 31 July 2023
PUBLISHED 21 August 2023

CITATION
Melano I, Lo Y-C and Su W-C (2023) Characterization of host substrates of SARS-CoV-2 main protease.
Front. Microbiol. 14:1251705.
doi: 10.3389/fmicb.2023.1251705

Characterization of host substrates of SARS-CoV-2 main protease

Ivonne Melano[1], Yan-Chung Lo[2] and Wen-Chi Su[1,3,4]*

[1]Graduate Institute of Biomedical Sciences, China Medical University, Taichung, Taiwan, [2]Sinphar Pharmaceutical Co., Ltd., Sinphar Group, Yilan, Taiwan, [3]International Master's Program of Biomedical Sciences, China Medical University, Taichung, Taiwan, [4]Department of Medical Research, China Medical University Hospital, Taichung, Taiwan

The main protease (M^{pro}) plays a crucial role in coronavirus, as it cleaves viral polyproteins and host cellular proteins to ensure successful replication. In this review, we discuss the preference in the recognition sequence of M^{pro} based on sequence-based studies and structural information and highlight the recent advances in computational and experimental approaches that have aided in discovering novel M^{pro} substrates. In addition, we provide an overview of the current understanding of M^{pro} host substrates and their implications for viral replication and pathogenesis. As M^{pro} has emerged as a promising target for the development of antiviral drugs, further insight into its substrate specificity may contribute to the design of specific inhibitors.

KEYWORDS

SARS-CoV-2, main protease, substrate, virus-host interaction, virus pathogenesis, viral replication

1. Introduction

Severe acute respiratory syndrome coronavirus 2 (SARS-CoV-2), the causative agent of the coronavirus disease 2019 (COVID-19) pandemic, is a positive-sense single-stranded RNA virus that utilizes its two cysteine proteases, nsp3/papain-like protease (PL^{pro}), and nsp5/3-chymotrypsin-like protease ($3CL^{pro}$), to cleave its polyproteins into functional viral proteins required for virus replication (Koudelka et al., 2021; Sabbah et al., 2021). Nsp3 cleaves three distinct sites of nsp1–nsp4, while nsp5 cleaves 11 distinct sites of nsp5–nsp16; thereby nsp5 is also referred to as the main protease (M^{pro}). M^{pro} is a conserved protease in the family Coronaviridae (Ullrich and Nitsche, 2020; Xiong et al., 2021). The mature M^{pro} is a dimeric cysteine protease and its catalytic dyad is formed by His41 and Cys145 (Ullrich and Nitsche, 2020; Hu et al., 2022). Besides viral polyproteins, viral proteases likewise cleave host proteins to hinder host immune responses and promote viral replication (Pablos et al., 2021). In this review, we first address the substrate specificity and further analyze the implication of M^{pro} cleavage on host substrates in various biological processes.

2. Substrate specificity of SARS-CoV-2 M^{pro}

The substrate specificity of SARS-CoV M^{pro} has been previously investigated. The recombinant protein substrates with saturation mutagenesis at each of the P5 to P3' positions were used to profile the sequence preference of M^{pro} substrates (Chuck et al., 2010). In addition, the 11 autoproteolytic cleavage site sequences in SARS-CoV-2 pp1ab and host substrates were applied

to analyze the sequence logo of the cleavage site. Thus far, the consensus sequence motif of M^{pro} substrates is recognized as (L/F/M)-Q↓(S/A/G/N), where ↓ is the cleavage site. In brief, this motif is composed of a conserved P1 residue Gln flanked by a hydrophobic (Leu, Phe, or Val) at P2 and a small aliphatic amino acid (Ser, Asn, Gly, or Ala) at P1' positions (Miczi et al., 2020; Koudelka et al., 2021; Moustaqil et al., 2021; Pablos et al., 2021; Zhang et al., 2021). The P1, P2, and P1' residues are important to determine substrate specificity, whereas the less conserved P3, P4, and P3' residues increase the recognition and binding stability of the substrates (Hu et al., 2022). P3 and P3' positions prefer positively charged residues to negatively charged ones (Chuck et al., 2010). Although M^{pro} primarily prefers Gln, it has also been found to recognize non-canonical Met or His at the P1 residue (Koudelka et al., 2021; Pablos et al., 2021). The identification of new substrate sequences can aid in the design of specific inhibitors that can target M^{pro} activity with higher affinity and selectivity.

3. Identification of host substrates

Computational and experimental methods are widely used for substrate identification. For computational methods, NetCorona 1.0, a publicly available web server originally designed to predict putative SARS-CoV M^{pro} cleavage sites, has been commonly used for identifying SARS-CoV-2 M^{pro} substrates (with a suggested threshold of 0.5), since the sequence of SARS-CoV-2 M^{pro} shares 96% identity with that of SARS-CoV M^{pro} (Miczi et al., 2020; Zhang et al., 2021; Scott et al., 2022). Another approach is to search for short stretches of homologous human-pathogen protein sequences (SSHHPS) using BLAST analysis, which is based on the principle that the cleavage site sequences found in the viral genome are identical to the cleavage sites on host cell substrates (Miczi et al., 2020). As to experimental methods, a commonly used screening procedure is the liquid chromatography–mass spectrometry (LC–MS)-based terminal amine isotopic labeling of substrates (TAILS) that not only identifies substrates but also their corresponding cleavage sites (Koudelka et al., 2021; Meyer et al., 2021; Pablos et al., 2021). Besides, Moustaqil et al. (2021) screened 71 human innate immune pathway proteins (HIIPs) using the cell-free *Leishmania tarentolae* protein expression system, which allows the direct visualization in SDS-PAGE of the target protein fused to GFP.

Table 1 lists the host proteins that have been identified as potential substrates for SARS-CoV-2 M^{pro} through computational or experimental methods, and further supported by the detection of cleaved products. Among the identified substrates, five proteins have available structure data in Protein Data Bank (PDB), while the rest were predicted by AlphaFold (Table 1). Through analysis of the structure information, we observed that the cleavage sites are commonly located in loops or loops connected to α-helixes or β-sheets (Figure 1), suggesting that most of the target sequences are accessible to M^{pro}. This implies that in addition to the prediction of cleavage sequences, structural analysis is also important for evaluation of the accessibility of putative cleavage sites (Miczi et al., 2020; Moustaqil et al., 2021).

4. Biological functions of substrates

Research on exploring the functional consequences of M^{pro} cleavage on host proteins is still ongoing. It is important to note that host proteins serve multiple functions, and their dysfunction may have implications for more than one biological process. The implications of M^{pro} cleavage, according to published information or the known biological function of the substrates, are discussed below.

4.1. Innate immune response

The innate immune system releases inflammatory cytokines and chemokines as an immediate defense against invading pathogens. However, viruses can manipulate the innate immune response to evade the host's antiviral defenses (Diamond and Kanneganti, 2022). M^{pro} was discovered to cleave interleukin-1 receptor-associated kinase 1 (IRAK1), a kinase involved in the regulation of the innate immune response (Miczi et al., 2020). Several viruses such as porcine epidemic diarrhea virus and borna disease virus 1 target IRAK1 to block IRAK1/TRAF6/NF-κB signaling pathway activation, consequently reducing the expression of the IFN-III subtypes, IFN-λ1, and -λ3 (Zhang et al., 2019; Zheng et al., 2022). Notably, inhibition of IRAK1 using pacritinib had effectively attenuated the pro-inflammatory cytokine release triggered by the GU-rich ssRNA sequence derived from the SARS-CoV-2 spike protein (Campbell et al., 2023). Similarly, the SARS-CoV-2 M^{pro} cleavage of the TAK1 binding protein (TAB1) results in decreased TAB1 protein levels in virus-infected cells and is proposed to inhibit cytokine production by disrupting the interaction between TAB1 and the transforming growth factor-β-activated kinase 1 (TAK1), which is necessary for constitutive activation of NF-κB (Jackson-Bernitsas et al., 2007; Moustaqil et al., 2021; Pablos et al., 2021). mRNA-decapping enzyme 1A (DCP1A), one of the interferon-stimulated genes (ISGs), was recently identified as an M^{pro} substrate (Song et al., 2023). Cleavage of DCP1A by porcine deltacoronavirus M^{pro} has been demonstrated to decrease antiviral activity (Zhu et al., 2020). It is conceivable that SARS-CoV-2 M^{pro} cleaves IRAK1, TAB1, and DCP1A to disturb the production of pro-inflammatory cytokines and attenuate the immune defense (Miczi et al., 2020).

On the other hand, hyperinflammation, characterized by cytokine storm, is a significant contributor to severe cases of COVID-19 (Diamond and Kanneganti, 2022). SARS-CoV-2 M^{pro} specifically cleaved Nod-like receptor protein 12 (NLRP12), as evidenced by significant reductions of NLRP12 protein levels in SARS-CoV-2 infected cells (Moustaqil et al., 2021). Its cleavage is proposed to enhance pro-inflammatory cytokine and chemokine production via NF-κB signaling, and perturb the NLRP3 inflammasome assembly to trigger the cleavage of pro-caspase-1, thereby enhancing the release of IL-1β, all associated with the hyperinflammation observed in severe COVID-19. Another ISG cleaved by M^{pro} is the solute carrier family 25 member 22 (SLC25A22; Zhang et al., 2021). Knockout of SLC25A22, a mitochondrial glutamate carrier, has been associated with decreased immunosuppressive function in colorectal cancer (Yoo et al., 2020; Zhou et al., 2021), implying its involvement in immune response activation.

Fas-associated factor 1 (FAF1) is a positive regulator of type I interferon (IFN) signaling and is involved in the activation of the Fas-mediated pathway of apoptosis. However, there are contrasting results on the role of FAF1 in regulating the antiviral immune response. FAF1 is suggested to reduce virus-induced type I IFN activation by inhibiting nuclear translocation of the transcription factor IRF3 (Song et al., 2016). In contrast, FAF1 is hypothesized to

TABLE 1 List of SARS-CoV-2 host substrates.

Gene symbol	Cleavage sequence	Proposed implications of M^{pro} cleavage	Reference	NetCorona score	PDB ID
IRAK1	^{453}QSTLQ↓AGL^{460}	Decrease cytokines production	Miczi et al. (2020)	0.859	Model
TAB1	^{128}KASLQ↓SQL^{135}	Inhibit cytokine production	Moustaqil et al. (2021); Pablos et al. (2021)	0.688	2J4O (a.a.16–371)
	^{440}TLTLQ↓STN^{447}			0.487	
DCP1A	^{339}STMMQ↓AVK^{346}	Abolish the activity of ISG effector	Song et al. (2023)	0.569	Model
NLRP12	^{237}GKLFQ↓GRF^{244}	Enhance the production of proinflammatory cytokines and chemokines	Moustaqil et al. (2021)	0.103	Model
	^{934}SVVLQ↓ANH^{941}			0.902	
SLC25A22	^{250}KTRLQ↓SLQ^{257}	Decrease immunosuppression	Zhang et al. (2021)	0.938	Model
FAF1	^{49}NGILQ↓SEY^{56}	Inhibit type 1 interferon signaling	Pablos et al. (2021)	0.224	Model
RPAP1	^{14}LLHFQ↓SQF^{21}	Divert transcription and translation machineries from host to virus	Pablos et al. (2021)	0.102	Model
	^{232}IARLQ↓AMA^{239}			0.768	
PTBP1	^{148}QAALQ↓AVN^{155}	Molecular switch from viral translation to replication	Pablos et al. (2021)	0.445	Model
PNN	^{109}KPALQ↓SSV^{116}	Transcriptional activation of immune response pathways and induce apoptosis	Meyer et al. (2021)	0.582	Model
CTBP1	^{153}GTRVQ↓SVE^{160}	Disturb the transcription of host antiviral response genes	Miczi et al. (2020); Scott et al. (2022)	0.946	6CDR
HDAC2	^{257}AVVLQ↓CGA^{264}	Impairment of ISG expression	Song et al. (2023)	0.328	6XEC (a.a. 1–376)
	^{379}GVQMQ↓AIP^{386}			0.503	
YAP1	^{129}PASLQ↓LGA^{136}	Inhibit IRF3 translocation and innate antiviral response	Pablos et al. (2021)	0.243	Model
MAP4K5	^{452}ISKLM↓SEN^{459}	Block Hippo pathway	Pablos et al. (2021)	NA	Model
CREB1	^{205}TTILQ↓YAQ^{212}	Regulate transcription of anti-apoptotic genes	Pablos et al. (2021)	0.262	Model
	^{225}QVVVQ↓AAS^{232}			0.195	
BIRC6	^{99}GATLQ↓ASA^{106}	Promote apoptosis and autophagy	Zhang et al. (2021)	0.861	N/A
TDP-43	^{327}QAALQ↓SSW^{334}	Induce cytotoxicity	Yang et al. (2023)	0.378	Model
LGALS8	^{154}SSDLQ↓STQ^{161}	Escape xenophagy	Pablos et al. (2021)	0.914	Model
FYCO1	^{975}LPGLQ↓AQL^{982}	Cause incomplete autophagy	Pablos et al. (2021)	0.551	Model
RNF20	^{517}SALLQ↓SQS^{524}	Stabilizes SREBP1-driven lipid metabolism	Zhang et al. (2021)	0.668	Model
PAICS	^{30}KVLLQ↓SKD^{37}	promote purine biosynthesis	Meyer et al. (2021)	0.864	7ALE
IRS2	^{1118}EAFLQ↓ASQ^{1125}	Insulin resistance	Pablos et al. (2021)	0.459	Model
GOLGA3	^{446}STKLQ↓AQV^{453}	Reconfigure endoplasmic reticulum and Golgi apparatus	Meyer et al. (2021)	0.606	Model
NUP107	^{31}RVLLQ↓ASQ^{38}	Hijack nuclear pore transport	Meyer et al. (2021); Pablos et al. (2021)	0.569	Model
KPNA3/IMA4	^{74}EAILQ↓NAT^{81}	Hijack nuclear pore transport	Pablos et al. (2021)	0.495	Model
SEPT2	^{336}IARMQ↓AQM^{343}	Destabilize filament structure and induce cilia dysfunction	Lee et al. (2023)	0.529	Model
SEPT6	^{76}QPGVQ↓LQS^{83}	Destabilize filament structure and induce cilia dysfunction	Pablos et al. (2021); Lee et al. (2023)	0.919	6UPA
SEPT9	^{216}VSQLQ↓SRL^{223}	Destabilize filament structure and induce cilia dysfunction	Pablos et al. (2021); Lee et al. (2023)	0.886	Model

Model: prediction of protein structure by AlphaFold.
N/A, not available.

bind competitively to NLRX1 to free the mitochondrial antiviral signaling protein (MAVS) upon RNA virus infection, which subsequently interacts with the retinoic acid-inducible gene (RIG)-I to initiate type I IFN signaling (Kim et al., 2017). Furthermore, virus infection is postulated to prevent aggregation of FAF1, which inhibits FAF1-dependent suppression of MAVS and then activates antiviral

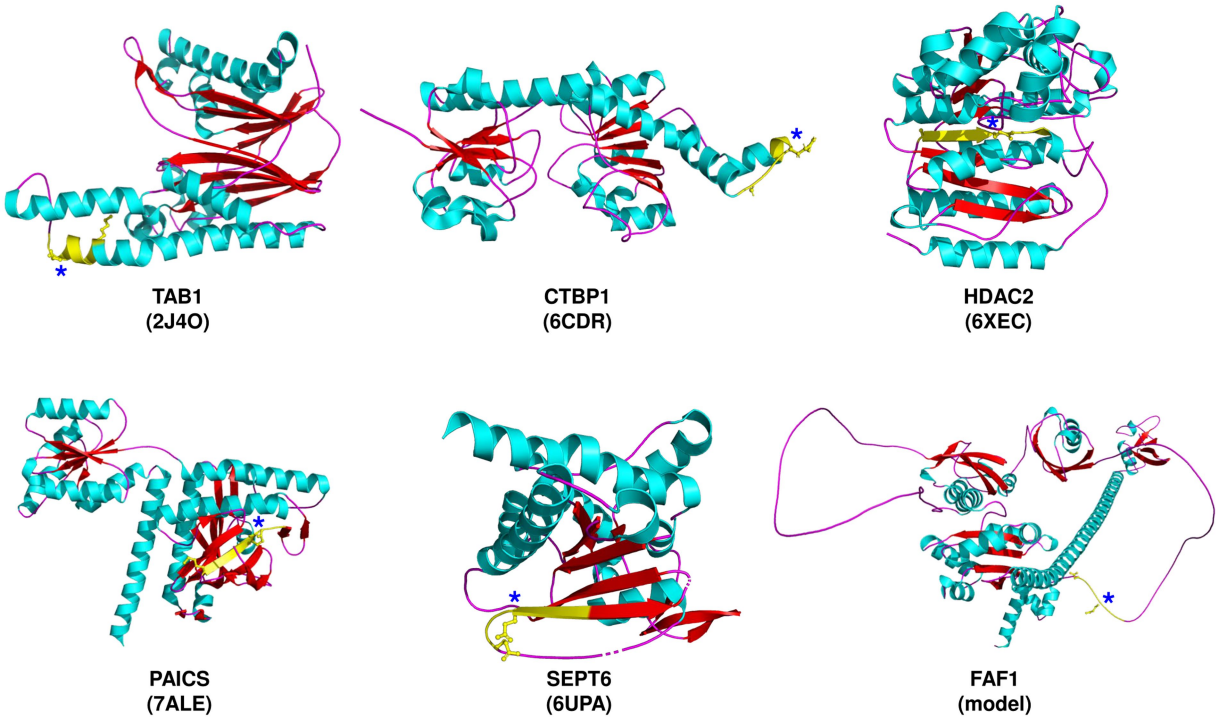

FIGURE 1
Severe acute respiratory syndrome coronavirus 2 (SARS-CoV-2) M^{pro} cleavage sites in selected target proteins. The proteins are depicted along with the corresponding PDB ID, except for FAF1, which is predicted by AlphaFold. The predicted cleavage sequences (yellow) are shown, with P1 and P5 residues, and an asterisk denoting the P1-Gln residue.

immunity (Dai et al., 2018). More studies are needed to confirm the role of FAF1 cleavage in virus infection.

4.2. Transcription and translation

Viruses can affect host gene expression at the transcriptional level. In addition, since viruses lack functional ribosomes, they attempt to usurp the host's translational apparatus by competing with cellular mRNA to achieve successful replication. For instance, RNA polymerase II-associated protein 1 (RPAP1), which is crucial to bridging RNA polymerase II with gene-enhancer elements to increase transcription, and the polypyrimidine tract-binding protein (PTBP1), essential for pre-mRNA splicing and mRNA export, are both cleaved by M^{pro}. Proteolysis of PTBP1 after SARS-CoV-2 infection leads to the redistribution of PTBP1 from the nucleus to the cytoplasm (Pablos et al., 2021). In polioviruses, proteolysis of PTBP1 is speculated to switch viral translation to replication (Back et al., 2002). Thus, M^{pro} might target RPAP1 and PTBP1 to divert transcription and translation machineries from host to virus.

Pinin (PNN), a multifunctional nuclear phosphoprotein involved in the regulation of transcription and alternative RNA splicing, has also been identified as a substrate of M^{pro} (Meyer et al., 2021). Depletion of PNN has been demonstrated to result in apoptosis *in vitro* and early lethality *in vivo* (Leu et al., 2012). Furthermore, PNN binds to the transcriptional co-repressor C-terminal binding protein 1 (CTBP1). The interaction of PNN and CTBP1 alters CTBP1 silencing function (Alpatov et al., 2004). The overlapping pathways enriched in PNN-KD and CTBP1-KD cells include the TNFα-induced canonical NFκB signaling pathway and the IFN response pathway (Zhang et al., 2016). CTBP1-mutated neuronal cells were more susceptible to West Nile virus than control cells, consistent with the lower expression of IFN-response genes in CTBP1-mutated cells (Vijayalingam et al., 2020). Cleavage of PNN and CTBP1 by M^{pro} is suggested to alter the transcription of host antiviral response genes and induce apoptosis (Miczi et al., 2020; Meyer et al., 2021). Furthermore, M^{pro} cleaves Histone deacetylase 2 (HDAC2), which primarily regulates gene transcription by modifying histones and is also required for ISG transcriptional elongation (Chang et al., 2004). In consequence, the cleavage of HDAC2 by M^{pro} results in the impairment of ISG expression (Song et al., 2023).

Yes-associated protein 1 (YAP1), a transcriptional co-activator, participates in Hippo pathway. Since YAP negatively regulated an antiviral immune response via inhibiting the translocation of IRF3 to the nucleus, cleavage of YAP1 is presumed to enhance innate immunity (Wang et al., 2017). The kinase activity of mitogen-activated kinase-kinase-kinase-kinase 5 (MAP4K5), another Hippo pathway regulator, can be inactivated by M^{pro} cleavage. cAMP response element binding protein 1 (CREB1) is a transcription factor that dimerizes with ATF1 to regulate the transcription of anti-apoptotic and cell proliferation genes. Besides, CREB1 binds YAP1 and forms a positive feedback loop with each other (Chen et al., 2018). M^{pro} cleavages of YAP1, MAP4K5, and CREB1 indicate that SARS-CoV-2 can hijack the Hippo-YAP signaling pathway (Pablos et al., 2021) for mediating a variety of cellular processes, including cell proliferation, differentiation, apoptosis, and immune response.

4.3. Apoptosis and autophagy

To maintain homeostasis, cells undergo two types of programmed cell death (PCD)-apoptosis and autophagy (Kennedy, 2015). Inhibition of these PCDs by SARS-CoV-2 aids the virus to avoid elimination in the cells and ensure viable cells for viral replication, while induction may benefit the virus by the regulation of immune response and virus release (Li et al., 2020, 2021, 2022). Moreover, SARS-CoV-2 exploits autophagy to prevent virus degradation (Chen et al., 2020). Several proteins involved in apoptosis and autophagy have been identified to be targeted by M^{pro}.

Baculoviral IAP repeat-containing protein 6 (BIRC6) functions as an inhibitor of apoptosis and autophagy by ubiquitinating pro-apoptotic factors and LC3B, leading to their proteasomal degradation (Ehrmann et al., 2022). M^{pro} cleavage of BIRC6 may promote apoptosis and autophagy, in line with the induction of apoptosis and autophagy upon SARS-CoV-2 infection (Li et al., 2020, 2021). Transactive response DNA binding protein 43 kDa (TDP-43) is critical in RNA regulation, including the expression of viral RNA (reviewed in Rahic et al., 2023). Cleavage of TDP-43 by M^{pro} induced cytotoxicity in neurons, which could contribute to the pathogenicity of SARS-CoV-2 in the nervous system (Yang et al., 2023).

Galectin-8 (LGALS8) is involved in the regulation of immune responses and directly binds to Spike S1 glycans and the autophagy adaptor NDP52 (Pablos et al., 2021). LGALS8 is proposed to sense the glycosylated Spike S1 protein and activate xenophagy, a type of selective autophagy targeting invading pathogens to lysosomes, to reduce SARS-CoV-2 infection (Pablos et al., 2021). Furthermore, the autophagy adaptor protein FYVE and the coiled coil domain containing 1 (FYCO1) has been identified as a candidate COVID-19 susceptibility and severity gene and is believed to be the key mediator that connects double-membrane vesicles (the main site of coronavirus replication) from the endoplasmic reticulum to the microtubule network in host cells (Reggiori et al., 2011; Parkinson et al., 2020; Lee et al., 2021; Jahanafrooz et al., 2022). The elimination of FYCO1 resulted in the accumulation of early autophagosomes (Pankiv et al., 2010). M^{pro} cleavage of LGALS8 and FYCO1 possibly enables SARS-CoV-2 to escape antiviral xenophagy (Pablos et al., 2021) and induce incomplete autophagy.

4.4. Cell metabolism

SARS-CoV-2 infection alters host cell metabolism (Andrade Silva et al., 2021; Mullen et al., 2021). In fact, proteins that play roles in cell metabolism were found to be substrates of M^{pro}. Cleavage of Ring finger protein 20 (RNF20) destabilizes the RNF20/RNF40 complex, which is essential for their ubiquitin E3 ligase activity. As a result, this blocks the degradation of the sterol regulatory element binding protein 1 (SREBP1), and subsequently increasing the lipid metabolism for promoting SARS-CoV-2 replication (Zhang et al., 2021).

Phosphoribosylaminoimidazole succinocarboxamide synthetase (PAICS), a *de novo* purine biosynthetic enzyme was previously identified to be crucial in influenza virus replication (Karlas et al., 2010; Generous et al., 2014). PAICS is proposed to be a candidate for a noncanonical route for SARS-CoV-2 infection in human placentas (Constantino et al., 2021). SARS-CoV-2 infection has been reported to promote *de novo* purine synthesis through nsp9 (Qin et al., 2022). Silencing of PAICS reduced virus titers (~10-fold), suggesting that cleavage of PAICS by M^{pro} results in altered function of PAICS (Meyer et al., 2021), which may influence the *de novo* purine synthesis.

Insulin receptor substrate 2 (IRS2) regulates insulin signaling and the control of glucose homeostasis. Hepatitis C virus infection downregulates IRS2 expression by upregulating the suppressor of cytokine signaling (SOCS) and by activating the mTOR/S6K1 signaling pathway, resulting in insulin resistance (Kawaguchi et al., 2004; Pazienza et al., 2007; Bose et al., 2012). Notably, new-onset hyperglycemia has been associated with SARS-CoV-2 because non-diabetic COVID-19 patients were found to have increased risk of insulin resistance (Chen et al., 2021; Wihandani et al., 2023), which may be associated with M^{pro} cleavage of IRS2 (Pablos et al., 2021).

4.5. Intracellular transport and cytoskeleton

The intracellular transport system and cytoskeletons are essential for viral infections, particularly for transporting viral components to specific subcellular compartment sites of translation, replication, and secretion. The Golgi apparatus is an integral component of the viral life cycle. SARS-CoV-2 remodels the Golgi structure for viral release, hence, M^{pro} cleavage of Golgin subfamily A member 3 (GOLGA3), which is involved in the organization of the Golgi apparatus and its associated vesicles (Meyer et al., 2021; Pablos et al., 2021), may also be linked to this modulation (Zhang et al., 2022). Moreover, GOLGA3 has been associated with COVID-19 and has been identified to interact with nsp13 (Gordon et al., 2020; Deng et al., 2021). M^{pro} cleavage of GOLGA3 may play a role in reconfiguring the endoplasmic reticulum to facilitate Golgi trafficking during virus assembly.

Although RNA viruses replicate in the cytoplasm, they also exploit the nucleocytoplasmic trafficking system to inhibit the host immune response (Sajidah et al., 2021), which may explain why SARS-CoV-2 M^{pro} cleaves the nuclear pore complex 107 kDa subunit (NUP107) and Importin subunit alpha-4 (IMA4), which are both important members of nuclear pore transport (Pablos et al., 2021). IMA4, also known as karyopherin subunit alpha-3 (KPNA3), has been shown to be targeted by the Japanese encephalitis virus NS5 protein to hinder the nuclear import of its cargo molecules IFN regulatory factor 3 and NF-κB, thereby subsequently inhibiting type 1 IFN production (Ye et al., 2017).

Septin (SEPT) is recognized as a component of the cytoskeleton (Mostowy and Cossart, 2012). Septin polymerizes into filaments at the cell cortex or in association with other cytoskeletal proteins, such as actin or microtubules. M^{pro} cleaves several septin proteins, including SEPT2, SEPT6, and SEPT9, to affect the septin complex, causing an unstable filament structure and inducing cilia dysfunction (Lee et al., 2023).

5. Discussion

With the help of computational and experimental methods, scientists have gained valuable insights into the substrates of M^{pro}.

NetCorona analysis is widely used for substrate prediction. Intriguingly, some of the identified substrates have low NetCorona scores (Table 1), implying other issues should be considered. Further information, like binding affinity, may improve the original algorithm. The steric effects on substrate specificity also play an important role for the assessment. Notably, the cleavage sites of HDAC2 and PAICS are buried in the structure, warranting further study regarding the mechanism of M^{pro} cleavage of these two proteins. Deep learning of sequenced-based prediction and structural analysis can likewise improve the accuracy of prediction.

Identification of viral host substrates helps determine specific virus-host interactions, including the cellular pathways involved, and the mechanisms of viral replication and pathogenesis. Consequently, researchers can gain valuable insights into how viruses cause diseases and develop strategies to control or treat viral infections. After COVID-19 infection, certain individuals developed post-acute sequelae of SARS-CoV-2 infection (PASC), known as long COVID. The persistence of viral RNA or proteins for weeks in these patients implies the presence of an impaired immune response. Exploring the potential role of M^{pro} in this aspect would be valuable. Besides, identifying the specific sequences of host substrates targeted by M^{pro} can have significant implications in developing peptidomimetic protease inhibitors. Discovering new substrate sequences can enhance the design of effective antiviral strategies. Continued research is essential to improve our understanding of M^{pro} function and develop potent antiviral therapies against coronaviruses.

Author contributions

W-CS conceived and supervised the review topic. IM, Y-CL, and W-CS participated in the writing and preparation of the manuscript. All authors contributed to the article and approved the submitted version.

Funding

This work is supported by the grant (MOST 111-2320-B-039-060) from the National Science and Technology Council, Taiwan, and the grant (CMU111-MF-29) from China Medical University.

Conflict of interest

Y-CL was employed by the company Sinphar Pharmaceutical Co, Ltd.

The remaining authors declare that the research was conducted in the absence of any commercial or financial relationships that could be construed as a potential conflict of interest.

Publisher's note

References

Alpatov, R., Munguba, G. C., Caton, P., Joo, J. H., Shi, Y., Shi, Y., et al. (2004). Nuclear speckle-associated protein Pnn/Drs binds to the transcriptional corepressor Ctbp and relieves Ctbp-mediated repression of the E-cadherin gene. *Mol. Cell. Biol.* 24, 10223–10235. doi: 10.1128/MCB.24.23.10223-10235.2004

Andrade Silva, M., Da Silva, A., Do Amaral, M. A., Fragas, M. G., and Câmara, N. O. S. (2021). Metabolic alterations in Sars-Cov-2 infection and its implication in kidney dysfunction. *Front. Physiol.* 12:624698. doi: 10.3389/fphys.2021.624698

Back, S. H., Kim, Y. K., Kim, W. J., Cho, S., Oh, H. R., Kim, J.-E., et al. (2002). Translation of polioviral mRNA is inhibited by cleavage of polypyrimidine tract-binding proteins executed by polioviral 3cPro. *J. Virol.* 76, 2529–2542. doi: 10.1128/jvi.76.5.2529-2542.2002

Bose, S. K., Shrivastava, S., Meyer, K., Ray, R. B., and Ray, R. (2012). Hepatitis C virus activates the Mtor/S6k1 signaling pathway in inhibiting Irs-1 function for insulin resistance. *J. Virol.* 86, 6315–6322. doi: 10.1128/JVI.00050-12

Campbell, G. R., Rawat, P., and Spector, S. A. (2023). Pacritinib inhibition of Irak1 blocks aberrant Tlr8 signalling by Sars-Cov-2 and Hiv-1-derived RNA. *J. Innate Immun.* 15, 96–106. doi: 10.1159/000525292

Chang, H. M., Paulson, M., Holko, M., Rice, C. M., Williams, B. R., Marie, I., et al. (2004). Induction of interferon-stimulated gene expression and antiviral responses require protein deacetylase activity. *Proc. Natl. Acad. Sci. U. S. A.* 101, 9578–9583. doi: 10.1073/pnas.0400567101

Chen, L., Feng, P., Peng, A., Qiu, X., Zhu, X., He, S., et al. (2018). Camp response element-binding protein and yes-associated protein form a feedback loop that promotes neurite outgrowth. *J. Cell. Mol. Med.* 22, 374–381. doi: 10.1111/jcmm.13324

Chen, S.-W., Himeno, M., Koui, Y., Sugiyama, M., Nishitsuji, H., Mizokami, M., et al. (2020). Modulation of hepatitis B virus infection by epidermal growth factor secreted from liver sinusoidal endothelial cells. *Sci. Rep.* 10:14349. doi: 10.1038/s41598-020-71453-5

Chen, M., Zhu, B., Chen, D., Hu, X., Xu, X., Shen, W. J., et al. (2021). Covid-19 may increase the risk of insulin resistance in adult patients without diabetes: a 6-month prospective study. *Endocr. Pract.* 27, 834–841. doi: 10.1016/j.eprac.2021.04.004

Chuck, C. P., Chong, L. T., Chen, C., Chow, H. F., Wan, D. C., and Wong, K. B. (2010). Profiling of substrate specificity of Sars-Cov 3cl. *PLoS One* 5:E13197. doi: 10.1371/journal.pone.0013197

Constantino, F. B., Cury, S. S., Nogueira, C. R., Carvalho, R. F., and Justulin, L. A. (2021). Prediction of non-canonical routes for Sars-Cov-2 infection in human placenta cells. *Front. Mol. Biosci.* 8:614728. doi: 10.3389/fmolb.2021.614728

Dai, T., Wu, L., Wang, S., Wang, J., Xie, F., Zhang, Z., et al. (2018). Faf1 regulates antiviral immunity by inhibiting mavs but is antagonized by phosphorylation upon viral infection. *Cell Host Microbe* 24, 776–790.E5. doi: 10.1016/j.chom.2018.10.006

Deng, H., Yan, X., and Yuan, L. (2021). Human genetic basis of coronavirus disease 2019. *Signal Transduct. Target. Ther.* 6:344. doi: 10.1038/s41392-021-00736-8

Diamond, M. S., and Kanneganti, T.-D. (2022). Innate immunity: the first line of defense against Sars-Cov-2. *Nat. Immunol.* 23, 165–176. doi: 10.1038/s41590-021-01091-0

Ehrmann, J. F., Grabarczyk, D. B., Heinke, M., Deszcz, L., Kurzbauer, R., Hudecz, O., et al. (2022). Structural basis of how the Birc6/SMAC complex regulates apoptosis and autophagy. Biorxiv [Preprint]. doi: 10.1126/science.ade8873

Generous, A., Thorson, M., Barcus, J., Jacher, J., Busch, M., and Sleister, H. (2014). Identification of putative interactions between swine and human influenza a virus nucleoprotein and human host proteins. *Virol. J.* 11:228. doi: 10.1186/s12985-014-0228-6

Gordon, D. E., Jang, G. M., Bouhaddou, M., Xu, J., Obernier, K., White, K. M., et al. (2020). A Sars-Cov-2 protein interaction map reveals targets for drug repurposing. *Nature* 583, 459–468. doi: 10.1038/s41586-020-2286-9

Hu, Q., Xiong, Y., Zhu, G. H., Zhang, Y. N., Zhang, Y. W., Huang, P., et al. (2022). The Sars-Cov-2 main protease (M(pro)): structure, function, and emerging therapies for Covid-19. *Medcomm* 3:E151. doi: 10.1002/mco2.151

Jackson-Bernitsas, D. G., Ichikawa, H., Takada, Y., Myers, J. N., Lin, X. L., Darnay, B. G., et al. (2007). Evidence that Tnf-Tnfr1-Tradd-Traf2-rip-Tak1-Ikk pathway mediates constitutive Nf-Kb activation and proliferation in human head and neck squamous cell carcinoma. *Oncogene* 26, 1385–1397. doi: 10.1038/sj.onc.1209945

Jahanafrooz, Z., Chen, Z., Bao, J., Li, H., Lipworth, L., and Guo, X. (2022). An overview of human proteins and genes involved in Sars-Cov-2 infection. *Gene* 808:145963. doi: 10.1016/j.gene.2021.145963

Karlas, A., Machuy, N., Shin, Y., Pleissner, K.-P., Artarini, A., Heuer, D., et al. (2010). Genome-wide RNAi screen identifies human host factors crucial for influenza virus replication. *Nature* 463, 818–822. doi: 10.1038/nature08760

Kawaguchi, T., Yoshida, T., Harada, M., Hisamoto, T., Nagao, Y., Ide, T., et al. (2004). Hepatitis C virus down-regulates insulin receptor substrates 1 and 2 through up-

regulation of suppressor of cytokine signaling 3. *Am. J. Pathol.* 165, 1499–1508. doi: 10.1016/S0002-9440(10)63408-6

Kennedy, P. G. E. (2015). Viruses, apoptosis, and neuroinflammation—a double-edged sword. *J. Neuro-Oncol.* 21, 1–7. doi: 10.1007/s13365-014-0306-y

Kim, J.-H., Park, M.-E., Nikapitiya, C., Kim, T.-H., Uddin, M. B., Lee, H.-C., et al. (2017). Fas-associated factor-1 positively regulates type i interferon response to RNA virus infection by targeting Nlrx1. *PLoS Pathog.* 13:E1006398. doi: 10.1371/journal.ppat.1006398

Koudelka, T., Boger, J., Henkel, A., Schonherr, R., Krantz, S., Fuchs, S., et al. (2021). N-terminomics for the identification of in vitro substrates and cleavage site specificity of the Sars-Cov-2 main protease. *Proteomics* 21:2000246. doi: 10.1002/pmic.202000246

Lee, A. R., Kweon, Y. C., Lee, S. M., and Park, C. Y. (2023). Human coronavirus 3cl proteases cleave septins and disrupt hedgehog signaling. *J. Med. Virol.* 95:E28618. doi: 10.1002/jmv.28618

Lee, J.-W., Lee, I.-H., Sato, T., Kong, S. W., and Iimura, T. (2021). Genetic variation analyses indicate conserved Sars-Cov-2–host interaction and varied genetic adaptation in immune response factors in modern human evolution. *Develop. Growth Differ.* 63, 219–227. doi: 10.1111/dgd.12717

Leu, S., Lin, Y.-M., Wu, C.-H., and Ouyang, P. (2012). Loss of PNN expression results in mouse early embryonic lethality and cellular apoptosis through Srsf1-mediated alternative expression of Bcl-Xs and Icad. *J. Cell Sci.* 125, 3164–3172. doi: 10.1242/jcs.100859

Li, F., Li, J., Wang, P. H., Yang, N., Huang, J., Ou, J., et al. (2021). Sars-Cov-2 spike promotes inflammation and apoptosis through autophagy by Ros-suppressed Pi3k/Akt/Mtor signaling. *Biochim. Biophys. Acta Mol. basis Dis.* 1867:166260. doi: 10.1016/j.bbadis.2021.166260

Li, S., Zhang, Y., Guan, Z., Li, H., Ye, M., Chen, X., et al. (2020). Sars-Cov-2 triggers inflammatory responses and cell death through Caspase-8 activation. *Signal Transduct. Target. Ther.* 5:235. doi: 10.1038/s41392-020-00334-0

Li, X., Zhang, Z., Wang, Z., Gutiérrez-Castrellón, P., and Shi, H. (2022). Cell deaths: involvement in the pathogenesis and intervention therapy of Covid-19. *Signal Transduct. Target. Ther.* 7:186. doi: 10.1038/s41392-022-01043-6

Meyer, B., Chiaravalli, J., Gellenoncourt, S., Brownridge, P., Bryne, D. P., Daly, L. A., et al. (2021). Characterising proteolysis during Sars-Cov-2 infection identifies viral cleavage sites and cellular targets with therapeutic potential. *Nat. Commun.* 12:5553. doi: 10.1038/s41467-021-25796-w

Miczi, M., Golda, M., Kunkli, B., Nagy, T., Tozser, J., and Motyan, J. A. (2020). Identification of host cellular protein substrates of Sars-Cov-2 main protease. *Int. J. Mol. Sci.* 21:9523. doi: 10.3390/ijms21249523

Mostowy, S., and Cossart, P. (2012). Septins: the fourth component of the cytoskeleton. *Nat. Rev. Mol. Cell Biol.* 13, 183–194. doi: 10.1038/nrm3284

Moustaqil, M., Ollivier, E., Chiu, H. P., Van Tol, S., Rudolffi-Soto, P., Stevens, C., et al. (2021). Sars-Cov-2 proteases Plpro and 3clpro cleave Irf3 and critical modulators of inflammatory pathways (NLRP12 and TAB1): implications for disease presentation across species. *Emerg. Microbes Infect.* 10, 178–195. doi: 10.1080/22221751.2020.1870414

Mullen, P. J., Garcia, G., Purkayastha, A., Matulionis, N., Schmid, E. W., Momcilovic, M., et al. (2021). Sars-Cov-2 infection rewires host cell metabolism and is potentially susceptible to Mtorc1 inhibition. *Nat. Commun.* 12:1876. doi: 10.1038/s41467-021-22166-4

Pablos, I., Machado, Y., De Jesus, H. C. R., Mohamud, Y., Kappelhoff, R., Lindskog, C., et al. (2021). Mechanistic insights into Covid-19 by global analysis of the Sars-Cov-2 3cl(pro) substrate degradome. *Cell Rep.* 37:109892. doi: 10.1016/j.celrep.2021.109892

Pankiv, S., Alemu, E. A., Brech, A., Bruun, J. A., Lamark, T., Overvatn, A., et al. (2010). Fyco1 is a Rab7 effector that binds to Lc3 and Pi3p to mediate microtubule plus end-directed vesicle transport. *J. Cell Biol.* 188, 253–269. doi: 10.1083/jcb.200907015

Parkinson, N., Rodgers, N., Head Fourman, M., Wang, B., Zechner, M., Swets, M. C., et al. (2020). Dynamic data-driven meta-analysis for prioritisation of host genes implicated in COVID-19. *Sci. Rep.* 10:22303. doi: 10.1038/s41598-020-79033-3

Pazienza, V., Clément, S., Pugnale, P., Conzelman, S., Foti, M., Mangia, A., et al. (2007). The hepatitis C virus core protein of genotypes 3a and 1b downregulates insulin receptor substrate 1 through genotype-specific mechanisms. *Hepatology* 45, 1164–1171. doi: 10.1002/hep.21634

Qin, C., Rao, Y., Yuan, H., Wang, T. Y., Zhao, J., Espinosa, B., et al. (2022). Sars-Cov-2 couples evasion of inflammatory response to activated nucleotide synthesis. *Proc. Natl. Acad. Sci. U. S. A.* 119:E2122897119. doi: 10.1073/pnas.2122897119

Rahic, Z., Buratti, E., and Cappelli, S. (2023). Reviewing the potential links between viral infections and Tdp-43 proteinopathies. *Int. J. Mol. Sci.* 24:1581. doi: 10.3390/ijms24021581

Reggiori, F., De Haan, C. A. M., and Molinari, M. (2011). Unconventional use of Lc3 by coronaviruses through the alleged subversion of the erad tuning pathway. *Viruses* 3, 1610–1623. doi: 10.3390/v3091610

Sabbah, D. A., Hajjo, R., Bardaweel, S. K., and Zhong, H. A. (2021). An updated review on Sars-Cov-2 main proteinase (M(pro)): protein structure and small-molecule inhibitors. *Curr. Top. Med. Chem.* 21, 442–460. doi: 10.2174/1568026620666201207095117

Sajidah, E. S., Lim, K., and Wong, R. W. (2021). How Sars-Cov-2 and other viruses build an invasion route to hijack the host nucleocytoplasmic trafficking system. *Cells* 10:1424. doi: 10.3390/cells10061424

Scott, B. M., Lacasse, V., Blom, D. G., Tonner, P. D., and Blom, N. S. (2022). Predicted coronavirus Nsp5 protease cleavage sites in the human proteome. *BMC Genom Data* 23:25. doi: 10.1186/s12863-022-01044-y

Song, S., Lee, J. J., Kim, H. J., Lee, J. Y., Chang, J., and Lee, K. J. (2016). FAS-associated factor 1 negatively regulates the antiviral immune response by inhibiting translocation of interferon regulatory factor 3 to the nucleus. *Mol. Cell. Biol.* 36, 1136–1151. doi: 10.1128/MCB.00744-15

Song, L., Wang, D., Abbas, G., Li, M., Cui, M., Wang, J., et al. (2023). The main protease of Sars-Cov-2 cleaves histone deacetylases and Dcp1a, attenuating the immune defense of the interferon-stimulated genes. *J. Biol. Chem.* 299:102990. doi: 10.1016/j.jbc.2023.102990

Ullrich, S., and Nitsche, C. (2020). The Sars-Cov-2 main protease as drug target. *Bioorg. Med. Chem. Lett.* 30:127377. doi: 10.1016/j.bmcl.2020.127377

Vijayalingam, S., Ezekiel, U. R., Xu, F., Subramanian, T., Geerling, E., Hoelscher, B., et al. (2020). Human IPSC-derived neuronal cells from Ctbp1-mutated patients reveal altered expression of neurodevelopmental gene networks. *Front. Neurosci.* 14:562292. doi: 10.3389/fnins.2020.562292

Wang, S., Xie, F., Chu, F., Zhang, Z., Yang, B., Dai, T., et al. (2017). Yap antagonizes innate antiviral immunity and is targeted for lysosomal degradation through Ikkε-mediated phosphorylation. *Nat. Immunol.* 18, 733–743. doi: 10.1038/ni.3744

Wihandani, D. M., Purwanta, M. L. A., Mulyani, W. R. W., Putra, I., and Supadmanaba, I. G. P. (2023). New-onset diabetes in Covid-19: the molecular pathogenesis. *Biomedicine* 13, 3–12. doi: 10.37796/2211-8039.1389

Xiong, M., Su, H., Zhao, W., Xie, H., Shao, Q., and Xu, Y. (2021). What coronavirus 3c-like protease tells us: from structure, substrate selectivity, to inhibitor design. *Med. Res. Rev.* 41, 1965–1998. doi: 10.1002/med.21783

Yang, J., Li, Y., Wang, S., Li, H., Zhang, L., Zhang, H., et al. (2023). The Sars-Cov-2 main protease induces neurotoxic Tdp-43 cleavage and aggregates. *Signal Transduct. Target. Ther.* 8:109. doi: 10.1038/s41392-023-01386-8

Ye, J., Chen, Z., Li, Y., Zhao, Z., He, W., Zohaib, A., et al. (2017). Japanese encephalitis virus Ns5 inhibits type I interferon (IFN) production by blocking the nuclear translocation of IFN regulatory factor 3 and Nf-Kb. *J. Virol.* 91, E00039–E00017. doi: 10.1128/JVI.00039-17

Yoo, H. C., Yu, Y. C., Sung, Y., and Han, J. M. (2020). Glutamine reliance in cell metabolism. *Exp. Mol. Med.* 52, 1496–1516. doi: 10.1038/s12276-020-00504-8

Zhang, X., Guo, Y., Xu, X., Tang, T., Sun, L., Wang, H., et al. (2019). Mir-146a promotes Borna disease virus 1 replication through Irak1/Traf6/Nf-Kb signaling pathway. *Virus Res.* 271:197671. doi: 10.1016/j.virusres.2019.197671

Zhang, J., Kennedy, A., Xing, L., Bui, S., Reid, W., Joppich, J., et al. (2022). Sars-Cov-2 triggers golgi fragmentation via down-regulation of Grasp55 to facilitate viral trafficking. Biorxiv [Preprint]. doi: 10.1101/2022.03.04.483074

Zhang, Y., Kwok, J. S.-L., Choi, P.-W., Liu, M., Yang, J., Singh, M., et al. (2016). Pinin interacts with C-terminal binding proteins for RNA alternative splicing and epithelial cell identity of human ovarian cancer cells. *Oncotarget* 7, 11397–11411. doi: 10.18632/oncotarget.7242

Zhang, S., Wang, J., and Cheng, G. (2021). Protease cleavage of Rnf20 facilitates coronavirus replication via stabilization of Srebp1. *Proc. Natl. Acad. Sci. U. S. A.* 118:e2107108118. doi: 10.1073/pnas.2107108118

Zheng, H.-Q., Li, C., Zhu, X.-F., Wang, W.-X., Yin, B.-Y., Zhang, W.-J., et al. (2022). Mir-615 facilitates porcine epidemic diarrhea virus replication by targeting Irak1 to inhibit type iii interferon expression. *Front. Microbiol.* 13:1071394. doi: 10.3389/fmicb.2022.1071394

Zhou, Q., Peng, Y., Chen, L.-S., Chen, H., Kang, W., Nie, Y., et al. (2021). Iddf2021-Abs-0183 Slc25a22 drives immune suppression in kras-mutant colorectal cancer. *Gut* 70, A53–A55. doi: 10.1136/gutjnl-2021-IDDF.51

Zhu, X., Chen, J., Tian, L., Zhou, Y., Xu, S., Long, S., et al. (2020). Porcine deltacoronavirus Nsp5 cleaves Dcp1a to decrease its antiviral activity. *J. Virol.* 94:e02162–19. doi: 10.1128/JVI.02162-19

frontiers | Frontiers in Microbiology

TYPE Review
PUBLISHED 13 September 2023
DOI 10.3389/fmicb.2023.1260543

OPEN ACCESS

EDITED BY
Shijian Zhang,
Dana–Farber Cancer Institute, United States

REVIEWED BY
Hao Hu,
Washington University in St. Louis, United States
Katrina Traber,
Boston University, United States

*CORRESPONDENCE
Yuying Zhang
bio_zhangyy@ujn.edu.cn
Fanhua Wei
weifanhua999@163.com

†These authors have contributed equally to this work

RECEIVED 18 July 2023
ACCEPTED 16 August 2023
PUBLISHED 13 September 2023

CITATION
Li H, Wang A, Zhang Y and Wei F (2023) Diverse roles of lung macrophages in the immune response to influenza A virus.
Front. Microbiol. 14:1260543.
doi: 10.3389/fmicb.2023.1260543

Diverse roles of lung macrophages in the immune response to influenza A virus

Haoning Li[1†], Aoxue Wang[1†], Yuying Zhang[2*] and Fanhua Wei[1*]

[1]College of Animal Science and Technology, Ningxia University, Yinchuan, China, [2]School of Biological Science and Technology, University of Jinan, Jinan, China

Influenza viruses are one of the major causes of human respiratory infections and the newly emerging and re-emerging strains of influenza virus are the cause of seasonal epidemics and occasional pandemics, resulting in a huge threat to global public health systems. As one of the early immune cells can rapidly recognize and respond to influenza viruses in the respiratory, lung macrophages play an important role in controlling the severity of influenza disease by limiting viral replication, modulating the local inflammatory response, and initiating subsequent adaptive immune responses. However, influenza virus reproduction in macrophages is both strain- and macrophage type-dependent, and ineffective replication of some viral strains in mouse macrophages has been observed. This review discusses the function of lung macrophages in influenza virus infection in order to better understand the pathogenesis of the influenza virus.

KEYWORDS

influenza virus, macrophage, antiviral, immune response, inflammation

1. Introduction

Influenza viruses include four major types A, B, C, and D, and belong to the family of *Orthomyxoviridae* family. Influenza A virus (IAV), influenza B virus (IBV), influenza C virus (ICV), and influenza D virus (IDV) can all infect mammals, with IAV, IBV, and ICV infecting humans. No human infections with IDV have been reported to date (Liu et al., 2020). Seasonal influenza viruses are responsible for most human respiratory infections, causing an estimated 290,000–650,000 deaths globally each year. IAVs are further divided into subtypes based on hemagglutinin (HA) and neuraminidase (NA) glycoproteins. There are 18 HA subtypes (H1–H18) and 11 NA subtypes (N1–N11) of IAV (Tong et al., 2013). Effective measures against IAV and IBV infection include the prevention of vaccine, or prophylactic or therapeutic treatment with antiviral drugs. However, the evolution of influenza viruses through antigenic drift and antigenic shift allows them to spread across different species and is responsible for the novel influenza viruses in pandemics (Taubenberger and Morens, 2008).

The innate immune system is the first line of defense against influenza virus infection consisting of physical barriers and innate cellular immune responses. During influenza virus infection, epithelial cells on the mucosa are infected and subsequently macrophages may be the cells that first responded to them immunologically and play a crucial role in virus resistance (Maines et al., 2008). Infection of respiratory epithelial cells with IAV is initiated by the binding of cell surface salivary acids to the viral HA proteins (Wiley and Skehel, 1987; Skehel and Wiley, 2000). Moreover, it is likely that viral entry into epithelial cells can be facilitated by the interaction with other cell surface receptors (Chu and Whittaker, 2004; Rapoport et al., 2006; Thompson et al., 2006; Oshansky et al., 2011). Alveolar macrophages (AMs) are also infected by seasonal

IAV strains (H1N1 and H3N2) and replication of seasonal IAV in AMs is not productive (Rodgers and Mims, 1982; van Riel et al., 2011; Yu et al., 2011). However, certain viral strains that can replicate in a productive manner in macrophages are now well known and this has a significant impact on the antiviral functions of macrophages (Cline et al., 2017). Following attachment, virus is internalized by receptor-mediated endocytosis using clathrin- or caveolin-dependent or -independent pathways, and conformational changes of HA in the low pH of the endosomal compartment leads to the fusion of viral and endosomal membranes. The fusion of the viral envelope with the endosomal membrane triggers the release of vRNP to the cytoplasm before entry into the nucleus to initiate viral replication. Inefficient attachment and entry (Londrigan et al., 2015) and a block downstream of virus internalization but upstream of nuclear entry (Cline et al., 2013; Marvin et al., 2017) are two cellular blocks that regulate the productive replication of influenza virus in macrophages. However, the HPAI H5N1 viruses and the H1N1 WSN strains are able to overcome these cellular barriers and further replicate in a productive manner in both mouse and primary human macrophages (Cline et al., 2013; Marvin et al., 2017). Therefore, IAV replication in macrophages is both strain- and macrophage type-dependent. These are described below and are summarized in Figure 1.

2. Macrophages heterogeneity following IAV infection

2.1. Macrophages plasticity during IAV infection

Macrophages exist in the body as a heterogeneous population of cells. According to different physiological anatomical locations in the lungs, macrophages are classified as AMs and alveolar interstitial macrophages (IMs; Hume et al., 2020). In mice, AMs are characterized as major histocompatibility complex (MHC) class II^{mod}CD11c^{high}Siglec-F^{high} in contrast to MHC II^{mod}CD11c^{low}Siglec-F^{neg}CD64^{pos} IMs (Misharin et al., 2013; Schneider et al., 2014b), whereas human AMs are MHC II^{high}CD11c^{high}CD14^{low} (Desch et al., 2016). Studies in granulocyte-macrophage colony-stimulating factor (GM-CSF)-deficient mice lacking functional Siglec-F^{high}CD11c^{high} AMs demonstrate for the first time the requirement for AMs in lung homeostasis (Dranoff et al., 1994). Upon influenza virus infection, AMs are implicated in viral clearance since depletion of AMs leads to a higher viral load, an increase in mortality, and a reduction in the production of type I IFN (IFN-I; Tumpey et al., 2005; Schneider et al., 2014a). Importantly, the depletion of AMs in pigs also increases the mortality and loss of body weight following IAV infection (Kim et al., 2008). In addition, the frequency of IMs is found to be twice as low as that of AMs in mice under steady-state conditions (Bedoret et al., 2009), but IMs expand at a much faster rate when responding to external stimuli than AMs do (Landsman and Jung, 2007). Indeed, the H5N1 infection leads to the rapid depletion of AMs from both bronchoalveolar lavage (BAL) and the lungs and the concurrent recruitment of IMs to the lungs (Corry et al., 2022).

Alveolar macrophages can be further subdivided into resident alveolar macrophages (TR-AMs) and recruited monocyte-derived macrophages (MO-AMs), while IMs can be classified as TR-IMs and MO-IMs. Currently, studies of lung macrophages are focused on AMs, mainly due to technical problems in the extraction of IMs and their similar phenotype to monocytes (Liegeois et al., 2018). Macrophages from the yolk sac and fetal liver precursors enter various tissues during the formation of embryonic organs and differentiate into tissue-resident macrophages by transforming growth factor-β (TGF-β) and GM-CSF in adulthood (Guilliams et al., 2013; Yu et al., 2017; Zhao et al., 2018). In steady-state conditions, TR-AMs are cells with a relatively long life span, which are fully established before birth and are maintained by self-replication without the need for replenishment by blood monocytes (Yona et al., 2013). In contrast, lung MO-AMs have a limited ability of self-maintenance and are replenished by macrophages recruited from circulating inflammatory monocytes in the peripheral blood (Iwasaki, 2016). Hence, location and origin are the two principal determinants of macrophage characteristics in the lungs (Zhou and Moore, 2018). TR-AMs appear to limit their own plasticity due to their prolonged residence in the tissue to facilitate tissue homeostasis, whereas MO-AMs are more plastic to an inflammatory state (Guilliams and Svedberg, 2021). For example, CCR2-deficient mic with fewer circulating monocytes (Serbina and Pamer, 2006) are showing less susceptibility to influenza virus infection and lower morbidity and mortality (Lin et al., 2008). MO-AMs and TR-AMs have similar phenotypes in the early stages of influenza virus infection, but have different transcriptional and epigenetic profiles and show unique functions (MacLean et al., 2022). Within 1 month of influenza infection, MO-AMs are transcriptionally similar to monocytes and produce more interleukin-6 (IL-6) upon stimulation. After 2 months of influenza infection, recruited and resident AMs become similar in transcription and function, whereas MO-AMs lose plasticity and are not providing antimicrobial protection, playing a similar role to TR-AMs in balancing lipolysis to remove surfactant from the alveoli at steady-state conditions (Aegerter et al., 2020; Kulikauskaite and Wack, 2020).

2.2. Variable polarization of macrophages in influenza virus infection

Macrophages can be imprinted with different roles depending on the microenvironment. Upon influenza virus infection, macrophage polarization has occurred in the presence of environmental stimuli, in which activated macrophages can become M1 related to Th1 cytokine responses, or M2 relevant to Th2 cytokines. The phenotype of proinflammatory M1 is referred to as classically activated macrophages. M2 macrophages are referred to as alternatively activated macrophages and exert anti-inflammatory cell functions and boost tissue recovery (Stein et al., 1992). On the basis of the cytokines that induce M2 macrophages and their gene expression profiles, M2 macrophages can be further classified into the categories (M2a, b, c, and d; Mantovani et al., 2004). An overview of the types of polarization, secretory molecules, and major functions of M1 and M2 macrophages is given in Table 1.

During the disease process, timely changes in the polarization status of M1/M2 macrophages are critical to the overall healing process. In early virus invasion, M1 macrophage dominance promotes an inflammatory response to clear pathogens, after which M2 type dominance can facilitate tissue healing (Alvarez et al., 2016). If M1 macrophages persistently survive predominantly, which results in immunopathological damage to the organism and impedes tissue

10.3389/fmicb.2023.1260543

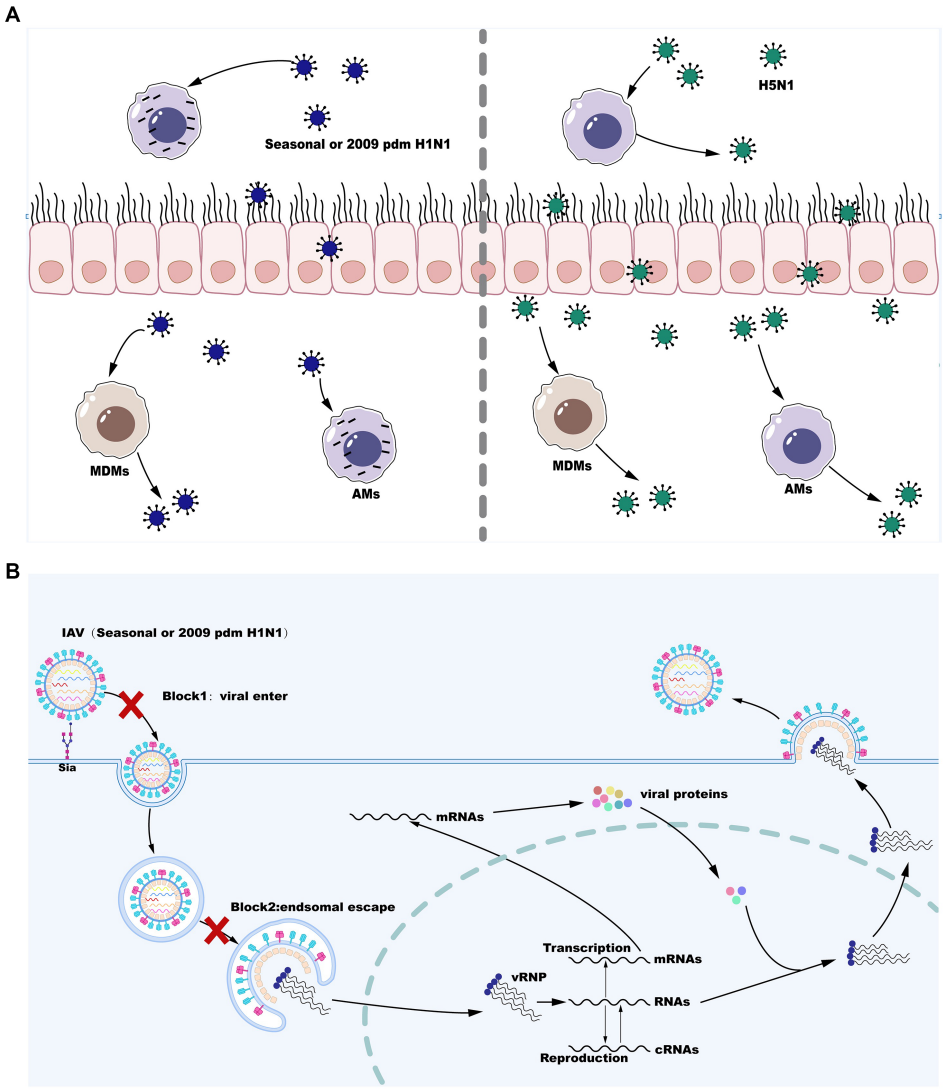

FIGURE 1
Influenza A virus (IAV) reproduction efficiency in MDMs and AMs. **(A)** Seasonal H1N1 or 2009 pdm H1N1 infection in MDMs is productively replicated, whereas seasonal H1N1 or 2009 pdm H1N1 infection in AMs is abortive. However, infection with some strains of H5N1 is productively replicated in both MDMs and AMs. **(B)** IAV replication blocks in AMs infection with seasonal H1N1 or 2009 pdm H1N1.

healing (Alvarez et al., 2016). Influenza virus-induced GM-CSF decreases proinflammatory macrophages by re-directing macrophages to a more "M2-like" activation state from a "M1-like" type by altering the ratio of CXCL9 to CCL17 in BAL (Halstead et al., 2018). In A(H1N1), A(H3N2), and A(H9N2) virus infection, macrophages undergo M1 polarization at 4 hpi and M2b polarization at 8 hpi, which is modulated by the PI3K/Akt signaling (Zhao et al., 2014) and by the autophagy and exosome production (Xia et al., 2022). In contrast to H1N1 virus infection, a well-defined set of dysregulated genes and pathways that occurred in the M1 subtype is specific to H5N1 virus-infected macrophages, leading to an exacerbation of pathology of H5N1 infection (Zhang et al., 2018). However, the AMs polarization following influenza virus infection is multifactorial and complex. Influenza virus infection induces M1-polarized AMs in early stages and M2b-polarized AMs in the middle stage (Zhao et al., 2014). M1-polarized AMs have a lower endosomal pH and facilitate viral replication, whereas M2-polarized AMs have a higher endosomal pH but a lower lysosomal pH and restrict SARS-CoV-2 infection (Lv et al., 2021; Wang Z. et al., 2022). The M1 state of AMs toward the M2 state is associated with the increased severity and inflammatory responses to influenza virus infection (Lauzon-Joset et al., 2019). Therefore, characterizing the variations and ratios of M1 and M2 in the lungs with different doses and infection times contributes to regulating lung injury following influenza virus infection (Yao et al., 2022).

Macrophages differ in their differentiation status after influenza virus infection. M1 macrophages produce the proinflammatory TNF-α and iNOS, while M2 macrophages express IL-10 and TGF-β. M2 macrophages express the macrophage mannose receptor CD206, produce high levels of arginase-1 (Arg-1), and enhanced phagocytic capacity, which has a protective role in influenza virus infection (Gordon, 2003; Campbell et al., 2015). It has been demonstrated that M2 macrophages are more susceptible to apoptotic cell death than M1 macrophages following IAV infection (Campbell et al., 2015). Expression of the macrophage mannose receptor is upregulated in

TABLE 1 The polarization types, secreted molecules, and main functions of macrophages.

Phenotypes	Secreted molecules	Main functions
M1	IL-1β, IL-12, IL-23, IL-10, TNF, IL-6, iNOS, CCL2, CCL3, CCL4, CCL5, CCL9, and CCL10	Th1 responses; antimicrobial properties; and tumor resistance
M2a	Arg, IL-10, IL-1Ra, TGF-β, CCL17, and CCL22	Th2 responses; tissue remodeling; wound healing; and anti-inflammatory
M2b	IL-10, IL-12, TNF, IL-1β, IL-6, and CCL1	Th2 activation; immune regulation; tumor progression; and promoting infections
M2c	IL-10, TGF-β, and MerTK	Immune regulation; tissue remodeling; and phagocyte apoptotic cells
M2d	IL-10, VEGF	Angiogenesis; tumor progression

M2-polarized macrophages (Jablonski et al., 2015; Roszer, 2015), this may explain why M2 macrophages are more susceptible to IAV infection. Importantly, although IAV-infected M1 macrophages produce the highest expression of proinflammatory cytokines including TNF-α, IAV-infected M2 macrophages can override the anti-inflammatory cytokines profile of these cells and cause them to secret TNF-α and other M1-like cytokines. Interestingly, these findings are only observed during the infection of macrophages with HPAI H5N1 and WSN viruses (Cline et al., 2013; Marvin et al., 2017), which have been shown to replicate productively in macrophages, these findings may explain the hypercytokinemia and enhanced inflammatory response in severe H5N1 infection.

3. Regulating inflammation

3.1. The sentinel role of macrophages

Alveolar macrophages display a state of relative quiescence, produce cytokines at low levels, and inhibit innate and adaptive immunity induction in the absence of infection (Hussell and Bell, 2014). After the influenza virus invades the epithelial barrier, AMs are the innate immune cells that can respond in the early stages of infection to initiate and evoke innate immunity. In addition to their vital phagocytic function, AMs also encode a variety of pattern-recognition receptors (PRRs) essential for the sensing of pathogens and tissue damage (Janeway and Medzhitov, 2002). Toll-like receptor (TLR) 3 is expressed by macrophages and recognizes viral RNA structures in phagocytosed IAV-infected cells (Schulz et al., 2005). TLR3 activation induces the upregulated expression of nuclear factor κB (NF-κB)-regulatory proinflammatory cytokines as well as the expression of IFN-I and IFN-stimulated genes (ISGs) regulated by interferon regulatory factor 3 (IRF3). When IFN-I binds to the IFNα/β receptor (IFNAR), a heterodimer consisting of two subunits, IFNAR1 and IFNAR2, it activates the Janus kinase/signal transducers and activators of transcription (JAK/STAT) pathway to induce the expression of ISGs, thereby inhibiting viral replication (Makris et al., 2017). Meanwhile, macrophages-expressed TLR7 and TLR8 sense IAV ssRNA liberated from engulfed cells (Diebold et al., 2004; Lund et al., 2004; Iwasaki and Pillai, 2014), which engage the viral RNA signal in a manner dependent on myeloid differentiation primary response gene 88 (MyD88) and then activate transcription factors NF-κB and IRF7. Following influenza virus infection, IAV proteins and nucleic acids produced by apoptotic cells are released into the extracellular space. For instance, IAV infection activates TLR4 pathway in lung macrophages by recognizing IAV nucleoprotein (NP), though whether NP triggers IFN-β production via TLR4 is not measured (Kim et al., 2022). Accumulating results suggest that and several host-derived damage-associated molecular patterns (DAMPs) can activate TLR4 pathway and trigger proinflammatory cytokines release, such as high-mobility group box 1 protein (HMGB1) and oxidized phospholipids (Imai et al., 2008; Shirey et al., 2016; Bertheloot and Latz, 2017). Moreover, RNA intermediates of IAV replication can be sensed by retinoic-acid inducible gene I (RIG-I) in the nucleus, resulting in the expression of IFN-I and proinflammatory cytokines (Liu et al., 2018). Viral ribonucleoproteins (vRNPs) are potentially recognized by Z-DNA-binding protein 1 (ZBP1), which triggers the activation of NLRP3 inflammasome to release IL-1β and IL-18 (Kuriakose et al., 2016). An overview of macrophage sensing implicated in IAV infection is provided in Figure 2.

It has been demonstrated that primary human macrophages can be infected by the avian H5N1 and seasonal H1N1 influenza viruses (Lee et al., 2009) and murine BMDMs can also be infected by the H1N1 and H5N1 viruses efficiently (Chan et al., 2012). Upon influenza virus infection, macrophages produced IFN-I and other cytokines including type III IFNs, IL-12, IL-1β, tumor necrosis factor-alpha (TNF-α), IL-6, and several chemokines are induced through different pathways. Responsiveness of macrophages and induction of IFN-I play a crucial role in protecting the lower respiratory tract, limiting viral spread, and effective immune protection against influenza virus infection. For instance, following influenza virus infection, AMs-produced IFN-I plays a role of immune protection through the promotion of hematopoietic cell proliferation and differentiation (Essers et al., 2009; Sato et al., 2009) and the upregulation of chemokine (C-C motif) ligand 2 (CCL2), which is necessary for CCR2-dependent Ly6C^{hi} monocyte egress from the bone marrow. However, IFNα/β IFNα/β may be exacerbated during virus infection by hindering viral control (Guarda et al., 2011; Teijaro et al., 2013) or by causing inflammation and tissue damage that exacerbate the disease (Hogner et al., 2013; Davidson et al., 2014). Moreover, IFN-γ is a major cytokine associated with M1 activation and is also involved in the M1/M2 paradigm together with LPS. The M1/M2 polarization following influenza virus infection will be discussed in the other section. In addition, IFN-λ is produced earlier and more frequently than IFN-I in influenza infection, which establishes the cellular state of viral resistance and induces a similar ISGs signature. Because of the abundant expression of IFN-λ in the initial stage of infection, IFN-λ signaling in macrophages likely plays a crucial role in combating influenza infection (Mallampalli et al., 2021). During influenza virus infection, IFN-λ is produced mainly by alveolar type II epithelial cells (ATIIs; Wang et al., 2009) and limits virus infection in respiratory and gastrointestinal epithelial cells since the expression of functional interferon λ receptor (IFNLR) complexes

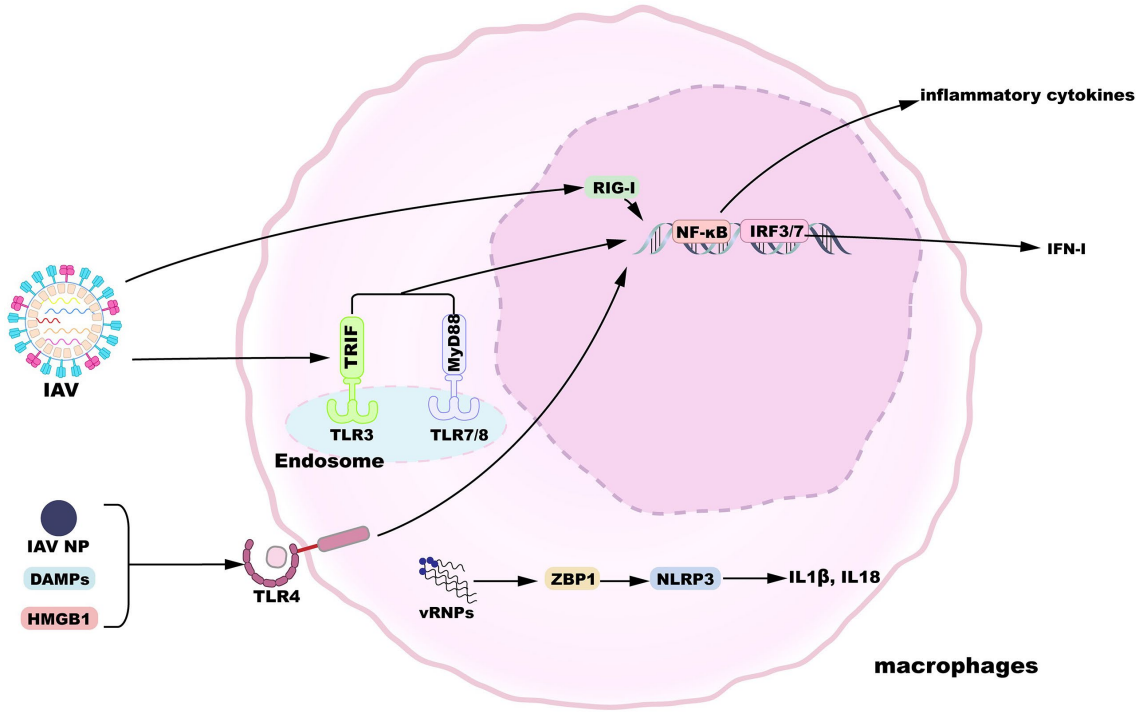

FIGURE 2
Macrophage sensing of influenza virus. TLR3, 7, and 8 can sense incoming virions. TLR4 is activated by HMGB1 or IAV nucleoprotein. TLR engagement results in the activation of proinflammatory or antiviral gene expression downstream of NF-κB or IRF3/7 signaling pathways. Additionally, replication products of IAV are recognized by nuclear RIG-I or ZBP1, inducing gene expression.

in the lungs and intestine is confined to epithelial cells (Mordstein et al., 2010). However, expression of IFNLR1 in macrophages is species-specific since macrophage colony-stimulating factor (M-CSF) or GM-CSF stimulation fails to induce ISGs after IFNL2 or IFNL3 stimulation in mice (Mallampalli et al., 2021). IFN-λ production reduces viral release and suppresses influenza virus-induced secretion of inflammatory cytokines including chemokines and IFN-β (Wang et al., 2009), facilitates the protective immune response of IAV-specific CD8+ T cells (Hemann et al., 2019), and promotes the proliferation and maturation of natural killer cells (Wang et al., 2017), with relatively fewer inflammatory side effects than IFN-α (Davidson et al., 2016).

3.2. The role of macrophages in the induction of excessive inflammatory response

Following influenza virus infection, the severity of the disease depends on the virulence of the influenza virus and host factors (Liu et al., 2016). In the 1918 H1N1 or the H5N1 viruses infection, cytokines and chemokines are excessively induced, causing a hypercytokinemia or "cytokine storm" that results in histopathological changes, systemic sepsis, and multi-organ dysfunction (Tisoncik et al., 2012; Liu et al., 2016; Wei et al., 2022). Recruitment of monocytes and expression of proinflammatory cytokines are upregulated in young mice during IAV infection, with increased secretion of IFN-I, monocyte chemotactic protein 1 (MCP-1), excessive recruitment of inflammatory monocytes, and persistent activation of NLR family pyrin domain containing 3 (NLRP3), resulting in increased mortality in young mice (Coates et al., 2018). Further studies have found that mice lacking NO synthase 2 (NOS2) or TNF have a decreased mortality during influenza virus infection, and that recruited macrophages are the major producers of inducible nitric oxide synthase (iNOS) production and directly responsible for NOS2 and TNF production, maybe the main cell population responsible for immunopathology (Karupiah et al., 1998; Jayasekera et al., 2006; Lin et al., 2008).

Macrophages can cause pathological immunity following influenza virus infection but also secrete cytokines to counteract the over-reactive inflammatory response. IL-10 is a robust anti-inflammatory factor mainly derived from macrophages, which inhibits the overproduction of inflammatory cytokines during infection or tissue injury through negative feedback regulation (Iyer et al., 2010). Inflammatory cytokines comprising IL-1β and TNF are produced in large quantities early in influenza virus infection, and homeostasis-related cytokines including IL-10 emerge later to inhibit the innate immune inflammatory response (Tisoncik et al., 2012; Wang et al., 2012). In addition to IL-10, macrophage-sourced peroxisome proliferator-activated receptor γ (PPAR-γ) suppresses overstated antiviral and inflammatory reactions caused by influenza virus infection (Huang et al., 2019). Level of PPAR-γ is downregulated in macrophages through IFN-dependent signaling during influenza virus infection, whereas expression of genes related to healing injured tissue in late disease such as endothelial and epithelial cell growth factors, is blocked in mice lacking PPAR-γ, suggesting that

macrophage-derived PPAR-γ promotes tissue repair (Huang et al., 2019). Transcription factors also play a key role in regulating the inflammatory and reparative effects of AMs after infection, such as β-catenin and HIF-1α, and deletion of these transcription factors in AMs results in accelerated rates of inflammation and lung repair (Zhu et al., 2021). In addition to AMs, IMs also exhibit another activation phenotype and play an immunomodulatory role in controlling excessive lung inflammation following influenza infection (Ural et al., 2020).

4. IAV infection and macrophage phagocytosis

As professional phagocytes, macrophages perform an instrumental role in clearing infectious organisms through the internalization and degradation of pathogens and by phagocytosis of apoptotic cells. Phagocytosis can be mediated through the phagocytic receptors on the surface of macrophages including mannose receptors, scavenger receptors (SRs), complement receptors, macrophage receptors with collagenous structure (MARCO), CD36, and Fc receptors. Phagocytosis by macrophages of apoptotic IAV-infected cells inhibits further transmission of the virus and facilitates disease control (Watanabe et al., 2005). When the IAV-infected epithelial cells undergo apoptosis, they can be effectively phagocytosed by macrophages at an early stage, which leads to the inhibition of virus growth (Fujimoto et al., 2000). Similarly, IAV-infected mice-derived BAL macrophages incorporate phagocytosed apoptotic cells and IAV-infected mice-derived AMs exhibit enhanced engulf capacity than uninfected mice-derived AMs (Watanabe et al., 2005; Hashimoto et al., 2007). The influenza virus-infected mice are treated with phagocytosis inhibitors, resulting in decreased levels of phagocytosis with BAL cells and increased lethality and lung inflammation in those mice (Watanabe et al., 2005). Further studies have demonstrated that phosphatidylserine (PS) and carbohydrate molecules on the macrophage surface mediate the process of phagocytosis of influenza virus-infected cells, and these molecules are modified by influenza NA expressed in virus-infected cells (Shiratsuchi et al., 2000; Watanabe et al., 2002). During virus-infected cell apoptosis, PS located in the inner layer of the plasmatic membrane is exposed on the cell surface and acts as a potent prophagocytic signal to attract phagocytes (Shiratsuchi and Nakanishi, 2006; Birkle and Brown, 2021). In steady-state conditions, "Do not eat me" signal is activated and prevents cells from being phagocytosed, while virus infection causes a profound reduction of surface silicic acid residues on live influenza virus-infected cells (Nita-Lazar et al., 2015), which promotes phagocytosis of the cells (Meesmann et al., 2010). During influenza virus infection, virus-infected alveolar type II cells and epithelial cells can release the find-me signals to direct macrophages toward their positions and facilitate their phagocytoses, such as C-X-C Motif chemokine ligand 10 (CXCL10) and other chemokines including CXCL8/12 (Birkle and Brown, 2021). Furthermore, the complement system and PPRs also play an important role in rapidly mobilizing macrophages to the destination location shortly after the infection with the influenza virus and promote phagocyte recognition (Birkle and Brown, 2021). Therefore, apoptosis of cells infected with the influenza virus causes phagocytosis of such cells, and direct clearance of the virus function as a mechanism for the antiviral immune response.

However, excessive clearance is detrimental to the inflammatory response. Further studies have demonstrated that MARCO plays a deleterious role for in early influenza viral immune responses (Ghosh et al., 2011). The enhanced proinflammatory gene induction in macrophages is observed in MARCO-deficient macrophages, and MARCO-deficient mice infected with IAV show improved survival and earlier relief from weight loss and morbidity symptoms (Ghosh et al., 2011). This is mainly due to the removal of proinflammatory oxidized lipoproteins from cellular debris by MARCO, which inhibits the early inflammatory response (Ghosh et al., 2011). Oxidized phospholipids are recognition signals released by apoptotic cells that promote phagocytosis of apoptotic cells, while inducing several proinflammatory genes such as MCP1 and IL-8 facilitate the resolution of acute inflammation (Kadl et al., 2004). Furthermore, it has been revealed that after sensing pathogens, macrophages can crawl through the pores of Kohn between alveoli and engulf pathogens with high phagocytic efficiency, whereas influenza virus infection impairs macrophages crawling through IFN-γ signaling, causing inappropriate inflammation and injury by excessive induction of neutrophil and increasing secondary bacterial infection (Neupane et al., 2020). Additionally, AMs have higher levels of phagocytic activity and faster phagocytic processes than IMs, while IMs located in interstitial locations with lower phagocytic capacity can engulf pathogens that escape from AMs, thus reducing the spread of pathogens within the organism (Fathi et al., 2001).

The phagocytic capacity of macrophages is also affected following influenza virus infection, and macrophage phagocytic activity against apoptotic cells is increased *in vitro* when macrophages are incubated with the supernatant from IAV-infected epithelial cells (Hashimoto et al., 2007). And cells infected with the influenza virus undergoing apoptosis can release heat-labile substances that stimulate the phagocytic activity of macrophages (Hashimoto et al., 2007). Environmental pollutants, cigarette smoke, and alcohol also can inhibit the phagocytosis of macrophages (Karavitis and Kovacs, 2011). Moreover, older adults have comparatively lower macrophage numbers and reproductive capacity, and exhibit higher mortality after influenza virus infection due to selective downregulation of the clearance receptor CD204 (Wong et al., 2017). The AMs of offspring of pregnant mice infected with the influenza virus have a reduced ability to clear influenza B virus and MRSA and are more susceptible to influenza virus infection (Jacobsen et al., 2021).

5. IAV-induced secondary bacterial pneumonia involves lung macrophages

Secondary bacterial pneumonia is another dominant cause of fatalities caused by IAV infection (Smith and McCullers, 2014) and is the main cause of human mortality for the 1918 Spanish flu (Morens et al., 2008). Many studies have shown that the progression of secondary bacterial infections is regulated by IAV proteins. For example, non-structural protein 1 (NS1) affects the regulation of the interferon response and its motif acts directly in influenza virus and *S. pneumoniae* co-infections (Shepardson et al., 2019). NA also facilitates access to receptors and nutrients for *S. pneumoniae* and thereby promotes the development of bacterial infection (Feng et al., 2013; Siegel et al., 2014), whereas matrix 1 protein (M1; Halder et al.,

2011), NP (Tripathi et al., 2013), M2 (Ichinohe et al., 2010), and HA (Klonoski et al., 2018) indirectly help in secondary bacterial infection development. In addition to functional defects, influenza virus infection decreases the number of AMs, resulting in increased susceptibility to bacterial superinfections (Ghoneim et al., 2013).

Multiple pathways of secondary bacterial pneumonia caused by IAV infection in relation to lung macrophages have been reported. As a preliminary point, AMs susceptibility to IAV-induced apoptosis promotes secondary bacterial infection by reducing anti-microbial lung macrophages (Ghoneim et al., 2013). This is also supported by the findings that the risk of secondary pneumococcal pneumonia decreased on the 14th day after infection with IAV, coinciding with a recovery in the number of AMs (Ghoneim et al., 2013). Moreover, inappropriate expression of cytokines can increase the risk of secondary bacterial infections by modulating macrophages. For example, IL-27 regulates the enhancement of *S. aureus* pneumonia susceptibility after influenza virus infection through the induction of IL-10 and the inhibition of IL-17 (Robinson et al., 2015). IFN-I production induced by IAV infection also enhances the susceptibility to secondary bacterial pneumonia because influenza-infected IFNAR−/− mice show increased survival and an increased capacity to clear secondary *S. pneumoniae* infection (Shahangian et al., 2009). In another study, IAV-induced IFN-γ inhibits the expression of MARCO by macrophages, thereby further inhibiting the uptake and killing *S. pneumoniae* during superinfections (Sun and Metzger, 2008). Additionally, influenza virus infection also chronically inhibits the ability of AMs to respond to TLR ligands. TLR9 expression on the surface of macrophages is upregulated after IAV infection (Martinez-Colon et al., 2019). It has been reported that TLR9-deficient mice show an increased expression of scavenger receptor A and iNOS on macrophages and an increased phagocytosis and killing of bacteria after influenza virus infection (Martinez-Colon et al., 2019). Anyway, these studies are mainly based on the findings that did not consider the lung microbiota, so it is imperative to include the role of the respiratory microbiome in influenza and secondary bacterial superinfections.

6. Involved in adaptive immune responses

Adaptive response, including CD4+ Th cells, CD8+ cytotoxic T lymphocytes (CTLs), B cells, and antigen-specific antibodies. Antigen-presenting cells (APCs) take up foreign substances and further degraded and presented them to T cells via MHC I or II molecules, or to T cells via other APCs. Endogenously processed viral peptides are presented by MHC I molecules on virus-infected cells surface and recognized by naive CD8+ T cells, which induces naive CD8+ T cells to differentiate into cytotoxic T cells that can recognize and kill virus-infected cells, whereas naive CD4+ T cells recognize exogenously processed peptides presented by MHC II molecules and differentiate through different pathways to generate effector subpopulations with different immune functions such as Th1 cells, Th2 cells, T follicular helper (Tfh), Th17 cells, and regulatory T cells (Tregs), which regulate the activation of target cells (Jin et al., 2012; Roche and Furuta, 2015). Th1 cells in the respiratory tract are activated following influenza virus infection, resulting in the production of TNF-α, IL-2, and IFN-γ (Zhu et al., 2010). Although T cell-mediated immune responses have a limited role in preventing initial viral replication, IFN-γ-producing Th1 cells are necessary for CD8+ T-cell activation and clearance of influenza virus and in preparation for recurrent infection. After influenza virus infection, Th2 cell-mediated immune responses aggravate lung tissue injury and postpone viral elimination (Graham et al., 1994). Highly specific and memorized humoral responses require the involvement of Tfh cells, whereas Th17 cells are involved in viral pathogenicity because influenza antigens-induced Th17 cells increase lung inflammation and morbidity after influenza virus challenging (Maroof et al., 2014; Miyauchi, 2017). However, other studies have suggested that the adoptive transfer of Th17 cells protects naive mice from a deadly flu challenge and defense against bacterial infections following influenza virus infection (McKinstry et al., 2009; Kudva et al., 2011). Furthermore, IAV stimulates the migration of Tregs into the lungs, this leads to a reduction in the cell number of Th17 cells and infiltrated neutrophils as well as diminished lung inflammation (Egarnes and Gosselin, 2018). Collectively, the viral sensing system detects influenza virus infection and releases chemokines to facilitate the migration of naive T cells, induce cytokines signaling, and convert APCs to effector T cells.

Antigen-presenting cells are important mediators that bridge the innate immune responses and adaptive immune system. The major APCs in activated naive T cells are DCs, which are the main initiating APCs and are induced to move toward local lymphatic tissues to present antigens and activate naive T cells under infection and inflammation conditions (Itano and Jenkins, 2003). Unlike DCs, tissue-resident macrophages are usually non-migratory and virus invasion does not cause them to migrate to lymphoid tissue, and therefore AMs have a limited role in antigen presentation and mostly maintain homeostasis of the lungs (Itano and Jenkins, 2003; Hou et al., 2021). Macrophages may be more important for the local amplification of T-cell responses already initiated by DCs. Macrophages rely on phagocytosis for antigen uptake, phagocytose and degrade them into peptides for presentation, while intracellular signaling is triggered by recognition of influenza virus by TLRs (Roche and Furuta, 2015; Koutsakos et al., 2019). Importantly, IMs are found to be more competent than AMs in driving T cell responses (Zaynagetdinov et al., 2013).

Efficacious humoral responses in the period of influenza virus infection encompass the induction of virus-specific neutralizing antibodies against viral HA and NA in an attempt to block infection, which is predominantly strain-specific (Waffarn and Baumgarth, 2011). It has been demonstrated that macrophages also promote humoral immunity. Recent studies have revealed that influenza virus rechallenge induces resident memory B (RMB) cell mobility and fast relocation to infected sites, subsequently differentiates into plasma cells and therefore leads to increased local antibody concentrations, this process is mediated by AMs, partly due to the induction of CXCL9 and CXCL10 expression (MacLean et al., 2022). These findings suggest that it will be useful to integrate strategies for inducing the concentration of cross-reactive antibodies at or near the location of viral entry (Iwasaki, 2016). Antigenic exposure at mucosal sites directly induces innate immune memory in tissue-resident macrophages populations, which are a new vaccine target for the development a novel type of adjuvants and of respiratory mucosal vaccine against influenza virus (Xing et al., 2020; Wang X. et al., 2022).

7. Conclusions and future perspective

The uncontrolled spread of influenza viruses places a burden on the public health of society and creates a serious threat to human life and health. The most seasonal and low pathogenic strains of the influenza virus cause an abortive infection in macrophages and therefore contribute to effective host defense, whereas some highly pathogenic strains of IAV infect macrophages productively. Given the diversity and plasticity of macrophages, elucidating the complicated interactions between macrophage phenotype and influenza virus infection will be helpful for deciphering the mechanisms implicating severe influenza disease. The development of single cell omics has led to new information regarding lung macrophages subtypes (Aegerter et al., 2022). Moreover, the advent of newer technologies of lineage tracing have improved our understanding of the plasticity of macrophages during and after infection, particularly in relation to AM subsets that originate from yolk sac macrophages versus MDMs. In the future, we can identify host restriction factors that determine abortive versus productive infection in macrophage types and distinguish different macrophages, and define biological agents that regulate the migration and differentiation of lung macrophages following influenza virus infection, these studies are also likely to provide new solutions for treatment and therapy options.

Author contributions

FW: Conceptualization, Project administration, Supervision, Writing – original draft, Writing – review & editing. HL: Writing – original draft, Writing – review & editing. YZ: Conceptualization, Supervision, Writing – original draft, Writing – review & editing. AW: Writing –original draft, Writing – review & editing.

Funding

The author(s) declare financial support was received for the research, authorship, and/or publication of this article. This work was supported by the Ningxia Natural Science Foundation of China (2021AAC05006) and the National Natural Science Foundation of China (NSFC; 31972669 and 81960297).

Conflict of interest

The authors declare that the research was conducted in the absence of any commercial or financial relationships that could be construed as a potential conflict of interest.

Publisher's note

All claims expressed in this article are solely those of the authors and do not necessarily represent those of their affiliated organizations, or those of the publisher, the editors and the reviewers. Any product that may be evaluated in this article, or claim that may be made by its manufacturer, is not guaranteed or endorsed by the publisher.

References

Aegerter, H., Kulikauskaite, J., Crotta, S., Patel, H., Kelly, G., Hessel, E. M., et al. (2020). Influenza-induced monocyte-derived alveolar macrophages confer prolonged antibacterial protection. *Nat. Immunol.* 21, 145–157. doi: 10.1038/s41590-019-0568-x

Aegerter, H., Lambrecht, B. N., and Jakubzick, C. V. (2022). Biology of lung macrophages in health and disease. *Immunity* 55, 1564–1580. doi: 10.1016/j.immuni.2022.08.010

Alvarez, M. M., Liu, J. C., Trujillo-de Santiago, G., Cha, B. H., Vishwakarma, A., Ghaemmaghami, A. M., et al. (2016). Delivery strategies to control inflammatory response: modulating M1-M2 polarization in tissue engineering applications. *J. Control. Release* 240, 349–363. doi: 10.1016/j.jconrel.2016.01.026

Bedoret, D., Wallemacq, H., Marichal, T., Desmet, C., Quesada Calvo, F., Henry, E., et al. (2009). Lung interstitial macrophages alter dendritic cell functions to prevent airway allergy in mice. *J. Clin. Invest.* 119, 3723–3738. doi: 10.1172/JCI39717

Bertheloot, D., and Latz, E. (2017). HMGB1, IL-1alpha, IL-33 and S100 proteins: dual-function alarmins. *Cell. Mol. Immunol.* 14, 43–64. doi: 10.1038/cmi.2016.34

Birkle, T., and Brown, G. C. (2021). I'm infected, eat me! Innate immunity mediated by live, infected cells Signaling to be phagocytosed. *Infect. Immun.* 89:e00476-20. doi: 10.1128/IAI.00476-20

Campbell, G. M., Nicol, M. Q., Dransfield, I., Shaw, D. J., Nash, A. A., and Dutia, B. M. (2015). Susceptibility of bone marrow-derived macrophages to influenza virus infection is dependent on macrophage phenotype. *J. Gen. Virol.* 96, 2951–2960. doi: 10.1099/jgv.0.000240

Chan, R. W., Leung, C. Y., Nicholls, J. M., Peiris, J. S., and Chan, M. C. (2012). Proinflammatory cytokine response and viral replication in mouse bone marrow derived macrophages infected with influenza H1N1 and H5N1 viruses. *PLoS One* 7:e51057. doi: 10.1371/journal.pone.0051057

Chu, V. C., and Whittaker, G. R. (2004). Influenza virus entry and infection require host cell N-linked glycoprotein. *Proc. Natl. Acad. Sci. U. S. A.* 101, 18153–18158. doi: 10.1073/pnas.0405172102

Cline, T. D., Beck, D., and Bianchini, E. (2017). Influenza virus replication in macrophages: balancing protection and pathogenesis. *J. Gen. Virol.* 98, 2401–2412. doi: 10.1099/jgv.0.000922

Cline, T. D., Karlsson, E. A., Seufzer, B. J., and Schultz-Cherry, S. (2013). The hemagglutinin protein of highly pathogenic H5N1 influenza viruses overcomes an early block in the replication cycle to promote productive replication in macrophages. *J. Virol.* 87, 1411–1419. doi: 10.1128/JVI.02682-12

Coates, B. M., Staricha, K. L., Koch, C. M., Cheng, Y., Shumaker, D. K., Budinger, G. R. S., et al. (2018). Inflammatory monocytes drive influenza a virus-mediated lung injury in juvenile mice. *J. Immunol.* 200, 2391–2404. doi: 10.4049/jimmunol.1701543

Corry, J., Kettenburg, G., Upadhyay, A. A., Wallace, M., Marti, M. M., Wonderlich, E. R., et al. (2022). Infiltration of inflammatory macrophages and neutrophils and widespread pyroptosis in lung drive influenza lethality in nonhuman primates. *PLoS Pathog.* 18:e1010395. doi: 10.1371/journal.ppat.1010395

Davidson, S., Crotta, S., McCabe, T. M., and Wack, A. (2014). Pathogenic potential of interferon alphabeta in acute influenza infection. *Nat. Commun.* 5:3864. doi: 10.1038/ncomms4864

Davidson, S., McCabe, T. M., Crotta, S., Gad, H. H., Hessel, E. M., Beinke, S., et al. (2016). IFNlambda is a potent anti-influenza therapeutic without the inflammatory side effects of IFNalpha treatment. *EMBO Mol. Med.* 8, 1099–1112. doi: 10.15252/emmm.201606413

Desch, A. N., Gibbings, S. L., Goyal, R., Kolde, R., Bednarek, J., Bruno, T., et al. (2016). Flow cytometric analysis of mononuclear phagocytes in nondiseased human lung and lung-draining lymph nodes. *Am. J. Respir. Crit. Care Med.* 193, 614–626. doi: 10.1164/rccm.201507-1376OC

Diebold, S. S., Kaisho, T., Hemmi, H., Akira, S., and Reis e Sousa, C. (2004). Innate antiviral responses by means of TLR7-mediated recognition of single-stranded RNA. *Science* 303, 1529–1531. doi: 10.1126/science.1093616

Dranoff, G., Crawford, A. D., Sadelain, M., Ream, B., Rashid, A., Bronson, R. T., et al. (1994). Involvement of granulocyte-macrophage colony-stimulating factor in pulmonary homeostasis. *Science* 264, 713–716. doi: 10.1126/science.8171324

Egarnes, B., and Gosselin, J. (2018). Contribution of regulatory T cells in nucleotide-binding oligomerization domain 2 response to influenza virus infection. *Front. Immunol.* 9:132. doi: 10.3389/fimmu.2018.00132

Essers, M. A., Offner, S., Blanco-Bose, W. E., Waibler, Z., Kalinke, U., Duchosal, M. A., et al. (2009). IFNalpha activates dormant haematopoietic stem cells in vivo. *Nature* 458, 904–908. doi: 10.1038/nature07815

Fathi, M., Johansson, A., Lundborg, M., Orre, L., Skold, C. M., and Camner, P. (2001). Functional and morphological differences between human alveolar and interstitial macrophages. *Exp. Mol. Pathol.* 70, 77–82. doi: 10.1006/exmp.2000.2344

Feng, C., Zhang, L., Nguyen, C., Vogel, S. N., Goldblum, S. E., Blackwelder, W. C., et al. (2013). Neuraminidase reprograms lung tissue and potentiates lipopolysaccharide-induced acute lung injury in mice. *J. Immunol.* 191, 4828–4837. doi: 10.4049/jimmunol.1202673

Fujimoto, I., Pan, J., Takizawa, T., and Nakanishi, Y. (2000). Virus clearance through apoptosis-dependent phagocytosis of influenza a virus-infected cells by macrophages. *J. Virol.* 74, 3399–3403. doi: 10.1128/JVI.74.7.3399-3403.2000

Ghoneim, H. E., Thomas, P. G., and McCullers, J. A. (2013). Depletion of alveolar macrophages during influenza infection facilitates bacterial superinfections. *J. Immunol.* 191, 1250–1259. doi: 10.4049/jimmunol.1300014

Ghosh, S., Gregory, D., Smith, A., and Kobzik, L. (2011). MARCO regulates early inflammatory responses against influenza: a useful macrophage function with adverse outcome. *Am. J. Respir. Cell Mol. Biol.* 45, 1036–1044. doi: 10.1165/rcmb.2010-0349OC

Gordon, S. (2003). Alternative activation of macrophages. *Nat. Rev. Immunol.* 3, 23–35. doi: 10.1038/nri978

Graham, M. B., Braciale, V. L., and Braciale, T. J. (1994). Influenza virus-specific CD4+ T helper type 2 T lymphocytes do not promote recovery from experimental virus infection. *J. Exp. Med.* 180, 1273–1282. doi: 10.1084/jem.180.4.1273

Guarda, G., Braun, M., Staehli, F., Tardivel, A., Mattmann, C., Forster, I., et al. (2011). Type I interferon inhibits interleukin-1 production and inflammasome activation. *Immunity* 34, 213–223. doi: 10.1016/j.immuni.2011.02.006

Guilliams, M., De Kleer, I., Henri, S., Post, S., Vanhoutte, L., De Prijck, S., et al. (2013). Alveolar macrophages develop from fetal monocytes that differentiate into long-lived cells in the first week of life via GM-CSF. *J. Exp. Med.* 210, 1977–1992. doi: 10.1084/jem.20131199

Guilliams, M., and Svedberg, F. R. (2021). Does tissue imprinting restrict macrophage plasticity? *Nat. Immunol.* 22, 118–127. doi: 10.1038/s41590-020-00849-2

Halder, U. C., Bagchi, P., Chattopadhyay, S., Dutta, D., and Chawla-Sarkar, M. (2011). Cell death regulation during influenza a virus infection by matrix (M1) protein: a model of viral control over the cellular survival pathway. *Cell Death Dis.* 2:e197. doi: 10.1038/cddis.2011.75

Halstead, E. S., Umstead, T. M., Davies, M. L., Kawasawa, Y. I., Silveyra, P., Howyrlak, J., et al. (2018). GM-CSF overexpression after influenza a virus infection prevents mortality and moderates M1-like airway monocyte/macrophage polarization. *Respir. Res.* 19:3. doi: 10.1186/s12931-017-0708-5

Hashimoto, Y., Moki, T., Takizawa, T., Shiratsuchi, A., and Nakanishi, Y. (2007). Evidence for phagocytosis of influenza virus-infected, apoptotic cells by neutrophils and macrophages in mice. *J. Immunol.* 178, 2448–2457. doi: 10.4049/jimmunol.178.4.2448

Hemann, E. A., Green, R., Turnbull, J. B., Langlois, R. A., Savan, R., and Gale, M. Jr. (2019). Interferon-lambda modulates dendritic cells to facilitate T cell immunity during infection with influenza a virus. *Nat. Immunol.* 20, 1035–1045. doi: 10.1038/s41590-019-0408-z

Hogner, K., Wolff, T., Pleschka, S., Plog, S., Gruber, A. D., Kalinke, U., et al. (2013). Macrophage-expressed IFN-beta contributes to apoptotic alveolar epithelial cell injury in severe influenza virus pneumonia. *PLoS Pathog.* 9:e1003188. doi: 10.1371/journal.ppat.1003188

Hou, F., Xiao, K., Tang, L., and Xie, L. (2021). Diversity of macrophages in lung homeostasis and diseases. *Front. Immunol.* 12:753940. doi: 10.3389/fimmu.2021.753940

Huang, S., Zhu, B., Cheon, I. S., Goplen, N. P., Jiang, L., Zhang, R., et al. (2019). PPAR-gamma in macrophages limits pulmonary inflammation and promotes host recovery following respiratory viral infection. *J. Virol.* 93:e00030-19. doi: 10.1128/JVI.00030-19

Hume, P. S., Gibbings, S. L., Jakubzick, C. V., Tuder, R. M., Curran-Everett, D., Henson, P. M., et al. (2020). Localization of macrophages in the human lung via design-based stereology. *Am. J. Respir. Crit. Care Med.* 201, 1209–1217. doi: 10.1164/rccm.201911-2105OC

Hussell, T., and Bell, T. J. (2014). Alveolar macrophages: plasticity in a tissue-specific context. *Nat. Rev. Immunol.* 14, 81–93. doi: 10.1038/nri3600

Ichinohe, T., Pang, I. K., and Iwasaki, A. (2010). Influenza virus activates inflammasomes via its intracellular M2 ion channel. *Nat. Immunol.* 11, 404–410. doi: 10.1038/ni.1861

Imai, Y., Kuba, K., Neely, G. G., Yaghubian-Malhami, R., Perkmann, T., van Loo, G., et al. (2008). Identification of oxidative stress and toll-like receptor 4 signaling as a key pathway of acute lung injury. *Cells* 133, 235–249. doi: 10.1016/j.cell.2008.02.043

Itano, A. A., and Jenkins, M. K. (2003). Antigen presentation to naive CD4 T cells in the lymph node. *Nat. Immunol.* 4, 733–739. doi: 10.1038/ni957

Iwasaki, A. (2016). Exploiting mucosal immunity for antiviral vaccines. *Annu. Rev. Immunol.* 34, 575–608. doi: 10.1146/annurev-immunol-032414-112315

Iwasaki, A., and Pillai, P. S. (2014). Innate immunity to influenza virus infection. *Nat. Rev. Immunol.* 14, 315–328. doi: 10.1038/nri3665

Iyer, S. S., Ghaffari, A. A., and Cheng, G. (2010). Lipopolysaccharide-mediated IL-10 transcriptional regulation requires sequential induction of type I IFNs and IL-27 in macrophages. *J. Immunol.* 185, 6599–6607. doi: 10.4049/jimmunol.1002041

Jablonski, K. A., Amici, S. A., Webb, L. M., Ruiz-Rosado Jde, D., Popovich, P. G., Partida-Sanchez, S., et al. (2015). Novel markers to delineate murine M1 and M2 macrophages. *PLoS One* 10:e0145342. doi: 10.1371/journal.pone.0145342

Jacobsen, H., Walendy-Gnirss, K., Tekin-Bubenheim, N., Kouassi, N. M., Ben-Batalla, I., Berenbrok, N., et al. (2021). Offspring born to influenza a virus infected pregnant mice have increased susceptibility to viral and bacterial infections in early life. *Nat. Commun.* 12:4957. doi: 10.1038/s41467-021-25220-3

Janeway, C. A. Jr., and Medzhitov, R. (2002). Innate immune recognition. *Annu. Rev. Immunol.* 20, 197–216. doi: 10.1146/annurev.immunol.20.083001.084359

Jayasekera, J. P., Vinuesa, C. G., Karupiah, G., and King, N. J. C. (2006). Enhanced antiviral antibody secretion and attenuated immunopathology during influenza virus infection in nitric oxide synthase-2-deficient mice. *J. Gen. Virol.* 87, 3361–3371. doi: 10.1099/vir.0.82131-0

Jin, B., Sun, T., Yu, X. H., Yang, Y. X., and Yeo, A. E. (2012). The effects of TLR activation on T-cell development and differentiation. *Clin. Dev. Immunol.* 2012:836485. doi: 10.1155/2012/836485

Kadl, A., Bochkov, V. N., Huber, J., and Leitinger, N. (2004). Apoptotic cells as sources for biologically active oxidized phospholipids. *Antioxid. Redox Signal.* 6, 311–320. doi: 10.1089/152308604322899378

Karavitis, J., and Kovacs, E. J. (2011). Macrophage phagocytosis: effects of environmental pollutants, alcohol, cigarette smoke, and other external factors. *J. Leukoc. Biol.* 90, 1065–1078. doi: 10.1189/jlb.0311114

Karupiah, G., Chen, J. H., Nathan, C. F., Mahalingam, S., and MacMicking, J. D. (1998). Identification of nitric oxide synthase 2 as an innate resistance locus against ectromelia virus infection. *J. Virol.* 72, 7703–7706. doi: 10.1128/JVI.72.9.7703-7706.1998

Kim, C. U., Jeong, Y. J., Lee, P., Lee, M. S., Park, J. H., Kim, Y. S., et al. (2022). Extracellular nucleoprotein exacerbates influenza virus pathogenesis by activating toll-like receptor 4 and the NLRP3 inflammasome. *Cell. Mol. Immunol.* 19, 715–725. doi: 10.1038/s41423-022-00862-5

Kim, H. M., Lee, Y. W., Lee, K. J., Kim, H. S., Cho, S. W., van Rooijen, N., et al. (2008). Alveolar macrophages are indispensable for controlling influenza viruses in lungs of pigs. *J. Virol.* 82, 4265–4274. doi: 10.1128/JVI.02602-07

Klonoski, J. M., Watson, T., Bickett, T. E., Svendsen, J. M., Gau, T. J., Britt, A., et al. (2018). Contributions of influenza virus hemagglutinin and host immune responses toward the severity of influenza virus: *Streptococcus pyogenes* superinfections. *Viral Immunol.* 31, 457–469. doi: 10.1089/vim.2017.0193

Koutsakos, M., McWilliam, H. E. G., Aktepe, T. E., Fritzlar, S., Illing, P. T., Mifsud, N. A., et al. (2019). Downregulation of MHC class I expression by influenza a and B viruses. *Front. Immunol.* 10:1158. doi: 10.3389/fimmu.2019.01158

Kudva, A., Scheller, E. V., Robinson, K. M., Crowe, C. R., Choi, S. M., Slight, S. R., et al. (2011). Influenza a inhibits Th17-mediated host defense against bacterial pneumonia in mice. *J. Immunol.* 186, 1666–1674. doi: 10.4049/jimmunol.1002194

Kulikauskaite, J., and Wack, A. (2020). Teaching old dogs new tricks? The plasticity of lung alveolar macrophage subsets. *Trends Immunol.* 41, 864–877. doi: 10.1016/j.it.2020.08.008

Kuriakose, T., Man, S. M., Malireddi, R. K., Karki, R., Kesavardhana, S., Place, D. E., et al. (2016). ZBP1/DAI is an innate sensor of influenza virus triggering the NLRP3 inflammasome and programmed cell death pathways. *Sci. Immunol.* 1:aag2045. doi: 10.1126/sciimmunol.aag2045

Landsman, L., and Jung, S. (2007). Lung macrophages serve as obligatory intermediate between blood monocytes and alveolar macrophages. *J. Immunol.* 179, 3488–3494. doi: 10.4049/jimmunol.179.6.3488

Lauzon-Joset, J. F., Scott, N. M., Mincham, K. T., Stumbles, P. A., Holt, P. G., and Strickland, D. H. (2019). Pregnancy induces a steady-state shift in alveolar macrophage M1/M2 phenotype that is associated with a heightened severity of influenza virus infection: mechanistic insight using mouse models. *J. Infect. Dis.* 219, 1823–1831. doi: 10.1093/infdis/jiy732

Lee, S. M., Gardy, J. L., Cheung, C. Y., Cheung, T. K., Hui, K. P., Ip, N. Y., et al. (2009). Systems-level comparison of host-responses elicited by avian H5N1 and seasonal H1N1 influenza viruses in primary human macrophages. *PLoS One* 4:e8072. doi: 10.1371/journal.pone.0008072

Liegeois, M., Legrand, C., Desmet, C. J., Marichal, T., and Bureau, F. (2018). The interstitial macrophage: a long-neglected piece in the puzzle of lung immunity. *Cell. Immunol.* 330, 91–96. doi: 10.1016/j.cellimm.2018.02.001

Lin, K. L., Suzuki, Y., Nakano, H., Ramsburg, E., and Gunn, M. D. (2008). CCR2+ monocyte-derived dendritic cells and exudate macrophages produce influenza-induced pulmonary immune pathology and mortality. *J. Immunol.* 180, 2562–2572. doi: 10.4049/jimmunol.180.4.2562

Liu, G., Lu, Y., Thulasi Raman, S. N., Xu, F., Wu, Q., Li, Z., et al. (2018). Nuclear-resident RIG-I senses viral replication inducing antiviral immunity. *Nat. Commun.* 9:3199. doi: 10.1038/s41467-018-05745-w

Liu, R., Sheng, Z., Huang, C., Wang, D., and Li, F. (2020). Influenza D virus. *Curr. Opin. Virol.* 44, 154–161. doi: 10.1016/j.coviro.2020.08.004

Liu, Q., Zhou, Y. H., and Yang, Z. Q. (2016). The cytokine storm of severe influenza and development of immunomodulatory therapy. *Cell. Mol. Immunol.* 13, 3–10. doi: 10.1038/cmi.2015.74

Londrigan, S. L., Short, K. R., Ma, J., Gillespie, L., Rockman, S. P., Brooks, A. G., et al. (2015). Infection of mouse macrophages by seasonal influenza viruses can be restricted at the level of virus entry and at a late stage in the virus life cycle. *J. Virol.* 89, 12319–12329. doi: 10.1128/JVI.01455-15

Lund, J. M., Alexopoulou, L., Sato, A., Karow, M., Adams, N. C., Gale, N. W., et al. (2004). Recognition of single-stranded RNA viruses by toll-like receptor 7. *Proc. Natl. Acad. Sci. U. S. A.* 101, 5598–5603. doi: 10.1073/pnas.0400937101

Lv, J., Wang, Z., Qu, Y., Zhu, H., Zhu, Q., Tong, W., et al. (2021). Distinct uptake, amplification, and release of SARS-CoV-2 by M1 and M2 alveolar macrophages. *Cell Discov.* 7:24. doi: 10.1038/s41421-021-00258-1

MacLean, A. J., Richmond, N., Koneva, L., Attar, M., Medina, C. A. P., Thornton, E. E., et al. (2022). Secondary influenza challenge triggers resident memory B cell migration and rapid relocation to boost antibody secretion at infected sites. *Immunity* 55, 718–733.e8. doi: 10.1016/j.immuni.2022.03.003

Maines, T. R., Szretter, K. J., Perrone, L., Belser, J. A., Bright, R. A., Zeng, H., et al. (2008). Pathogenesis of emerging avian influenza viruses in mammals and the host innate immune response. *Immunol. Rev.* 225, 68–84. doi: 10.1111/j.1600-065X.2008.00690.x

Makris, S., Paulsen, M., and Johansson, C. (2017). Type I interferons as regulators of lung inflammation. *Front. Immunol.* 8:259. doi: 10.3389/fimmu.2017.00259

Mallampalli, R. K., Adair, J., Elhance, A., Farkas, D., Chafin, L., Long, M. E., et al. (2021). Interferon lambda Signaling in macrophages is necessary for the antiviral response to influenza. *Front. Immunol.* 12:735576. doi: 10.3389/fimmu.2021.735576

Mantovani, A., Sica, A., Sozzani, S., Allavena, P., Vecchi, A., and Locati, M. (2004). The chemokine system in diverse forms of macrophage activation and polarization. *Trends Immunol.* 25, 677–686. doi: 10.1016/j.it.2004.09.015

Maroof, A., Yorgensen, Y. M., Li, Y., and Evans, J. T. (2014). Intranasal vaccination promotes detrimental Th17-mediated immunity against influenza infection. *PLoS Pathog.* 10:e1003875. doi: 10.1371/journal.ppat.1003875

Martinez-Colon, G. J., Warheit-Niemi, H., Gurczynski, S. J., Taylor, Q. M., Wilke, C. A., Podsiad, A. B., et al. (2019). Influenza-induced immune suppression to methicillin-resistant *Staphylococcus aureus* is mediated by TLR9. *PLoS Pathog.* 15:e1007560. doi: 10.1371/journal.ppat.1007560

Marvin, S. A., Russier, M., Huerta, C. T., Russell, C. J., and Schultz-Cherry, S. (2017). Influenza virus overcomes cellular blocks to productively replicate. *Impact. Macrophage Funct. J. Virol.* 91:e01417-16. doi: 10.1128/JVI.01417-16

McKinstry, K. K., Strutt, T. M., Buck, A., Curtis, J. D., Dibble, J. P., Huston, G., et al. (2009). IL-10 deficiency unleashes an influenza-specific Th17 response and enhances survival against high-dose challenge. *J. Immunol.* 182, 7353–7363. doi: 10.4049/jimmunol.0900657

Meesmann, H. M., Fehr, E. M., Kierschke, S., Herrmann, M., Bilyy, R., Heyder, P., et al. (2010). Decrease of sialic acid residues as an eat-me signal on the surface of apoptotic lymphocytes. *J. Cell Sci.* 123, 3347–3356. doi: 10.1242/jcs.066696

Misharin, A. V., Morales-Nebreda, L., Mutlu, G. M., Budinger, G. R., and Perlman, H. (2013). Flow cytometric analysis of macrophages and dendritic cell subsets in the mouse lung. *Am. J. Respir. Cell Mol. Biol.* 49, 503–510. doi: 10.1165/rcmb.2013-0086MA

Miyauchi, K. (2017). Helper T cell responses to respiratory viruses in the lung: development, virus suppression, and pathogenesis. *Viral Immunol.* 30, 421–430. doi: 10.1089/vim.2017.0018

Mordstein, M., Neugebauer, E., Ditt, V., Jessen, B., Rieger, T., Falcone, V., et al. (2010). Lambda interferon renders epithelial cells of the respiratory and gastrointestinal tracts resistant to viral infections. *J. Virol.* 84, 5670–5677. doi: 10.1128/JVI.00272-10

Morens, D. M., Taubenberger, J. K., and Fauci, A. S. (2008). Predominant role of bacterial pneumonia as a cause of death in pandemic influenza: implications for pandemic influenza preparedness. *J. Infect. Dis.* 198, 962–970. doi: 10.1086/591708

Neupane, A. S., Willson, M., Chojnacki, A. K., Vargas, E. S. C. F., Morehouse, C., Carestia, A., et al. (2020). Patrolling alveolar macrophages conceal bacteria from the immune system to maintain homeostasis. *Cells* 183, 110–125.e11. doi: 10.1016/j.cell.2020.08.020

Nita-Lazar, M., Banerjee, A., Feng, C., Amin, M. N., Frieman, M. B., Chen, W. H., et al. (2015). Desialylation of airway epithelial cells during influenza virus infection enhances pneumococcal adhesion via galectin binding. *Mol. Immunol.* 65, 1–16. doi: 10.1016/j.molimm.2014.12.010

Oshansky, C. M., Pickens, J. A., Bradley, K. C., Jones, L. P., Saavedra-Ebner, G. M., Barber, J. P., et al. (2011). Avian influenza viruses infect primary human bronchial epithelial cells unconstrained by sialic acid alpha2,3 residues. *PLoS One* 6:e21183. doi: 10.1371/journal.pone.0021183

Rapoport, E. M., Mochalova, L. V., Gabius, H. J., Romanova, J., and Bovin, N. V. (2006). Search for additional influenza virus to cell interactions. *Glycoconj. J.* 23, 115–125. doi: 10.1007/s10719-006-5444-x

Robinson, K. M., Lee, B., Scheller, E. V., Mandalapu, S., Enelow, R. I., Kolls, J. K., et al. (2015). The role of IL-27 in susceptibility to post-influenza *Staphylococcus aureus* pneumonia. *Respir. Res.* 16:10. doi: 10.1186/s12931-015-0168-8

Roche, P. A., and Furuta, K. (2015). The ins and outs of MHC class II-mediated antigen processing and presentation. *Nat. Rev. Immunol.* 15, 203–216. doi: 10.1038/nri3818

Rodgers, B. C., and Mims, C. A. (1982). Influenza virus replication in human alveolar macrophages. *J. Med. Virol.* 9, 177–184. doi: 10.1002/jmv.1890090304

Roszer, T. (2015). Understanding the mysterious M2 macrophage through activation markers and effector mechanisms. *Mediat. Inflamm.* 2015:816460. doi: 10.1155/2015/816460

Sato, T., Onai, N., Yoshihara, H., Arai, F., Suda, T., and Ohteki, T. (2009). Interferon regulatory factor-2 protects quiescent hematopoietic stem cells from type I interferon-dependent exhaustion. *Nat. Med.* 15, 696–700. doi: 10.1038/nm.1973

Schneider, C., Nobs, S. P., Heer, A. K., Kurrer, M., Klinke, G., van Rooijen, N., et al. (2014a). Alveolar macrophages are essential for protection from respiratory failure and associated morbidity following influenza virus infection. *PLoS Pathog.* 10:e1004053. doi: 10.1371/journal.ppat.1004053

Schneider, C., Nobs, S. P., Kurrer, M., Rehrauer, H., Thiele, C., and Kopf, M. (2014b). Induction of the nuclear receptor PPAR-gamma by the cytokine GM-CSF is critical for the differentiation of fetal monocytes into alveolar macrophages. *Nat. Immunol.* 15, 1026–1037. doi: 10.1038/ni.3005

Schulz, O., Diebold, S. S., Chen, M., Naslund, T. I., Nolte, M. A., Alexopoulou, L., et al. (2005). Toll-like receptor 3 promotes cross-priming to virus-infected cells. *Nature* 433, 887–892. doi: 10.1038/nature03326

Serbina, N. V., and Pamer, E. G. (2006). Monocyte emigration from bone marrow during bacterial infection requires signals mediated by chemokine receptor CCR2. *Nat. Immunol.* 7, 311–317. doi: 10.1038/ni1309

Shahangian, A., Chow, E. K., Tian, X., Kang, J. R., Ghaffari, A., Liu, S. Y., et al. (2009). Type I IFNs mediate development of postinfluenza bacterial pneumonia in mice. *J. Clin. Invest.* 119, 1910–1920. doi: 10.1172/JCI35412

Shepardson, K., Larson, K., Cho, H., Johns, L. L., Malkoc, Z., Stanek, K., et al. (2019). A novel role for PDZ-binding motif of influenza a virus nonstructural protein 1 in regulation of host susceptibility to Postinfluenza bacterial superinfections. *Viral Immunol.* 32, 131–143. doi: 10.1089/vim.2018.0118

Shiratsuchi, A., Kaido, M., Takizawa, T., and Nakanishi, Y. (2000). Phosphatidylserine-mediated phagocytosis of influenza a virus-infected cells by mouse peritoneal macrophages. *J. Virol.* 74, 9240–9244. doi: 10.1128/JVI.74.19.9240-9244.2000

Shiratsuchi, A., and Nakanishi, Y. (2006). Elimination of influenza virus-infected cells by phagocytosis. *Yakugaku Zasshi* 126, 1245–1251. doi: 10.1248/yakushi.126.1245

Shirey, K. A., Lai, W., Patel, M. C., Pletneva, L. M., Pang, C., Kurt-Jones, E., et al. (2016). Novel strategies for targeting innate immune responses to influenza. *Mucosal Immunol.* 9, 1173–1182. doi: 10.1038/mi.2015.141

Siegel, S. J., Roche, A. M., and Weiser, J. N. (2014). Influenza promotes pneumococcal growth during coinfection by providing host sialylated substrates as a nutrient source. *Cell Host Microbe* 16, 55–67. doi: 10.1016/j.chom.2014.06.005

Skehel, J. J., and Wiley, D. C. (2000). Receptor binding and membrane fusion in virus entry: the influenza hemagglutinin. *Annu. Rev. Biochem.* 69, 531–569. doi: 10.1146/annurev.biochem.69.1.531

Smith, A. M., and McCullers, J. A. (2014). Secondary bacterial infections in influenza virus infection pathogenesis. *Curr. Top. Microbiol. Immunol.* 385, 327–356. doi: 10.1007/82_2014_394

Stein, M., Keshav, S., Harris, N., and Gordon, S. (1992). Interleukin 4 potently enhances murine macrophage mannose receptor activity: a marker of alternative immunologic macrophage activation. *J. Exp. Med.* 176, 287–292. doi: 10.1084/jem.176.1.287

Sun, K., and Metzger, D. W. (2008). Inhibition of pulmonary antibacterial defense by interferon-gamma during recovery from influenza infection. *Nat. Med.* 14, 558–564. doi: 10.1038/nm1765

Taubenberger, J. K., and Morens, D. M. (2008). The pathology of influenza virus infections. *Annu. Rev. Pathol.* 3, 499–522. doi: 10.1146/annurev.pathmechdis.3.121806.154316

Teijaro, J. R., Ng, C., Lee, A. M., Sullivan, B. M., Sheehan, K. C., Welch, M., et al. (2013). Persistent LCMV infection is controlled by blockade of type I interferon signaling. *Science* 340, 207–211. doi: 10.1126/science.1235214

Thompson, C. I., Barclay, W. S., Zambon, M. C., and Pickles, R. J. (2006). Infection of human airway epithelium by human and avian strains of influenza a virus. *J. Virol.* 80, 8060–8068. doi: 10.1128/JVI.00384-06

Tisoncik, J. R., Korth, M. J., Simmons, C. P., Farrar, J., Martin, T. R., and Katze, M. G. (2012). Into the eye of the cytokine storm. *Microbiol. Mol. Biol. Rev.* 76, 16–32. doi: 10.1128/MMBR.05015-11

Tong, S., Zhu, X., Li, Y., Shi, M., Zhang, J., Bourgeois, M., et al. (2013). New world bats harbor diverse influenza a viruses. *PLoS Pathog.* 9:e1003657. doi: 10.1371/journal.ppat.1003657

Tripathi, S., Batra, J., Cao, W., Sharma, K., Patel, J. R., Ranjan, P., et al. (2013). Influenza a virus nucleoprotein induces apoptosis in human airway epithelial cells: implications of a novel interaction between nucleoprotein and host protein Clusterin. *Cell Death Dis.* 4:e562. doi: 10.1038/cddis.2013.89

Tumpey, T. M., Garcia-Sastre, A., Taubenberger, J. K., Palese, P., Swayne, D. E., Pantin-Jackwood, M. J., et al. (2005). Pathogenicity of influenza viruses with genes from the 1918 pandemic virus: functional roles of alveolar macrophages and neutrophils in

limiting virus replication and mortality in mice. *J. Virol.* 79, 14933–14944. doi: 10.1128/JVI.79.23.14933-14944.2005

Ural, B. B., Yeung, S. T., Damani-Yokota, P., Devlin, J. C., de Vries, M., Vera-Licona, P., et al. (2020). Identification of a nerve-associated, lung-resident interstitial macrophage subset with distinct localization and immunoregulatory properties. *Sci. Immunol.* 5:eaax8756. doi: 10.1126/sciimmunol.aax8756

van Riel, D., Leijten, L. M., van der Eerden, M., Hoogsteden, H. C., Boven, L. A., Lambrecht, B. N., et al. (2011). Highly pathogenic avian influenza virus H5N1 infects alveolar macrophages without virus production or excessive TNF-alpha induction. *PLoS Pathog.* 7:e1002099. doi: 10.1371/journal.ppat.1002099

Waffarn, E. E., and Baumgarth, N. (2011). Protective B cell responses to flu--no fluke! *J. Immunol.* 186, 3823–3829. doi: 10.4049/jimmunol.1002090

Wang, Y., Li, T., Chen, Y., Wei, H., Sun, R., and Tian, Z. (2017). Involvement of NK cells in IL-28B-mediated immunity against influenza virus infection. *J. Immunol.* 199, 1012–1020. doi: 10.4049/jimmunol.1601430

Wang, Z., Li, S., and Huang, B. (2022). Alveolar macrophages: Achilles' heel of SARS-CoV-2 infection. *Signal Transduct. Target. Ther.* 7:242. doi: 10.1038/s41392-022-01106-8

Wang, J., Nikrad, M. P., Travanty, E. A., Zhou, B., Phang, T., Gao, B., et al. (2012). Innate immune response of human alveolar macrophages during influenza a infection. *PLoS One* 7:e29879. doi: 10.1371/journal.pone.0053383

Wang, J., Oberley-Deegan, R., Wang, S., Nikrad, M., Funk, C. J., Hartshorn, K. L., et al. (2009). Differentiated human alveolar type II cells secrete antiviral IL-29 (IFN-lambda 1) in response to influenza a infection. *J. Immunol.* 182, 1296–1304. doi: 10.4049/jimmunol.182.3.1296

Wang, X., Yin, X., Zhang, B., Liu, C., Lin, Y., Huang, X., et al. (2022). A prophylactic effect of aluminium-based adjuvants against respiratory viruses via priming local innate immunity. *Emerg. Microbes Infect.* 11, 914–925. doi: 10.1080/22221751.2022.2050951

Watanabe, Y., Hashimoto, Y., Shiratsuchi, A., Takizawa, T., and Nakanishi, Y. (2005). Augmentation of fatality of influenza in mice by inhibition of phagocytosis. *Biochem. Biophys. Res. Commun.* 337, 881–886. doi: 10.1016/j.bbrc.2005.09.133

Watanabe, Y., Shiratsuchi, A., Shimizu, K., Takizawa, T., and Nakanishi, Y. (2002). Role of phosphatidylserine exposure and sugar chain desialylation at the surface of influenza virus-infected cells in efficient phagocytosis by macrophages. *J. Biol. Chem.* 277, 18222–18228. doi: 10.1074/jbc.M201074200

Wei, F., Gao, C., and Wang, Y. (2022). The role of influenza a virus-induced hypercytokinemia. *Crit. Rev. Microbiol.* 48, 240–256. doi: 10.1080/1040841X.2021.1960482

Wiley, D. C., and Skehel, J. J. (1987). The structure and function of the hemagglutinin membrane glycoprotein of influenza virus. *Annu. Rev. Biochem.* 56, 365–394. doi: 10.1146/annurev.bi.56.070187.002053

Wong, C. K., Smith, C. A., Sakamoto, K., Kaminski, N., Koff, J. L., and Goldstein, D. R. (2017). Aging impairs alveolar macrophage phagocytosis and increases influenza-induced mortality in mice. *J. Immunol.* 199, 1060–1068. doi: 10.4049/jimmunol.1700397

Xia, C., Xu, W., Ai, X., Zhu, Y., Geng, P., Niu, Y., et al. (2022). Autophagy and exosome Coordinately enhance macrophage M1 polarization and recruitment in influenza a virus infection. *Front. Immunol.* 13:722053. doi: 10.3389/fimmu.2022.926781

Xing, Z., Afkhami, S., Bavananthasivam, J., Fritz, D. K., D'Agostino, M. R., Vaseghi-Shanjani, M., et al. (2020). Innate immune memory of tissue-resident macrophages and trained innate immunity: re-vamping vaccine concept and strategies. *J. Leukoc. Biol.* 108, 825–834. doi: 10.1002/JLB.4MR0220-446R

Yao, D., Bao, L., Li, F., Liu, B., Wu, X., Hu, Z., et al. (2022). H1N1 influenza virus dose dependent induction of dysregulated innate immune responses and STAT1/3 activation are associated with pulmonary immunopathological damage. *Virulence* 13, 1558–1572. doi: 10.1080/21505594.2022.2120951

Yona, S., Kim, K. W., Wolf, Y., Mildner, A., Varol, D., Breker, M., et al. (2013). Fate mapping reveals origins and dynamics of monocytes and tissue macrophages under homeostasis. *Immunity* 38, 79–91. doi: 10.1016/j.immuni.2012.12.001

Yu, X., Buttgereit, A., Lelios, I., Utz, S. G., Cansever, D., Becher, B., et al. (2017). The cytokine TGF-beta promotes the development and homeostasis of alveolar macrophages. *Immunity* 47, 903–912 e4. doi: 10.1016/j.immuni.2017.10.007

Yu, W. C., Chan, R. W., Wang, J., Travanty, E. A., Nicholls, J. M., Peiris, J. S., et al. (2011). Viral replication and innate host responses in primary human alveolar epithelial cells and alveolar macrophages infected with influenza H5N1 and H1N1 viruses. *J. Virol.* 85, 6844–6855. doi: 10.1128/JVI.02200-10

Zaynagetdinov, R., Sherrill, T. P., Kendall, P. L., Segal, B. H., Weller, K. P., Tighe, R. M., et al. (2013). Identification of myeloid cell subsets in murine lungs using flow cytometry. *Am. J. Respir. Cell Mol. Biol.* 49, 180–189. doi: 10.1165/rcmb.2012-0366MA

Zhang, N., Bao, Y. J., Tong, A. H., Zuyderduyn, S., Bader, G. D., Malik Peiris, J. S., et al. (2018). Whole transcriptome analysis reveals differential gene expression profile reflecting macrophage polarization in response to influenza a H5N1 virus infection. *BMC Med. Genet.* 11:20. doi: 10.1186/s12920-018-0335-0

Zhao, X., Dai, J., Xiao, X., Wu, L., Zeng, J., Sheng, J., et al. (2014). PI3K/Akt signaling pathway modulates influenza virus induced mouse alveolar macrophage polarization to M1/M2b. *PLoS One* 9:e104506. doi: 10.1371/journal.pone.0115872

Zhao, Y., Zou, W., Du, J., and Zhao, Y. (2018). The origins and homeostasis of monocytes and tissue-resident macrophages in physiological situation. *J. Cell. Physiol.* 233, 6425–6439. doi: 10.1002/jcp.26461

Zhou, X., and Moore, B. B. (2018). Location or origin? What is critical for macrophage propagation of lung fibrosis? *Eur. Respir. J.* 51:1800103. doi: 10.1183/13993003.00103-2018

Zhu, B., Wu, Y., Huang, S., Zhang, R., Son, Y. M., Li, C., et al. (2021). Uncoupling of macrophage inflammation from self-renewal modulates host recovery from respiratory viral infection. *Immunity* 54, 1200–1218.e9. doi: 10.1016/j.immuni.2021.04.001

Zhu, J., Yamane, H., and Paul, W. E. (2010). Differentiation of effector CD4 T cell populations (*). *Annu. Rev. Immunol.* 28, 445–489. doi: 10.1146/annurev-immunol-030409-101212

frontiers | Frontiers in Microbiology

TYPE Review
PUBLISHED 02 October 2023
DOI 10.3389/fmicb.2023.1277552

OPEN ACCESS

EDITED BY
Shijian Zhang,
Dana–Farber Cancer Institute, United States

REVIEWED BY
Agnieszka Kwiatek,
University of Warsaw, Poland
Zhen Luo,
Jinan University, China

*CORRESPONDENCE
Yonggang Wang
✉ wangyg1982@jlu.edu.cn

RECEIVED 14 August 2023
ACCEPTED 18 September 2023
PUBLISHED 02 October 2023

CITATION
Zhao Y, Li C, Zhang S, Cheng J, Liu Y, Han X, Wang Y and Wang Y (2023) Inhaled nitric oxide: can it serve as a savior for COVID-19 and related respiratory and cardiovascular diseases? *Front. Microbiol.* 14:1277552. doi: 10.3389/fmicb.2023.1277552

Inhaled nitric oxide: can it serve as a savior for COVID-19 and related respiratory and cardiovascular diseases?

Yifan Zhao[1], Cheng Li[1], Shuai Zhang[1], Jiayu Cheng[1], Yucheng Liu[2], Xiaorong Han[3], Yinghui Wang[1] and Yonggang Wang[1]*

[1]Department of Cardiovascular Center, The First Hospital of Jilin University, Changchun, China, [2]Department of Family and Community Medicine, Feinberg School of Medicine, McGaw Medical Center of Northwestern University, Chicago, IL, United States, [3]Department of Special Care Center, Fuwai Hospital, National Clinical Research Center for Cardiovascular Diseases, National Center for Cardiovascular Diseases, Chinese Academy of Medical Science and Peking Union Medical College, Beijing, China

Nitric oxide (NO), as an important gaseous medium, plays a pivotal role in the human body, such as maintaining vascular homeostasis, regulating immune-inflammatory responses, inhibiting platelet aggregation, and inhibiting leukocyte adhesion. In recent years, the rapid prevalence of coronavirus disease 2019 (COVID-19) has greatly affected the daily lives and physical and mental health of people all over the world, and the therapeutic efficacy and resuscitation strategies for critically ill patients need to be further improved and perfected. Inhaled nitric oxide (iNO) is a selective pulmonary vasodilator, and some studies have demonstrated its potential therapeutic use for COVID-19, severe respiratory distress syndrome, pulmonary infections, and pulmonary hypertension. In this article, we describe the biochemistry and basic characteristics of NO and discuss whether iNO can act as a "savior" for COVID-19 and related respiratory and cardiovascular disorders to exert a potent clinical protective effect.

KEYWORDS

nitric oxide, inhaled nitric oxide, COVID-19, pulmonary arterial hypertension, lung infection, acute respiratory distress syndrome

1. Introduction

Nitric oxide (NO) is an important pleiotropic regulator that is enzymatically synthesized *in vivo* from L-arginine by nitric oxide synthase (NOS), which precisely regulates cardiovascular, respiratory, neurological, and other multi-systems as well as a wide range of life activities by sending signals to specific targets. NOS has three different subtypes, namely endothelial nitric oxide synthase (eNOS), neuronal nitric oxide synthase (nNOS), and inducible nitric oxide synthase (iNOS), and the resulting NO can perform a variety of biological functions *in vivo*, such as vasodilatation, metabolic regulation, host defense, neurotransmitters, and so on (Mac Micking et al., 1997; Kashiwagi et al., 2023; Soundararajan et al., 2023). The coronavirus disease 2019 (COVID-19) has swept over the globe in recent years, with far-reaching consequences for people's physical and mental health as well as the global social economy. When the human body is infected with severe acute respiratory syndrome coronavirus 2 (SARS-CoV-2), several

clinical symptoms and pathologic features might arise, and some patients may continue to have some chronic sequelae after recovery (Chen et al., 2021; Yong, 2021). Inhaled nitric oxide (iNO), a therapeutic agent that delivers NO, has been approved for the treatment of neonatal pulmonary hypertension, and its role as an unconventional treatment with improved oxygenation and selective pulmonary vasodilatation appears to offer a promising therapeutic option for critically ill patients with COVID-19 (Kamenshchikov et al., 2022; Shei and Baranauskas, 2022). In addition to this, encouraging clinical benefits have been shown for cardiopulmonary diseases such as acute respiratory distress syndrome, lung infections, and pulmonary hypertension in adults (Sokol et al., 2016; Lisi et al., 2021). In this review, we present the sources and biological functions of NO, describe whether iNO can provide safe and effective therapeutic effects in the context of COVID-19, and discuss clinical applications in COVID-19-related cardiovascular and respiratory diseases.

2. The biosynthesis, biological functions, and therapeutic uses of NO

Because of its uncharged lipophilic feature, NO, as a key gas molecule in the living system, can freely travel between cells through the cell membrane and assist in the regulation of numerous physiological functions in the human body (Cinelli et al., 2020). Endogenous nitric oxide is created by macrophages, neurons, vascular smooth muscle, and cardiomyocytes via nitric oxide synthase's conversion of L-arginine to L-citrulline (Nasyrova et al., 2020; Burov et al., 2022). Nitric oxide synthase has three isoforms. eNOS is normally expressed in vascular endothelial cells, and its mediated production of NO can diffuse into smooth muscle cells, activate soluble guanylate cyclase (sGC) to produce cyclic guanosine monophosphate (cGMP), and activate protein kinase G (PKG), which phosphorylates myosin light chain kinase (MLCK), thereby relaxing the smooth muscle and leading to vasodilation (Arnold et al., 1977; Ataei Ataabadi et al., 2020; Ma et al., 2023). In addition, NO produced by eNOS has physiological functions such as inhibition of platelet aggregation and adhesion, inhibition of leukocyte adhesion and vascular inflammation, inhibition of smooth muscle cell proliferation, anti-atherosclerosis, etc., which are important for maintaining the normal function of the cardiovascular system (Förstermann and Sessa, 2012; Li et al., 2014; Russo et al., 2023). nNOS regulates neurotransmitter release via the NO-NOsCG-cGMP signaling pathway and is also involved in the regulation of sympathetic nerves. When numerous pathologic causes cause a decrease in NO generation by nNOS, illnesses such as heart failure, hypertension, and renal insufficiency proceed (Sharma and Patel, 2017; Lundberg and Weitzberg, 2022). Cytokines, bacterial products, and other substances act as inducers to induce the release of large amounts of NO, i.e., inducible NOS (iNOS), from nitric oxide synthase in cells. iNOS is not often found in cells but is expressed in endothelial cells and immune cells after stimulation by certain inducers and exerts cytostatic or cytotoxic effects on tumor cells, microorganisms, or parasites. It is important to note that when NO is overexpressed, it can also have deleterious effects on normal tissues, such as infectious shock, pain, cancer, diabetes, etc. (Förstermann and Sessa, 2012; Cinelli et al., 2020; Lundberg and Weitzberg, 2022).

With the NO-NOsCG-cGMP signaling pathway playing a significant role, NO is a key signaling molecule for the control of vascular function, neurotransmission, the immune-inflammatory response, and other physiological activities. Through this signaling system, scientists are attempting to investigate treatment approaches for respiratory and cardiovascular illnesses. In addition to nitroglycerin and nitroprusside, which are known to be important NO donors for the treatment of angina pectoris and hypertensive crises (Miller and Megson, 2007), measurement of exhaled NO in a single breath can be used to monitor the treatment of allergic asthma (Rupani and Kent, 2022), and sGC activators (e.g., Riociguat, Vericiguat) and PDF5 inhibitors (e.g., sildenafil), which can synergize with endogenous NO, have shown promising therapeutic effects in the treatment of pulmonary hypertension (Lundberg and Weitzberg, 2022; Grześk et al., 2023). Since NO is highly reactive and easily passes through biological membranes, researchers have attempted to explore strategies to enhance NO release and exogenous NO supplementation. Roberts et al. discovered that iNO not only diffuses through the lungs but at the same time selectively dilates the pulmonary vasculature, innovatively applying NO to clinical practice (Roberts et al., 1992). Since 1993, iNO has been extensively studied as one of the potential treatments for acute respiratory distress syndrome (ARDS) and was approved by the FDA in 1999 for the treatment of persistent pulmonary hypertension in neonates (American Academy of Pediatrics, 2000; Redaelli et al., 2023). iNO is potentially beneficial in reducing right heart load and reducing hypoxemia due to ARDS when used in the low dose range (10–80 ppm). Systemic vasodilatory effects were not demonstrated at inhalation concentrations up to 160 ppm. At high doses (>160 ppm), iNO kills a wide range of pathogens, including bacteria, fungi, and viruses, and its antimicrobial activity is enhanced when used in combination with antibiotics (Barnes and Brisbois, 2020; Sorbo et al., 2022). Additionally, iNO is advantageous for myocardial damage, cardiac arrest, neuroprotection, recovering organ function following organ transplantation, and patient survival (Barnes and Brisbois, 2020; Redaelli et al., 2022). In this article, we focus on the possible therapeutic potential of iNO in COVID-19, focusing on its clinical applications and therapeutic perspectives in the respiratory and cardiovascular systems (Figure 1).

3. Clinical application of iNO in COVID-19

3.1. The role of NO in COVID-19

SARS-CoV-2 is the pathogen responsible for COVID-19. When it infects a person, it can cause structural and functional damage to a number of organs, with the respiratory system being the primary manifestation. Affected individuals may experience no symptoms, mild symptoms, severe illness, or even death (Guimarães et al., 2021; Stratton et al., 2021). Infection with SARS-CoV-2 can lead to decreased NO production and utilization by a number of mechanisms, including direct infection of endothelial cells, amplification of the detrimental effects of the angiotensin-converting enzyme (ACE)/angiotensin II (AngII)/angiotensin II type 1 (AT1) axis following down-regulation of angiotensin-converting enzyme 2 (ACE2) expression, and further development of the hyperinflammatory state as a cytokine storm (Dominic et al., 2021; Fang et al., 2021; Ferrari and

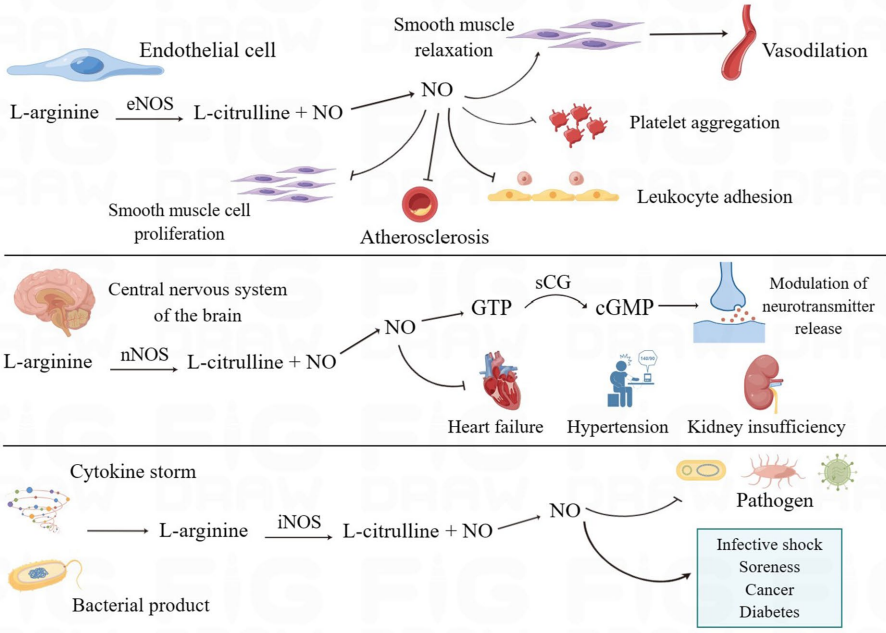

FIGURE 1
The biosynthesis and biological functions of NO. eNOS, nNOS, and iNOS catalyze the production of NO through L-arginine and perform different biological functions in the human body. eNOS mediates vasodilatation and inhibits platelet aggregation, leukocyte adhesion, smooth muscle cell proliferation, and atherosclerosis. nNOS, in addition to regulating the release of neurotransmitters, increases the development of cardiac and renal insufficiency and hypertension when NO production decreases. iNOS can produce large amounts of NO when stimulated, which on the one hand helps to enhance the ability of antibacterial and inflammatory responses and on the other hand can have adverse effects on normal tissues. (By Figdraw).

Protti, 2022; Montiel et al., 2022). On the other hand, studies have demonstrated that NO has direct or indirect antiviral effects (Lisi et al., 2021). The inflammatory response caused by viral infection activates macrophages with increased expression of iNOS and the release of large amounts of NO, which plays a role in regulating host immune function against pathogens (Guimarães et al., 2021). SARS-CoV-2 can infect the nervous system and damage the blood–brain barrier via binding to ACE2 in vascular smooth muscle cells and brain capillary endothelial cells. Large levels of NO are consequently created to prevent viral replication after iNOS is triggered. It is important to keep in mind, though, that excessive NO-related free radical generation might harm the brain, leaving some patients with neurological deficiencies like sleep difficulties (Cespuglio et al., 2021). In addition, NO inhibits or impairs SARS-CoV-2 by acting on the viral spiking protein and the cysteine protease encoded by SARS-CoV-2 Orf1a (Stefano et al., 2020). The antiviral effect of NO was similarly demonstrated in a study by Akaberi et al. The viral inhibition following release of NO from the NO-donor nitroso-N-acetylpenicillamine (SNAP) was dose-dependent, with a delayed or blocking effect on the occurrence of cytopathic effects (CPE) in virus-infected cells. The reduction in viral replication may be related to the nitrosylation of the SARS-CoV-2 3CL cysteine protease, although this has to be further validated (Akaberi et al., 2020). The antiviral capacity of NO was further explored in a clinical study. The patients with mild COVID-19 infection were randomly assigned to a nitric oxide nasal spray (NONS) treatment group and a placebo group, and the results demonstrated that NONS can play a clinically beneficial role by effectively and safely reducing the RNA load of SARS-CoV-2 and decreasing further virus transmission (Winchester et al., 2021). However, an *in vitro* experiment conducted by Rousseaud's team negated the antiviral properties of gaseous NO. No effect on viral load was observed after exposing SARS-CoV-2-infected cells to high doses of gaseous NO (Rousseaud et al., 2023). In addition to this, the massive production of NO can cause tissue and cell death, and the cytotoxic effects of reactive oxygen and nitrogen species can be damaging to the body (Lisi et al., 2021). Therefore, further investigation and refinement are needed regarding the antiviral treatment and clinical safety of NO.

SARS-CoV-2 is a respiratory pathogen that can damage the respiratory system, resulting in severe hypoxemia and dyspnea; however, some patients present with silent hypoxia, i.e., severe hypoxemia without significant dyspnea (Yuki et al., 2020; Mandal, 2023). Mortaz et al. found that the NO content of erythrocytes in COVID-19 patients was higher than that in non-COVID-19 patients. When tissue hypoxia and oxidative stress occur *in vivo*, erythrocytes produce NO through S-nitrosoprotein (SNO-Hb) transfer and erythrocyte nitric oxide synthase, which diastole the small blood vessels, regulate the local blood flow, and promote the release of oxygen into hypoxic tissues, thereby playing a role in the protection of COVID-19 patients suffering from silent hypoxia (Mortaz et al., 2020; Mandal, 2023). It has been shown that patients with severe COVID-19 have reduced HbNO compared to non-COVID-19 patients with similar cardiovascular risk, which correlates with reduced NO bioavailability and is a potential specific biomarker of endothelial dysfunction (Ferrari and Protti, 2022). The results,

however, were disputed. Nogueira et al. came to the conclusion that endogenous nitrite is influenced by outside factors such as diet, lifestyle, and oral flora and that treatment of the blood with N-acetylcysteine and ascorbic acid artificially increases HbNO when endogenous nitrite is present. This means that HbNO does not reflect endothelial function at an early stage and that further assay method optimization is required (Nogueira et al., 2022).

The COVID-19 pandemic has placed a significant burden on healthcare systems around the world, and the rational allocation and utilization of healthcare resources and the economy in response to the severity of the disease is an urgent issue, so researchers are looking for a convenient, safe, and non-invasive biomarker to stratify the risk level of the disease. Fraction of exhaled nitric oxide (FeNO) is a simple, reproducible, non-invasive biomarker with diagnostic value for nonspecific respiratory symptoms and airway inflammation and is used as an adjunctive assessment for the diagnosis of asthma, predicting the response to inhaled corticosteroids, and guiding clinical treatment (Guida et al., 2023; Murugesan et al., 2023). FeNO levels in COVID-19 patients and the clinical value of FeNO in COVID-19 are controversial. On the one hand, SARS-CoV-2 infection induces an inflammatory response with a cytokine storm that induces NO production by iNOS (Karki et al., 2021), and on the other hand, it was shown that the severity of SARS-CoV-2 infection was negatively correlated with FeNO production, which was related to the fact that ACE2 attenuated the production of NO by iNOS in airway epithelial cells, whereas high expression of ACE2 had a stronger susceptibility to SARS-CoV-2 (Betancor et al., 2022a). It has been suggested that FeNO levels are elevated in COVID-19 patients compared to healthy individuals. Kerget et al. concluded that FeNO levels can be used to assess lung parenchymal involvement in COVID-19 patients and that patients with cytokine storms have higher levels of FeNO (Kerget et al., 2022). Whereas the results of a single-center prospective study showed that the more severe the disease, the lower the FeNO levels in those with COVID-19, with patients with measurements $\leq$ 11.8 PPB having worse clinical outcomes (Lior et al., 2022). It has been questioned whether FeNO levels in COVID-19 patients can be used to predict the severity and prognosis of the disease. Betancor et al. demonstrated that FeNO levels were normal during the acute phase of SARS-CoV-2 infection and increased slightly during the recovery phase, independently of disease severity (Betancor et al., 2022a,b). Even in the group with post-COVID-19 syndrome, FeNO does not have a clear clinical value (Maniscalco et al., 2022). Age, gender, smoking, concurrent respiratory conditions, and whether or not the patient has had corticosteroid therapy are some of the variables that can affect FeNO levels. The sample size and the FeNO instruments also have an impact on the study's outcome (Betancor et al., 2022a). Therefore, it is unknown whether FeNO truly has potential therapeutic value for COVID-19 disease risk categorization and treatment regimen advice. Multicenter, large-sample trials are still required to make this determination.

3.2. Clinical application of iNO in COVID-19

Numerous studies have investigated and talked about the clinical use of iNO in COVID-19. The idea that iNO can improve oxygenation to varying degrees in this subset of patients and lessen the use of invasive respiratory support techniques is supported by a number of pieces of evidence, despite the fact that iNO cannot be used as a conventional treatment for refractory hypoxemia and ARDS brought on by COVID-19 and does not significantly improve mortality or prognosis (Parikh et al., 2020; Garfield et al., 2021; Lotz et al., 2021; Safaee Fakhr et al., 2021; Al Sulaiman et al., 2022). It has been suggested that appropriate iNO therapy given in the early stages of COVID-19 infection may delay disease progression, especially in patients who are older or have multiple comorbidities that result in decreased endogenous nitric oxide production (Adusumilli et al., 2020). There is even proof that pregnant individuals with severe or critical COVID-19 benefit from high-dose iNO therapy (Safaee Fakhr et al., 2020).

Smoking puts human health in danger, raises the prevalence of respiratory and cardiovascular disorders, and lowers life expectancy rates (Ambrose and Barua, 2004; Lugg et al., 2022). However, according to other research, smoking appears to protect against COVID-19 and reduce SARS-CoV-2 infection, which is known as the smoker's paradox (Usman et al., 2021; Papadopoulos et al., 2023). Epidemiologic studies have found that only a small proportion of patients in the smoking population, which makes up a relatively large proportion of the smoking population in several countries around the world, have COVID-19 (Berlin et al., 2020; Hedenstierna et al., 2020; Usman et al., 2021). Although the idea that smoking has a protective effect may seem naive, a partially plausible explanation exists from a pathophysiological point of view:1. It has been suggested that the large elevation of NO in the lower respiratory tract after smoking, present in the epithelial lining fluid, leads to an increase in the reactivity of a bioequivalent form with a similar bioactivity to that of NO, thus protecting against SARS-CoV-2 infection (Chambers et al., 1998; Zhao et al., 2015). 2. Tobacco smoke may enhance the uncoupling of eNOS and promote transcription, leading to increased NO production (Papadopoulos et al., 2023). 3. CYP450 in the liver mediates NO release from nitrate when the typical eNOS pathway is impaired (Papadopoulos et al., 2023). 4. The anti-inflammatory effects of nicotine and the suppression of systemic cytokines in smokers help to attenuate the cytokine storm of COVID-19 (Wang et al., 2003; Garufi et al., 2020; Usman et al., 2021). 5. Smoking may upregulate ACE2 expression and thus reduce disease severity (Usman et al., 2021). Hedenstierna et al. suggested that short, high doses of iNO have a preventive effect on COVID-19. This is because cigarettes contain a high amount of NO, and a high concentration of NO during a single inhalation can quickly reach the virus by diffusion. As a result, COVID-19 prophylaxis may be possible with high-dose, intermittent delivery of iNO over a short period of time. But smoking is undeniably a risk factor for COVID-19, and continuing to smoke over time raises the likelihood of contracting the virus (Hedenstierna et al., 2020).

Regarding the clinical effectiveness and safety of iNO, there is still some disagreement. Because COVID-19-induced ARDS has more significant vascular endothelial damage and microthrombosis than non-COVID-19-induced ARDS, in addition to diffuse loss of pulmonary vasoconstriction and peri-alveolar solidity, which may affect iNO's ability to improve oxygenation (Longobardo et al., 2021; Bonizzoli et al., 2022). In terms of safety, Lotz et al. found that iNO appears to be associated with an increase in acute kidney injury with hospital-acquired pneumonia (Al Sulaiman et al., 2022). iNO therapy is an innovative tool in COVID-19, but due to the complexity of the pathogenesis of COVID-19 and the variety of clinical symptoms, the

patient population, timing, dosage, and mode of administration of iNO therapy are still unknown, and these are the difficulties that need to be overcome in future studies (Frostell and Hedenstierna, 2021; Shei and Baranauskas, 2022).

4. Application of iNO in respiratory and cardiovascular diseases

4.1. Acute respiratory distress syndrome

Acute respiratory distress syndrome (ARDS) is caused by various pathogenic factors that damage alveolar epithelial cells and capillary endothelial cells, resulting in pulmonary edema and severe hypoxemia, thus causing acute respiratory distress (Meyer et al., 2021; Bos and Ware, 2022). Previous research has concluded that iNO is a valuable therapeutic option for severe hypoxemia caused by ARDS because of its ability to selectively dilate the pulmonary vasculature and improve the ventilation-to-blood flow ratio, and that iNO's therapeutic efficacy can be improved when used in combination with other therapeutic means (Kaisers et al., 2003). Several studies, however, have indicated that iNO only increases the oxygenation index temporarily, does not improve long-term patient survival appreciably, and may even increase the risk of mortality and renal impairment (Adhikari et al., 2007; Afshari et al., 2011; Gebistorf et al., 2016). As a result, iNO is not indicated as a first-line treatment for ARDS (Gebistorf et al., 2016).

However, it is worth noting that iNO seems to have a wider use in patients with COVID-19-associated acute respiratory distress syndrome (C-ARDS; Mekontso Dessap et al., 2023). For persistent refractory hypoxemia due to COVID-19, inhaled 5–20 ppm NO appears to be beneficial in improving oxygenation in addition to neuromuscular blockade and optimizing positive end-expiratory pressure therapy (Matthay et al., 2020). The results of a multicenter retrospective study also confirmed the clinical value of iNO, with nearly half of the patients having a better oxygenation response after iNO, and about half of the patients who met the indications for ECMO no longer needed to be dependent on ECMO after iNO (51.6%), and this group of patients who responded well to iNO had a better prognosis than those who still met the indications for ECMO after iNO (Mekontso Dessap et al., 2023). However, as mentioned earlier, the role of iNO in improving hypoxemia remains controversial, which is related to the complex pathogenesis of severe hypoxemia in patients with C-ARDS (Archer et al., 2020; Bonizzoli et al., 2022; Mekontso Dessap et al., 2023). In addition to this, the safety of iNO and whether it is synergistic with other therapeutic measures are not yet known; therefore, further research and exploration are needed.

4.2. Lung infections

Antibiotic misuse can result in the growth of bacteria that are multidrug resistant, which can prolong hospital stays, necessitate the use of stronger drugs, raise their dosage, and cause complications from various infections that increase the likelihood of negative clinical outcomes (Santacroce et al., 2023; Yao et al., 2023). Contrary to conventional treatments, iNO is not linked to drug resistance, and because it diffuses quickly across biological fluids and membranes, NO can get into places where intravenous medications cannot. Because it may efficiently suppress or kill germs, iNO has great therapeutic potential in the field of anti-infective therapy (Sorbo et al., 2022).

In vitro studies have demonstrated that the antimicrobial capacity of iNO is dose-dependent. Low doses of iNO less than 160 ppm have only an inhibitory effect on bacteria, but doses greater than 160 ppm can kill bacterial colonies of *Escherichia coli*, *Pseudomonas aeruginosa*, and *Staphylococcus aureus*, and when applied at higher doses (200 ppm), it has a significant bactericidal effect on multidrug-resistant cocci (Ghaffari et al., 2006; Sorbo et al., 2022). It is unavoidable that NO can bind to hemoglobin and generate methemoglobin when it is injected into the body in large concentrations, interfering with normal oxygen transport even if *in vitro* studies have strongly supported the antibacterial impact of iNO (Signori et al., 2022). High-dose, intermittent dosing therefore seems to be an effective solution. With such a solution in mind, researchers have conducted numerous *in vivo* studies. Several animal studies have shown that iNO has good antimicrobial activity and no side effects when the dose is well balanced with the duration of exposure, and even Michaelsen et al. have demonstrated the safety of high doses of continuous iNO in healthy animals (Miller et al., 2013; Michaelsen et al., 2021; Wiegand et al., 2021; Sorbo et al., 2022). Also, this regimen showed better clinical efficacy in clinical studies. The researchers showed no significant adverse events and a good safety profile after giving high doses of intermittent iNO to healthy individuals and patients with pulmonary infections (Miller et al., 2012; Sorbo et al., 2022). Flume et al. administered iNO to nine patients with nontuberculous mycobacterial lung disease (NTM-PD), four of whom tested negative on sputum culture after 3 weeks and had no safety concerns with the treatment. Although three of the patients were found to have positive sputum cultures after retesting 3 months after stopping treatment, the NTM load was lower than before (Flume et al., 2023). In a prospective double-blind randomized controlled study, infants with acute bronchiolitis were randomly assigned to a standard treatment group and to different iNO concentrations in combination with standard treatment. The results showed that high-dose intermittent injections of 150 ppm iNO were clinically more effective and well tolerated than the other groups (Goldbart et al., 2023). However, iNO has not shown bactericidal efficacy in clinical studies or *in vitro* experiments, and further exploration is needed to increase the dosage and prolong the exposure time to achieve complete eradication of pathogenic microorganisms while ensuring human safety (Deppisch et al., 2016; Sorbo et al., 2022).

4.3. Pulmonary arterial hypertension

Pulmonary hypertension (PH) is a life-threatening vascular disease in which persistent vasoconstriction, increased vessel wall stiffness, pulmonary vascular remodeling, and *in situ* thrombus can cause increased pulmonary vascular resistance (PVR), leading to increased pulmonary artery pressures, which can lead to progressive right heart insufficiency and heart failure (Keshavarz et al., 2020; Zolty, 2020). The disease has diverse etiologies, an insidious onset, and complex pathophysiologic mechanisms and is usually diagnosed when the patient presents with dyspnea, fatigue, and cyanosis of the lips and mouth (Keshavarz et al., 2020). Based on the pathogenesis of PH, a number of specific therapeutic options have been developed, including

prostacyclin analogs (Montani et al., 2014), endothelin receptor antagonists (Goldberg et al., 2017), soluble guanylate cyclase agonists (Stasch et al., 2011), and phosphodiesterase inhibitors (Triposkiadis et al., 2022).

The NO-sCG-cGMP signaling pathway plays an important role in the pathogenesis of PH, and several targeted therapies have been developed based on this signaling pathway (Keshavarz et al., 2020). Studies have shown that NOS expression is reduced and NO bioavailability is decreased in patients with PH (Giaid and Saleh, 1995; Demoncheaux et al., 2005). iNO selectively lowers pulmonary arterial pressure without systemic hypotensive effects and improves mean pulmonary arterial pressure, pulmonary vascular resistance, and oxygenation in adult PH patients with severe hypoxemia and respiratory failure as a "rescue" therapy (Keshavarz et al., 2020). Feng et al. found that iNO improved oxygenation status while reducing the risk of right heart failure in COVID-19 patients with preexisting pulmonary hypertension (Feng et al., 2021). A clinical trial has shown that pulsed iNO improves daily physical activity in patients with pulmonary hypertension due to pulmonary fibrosis and is beneficial and safe in the clinical management of the disease (Nathan et al., 2020). In addition, for pulmonary hypertension after cardiac surgery, iNO not only improves hemodynamics, but also has a protective effect on systemic organ function (Nakane et al., 2021). However, iNO is currently only approved for the treatment of persistent pulmonary hypertension in neonates, and there is much controversy over adult pulmonary hypertension. For example, iNO has a short half-life, can produce toxic metabolites, has low outpatient penetration, is costly, and appears to have no clinical benefit in terms of prognosis for some patients (Sardo et al., 2018; Keshavarz et al., 2020; Redaelli et al., 2022). Therefore, although iNO is being considered as a therapeutic option for patients with severely impaired respiratory function, large randomized controlled trials are needed to further judge its clinical benefits and safety.

In addition to its therapeutic applications, the vascular reactivity test for iNO is used to identify patients with pulmonary hypertension in whom elevated pulmonary vascular resistance is not accompanied by severe vascular remodeling. The test is only used to determine whether calcium channel blockers are necessary for treatment in patients with idiopathic, hereditary, or drug-induced pulmonary hypertension, and there is a chance that giving iNO to patients with other types of pulmonary hypertension could cause pulmonary edema (Redaelli et al., 2022). iNO can be used to determine the response to calcium channel blockers in patients with pulmonary hypertension, and whether this test of vascular reactivity is indicative of patient prognosis was studied by Malhotra et al. The results of the study showed that a decrease in PVR and mPAP after iNO implies better long-term survival, is an independent predictor of survival, and facilitates risk stratification of patients with pulmonary hypertension, even in patients who are not suitable for treatment with calcium channel blockers (Malhotra et al., 2011). The clinical value of repeated iNO vascular reactivity testing in patients with pulmonary hypertension was first investigated by Tooba et al. The results showed that the reactivity of the pulmonary vasculature to iNO decreased over time, which may be related to disease progression leading to vasoconstrictive hypoplasia and to the impact of vasodilatory reserve by specific treatments for pulmonary arterial hypertension (Tooba et al., 2020). Ishii et al. confirmed Tooba's findings on altered pulmonary vascular reactivity but differed from them by suggesting that the results of vascular reactivity testing after treatment of pulmonary hypertension could suggest prognostic information. Patients with reduced vascular reactivity had worse clinical outcomes than those with preserved vascular reactivity, which facilitates earlier identification of high-risk individuals in the follow-up of pulmonary hypertension and facilitates early intervention and treatment (Ishii et al., 2023; Figure 2).

5. Summary and outlook

NO, as a free radical gas, is involved in numerous life activities through direct interaction with target cells or the formation of multiple nitrogen oxides. The biochemistry and mediated signaling pathways of NO are complex and diverse, and therapeutic agents and treatments derived from them are widely used in clinical practice. iNO is a method of delivering nitric oxide as a selective pulmonary vasodilator with excellent therapeutic potential for COVID-19 and other related respiratory and cardiovascular diseases. It has also recently inspired the creation of portable NO generators, an area of

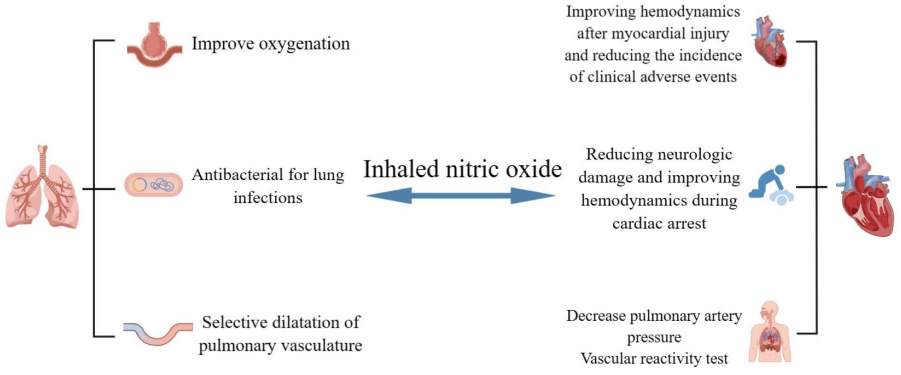

FIGURE 2
Potential clinical applications of iNO in respiratory and cardiovascular diseases. iNO can be used as a "rescue" or "innovative" therapy for COVID-19-related respiratory and cardiovascular diseases, with potential clinical benefits in hypoxemia, pulmonary infections, dilated pulmonary vessels, myocardial injury, cardiac arrest, and pulmonary hypertension. The potential clinical benefits of these therapies in hypoxemia However, high-quality evidence for these clinical applications is still lacking and needs to be explored and refined. (By Figdraw).

research that is currently quite active. Even though iNO appears to be a rescue therapy for seriously ill patients, there are toxicity concerns that must be carefully considered, as they are driven by pathophysiological signals *in vivo*. Clinical studies on iNO have been somewhat successful, but there is still a long way to go before it becomes a mature and safe therapy.

Author contributions

YZ: Writing – original draft. CL: Writing – review & editing. SZ: Writing – review & editing. JC: Writing – review & editing. YL: Writing – review & editing. XH: Writing – review & editing. YiW: Writing – review & editing. YoW: Writing – review & editing.

Funding

The author(s) declare financial support was received for the research, authorship, and/or publication of this article. The study was supported by the National Natural Science Foundation of China (CL, grant number: 82000347). This study was also supported by Jilin Province Science and technology development plan project (CL, grant number: YDZJ202301ZYTS441).

Conflict of interest

The authors declare that the research was conducted in the absence of any commercial or financial relationships that could be construed as a potential conflict of interest.

Publisher's note

All claims expressed in this article are solely those of the authors and do not necessarily represent those of their affiliated organizations, or those of the publisher, the editors and the reviewers. Any product that may be evaluated in this article, or claim that may be made by its manufacturer, is not guaranteed or endorsed by the publisher.

References

Adhikari, N. K., Burns, K. E., Friedrich, J. O., Granton, J. T., Cook, D. J., and Meade, M. O. (2007). Effect of nitric oxide on oxygenation and mortality in acute lung injury: systematic review and meta-analysis. *BMJ* 334:779. doi: 10.1136/bmj.39139.716794.55

Adusumilli, N. C., Zhang, D., Friedman, J. M., and Friedman, A. J. (2020). Harnessing nitric oxide for preventing, limiting and treating the severe pulmonary consequences of COVID-19. *Nitric Oxide* 103, 4–8. doi: 10.1016/j.niox.2020.07.003

Afshari, A., Brok, J., Møller, A. M., and Wetterslev, J. (2011). Inhaled nitric oxide for acute respiratory distress syndrome and acute lung injury in adults and children: a systematic review with meta-analysis and trial sequential analysis. *Anesth. Analg.* 112, 1411–1421. doi: 10.1213/ANE.0b013e31820bd185

Akaberi, D., Krambrich, J., Ling, J., Luni, C., Hedenstierna, G., Järhult, J. D., et al. (2020). Mitigation of the replication of SARS-CoV-2 by nitric oxide in vitro. *Redox Biol.* 37:101734. doi: 10.1016/j.redox.2020.101734

Al Sulaiman, K., Korayem, G. B., Altebainawi, A. F., Al Harbi, S., Alissa, A., Alharthi, A., et al. (2022). Evaluation of inhaled nitric oxide (iNO) treatment for moderate-to-severe ARDS in critically ill patients with COVID-19: a multicenter cohort study. *Crit. Care* 26:304. doi: 10.1186/s13054-022-04158-y

Ambrose, J. A., and Barua, R. S. (2004). The pathophysiology of cigarette smoking and cardiovascular disease: an update. *J. Am. Coll. Cardiol.* 43, 1731–1737. doi: 10.1016/j.jacc.2003.12.047

American Academy of Pediatrics (2000). Committee on fetus and newborn. Use of inhaled nitric oxide. *Pediatrics* 106, 344–345. doi: 10.1542/peds.106.2.344

Archer, S. L., Sharp, W. W., and Weir, E. K. (2020). Differentiating COVID-19 pneumonia from acute respiratory distress syndrome and high altitude pulmonary edema: therapeutic implications. *Circulation* 142, 101–104. doi: 10.1161/circulationaha.120.047915

Arnold, W. P., Mittal, C. K., Katsuki, S., and Murad, F. (1977). Nitric oxide activates guanylate cyclase and increases guanosine 3′:5′-cyclic monophosphate levels in various tissue preparations. *Proc. Natl. Acad. Sci. U. S. A.* 74, 3203–3207. doi: 10.1073/pnas.74.8.3203

Ataei Ataabadi, E., Golshiri, K., Jüttner, A., Krenning, G., Danser, A. H. J., and Roks, A. J. M. (2020). Nitric oxide-cGMP signaling in hypertension: current and future options for pharmacotherapy. *Hypertension* 76, 1055–1068. doi: 10.1161/hypertensionaha.120.15856

Barnes, M., and Brisbois, E. J. (2020). Clinical use of inhaled nitric oxide: local and systemic applications. *Free Radic. Biol. Med.* 152, 422–431. doi: 10.1016/j.freeradbiomed.2019.11.029

Berlin, I., Thomas, D., Le Faou, A. L., and Cornuz, J. (2020). COVID-19 and smoking. *Nicotine Tob. Res.* 22, 1650–1652. doi: 10.1093/ntr/ntaa059

Betancor, D., Olaguibel, J. M., and Sastre, J. (2022a). The discrepant role of fractional exhaled nitric oxide in SARS-CoV-2 infection. *J. Investig. Allergol. Clin. Immunol.* 32, 417–418. doi: 10.18176/jiaci.0842

Betancor, D., Valverde-Mongue, M., Gomez-Lopez, A., Barroso, B., Ruete, L., Olaguibel, J. M., et al. (2022b). Evaluation of fractional exhaled nitric oxide during SARS-CoV-2 infection. *J. Investig. Allergol. Clin. Immunol.* 32, 301–303. doi: 10.18176/jiaci.0762

Bonizzoli, M., Lazzeri, C., Cianchi, G., Guetti, C., Fulceri, G. E., Socci, F., et al. (2022). Effects of rescue inhaled nitric oxide on right ventricle and pulmonary circulation in severe COVID-related acute respiratory distress syndrome. *J. Crit. Care* 72:153987. doi: 10.1016/j.jcrc.2022.153987

Bos, L. D. J., and Ware, L. B. (2022). Acute respiratory distress syndrome: causes, pathophysiology, and phenotypes. *Lancet* 400, 1145–1156. doi: 10.1016/s0140-6736(22)01485-4

Burov, O. N., Kletskii, M. E., Kurbatov, S. V., Lisovin, A. V., and Fedik, N. S. (2022). Mechanisms of nitric oxide generation in living systems. *Nitric Oxide* 118, 1–16. doi: 10.1016/j.niox.2021.10.003

Cespuglio, R., Strekalova, T., Spencer, P. S., Román, G. C., Reis, J., Bouteille, B., et al. (2021). SARS-CoV-2 infection and sleep disturbances: nitric oxide involvement and therapeutic opportunity. *Sleep* 44:zsab009. doi: 10.1093/sleep/zsab009

Chambers, D. C., Tunnicliffe, W. S., and Ayres, J. G. (1998). Acute inhalation of cigarette smoke increases lower respiratory tract nitric oxide concentrations. *Thorax* 53, 677–679. doi: 10.1136/thx.53.8.677

Chen, Y., Klein, S. L., Garibaldi, B. T., Li, H., Wu, C., Osevala, N. M., et al. (2021). Aging in COVID-19: vulnerability, immunity and intervention. *Ageing Res. Rev.* 65:101205. doi: 10.1016/j.arr.2020.101205

Cinelli, M. A., Do, H. T., Miley, G. P., and Silverman, R. B. (2020). Inducible nitric oxide synthase: regulation, structure, and inhibition. *Med. Res. Rev.* 40, 158–189. doi: 10.1002/med.21599

Demoncheaux, E. A., Higenbottam, T. W., Kiely, D. G., Wong, J. M., Wharton, S., Varcoe, R., et al. (2005). Decreased whole body endogenous nitric oxide production in patients with primary pulmonary hypertension. *J. Vasc. Res.* 42, 133–136. doi: 10.1159/000083502

Deppisch, C., Herrmann, G., Graepler-Mainka, U., Wirtz, H., Heyder, S., Engel, C., et al. (2016). Gaseous nitric oxide to treat antibiotic resistant bacterial and fungal lung infections in patients with cystic fibrosis: a phase I clinical study. *Infection* 44, 513–520. doi: 10.1007/s15010-016-0879-x

Dominic, P., Ahmad, J., Bhandari, R., Pardue, S., Solorzano, J., Jaisingh, K., et al. (2021). Decreased availability of nitric oxide and hydrogen sulfide is a hallmark of COVID-19. *Redox Biol.* 43:101982. doi: 10.1016/j.redox.2021.101982

Fang, W., Jiang, J., Su, L., Shu, T., Liu, H., Lai, S., et al. (2021). The role of NO in COVID-19 and potential therapeutic strategies. *Free Radic. Biol. Med.* 163, 153–162. doi: 10.1016/j.freeradbiomed.2020.12.008

Feng, W. X., Yang, Y., Wen, J., Liu, Y. X., Liu, L., and Feng, C. (2021). Implication of inhaled nitric oxide for the treatment of critically ill COVID-19 patients with pulmonary hypertension. *ESC Heart Fail* 8, 714–718. doi: 10.1002/ehf2.13023

Ferrari, M., and Protti, A. (2022). Nitric oxide in COVID-19: too little of a good thing? *EBioMedicine* 77:103925. doi: 10.1016/j.ebiom.2022.103925

Flume, P. A., Garcia, B. A., Wilson, D., Steed, L., Dorman, S. E., and Winthrop, K. (2023). Inhaled nitric oxide for adults with pulmonary non-tuberculous mycobacterial infection. *Respir. Med.* 206:107069. doi: 10.1016/j.rmed.2022.107069

Förstermann, U., and Sessa, W. C. (2012). Nitric oxide synthases: regulation and function. *Eur. Heart J.* 33, 829–837. doi: 10.1093/eurheartj/ehr304

Frostell, C. G., and Hedenstierna, G. (2021). Nitric oxide and COVID-19: dose, timing and how to administer it might be crucial. *Acta Anaesthesiol. Scand.* 65, 576–577. doi: 10.1111/aas.13788

Garfield, B., McFadyen, C., Briar, C., Bleakley, C., Vlachou, A., Baldwin, M., et al. (2021). Potential for personalised application of inhaled nitric oxide in COVID-19 pneumonia. *Br. J. Anaesth.* 126, e72–e75. doi: 10.1016/j.bja.2020.11.006

Garufi, G., Carbognin, L., Orlandi, A., Tortora, G., and Bria, E. (2020). Smoking habit and hospitalization for severe acute respiratory syndrome coronavirus 2 (SARS-CoV-2)-related pneumonia: the unsolved paradox behind the evidence. *Eur. J. Intern. Med.* 77, 121–122. doi: 10.1016/j.ejim.2020.04.042

Gebistorf, F., Karam, O., Wetterslev, J., and Afshari, A. (2016). Inhaled nitric oxide for acute respiratory distress syndrome (ARDS) in children and adults. *Cochrane Database Syst. Rev.* 2018:CD002787. doi: 10.1002/14651858.CD002787.pub3

Ghaffari, A., Miller, C. C., McMullin, B., and Ghahary, A. (2006). Potential application of gaseous nitric oxide as a topical antimicrobial agent. *Nitric Oxide* 14, 21–29. doi: 10.1016/j.niox.2005.08.003

Giaid, A., and Saleh, D. (1995). Reduced expression of endothelial nitric oxide synthase in the lungs of patients with pulmonary hypertension. *N. Engl. J. Med.* 333, 214–221. doi: 10.1056/nejm199507273330403

Goldbart, A., Lavie, M., Lubetzky, R., Pillar, G., Landau, D., Schlesinger, Y., et al. (2023). Inhaled nitric oxide for the treatment of acute bronchiolitis: a multicenter randomized controlled clinical trial to evaluate dose response. *Ann. Am. Thorac. Soc.* 20, 236–244. doi: 10.1513/AnnalsATS.202103-348OC

Goldberg, A. B., Mazur, W., and Kalra, D. K. (2017). Pulmonary hypertension: diagnosis, imaging techniques, and novel therapies. *Cardiovasc Diagn Ther* 7, 405–417. doi: 10.21037/cdt.2017.04.11

Grześk, G., Witczyńska, A., Węglarz, M., Wołowiec, Ł., Nowaczyk, J., Grześk, E., et al. (2023). Soluble guanylyl cyclase activators-promising therapeutic option in the pharmacotherapy of heart failure and pulmonary hypertension. *Molecules* 28:861. doi: 10.3390/molecules28020861

Guida, G., Carriero, V., Bertolini, F., Pizzimenti, S., Heffler, E., Paoletti, G., et al. (2023). Exhaled nitric oxide in asthma: from diagnosis to management. *Curr. Opin. Allergy Clin. Immunol.* 23, 29–35. doi: 10.1097/aci.0000000000000877

Guimarães, L. M. F., Rossini, C. V. T., and Lameu, C. (2021). Implications of SARS-Cov-2 infection on eNOS and iNOS activity: consequences for the respiratory and vascular systems. *Nitric Oxide* 111-112, 64–71. doi: 10.1016/j.niox.2021.04.003

Hedenstierna, G., Chen, L., Hedenstierna, M., Lieberman, R., and Fine, D. H. (2020). Nitric oxide dosed in short bursts at high concentrations may protect against Covid 19. *Nitric Oxide* 103, 1–3. doi: 10.1016/j.niox.2020.06.005

Ishii, S., Hatano, M., Maki, H., Minatsuki, S., Saito, A., Yagi, H., et al. (2023). Prognostic value of follow-up vasoreactivity test in pulmonary arterial hypertension. *J. Cardiol.* 82, 69–75. doi: 10.1016/j.jjcc.2023.01.005

Kaisers, U., Busch, T., Deja, M., Donaubauer, B., and Falke, K. J. (2003). Selective pulmonary vasodilation in acute respiratory distress syndrome. *Crit. Care Med.* 31, S337–S342. doi: 10.1097/01.Ccm.0000057913.45273.1a

Kamenshchikov, N. O., Berra, L., and Carroll, R. W. (2022). Therapeutic effects of inhaled nitric oxide therapy in COVID-19 patients. *Biomedicine* 10:20369. doi: 10.3390/biomedicines10020369

Karki, R., Sharma, B. R., Tuladhar, S., Williams, E. P., Zalduondo, L., Samir, P., et al. (2021). Synergism of TNF-α and IFN-γ triggers inflammatory cell death, tissue damage, and mortality in SARS-CoV-2 infection and cytokine shock syndromes. *Cells* 184, 149–168.e17. doi: 10.1016/j.cell.2020.11.025

Kashiwagi, S., Morita, A., Yokomizo, S., Ogawa, E., Komai, E., Huang, P. L., et al. (2023). Photobiomodulation and nitric oxide signaling. *Nitric Oxide* 130, 58–68. doi: 10.1016/j.niox.2022.11.005

Kerget, B., Araz, Ö., and Akgün, M. (2022). The role of exhaled nitric oxide (FeNO) in the evaluation of lung parenchymal involvement in COVID-19 patients. *Intern. Emerg. Med.* 17, 1951–1958. doi: 10.1007/s11739-022-03035-4

Keshavarz, A., Kadry, H., Alobaida, A., and Ahsan, F. (2020). Newer approaches and novel drugs for inhalational therapy for pulmonary arterial hypertension. *Expert Opin. Drug Deliv.* 17, 439–461. doi: 10.1080/17425247.2020.1729119

Li, H., Horke, S., and Förstermann, U. (2014). Vascular oxidative stress, nitric oxide and atherosclerosis. *Atherosclerosis* 237, 208–219. doi: 10.1016/j.atherosclerosis.2014.09.001

Lior, Y., Yatzkan, N., Brami, I., Yogev, Y., Riff, R., Hekselman, I., et al. (2022). Fractional exhaled nitric oxide (FeNO) level as a predictor of COVID-19 disease severity. *Nitric Oxide* 124, 68–73. doi: 10.1016/j.niox.2022.05.002

Lisi, F., Zelikin, A. N., and Chandrawati, R. (2021). Nitric oxide to fight viral infections. *Adv. Sci.* 8:2003895. doi: 10.1002/advs.202003895

Longobardo, A., Montanari, C., Shulman, R., Benhalim, S., Singer, M., and Arulkumaran, N. (2021). Inhaled nitric oxide minimally improves oxygenation in COVID-19 related acute respiratory distress syndrome. *Br. J. Anaesth.* 126, e44–e46. doi: 10.1016/j.bja.2020.10.011

Lotz, C., Muellenbach, R. M., Meybohm, P., Mutlak, H., Lepper, P. M., Rolfes, C. B., et al. (2021). Effects of inhaled nitric oxide in COVID-19-induced ARDS—is it worthwhile? *Acta Anaesthesiol. Scand.* 65, 629–632. doi: 10.1111/aas.13757

Lugg, S. T., Scott, A., Parekh, D., Naidu, B., and Thickett, D. R. (2022). Cigarette smoke exposure and alveolar macrophages: mechanisms for lung disease. *Thorax* 77, 94–101. doi: 10.1136/thoraxjnl-2020-216296

Lundberg, J. O., and Weitzberg, E. (2022). Nitric oxide signaling in health and disease. *Cells* 185, 2853–2878. doi: 10.1016/j.cell.2022.06.010

Ma, J., Li, Y., Yang, X., Liu, K., Zhang, X., Zuo, X., et al. (2023). Signaling pathways in vascular function and hypertension: molecular mechanisms and therapeutic interventions. *Signal Transduct. Target. Ther.* 8:168. doi: 10.1038/s41392-023-01430-7

Mac Micking, J., Xie, Q. W., and Nathan, C. (1997). Nitric oxide and macrophage function. *Annu. Rev. Immunol.* 15, 323–350. doi: 10.1146/annurev.immunol.15.1.323

Malhotra, R., Hess, D., Lewis, G. D., Bloch, K. D., Waxman, A. B., and Semigran, M. J. (2011). Vasoreactivity to inhaled nitric oxide with oxygen predicts long-term survival in pulmonary arterial hypertension. *Pulm Circ* 1, 250–258. doi: 10.4103/2045-8932.83449

Mandal, S. M. (2023). Nitric oxide mediated hypoxia dynamics in COVID-19. *Nitric Oxide* 133, 18–21. doi: 10.1016/j.niox.2023.02.002

Maniscalco, M., Ambrosino, P., Poto, R., Fuschillo, S., Poto, S., Matera, M. G., et al. (2022). Can FeNO be a biomarker in the post-COVID-19 patients monitoring? *Respir. Med.* 193:106745. doi: 10.1016/j.rmed.2022.106745

Matthay, M. A., Aldrich, J. M., and Gotts, J. E. (2020). Treatment for severe acute respiratory distress syndrome from COVID-19. *Lancet Respir. Med.* 8, 433–434. doi: 10.1016/s2213-2600(20)30127-2

Mekontso Dessap, A., Papazian, L., Schaller, M., Nseir, S., Megarbane, B., Haudebourg, L., et al. (2023). Inhaled nitric oxide in patients with acute respiratory distress syndrome caused by COVID-19: treatment modalities, clinical response, and outcomes. *Ann. Intensive Care* 13:57. doi: 10.1186/s13613-023-01150-9

Meyer, N. J., Gattinoni, L., and Calfee, C. S. (2021). Acute respiratory distress syndrome. *Lancet* 398, 622–637. doi: 10.1016/s0140-6736(21)00439-6

Michaelsen, V. S., Ribeiro, R. V. P., Brambate, E., Ali, A., Wang, A., Pires, L., et al. (2021). A novel pre-clinical strategy to deliver antimicrobial doses of inhaled nitric oxide. *PloS One* 16:e0258368. doi: 10.1371/journal.pone.0258368

Miller, C. C., Hergott, C. A., Rohan, M., Arsenault-Mehta, K., Döring, G., and Mehta, S. (2013). Inhaled nitric oxide decreases the bacterial load in a rat model of *Pseudomonas aeruginosa* pneumonia. *J. Cyst. Fibros.* 12, 817–820. doi: 10.1016/j.jcf.2013.01.008

Miller, M. R., and Megson, I. L. (2007). Recent developments in nitric oxide donor drugs. *Br. J. Pharmacol.* 151, 305–321. doi: 10.1038/sj.bjp.0707224

Miller, C., Miller, M., McMullin, B., Regev, G., Serghides, L., Kain, K., et al. (2012). A phase I clinical study of inhaled nitric oxide in healthy adults. *J. Cyst. Fibros.* 11, 324–331. doi: 10.1016/j.jcf.2012.01.003

Montani, D., Chaumais, M. C., Guignabert, C., Günther, S., Girerd, B., Jaïs, X., et al. (2014). Targeted therapies in pulmonary arterial hypertension. *Pharmacol. Ther.* 141, 172–191. doi: 10.1016/j.pharmthera.2013.10.002

Montiel, V., Lobysheva, I., Gérard, L., Vermeersch, M., Perez-Morga, D., Castelein, T., et al. (2022). Oxidative stress-induced endothelial dysfunction and decreased vascular nitric oxide in COVID-19 patients. *EBioMedicine* 77:103893. doi: 10.1016/j.ebiom.2022.103893

Mortaz, E., Malkmohammad, M., Jamaati, H., Naghan, P. A., Hashemian, S. M., Tabarsi, P., et al. (2020). Silent hypoxia: higher NO in red blood cells of COVID-19 patients. *BMC Pulm. Med.* 20:269. doi: 10.1186/s12890-020-01310-8

Murugesan, N., Saxena, D., Dileep, A., Adrish, M., and Hanania, N. A. (2023). Update on the role of FeNO in asthma management. *Diagnostics* 13:1428. doi: 10.3390/diagnostics13081428

Nakane, T., Esaki, J., Ueda, R., Honda, M., and Okabayashi, H. (2021). Inhaled nitric oxide improves pulmonary hypertension and organ functions after adult heart valve surgeries. *Gen. Thorac. Cardiovasc. Surg.* 69, 1519–1526. doi: 10.1007/s11748-021-01651-z

Nasyrova, R. F., Moskaleva, P. V., Vaiman, E. E., Shnayder, N. A., Blatt, N. L., and Rizvanov, A. A. (2020). Genetic factors of nitric Oxide's system in Psychoneurologic disorders. *Int. J. Mol. Sci.* 21:604. doi: 10.3390/ijms21051604

Nathan, S. D., Flaherty, K. R., Glassberg, M. K., Raghu, G., Swigris, J., Alvarez, R., et al. (2020). A randomized, double-blind, placebo-controlled study of pulsed, inhaled nitric oxide in subjects at risk of pulmonary hypertension associated with pulmonary fibrosis. *Chest* 158, 637–645. doi: 10.1016/j.chest.2020.02.016

Nogueira, R. C., Minnion, M., Clark, A. D., Dyson, A., Tanus-Santos, J. E., and Feelisch, M. (2022). On the origin of nitrosylated hemoglobin in COVID-19: endothelial NO capture or redox conversion of nitrite?: experimental results and a cautionary note on challenges in translational research. *Redox Biol.* 54:102362. doi: 10.1016/j.redox.2022.102362

Papadopoulos, K. I., Papadopoulou, A., and Aw, T. C. (2023). Live to die another day: novel insights may explain the pathophysiology behind smoker's paradox in SARS-CoV-2 infection. *Mol. Cell. Biochem.* 1-10, 1–10. doi: 10.1007/s11010-023-04681-8

Parikh, R., Wilson, C., Weinberg, J., Gavin, D., Murphy, J., and Reardon, C. C. (2020). Inhaled nitric oxide treatment in spontaneously breathing COVID-19 patients. *Ther. Adv. Respir. Dis.* 14:1753466620933510. doi: 10.1177/1753466620933510

Redaelli, S., Magliocca, A., Malhotra, R., Ristagno, G., Citerio, G., Bellani, G., et al. (2022). Nitric oxide: clinical applications in critically ill patients. *Nitric Oxide* 121, 20–33. doi: 10.1016/j.niox.2022.01.007

Redaelli, S., Pozzi, M., Giani, M., Magliocca, A., Fumagalli, R., Foti, G., et al. (2023). Inhaled nitric oxide in acute respiratory distress syndrome subsets: rationale and clinical applications. *J. Aerosol Med. Pulm. Drug Deliv.* 36, 112–126. doi: 10.1089/jamp.2022.0058

Roberts, J. D., Polaner, D. M., Lang, P., and Zapol, W. M. (1992). Inhaled nitric oxide in persistent pulmonary hypertension of the newborn. *Lancet* 340, 818–819. doi: 10.1016/0140-6736(92)92686-a

Rousseaud, A., Prot, M., Loriere, E. S., Katz, I., Ramirez-Gil, J. F., and Farjot, G. (2023). Gaseous nitric oxide failed to inhibit the replication cycle of SARS-CoV-2 in vitro. *Nitric Oxide* 132, 27–33. doi: 10.1016/j.niox.2023.01.004

Rupani, H., and Kent, B. D. (2022). Using fractional exhaled nitric oxide measurement in clinical asthma management. *Chest* 161, 906–917. doi: 10.1016/j.chest.2021.10.015

Russo, I., Barale, C., Melchionda, E., Penna, C., and Pagliaro, P. (2023). Platelets and Cardioprotection: the role of nitric oxide and carbon oxide. *Int. J. Mol. Sci.* 24:6107. doi: 10.3390/ijms24076107

Safaee Fakhr, B., Di Fenza, R., Gianni, S., Wiegand, S. B., Miyazaki, Y., Araujo Morais, C. C., et al. (2021). Inhaled high dose nitric oxide is a safe and effective respiratory treatment in spontaneous breathing hospitalized patients with COVID-19 pneumonia. *Nitric Oxide* 116, 7–13. doi: 10.1016/j.niox.2021.08.003

Safaee Fakhr, B., Wiegand, S. B., Pinciroli, R., Gianni, S., Morais, C. C. A., Ikeda, T., et al. (2020). High concentrations of nitric oxide inhalation therapy in pregnant patients with severe coronavirus disease 2019 (COVID-19). *Obstet. Gynecol.* 136, 1109–1113. doi: 10.1097/aog.0000000000004128

Santacroce, L., Di Domenico, M., Montagnani, M., and Jirillo, E. (2023). Antibiotic resistance and microbiota response. *Curr. Pharm. Des.* 29, 356–364. doi: 10.2174/1381612829666221219093450

Sardo, S., Osawa, E. A., Finco, G., Gomes Galas, F. R. B., de Almeida, J. P., Cutuli, S. L., et al. (2018). Nitric oxide in cardiac surgery: a Meta-analysis of randomized controlled trials. *J. Cardiothorac. Vasc. Anesth.* 32, 2512–2519. doi: 10.1053/j.jvca.2018.02.003

Sharma, N. M., and Patel, K. P. (2017). Post-translational regulation of neuronal nitric oxide synthase: implications for sympathoexcitatory states. *Expert Opin. Ther. Targets* 21, 11–22. doi: 10.1080/14728222.2017.1265505

Shei, R. J., and Baranauskas, M. N. (2022). More questions than answers for the use of inhaled nitric oxide in COVID-19. *Nitric Oxide* 124, 39–48. doi: 10.1016/j.niox.2022.05.001

Signori, D., Magliocca, A., Hayashida, K., Graw, J. A., Malhotra, R., Bellani, G., et al. (2022). Inhaled nitric oxide: role in the pathophysiology of cardio-cerebrovascular and respiratory diseases. *Intensive Care Med. Exp.* 10:28. doi: 10.1186/s40635-022-00455-6

Sokol, G. M., Konduri, G. G., and Van Meurs, K. P. (2016). Inhaled nitric oxide therapy for pulmonary disorders of the term and preterm infant. *Semin. Perinatol.* 40, 356–369. doi: 10.1053/j.semperi.2016.05.007

Sorbo, L. D., Michaelsen, V. S., Ali, A., Wang, A., Ribeiro, R. V. P., and Cypel, M. (2022). High doses of inhaled nitric oxide as an innovative antimicrobial strategy for lung infections. *Biomedicine* 10:1525. doi: 10.3390/biomedicines10071525

Soundararajan, L., Dharmarajan, A., and Samji, P. (2023). Regulation of pleiotropic physiological roles of nitric oxide signaling. *Cell. Signal.* 101:110496. doi: 10.1016/j.cellsig.2022.110496

Stasch, J. P., Pacher, P., and Evgenov, O. V. (2011). Soluble guanylate cyclase as an emerging therapeutic target in cardiopulmonary disease. *Circulation* 123, 2263–2273. doi: 10.1161/circulationaha.110.981738

Stefano, G. B., Esch, T., and Kream, R. M. (2020). Potential Immunoregulatory and antiviral/SARS-CoV-2 activities of nitric oxide. *Med. Sci. Monit.* 26:e925679. doi: 10.12659/msm.925679

Stratton, C. W., Tang, Y. W., and Lu, H. (2021). Pathogenesis-directed therapy of 2019 novel coronavirus disease. *J. Med. Virol.* 93, 1320–1342. doi: 10.1002/jmv.26610

Tooba, R., Almoushref, A., and Tonelli, A. R. (2020). Is there value in repeating inhaled nitric oxide Vasoreactivity tests in patients with pulmonary arterial hypertension? *Lung* 198, 87–94. doi: 10.1007/s00408-019-00318-0

Triposkiadis, F., Xanthopoulos, A., Skoularigis, J., and Starling, R. C. (2022). Therapeutic augmentation of NO-sGC-cGMP signalling: lessons learned from pulmonary arterial hypertension and heart failure. *Heart Fail. Rev.* 27, 1991–2003. doi: 10.1007/s10741-022-10239-5

Usman, M. S., Siddiqi, T. J., Khan, M. S., Patel, U. K., Shahid, I., Ahmed, J., et al. (2021). Is there a smoker's paradox in COVID-19? *BMJ Evid Based Med* 26, 279–284. doi: 10.1136/bmjebm-2020-111492

Wang, H., Yu, M., Ochani, M., Amella, C. A., Tanovic, M., Susarla, S., et al. (2003). Nicotinic acetylcholine receptor alpha 7 subunit is an essential regulator of inflammation. *Nature* 421, 384–388. doi: 10.1038/nature01339

Wiegand, S. B., Traeger, L., Nguyen, H. K., Rouillard, K. R., Fischbach, A., Zadek, F., et al. (2021). Antimicrobial effects of nitric oxide in murine models of Klebsiella pneumonia. *Redox Biol.* 39:101826. doi: 10.1016/j.redox.2020.101826

Winchester, S., John, S., Jabbar, K., and John, I. (2021). Clinical efficacy of nitric oxide nasal spray (NONS) for the treatment of mild COVID-19 infection. *J. Infect.* 83, 237–279. doi: 10.1016/j.jinf.2021.05.009

Yao, J., Zou, P., Cui, Y., Quan, L., Gao, C., Li, Z., et al. (2023). Recent advances in strategies to combat bacterial drug resistance: antimicrobial materials and drug delivery systems. *Pharmaceutics* 15:1188. doi: 10.3390/pharmaceutics15041188

Yong, S. J. (2021). Long COVID or post-COVID-19 syndrome: putative pathophysiology, risk factors, and treatments. *Infect. Dis.* 53, 737–754. doi: 10.1080/23744235.2021.1924397

Yuki, K., Fujiogi, M., and Koutsogiannaki, S. (2020). COVID-19 pathophysiology: a review. *Clin. Immunol.* 215:108427. doi: 10.1016/j.clim.2020.108427

Zhao, Y., Vanhoutte, P. M., and Leung, S. W. (2015). Vascular nitric oxide: Beyond eNOS. *J. Pharmacol. Sci.* 129, 83–94. doi: 10.1016/j.jphs.2015.09.002

Zolty, R. (2020). Pulmonary arterial hypertension specific therapy: the old and the new. *Pharmacol. Ther.* 214:107576. doi: 10.1016/j.pharmthera.2020.107576

frontiers | Frontiers in Microbiology

TYPE Original Research
PUBLISHED 03 November 2023
DOI 10.3389/fmicb.2023.1237913

OPEN ACCESS

EDITED BY
Wei Wei,
First Affiliated Hospital of Jilin University, China

REVIEWED BY
Zhiwen Xu,
Sichuan Agricultural University, China
Changxu Song,
South China Agricultural University, China

*CORRESPONDENCE
Xingcui Zhang
✉ zhangxc923@163.com
ZhenHui Song
✉ szh7678@126.com

†These authors have contributed equally to this work

RECEIVED 10 June 2023
ACCEPTED 16 October 2023
PUBLISHED 03 November 2023

CITATION
Zhang Y, Zhang S, Sun Z, Liu X, Liao G, Niu Z, Kan Z, Xu S, Zhang J, Zou H, Zhang X and Song Z (2023) Porcine epidemic diarrhea virus causes diarrhea by activating EGFR to regulates NHE3 activity and mobility on plasma membrane.
Front. Microbiol. 14:1237913.
doi: 10.3389/fmicb.2023.1237913

Porcine epidemic diarrhea virus causes diarrhea by activating EGFR to regulates NHE3 activity and mobility on plasma membrane

YiLing Zhang[1,2†], Shujuan Zhang[1†], Zhiwei Sun[1†], Xiangyang Liu[1,3], Guisong Liao[1], Zheng Niu[4], ZiFei Kan[1,5], ShaSha Xu[1], JingYi Zhang[1], Hong Zou[1], Xingcui Zhang[1*] and ZhenHui Song[1,6*]

[1]School of Animal Medicine, Southwest University Rongchang Campus, Chongqing, China, [2]Department of Animal Science and Technology, Three Gorges Vocational College, Chongqing, China, [3]Department of Preventive Veterinary Medicine, College of Animal Medicine, Xinjiang Agricultural University, Xinjiang, China, [4]College of Veterinary Medicine, Northwest Agriculture and Forestry University, Shanxi, China, [5]School of Medicine, University of Electronic Science and Technology, Chengdu, China, [6]Immunology Research Center, Institute of Medical Research, Southwest University, Chongqing, China

As part of the genus Enteropathogenic Coronaviruses, Porcine Epidemic Diarrhea Virus (PEDV) is an important cause of early diarrhea and death in piglets, and one of the most difficult swine diseases to prevent and control in the pig industry. Previously, we found that PEDV can block Na^+ absorption and induce diarrhea in piglets by inhibiting the activity of the sodium-hydrogen ion transporter NHE3 in pig intestinal epithelial cells, but the mechanism needs to be further explored. The epidermal growth factor receptor (EGFR) has been proved to be one of the co-receptors involved in many viral infections and a key protein involved in the regulation of NHE3 activity in response to various pathological stimuli. Based on this, our study used porcine intestinal epithelial cells (IPEC-J2) as an infection model to investigate the role of EGFR in regulating NHE3 activity after PEDV infection. The results showed that EGFR mediated viral invasion by interacting with PEDV S1, and activated EGFR regulated the downstream EGFR/ERK signaling pathway, resulting in decreased expression of NHE3 and reduced NHE3 mobility at the plasma membrane, which ultimately led to decreased NHE3 activity. The low level of NHE3 expression in intestinal epithelial cells may be a key factor leading to PEDV-induced diarrhea in newborn piglets. This study reveals the importance of EGFR in the regulation of NHE3 activity by PEDV and provides new targets and clues for the prevention and treatment of PEDV-induced diarrhea in piglets.

KEYWORDS

PEDV, sodium-hydrogen exchanger NHE3, EGFR, diarrhea, piglets

1. Introduction

PEDV is one of the main pathogens that cause diarrhea in piglets, it is a gastrointestinal infection with high mortality, manifested by jet diarrhea, rapid dehydration and severe vomiting (No et al., 2015; Chen et al., 2019; Niu et al., 2021). Indeed, 80–100% of piglets die within a few days after infection (Alvarez et al., 2015; Lee, 2015). In recent years, because of the continuous emergence of new epidemic strains of PEDV, traditional vaccination has not achieved the expected prevention and control effect, and large-scale outbreaks continue to occur, bringing

serious economic losses to the pig industry (Wang et al., 2020). The target organ of PEDV infection in the host is the pig's small intestine, which can cause intestinal cell dysfunction and abnormal expression of channel proteins related to water and salt metabolism, resulting in disruption of the balance between absorption and secretion of intestinal substances and loss of water and electrolytes, ultimately leading to vomiting, reduced appetite, and impaired absorption diarrhea (Song et al., 2015). Therefore, determining the etiology and pathogenic mechanism of PEDV-induced diarrhea could provide a more effective method to its prevention and control.

Severe dehydration due to acute diarrhea is the key factor leading to death in newborn piglets. Diarrhea is associated with impaired Na^+ absorption by IPEC-J2 cells (Field, 2003); but the mechanism of sodium imbalance diarrhea due to PEDV needs to be further investigated. Na^+/H^+ exchanger 3 is one of the transmembrane transporter proteins that are essential for mediating Na^+/H^+ homeostasis in the gut, playing a major role in regulating cellular pH and the homeostasis of the intestinal microenvironment (No et al., 2015). Changes in its activity and the amount of expression are closely related to the onset of diarrhea. When the activity of NHE3 is inhibited for a long time, it can lead to the occurrence of disease, and even death in severe cases (Anbazhagan et al., 2018). NHE3 is transported in the plasma membrane and the intracellular circulation of small intestinal villous epithelial cells, and the sodium-hydrogen exchange activity is mainly influenced by the amount of NHE3 transferred to the plasma membrane. Therefore, regulation of the functional activity of NHE3 is closely related to its mobility at the plasma membrane.

Signaling pathways activated by the epidermal growth factor receptor (EGFR) play an important role in cell proliferation, apoptosis and viral infection. EGFR is the transmembrane receptor for most viruses, including TGEV, which helps the virus invade the host and activates related signaling pathways (Hu et al., 2018). A recent study found that activation of EGFR occurs at an early stage of PEDV infection and might interact directly with viral S proteins to mediate PEDV invasion (Yang L. et al., 2018), the mechanism of action of which is unclear.

Further studies in our laboratory have shown that specific inhibition of NHE3 activity in IPEC-J2 cells leads to watery diarrhea and severe dehydration in piglets (Niu et al., 2021). Furthermore, PEDV infection inhibited the expression of NHE3 in IPEC-J2 cells and reduced extracellular Na^+ uptake by the cells. Thus, the aim of this study was to explore the role of EGFR in the regulation of NHE3 activity by PEDV infection is an important reference for finding the targets of action against PEDV diarrhea.

2. Materials and methods

2.1. Cells, viruses, and reagents

IPEC-J2 and African green monkey kidney cells (Vero) were both cultured in DMEM medium containing 10% fetal bovine serum, 1% double antibody in a 37°C, 5% CO_2 cell culture incubator. The cells mentioned above were all pre-preserved in the laboratory. The PEDV-LJX variant was kindly presented by Guangliang Liu, a researcher from Lanzhou Veterinary Research Institute. Recombinant human EGF from Gibco (Grand Island, NY, USA) at 10 ng/mL. The tyrosinase inhibitor AG1478 was purchased from Apexbio (Houston, TX, USA) and used at a dose of 30 μM.

2.2. Total cellular proteins and membrane protein extraction

IPEC-J2 cells were seeded in 60 mm dishes. An experimental group and a control group were set up, and each group was replicated three times independently. When cells grew to 90%, PEDV virus fluid (MOI = 0.1), or an optimal dose of EGFR modulator, was inoculated at 2 h and 72 h, respectively. The proteins were extracted using Beyotime's cell membrane and plasma protein extraction kits, added with 6 × Loading Buffer (TransGen Biotech, China), denatured at 100°C for 10 min, cooled, and stored at −20°C before use.

2.3. Western blotting

Equal amounts of protein samples were separated by SDS-PAGE gel electro-phoresis and transferred to polyvinylidene fluoride membranes. The membranes was blocked with 5% skimmed milk powder diluted by TBST. After incubation overnight at 4°C with the appropriate primary antibody, the membrane was washed three times with 1 × TBST for 10 min/time and then incubated with goat anti-rabbit secondary antibody or goat anti-mouse secondary antibody (Proteintech, Rosemont, IL, USA) for 90 min on a shaker at room temperature. Images of the immunoreactive proteins on the membrane were chromogenic using the FX5 imaging system (VILBER, Marne-la-Vallée cedex 3, France). The grayscale values were analyzed. The phospho-EGFR (Tyr1068) antibody was purchased from Cell Signaling Technology (Danvers, MA, USA). Antibodies recognizing EGFR, SLC9A3 (NHE3), β-Actin, β-Tubulin (Rabbit Antibody), 6 × His (His-Tag), and FLAG® tag were purchased from Proteintech. The phospho-extracellular kinase (ERK)1/2 (Thr202 + Tyr204) antibody was purchased from Beijing BoaoSen Biotechnology Co. (Beijing, China).

2.4. Half of the tissue culture infected dose ($TCID_{50}$)

After IPEC-J2 cells had grown to spread all over the cell bottles, pre-treatment of cells with 10 ng/mL of EGF or 30 μM of AG1478 in 2 mL, and then inoculated with 10^5 $TCID_{50}$/mL PEDV-LJX strain, and both virus-infected and blank control groups were established. After incubation with the virus for 1.5 h, the cells were freeze-thawed three times and then centrifuged at 12000 × g for 10 min. The supernatant was collected into centrifuge tubes, and the $TCID_{50}$ of each group of PEDV was determined in Vero cells according to the Reed-Muench method.

2.5. Co-immunoprecipitation (Co-IP)

Sequences of the coding regions of the PEDV S and EGFR genes registered in GenBank according to the NCBI, PEDV S1 (637–2,127 bp) was selected and constructed into vector pTT5 as a Flag tag fusion. The fragment of EGFR encoding the extracellular region (139–1,473 bp) was constructed into vector pTT5 as a His tag fusion. The above gene fragments were synthesized, and the recombinant plasmids were constructed, and sequenced by Wuhan GeneCreate Biological

Engineering Co., Ltd. (Wuhan, China). Splicing HEK-293 T cells into 60 mm dishes, and when the cells grew to about 80% confluence, they were transfected with the constructed eukaryotic expression vector plasmids of PEDV S1 and EGFR extracellular region. At 48 h after transfection, samples were prepared for immunoprecipitation and the target bands were detected using western blotting.

2.6. Fluorescence recovery after photobleaching (FRAP)

IPEC-J2 cells were inoculated with 1×10^4 cells per well in a confocal dish (medium without antibiotics), and when the cells reached 80% growth, the cells were washed 3 times with PBS. After 6 h of plasmid transfection, the AG1478 treatment solution was slowly added from the edge of the confocal dish, mixed well and incubated at 37°C with 5% CO_2 for 24 h. The pEGFP-NHE3 DMSO treatment group was treated with the same dose of DMSO for 24 h. The pEGFP-NHE3 EGF treatment group was replaced with serum-free phenol red-free DMEM after 6 h of plasmid transfection. After the above groups had reached the treatment time point, they were washed twice with PBS and replaced with phenol red-free maintenance medium for FRAP assay. A Zeiss LSM 800 laser confocal microscope with a 63 × oil objective (numerical aperture of 1.4) was used to observe and photograph the cell samples, and the ROI was used to observe the real-time fluorescence intensity of the three areas. Finally, the ZEN (blue) software was used to export the data and to compare the fluorescence intensity of the bleached areas throughout the process. When the test is completed for all groups, use ZEN (blue) software to export the data and analyze the fluorescence intensity of the bleached area throughout the process (Yang Z. et al., 2018).

2.7. Animal experiments

Nine 3-day-old lactating Rongchang piglets were randomly divided into Control, PEDV-infected and Tenapanor groups, with three piglets in each group. 10 mL of saline was administered to the Mock group, 10 mL of 1×10^6 $TCID_{50}$/mL of PEDV LJX strain was administered orally to the PEDV-infected group, and 10 mL of Tenapanor was administered to the Tenapanor group. After inoculation, clinical signs, such as diarrhea, were assessed daily. After significant diarrhea developed in the PEDV group, piglets from both groups were uniformly dissected to observe intestinal lesions.

All animal experiments were approved by the Southwestern University Institutional Animal Care and Use Committee (animal protocol approval number: CQLA-2021-0122). The National Institutes of Health guidelines for the performance of animal experiments were followed.

2.8. Data analysis

All statistical analyses were performed using GraphPad Prism 8.0 (GraphPad Inc., La Jolla, CA, USA). All data are expressed as the mean ± SD or standard error of the mean (SEM) of three separate repetitions. ANOVA and *t*-tests were used to analyze significant differences in *p* values ($p^* < 0.05$; $p^{**} < 0.01$; $p^{***} < 0.001$).

3. Results

3.1. NHE3 inhibitor induces diarrhea in piglets

To determine whether NHE3 is associated with piglet diarrhea, piglets in the control group received 10 mL of saline orally, PEDV-infected groups were orally infected with the PEDV-LJX strain, and the NHE3 inhibitor-fed piglets received Tenapanor at a concentration of 15 mg/kg. The anatomical results showed that control piglets had normal, dry, and formed stools (Figure 1A). However, the PEDV-infected piglets and the NHE3 inhibitor-fed piglets showed dilute watery diarrhea and their gastrointestinal tracts were thinning with transparency, and swollen (Figures 1B,C). These studies demonstrate that reducing the activity of the transporter protein NHE3 in piglet small intestinal epithelial cells leads to severe diarrhea and rapid dehydration in piglets.

3.2. The protein expression level of NHE3 protein was dose-dependent with PEDV titers

To further investigate the relationship between PEDV and NHE3, we detected the NHE3 protein expression levels at different titers of PEDV by Western blot. The results showed that when PEDV was infected at MOI = 1.0 or 0.5 for 2 h, the level of NHE3 decreased significantly at MOI = 0.1 (Figures 2A,C). 72 h after PEDV infection, the level of NHE3 decreased significantly at MOI = 0.1, 0.5 and 1 (Figures 2B,C). These results indicated that NHE3 levels decreased in a dose-dependent manner according to PEDV titers. The higher of PEDV titer, the more pronounced of the decrease in NHE3 levels.

3.3. PEDV infection induces EGFR phosphorylation on IPEC-J2 cells

To verify that PEDV infection activates EGFR, activation of the EGFR was evaluated by detecting the level of phosphorylated EGFR (p-EGFR) at different time points after PEDV infection of IPEC-J2 cells. The Western-blot results (Figure 3) indicated that the level of p-EGFR increased significantly during the pre-PEDV infection stage (10, 30, and 60 min) compared with the control group. In the advanced stages of PEDV infection (24, 48 h), p-EGFR levels remained upregulated but not significantly, then significantly higher at 72 h ($0.01 < p < 0.05$). These findings showed that PEDV infection rapidly activates EGFR, contributing to its phosphorylation and increased its expression.

3.4. PEDV interacts with the EGFR extracellular region through the S1 protein

The S protein of PEDV is a type I transmembrane glycoprotein consisting of two structural domains, S1 and S2, responsible for binding and fusion with the host cell. EGFR exists as a dimer on the cell membrane surface and the functional region is divided into an extracellular receptor binding region, a transmembrane region and an

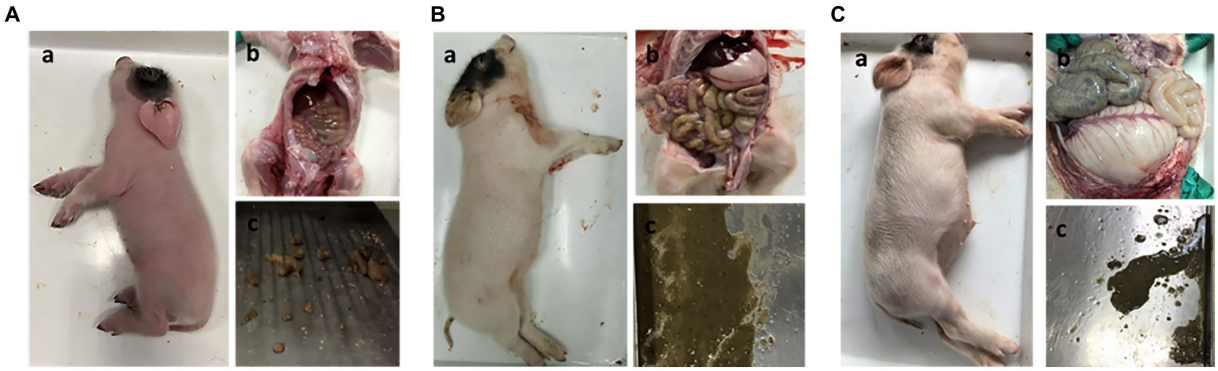

FIGURE 1
Clinical autopsy diagram of piglets with diarrhea. **(A)** Anatomy of a normal piglet; **(B)** Anatomy of a PEDV-infected piglet; **(C)** Anatomy of a NHE3 inhibitor-fed piglet.

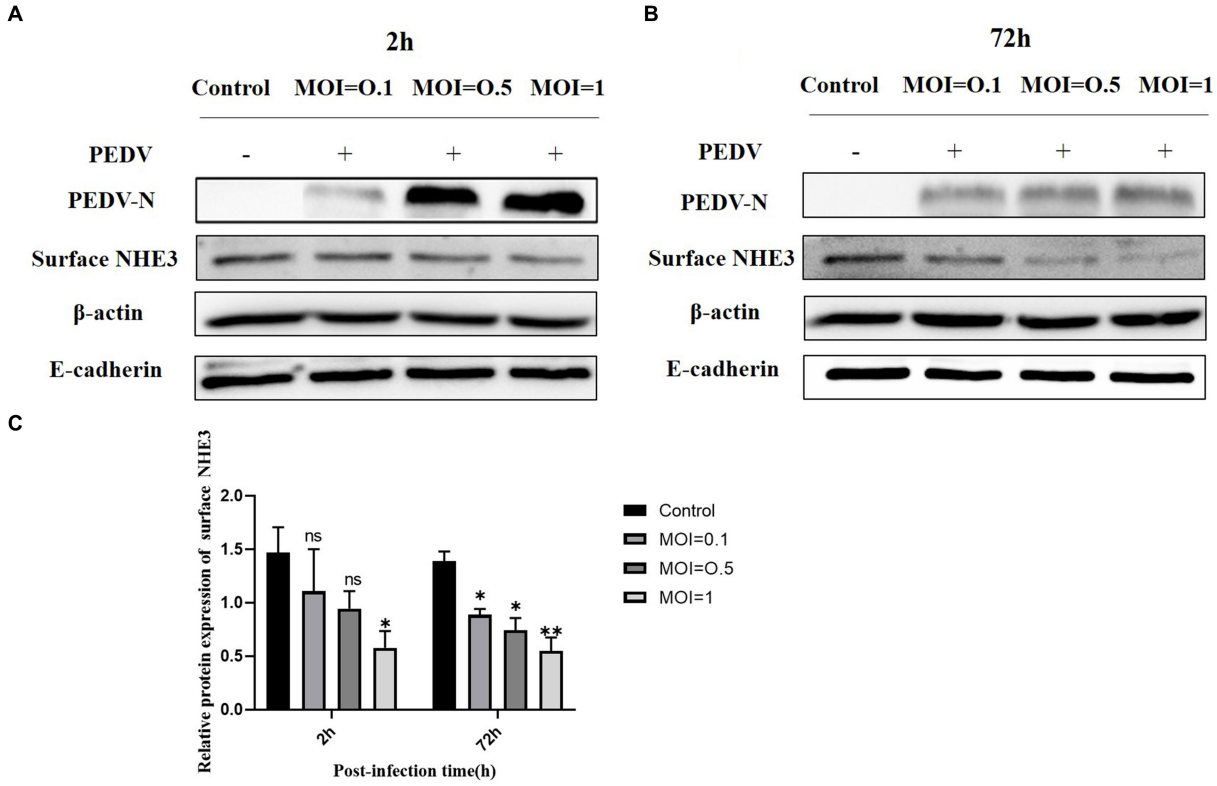

FIGURE 2
NHE3 protein levels at different titres of PEDV infection. **(A)** Western blotting results for surface NHE3 at 2 h after PEDV infection; **(B)** Western blotting results for surface NHE3 at 72 h after PEDV infection; **(C)** Grayscale analysis results for surface NHE3 protein at 2 and 72 h post PEDV infection.

intracellular kinase structural domain (Figure 4B). To investigate the interaction between the S protein and EGFR, the PEDV S gene (637 bp-2127 bp) (Figure 4A) and the EGFR gene (139-1473 bp) were ligated onto the ptt5 vector (Figure 4B) with different tags (flag and his) to identify the size by PCR through Wuhan GeneCreat (Figures 4C,D). Immunoprecipitation was used to test whether the PEDV S1 structural domain could directly interact with the extracellular region of EGFR. Lysates from HEK 293 T cells co-transfected with pTT5-PEDV S1 and pTT5-EGFR plasmids were subjected to western-blot after Co-IP to detect the results. The results confirmed the interaction of the PEDV S1 structural domain with the extracellular region of EGFR (Figure 4E), indicating that EGFR mediates PEDV invasion through binding of the extracellular receptor binding region to the PEDV S1 structural domain.

3.5. EGFR is involved in PEDV invasion of IPEC-J2 cells

Based on the fact that PEDV infection activates EGFR, we investigated whether altering the phosphorylation level of EGFR would affect PEDV invasion. In this experiment, EGFR

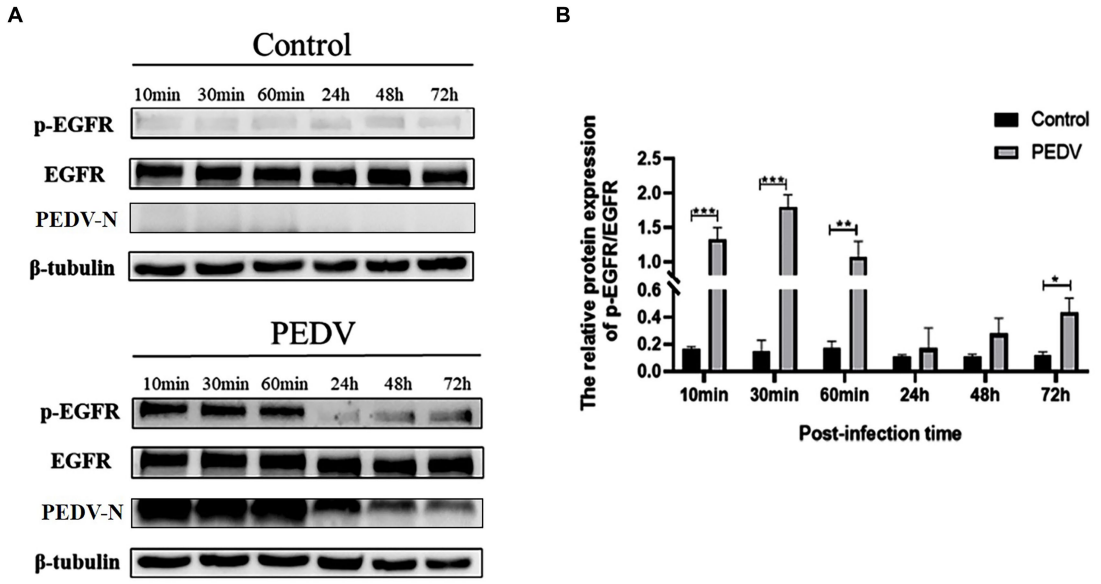

FIGURE 3
Levels of p-EGFR/EGFR at different points of time after PEDV infection of IPEC-J2 cells. **(A)** Graph of p-EGFR/EGFR at different points of time after PEDV infection with IPEC-J2 cells according to the western blotting results; **(B)** Grayscale analysis of p-EGFR/EGFR levels.

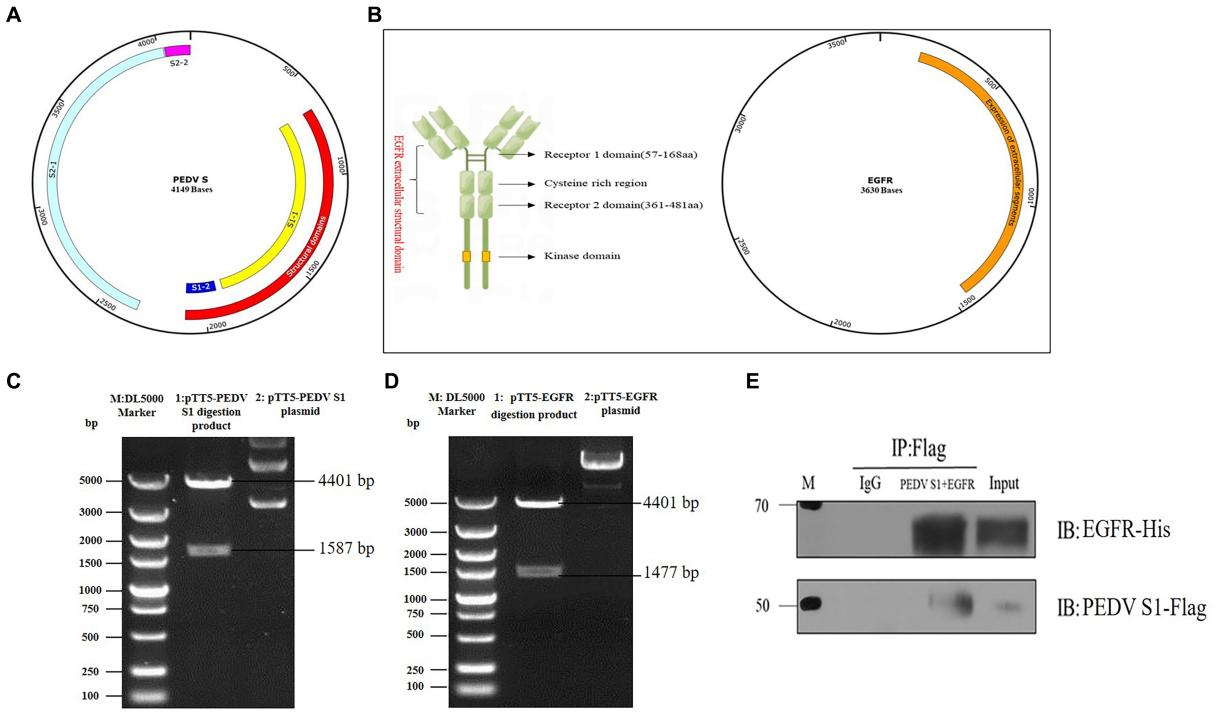

FIGURE 4
Vector construction of PEDV S1 and EGFR. **(A)** Construction of PEDV S1 eukaryotic expression vector (red); **(B)** Construction of EGFR extracellular structural domain and eukaryotic expression vector (orange); **(C)** Double digestion identification of the PEDV S1 eukaryotic expression vector (M: DL5000 Marker; 1: pTT5-PEDV S1 digestion product; 2: pTT5-PEDV S1 plasmid); **(D)** Double digestion identification of the EGFR eukaryotic expression vector (M:DL5000 Marker; 1: pTT5-EGFR digestion product; 2: pTT5-EGFR plasmid); **(E)** Co-IP of PEDV S1 and the EGFR extracellular region.

phosphorylation was regulated by EGF (a specific activator of EGFR) and AG1478 (a specific inhibitor of EGFR). It has been shown that EGFR phosphorylation can be induced by treating cells with 10 ng/mL of EGF, and previous studies in our laboratory have shown that 30 μM of AG1478 has the best inhibitory effect on EGFR phosphorylation and it is not toxic to IPEC-J2 cells (Yang Z. et al., 2018). The effect of

EGFR modulators on phosphorylated EGFR levels was examined using western blotting, which showed that the optimal duration of action was 15 min for EGF (Figures 5A,B) and 24 h for AG1478 (Figures 5C,D). IPEC-J2 cells were pretreated with the optimal dose and duration of the EGFR modulators determined above, the expression of PEDV N protein was detected by western blotting and the viral titer was determined by $TCID_{50}$ after 1 h and 2 h of PEDV incubation. The results indicated that PEDV infection increased and EGFR phosphorylation levels were elevated after EGF pretreatment (Figures 5E–G,K), and was significantly higher at 1 h of PEDV infection ($0.01 < p < 0.05$), indicating that activation of EGFR promotes PEDV infection. In contrast, PEDV infection as well as EGFR phosphorylation levels was significantly reduced after 24 h of AG1478 pretreatment ($0.01 < p < 0.05$), indicating that inhibition of EGFR activity reduced PEDV infection (Figures 5H–J,L).

3.6. Regulation of EGFR activity affects the level of NHE3 protein

To investigate whether there is a direct correlation between EGFR and changes in NHE3, the level of NHE3 was detected after modulating EGFR activity. Western blotting showed that total NHE3 protein levels remained essentially unchanged for the first 60 min after EGFR activation using EGF, and surface NHE3 levels were slightly upregulated in the first 30 min, but decreased at both 24 h and 72 h, in which the decrease at 72 h was significant (Figures 6A–D). Total NHE3 levels and surface NHE3 levels were upregulated for 48 h after EGFR inhibition using AG1478, but were slightly downregulated at 72 h (Figures 6E–H). The above results proved that there is a correlation between EGFR activity and NHE3 levels, and when EGFR activity is inhibited, NHE3 protein levels are upregulated.

3.7. PEDV infection regulates NHE3 levels through the EGFR/ERK signaling pathway

To investigate whether PEDV can regulate the level of NHE3 through the EGFR/ERK signaling pathways, PEDV was used to infect IPEC-J2 cells after activation of EGFR, and the levels of key signaling factors in the EGFR/ERK signaling pathway, and the level of NHE3 was examined. The results showed that EGFR was activated after PEDV infected cells for 2 h and 72 h, there was a significant increase in the level of p-EGFR (Figures 7A,B), and the change in level of p-ERK was basically consistent with that of p-EGFR (Figures 7A,C). However, the NHE3 level was downregulated at both 2 h and 72 h of PEDV infection after activation of EGFR activity ($0.01 < p < 0.05$), and the level was lower than that of the PEDV infection alone group (Figures 7A,D). PEDV infection at 2 h and 72 h after inhibition of EGFR activity continued to elevate p-EGFR levels. However, the

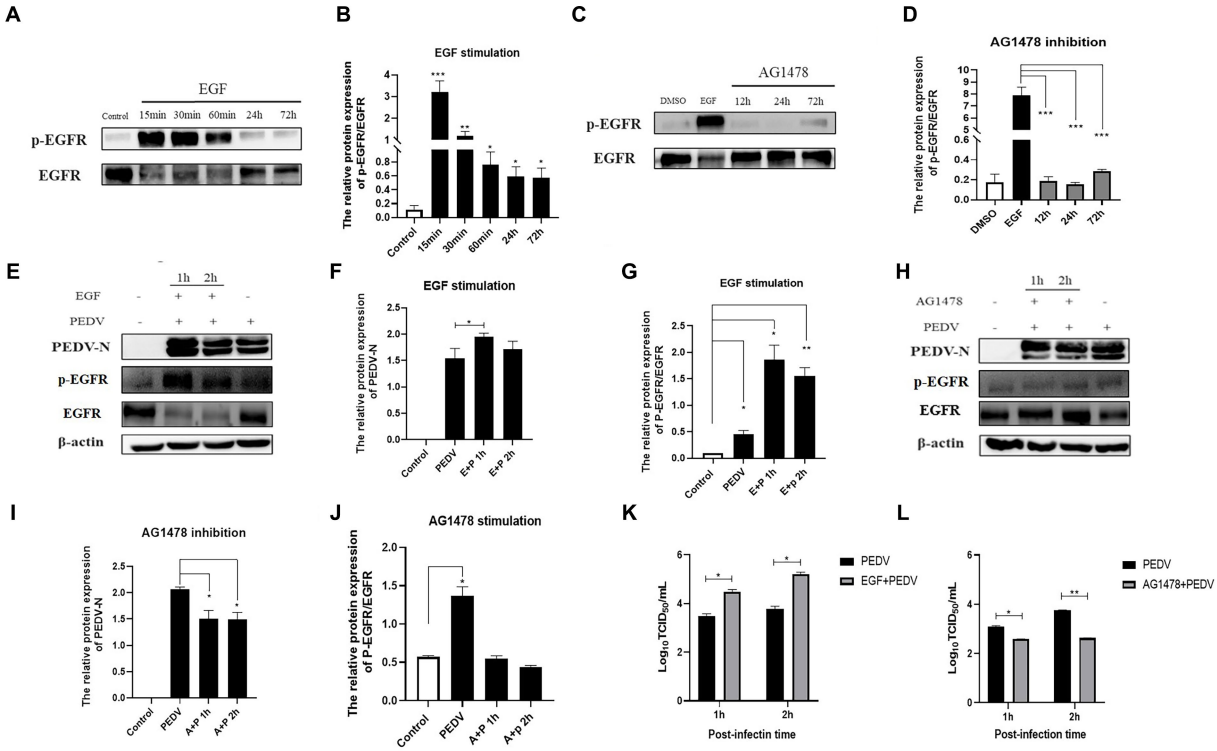

FIGURE 5
EGFR regulates PEDV invasion into IPEC-J2 cells. **(A)** Western blotting results for p-EGFR/EGFR after EGF treatment; **(B)** Grayscale analysis results for p-EGFR/EGFR after EGF treatment; **(C)** Results of western-blot for p-EGFR/EGFR after AG1478 treatment; **(D)** Grayscale analysis results for p-EGFR/EGFR after AG1478 treatment; **(E)** Results of western-blot for PEDV N, p-EGFR, EGFR protein after EGF treatment; **(F)** Grayscale analysis results of PEDV N protein after EGF treatment; **(G)** Grayscale analysis results for p-EGFR/EGFR after EGF treatment; **(H)** Western blotting results for PEDV N, p-EGFR, EGFR protein after AG1478 treatment; **(I)** Grayscale analysis results for PEDV N protein after AG1478 treatment; **(J)** Grayscale analysis results for p-EGFR/EGFR after AG1478 treatment; **(K)** Virus titer detected by $TCID_{50}$ after EGF treatment; **(L)** Virus titer detected by $TCID_{50}$ after AG1478 treatment.

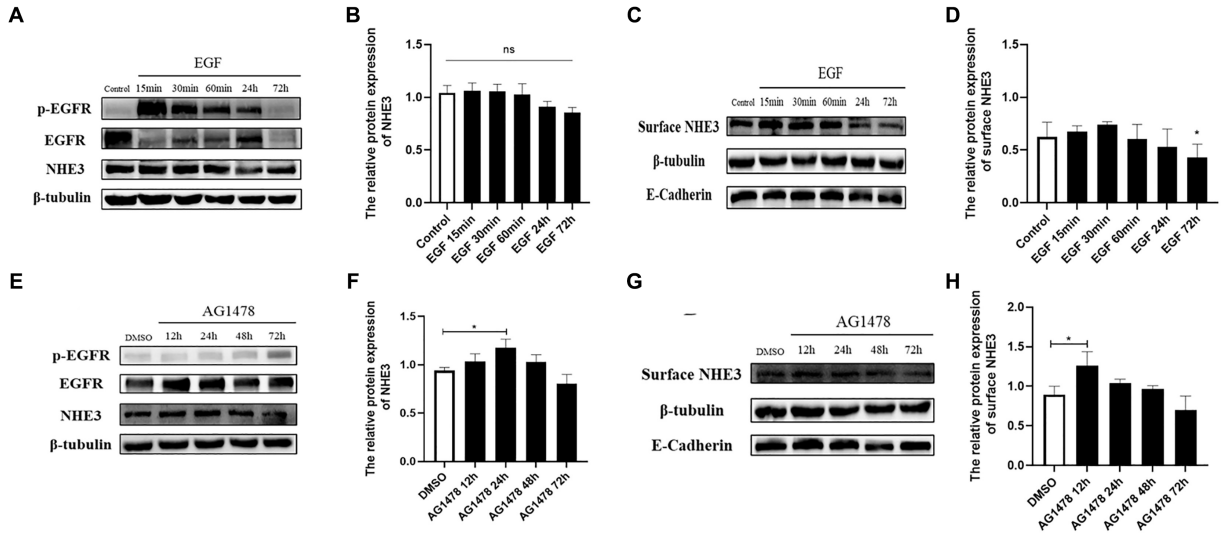

FIGURE 6
Levels of NHE3 at different time points after regulation of EGFR activity. **(A)** Western blotting results for total NHE3 after EGF treatment; **(B)** Grayscale analysis results for total NHE3 after EGF treatment; **(C)** Western blotting results for membrane-bound NHE3 after EGF treatment; **(D)** Grayscale analysis results for membrane-bound NHE3 after EGF treatment; **(E)** Western blotting results for total NHE3 after AG1478 treatment; **(F)** Grayscale analysis results for total NHE3 after AG1478 treatment; **(G)** Western blotting results for membrane-bound NHE after AG1478 treatment; **(H)** Grayscale analysis results for membrane-bound NHE3 after AG1478 treatment.

elevated levels of p-EGFR were significantly higher in the PEDV-infected group than in the group with inhibition of EGFR activity (Figures 7E,F). Changes in the levels of p-ERK were largely consistent with those of p-EGFR and were also elevated (Figures 7E,G). NHE3 was downregulated after PEDV infection at both 2 h and 72 h compared with that of control group after inhibition of EGFR activity (Figures 7E,H), which was significant at 72 h ($0.01 < p < 0.05$). However, its level of downregulation was less significant than that in the PEDV-infected group, with a significant difference at 72 h ($0.01 < p < 0.05$). The above results suggest that PEDV infection leads to notable upregulation of p-EGFR and p-ERK following activation of EGFR activity in IPEC-J2 cells, and that ERK is regulated by EGFR following PEDV infection. This demonstrates that the effect of PEDV infection on NHE3 is regulated by the EGFR/ERK signaling pathway. Activation of EGFR downregulated NHE3 levels more significantly, while inhibition of EGFR activity somewhat attenuated the downregulation of NHE3 in IPEC-J2 induced by PEDV infection.

3.8. PEDV infection regulates the mobility of plasma membrane NHE3 through EGFR

To better observe the dynamic changes in NHE3 induced by PEDV processing, the impacts of modulating EGFR activity on the mobility of NHE3 across the plasma membrane of IPEC-J2 cells after PEDV infection was examined using FRAP. The fluorescence intensity of the bleached areas in all groups decreased significantly after bleaching and started to recover again with time, indicating that the NHE3 fluorescent molecules remained mobile after PEDV infection (Figures 8A, 9A). The pEGFP-NHE3 group (Control) showed stronger recovery of fluorescence intensity than all PEDV-infected groups, while the pEGFP-NHE3 EGF + PEDV group had the weakest recovery of bleached areas post-bleaching. The fluorescence intensity of the anchored bleached area before and during recovery was analyzed for each group using ZEN (blue) software, which was used to detect the fluorescence recovery rates and dynamic fraction (Mobile fraction, Mf) of each group.

The results showed that the NHE3 fluorescence recovery rate was significantly lower in the EGF-treated group compared with that in the pEGFP-NHE3 group. The fluorescence recovery rate in the AG1478-treated group was higher than that in the DMSO group in the first 6 min and lower than that in the DMSO group after 6 min (Figures 8A,B). However, the NHE3 fluorescence recovery rate in all three groups was lower than the pEGFP-NHE3 group (Figure 8C). This indicated that NHE3 fluorescent bleaching recovery rate was relatively reduced after activation of EGFR, and inhibition of EGFR activity upregulated the fluorescence recovery rate of NHE3. Compared with that in the control group, NHE3 fluorescent bleaching recovery rate in all PEDV-infected groups was weaker at each time point (Figures 9A–C). After activating EGFR, infection with PEDV induced a more noticeable decline in the NHE3 fluorescence recovery rate at 72 h, while inhibiting EGFR activity followed by infection with PEDV relatively upregulated the fluorescence recovery rate of NHE3, and the effect was better at 2 h (Figure 9D). The above results show that compared with the control group, PEDV infection of IPEC-J2 cells reduced the fluidity of NHE3 on the plasma membrane. When EGFR was activated, PEDV infection further reduced the fluidity of NHE3, whereas infection with PEDV after inhibition of EGFR activity could enhance the fluidity of NHE3, indicating that during PEDV infection, the stronger the activity of EGFR on the IPEC-J2 cell membrane, the weaker the fluidity of NHE3, i.e., negative feedback by EGFR regulates the fluidity of NHE3 on the plasma membrane.

4. Discussion

It has been well documented that EGFR can act as one of the co-receptors involved in viral infection. Previous studies in our

10.3389/fmicb.2023.1237913

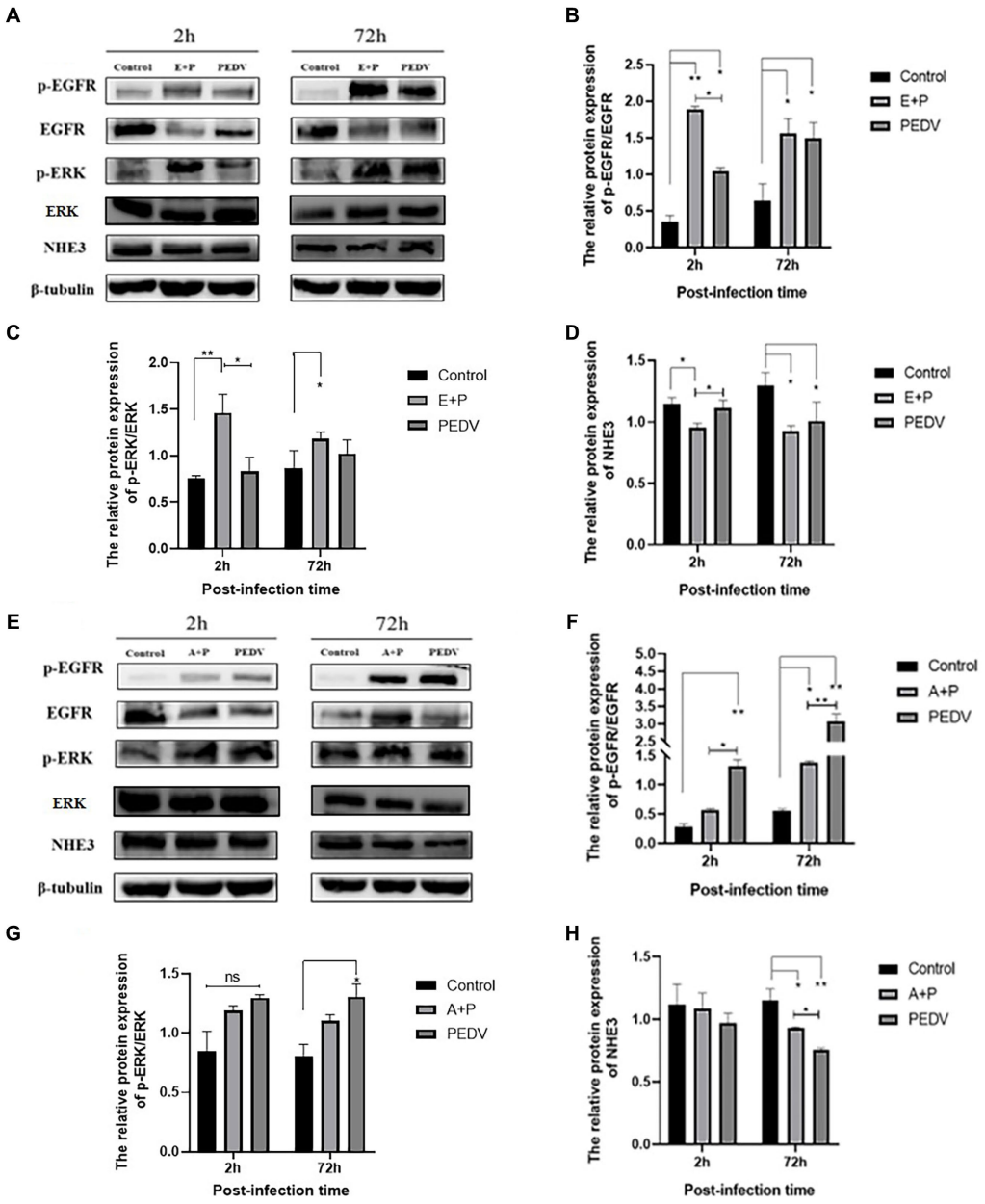

FIGURE 7
Level of EGFR, ERK, and NHE3 proteins at different times of PEDV infection after regulation of EGFR. **(A)** Western blotting results for p-EGFR, EGFR, p-ERK, ERK, and NHE3 after activation of EGFR; **(B)** Grayscale analysis results for p-EGFR/EGFR; **(C)** Grayscale analysis results for p-ERK/ERK; **(D)** Grayscale analysis results for NHE3; **(E)** Western blotting results of p-EGFR, EGFR, p-ERK, ERK, and NHE3 after inhibition of EGFR; **(F)** Grayscale analysis results for p-EGFR/EGFR; **(G)** Grayscale analysis results for p-ERK/ERK; **(H)** Grayscale analysis results for the NHE3.

laboratory have found that EGFR promotes the intracellular proliferation of TGEV (Yang Z. et al., 2018), and it is unknown whether EGFR plays an equivalent role in the process of PEDV infection. Therefore, we first verified that PEDV infection could cause EGFR phosphorylation, and the results showed that EGFR phosphorylation levels increased significantly at 10 min of PEDV infection and peaked at 30 min, indicating that viral infection could rapidly induce intracellular EGFR activation, resulting in enhanced EGFR activity (Figure 3). However, in contrast to the results of the identified studies, we found that EGFR phosphorylation levels were again elevated at later stages of PEDV infection (48 h, 72 h), but not as significantly as at earlier stages. It is possible that this is caused by the massive replication of PEDV after cell invasion and in the subsequent release of new viral particles that infect the surrounding host cells.

Viral invasion is the initial step of viral infection. PEDV invasion into host cells is mediated by S glycoproteins attached to specific host receptors, and S proteins can be subdivided into two subunits, S1, which mediates the binding of viruses to surface-specific receptors on host cells, and S2, which is involved in the fusion process of viral and host cell membranes (Kirchdoerfer et al., 2021). In Hu W's study, p-APN and EGFR were found to be synergistically involved in TGEV invasion, and EGFR can be activated early in PEDV infection to

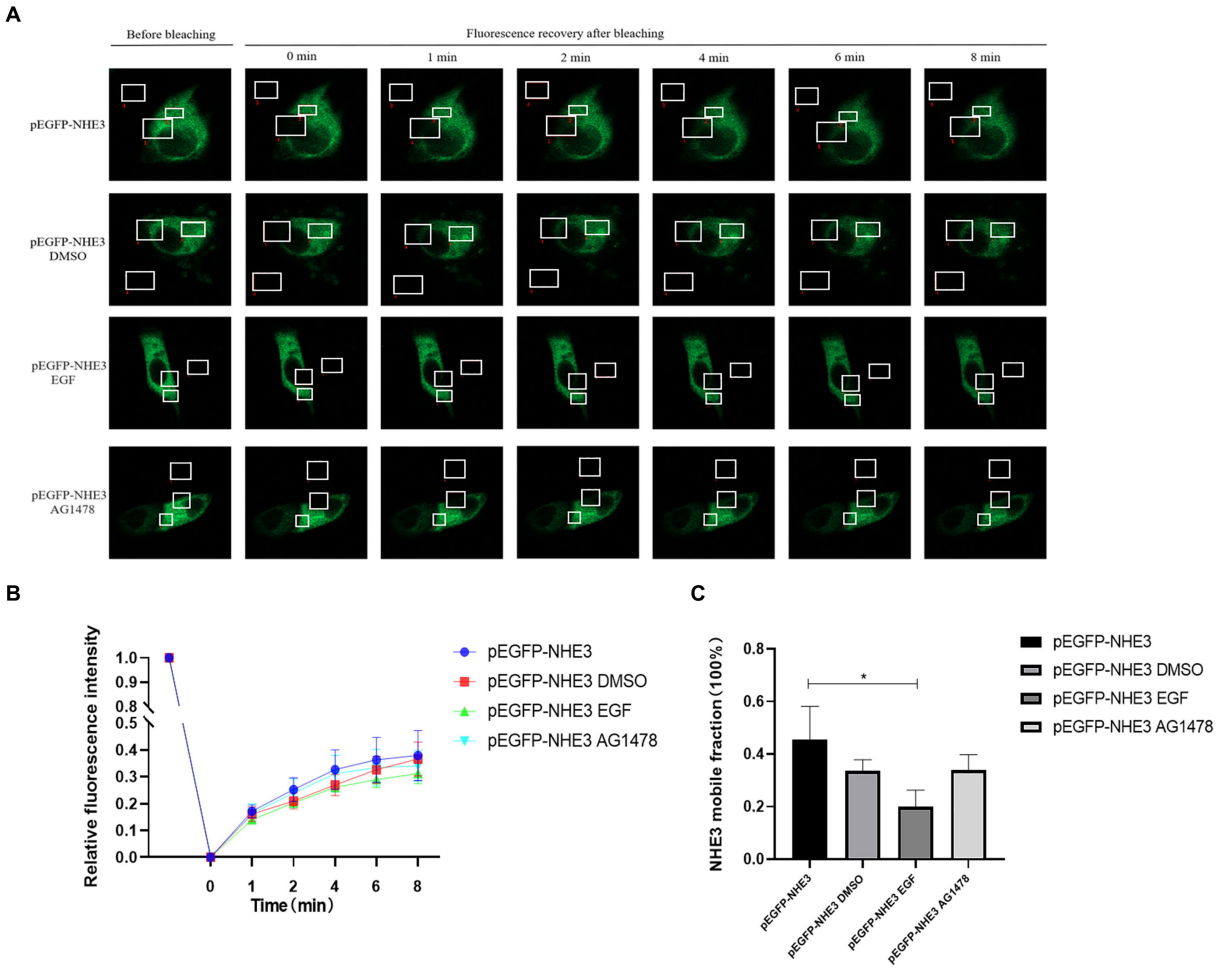

FIGURE 8
Rate of recovery of NHE3 fluorescence and dynamics at the plasma membrane following modulation of EGFR. **(A)** Dynamics of fluorescent molecules in the bleaching region during FRAP (63×/1.4NA); **(B)** Fluorescence bleaching recovery of NHE3 on cell membranes; **(C)** Dynamic analysis of NHE3 on membranes.

promote adsorption of virus invasion, suggesting that EGFR is most likely one of the invasion receptors of PEDV (Hu et al., 2018). Therefore, this experiment confirmed the direct interaction between the PEDV S1 structural domain and the EGFR extracellular region by constructing eukaryotic expression vectors for PEDV S1 and EGFR extracellular region and immunoprecipitating them after co-transfection with HEK 293 T cells (Figure 4). It indicates that EGFR activation induced by PEDV infection may be mediated by a direct interaction between the EGFR extracellular receptor binding region and PEDV S1 protein.

Since the invasion process of PEDV occurs early in the infection, it has been shown that viral infection can competitively exploit the endocytosis of EGFR and activate EGFR downstream signaling pathways to counteract the host's antiviral response (Zheng et al., 2014; Perez Verdaguer et al., 2021). Therefore, this experiment next investigated the relationship between EGFR and PEDV invasion. After modulating EGFR activity by EGFR-specific regulators epidermal growth factor (EGF) and tyrosinase inhibitor (AG1478), we examined the viral titer and N protein expression in PEDV-infected IPEC-J2 cells at 1 h and 2 h. We found that activation of EGFR promoted PEDV infection and inhibition of EGFR activity reduced PEDV infection (Figure 5). This validates our conjecture that EGFR can be involved in PEDV invasion of IPEC-J2 cells and that EGFR activation induced by PEDV infection enhances the ability of PEDV to infiltrate.

Epidermal growth factor (EGF) is the most primitive member of the EGF ligand family. In normal physiological regulation, EGF binds specifically to EGFR, promotes EGFR and ERK phosphorylation, and activates its downstream signaling pathway molecules to exert regulatory functions (Singh et al., 2016; Abud et al., 2021). By the results we found that the total protein level of NHE3 remained basically unchanged for a short time after activation of EGFR with EGF, while the level of surface NHE3 protein was slightly up-regulated, but prolonged EGF treatment caused a slight decrease in the protein level of NHE3. The slight upregulation of NHE3 expression on the membrane in the short term after EGF stimulation may be an acute regulation occurring within a short period of time after cell activation, and the acute regulation is rapid and reversible, so the level of surface NHE3 protein returned to normal after 60 min of EGF treatment. However, continuous EGF stimulation leads to rapid cell growth and differentiation, causing cell growth inhibition in the presence of limited space and nutrient supply, which may explain the relative decrease in NHE3 expression and mobility after continuous activation of EGFR instead. Tyrphostin AG-1478 is a selective EGFR

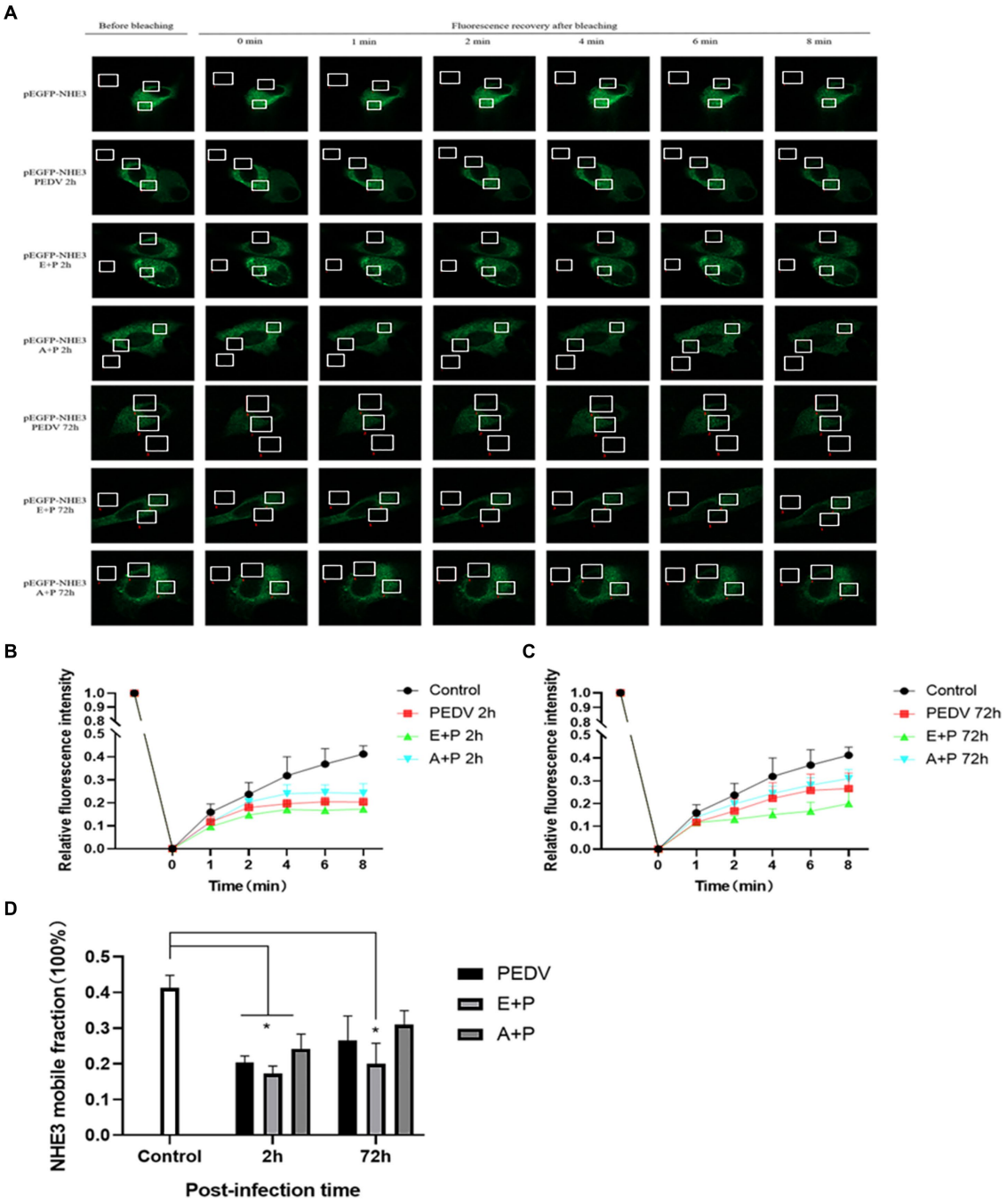

FIGURE 9
PEDV infection regulates the mobility of plasma surface NHE3 through EGFR. **(A)** Dynamics of fluorescent molecules in the bleaching region during FRAP (63×/1.4NA); **(B)** Fluorescence recovery rate of NHE3 on the cell membrane 2 h after PEDV invasion; **(C)** Fluorescence recovery rate of NHE3 on the cell membrane 72 h after PEDV invasion; **(D)** Analysis of the dynamic fraction of NHE3 on the cell membrane after PEDV invasion.

tyrosine kinase inhibitor with clinically proven antiviral activity against HCV and encephalomyocarditis virus (EMCV) (Dorobantu et al., 2016). After using AG1478 to inhibit EGFR activity, the phosphorylation levels of EGFR and ERK were significantly down-regulated and the relative expression of NHE3 was significantly up-regulated after EGFR inhibition. The above results indicate that PEDV infection is regulated by the EGFR/ERK signaling pathway to regulate NHE3 expression, and a certain negative phase between EGFR and NHE3 (Figure 6). When EGFR activity was inhibited, the phosphorylation level of ERK was also inhibited, while the activity of NHE3 was increased. Our laboratory studies demonstrated that NHE3 activity was regulated through the EGFR/ERK pathway. Importantly, NHE3 mobility on the plasma membrane of TGEV infected cells was significantly weaker than that in normal cells, and EGFR inhibition and knockdown recovered this mobility (Yang Z. et al., 2018). Therefore, we speculate that the activity and mobility of NHE3, regulated through the EGFR/ERK pathway on the brush border membrane of small intestinal epithelial cells, decreased after PEDV infection.

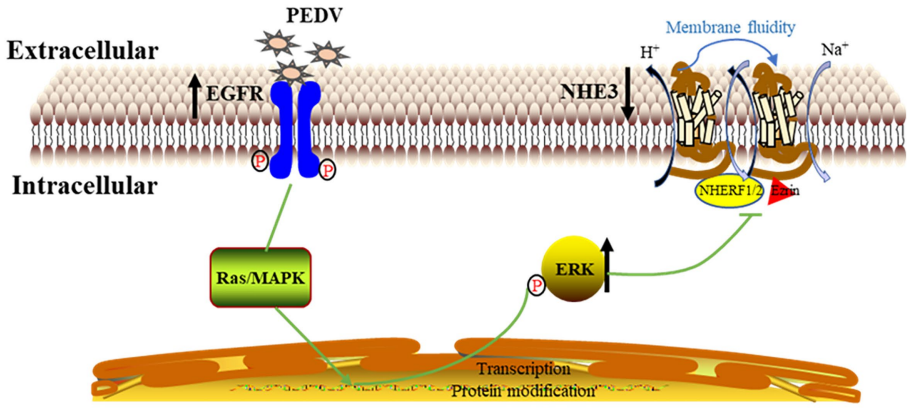

FIGURE 10
Mechanistic model of PEDV infection regulating NHE3 activity by activating EGFR.

In order to further study the mechanism of PEDV regulating NHE3, the expression of key signaling factors in NHE3 and EGFR pathways was detected by regulating the activity of EGFR after infection with PEDV. EGFR promotes PEDV infection to downregulate NHE3 expression and mobility (Figure 7). This result indicated that after EGFR was activated by PEDV infection, the invasion and proliferation of PEDV could be affected by EGFR, and the expression and mobility of NHE3 could be regulated. The following regulatory mechanisms exist for EGFR and NHE3 in porcine transmissible gastroenteritis virus (TGEV), which is also an alphacoronavirus: infection with TGEV enhances intestinal glucose uptake and increases the expression of EGFR, SGLT1, and GLUT2 in intestinal epithelial cells, and there is a positive regulatory relationship between EGFR and SGLT1 (Ren et al., 2013; Dai et al., 2016). In the case of TGEV infection, down-regulation of SGLT1 expression promotes the translocation of NHE3, which increases the expression of NHE3 on the plasma membrane (Yang et al., 2020). Inhibition of EGFR activity can promote the fluidity of NHE3 on the plasma membrane and promote the absorption of Na^+ (Yang Z. et al., 2018). Combined with the results of this experiment, we preliminarily speculate that PEDV can activate EGFR, causing the decrease of NHE3 activity in small intestinal epithelial cells, and the Na^+/H^+ exchange barrier, which can promote the occurrence of diarrhea (Gekle et al., 2001; Dominguez et al., 2016).

In conclusion, EGFR may be one of the receptors involved in PEDV invasion of intestinal epithelial cells, and PEDV infection activates EGFR, which then phosphorylates ERK and thereby regulates the expression and mobility of NHE3 on the plasma membrane, ultimately leading to reduced NHE3 activity. Decreased NHE3 activity and impaired Na^+/H^+ exchange may be key factors in the development of diarrhea induced by PEDV infection in newborn piglets (Figure 10).

Data availability statement

The raw data supporting the conclusions of this article will be made available by the authors, without undue reservation.

Ethics statement

The animal study was approved by Southwest University Laboratory Animal Ethics Review Committee/Southwestern University Animal Experiment Institutional Review Committee. The study was conducted in accordance with the local legislation and institutional requirements.

Author contributions

YZ and SZ wrote the first draft of the manuscript. ZHS, XL, and GL wrote parts of the manuscript. ZK performed the statistical analysis. HZ, SX, and JZ contributed to the conception and design of the study. ZHS organized the database. All authors contributed to the revision of the manuscript, read and approved the submitted version.

Funding

This work was supported by the Central University Basic Research Fund of China (XDJK2020RC001); Venture and Innovation Support Program for Chongqing Overseas Returnees (cx2019097); 2020 Chongqing Rongchang Agricultural and Animal Hi-Tech Specialization.

Acknowledgments

Thanks to my supervisor and colleagues in the lab.

Conflict of interest

The authors declare that the research was conducted in the absence of any commercial or financial relationships that could be construed as a potential conflict of interest.

Publisher's note

References

Abud, H. E., Chan, W. H., and Jarde, T. (2021). Source and impact of the EGF family of ligands on intestinal stem cells. *Front. Cell Dev. Biol.* 9:685665. doi: 10.3389/fcell.2021.685665

Alvarez, J., Sarradell, J., Morrison, R., and Perez, A. (2015). Impact of porcine epidemic diarrhea on performance of growing pigs. *PLoS One* 10:e0120532. doi: 10.1371/journal.pone.0120532

Anbazhagan, A. N., Priyamvada, S., Alrefai, W. A., and Dudeja, P. K. (2018). Pathophysiology of IBD associated diarrhea. *Tissue Barriers* 6:e1463897. doi: 10.1080/21688370.2018.1463897

Chen, X., Zhang, X. X., Li, C., Wang, H., Wang, H., Meng, X. Z., et al. (2019). Epidemiology of porcine epidemic diarrhea virus among Chinese pig populations: a meta-analysis. *Microb. Pathog.* 129, 43–49. doi: 10.1016/j.micpath.2019.01.017

Dai, L., Hu, W. W., Xia, L., Xia, M., and Yang, Q. (2016). Transmissible gastroenteritis virus infection enhances SGLT1 and GLUT2 expression to increase glucose uptake. *PLoS One* 11:e165585:e0165585. doi: 10.1371/journal.pone.0165585

Dominguez, R. J., de la Mora, C. S., and Rieg, T. (2016). Novel developments in differentiating the role of renal and intestinal sodium hydrogen exchanger 3. *Am. J. Physiol. Regul. Integr. Comp. Physiol.* 311, R1186–R1191. doi: 10.1152/ajpregu.00372.2016

Dorobantu, C. M., Harak, C., Klein, R., van der Linden, L., Strating, J. R. P. M., van der Schaar, H. M., et al. (2016). Tyrphostin AG1478 inhibits Encephalomyocarditis virus and hepatitis C virus by targeting phosphatidylinositol 4-kinase IIIα. *Antimicrob. Agents Chemother.* 60, 6402–6406. doi: 10.1128/AAC.01331-16

Field, M. (2003). Intestinal ion transport and the pathophysiology of diarrhea. *J. Clin. Invest.* 111, 931–943. doi: 10.1172/JCI200318326

Gekle, M., Freudinger, R., Mildenberger, S., Schenk, K., Marschitz, I., and Schramek, H. (2001). Rapid activation of Na+/H+-exchange in MDCK cells by aldosterone involves MAP-kinases ERK 1/2. *Pflugers Arch.* 441, 781–786. doi: 10.1007/s004240000507

Hu, W., Zhang, S., Shen, Y., and Yang, Q. (2018). Epidermal growth factor receptor is a co-factor for transmissible gastroenteritis virus entry. *Virology* 521, 33–43. doi: 10.1016/j.virol.2018.05.009

Kirchdoerfer, R. N., Bhandari, M., Martini, O., Sewall, L. M., Bangaru, S., Yoon, K. J., et al. (2021). Structure and immune recognition of the porcine epidemic diarrhea virus spike protein. *Structure* 29, 385–392.e5. doi: 10.1016/j.str.2020.12.003

Lee, C. (2015). Porcine epidemic diarrhea virus: an emerging and re-emerging epizootic swine virus. *Virol. J.* 12:193. doi: 10.1186/s12985-015-0421-2

Niu, Z., Zhang, Y., Kan, Z., Ran, L., Yan, T., Xu, S. S., et al. (2021). Decreased NHE3 activity in intestinal epithelial cells in TGEV and PEDV-induced piglet diarrhea. *Vet. Microbiol.* 263:109263. doi: 10.1016/j.vetmic.2021.109263

No, Y. R., He, P., Yoo, B. K., and Yun, C. C. (2015). Regulation of NHE3 by lysophosphatidic acid is mediated by phosphorylation of NHE3 by RSK2. *Am. J. Physiol. Cell Physiol.* 309, C14–C21. doi: 10.1152/ajpcell.00067.2015

Perez Verdaguer, M., Zhang, T., Paulo, J. A., Gygi, S., Watkins, S. C., Sakurai, H., et al. (2021). Mechanism of p38 MAPK–induced EGFR endocytosis and its crosstalk with ligand-induced pathways. *J. Cell Biol.* 220:e202102005. doi: 10.1083/jcb.202102005

Ren, J., Bollu, L. R., Su, F., Gao, G., Xu, L., Huang, W. C., et al. (2013). EGFR-SGLT1 interaction does not respond to EGFR modulators, but inhibition of SGLT1 sensitizes prostate cancer cells to EGFR tyrosine kinase inhibitors. *Prostate* 73, 1453–1461. doi: 10.1002/pros.22692

Singh, B., Carpenter, G., and Coffey, R. J. (2016). EGF receptor ligands: recent advances. *F1000Res* 8:F1000 Faculty Rev-2270. doi: 10.12688/f1000research.9025.1.

Song, D., Moon, H., and Kang, B. (2015). Porcine epidemic diarrhea: a review of current epidemiology and available vaccines. *Clin. Exp. Vaccine Res.* 4, 166–176. doi: 10.7774/cevr.2015.4.2.166

Wang, Z., Li, X., Shang, Y., Wu, J., Dong, Z., Cao, X., et al. (2020). Rapid differentiation of PEDV wild-type strains and classical attenuated vaccine strains by fluorescent probe-based reverse transcription recombinase polymerase amplification assay. *BMC Vet. Res.* 16:208. doi: 10.1186/s12917-020-02424-1

Yang, Z., Ran, L., Yuan, P., Yang, Y., Wang, K., Xie, L., et al. (2018). EGFR as a negative regulatory protein adjusts the activity and mobility of NHE3 in the cell membrane of IPEC-J2 cells with TGEV infection. *Front. Microbiol.* 9:2734. doi: 10.3389/fmicb.2018.02734

Yang, L., Xu, J., Guo, L., Guo, T., Zhang, L., Feng, L., et al. (2018). Porcine epidemic diarrhea virus-induced epidermal growth factor receptor activation impairs the antiviral activity of type I interferon. *J. Virol.* 92:e02095-17. doi: 10.1128/JVI.02095-17

Yang, Y., Yu, Q., Song, H., Ran, L., Wang, K., Xie, L., et al. (2020). Decreased NHE3 activity and trafficking in TGEV-infected IPEC-J2 cells via the SGLT1-mediated P 38 MAPK/AKt2 pathway. *Virus Res.* 280:197901. doi: 10.1016/j.virusres.2020.197901

Zheng, K., Kitazato, K., and Wang, Y. (2014). Viruses exploit the function of epidermal growth factor receptor. *Rev. Med. Virol.* 24, 274–286. doi: 10.1002/rmv.1796

frontiers | Frontiers in Microbiology

TYPE Mini Review
PUBLISHED 10 November 2023
DOI 10.3389/fmicb.2023.1294056

OPEN ACCESS

EDITED BY
Qiang Ding,
Tsinghua University, China

REVIEWED BY
Leiliang Zhang,
Shandong First Medical University and Shandong Academy of Medical Sciences, China
Huahao Fan,
Beijing University of Chemical Technology, China

*CORRESPONDENCE
Junfeng Zhou
ttxs21ct@jlu.edu.cn

RECEIVED 14 September 2023
ACCEPTED 26 October 2023
PUBLISHED 10 November 2023

CITATION
Song Y, Yao L, Li SS and Zhou JF (2023) Psoriasis comorbidity management in the COVID era: a pressing challenge. *Front. Microbiol.* 14:1294056. doi: 10.3389/fmicb.2023.1294056

Psoriasis comorbidity management in the COVID era: a pressing challenge

Yang Song, Lei Yao, Shanshan Li and Junfeng Zhou*

Department of Dermatology, Hospital of Jilin University, Changchun, China

The global COVID-19 pandemic has presented a significant, ongoing challenge since its emergence in late 2019. Today, the Omicron strain, which is less lethal but more contagious than the original outbreak strain, continues to pose substantial health risks. In this background, the management of psoriatic comorbidities has become even more complex, particularly for patients with underlying inflammatory, metabolic, or cardiovascular diseases. This review aims to summarize current research on comorbid COVID-19 and psoriasis, and provide insights into the development of evidence-based management strategies. By providing appropriate patient instruction, implementing protective measures, and re-evaluating medication prescriptions based on each patient's unique situation, healthcare professionals can effectively address the challenges faced by patients with comorbid psoriasis in the COVID-19 era.

KEYWORDS

COVID-19, SARS-CoV-2, psoriasis, comorbidity, management, biologics

1. Introduction

The COVID-19 outbreak caused by Severe Acute Respiratory Syndrome Coronavirus type-2 (SARS-CoV-2) has been spreading worldwide. Because of the frequent genetic mutation and recombination of SARS-CoV-2, many new variants of this coronavirus have emerged. Although less lethal than previous strains, these prevalent, mildly virulent variants (e.g. BQ and XBB subvariants of Omicron) are capable of spreading much more efficiently, and harbor an advantage in antibody evasion (Wang et al., 2023), causing less urgent, but long-lasting health problems. Patients with immunosuppressed and impaired organ functions are the most susceptible to SARS-CoV-2 infection in this post-COVID era.

Psoriasis is a common chronic inflammatory skin problem worldwide. Complete cure of this disease is considered impossible due to the complex underlying pathogenic mechanisms, which include genetic, epigenetic, environmental, and autoimmune factors (mainly induced by IL-17 and TNF-α). Long-lasting or recurrent lesions may cause discomfort that consequently lowers the quality of life of patients. Traditionally, management of psoriasis has been relatively challenging due to the lack of a single effective treatment. Approaches that include both customized combined therapy and patient education are necessary. Recently, biologics (including TNF-α inhibitors, IL-17, and IL-12/23 inhibitors) have become a revolutionary modality in the management of psoriasis based on randomized controlled trial evidence and large sample size real-world research. TNF-α inhibitors have been used to treat autoimmune disease for many years before they are introduced to psoriasis. Major adverse effects are serious infections like tuberculosis and hepatitis, along with increased risk of tumors. IL-17 and IL-23, IL-12/23 inhibitors are new biotics with a better safe profile. Overall, biotics are quick-acting, highly effective, and

safe; Other small molecular agents like Janus kinase (JAK) inhibitors also have satisfactory therapeutic effect and safety, however, a maintenance treatment with biotics or JAK inhibitors is still necessary for a long-lasting relief.

Comorbidity management is another challenge for psoriasis patients, especially those with a very long course of disease, high Psoriasis Area and Severity Index (PASI) score, or resistance to treatments. Patients with psoriasis clearly have higher risks of developing cardiovascular, metabolic, and autoimmune diseases. These comorbidities can further damage the patient's health, and bring complexity to the management of their psoriasis. Today as COVID has become a new global health challenge, it has brought greater difficulties for psoriasis patients with comorbidities. Because underlying diseases, such as inflammatory, metabolic, and cardiovascular diseases are risk factors for COVID infection and more severe disease courses.

This review summarizes the research on the comorbidity of COVID-19 and psoriasis, and aims to shed light on the current thinking around management strategies based on existing evidence.

1.1. Psoriasis and its comorbidities

Patients with psoriasis are more likely to develop systemic disorders, such as eye complications (sclerotitis, uveitis), gastrointestinal diseases (colitis gravis, Crohn's disease), metabolic syndrome (hypertension, obesity, cardiovascular disease, diabetes, hyperlipidemia, hyperuricemia/gout), psoriatic arthritis (PsA), and other autoimmune diseases (vitiligo, alopecia areata). These comorbidities are collectively known as "psoriatic disease" (Aggarwal et al., 2018). Although the underlying mechanisms of these disorders in psoriasis have not been completely elucidated, they share similar triggers with psoriasis (Gisondi et al., 2020), such as genetic, environmental, and psychological factors. Additionally, the release of inflammatory cytokines, such as tumor necrosis factor TNF- α and interleukin (IL)-17 by psoriasis patients (Brembilla et al., 2018), leads to a systemically high inflammation burden that contributes to the development and exacerbation of psoriatic diseases. Research has shown that inflammation exists in many organs (e.g., aorta, liver, joints) other than skin, even in patients with mild lesions (Youn et al., 2015). In addition to the direct harm to different organs, a chain of events drives the development of psoriasis comorbidities (Figure 1). Chronic inflammation increases risks of obesity and insulin resistance (Boehncke et al., 2007), and injury to the blood vessel endothelium accelerates atherosclerotic plaque formation and lowers blood vessel elasticity. Together with conditions such as diabetes and dyslipidemia, atherosclerosis develops gradually and may eventually lead to severe cardiovascular diseases.

Conversely, these diseases can also worsen the autoimmune disorder in psoriasis, making it challenging to control lesions and prevent recurrence. Psoriatic diseases also have negative impacts on the treatment options in patients with certain comorbidities as they may be contraindications of some drugs. Considering the significant influence of comorbidity on psoriasis, guidelines, and expert consensuses recommend monitoring of psoriatic disease as an important part of psoriasis management (Elmets et al., 2019).

1.2. Psoriasis comorbidity and the risk of COVID-19 infection and severity

Today, although the risk to healthy people is greatly reduced, SARS-CoV-2 remains an imposing menace to people with underlying health conditions and older age (Espinosa et al., 2020; Gallo Marin et al., 2021).

There are controversies regarding susceptibility to COVID-19 infection of patients with cutaneous psoriasis. A large amount of research has lifted the veil of the immune response and pathogenic mechanisms of COVID-19 (Hosseini et al., 2020). The T-cell disorders of psoriasis may interfere with the anti-coronavirus immune response, which relies on CD4+ and CD8+ T-cell function (Sette and Crotty, 2021). The inflammatory status can also facilitate invasion of SARS-CoV-2 through an environmental elastase pathway. Comparative analysis of gene expression revealed that ACE2 and FURIN, which are genes significantly associated with SARS-CoV-2 infection, are upregulated in psoriasis patients, and 48 of 161 genes that are upregulated in the lungs of COVID-19 patients are also positively regulated in psoriasis (Singh et al., 2021). Surprisingly, however, some clinical studies reported that in psoriasis patients with skin involvement only, the chances of getting infected or developing a severe case were not higher than those in healthy populations. Although the underlying reasons for these contrary findings have not been well investigated, two hypotheses have been proposed: (1) genetic background may impact the development of the COVID-19-induced cytokine storm; and (2) anti-inflammation therapy to treat psoriasis may help to control the cytokine storm and/or lung fibrosis. Basic research and additional clinical studies of larger samples are needed to elucidate this issue.

Unlike the confusion in determining the role of cutaneous psoriasis in coronavirus infection, comorbidities like obesity, diabetes, and cardiovascular diseases, surely put patients at a higher risk of COVID-19 infection. Obesity, which is common among psoriasis patients suffering from metabolic syndrome, contributes to immune disorders and leads to an inhibited immune response against SARS-CoV-2 (Magdy Beshbishy et al., 2020). Obesity also damages lung function (Dixon and Peters, 2018), increasing the vulnerability to respiratory viral diseases (Green and Beck, 2017; Llamas-Velasco et al., 2021). Indeed, the increased risk of pulmonary fibrosis in patients with obesity raises the likelihood that they will develop a more severe course of COVID-19 (Steenblock et al., 2022).

Diabetes, like cutaneous psoriasis, does not appear to increase the risk of SARS-CoV-2 infection (Albulescu et al., 2020); however, it is a risk factor for severe COVID-19 disease and death. ACE2 is also upregulated in patients with type 2 diabetes (Gutta et al., 2018), which may exacerbate the damage to alveolar epithelial cells (Albulescu et al., 2020) and lead to a rapidly progressing course of COVID-19. Furthermore, the increased risk of acquiring bacterial infections among patients with high blood sugar levels, and the chronic inflammation status and high platelet reactivity of patients with diabetes (Demirtunc et al., 2009; Maiocchi et al., 2018), put these individuals at higher risks of developing severe COVID-19 disease or death.

Pre-existing cardiovascular diseases are associated with higher rates of severity and morbimortality from COVID-19 and, among patients requiring hospitalization, hypertension is the most common concomitant cardiovascular condition (Richardson et al., 2020; Zheng

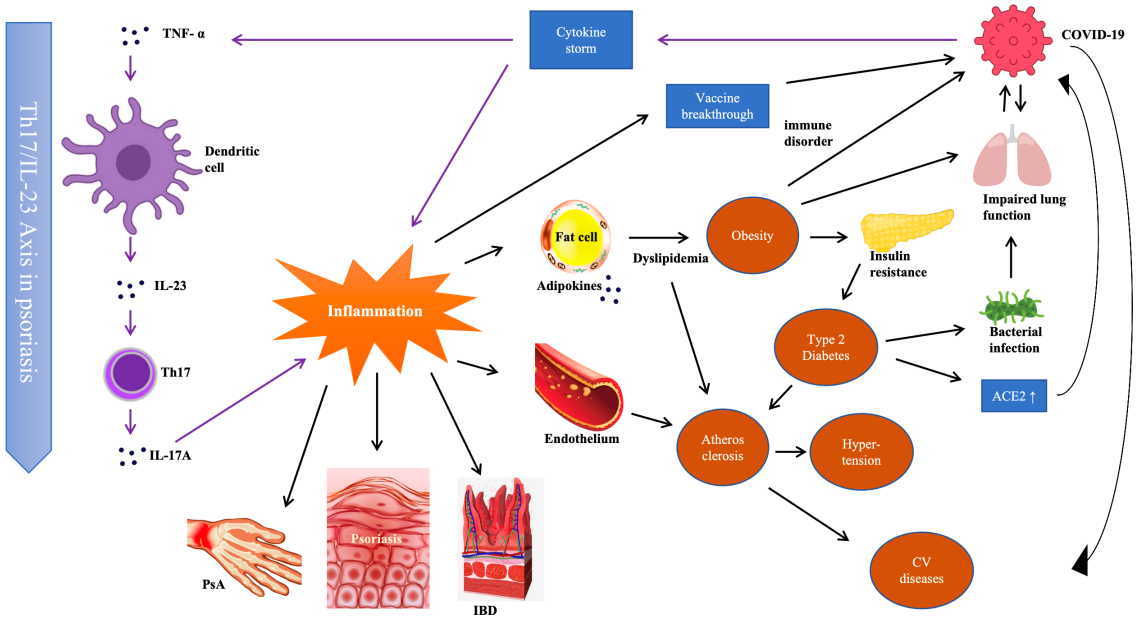

FIGURE 1
Immunological correlation among psoriasis, its comorbidities and COVID-19.

et al., 2020). Acute myocardial infarction and heart failure are also correlated with SARS-CoV-2 infection. The cellular damage to blood vessel epithelium by the chronic inflammatory status in psoriasis patients leads to a higher rate of hypertension and accelerated atherosclerotic plaque formation (Lowes et al., 2014; Boehncke, 2018). The hypercoagulative state of psoriasis patients especially after COVID-19 infection also raises the possibility of thrombogenesis, which may have life-threatening consequences in patients with cytokine storm or impaired lung function.

Another possible explanation for why patients with these comorbidities are at high risk during COVID-19 is that the damaged immune system leads to vaccine breakthrough (Hanckova and Betakova, 2021; Juthani et al., 2021).

1.3. Interference of SARS-CoV-2 in psoriasis patients with comorbidity

After the acute phase of COVID-19, some patients develop long-term health problems, which are also called "long COVID" (Lai et al., 2023), and include fatigue, chest tightness, anxiety, and other specific presentations if other organs are involved (Desai et al., 2022). Psoriasis patients are also vulnerable.

A common feature of the complex relationships encompassing psoriasis, its related comorbidities, and coronavirus infection, is inflammation. As stated above, psoriasis patients with comorbidities usually exhibit a more severe inflammatory status driven by IL-17 and TNF-α. SARS-CoV-2 infection can trigger an adaptive immune response in which fluctuations in immune function may cause onset, worsening, or recurrence of psoriasis (Zahedi Niaki et al., 2020; Silva Andrade et al., 2021). The COVID-19 induced IL-17 immune response (Queiroz et al., 2022) and TNF-α release (Vianello et al., 2022; Davis et al., 2023) can worsen psoriasis and its comorbidities. Therefore, patients with psoriasis comorbidities are more likely to be negatively impacted by post-COVID-19 effects.

Besides COVID-19 infection, dermatologists, and patients alike should be made aware that the COVID-19 vaccination itself may also induce or exacerbate psoriasis (Potestio et al., 2023).

1.4. Management of the COVID-19 and psoriasis comorbidity

Seasonal reinfection of SARS-CoV-2 variants has become a health problem that seems to be unavoidable. Proper patient education is necessary to help psoriasis patients with comorbidities experience increased quality of life, lower the frequency of recurrence, and control systemic complications. Patients should avoid factors that may further suppress immune function and adopt protective measures, such as mask-wearing. Upon noticing signs of COVID-19 infection, patients should quickly seek a diagnosis and early active treatment because prolonged infection may increase inflammatory damage. Prescriptions for patients with comorbidities should also be re-evaluated during the COVID-19 era. Below, we highlight treatment recommendations in specific patient comorbidity groups in the COVID era (Table 1).

2. PsA

For patients with moderate-to-severe PsA, early use of MTX is recommended to prevent disease progression and joint destruction (Michelsen et al., 2023). Despite the suggestion by some studies that MTX administered within 2 weeks after vaccination may affect the vaccine response (Arnold et al., 2021), there is no evidence of an increased risk of COVID-19 in patients receiving MTX therapy. It is

TABLE 1 Common comorbidities of psoriasis and the recommended treatment options in the COVID era.

Comorbidities of psoriasis	Treatment recommendations in the COVID era
Psoriatic arthritis	IL-17 inhibitor, IL-23 inhibitor, or IL-12/23 inhibitor for initial treatment; MTX, TNF-α, or JAK inhibitor can be continued in patients who are already in the course of treatment with these agents.
Inflammatory bowel disease	Infliximab, adalimumab, certolizumab, or ustekinumab are approved in patients with Crohn's disease; infliximab, adalimumab or ustekinumab are approved in patients with ulcerative colitis; IL-23 and IL-12/23 inhibitors are effective treatment option; Avoid IL-17 inhibitors.
Metabolic syndrome	IL-12/23 inhibitors and IL-17 inhibitors; Cyclosporine, MTX and retinoids are not recommended.
Ischemic heart disease and atherosclerosis	MTX, IL-17 inhibitors, IL-12/23 inhibitors, and TNF-α inhibitors. Cyclosporine and retinoids are not recommended.
Congestive heart failure	MTX, retinoids, IL-17 inhibitors, and IL-12/23 inhibitors; Avoid TNF-α inhibitors and cyclosporine in COVID-19 patients.
Hepatitis	IL-17 inhibitors, IL-23 inhibitors, and IL-12/23 inhibitors.
Latent tuberculosis	IL-17 inhibitors, IL-23 inhibitors, and IL-12/23 inhibitors; Avoid TNF-α inhibitors.

recommended to continue this medication during COVID-19 (Sadeghinia and Daneshpazhooh, 2021). For active unilateral or oligo-arthritis and enthesitis, local injection of corticosteroid is an option.

When peripheral joint disease cannot be controlled, or when the axial joints are involved, biologic treatment is recommended. The US Food and Drug Administration has approved five TNF-α inhibitors (etanercept, adalimumab, infliximab, pexelizumab, golimumab), two IL-17A inhibitors (secukinumab, ixekizumab), and one IL-12/23 inhibitor (ustekinumab) for the treatment of PsA. Previous guidelines prioritized TNF-α inhibitors, but recent studies suggest that the adoption of a TNF-α inhibitor should no longer be mandatory because ustekinumab and IL-17A antibodies may be equally effective (Sadeghinia and Daneshpazhooh, 2021). The risk of COVID-19 infection in psoriasis patients receiving TNF-α, IL-17, IL-12, and IL-23 inhibitors was also investigated in different cohort studies, systematic evaluations, and meta-analyses. The effects of TNF-α inhibitors on COVID-19 infection remain controversial. Some studies showed a higher risk of infection with TNF-α inhibitor therapy, whereas others showed no significant differences (Dommasch et al., 2019; Jin et al., 2022; Schneeweiss et al., 2023). For instance, In a study on psoriasis patients, the use of TNF-α inhibitors increased overall infection and upper respiratory tract infection by up to 7% compared with placebo, higher than the rates with IL-17 and IL-12/23 inhibitors (Lebwohl et al., 2020).

In studies of JAK inhibitors, ruxolitinib, and baricitinib were found to contribute to a hyperinflammatory state in critical COVID-19 patients, but simultaneously inhibited the receptor-mediated endocytosis of SARS-CoV-2 viral particles, thereby exhibiting antiviral potential (Zahedi Niaki et al., 2020). Currently, there is insufficient evidence of harm or benefit of JAK inhibition therapy in patients with SARS-CoV-2 infection.

For PsA patients with skin involvement, IL-17A, IL-23, or IL-12/23 inhibitors are recommended. For patients with inflammatory bowel disease (IBD), TNF-α, IL-12/23, IL-23, or JAK inhibitors are recommended (Michelsen et al., 2023). For patients with PsA infected with COVID-19, the initial biologic treatment should be one of the safer agents, such as an IL-17, IL-23, or IL-12/23 inhibitor. Among patients already under TNF-α or JAK inhibitor therapy, the treatment can be continued during COVID-19 infection (Sadeghinia and Daneshpazhooh, 2021).

3. IBD

Approved targeted therapies are preferred for patients with psoriasis and active IBD or history of IBD. Infliximab, adalimumab, pexelizumab, and ustekinumab were approved for the treatment of Crohn's disease, and infliximab, adalimumab, and upadacitinibi for the treatment of ulcerative colitis. Notably, etanercept failed in clinical trials in patients with Crohn's disease. There is a warning in the prescribing information for IL-17A antibodies for patients with IBD, and active Crohn's disease is a contraindication to the use of the IL-17 antibody brodalumab (Whitlock et al., 2018). The IL-23 inhibitors guselkumab and risankizumab and the JAK inhibitor upadacitinib have shown good efficacy in Crohn's disease and ulcerative colitis, with prolonged efficacy and safety (Barberio et al., 2023; Friedberg et al., 2023). Studies also showed efficacy of guselkumab in controlling intestinal inflammation (Higashiyama and Hokaria, 2023).

One study reported an increase of up to 9% in the overall infection rate and a slight increase in the upper respiratory tract infection rate in users of IL-23 blockers (Lebwohl et al., 2020). However, other research did not detect a difference in infection risk among users of TNF-α, IL-17, or IL-12/23 inhibitors in psoriasis or PsA (Li et al., 2020). Additional randomized controlled trials showed that the risk of upper respiratory tract infection in users of IL-23 inhibitors was similar to that with placebo (Brownstone et al., 2020). Today, in the post-pandemic era, IL-12/23 inhibitors are associated with a lower risk of infection, enabling a favorable outcome after COVID-19; thus, it is recommended to initiate or continue their application in psoriasis patients with IBD (Machado et al., 2023).

4. Metabolic syndrome

MTX should be used with caution in patients with diabetes, obesity, and non-alcoholic fatty liver disease because the risk of liver fibrosis increases when the cumulative dose exceeds 1.5 g (Singh et al., 2019). Cyclosporine can increase insulin resistance, and interfere with fatty acid metabolism, thereby leading to dyslipidemia and elevated serum uric acid (Gisondi et al., 2013). Furthermore, a Danish cohort study found that patients receiving cyclosporin had a significantly increased risk of hospitalization for COVID-19 (Galvez-Romero et al., 2021), suggesting caution when administering cyclosporin in patients with metabolic syndrome.

About obesity and biologics, Studies have shown that weight gain may occur in patients treated with TNF-α inhibitors. In contrast, ustekinumab and IL-17 inhibitors generally do not increase body weight (Onsun et al., 2022).

Regarding diabetes and biotics, studies of patients receiving TNF-α antagonists had a lower risk of new diabetes compared with those receiving other drugs, with an adjusted diabetes risk ratio of 0.62 (95%CI: 0.42–0.91) (Solomon et al., 2011). Other studies have found that patients with underlying diabetes or metabolic syndrome receiving anti-TNF-α therapy exhibit improved insulin resistance (Dal Bello et al., 2020). A phase III randomized controlled trial of secukinumab showed that patients on the drug had a trend of lower fasting glucose level compared with placebo during the first 12 weeks (Gerdes et al., 2020).

For COVID-19 patients with psoriasis, IL-17 inhibitors have demonstrated good efficacy and safety. In psoriasis, the incidences of upper respiratory tract infections were comparable in patients treated with IL-17 inhibitors and placebo (Langley et al., 2019). IL-17 may have a pathogenic role in the acute respiratory distress syndrome and lung inflammation associated with severe COVID-19. COVID-19 patients with pulmonary complications have increased populations and activation of Th17 cells. Th17 pathway blockers can downregulate the abnormal immune response of COVID-19 and reduce mortality (Bashyam and Feldman, 2020; Machado et al., 2023).

5. Cardiovascular disease

5.1. Ischemic heart disease and atherosclerosis

Systemic retinoids increase the levels of serum triglycerides and cholesterol by transforming high-density lipoprotein to low-density lipoprotein, which contributes to elevated risk of coronary heart disease (Balak et al., 2020). Similarly, cyclosporin can induce or aggravate arterial hypertension (in a dose-dependent manner), aggravate dyslipidemia, and raise blood glucose levels. Cyclosporine may interfere with drugs used in patients with ischemic heart disease, such as beta-blockers, calcium antagonists, fibrates and most statins (Berth-Jones et al., 2019). By contrast, MTX improved arteriosclerosis and reduced the carotid intima-media thickness in patients with moderate-to-severe psoriasis (Martinez-Lopez et al., 2018). MTX was also found to reduce risks of cardiovascular morbidity and mortality compared with cyclosporine and retinoids (Roubille et al., 2015; Tsai et al., 2021).

Treatment with TNF-α monoclonal antibodies and ustekinumab has been shown to reduce aortic vascular inflammation and systemic inflammatory biomarkers (Eder et al., 2018; Gelfand et al., 2020). Furthermore, TNF-α treatment reduces intima-media thickness and arterial stiffness and consequently lower the risk of myocardial infarction (Terui and Asano, 2023) and myocardial damage (Atzeni et al., 2020). Secukinumab may exert beneficial effects on the cardiovascular system in psoriasis patients by improving endothelial function (von Stebut et al., 2019). Anti IL-23 therapy is also beneficial as IL-23 is a proatherogenic cytokine.

Overall, considering efficacy, safety, and impact on COVID infection, MTX is recommended as the preferred conventional medication for patients with psoriasis and ischemic heart disease. Anti-TNF-α antibodies, ustekinumab, and IL-17 inhibitors are suggested as preferred targeted therapies in these patients (without heart failure) in the COVID-19 era.

5.2. Congestive heart failure

Cyclosporine is not recommended in patients with psoriasis and advanced congestive heart failure (CHF) because it may increase blood pressure and decrease renal function (Berth-Jones et al., 2019).

A study of patients with heart failure showed a trend of increased mortality and hospital admission rates among patients who received etanercept compared with those who received placebo (Deswal et al., 1999). Infliximab was evaluated in a randomized, double-blind, placebo-controlled phase II pilot study that showed an association between high-dose infliximab (10 mg/kg) and increased mortality and hospitalization rates in patients with heart failure (Chung et al., 2003). TNF is usually considered as a cardiotoxic factor (Kotyla, 2018), the reason why anti-TNF therapy may increase heart failure risk is still unclear.

In the COVID-19 era, expert opinion on the treatment of patients with psoriasis and heart failure with MTX, retinoids, and ustekinumab, IL-17, and IL-23 inhibitors is neutral, depending on the underlying cause of heart failure. MTX and retinoids can be recommended as treatment options for patients with psoriasis and advanced congestive heart failure. Ustekinumab, IL-17, and IL-23 inhibitors are also considered. TNF-α inhibitors, especially adalimumab and infliximab, are contraindicated in patients with congestive heart failure III/IV and should be cautioned in patients with mild congestive heart failure (New York Heart Association I/II). The use of etanercept in patients with CHF should be closely monitored (Campanati et al., 2020). In patients already infected with SARS-Cov-2, concomitant heart failure may deteriorate rapidly, it is reasonable to avoid anti-TNF therapy in all heart failure level patients who are suffering from COVID-19.

6. Hepatitis

TNF-α has been associated with the risk of hepatitis B virus (HBV) reactivation and drug-induced liver injury. A multicenter study in psoriasis patients with hepatitis B or C reported the occurrence of viral reactivation, showing a higher risk with TNF-α inhibitors than with IL-17 inhibitors (Chiu et al., 2021). Three phase III randomized controlled trials ($n = 3,736$) confirmed the clinical efficacy of ixekizumab in treating patients with psoriasis, and reported no cases of hepatitis B reactivation as of Week 60 (Gordon et al., 2016). A study of 30 patients with chronic inactive HBV infection who were treated with secukinumab indicated that this drug did not increase the risk of hepatitis during treatment (Qin et al., 2022). In a prospective cohort study of ustekinumab in patients with psoriasis ($n = 93$), the reactivation rate among HBV carriers was 17.4% without prophylaxis (Ting et al., 2018). IL-17 and IL-23 inhibitors, as well as ustekinumab were recommended as preferred systemic treatments for this patient group (Nast et al., 2021).

7. Latent tuberculosis

There are few data on the risk of TB reactivation with retinoids, cyclosporine, and MTX. To date, most published guidelines do not recommend TB screening for these drugs. However, the World Health Organization has issued black box warnings about the risk of TB and other serious infections with TNF-α inhibitors. Furthermore, a review suggested that patients with latent TB who received TNF-α had an approximately two to four-fold increased risk of active TB (Baddley et al., 2018). The mechanism maybe related to the effects of anti-TNF-α therapy on cellular interactions in a latent TB granuloma (Robert and Miossec, 2021). Patients receiving IL-17 as well as IL23 inhibitors had the lowest risk of activating latent TB than other previously approved drugs including TNF-α inhibitors and IL12/23 inhibitors (Nogueira et al., 2021).

8. Conclusion

The interplay between comorbid COVID-19 and psoriasis presents a compounding challenge for the management of both conditions. Despite the decreased virulence of the prevalent SARS-CoV-2 strains, small seasonal waves of infection continue to cause severe illness, especially among vulnerable populations. Psoriasis patients with comorbidities are particularly at risk. To effectively manage comorbidities in psoriasis patients during the COVID-19 era, it is essential to provide patients with properly individualized therapeutic modalities that improve their quality of life, reduce recurrence rates, and control systemic complications.

Author contributions

YS: Funding acquisition, Writing – original draft, Writing – review & editing. LY: Validation, Writing – review & editing. SL: Methodology, Resources, Writing – review & editing. JZ: Funding acquisition, Writing-original draft, Writing-review & editing, Project administration.

Funding

The author(s) declare financial support was received for the research, authorship, and/or publication of this article. This work was funded by the Natural Science Foundation of Jilin Province (Project nos. YDZJ202201ZYTS030 and 20220204095YY); and by the Jilin Provincial Healthcare Talent Special Program of Jilin Province Department of Finance (Project number JLSWSRCZX2021-67).

Acknowledgments

We thank Michelle Kahmeyer-Gabbe, PhD, from Liwen Bianji (Edanz) (www.liwenbianji.cn) for editing the English text of a draft of this manuscript.

Conflict of interest

The authors declare that the research was conducted in the absence of any commercial or financial relationships that could be construed as a potential conflict of interest.

Publisher's note

References

Aggarwal, D., Arumalla, N., Jethwa, H., and Abraham, S. (2018). The use of biomarkers as a tool for novel psoriatic disease drug discovery. *Exp. Opin. Drug Discov.* 13, 875–887. doi: 10.1080/17460441.2018.1508206

Albulescu, R., Dima, S. O., Florea, I. R., Lixandru, D., Serban, A. M., Aspritoiu, V. M., et al. (2020). COVID-19 and diabetes mellitus: unraveling the hypotheses that worsen the prognosis (review). *Exp. Ther. Med.* 20:194. doi: 10.3892/etm.2020.9324

Arnold, J., Winthrop, K., and Emery, P. (2021). COVID-19 vaccination and antirheumatic therapy. *Rheumatology (Oxford)* 60, 3496–3502. doi: 10.1093/rheumatology/keab223

Atzeni, F., Nucera, V., Galloway, J., Zoltan, S., and Nurmohamed, M. (2020). Cardiovascular risk in ankylosing spondylitis and the effect of anti-TNF drugs: a narrative review. *Expert. Opin. Biol. Ther.* 20, 517–524. doi: 10.1080/14712598.2020.1704727

Baddley, J. W., Cantini, F., Goletti, D., Gomez-Reino, J. J., Mylonakis, E., San-Juan, R., et al. (2018). ESCMID study Group for Infections in compromised hosts (ESGICH) consensus document on the safety of targeted and biological therapies: an infectious diseases perspective (soluble immune effector molecules [I]: anti-tumor necrosis factor-alpha agents). *Clin. Microbiol. Infect.* 24, S10–S20. doi: 10.1016/j.cmi.2017.12.025

Balak, D. M. W., Gerdes, S., Parodi, A., and Salgado-Boquete, L. (2020). Long-term safety of Oral systemic therapies for psoriasis: a comprehensive review of the literature. *Dermatol. Ther. (Heidelb)* 10, 589–613. doi: 10.1007/s13555-020-00409-4

Barberio, B., Gracie, D. J., Black, C. J., and Ford, A. C. (2023). Efficacy of biological therapies and small molecules in induction and maintenance of remission in luminal Crohn's disease: systematic review and network meta-analysis. *Gut* 72, 264–274. doi: 10.1136/gutjnl-2022-328052

Bashyam, A. M., and Feldman, S. R. (2020). Should patients stop their biologic treatment during the COVID-19 pandemic. *J. Dermatolog. Treat.* 31, 317–318. doi: 10.1080/09546634.2020.1742438

Berth-Jones, J., Exton, L. S., Ladoyanni, E., Mohd Mustapa, M. F., Tebbs, V. M., Yesudian, P. D., et al. (2019). British Association of Dermatologists guidelines for the safe and effective prescribing of oral ciclosporin in dermatology 2018. *Br. J. Dermatol.* 180, 1312–1338. doi: 10.1111/bjd.17587

Boehncke, W. H. (2018). Systemic inflammation and cardiovascular comorbidity in psoriasis patients: causes and consequences. *Front. Immunol.* 9:579. doi: 10.3389/fimmu.2018.00579

Boehncke, S., Thaci, D., Beschmann, H., Ludwig, R. J., Ackermann, H., Badenhoop, K., et al. (2007). Psoriasis patients show signs of insulin resistance. *Br. J. Dermatol.* 157, 1249–1251. doi: 10.1111/j.1365-2133.2007.08190.x

Brembilla, N. C., Senra, L., and Boehncke, W. H. (2018). The IL-17 family of cytokines in psoriasis: IL-17A and beyond. *Front. Immunol.* 9:1682. doi: 10.3389/fimmu.2018.01682

Brownstone, N. D., Thibodeaux, Q. G., Reddy, V. D., Myers, B. A., Chan, S. Y., Bhutani, T., et al. (2020). Novel coronavirus disease (COVID-19) and biologic therapy in psoriasis: infection risk and patient counseling in uncertain times. *Dermatol. Ther.* 10, 339–349. doi: 10.1007/s13555-020-00377-9

Campanati, A., Diotallevi, F., Martina, E., Paolinelli, M., Radi, G., and Offidani, A. (2020). Safety update of etanercept treatment for moderate to severe plaque psoriasis. *Expert Opin. Drug Saf.* 19, 439–448. doi: 10.1080/14740338.2020.1740204

Chiu, H. Y., Chiu, Y. M., Chang Liao, N. F., Chi, C. C., Tsai, T. F., Hsieh, C. Y., et al. (2021). Predictors of hepatitis B and C virus reactivation in patients with psoriasis

treated with biologic agents: a 9-year multicenter cohort study. *J. Am. Acad. Dermatol.* 85, 337–344. doi: 10.1016/j.jaad.2019.12.001

Chung, E. S., Packer, M., Lo, K. H., Fasanmade, A. A., Willerson, J. T., and Anti, T. N. (2003). Randomized, double-blind, placebo-controlled, pilot trial of infliximab, a chimeric monoclonal antibody to tumor necrosis factor-alpha, in patients with moderate-to-severe heart failure: results of the anti-TNF therapy against congestive heart failure (ATTACH) trial. *Circulation* 107, 3133–3140. doi: 10.1161/01.CIR.0000077913.60364.D2

Dal Bello, G., Gisondi, P., Idolazzi, L., and Girolomoni, G. (2020). Psoriatic arthritis and diabetes mellitus: a narrative review. *Rheumatol. Ther.* 7, 271–285. doi: 10.1007/s40744-020-00206-7

Davis, H. E., McCorkell, L., Vogel, J. M., and Topol, E. J. (2023). Long COVID: major findings, mechanisms and recommendations. *Nat. Rev. Microbiol.* 21, 133–146. doi: 10.1038/s41579-022-00846-2

Demirtunc, R., Duman, D., Basar, M., Bilgi, M., Teomete, M., and Garip, T. (2009). The relationship between glycemic control and platelet activity in type 2 diabetes mellitus. *J. Diabetes Complicat.* 23, 89–94. doi: 10.1016/j.jdiacomp.2008.01.006

Desai, A. D., Lavelle, M., Boursiquot, B. C., and Wan, E. Y. (2022). Long-term complications of COVID-19. *Am. J. Physiol. Cell Physiol.* 322, C1–C11. doi: 10.1152/ajpcell.00375.2021

Deswal, A., Bozkurt, B., Seta, Y., Parilti-Eiswirth, S., Hayes, F. A., Blosch, C., et al. (1999). Safety and efficacy of a soluble P75 tumor necrosis factor receptor (Enbrel, etanercept) in patients with advanced heart failure. *Circulation* 99, 3224–3226. doi: 10.1161/01.cir.99.25.3224

Dixon, A. E., and Peters, U. (2018). The effect of obesity on lung function. *Expert Rev. Respir. Med.* 12, 755–767. doi: 10.1080/17476348.2018.1506331

Dommasch, E. D., Kim, S. C., Lee, M. P., and Gagne, J. J. (2019). Risk of serious infection in patients receiving systemic medications for the treatment of psoriasis. *JAMA Dermatol.* 155, 1142–1152. doi: 10.1001/jamadermatol.2019.1121

Eder, L., Joshi, A. A., Dey, A. K., Cook, R., Siegel, E. L., Gladman, D. D., et al. (2018). Association of Tumor Necrosis Factor Inhibitor Treatment with Reduced Indices of subclinical atherosclerosis in patients with psoriatic disease. *Arthritis Rheumatol.* 70, 408–416. doi: 10.1002/art.40366

Elmets, C. A., Leonardi, C. L., Davis, D. M. R., Gelfand, J. M., Lichten, J., Mehta, N. N., et al. (2019). Joint AAD-NPF guidelines of care for the management and treatment of psoriasis with awareness and attention to comorbidities. *J. Am. Acad. Dermatol.* 80, 1073–1113. doi: 10.1016/j.jaad.2018.11.058

Espinosa, O. A., Zanetti, A. D. S., Antunes, E. F., Longhi, F. G., Matos, T. A., and Battaglini, P. F. (2020). Prevalence of comorbidities in patients and mortality cases affected by SARS-CoV2: a systematic review and meta-analysis. *Rev. Inst. Med. Trop. São Paulo* 62:e43. doi: 10.1590/S1678-9946202062043

Friedberg, S., Choi, D., Hunold, T., Choi, N. K., Garcia, N. M., Picker, E. A., et al. (2023). Upadacitinib is effective and safe in both ulcerative colitis and Crohn's disease: prospective Real-world experience. *Clin. Gastroenterol. Hepatol.* 21, 1913–1923.e2. doi: 10.1016/j.cgh.2023.03.001

Gallo Marin, B., Aghagoli, G., Lavine, K., Yang, L., Siff, E. J., Chiang, S. S., et al. (2021). Predictors of COVID-19 severity: a literature review. *Rev. Med. Virol.* 31, 1–10. doi: 10.1002/rmv.2146

Galvez-Romero, J. L., Palmeros-Rojas, O., Real-Ramirez, F. A., Sanchez-Romero, S., Tome-Maxil, R., Ramirez-Sandoval, M. P., et al. (2021). Cyclosporine a plus low-dose steroid treatment in COVID-19 improves clinical outcomes in patients with moderate to severe disease: a pilot study. *J. Intern. Med.* 289, 906–920. doi: 10.1111/joim.13223

Gelfand, J. M., Shin, D. B., Alavi, A., Torigian, D. A., Werner, T., Papadopoulos, M., et al. (2020). A phase IV, randomized, double-blind, placebo-controlled crossover study of the effects of Ustekinumab on vascular inflammation in psoriasis (the VIP-U trial). *J. Invest. Dermatol.* 140, 85–93.e2. doi: 10.1016/j.jid.2019.07.679

Gerdes, S., Pinter, A., Papavassilis, C., and Reinhardt, M. (2020). Effects of secukinumab on metabolic and liver parameters in plaque psoriasis patients. *J. Eur. Acad. Dermatol. Venereol.* 34, 533–541. doi: 10.1111/jdv.16004

Gisondi, P., Bellinato, F., Girolomoni, G., and Albanesi, C. (2020). Pathogenesis of chronic plaque psoriasis and its intersection with cardio-metabolic comorbidities. *Front. Pharmacol.* 11:117. doi: 10.3389/fphar.2020.00117

Gisondi, P., Cazzaniga, S., Chimenti, S., Giannetti, A., Maccarone, M., Picardo, M., et al. (2013). Metabolic abnormalities associated with initiation of systemic treatment for psoriasis: evidence from the Italian Psocare registry. *J. Eur. Acad. Dermatol. Venereol.* 27, e30–e41. doi: 10.1111/j.1468-3083.2012.04450.x

Gordon, K. B., Blauvelt, A., Papp, K. A., Langley, R. G., Luger, T., Ohtsuki, M., et al. (2016). Phase 3 trials of Ixekizumab in moderate-to-severe plaque psoriasis. *N. Engl. J. Med.* 375, 345–356. doi: 10.1056/NEJMoa1512711

Green, W. D., and Beck, M. A. (2017). Obesity impairs the adaptive immune response to influenza virus. *Ann. Am. Thorac. Soc.* 14, S406–S409. doi: 10.1513/AnnalsATS.201706-447AW

Gutta, S., Grobe, N., Kumbaji, M., Osman, H., Saklayen, M., Li, G., et al. (2018). Increased urinary angiotensin converting enzyme 2 and neprilysin in patients with type 2 diabetes. *Am. J. Physiol. Renal Physiol.* 315, F263–F274. doi: 10.1152/ajprenal.00565.2017

Hanckova, M., and Betakova, T. (2021). Pandemics of the 21st century: the risk factor for obese people. *Viruses* 14:25. doi: 10.3390/v14010025

Higashiyama, M., and Hokaria, R. (2023). New and emerging treatments for inflammatory bowel disease. *Digestion* 104, 74–81. doi: 10.1159/000527422

Hosseini, A., Hashemi, V., Shomali, N., Asghari, F., Gharibi, T., Akbari, M., et al. (2020). Innate and adaptive immune responses against coronavirus. *Biomed. Pharmacother.* 132:110859. doi: 10.1016/j.biopha.2020.110859

Jin, Y., Lee, H., Lee, M. P., Landon, J. E., Merola, J. F., Desai, R. J., et al. (2022). Risk of hospitalization for serious infection after initiation of Ustekinumab or other biologics in patients with psoriasis or psoriatic arthritis. *Arthritis Care Res. (Hoboken)* 74, 1792–1805. doi: 10.1002/acr.24630

Juthani, P. V., Gupta, A., Borges, K. A., Price, C. C., Lee, A. I., Won, C. H., et al. (2021). Hospitalisation among vaccine breakthrough COVID-19 infections. *Lancet Infect. Dis.* 21, 1485–1486. doi: 10.1016/S1473-3099(21)00558-2

Kotyla, P. J. (2018). Bimodal function of Anti-TNF treatment: shall we be concerned about Anti-TNF treatment in patients with rheumatoid arthritis and heart failure? *Int. J. Mol. Sci.* 19:1739. doi: 10.3390/ijms19061739

Lai, C. C., Hsu, C. K., Yen, M. Y., Lee, P. I., Ko, W. C., and Hsueh, P. R. (2023). Long COVID: an inevitable sequela of SARS-CoV-2 infection. *J. Microbiol. Immunol. Infect.* 56, 1–9. doi: 10.1016/j.jmii.2022.10.003

Langley, R. G., Kimball, A. B., Nak, H., Xu, W., Pangallo, B., Osuntokun, O. O., et al. (2019). Long-term safety profile of ixekizumab in patients with moderate-to-severe plaque psoriasis: an integrated analysis from 11 clinical trials. *J. Eur. Acad. Dermatol. Venereol.* 33, 333–339. doi: 10.1111/jdv.15242

Lebwohl, M., Rivera-Oyola, R., and Murrell, D. F. (2020). Should biologics for psoriasis be interrupted in the era of COVID-19? *J. Am. Acad. Dermatol.* 82, 1217–1218. doi: 10.1016/j.jaad.2020.03.031

Li, X., Andersen, K. M., Chang, H. Y., Curtis, J. R., and Alexander, G. C. (2020). Comparative risk of serious infections among real-world users of biologics for psoriasis or psoriatic arthritis. *Ann. Rheum. Dis.* 79, 285–291. doi: 10.1136/annrheumdis-2019-216102

Llamas-Velasco, M., Ovejero-Merino, E., and Salgado-Boquete, L. (2021). Obesity - a risk factor for psoriasis and COVID-19. *Actas Dermosifiliogr.* 112, 489–494. doi: 10.1016/j.ad.2020.12.001

Lowes, M. A., Suarez-Farinas, M., and Krueger, J. G. (2014). Immunology of psoriasis. *Annu. Rev. Immunol.* 32, 227–255. doi: 10.1146/annurev-immunol-032713-120225

Machado, P. M., Schafer, M., Mahil, S. K., Liew, J., Gossec, L., Dand, N., et al. (2023). Characteristics associated with poor COVID-19 outcomes in people with psoriasis, psoriatic arthritis and axial spondyloarthritis: data from the COVID-19 PsoProtect and global rheumatology Alliance physician-reported registries. *Ann. Rheum. Dis.* 82, 698–709. doi: 10.1136/ard-2022-223499

Magdy Beshbishy, A., Hetta, H. F., Hussein, D. E., Saati, A. A., C Uba, C., Rivero-Perez, N., et al. (2020). Factors associated with increased morbidity and mortality of obese and overweight COVID-19 patients. *Biology (Basel)* 9:280. doi: 10.3390/biology9090280

Maiocchi, S., Alwis, I., Wu, M. C. L., Yuan, Y., and Jackson, S. P. (2018). Thromboinflammatory functions of platelets in ischemia-reperfusion injury and its dysregulation in diabetes. *Semin. Thromb. Hemost.* 44, 102–113. doi: 10.1055/s-0037-1613694

Martinez-Lopez, A., Blasco-Morente, G., Perez-Lopez, I., Tercedor-Sanchez, J., and Arias-Santiago, S. (2018). Studying the effect of systemic and biological drugs on intima-media thickness in patients suffering from moderate and severe psoriasis. *J. Eur. Acad. Dermatol. Venereol.* 32, 1492–1498. doi: 10.1111/jdv.14841

Michelsen, B., Ostergaard, M., Nissen, M. J., Ciurea, A., Moller, B., Ornbjerg, L. M., et al. (2023). Differences and similarities between the EULAR/ASAS-EULAR and national recommendations for treatment of patients with psoriatic arthritis and axial spondyloarthritis across Europe. *Lancet Reg. Health Eur.* 33:100706. doi: 10.1016/j.lanepe.2023.100706

Nast, A., Smith, C., Spuls, P. I., Avila Valle, G., Bata-Csorgo, Z., Boonen, H., et al. (2021). EuroGuiDerm guideline on the systemic treatment of psoriasis vulgaris - part 2: specific clinical and comorbid situations. *J. Eur. Acad. Dermatol. Venereol.* 35, 281–317. doi: 10.1111/jdv.16926

Nogueira, M., Warren, R. B., and Torres, T. (2021). Risk of tuberculosis reactivation with interleukin (IL)-17 and IL-23 inhibitors in psoriasis - time for a paradigm change. *J. Eur. Acad. Dermatol. Venereol.* 35, 824–834. doi: 10.1111/jdv.16866

Onsun, N., Akaslan, T. C., Sallahoglu, K., Gulcan, A. S., Bulut, H., and Yabaci, A. (2022). Effects of TNF inhibitors and an IL12/23 inhibitor on changes in body weight and adipokine levels in psoriasis patients: a 48-week comparative study. *J. Dermatolog. Treat.* 33, 1727–1732. doi: 10.1080/09546634.2021.1901845

Potestio, L., Battista, T., Cacciapuoti, S., Ruggiero, A., Martora, F., Fornaro, L., et al. (2023). New onset and exacerbation of psoriasis following COVID-19 vaccination: a review of the current knowledge. *Biomedicine* 11:2191. doi: 10.3390/biomedicines11082191

Qin, H., Liu, N., Hu, Y., Yu, N., Yi, X., Gao, Y., et al. (2022). Safety and efficacy of secukinumab in psoriasis patients infected with hepatitis B virus: a retrospective study. *Eur. J. Dermatol.* 32, 394–400. doi: 10.1684/ejd.2022.4263

Queiroz, M. A. F., Neves, P., Lima, S. S., Lopes, J. D. C., Torres, M., Vallinoto, I., et al. (2022). Cytokine profiles associated with acute COVID-19 and long COVID-19 syndrome. *Front. Cell. Infect. Microbiol.* 12:922422. doi: 10.3389/fcimb.2022.922422

Richardson, S., Hirsch, J. S., Narasimhan, M., Crawford, J. M., McGinn, T., Davidson, K. W., et al. (2020). Presenting characteristics, comorbidities, and outcomes among 5700 patients hospitalized with COVID-19 in the new York City area. *JAMA* 323, 2052–2059. doi: 10.1001/jama.2020.6775

Robert, M., and Miossec, P. (2021). Reactivation of latent tuberculosis with TNF inhibitors: critical role of the beta 2 chain of the IL-12 receptor. *Cell. Mol. Immunol.* 18, 1644–1651. doi: 10.1038/s41423-021-00694-9

Roubille, C., Richer, V., Starnino, T., McCourt, C., McFarlane, A., Fleming, P., et al. (2015). The effects of tumour necrosis factor inhibitors, methotrexate, non-steroidal anti-inflammatory drugs and corticosteroids on cardiovascular events in rheumatoid arthritis, psoriasis and psoriatic arthritis: a systematic review and meta-analysis. *Ann. Rheum. Dis.* 74, 480–489. doi: 10.1136/annrheumdis-2014-206624

Sadeghinia, A., and Daneshpazhooh, M. (2021). Immunosuppressive drugs for patients with psoriasis during the COVID-19 pandemic era a review. *Dermatol. Ther.* 34:e14498. doi: 10.1111/dth.14498

Schneeweiss, M. C., Savage, T. J., Wyss, R., Jin, Y., Schoder, K., Merola, J. F., et al. (2023). Risk of infection in children with psoriasis receiving treatment with Ustekinumab, Etanercept, or methotrexate before and after labeling expansion. *JAMA Dermatol.* 159, 289–298. doi: 10.1001/jamadermatol.2022.6325

Sette, A., and Crotty, S. (2021). Adaptive immunity to SARS-CoV-2 and COVID-19. *Cells* 184, 861–880. doi: 10.1016/j.cell.2021.01.007

Silva Andrade, B., Siqueira, S., de Assis Soares, W. R., de Souza Rangel, F., Santos, N. O., Dos Santos Freitas, A., et al. (2021). Long-COVID and post-COVID health complications: an up-to-date review on clinical conditions and their possible molecular mechanisms. *Viruses* 13:700. doi: 10.3390/v13040700

Singh, J. A., Guyatt, G., Ogdie, A., Gladman, D. D., Deal, C., Deodhar, A., et al. (2019). Special article: 2018 American College of Rheumatology/National Psoriasis Foundation guideline for the treatment of psoriatic arthritis. *Arthritis Rheumatol.* 71, 5–32. doi: 10.1002/art.40726

Singh, M. K., Mobeen, A., Chandra, A., Joshi, S., and Ramachandran, S. (2021). A meta-analysis of comorbidities in COVID-19: which diseases increase the susceptibility of SARS-CoV-2 infection? *Comput. Biol. Med.* 130:104219. doi: 10.1016/j.compbiomed.2021.104219

Solomon, D. H., Massarotti, E., Garg, R., Liu, J., Canning, C., and Schneeweiss, S. (2011). Association between disease-modifying antirheumatic drugs and diabetes risk in patients with rheumatoid arthritis and psoriasis. *JAMA* 305, 2525–2531. doi: 10.1001/jama.2011.878

Steenblock, C., Hassanein, M., Khan, E. G., Yaman, M., Kamel, M., Barbir, M., et al. (2022). Obesity and COVID-19: what are the consequences? *Horm. Metab. Res.* 54, 496–502. doi: 10.1055/a-1878-9757

Terui, H., and Asano, Y. (2023). Biologics for reducing cardiovascular risk in psoriasis patients. *J. Clin. Med.* 12:1162. doi: 10.3390/jcm12031162

Ting, S. W., Chen, Y. C., and Huang, Y. H. (2018). Risk of hepatitis B reactivation in patients with psoriasis on Ustekinumab. *Clin. Drug Investig.* 38, 873–880. doi: 10.1007/s40261-018-0671-z

Tsai, M. H., Chan, T. C., Lee, M. S., and Lai, M. S. (2021). Cardiovascular risk associated with methotrexate versus Retinoids in patients with psoriasis: a Nationwide Taiwanese cohort study. *Clin. Epidemiol.* 13, 693–705. doi: 10.2147/CLEP.S305126

Vianello, A., Guarnieri, G., Braccioni, F., Lococo, S., Molena, B., Cecchetto, A., et al. (2022). The pathogenesis, epidemiology and biomarkers of susceptibility of pulmonary fibrosis in COVID-19 survivors. *Clin. Chem. Lab. Med.* 60, 307–316. doi: 10.1515/cclm-2021-1021

von Stebut, E., Reich, K., Thaci, D., Koenig, W., Pinter, A., Korber, A., et al. (2019). Impact of Secukinumab on endothelial dysfunction and other cardiovascular disease parameters in psoriasis patients over 52 weeks. *J. Invest. Dermatol.* 139, 1054–1062. doi: 10.1016/j.jid.2018.10.042

Wang, Q., Iketani, S., Li, Z., Liu, L., Guo, Y., Huang, Y., et al. (2023). Alarming antibody evasion properties of rising SARS-CoV-2 BQ and XBB subvariants. *Cells* 186, 279–286.e8. doi: 10.1016/j.cell.2022.12.018

Whitlock, S. M., Enos, C. W., Armstrong, A. W., Gottlieb, A., Langley, R. G., Lebwohl, M., et al. (2018). Management of psoriasis in patients with inflammatory bowel disease: from the medical Board of the National Psoriasis Foundation. *J. Am. Acad. Dermatol.* 78, 383–394. doi: 10.1016/j.jaad.2017.06.043

Youn, S. W., Kang, S. Y., Kim, S. A., Park, G. Y., and Lee, W. W. (2015). Subclinical systemic and vascular inflammation detected by (18) F-fluorodeoxyglucose positron emission tomography/computed tomography in patients with mild psoriasis. *J. Dermatol.* 42, 559–566. doi: 10.1111/1346-8138.12859

Zahedi Niaki, O., Anadkat, M. J., Chen, S. T., Fox, L. P., Harp, J., Micheletti, R. G., et al. (2020). Navigating immunosuppression in a pandemic: a guide for the dermatologist from the COVID task force of the medical dermatology society and Society of Dermatology Hospitalists. *J. Am. Acad. Dermatol.* 83, 1150–1159. doi: 10.1016/j.jaad.2020.06.051

Zheng, Z., Peng, F., Xu, B., Zhao, J., Liu, H., Peng, J., et al. (2020). Risk factors of critical & mortal COVID-19 cases: a systematic literature review and meta-analysis. *J. Infect.* 81, e16–e25. doi: 10.1016/j.jinf.2020.04.021

frontiers | Frontiers in Microbiology

TYPE Original Research
PUBLISHED 20 December 2023
DOI 10.3389/fmicb.2023.1289387

OPEN ACCESS

EDITED BY
Wei Wei,
First Affiliated Hospital of Jilin University, China

REVIEWED BY
Fares Z. Najar,
Oklahoma State University, United States
Sanghita Sarkar,
University of Alabama at Birmingham,
United States

*CORRESPONDENCE
David J. Marchant
✉ marchant@ualberta.ca

RECEIVED 05 September 2023
ACCEPTED 29 November 2023
PUBLISHED 20 December 2023

CITATION
McClelland RD, Lin Y-CJ, Culp TN, Noyce R, Evans D, Hobman TC, Meier-Stephenson V and Marchant DJ (2023) The domestication of SARS-CoV-2 into a seasonal infection by viral variants.
Front. Microbiol. 14:1289387.
doi: 10.3389/fmicb.2023.1289387

The domestication of SARS-CoV-2 into a seasonal infection by viral variants

Ryley D. McClelland[1], Yi-Chan James Lin[1], Tyce N. Culp[1], Ryan Noyce[1], David Evans[1], Tom C. Hobman[1,2], Vanessa Meier-Stephenson[1,3] and David J. Marchant[1]*

[1]Department of Medical Microbiology and Immunology, University of Alberta, Edmonton, AB, Canada, [2]Department of Cell Biology, University of Alberta, Edmonton, AB, Canada, [3]Department of Medicine, University of Alberta, Edmonton, AB, Canada

Introduction: The COVID-19 pandemic was caused by the zoonotic betacoronavirus SARS-CoV-2. SARS-CoV-2 variants have emerged due to adaptation in humans, shifting SARS-CoV-2 towards an endemic seasonal virus. We have termed this process 'virus domestication'.

Methods: We analyzed aggregate COVID-19 data from a publicly funded healthcare system in Canada from March 7, 2020 to November 21, 2022. We graphed surrogate calculations of COVID-19 disease severity and SARS-CoV-2 variant plaque sizes in tissue culture.

Results and Discussion: Mutations in SARS-CoV-2 adapt the virus to better infect humans and evade the host immune response, resulting in the emergence of variants with altered pathogenicity. We observed a decrease in COVID-19 disease severity surrogates after the arrival of the Delta variant, coinciding with significantly smaller plaque sizes. Overall, we suggest that SARS-CoV-2 has become more infectious and less virulent through viral domestication. Our findings highlight the importance of SARS-CoV-2 vaccination and help inform public policy on the highest probability outcomes during viral pandemics.

KEYWORDS

seasonal infection, virus, adaptation, COVID19, coronavirus, SARS, surrogates

Introduction

Domestication refers to the act of gradual adaptation and taming towards humans such that the organism is genetically distinct from its wild counterparts. There are many accepted definitions of domestication and many whose wording applies to the description of our evolving relationship with the SARS-CoV-2 virus. Like many domesticated animal species, the term "domestication" does not equate to safety; both domesticated animals and seasonal viruses like influenza and respiratory syncytial virus are significant burdens to global mortality each year (Forrester et al., 2018; Paget et al., 2019; Du et al., 2023).

The spillover of the SARS-CoV-2 virus from bats through an unknown intermediate species into the human population precipitated the COVID-19 pandemic (Worobey et al., 2022). Prior to COVID-19, coronavirus outbreaks of SARS-CoV and MERS-CoV occurred in 2003 and 2012, respectively. The 2003 SARS-CoV is no longer circulating in humans and human MERS-CoV cases occur sporadically. The propensity of SARS-CoV-2 to rapidly spread within the human population is linked to its ability to be transmitted by infected persons before symptoms develop and by those who are asymptomatic.

We expect the eventual domestication of SARS-CoV-2 to occur akin to seasonal human coronaviruses (HCoV) such as HKU1, OC43 and NL63. These seasonal coronaviruses share distinct

similarities in genome sequence, receptor usage and biology of infection. Indeed, HCoV-OC43 likely originated as a zoonotic bovine coronavirus that became seasonal in humans due to a pandemic that occurred in 1890 (Vijgen et al., 2005). We believe that immune processes such as vaccination and immune memory will continue to drive the emergence of SARS-CoV-2 variants. This serves as an indication that domestication of SARS-CoV-2 is underway and will eventually become another endemic seasonal infection like HCoV-OC43.

In this study, we provide support that SARS-CoV-2 emerged into humans as a more virulent infection that has reduced in pathogenesis with an increase in infectiousness over time, coinciding with the emergence and dominance of SARS-CoV-2 variants of concern (VOCs). We warn that this process could make long-COVID more difficult to diagnose as infection becomes insidious and there is an increased risk of misdiagnosis. We have called this process of "virus domestication."

Methods

Data sources

This was a population-based longitudinal study using publicly available data on COVID-19 case statistics and vaccination rates in Alberta retrieved from the Government of Alberta website. The Canadian Province of Alberta has a publicly funded and publicly accessible health care system. Throughout the pandemic the Government of Alberta has recorded case, hospitalization, ICU admission and deaths due to SARS-CoV-2 infection and made the data publicly available. In this data set, there was 618,030 cumulative COVID-19 cases and 5,177 cumulative deaths attributed to COVID-19 in Alberta. The number of new hospitalizations and ICU admissions were recorded daily.

Calculation of surrogate markers of COVID-19 disease severity

The daily ICU admissions and deaths from aggregate data on COVID-19 cases in Alberta were divided by the hospitalizations at each respective day and tabulated.

Culture and plaque assay of SARS-CoV-2 variants

Culture of SARS-CoV-2 variants has been described previously with the following modifications: Vero E6/TMPRSS2 was used instead of Vero CCL-81 cells (Lin et al., 2022). Results are the product of one experiment but are representative of at least three independent replicate experiments per strain. Plaque sizes were measured using ImageJ (NIH) and reported as plaque area (mm^2).

Statistical analysis

Plaque diameters were measured and reported as plaque area (mm^2). Statistical significance between plaque areas was by one-way ANOVA with Tukey's test of significance using Graphpad Prism 10.

Results

We charted cases, hospitalizations, ICU admissions and deaths due to COVID-19 in the Canadian province of Alberta (Figure 1). Aggregate data show the detection of SARS-CoV-2 cases in the general population after March 7th, 2020 when Alberta Clinical Laboratories began testing for SARS-CoV-2 by PCR (Pabbaraju et al., 2022; Stokes et al., 2022). The World Health Organization declared a pandemic on March 11th, 2020. Figure 1 shows that there was an initial rise in daily infections, hospitalizations, and deaths, that then decreased with the enactment of COVID-19 health protection laws (Figure 1; i to x). In the weeks following the reopening of schools for in-class instruction after week 28 (day 200; health measure xiii) of the pandemic there was a wave of cases, hospitalizations, and deaths that occurred.

The arrival of variants coincided with a decrease in surrogate indicators of COVID-19 severity

Consistent with the domestication model, we observed a decrease in daily deaths (Figure 1C) whereas daily cases increased to their highest levels with the peak of Omicron BA1 prevalence (Figure 1A). We postulated that this was an indicator of mean reduced pathogenesis in the population, so we defined surrogates of COVID-19 disease severity. Here we chose hospitalization as the denominator because ICU cases and deaths would often be recorded as hospitalization initially, prior to ICU admission or death. We divided the daily number of intensive care unit (ICU) admissions or deaths (Figures 2A–D) by the number of hospitalized cases, so the calculation serves as an approximation of COVID-19 severity within a one-week to one-month time frame of hospital admission. There was a considerable reduction in ICU admissions versus hospitalizations coinciding with the arrival of variants Delta and Omicron, in particular.

Surrogate pathogenicity coincided with VOC plaque sizes

Viral escape from immune pressure and increased infectivity are the result of mutations in the VOCs, but these mutations come at a cost to viral replication. In a cell monolayer, the size of the virus plaques are related to the replicative fitness of the virus (Mandary et al., 2020). Consistently, we previously reported that respiratory syncytial virus (RSV) plaque sizes were associated with RSV viral load in patient samples (Elawar et al., 2017). Since SARS-CoV-2 viral loads are related to disease severity (Fajnzylber et al., 2020), we asked if SARS-CoV-2 plaque size was associated with disease surrogates of COVID-19. In a cell monolayer of Vero E6/TMPRSS2 cells, VOC plaque sizes were measured using ImageJ and reported as plaque area (mm^2) (Figure 2F). As we move from wild type to Delta, plaque size increased, relating to increased viral production and therefore improved replicative fitness. This coincided with the increased infectivity seen at the population level (Hui et al., 2022). This was

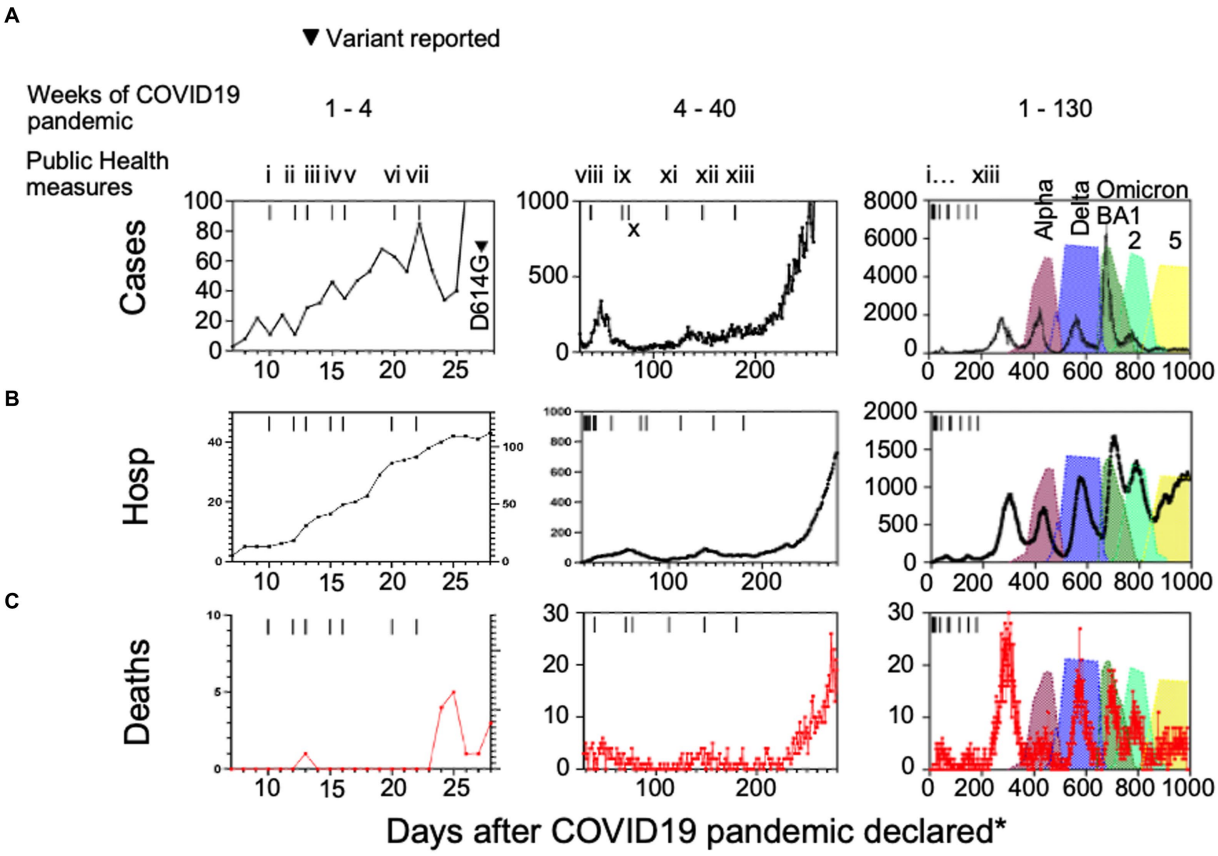

FIGURE 1
(A) Case numbers, **(B)** hospitalizations, and **(C)** deaths compared to public health measures and variants of interest introduced in Alberta, Canada. (i) school closures province-wide, (ii) public health emergency declared in Alberta, (iii) non-emergency health care procedure cancellations, (iv) care home lockdown, (v) US-Canada border closed, (vi) quarantine measures for international travelers introduced, (vii) restaurant and retail closures, (viii) test all who are symptomatic, (ix) mask wearing advised in Alberta and (x) Canada-wide, (xi) 2 m social distancing in public places, (xii) masks mandatory in public settings across Canada, (xiii) in-class grades kindergarten to 12 resume with masking, hand hygiene, and social distancing protocols. Hosp = hospitalizations, *days after the COVID-19 pandemic was declared by the World Health Organization on March 7th, 2020.

paired with evidence of stronger spike protein affinity leading to higher viral loads, potentially explaining its greater infectivity in the population (Kissler et al., 2021; Mannar et al., 2022). The spike proteins of Delta and Omicron variants have similar binding affinities for ACE2 (Mannar et al., 2022). However, we found that Omicron plaque sizes were significantly smaller than Delta plaque sizes (Figure 2F). This suggests that a process distinct from attachment is impacting viral fitness and leading to less viral replication in VOCs (Mannar et al., 2022). As the COVID-19 pandemic progressed and mutations arose from immune escape, we observed a coincident change in behavior in cell culture, including a reduction in variant plaque sizes as variants emerged over time. We noted that the ICU: hospitalization surrogates and plaque sizes decreased by about 10-fold and 17-fold with Omicron as compared to Delta variants, respectively (Figures 2A,B,F).

Vaccination efficacy, variants, and COVID-19 severity surrogates

COVID-19 vaccinations have prevented considerable morbidity and mortality worldwide. Having antibodies at the ready, whether through vaccination or natural infection has clear advantages at the individual level to clear the infection more readily. Average viral loads between vaccinated and unvaccinated individuals have not been shown to be significantly different in acute infections (Kissler et al., 2021). Studies on Omicron have suggested that it can evade most pre-existing neutralizing antibodies though some indicate that broadly neutralizing antibodies maintain their efficacy (Cameroni et al., 2022). Though the mutations of SARS-CoV-2 that affect receptor affinity and antibody sensitivity have been accurately and exhaustively studied, many of these mutations are compensatory so it is very difficult to ascribe these traits to any one mutation (Moulana et al., 2022).

We suggest that our COVID-19 disease severity surrogates can serve as indicators of population immunity. To determine whether the emergence of the variants affected disease severity we graphed Alberta vaccination rates (for the purpose of completeness) with ICU and death surrogate ratios (Figures 2C,D). From these data, we noted that the emergence of Delta and other SARS-CoV-2 variants in Alberta coincided with one and two dose vaccination rates of 60% and 57.3%, respectively (Figure 2E).

The Delta variant arrived after en-masse vaccination on day 501 and the first Omicron BA1 strain arrived on day 648 with BA2 and BA5 arriving on days 713 and 835, respectively. Vaccination coverage with 1 and 2 doses were 82% and 77.6% of the population, respectively, by August 29th 2022 (day 907). If we were to incorporate immunity from the natural infection itself, these numbers would be even higher.

10.3389/fmicb.2023.1289387

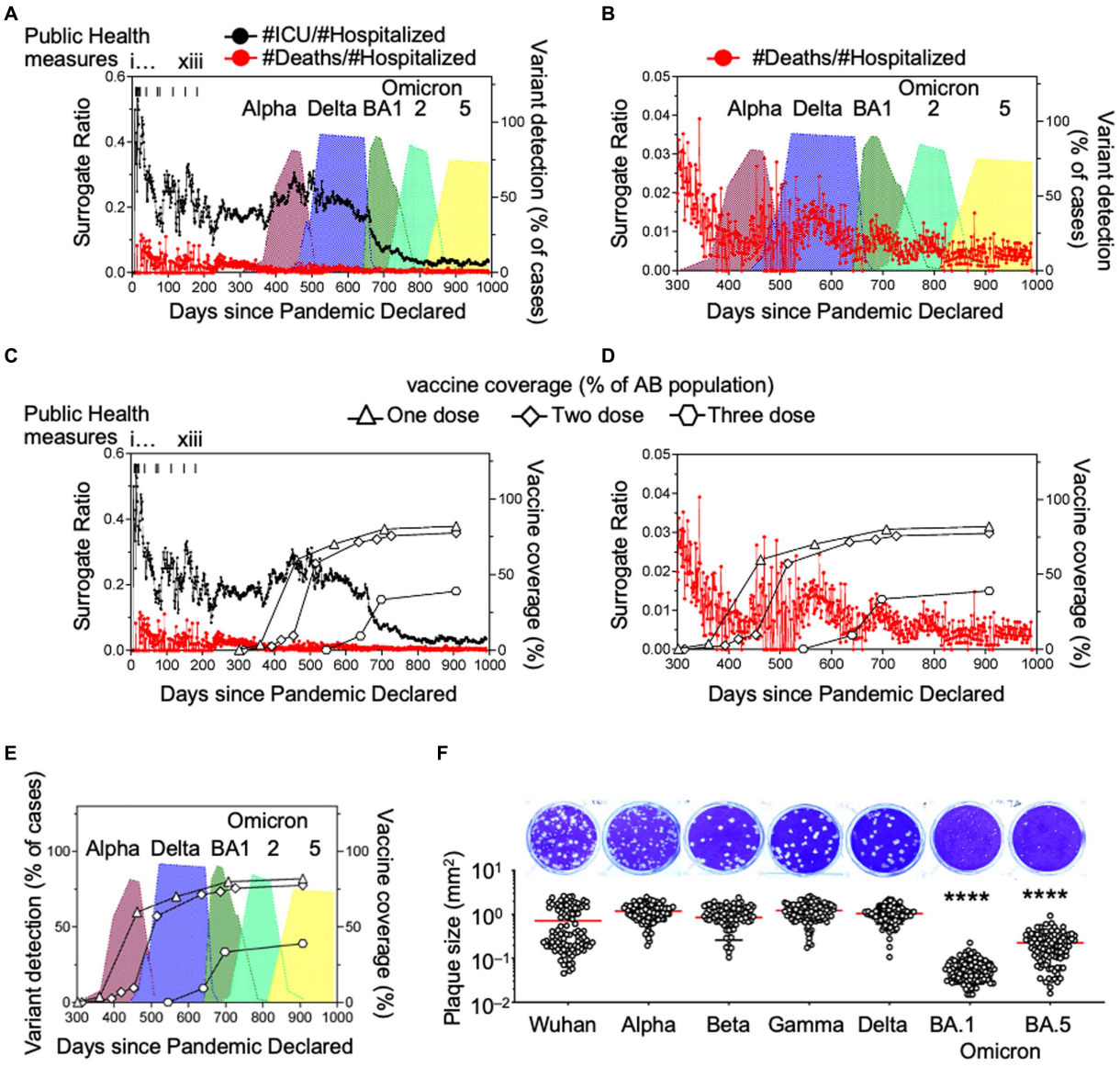

FIGURE 2
Ratios of daily hospitalizations to ICU admissions and daily hospitalizations to deaths as surrogate markers of COVID-19 disease severity and *in vitro* plaque sizes of variants. **(A,B)** Daily ICU admissions or deaths due to SARS-CoV-2 were divided by daily hospitalizations due to SARS-CoV-2 to illustrate the association of the death surrogate with variants Alpha, Gamma, Delta and Omicron introduction in Alberta, Canada and **(C–E)** association with vaccination rate with one, two, and three doses of SARS-CoV-2 vaccine. **(F)** SARS-CoV-2 isolates of each variant were plated on cells simultaneously with methylcellulose overlay, stained and imaged 3 days later. Diameters of the plaques were measured and reported as plaque area (mm^2). Significance was determined by one-way ANOVA with Tukey's test of significance. $^*p < 0.0001$.

Consistent with our observation, others observed a 91% decrease in mortality with Omicron infections compared to the Delta variant (Lewnard et al., 2022). Though our data does not consider immunity at the individual level, if there was immune escape by a mutation or set of mutations, we expect that ICU admissions and death surrogates would have increased after arrival of Delta and Omicron (Andrews et al., 2022).

Discussion

The emergence of seasonal coronaviruses from their pandemic predecessors suggests that a virus domestication process occurs. That is, mutations adapt the virus to infect humans and evade the host immune response at the cost of replicative fitness and pathogenicity. This adaptation process is evident in the emergence of SARS-CoV-2 VOCs. Mutations in SARS-CoV-2 have resulted in increased human ACE2 receptor affinity at the cost of the rate of replication (Moulana et al., 2022) and higher tropism for the upper respiratory tract (Hui et al., 2022) that may represent the domestication process toward a less severe but more common seasonal infection. Importantly, the reduced pathogenicity of SARS-CoV-2 could make long-term COVID-19 sequelae more insidious, harder to diagnose and therefore highlights the increased importance of vaccination.

As we report here, mutation and outgrowth of variants is a normal part of virus domestication and overall leads to less pathogenic

outcomes in the population over time. At this point we do not know if SARS-CoV-2 has become completely domesticated into a seasonal virus. However, we predict that this will likely be the point at which hospitalized cases occur primarily during Winter months, coinciding with other seasonal respiratory viruses. We outline these principles to help inform on highest probability outcomes during viral pandemics. In the face of virus mutation, these principles may help inform public policy.

Data availability statement

The data presented in this study were retrieved from the Government of Alberta website. The dataset contains no potential identifiers and is available in the Supplementary files.

Ethics statement

The studies involving humans were approved by University of Alberta Human Research Ethics Board 2. The studies were conducted in accordance with the local legislation and institutional requirements. Written informed consent for participation was not required from the participants or the participants' legal guardians/next of kin in accordance with the national legislation and institutional requirements.

Author contributions

RM: Conceptualization, Data curation, Formal analysis, Investigation, Methodology, Visualization, Writing – original draft, Writing – review & editing. Y-CL: Data curation, Methodology, Writing – review & editing. TC: Conceptualization, Investigation, Methodology, Writing – review & editing. RN: Conceptualization, Writing – review & editing. DE: Writing – review & editing. TH: Conceptualization, Writing – review & editing. VM-S: Conceptualization, Visualization, Writing – original draft, Writing – review & editing. DM: Conceptualization, Data curation, Funding acquisition, Investigation, Methodology, Supervision, Writing – original draft, Writing – review & editing.

Funding

The author(s) declare financial support was received for the research, authorship, and/or publication of this article. This study was supported by project grants from the Canadian Institutes of Health Research, and studentship funding for RM from Smiths Landing First Nation, NT (Grant No: CIHR: RN382934-418735 and CIHR: RN422598-443427).

Acknowledgments

The authors thank Dr. Graham Tipples (Scientific Director, Alberta Precision Laboratories Alberta Health Services) for reading the manuscript and providing useful criticism.

Conflict of interest

The authors declare that the research was conducted in the absence of any commercial or financial relationships that could be construed as a potential conflict of interest.

The author(s) declared that they were an editorial board member of Frontiers, at the time of submission. This had no impact on the peer review process and the final decision.

Publisher's note

Supplementary material

The Supplementary material for this article can be found online at: https://www.frontiersin.org/articles/10.3389/fmicb.2023.1289387/full#supplementary-material

References

Andrews, N., Stowe, J., Kirsebom, F., Toffa, S., Rickeard, T., Gallagher, E., et al. (2022). Covid-19 vaccine effectiveness against the Omicron (B.1.1.529) variant. *N. Engl. J. Med.* 386, 1532–1546. doi: 10.1056/NEJMoa2119451

Cameroni, E., Bowen, J. E., Rosen, L. E., Saliba, C., Zepeda, S. K., Culap, K., et al. (2022). Broadly neutralizing antibodies overcome SARS-CoV-2 Omicron antigenic shift. *Nature* 602, 664–670. doi: 10.1038/s41586-021-04386-2

Du, Y., Yan, R., Wu, X., Zhang, X., Chen, C., Jiang, D., et al. (2023). Global burden and trends of respiratory syncytial virus infection across different age groups from 1990 to 2019: a systematic analysis of the global burden of disease 2019 study. *Int. J. Infect. Dis.* 135, 70–76. doi: 10.1016/j.ijid.2023.08.008

Elawar, F., Griffiths, C. D., Zhu, D., Bilawchuk, L. M., Jensen, L. D., Forss, L., et al. (2017). A virological and phylogenetic analysis of the emergence of new clades of respiratory syncytial virus. *Sci. Rep.* 7:12232. doi: 10.1038/s41598-017-12001-6

Fajnzylber, J., Regan, J., Coxen, K., Corry, H., Wong, C., Rosenthal, A., et al. (2020). Massachusetts consortium for pathogen, SARS-CoV-2 viral load is associated with increased disease severity and mortality. *Nat. Commun.* 11:5493. doi: 10.1038/s41467-020-19057-5

Forrester, J. A., Weiser, T. G., and Forrester, J. D. (2018). An update on fatalities due to venomous and nonvenomous animals in the United States (2008–2015). *Wilderness Environ. Med.* 29, 36–44. doi: 10.1016/j.wem.2017.10.004

Hui, K. P. Y., Ho, J. C. W., Cheung, M. C., Ng, K. C., Ching, R. H. H., Lai, K. L., et al. (2022). SARS-CoV-2 Omicron variant replication in human bronchus and lung *ex vivo*. *Nature* 603, 715–720. doi: 10.1038/s41586-022-04479-6

Kissler, S. M., Fauver, J. R., Mack, C., Tai, C. G., Breban, M. I., Watkins, A. E., et al. (2021). Viral dynamics of SARS-CoV-2 variants in vaccinated and unvaccinated persons. *N. Engl. J. Med.* 385, 2489–2491. doi: 10.1056/NEJMc2102507

Lewnard, J. A., Hong, V. X., Patel, M. M., Kahn, R., Lipsitch, M., and Tartof, S. Y. (2022). Clinical outcomes associated with SARS-CoV-2 Omicron (B.1.1.529) variant and BA.1/BA.1.1 or BA.2 subvariant infection in Southern California. *Nat. Med.* 28, 1933–1943. doi: 10.1038/s41591-022-01887-z

Lin, Y. C., Malott, R. J., Ward, L., Kiplagat, L., Pabbaraju, K., Gill, K., et al. (2022). Detection and quantification of infectious severe acute respiratory coronavirus-2 in diverse clinical and environmental samples. *Sci. Rep.* 12:5418. doi: 10.1038/s41598-022-09218-5

Mandary, M. B., Masomian, M., Ong, S. K., and Poh, C. L. (2020). Characterization of plaque variants and the involvement of quasi-species in a population of EV-A71. *Viruses* 12:651. doi: 10.3390/v12060651

Mannar, D., Saville, J. W., Zhu, X., Srivastava, S. S., Berezuk, A. M., Tuttle, K. S., et al. (2022). SARS-CoV-2 Omicron variant: antibody evasion and cryo-EM structure of spike protein-ACE2 complex. *Science* 375, 760–764. doi: 10.1126/science.abn7760

Moulana, A., Dupic, T., Phillips, A. M., Chang, J., Nieves, S., Roffler, A. A., et al. (2022). Compensatory epistasis maintains ACE2 affinity in SARS-CoV-2 Omicron BA.1. *Nat. Commun.* 13:7011. doi: 10.1038/s41467-022-34506-z

Pabbaraju, K., Zelyas, N., Wong, A., Croxen, M. A., Lynch, T., Buss, E., et al. (2022). Evolving strategy for an evolving virus: development of real-time PCR assays for detecting all SARS-CoV-2 variants of concern. *J. Virol. Methods* 307:114553. doi: 10.1016/j.jviromet.2022.114553

Paget, J., Spreeuwenberg, P., Charu, V., Taylor, R. J., Iuliano, A. D., Bresee, J., et al. (2019). Global mortality associated with seasonal influenza epidemics: new burden estimates and predictors from the GLaMOR project. *J. Glob. Health* 9:020421. doi: 10.7189/jogh.09.020421

Stokes, W., Berenger, B. M., Scott, B., Szelewicki, J., Singh, T., Portnoy, D., et al. (2022). One swab fits all: performance of a rapid, antigen-based SARS-CoV-2 test using a nasal swab, nasopharyngeal swab for nasal collection, and RT-PCR confirmation from residual extraction buffer. *J. Appl. Lab. Med.* 7, 834–841. doi: 10.1093/jalm/jfac004

Vijgen, L., Keyaerts, E., Moes, E., Thoelen, I., Wollants, E., Lemey, P., et al. (2005). Complete genomic sequence of human coronavirus OC43: molecular clock analysis suggests a relatively recent zoonotic coronavirus transmission event. *J. Virol.* 79, 1595–1604. doi: 10.1128/JVI.79.3.1595-1604.2005

Worobey, M., Levy, J. I., Malpica Serrano, L., Crits-Christoph, A., Pekar, J. E., Goldstein, S. A., et al. (2022). The Huanan seafood wholesale market in Wuhan was the early epicenter of the COVID-19 pandemic. *Science* 377, 951–959. doi: 10.1126/science.abp8715

frontiers | Frontiers in Microbiology

TYPE Review
PUBLISHED 20 December 2023
DOI 10.3389/fmicb.2023.1282112

OPEN ACCESS

EDITED BY
Wei Wei,
First Affiliated Hospital of Jilin University, China

REVIEWED BY
Mohsan Ullah Goraya,
Huaqiao University, China
Verónica Martín García,
Immunology and Infectious Diseases Control Director (CISA-INIA-CSIC), Spain

*CORRESPONDENCE
Jingqiang Ren
✉ rjq207@163.com
Shubo Wen
✉ wen0516@126.com
Hewei Zhang
✉ 201818008@lypt.edu.cn

†These authors have contributed equally to this work

RECEIVED 23 August 2023
ACCEPTED 29 November 2023
PUBLISHED 20 December 2023

CITATION
Cheng H, Zhang H, Cai H, Liu M, Wen S and Ren J (2023) Molecular biology of canine parainfluenza virus V protein and its potential applications in tumor immunotherapy. *Front. Microbiol.* 14:1282112. doi: 10.3389/fmicb.2023.1282112

Molecular biology of canine parainfluenza virus V protein and its potential applications in tumor immunotherapy

Huai Cheng[1†], Hewei Zhang[2,3*†], Huanchang Cai[1], Min Liu[1], Shubo Wen[4*] and Jingqiang Ren[1,3*]

[1]Wenzhou Key Laboratory for Virology and Immunology, Institute of Virology, Wenzhou University, Wenzhou, China, [2]College of Food and Drugs, Luoyang Polytechnic, Luoyang, China, [3]Animal Diseases and Public Health Engineering Research Center of Henan Province, Luoyang, China, [4]Preventive Veterinary Laboratory, College of Animal Science and Technology, Inner Mongolia Minzu University, Tongliao, China

Canine parainfluenza virus (CPIV) is a zoonotic virus that is widely distributed and is the main pathogen causing canine infectious respiratory disease (CIRD), also known as "kennel cough," in dogs. The CPIV-V protein is the only nonstructural protein of the virus and plays an important role in multiple stages of the virus life cycle by inhibiting apoptosis, altering the host cell cycle and interfering with the interferon response. In addition, studies have shown that the V protein has potential applications in the field of immunotherapy in oncolytic virus therapy or self-amplifying RNA vaccines. In this review, the biosynthesis, structural characteristics and functions of the CPIV-V protein are reviewed with an emphasis on how it facilitates viral immune escape and its potential applications in the field of immunotherapy. Therefore, this review provides a scientific basis for research into the CPIV-V protein and its potential applications.

KEYWORDS

canine parainfluenza virus, V protein, molecular mechanism, structure, viral replication, immune escape, tumor immunotherapy

1 Introduction

Canine parainfluenza virus (CPIV) is a single-stranded negative RNA virus with non-segmented segments that belongs to the *Paramyxoviridae* family and *Rubulavirus* genus (Yang, 2022). When the virus was first isolated from rhesus monkey and cynomolgus monkey kidney cells, it was named as simian virus 5 (SV5) (Hull et al., 1956). However, because it is a canine pathogen that causes infectious tracheobronchitis and even secondary pneumonia and other diseases of the respiratory tract, resulting in 'kennel cough', it is also called CPIV (Yang, 2022). Notably, CPIV infection has been reported in cats, hamsters, guinea pigs, pigs and humans, but most of these infections do not lead to disease (Charoenkul et al., 2021; Ibrahim et al., 2022; Wang et al., 2023). In recent years, arthropod ticks have been mechanical carriers of CPIV (Yang et al., 2022). Since CPIV has been isolated from multiple species and because all its natural hosts have not been identified, CPIV was named parainfluenza virus 5 (PIV5) by the International Committee on Virus Classification in 2009 (Chen, 2018). In 2016, the virus was renamed mammalian orthorubulavirus 5 (Yang, 2022). Since CPIV is commonly used to

represent the virus causing kennel cough in veterinary medicine, it is referred to as CPIV in this paper.

The CPIV genome is 15,246 bp long, which is the smallest paramyxovirus genome (Wang et al., 2023), and follows the "rule of six", which means that efficient replication of most paramyxoviruses occurs only when the length of the viral genome is a multiple of six (Kolakofsky et al., 1998). From the 3′ end to the −5′ end, the CPIV genome sequentially encodes a nucleocapsid protein (NP), a phosphoprotein (P), a matrix protein (M), a small hydrophobic protein (SH), a hemagglutinin neuraminidase (HN) and a large polymerase protein (L). The V protein is a viral nonstructural protein produced by RNA editing of the P gene (Chen, 2018). Many studies have shown that the V protein not only controls viral RNA synthesis and promotes viral replication but is also extensively involved in the interaction between the virus and host, preventing apoptosis and inhibiting the interferon (IFN) response, immune-related cytokine expression, and other processes.

2 Molecular mechanism underlying CPIV-V protein effects

Overlapping genes, also known as overprinting genes, are defined as two or more genes that share a single DNA sequence. Due to the limits on viral genome length, overprinting is widespread in the viral genome (Wright et al., 2022), and differentiation between genes can occur in gene transcription or mRNA translation. At the transcriptional level, viruses typically employ a cotranscriptional RNA editing strategy by adding several nontemplated nucleotides into nascent RNA during the process of transcription (Rao et al., 2020). At the translation level, viruses undergo overprinting through noncanonical translation initiation and extension (Sorokin et al., 2021). The process mainly involves non-AUG codon initiation, ribosome frameshifting and other mechanisms (Douglas et al., 2021).

CPIV belongs to the paramyxovirus family, and many studies have shown that RNA editing occurs in the transcription of the paramyxovirus P gene, which produces V, W and other proteins that antagonize the host innate immune response (Kolakofsky, 2016). Currently, two models have been established for this editing process: the P and V models (Douglas et al., 2021). The former involves the P protein encoded by the original gene sequence, while V, W and other proteins are translated after the insertion of one or two guanylate acids (G) into the conserved region of the transcribed mRNA of the P gene. In the V model, the V protein is encoded by the original gene sequence, the mRNA encoding the W protein acquires a G that is inserted during transcription, and P carries two G inserted at the same location. CPIV is a V model virus. During V gene transcription, two unpaired G are added at the 551th nucleotide of its mRNA sequence, and thus, the open read frame (ORF) is changed to generate P mRNA (Figure 1B), and the number of V gene transcripts is slightly higher than that of the P gene (Thomas et al., 1988; Wang et al., 2023). Other viruses in the same genus, such as human parainfluenza virus type 2 (HPIV2) (Ohta et al., 2021), belong to the V model. However, the well-characterized Newcastle disease virus (NDV) (Jadhav et al., 2020) and measles virus (MeV) (Nagano et al., 2020) are P model viruses. Although the mechanism underlying V protein biosynthesis varies among paramyxoviruses, all V proteins share an N-terminal domain (NTD) with the P protein, and the C-terminal domain (CTD) is highly conserved among paramyxoviruses. Notably, it was originally found that the V protein is not necessary for viral replication and was naturally called an accessory protein (Peluso et al., 1977); however, in 1995, Paterson confirmed that the V protein is also a structural viral protein and a component of the nucleocapsid core through polypeptide analysis and immunoelectron microscopy (Paterson et al., 1995), revealing the potential functions of the V protein in the viral cycle.

3 Structure of the V protein

The V protein of CPIV contains 222 amino acids, including the NTD, which shares 164 amino acid residues with the P protein, and a unique cysteine-rich CTD (Figure 1A) (Wang et al., 2023). The CTD has a conserved motif containing seven cysteines, which can bind two zinc atoms to form a zinc finger structure (Figure 1C) (Paterson et al., 1995). Many studies have shown that the C-terminal zinc finger domain of the V protein is crucial for its normal function. Initial studies found that it can inhibit the transcription of viral RNA (Yang et al., 2015). Moreover, it can inhibit the apoptosis of host cells (Sun et al., 2004) and contributes to the regulation of viral replication (He et al., 2002). In addition, the zinc finger structure can interact with damage-specific DNA binding protein 1 (DDB1), causing a conformational change in DDB1, which enables binding to the signal transducer and activator of transcription 2 (STAT2) and ultimately promotes the ubiquitination of the signal transducer and activator of transcription 1 (STAT1) (Precious et al., 2005), thereby negatively regulating the IFN signaling pathway. Notably, a conserved Trp motif (W-X3-W-X9-W) lies upstream of the zinc finger domain, and it is also involved in the degradation of the STAT1 and inhibition of the IFN signaling pathway (Nishio et al., 2005). In addition, some studies have revealed that the CTD of the V protein is an oligomerization domain that can mediate the oligomerization of homologous or heterologous V proteins, forming V protein-dependent degradation complexes (VDC) and then rapidly degrading the STAT1 (Ulane et al., 2005).

The NTD of the V protein is not specific; it is similar to that of the P protein, which did not initially attract attention from scientists. However, with the deepening of research into the V protein, scientists have found that its NTD plays an indispensable role in its function. Studies have revealed that there are several key amino acids in the NTD of the V protein that are involved in the binding of the V protein to RNA (K74, K76, K77, R79, K81) (Lin et al., 1997), regulation of viral RNA transcription (L16, I17) (Yang et al., 2015), degradation of STAT1 (Y26, L50, L102) (Chatziandreou et al., 2002) (Table 1).

4 Current progress on the regulation of viral growth and replication by the V protein

4.1 The role of the V protein in the viral life cycle

Studies have shown that in CPIV-infected cells, the V protein is distributed in both the cytoplasm and nucleus (Precious et al., 1995), indicating that the V protein may be a multifunctional viral protein and participate in multiple processes of the viral life cycle. Lin et al. used the SV5 minigenome system to show that the V protein inhibited

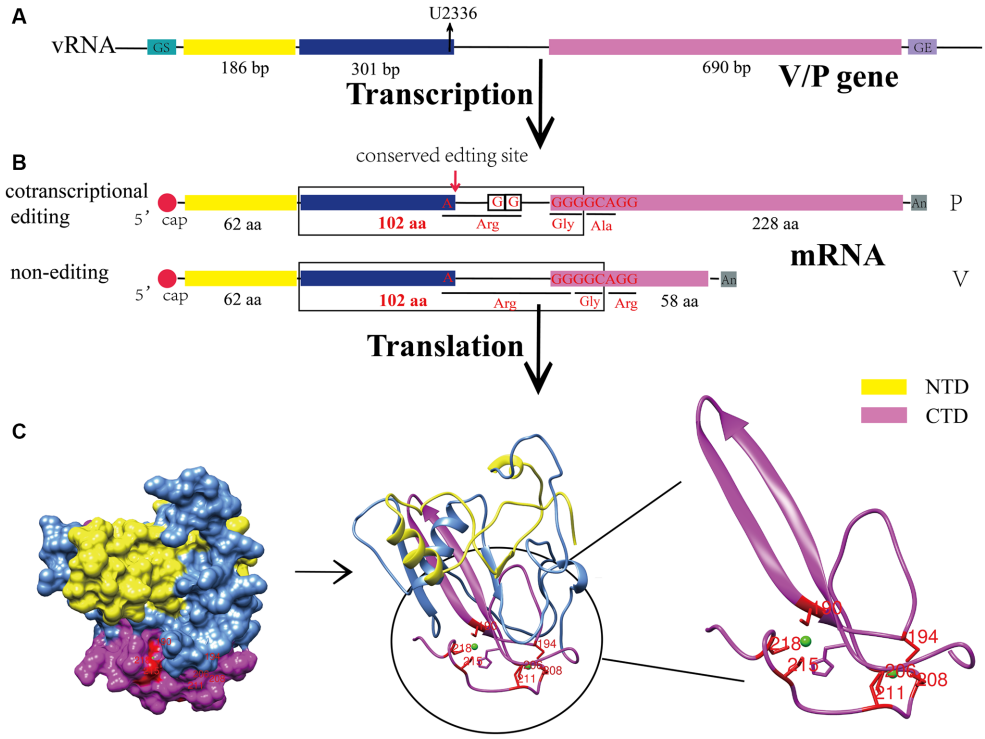

FIGURE 1
Biosynthesis process and structural characteristics of the CPIV-V protein. **(A)** Genomic characteristics of the V/P gene. U2336 is the conserved editing site in the viral genome. **(B)** V/P mRNA is produced by different modes of transcription. **(C)** Sphere model, cartoon representation and C-terminal zinc finger domain of the CPIV-V protein. All protein structures were created on UCSF Chimera. bp, base pairs; aa, amino acid; vRNA, viral RNA; GS, gene start; GE, gene end; NTD, N-terminal domain; CTD, C-terminal domain.

TABLE 1 **Contributions of key amino acid residues in NTD to the functions of V protein.**

Key amino acid residues in NTD	Functions	References
K74, K76, K77, R79, K81	Assisting V protein bind to RNA	Lin et al. (1997)
L16, I17	Regulating viral RNA transcription	Yang et al. (2015)
Y26, L50, L102	Participating in the degradation of STAT1	Chatziandreou et al. (2002)

CPIV-RNA replication and transcription (Lin et al., 2005). Sun et al. found that the V protein interacted with the Akt kinase in host cells and promoted virus replication by phosphorylating the P protein (Sun et al., 2008). In addition, the recombinant SV5 virus in which the V protein does not harbor a CTD replicated slowly in infection-susceptible cells and became a pseudovirus after multiple passages, indicating the importance of the V protein for CPIV replication (He et al., 2002).

4.2 Interactions between the V protein and other CPIV viral proteins

Generally, the structural and nonstructural proteins of a virus cooperate to facilitate viral replication and spread throughout the viral life cycle. Studies have shown that the V protein interacts with the NP protein to ensure the solubility of the NP protein before it binds to the viral genome, but the P protein inhibits the binding of the V protein to the NP protein, indicating that the binding site may lie in the NTD shared with the P protein (Precious et al., 1995). It was also revealed that the mutation of three amino acids in the N-terminus of the V protein led to the aggregation of the NP protein and formation of inclusion bodies and reduced the expression of the HN protein (Chatziandreou et al., 2002). In addition, the NTD of the V protein regulates viral RNA transcription by regulating the NP-P interaction, and amino acid residue V120 in the V protein is a key site in this interaction (Yang et al., 2015). In addition, the V protein binds to the L protein and contributes to viral genome replication regulation (Nishio et al., 2008).

5 Research progress into the interaction between the V protein and a host

5.1 The V protein promotes viral replication and growth by delaying host cell division, inhibiting cell apoptosis, promoting actin synthesis, and antagonizing tetherin

After infecting cells, viruses generally hijack host cells and drive preferential replication of the virus. In CPIV-infected cells, the V

protein delays the cell cycle by interfering with the phosphorylation and dephosphorylation of retinoblastoma protein (RB), promotes the transport of virus envelope glycoproteins HN and F to the cell membrane, and then promotes the assembly and budding of the virus (Lin and Lamb, 2000). In addition, the V protein elevates the induction of endoplasmic reticulum (ER) stress and inhibits the activation of cysteine aspartate-specific protease 12 (caspase 12) activity, thereby blocking cell apoptosis (Sun et al., 2004). Wansley et al. found that the recombinant SV5 virus with a mutation in the amino terminus of the P/V gene (rSV5-P/V-CPI$^-$) caused the apoptosis of infected cells and activated the host IFN signaling pathway. The V protein in a coinfected wild-type virus (rSV5-WT) functions as a trans-acting factor to block the apoptosis and IFN signaling pathways induced by rSV5-P/V-CPI$^-$ (Wansley et al., 2003). In addition to affecting the cell cycle and inhibiting apoptosis, the V protein regulates the actin-binding protein Profilin2 by binding to Rhoa (Ras homolog gene family member A) and promotes the elongation of F-actin, thereby promoting the growth and replication of the virus (Figure 2 left) (Ohta et al., 2020).

Tetherin, also known as bone marrow stromal cell antigen 2 (BST2) or CD317, is a Type II transmembrane glycoprotein (Berry et al., 2018). Studies have shown that Tetherin is an antiviral factor that is activated and anchored to the cell membrane by type I interferon (IFN-I) and type II interferon (IFN-II) (Foster et al., 2017). When the virus buds, the glycol phosphatidyl-inositol (GPI) anchor at the C-terminus of Tetherin binds to the virus, anchoring it to the cell membrane and initiating endocytosis, promoting the transport of the virus to lysosomes for degradation. Then, pattern recognition receptors (PRRs) recognize the virus in the inner compartment and activate downstream signaling pathways to induce IFN-I responses (Zhao et al., 2022). The V protein of CPIV binds to and antagonizes tetherin, thereby promoting viral budding and spread (Figure 2 left) (Ohta et al., 2017).

5.2 V protein maintains efficient viral protein synthesis by inhibiting PKR activation

During viral infection, most host cells recognize and bind the double-stranded RNA produced during viral replication through protein kinase R (PKR), which is then activated through homodimerization and autophosphorylation. Ultimately, it phosphorylates eIF-2α and inhibits protein translation (Chukwurah et al., 2021). For CPIV, the V protein limits the activation of PKR by reducing the production of aberrant viral mRNA and double-stranded viral RNA (Figure 2 left), thereby maintaining the protein translation process of the virus and host cells (Gainey et al., 2008a).

5.3 Interactions between the V protein and host immune system

5.3.1 The V protein facilitates CPIV escape from the host innate immune response

The host innate immune response refers to the first line of defense against the invasion of pathogenic microorganisms in hosts, including humans and animals. They mainly recognize the pathogen-associated molecular patterns (PAMPs) of invading pathogens through PRRs, produce IFNs and a series of cytokines to resist invasive viruses, and ultimately initiate and participate in the adaptive immune response (Kikkert, 2020). Many studies have shown that the CPIV-V protein inhibits the host innate immune response mainly by inhibiting the production of IFN and blocking the IFN antiviral signaling pathway (Figure 2) (He et al., 2002; Young and Parks, 2003; Sun et al., 2004; Precious et al., 2005; Douglas et al., 2021).

After viral infection, the PRRs melanoma differentiation-associated gene 5 (MDA5), retinoic acid-inducible gene-1 (RIG-1) and laboratory of genetics and physiology 2 (LGP2) are activated in cells and identify viral dsRNA or double 5′ capped-pppRNA structures (Negishi et al., 2018). They then activate the downstream virus-induced signaling adaptor (VISA)/mitochondrial antiviral signaling protein (MAVS)/interferon β (IFN-β) promoter stimulator 1 (IPS-1) complex, which mediates two distinct signaling pathways to defend against viral infection (Figure 2 left) (Vignuzzi and López, 2019; Iuliano et al., 2021; Zheng et al., 2023). One pathway recruits the IKK-related TANK-binding kinase 1 (TBK1) by interacting with tumor necrosis factor receptor-associated factor 3 (TRAF3) and inhibitor of nuclear factor κB kinase-ε (IKKε); these factors form a complex on the mitochondria, which activates the IFN regulatory factor 3 (IRF3) by phosphorylating it. The second pathway recruits the tumor necrosis factor receptor-associated factor 6 (TRAF6) and nuclear factor-κb (NF-κB) inhibitor IKK complex to phosphorylate the inhibitor of κB (IκB), after which phosphorylated IκB is recognized by the β-Transducin repeats-containing protein (β-TrCP), the substrate recognition subunit of the SCF (SKP1, CUL1, and F-box protein)-type E3 ubiquitin ligase complex and is then cleaved by the proteasome to release NF-κB. Finally, activated IRF3 and NF-κB are transported to the nucleus to promote the expression of IFNs and proinflammatory cytokines (Hou, 2021; Ke, 2023). After secretion, IFN binds to specific receptors on the cell surface to activate the intracellular Janus kinase/signal transducer and activator of transcription (JAK/STAT) signaling pathway, which ultimately leads to the expression of hundreds of interferon-stimulated genes (ISGs), activating host immune responses and inflammation (Figure 2 right) (Ke, 2023).

However, in CPIV-infected cells, V proteins can inhibit upstream signaling pathways in several ways to antagonize the host antiviral response and promote viral replication. First, the CTD of the V protein can bind to the minimal V protein binding region (MVBR) of MDA5 and inhibit its ATP hydrolysis activity, thereby inhibiting the normal folding and aggregation of MDA5 to form a filamentous structure, which makes it unable to activate the downstream VISA/MAVS/IPS-1 complex (Motz et al., 2013; Mandhana et al., 2018). In addition, the V protein interacts with LGP2 in the same manner, inhibiting the potentiating effect of LGP2 on MDA5 signaling (Rodriguez and Horvath, 2014). Second, the V protein can be phosphorylated as an alternative substrate for IKKε/TBK1, thereby inhibiting IKKε/TBK1 activation of IRF3 (Lu et al., 2008). These two effects eventually lead to a decrease in the synthesis of IFN-I. Notably, an article published in 2018 reported that the V protein interacts with RIG-1 and its regulatory protein tripartite motif-containing 25 (TRIM25) and inhibits RIG-1 downstream signaling pathways by inhibiting TRIM25 ubiquitination of RIG-1 (Sánchez-Aparicio et al., 2018). However, previous studies have suggested that the V protein does not interact with RIG-1 (Childs et al., 2007); these differences may have been due to the different research methods used in the two

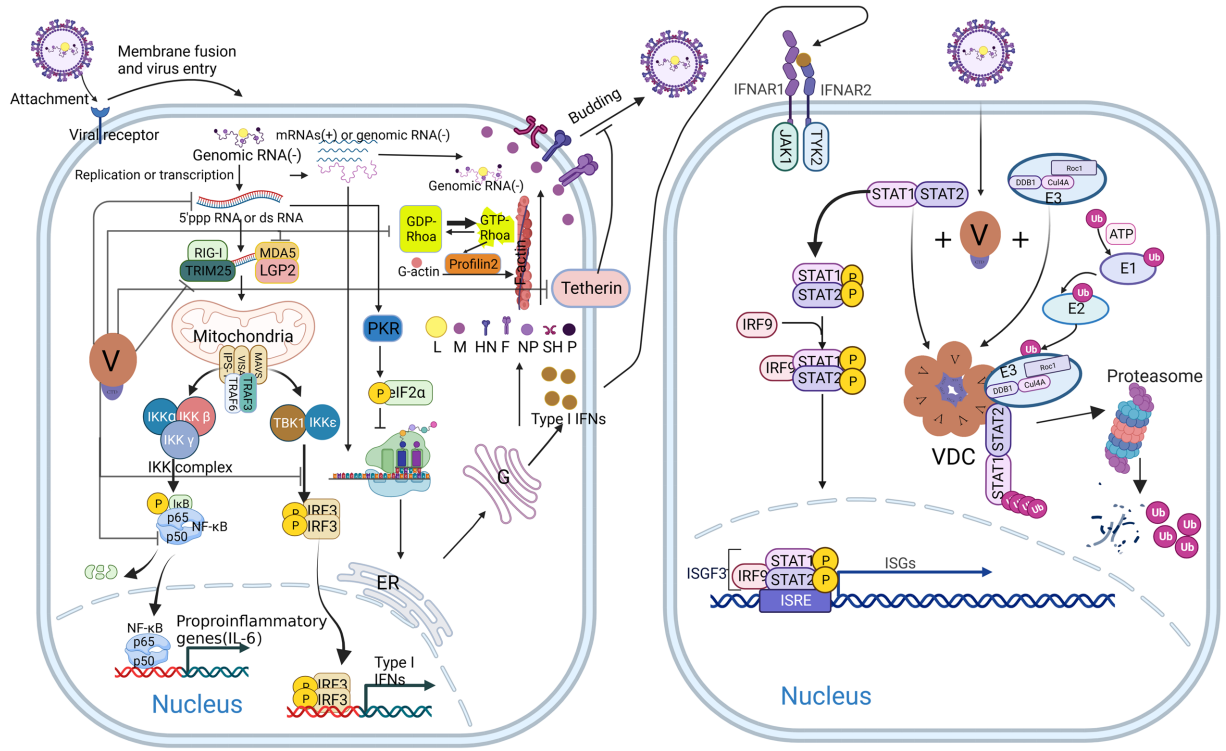

FIGURE 2
Host antiviral response and multiple antagonistic effects of V protein after CPIV infection. V protein inhibits type I IFN (IFN I) production by antagonizing TRIM25, MDA5, LGP2, TBK1/IKKε, and NFκB and promotes viral replication, budding, and spread by reducing the production of dsRNA, inhibiting tetherin, and binding Rhoa (left). V protein inhibits the IFN response by forming VDC to degrade STAT1 (right).

studies. The interaction between the V protein and RIG-1 needs to be confirmed by further studies. In addition, the V protein interacts with the DDB1 (Lin et al., 1998) and STAT2 (Parisien et al., 2002; Omagari et al., 2021) and then forms a globular VDC through its C-terminal oligomerization domain; DDB1 then interacts with Rbx1 (a small RING finger protein) and Cullin 4a (Cul4a) in the E3 ubiquitin ligase complex to ubiquitinate the STAT2 and ultimately inhibit JAK–STAT signaling (Ulane et al., 2005). Notably, the conserved cysteine-rich domain in the C-terminus of the V protein plays a decisive role in these processes. The loss of this domain leads to a large amount of IFN-β production and recovery of the IFN signaling pathway, resulting in extensive cytopathic effects (CPEs) (He et al., 2002).

In addition to inhibiting the synthesis of IFN-β and blocking the IFN signaling pathway, the V protein also inhibits the activation of the NF-κB family p50 protein in a virus-specific manner (Figure 2 left), thereby inhibiting its transcriptional activation of interleukin-6 (IL-6) (Lin et al., 2007). In contrast to HPIV2, the CPIV-V protein inhibits the secretion of the proinflammatory cytokines interleukin-8 (IL-8) and macrophage chemoattractant protein-1 (MCP-1) (Young and Parks, 2003) in an NF-κB-independent manner. However, CPIV-V exerted no significant effect on the secretion of the CC chemokine RANTES (Young et al., 2006). The V protein is involved in regulating the secretion of proinflammatory cytokines, chemokines and other cytokines.

Recent studies have shown that virus-mediated autophagy activation negatively regulates the host innate immune response mediated by PRRs such as RIG-1 and MDA5, thereby promoting virus replication (Wu et al., 2021; Ke, 2023). In addition, in a study of Sendai virus (SeV), autophagy-related receptor coiled-coil domain containing protein 50 (CCDC50) inhibited the recruitment of downstream MAVS proteins by RIG-1/MDA5 and targeted them for autophagic degradation. Moreover, CCDC50 inhibited the IFR3/7-mediated IFN response and NF-KB-mediated inflammatory response (Hou et al., 2021). It can be concluded from these studies that autophagy plays an important role in the virus-induced host innate immune response, similar to the role of V protein. However, there is no report on the interaction between the V protein and autophagy, and further exploration and research are needed.

5.3.2 The V protein assists CPIV in escaping the host adaptive immune response

Dendritic cells (DCs) are key hub cells connecting host innate immunity and adaptive immunity. Immature DCs sense a virus through PRRs, including RIG-1 and MDA5, and then initiate the innate immune response, which promotes the expression of IFN-I, costimulatory molecules CD80 and CD86 and cytokines on the surface of DC cells and contributes to DC maturation. Mature DCs then migrate to lymph nodes, promote the maturation of naive T cells, and eventually activate the host adaptive immune response (Jr and Dl, 2021). Previous research results showed that recombinant CPIV (rCPIV) generated by V gene mutation promoted DC maturation, but wild-type CPIV did not. Only high-MOI (50 pfu/cell) rCPIV-infected DCs underwent DC maturation (CD80, CD86 expression), and

infection at a low MOI (10 pfu/cell) caused only high expression of CD86 and partial maturation of DCs (Pejawar et al., 2005; Parks and Alexander-Miller, 2013). Therefore, the V protein plays an important role in promoting the maturation of DCs and further inhibiting host adaptive immunity.

In addition, CPIV (CPI^-) generated by three amino acid mutations in the N-terminus of the V protein was less susceptible to killing by killer T cells or antibody-mediated killing than wild-type virus (CPI^+), which allowed CPI^- to establish long-lasting infection in a host. This study proposed a model of virus persistence: during the interaction between CPIV and the host, the virus selectively evolved into a CPI^+/CPI^- virus via V gene mutation on the basis of the host adaptive immunity status to establish persistent infection (Chatziandreou et al., 2002). The V gene clearly plays an important role in virus evolution and persistent infection.

5.3.3 Could V protein antagonize the production of viral DVG?

Virus-defective genomes (DVGs) are products of the viral genome caused by mutation, modification and truncation during replication. In the absence of standard virus coinfection, DVGS cannot replicate normally in cells (Vignuzzi and López, 2019). There are two main forms of DVGs in RNA viruses: deletion DVGs and snapback or copyback DVGs (Manzoni and López, 2018). The former refers to a mutation in which the middle sequence of a virus is deleted but the two ends of the viral genome are retained, and the latter refers to a mutation in which the viral genome carries a viral 5′ structure and a loop. Snapback or copy-back DVGs are more common in RNA viruses than in DNA viruses (Genoyer and López, 2019). In infected cells, DVGs promote the establishment of persistent viral infection, induce the production of defective virions, and activate the host innate immune response (Manzoni and López, 2018; Ziegler and Botten, 2020). In paramyxoviruses, the C protein of MeV, Sendai virus (SeV) and human parainfluenza virus type 1 (HPIV1) limit the production of DVGs, but the accumulation of DVGs in cells can inhibit the expression of C protein (Genoyer and López, 2019), suggesting that there may be multiple modes of mutual regulation between paramyxovirus C protein and viral DVGs. As mentioned above, the V protein of CPIV inhibits host innate immune responses through multiple pathways; however, consistent with the paramyxovirus described above, CPIV generates snapback DVGs during replication and induces host innate immune responses during replication (Wignall-Fleming et al., 2020). However, similar to the C protein, the V protein is a product of RNA editing of the P gene (Siering et al., 2022). Whether the V protein inhibits the production of viral DVGs is unclear, and this possibility and the intrinsic mechanism need to be further studied.

6 V protein application to tumor immunotherapy

6.1 Application of P/V-CPI- to oncolytic virotherapy

Oncolytic viruses (OVs) are new types of tumor immunotherapies that replicate and lyse tumor cells through different regulatory mechanisms without affecting normal cell growth (Lin et al., 2023). Most oncolytic viruses being studied (adenoviruses, poxviruses, herpesviruses, reovirus and coxsackieviruses) are genetically edited to increase their tropism and reduce their virulence in non-tumorigenic host cells (Raja et al., 2018; Huang et al., 2023; Jiang et al., 2023). In recent years, oncolytic viruses among paramyxoviruses have been extensively studied. Through attachment protein on the surface of the virus, a virus specifically infects and kills tumor cells. For example, the recombinant measles virus that specifically binds to Nectin4 but not to the original receptor SLAM (rMV-SLAMblind). rMV-SLAMblind specifically infects and lyses tumor cells that express high levels of Nectin4 (Matveeva and Shabalina, 2020; Moritoh et al., 2023).

6.1.1 Advantages of P/V-CPI- as an OV

Many studies have focused on the application of CPIV to oncolytic therapy. Initially, Wansley and Parks discovered that naturally occurring mutations in the P/V overlapping gene region could convert CPIV into a cytopathic virus (P/V-CPI-), which induced IFN production and apoptosis (Wansley and Parks, 2002). Thus, the oncolytic CPIV virus used in subsequent studies was P/V-CPI-. P/V-CPI- also induced proinflammatory cytokines and caused severe CPE in infected cells, which eventually underwent apoptosis (Wansley and Parks, 2002; Dillon et al., 2006). Currently, numerous studies have shown that P/V-CPI- increases the killing effect on tumor cells by promoting the production of double-stranded RNA, activating caspase-dependent death pathways, interfering with the DNA damage repair response in tumor cells, abrogating PKR-mediated protein synthesis, and forming extensive syncytia, etc., (Wansley et al., 2003, 2005; Dillon et al., 2006; Gainey et al., 2008a; Kedarinath and Parks, 2022).

A concerning danger of oncolytic viruses for cancer therapy is the specificity of the virus in targeting tumor cells. Surprisingly, P/V-CPI- could induce apoptosis in most human tumor cell lines currently studied in the laboratory but did not affect the growth of normal cells (Wansley et al., 2005). Meanwhile, P/V-CPI-has two major advantages as an OV. First, P/V-CPI- could induce the production of IFNs but maintain normal IFN signaling pathways, suggesting that IFN responses within normal cells limited viral growth and spread on normal cells rather than tumor cells, in which case IFN responses are dysfunctional (Capraro et al., 2008). Second is an advantage of the genome itself: CPIV is a cytoplasmic-replicating negative sense RNA virus, whose life cycles lack a DNA stage, thus posing a minimal risk of recombining the host genome (Wang et al., 2023). Moreover, there is no pathogenic gene in the CPIV genome, making it safe for infection and treatment. Correspondingly, *in vivo* experiments showed that the virus-infected mice did not have obvious pathological characteristics and could significantly reduce the tumor burden of mice (Capraro et al., 2008; Gainey et al., 2008b), indicating that the recombinant virus has high safety for mammals and has potential for clinical transformation.

6.1.2 Preclinical study of P/V-CPI- as an OV

Researchers from Griffith D. Park's team have investigated the viability and mechanisms of rCPIV as an oncolytic virus (Table 2). Preliminary studies found that P/V-CPI- was oncolytic and reduced tumor burden in mice. Further research disclosed that P/V-CPI- activated the caspase apoptosis pathway and formed syncytia to kill tumors; surprisingly, it is safe for normal or benign human cells (Capraro et al., 2008; Gainey et al., 2008b; Kedarinath and Parks, 2022). To improve its killing ability, a mutation (G3A) was introduced

TABLE 2 The application of P/V-CPI- in the treatment of different tumors.

Tumor types	Combined therapeutic agents	Molecular mechanisms of killing tumors	References
Human lung cancer	Membrane-anchored Fc chimera (NA-Fc) and adoptive PM21-NK cells	Increasing release of TNF-α and IFN-γ cytokines from NK cells and enhancing CD16-Fc interactions, thus increasing PM21-NK cell killing ability	Varudkar et al. (2023)
	Adoptive PM21-NK cells	1. Infected cells: NK cells receptors recognize viral glycoprotein to activate NK cells 2. Uninfected cells: Those tumor cells IFN-I and IFN-III receptors bind IFN secreted from infected cells to activate NK cells	Varudkar et al. (2021)
	Histone deacetylase inhibitors (scriptaid)	1. Increasing in cell killing through increasing in caspase-9 and − 3/7 activity 2. Enhancing spread of the P/V-CPI- by reducing nuclear localization of IRF-3 and then downregulating IFN-β induction	Fox and Parks (2019)
Human prostate cancer	Hyperfusogenic F Protein	Increasing cell-killing by enhancing cancer cell–cell fusion	Gainey et al. (2008b)
Neuroblastoma	DNA methyltransferase inhibitor (5-azacytidine)	Enhanced cancer killing by inducing dsRNA production and activating downstream signaling (hypothesis)	Kedarinath et al. (2023)
Human laryngeal cancer	DNA-damaging agents (cisplatin)	Inhibiting DDB1 protein entry into the nucleus, leading to DNA damage-induced death	Fox and Parks (2018)

at the third position of the F protein fusion peptide, resulting in increased fusogenicity and tumor killing through necrosis and inflammatory responses. Notably, G3A mutation did not affect viral susceptibility to IFNs. However, F protein-induced cell death may lead to a strong immune response, which could affect the growth and dissemination of lysogenic viruses (Gainey et al., 2008b).

DNA-damaging drugs, such as cisplatin, are general chemotherapeutic drugs for tumor treatment. However, some tumors develop strong drug resistance during clinical treatment, which is mostly related to the gradual enhancement of the DNA repair ability in tumor cells, leading to tumor recurrence in patients (Agarwal and Kaye, 2003; Eskander et al., 2023). It is crucial to address this drug resistance to improve the efficacy of chemotherapy. Therapies combining P/V-CPI- with DNA-damaging drugs showed that virus infection inhibited DDB1 nuclear translocation, altered DNA repair pathways, and increased apoptosis, thus inducing the death of tumor cells (Fox and Parks, 2018). This finding is a promising new strategy for treating drug-resistant tumors. The combination of P/V-CPI- with histone deacetylase (HDAC) inhibitors and DNA methyltransferase inhibitors (DNMTi) also improved its killing efficacy and expanded its applicability (Fox and Parks, 2019; Kedarinath et al., 2023).

It has been established that utilizing 3D spheroid cultured tumor cells is a more effective research model for investigating cancer therapies when compared to conventional 2D cultured cells (Jensen and Teng, 2020). In one study using 3D spheroid lung cancer cells, researchers discovered that combining P/V-CPI- with PM21-NK adoptive therapies effectively killed cells of 3D spheroid tumors through activated NK cells. Notably, NK cells killed cells within spheroids that were not infected by oncolytic viruses. This was achieved through IFN-I/IFN-III released by surface cells infected with P/V-CPI- (Varudkar et al., 2021). Additionally, delivering a novel membrane-anchored Fc chimera (NA-Fc) to P/V-CPI-infected tumor cells enhanced the killing effect of adoptive NK cell killing through antibody-dependent cellular cytotoxicity (ADCC) (Varudkar et al., 2023). In conclusion, the oncolytic effect and killing mechanism of P/V-CPI- have been investigated in various tumor cells, such as lung and prostate cancers. Nevertheless, additional experiments must be carried out to verify the safety and half-life period of the treatment for future clinical studies.

6.1.3 Existing problems and prospects of P/V-CPI- as an OV

As studies on CPIV have progressed, researchers have identified potential risks and problems with P/V-CPI- as an OV. While acute infection can cause apoptosis in tumor cells, some cells survive and transition to persistent infection (PI) cells over time (Gainey et al., 2008b). This poses a risk of tumor escape and recurrence. Additionally, PI tumor cells become resistant to the killing effects of adoptive NK cells, reducing the efficacy of adoptive NK cell therapy (Varudkar et al., 2023). To address these risks, it is suggested to combine chemotherapeutic drugs targeting DNA damage or delivery of NA-Fc to P/V-CPI-infected tumor cells with oncolytic viruses to enhance their efficiency (Fox and Parks, 2018; Varudkar et al., 2023). Further research is needed to understand the mechanisms by which viruses establish PI, monitor the occurrence of PI cells in real time, and optimize viral vectors to reduce the likelihood of PI cells appearing. Adoptive cell transfer (ACT) therapies are procedures that transfer qualified and active antitumor lymphocytes (T/NK cells), which are cultured *in vitro*, to patients for tumor regression. These therapies include chimeric antigen receptor T/NK cell (CAR-T/NK) therapy, T-cell receptor-engineered T-cell (TCR-T) therapy, and tumor-infiltrating lymphocyte (TIL) therapy (Lin et al., 2023). Saul J. Priceman discovered that recombinant oncolytic poxviruses containing truncated CD19 (CD19t), a tumor-specific antigen, can promote the labeling of tumor cells by viral infection, leading to improved targeting of CAR-T cells. Furthermore, the clearance of targeted tumor cells by CAR-T cells contributes to virus release, leading to the establishment of PI in these cells, which increases the duration of OV (Park et al., 2020). It is evident that the viral vector composition can be optimized, leading to lysis and death of PI tumor

cells. Meanwhile, in combination with ACT therapies, PI can also become a good weapon for tumor killing.

Safety is an important consideration for all new therapies. As previously discussed, P/V-CPI- was first employed as an OV because viral growth and spread in normal cells were considerably hindered by the IFN response. It is important to test the integrity of IFN synthesis and downstream signaling pathways in tumor cells before deploying P/V-CPI- for tumor therapy. Gainey et al. improved the oncolytic effect of P/V-CPI- by introducing a hyperfusogenic F Protein to P/V-CPI- through G3A mutation. Additionally, her findings show that the mutation did not affect viral IFN sensitivity (Gainey et al., 2008b). This also implies that, during the optimization of OV vectors, it is important to test their IFN sensitivity. Even though P/V-CPI- does not have a oncolytic effect on normal or benign human cells, however, due to its extensive host tropism, highly mutable RNA viral genome, and capacity for recombination with wild-type strains make it necessary to implement several safety measures for its enhancement. These measures encompass strict strain screening, virus mutant detection, and genetic recombination detection, etc.

In conclusion, while numerous studies have shown the potential of P/V-CPI as an OV, they have only been conducted *in vitro* at the cell level. Therefore, more comprehensive research is needed to determine the oncolytic impact of P/V-CPI on various types of tumors *in vivo* and the immune response changes initiated by P/V-CPI, as well as the organism's long-term well-being. In addition, oncolytic paramyxoviruses (Measles virus, Newcastle disease virus) currently being tested in clinical trials have implemented multiple strategies to enhance their efficacy and safety, such as fusing single-chain antibodies targeting tumor-specific antigens to enhance viral targeting (Yaiw et al., 2011), inserting exogenous cytokine genes to trigger immunogenic cell death (ICD) in tumor cells (Huang et al., 2020), and constructing viral vectors expressing bispecific T-cell engagers (BiTE) or trispecific T cells (TriTE) that activate T-cell immunity directly, which bypass the antigen-presenting cells (APCs) antigen presentation process and improve the killing ability (Freedman et al., 2017; Lin et al., 2023), and combination therapy with immune checkpoint inhibitors (ICIs) (Zamarin et al., 2014). Together, continuously optimizing the composition of P/V-CPI viral vectors, along with attempting to combine them with different therapies, will enhance the targeting selectivity, application prospects, and oncolytic ability of P/V-CPI-. Meanwhile, experiments are needed to confirm its safe dosage and duration for the next step of possible clinical studies.

6.2 Application of the V protein in the self-amplifying RNA vaccine

The development of messenger RNA (mRNA) vaccines, or mRNA technology, has advanced dramatically with the advent of the coronavirus disease 2019 (COVID-19) pandemic. Notably, Karikó et al. were awarded this year's Nobel Prize in Physiology or Medicine for their discoveries concerning nucleoside base modifications (Karikó et al., 2005), which made possible the development of an effective mRNA vaccine against COVID-19. The self-amplifying RNA (saRNA) vaccine, an emerging mRNA vaccine derived from the genome of α virus that comprises an mRNA sequence of α virus replicase and antigen protein, is able to self-amplify the gene of interest (GOI) sequence *in vivo* (Figure 3A) (Schmidt and Schnierle, 2023). In recent years, saRNA vaccines have received widespread attention in the field of infectious diseases and tumor treatment (Ballesteros-Briones et al., 2020; Lundstrom, 2020; Karam and Daoud, 2022). The main advantage of saRNA is that a lower dose of vaccine can obtain the same protective efficiency as a conventional mRNA vaccine(Papukashvili et al., 2022). With further study of saRNA vaccines, it has been shown that saRNA induces side effects. Since saRNA replicates itself *in vivo*, it produces a large amount of RNA, particularly double-stranded RNA in the cytoplasm, which is recognized by multiple PRRs, including RIG-I, MDA5, Toll-like receptor3 (TLR3), TLR7, PKR, and 2′-5′oligoadenylate synthetase (OAS), and then induces remarkable IFN responses and pro-inflammatory cytokine release (Figure 3B), which inhibits the translation of saRNA (Linares-Fernández et al., 2020; Comes et al., 2023).

To date, strategies to resolve these issues have been described in detail, the most promising of which is to introduce the mRNA sequences of innate inhibiting proteins (IIPs) to saRNAs, which enable their escape from host immune recognition and the IFN response(Devasthanam, 2014). Studies have revealed that the V protein of CPIV promotes the expression of a saRNA protein by inhibiting the activation of NF-κB and IRF3 (Figure 3B), thereby increasing the expression of saRNA vaccines (Blakney et al., 2021). However, there is no evidence indicating that the V protein could enhance the immunogenicity of tested animals. Encouragingly, V protein was found to increase the proportion of saRNA-expressing cells in human skin explants(Blakney et al., 2021), suggesting that it may enhance the immunogenicity of saRNA in human cells, but more experiments are needed to confirm this.

Overall, from the present point of view, the introduction of V protein into the saRNA vector backbone indeed helps to suppress the level of innate immunity *in vivo*, which in turn enhances the expression level of the target antigen. However, because RNA viral genomes are highly mutated and prone to recombination, more experiments should be designed to verify their safety, especially their sensitivity to different types of human cells, before clinical application.

7 Interaction of the V protein with other viruses

As mentioned above, the V protein can promote the replication and spread of CPIV by inhibiting apoptosis, hijacking the host PKB kinase, and interfering with the host immune response and other processes. Some studies have shown that in primary human fetal liver cells (HFLC), the V protein promotes the expression of the hepatitis C virus (HCV) protein by inhibiting the IFN pathway and antagonizing the induction of type III IFN, IL-29, ultimately promoting the replication and spread of HCV (Figure 4) (Andrus et al., 2011). This finding indicates that the V protein is beneficial for elucidating the mechanism of other viral infections, particularly viral replication, spread and other processes.

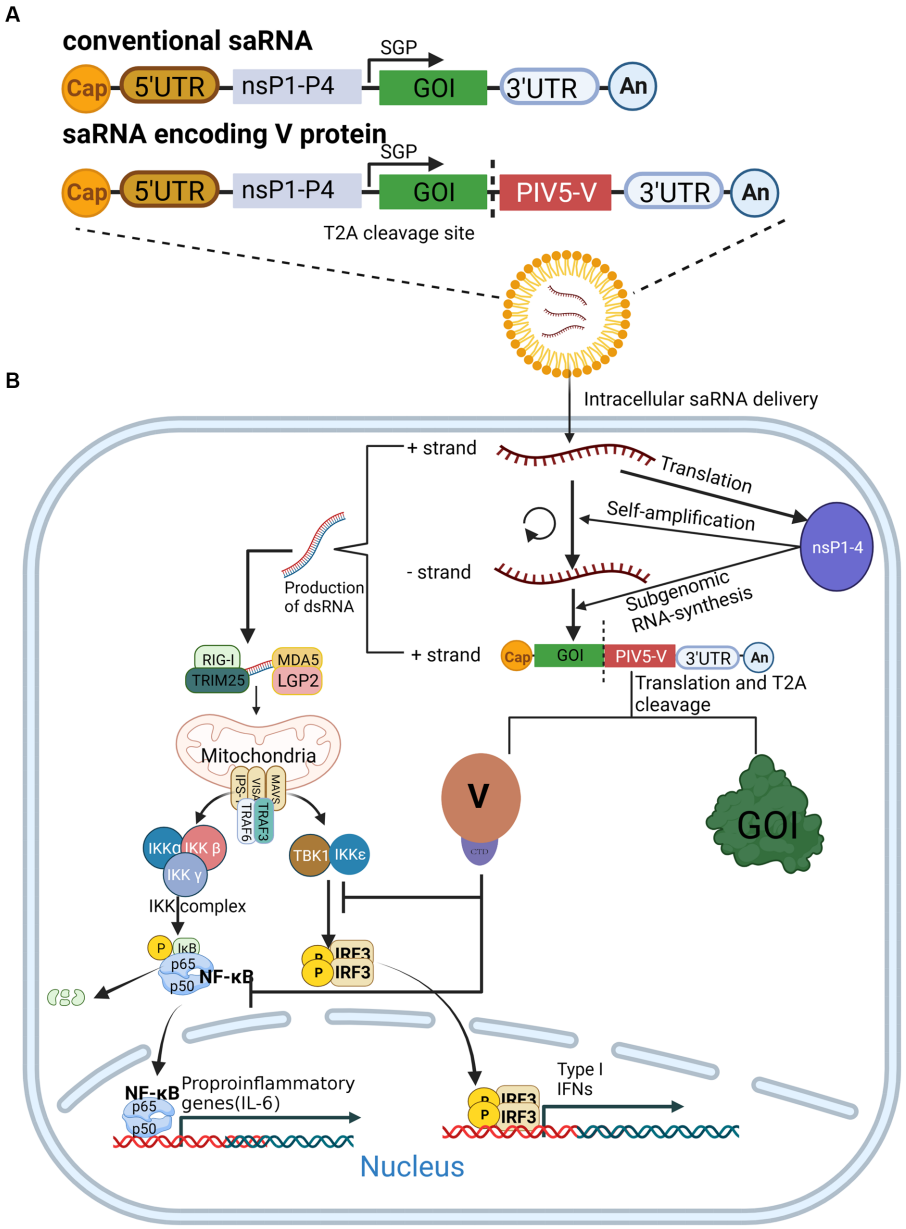

FIGURE 3
The expression of saRNA is enhanced by the V protein. **(A)** Composition of conventional saRNAs and V-protein-encoding saRNAs. **(B)** V protein antagonizes the innate immune response by inhibiting NF-κB and IFR3 activation, which in turn enhances saRNA expression.

8 Conclusion and future perspectives

With in-depth research on the paramyxovirus V protein, research into the CPIV-V protein has gradually become a research hotspot. Based on the above studies, it can be seen that the V protein may not only be a nonstructural protein of the virus but also function as a structural protein that participates in multiple processes of the virus life cycle and facilitates viral escape from the host immune response by delaying the cell cycle, inhibiting cell apoptosis, resisting the IFN response, inhibiting dendritic cell maturation, etc. Although the structure and function of the V protein CTD have been extensively studied, the function of the NTD of the V protein and its functional difference from the NTD of the P protein have been less intensively studied. In addition, NVGs and autophagy show a very strong correlation with the host innate immune response, and whether the V protein interacts with these components and the potential mechanism underlying this interaction and its importance need to be further studied.

Oncolytic virus and saRNA vaccines are two emerging tumor immunotherapies, and the application of the V protein shows that research into the V protein has great reference value and importance for the development of new diagnostic and treatment methods. However, V-Protein research in those fields has focused mainly on *in*

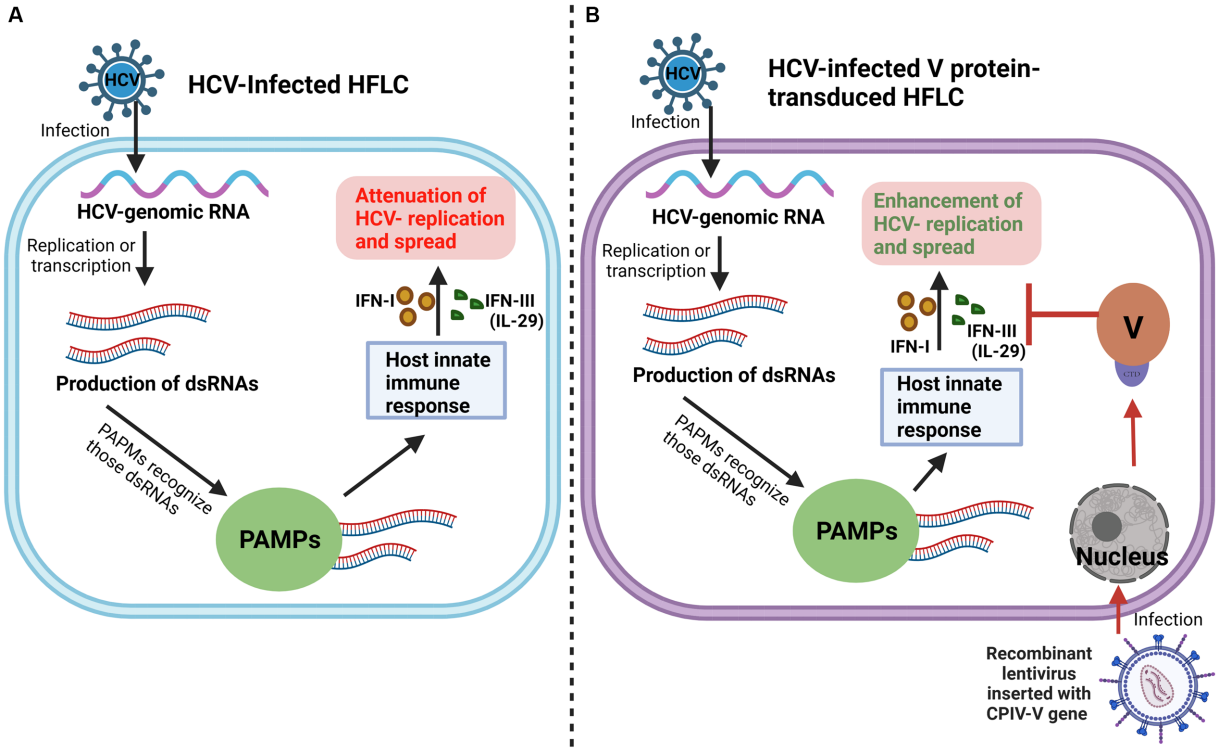

FIGURE 4
V protein promotes HCV replication and spread. **(A)** Conventionally, in HCV-Infected HFLC, PAMPs recognize dsRNAs derived from HCV replication, activate the HFLC innate immune response, and inhibit HCV replication and spread. **(B)** When the V protein is introduced into HFLC by a lentiviral vector, the V protein promotes the replication and spread of HCV by antagonizing IFN-I and IFN-III (IL-29) induced by the HFLC innate immune response.

vitro experiments, and many scientific experiments will be needed in the future to verify the safety, dosage and half-life *in vivo*.

Author contributions

HCh: Data curation, Software, Writing – original draft. HZ: Investigation, Supervision, Writing – review & editing. HCa: Data curation, Methodology, Software, Writing – original draft. ML: Software, Conceptualization, Writing – review & editing. SW: Writing – review & editing, Supervision, Validation. JR: Supervision, Writing – review & editing, Investigation, Project administration.

Funding

The author(s) declare financial support was received for the research, authorship, and/or publication of this article. This research was funded by the Youth Growth Technology Project of Jilin Provincial Science and Technology Development Program (no. 20210508019RQ) and the Start-Up Research Fund from Wenzhou University (no. QD2023014).

Conflict of interest

The authors declare that the research was conducted in the absence of any commercial or financial relationships that could be construed as a potential conflict of interest.

Publisher's note

All claims expressed in this article are solely those of the authors and do not necessarily represent those of their affiliated organizations, or those of the publisher, the editors and the reviewers. Any product that may be evaluated in this article, or claim that may be made by its manufacturer, is not guaranteed or endorsed by the publisher.

References

Agarwal, R., and Kaye, S. B. (2003). Ovarian cancer: strategies for overcoming resistance to chemotherapy. *Nat. Rev. Cancer* 3, 502–516. doi: 10.1038/nrc1123

Andrus, L., Marukian, S., Jones, C. T., Catanese, M. T., Sheahan, T. P., Schoggins, J. W., et al. (2011). Expression of paramyxovirus V proteins promotes replication and spread of hepatitis C virus in cultures of primary human fetal liver cells. *Hepatology* 54, 1901–1912. doi: 10.1002/hep.24557

Ballesteros-Briones, M. C., Silva-Pilipich, N., Herrador-Cañete, G., Vanrell, L., and Smerdou, C. (2020). A new generation of vaccines based on alphavirus self-amplifying RNA. *Curr. Opin. Virol.* 44, 145–153. doi: 10.1016/j.coviro.2020.08.003

Berry, K. N., Kober, D. L., Su, A., and Brett, T. J. (2018). Limiting respiratory viral infection by targeting antiviral and immunological functions of BST-2/Tetherin: knowledge and gaps. *BioEssays* 40:e1800086. doi: 10.1002/bies.201800086

Blakney, A. K., McKay, P. F., Bouton, C. R., Hu, K., Samnuan, K., and Shattock, R. J. (2021). Innate inhibiting proteins enhance expression and immunogenicity of self-amplifying RNA. *Mol. Ther.* 29, 1174–1185. doi: 10.1016/j.ymthe.2020.11.011

Capraro, G. A., Johnson, J. B., Kock, N. D., and Parks, G. D. (2008). Virus growth and antibody responses following respiratory tract infection of ferrets and mice with WT and P/V mutants of the paramyxovirus simian virus 5. *Virology* 376, 416–428. doi: 10.1016/j.virol.2008.03.034

Charoenkul, K., Nasamran, C., Janetanakit, T., Chaiyawong, S., Bunpapong, N., Boonyapisitsopa, S., et al. (2021). Molecular detection and whole genome characterization of canine parainfluenza type 5 in Thailand. *Sci. Rep.* 11:3866. doi: 10.1038/s41598-021-83323-9

Chatziandreou, N., Young, D., Andrejeva, J., Goodbourn, S., and Randall, R. E. (2002). Differences in interferon sensitivity and biological properties of two related isolates of simian virus 5: a model for virus persistence. *Virology* 293, 234–242. doi: 10.1006/viro.2001.1302

Chen, Z. (2018). Parainfluenza virus 5-vectored vaccines against human and animal infectious diseases. *Rev. Med. Virol.* 28:e1965. doi: 10.1002/rmv.1965

Childs, K., Stock, N., Ross, C., Andrejeva, J., Hilton, L., Skinner, M., et al. (2007). Mda-5, but not RIG-I, is a common target for paramyxovirus V proteins. *Virology* 359, 190–200. doi: 10.1016/j.virol.2006.09.023

Chukwurah, E., Farabaugh, K. T., Guan, B.-J., Ramakrishnan, P., and Hatzoglou, M. (2021). A tale of two proteins: PACT and PKR and their roles in inflammation. *FEBS J.* 288, 6365–6391. doi: 10.1111/febs.15691

Comes, J. D. G., Pijlman, G. P., and Hick, T. A. H. (2023). Rise of the RNA machines - self-amplification in mRNA vaccine design. *Trends Biotechnol.* 41, 1417–1429. doi: 10.1016/j.tibtech.2023.05.007

Devasthanam, A. S. (2014). Mechanisms underlying the inhibition of interferon signaling by viruses. *Virulence* 5, 270–277. doi: 10.4161/viru.27902

Dillon, P. J., Wansley, E. K., Young, V. A., Alexander-Miller, M. A., and Parks, G. D. (2006). Exchange of P/V genes between two non-cytopathic simian virus 5 variants results in a recombinant virus that kills cells through death pathways that are sensitive to caspase inhibitors. *J. Gen. Virol.* 87, 3643–3648. doi: 10.1099/vir.0.82242-0

Douglas, J., Drummond, A. J., and Kingston, R. L. (2021). Evolutionary history of cotranscriptional editing in the paramyxoviral phosphoprotein gene. *Virus Evolution* 7:veab028. doi: 10.1093/ve/veab028

Eskander, R. N., Moore, K. N., Monk, B. J., Herzog, T. J., Annunziata, C. M., O'Malley, D. M., et al. (2023). Overcoming the challenges of drug development in platinum-resistant ovarian cancer. *Front. Oncol.* 13:1258228. doi: 10.3389/fonc.2023.1258228

Foster, T. L., Pickering, S., and Neil, S. J. D. (2017). Inhibiting the ins and outs of HIV replication: cell-intrinsic antiretroviral restrictions at the plasma membrane. *Front. Immunol.* 8:1853. doi: 10.3389/fimmu.2017.01853

Fox, C. R., and Parks, G. D. (2018). Parainfluenza virus infection sensitizes Cancer cells to DNA-damaging agents: implications for oncolytic virus therapy. *J. Virol.* 92, e01948–e01917. doi: 10.1128/JVI.01948-17

Fox, C. R., and Parks, G. D. (2019). Histone deacetylase inhibitors enhance cell killing and block interferon-Beta synthesis elicited by infection with an oncolytic parainfluenza virus. *Viruses* 11:431. doi: 10.3390/v11050431

Freedman, J. D., Hagel, J., Scott, E. M., Psallidas, I., Gupta, A., Spiers, L., et al. (2017). Oncolytic adenovirus expressing bispecific antibody targets T-cell cytotoxicity in cancer biopsies. *EMBO Mol. Med.* 9, 1067–1087. doi: 10.15252/emmm.201707567

Gainey, M. D., Dillon, P. J., Clark, K. M., Manuse, M. J., and Parks, G. D. (2008a). Paramyxovirus-induced shutoff of host and viral protein synthesis: role of the P and V proteins in limiting PKR activation. *J. Virol.* 82, 828–839. doi: 10.1128/JVI.02023-07

Gainey, M. D., Manuse, M. J., and Parks, G. D. (2008b). A hyperfusogenic F protein enhances the oncolytic potency of a paramyxovirus simian virus 5 P/V mutant without compromising sensitivity to type I interferon. *J. Virol.* 82, 9369–9380. doi: 10.1128/JVI.01054-08

Genoyer, E., and López, C. B. (2019). The impact of defective viruses on infection and immunity. *Annu Rev Virol* 6, 547–566. doi: 10.1146/annurev-virology-092818-015652

He, B., Paterson, R. G., Stock, N., Durbin, J. E., Durbin, R. K., Goodbourn, S., et al. (2002). Recovery of paramyxovirus simian virus 5 with a V protein lacking the conserved cysteine-rich domain: the multifunctional V protein blocks both interferon-beta induction and interferon signaling. *Virology* 303, 15–32. doi: 10.1006/viro.2002.1738

Hou, W. (2021) *ATP6V1G1 Positively Regulates RLR Antiviral Innate Immune Signaling Pathway by Targeting RIG-I. [Dissertation]*. [Nanchang (China)]: Jiangxi Normal University.

Hou, P., Yang, K., Jia, P., Liu, L., Lin, Y., Li, Z., et al. (2021). A novel selective autophagy receptor, CCDC50, delivers K63 polyubiquitination-activated RIG-I/MDA5 for degradation during viral infection. *Cell Res.* 31, 62–79. doi: 10.1038/s41422-020-0362-1

Huang, Z., Guo, H., Lin, L., Li, S., Yang, Y., Han, Y., et al. (2023). Application of oncolytic virus in tumor therapy. *J. Med. Virol.* 95:e28729. doi: 10.1002/jmv.28729

Huang, F.-Y., Wang, J.-Y., Dai, S.-Z., Lin, Y.-Y., Sun, Y., Zhang, L., et al. (2020). A recombinant oncolytic Newcastle virus expressing MIP-3α promotes systemic antitumor immunity. *J. Immunother. Cancer* 8:e000330. doi: 10.1136/jitc-2019-000330

Hull, R. N., Minner, J. R., and Smith, J. W. (1956). New viral agents recovered from tissue cultures of monkey kidney cells. I. Origin and properties of cytopathogenic agents S.V.1, S.V.2, S.V.4, S.V.5, S.V.6, S.V.11, S.V.12 and S.V.15. *Am. J. Hyg.* 63, 204–215. doi: 10.1093/oxfordjournals.aje.a119804

Ibrahim, Y. M., Zhang, W., Werid, G. M., Zhang, H., Pan, Y., Zhang, L., et al. (2022). Characterization of parainfluenza virus 5 from diarrheic piglet highlights its zoonotic potential. *Transbound. Emerg. Dis.* 69, e1510–e1525. doi: 10.1111/tbed.14482

Iuliano, M., Mangino, G., Chiantore, M. V., Di Bonito, P., Rosa, P., Affabris, E., et al. (2021). Virus-induced tumorigenesis and IFN system. *Biology (Basel)* 10:994. doi: 10.3390/biology10100994

Jadhav, A., Zhao, L., Ledda, A., Liu, W., Ding, C., Nair, V., et al. (2020). Patterns of RNA editing in Newcastle disease virus infections. *Viruses* 12:1249. doi: 10.3390/v12111249

Jensen, C., and Teng, Y. (2020). Is it time to start transitioning from 2D to 3D cell culture? *Front. Mol. Biosci.* 7:33. doi: 10.3389/fmolb.2020.00033

Jiang, Y., Zhang, H., Wang, J., Chen, J., Guo, Z., Liu, Y., et al. (2023). Exploiting RIG-I-like receptor pathway for cancer immunotherapy. *J. Hematol. Oncol.* 16:8. doi: 10.1186/s13045-023-01405-9

Jr, T., and Dl, F. (2021). COVID-19 vaccines: modes of immune activation and future challenges. *Nat. Rev. Immunol.* 21, 195–197. doi: 10.1038/s41577-021-00526-x

Karam, M., and Daoud, G. (2022). mRNA vaccines: Past, present, future. *Asian J Pharm Sci* 17, 491–522. doi: 10.1016/j.ajps.2022.05.003

Karikó, K., Buckstein, M., Ni, H., and Weissman, D. (2005). Suppression of RNA recognition by toll-like receptors: the impact of nucleoside modification and the evolutionary origin of RNA. *Immunity* 23, 165–175. doi: 10.1016/j.immuni.2005.06.008

Ke, P.-Y. (2023). Crosstalk between autophagy and RLR signaling. *Cells* 12:956. doi: 10.3390/cells12060956

Kedarinath, K., and Parks, G. D. (2022). Differential in vitro growth and cell killing of Cancer versus benign prostate cells by oncolytic parainfluenza virus. *Pathogens* 11:493. doi: 10.3390/pathogens11050493

Kedarinath, K., Shiffer, E. M., and Parks, G. D. (2023). DNA methyltransferase inhibitor 5-azacytidine enhances neuroblastoma cell lysis by an oncolytic parainfluenza virus. *Anti-Cancer Drugs* 34, 916–928. doi: 10.1097/CAD.0000000000001525

Kikkert, M. (2020). Innate immune evasion by human respiratory RNA viruses. *J. Innate Immun.* 12, 4–20. doi: 10.1159/000503030

Kolakofsky, D. (2016). Paramyxovirus RNA synthesis, mRNA editing, and genome hexamer phase: a review. *Virology* 498, 94–98. doi: 10.1016/j.virol.2016.08.018

Kolakofsky, D., Pelet, T., Garcin, D., Hausmann, S., Curran, J., and Roux, L. (1998). Paramyxovirus RNA synthesis and the requirement for hexamer genome length: the rule of six revisited. *J. Virol.* 72, 891–899. doi: 10.1128/JVI.72.2.891-899.1998

Lin, Y., Horvath, F., Aligo, J. A., Wilson, R., and He, B. (2005). The role of simian virus 5 V protein on viral RNA synthesis. *Virology* 338, 270–280. doi: 10.1016/j.virol.2005.05.014

Lin, G. Y., and Lamb, R. A. (2000). The paramyxovirus simian virus 5 V protein slows progression of the cell cycle. *J. Virol.* 74, 9152–9166. doi: 10.1128/jvi.74.19.9152-9166.2000

Lin, G. Y., Paterson, R. G., and Lamb, R. A. (1997). The RNA binding region of the paramyxovirus SV5 V and P proteins. *Virology* 238, 460–469. doi: 10.1006/viro.1997.8866

Lin, G. Y., Paterson, R. G., Richardson, C. D., and Lamb, R. A. (1998). The V protein of the paramyxovirus SV5 interacts with damage-specific DNA binding protein. *Virology* 249, 189–200. doi: 10.1006/viro.1998.9317

Lin, D., Shen, Y., and Liang, T. (2023). Oncolytic virotherapy: basic principles, recent advances and future directions. *Signal Transduct. Target. Ther.* 8:156. doi: 10.1038/s41392-023-01407-6

Lin, Y., Sun, M., Fuentes, S. M., Keim, C. D., Rothermel, T., and He, B. (2007). Inhibition of interleukin-6 expression by the V protein of parainfluenza virus 5. *Virology* 368, 262–272. doi: 10.1016/j.virol.2007.07.009

Linares-Fernández, S., Lacroix, C., Exposito, J.-Y., and Verrier, B. (2020). Tailoring mRNA vaccine to balance innate/adaptive immune response. *Trends Mol. Med.* 26, 311–323. doi: 10.1016/j.molmed.2019.10.002

Lu, L. L., Puri, M., Horvath, C. M., and Sen, G. C. (2008). Select paramyxoviral V proteins inhibit IRF3 activation by acting as alternative substrates for inhibitor of kappaB kinase epsilon (IKKe)/TBK1. *J. Biol. Chem.* 283, 14269–14276. doi: 10.1074/jbc.M710089200

Lundstrom, K. (2020). Self-amplifying RNA viruses as RNA vaccines. *Int. J. Mol. Sci.* 21:5130. doi: 10.3390/ijms21145130

Mandhana, R., Qian, L. K., and Horvath, C. M. (2018). Constitutively active MDA5 proteins are inhibited by paramyxovirus V proteins. *J. Interf. Cytokine Res.* 38, 319–332. doi: 10.1089/jir.2018.0049

Manzoni, T. B., and López, C. B. (2018). Defective (interfering) viral genomes re-explored: impact on antiviral immunity and virus persistence. *Future Virol* 13, 493–503. doi: 10.2217/fvl-2018-0021

Matveeva, O. V., and Shabalina, S. A. (2020). Prospects for using expression patterns of paramyxovirus receptors as biomarkers for oncolytic Virotherapy. *Cancers (Basel)* 12:3659. doi: 10.3390/cancers12123659

Moritoh, K., Shoji, K., Amagai, Y., Fujiyuki, T., Sato, H., Yoneda, M., et al. (2023). Immune response elicited in the tumor microenvironment upon rMV-SLAMblind cancer virotherapy. *Cancer Sci.* 114, 2158–2168. doi: 10.1111/cas.15740

Motz, C., Schuhmann, K. M., Kirchhofer, A., Moldt, M., Witte, G., Conzelmann, K.-K., et al. (2013). Paramyxovirus V proteins disrupt the fold of the RNA sensor MDA5 to inhibit antiviral signaling. *Science* 339, 690–693. doi: 10.1126/science.1230949

Nagano, Y., Sugiyama, A., Kimoto, M., Wakahara, T., Noguchi, Y., Jiang, X., et al. (2020). The measles virus V protein binding site to STAT2 overlaps that of IRF9. *J. Virol.* 94, e01169–e01120. doi: 10.1128/JVI.01169-20

Negishi, H., Taniguchi, T., and Yanai, H. (2018). The interferon (IFN) class of cytokines and the IFN regulatory factor (IRF) transcription factor family. *Cold Spring Harb. Perspect. Biol.* 10:a028423. doi: 10.1101/cshperspect.a028423

Nishio, M., Ohtsuka, J., Tsurudome, M., Nosaka, T., and Kolakofsky, D. (2008). Human parainfluenza virus type 2 V protein inhibits genome replication by binding to the L protein: possible role in promoting viral fitness. *J. Virol.* 82, 6130–6138. doi: 10.1128/JVI.02635-07

Nishio, M., Tsurudome, M., Ito, M., Garcin, D., Kolakofsky, D., and Ito, Y. (2005). Identification of paramyxovirus V protein residues essential for STAT protein degradation and promotion of virus replication. *J. Virol.* 79, 8591–8601. doi: 10.1128/JVI.79.13.8591-8601.2005

Ohta, K., Matsumoto, Y., Ito, M., and Nishio, M. (2017). Tetherin antagonism by V proteins is a common trait among the genus Rubulavirus. *Med. Microbiol. Immunol.* 206, 319–326. doi: 10.1007/s00430-017-0509-y

Ohta, K., Matsumoto, Y., and Nishio, M. (2020). Common and unique mechanisms of filamentous actin formation by viruses of the genus Orthorubulavirus. *Arch. Virol.* 165, 799–807. doi: 10.1007/s00705-020-04565-y

Ohta, K., Saka, N., and Nishio, M. (2021). Human parainfluenza virus type 2 V protein modulates Iron homeostasis. *J. Virol.* 95, e01861–e01820. doi: 10.1128/JVI.01861-20

Omagari, K., Asamitsu, K., and Tanaka, Y. (2021). Application of fluorescent-based technology detecting protein-protein interactions to monitor the binding of hepatitis B virus X protein to DNA-damage-binding protein 1. *Biophys Physicobiol* 18, 67–77. doi: 10.2142/biophysico.bppb-v18.008

Papukashvili, D., Rcheulishvili, N., Liu, C., Ji, Y., He, Y., and Wang, P. G. (2022). Self-amplifying RNA approach for protein replacement therapy. *Int. J. Mol. Sci.* 23:12884. doi: 10.3390/ijms232112884

Parisien, J.-P., Lau, J. F., Rodriguez, J. J., Ulane, C. M., and Horvath, C. M. (2002). Selective STAT protein degradation induced by paramyxoviruses requires both STAT1 and STAT2 but is independent of alpha/beta interferon signal transduction. *J. Virol.* 76, 4190–4198. doi: 10.1128/jvi.76.9.4190-4198.2002

Park, A. K., Fong, Y., Kim, S.-I., Yang, J., Murad, J. P., Lu, J., et al. (2020). Effective combination immunotherapy using oncolytic viruses to deliver CAR targets to solid tumors. *Sci. Transl. Med.* 12:eaaz1863. doi: 10.1126/scitranslmed.aaz1863

Parks, G. D., and Alexander-Miller, M. A. (2013). Paramyxovirus activation and inhibition of innate immune responses. *J. Mol. Biol.* 425, 4872–4892. doi: 10.1016/j.jmb.2013.09.015

Paterson, R. G., Leser, G. P., Shaughnessy, M. A., and Lamb, R. A. (1995). The paramyxovirus SV5 V protein binds two atoms of zinc and is a structural component of virions. *Virology* 208, 121–131. doi: 10.1006/viro.1995.1135

Pejawar, S. S., Parks, G. D., and Alexander-Miller, M. A. (2005). Abortive versus productive viral infection of dendritic cells with a paramyxovirus results in differential upregulation of select costimulatory molecules. *J. Virol.* 79, 7544–7557. doi: 10.1128/JVI.79.12.7544-7557.2005

Peluso, R. W., Lamb, R. A., and Choppin, P. W. (1977). Polypeptide synthesis in simian virus 5-infected cells. *J. Virol.* 23, 177–187. doi: 10.1128/JVI.23.1.177-187.1977

Precious, B., Childs, K., Fitzpatrick-Swallow, V., Goodbourn, S., and Randall, R. E. (2005). Simian virus 5 V protein acts as an adaptor, linking DDB1 to STAT2, to facilitate the ubiquitination of STAT1. *J. Virol.* 79, 13434–13441. doi: 10.1128/JVI.79.21.13434-13441.2005

Precious, B., Young, D. F., Bermingham, A., Fearns, R., Ryan, M., and Randall, R. E. (1995). Inducible expression of the P, V, and NP genes of the paramyxovirus simian virus 5 in cell lines and an examination of NP-P and NP-V interactions. *J. Virol.* 69, 8001–8010. doi: 10.1128/JVI.69.12.8001-8010.1995

Raja, J., Ludwig, J. M., Gettinger, S. N., Schalper, K. A., and Kim, H. S. (2018). Oncolytic virus immunotherapy: future prospects for oncology. *J. Immunother. Cancer* 6:140. doi: 10.1186/s40425-018-0458-z

Rao, P. L., Gandham, R. K., and Subbiah, M. (2020). Molecular evolution and genetic variations of V and W proteins derived by RNA editing in avian paramyxoviruses. *Sci. Rep.* 10:9532. doi: 10.1038/s41598-020-66252-x

Rodriguez, K. R., and Horvath, C. M. (2014). Paramyxovirus V protein interaction with the antiviral sensor LGP2 disrupts MDA5 signaling enhancement but is not relevant to LGP2-mediated RLR signaling inhibition. *J. Virol.* 88, 8180–8188. doi: 10.1128/JVI.00737-14

Sánchez-Aparicio, M. T., Feinman, L. J., García-Sastre, A., and Shaw, M. L. (2018). Paramyxovirus V proteins interact with the RIG-I/TRIM25 regulatory complex and inhibit RIG-I signaling. *J. Virol.* 92, e01960–e01917. doi: 10.1128/JVI.01960-17

Schmidt, C., and Schnierle, B. S. (2023). Self-amplifying RNA vaccine candidates: alternative platforms for mRNA vaccine development. *Pathogens* 12:138. doi: 10.3390/pathogens12010138

Siering, O., Cattaneo, R., and Pfaller, C. K. (2022). C proteins: controllers of orderly paramyxovirus replication and of the innate immune response. *Viruses* 14:137. doi: 10.3390/v14010137

Sorokin, I. I., Vassilenko, K. S., Terenin, I. M., Kalinina, N. O., Agol, V. I., and Dmitriev, S. E. (2021). Non-canonical translation initiation mechanisms employed by eukaryotic viral mRNAs. *Biochemistry (Mosc)* 86, 1060–1094. doi: 10.1134/S0006297921090042

Sun, M., Fuentes, S. M., Timani, K., Sun, D., Murphy, C., Lin, Y., et al. (2008). Akt plays a critical role in replication of nonsegmented negative-stranded RNA viruses. *J. Virol.* 82, 105–114. doi: 10.1128/JVI.01520-07

Sun, M., Rothermel, T. A., Shuman, L., Aligo, J. A., Xu, S., Lin, Y., et al. (2004). Conserved cysteine-rich domain of paramyxovirus simian virus 5 V protein plays an important role in blocking apoptosis. *J. Virol.* 78, 5068–5078. doi: 10.1128/jvi.78.10.5068-5078.2004

Thomas, S. M., Lamb, R. A., and Paterson, R. G. (1988). Two mRNAs that differ by two nontemplated nucleotides encode the amino coterminal proteins P and V of the paramyxovirus SV5. *Cells* 54, 891–902. doi: 10.1016/s0092-8674(88)91285-8

Ulane, C. M., Kentsis, A., Cruz, C. D., Parisien, J.-P., Schneider, K. L., and Horvath, C. M. (2005). Composition and assembly of STAT-targeting ubiquitin ligase complexes: paramyxovirus V protein carboxyl terminus is an oligomerization domain. *J. Virol.* 79, 10180–10189. doi: 10.1128/JVI.79.16.10180-10189.2005

Varudkar, N., Oyer, J. L., Copik, A., and Parks, G. D. (2021). Oncolytic parainfluenza virus combines with NK cells to mediate killing of infected and non-infected lung cancer cells within 3D spheroids: role of type I and type III interferon signaling. *J. Immunother. Cancer* 9:e002373. doi: 10.1136/jitc-2021-002373

Varudkar, N., Shiffer, E. M., Oyer, J. L., Copik, A., and Parks, G. D. (2023). Delivery of a novel membrane-anchored fc chimera enhances NK cell-mediated killing of tumor cells and persistently virus-infected cells. *PLoS One* 18:e0285532. doi: 10.1371/journal.pone.0285532

Vignuzzi, M., and López, C. B. (2019). Defective viral genomes are key drivers of the virus-host interaction. *Nat. Microbiol.* 4, 1075–1087. doi: 10.1038/s41564-019-0465-y

Wang, T., Zheng, L., Zhao, Q., Yao, Y., Zhou, F., Wei, F., et al. (2023). Parainfluenza virus 5 is a next-generation vaccine vector for human infectious pathogens. *J. Med. Virol.* 95:e28622. doi: 10.1002/jmv.28622

Wansley, E. K., Dillon, P. J., Gainey, M. D., Tam, J., Cramer, S. D., and Parks, G. D. (2005). Growth sensitivity of a recombinant simian virus 5 P/V mutant to type I interferon differs between tumor cell lines and normal primary cells. *Virology* 335, 131–144. doi: 10.1016/j.virol.2005.02.004

Wansley, E. K., Grayson, J. M., and Parks, G. D. (2003). Apoptosis induction and interferon signaling but not IFN-beta promoter induction by an SV5 P/V mutant are rescued by coinfection with wild-type SV5. *Virology* 316, 41–54. doi: 10.1016/s0042-6822(03)00584-1

Wansley, E. K., and Parks, G. D. (2002). Naturally occurring substitutions in the P/V gene convert the noncytopathic paramyxovirus simian virus 5 into a virus that induces alpha/beta interferon synthesis and cell death. *J. Virol.* 76, 10109–10121. doi: 10.1128/jvi.76.20.10109-10121.2002

Wignall-Fleming, E. B., Vasou, A., Young, D., Short, J. A. L., Hughes, D. J., Goodbourn, S., et al. (2020). Innate intracellular antiviral responses restrict the amplification of defective virus genomes of parainfluenza virus 5. *J. Virol.* 94, e00246–e00220. doi: 10.1128/JVI.00246-20

Wright, B. W., Molloy, M. P., and Jaschke, P. R. (2022). Overlapping genes in natural and engineered genomes. *Nat. Rev. Genet.* 23, 154–168. doi: 10.1038/s41576-021-00417-w

Wu, Y., Jin, S., Liu, Q., Zhang, Y., Ma, L., Zhao, Z., et al. (2021). Selective autophagy controls the stability of transcription factor IRF3 to balance type I interferon production and immune suppression. *Autophagy* 17, 1379–1392. doi: 10.1080/15548627.2020.1761653

Yaiw, K.-C., Miest, T. S., Frenzke, M., Timm, M., Johnston, P. B., and Cattaneo, R. (2011). CD20-targeted measles virus shows high oncolytic specificity in clinical samples from lymphoma patients independent of prior rituximab therapy. *Gene Ther.* 18, 313–317. doi: 10.1038/gt.2010.150

Yang, Y.P. (2022) *Establishment of a Rapid Detection Method for Canine Parainfluenza Virus. [Dissertation]*. Wuhan (China): Huazhong Agricultural University.

Yang, M., Ma, Y., Jiang, Q., Song, M., Kang, H., Liu, J., et al. (2022). Isolation, identification and pathogenic characteristics of tick-derived parainfluenza virus 5 in Northeast China. *Transbound. Emerg. Dis.* 69, 3300–3316. doi: 10.1111/tbed.14681

Yang, Y., Zengel, J., Sun, M., Sleeman, K., Timani, K. A., Aligo, J., et al. (2015). Regulation of viral RNA synthesis by the V protein of parainfluenza virus 5. *J. Virol.* 89, 11845–11857. doi: 10.1128/JVI.01832-15

Young, V. A., Dillon, P. J., and Parks, G. D. (2006). Variants of the paramyxovirus simian virus 5 with accelerated or delayed viral gene expression activate proinflammatory cytokine synthesis. *Virology* 350, 90–102. doi: 10.1016/j.virol.2006.01.006

Young, V. A., and Parks, G. D. (2003). Simian virus 5 is a poor inducer of chemokine secretion from human lung epithelial cells: identification of viral mutants that activate interleukin-8 secretion by distinct mechanisms. *J. Virol.* 77, 7124–7130. doi: 10.1128/jvi.77.12.7124-7130.2003

Zamarin, D., Holmgaard, R. B., Subudhi, S. K., Park, J. S., Mansour, M., Palese, P., et al. (2014). Localized oncolytic virotherapy overcomes systemic tumor resistance to immune checkpoint blockade immunotherapy. *Sci. Transl. Med.* 6:226ra32. doi: 10.1126/scitranslmed.3008095

Zhao, Y., Zhao, K., Wang, S., and Du, J. (2022). Multi-functional BST2/tetherin against HIV-1, other viruses and LINE-1. *Front. Cell. Infect. Microbiol.* 12:979091. doi: 10.3389/fcimb.2022.979091

Zheng, J., Shi, W., Yang, Z., Chen, J., Qi, A., Yang, Y., et al. (2023). "RIG-I-like receptors: molecular mechanism of activation and signaling" in *Advances in Immunology*. Frederick W. Alt and Kenneth Murphy Eds. (Elsevier, Amsterdam: Academic Press).

Ziegler, C. M., and Botten, J. W. (2020). Defective interfering particles of negative-Strand RNA viruses. *Trends Microbiol.* 28, 554–565. doi: 10.1016/j.tim.2020.02.006

10.3389/fmicb.2023.1282112

Glossary

CPIV	Canine parainfluenza virus
CIRD	Canine infectious respiratory disease
SV5	Simian virus 5
PIV5	Parainfluenza virus 5
NP	Nucleocapsid protein
P	Phosphoprotein
M	Matrix protein
SH	Small hydrophobic protein
HN	Hemagglutinin neuraminidase
L	Large polymerase protein
IFN	Interferon
ORF	Open read frame
HPIV2	Human parainfluenza virus type 2
NDV	Newcastle disease virus
MeV	Measles virus
NTD	N-terminal domain
CTD	C-terminal domain
DDB1	Damage-specific DNA binding protein 1
STAT2	Signal transducer and activator of transcription 2
STAT1	Signal transducer and activator of transcription 1
VDC	V protein-dependent degradation complexes
PKB	Protein kinase B
RB	Retinoblastoma protein
ER	Endoplasmic reticulum
Caspase	Cysteine aspartate-specific protease
RhoA	Ras homolog gene family member A
F-actin	Filamentous actin
BST2	Bone marrow stromal cell antigen 2
GPI	Glycol phosphatidyl-inositol
PRRs	Pattern recognition receptors
PKR	Protein kinase R
eIF-2α	Eukaryotic initiation factor 2 alpha
PAMPs	Pathogen-associated molecular patterns
MDA5	Melanoma differentiation-associated gene 5
RIG-1	Retinoic acid-inducible gene-1
LGP2	Laboratory of genetics and physiology 2
VISA	Virus-induced signaling adaptor
MAVS	Mitochondrial antiviral signaling protein
IPS-1	IFN β promoter stimulator 1
TRAF3	Tumor necrosis factor receptor-associated factor 3
IKKε	Nuclear factor κB kinase-ε
IRF3	IFN regulatory factor 3
TRAF6	Tumor necrosis factor receptor-associated factor 6
NF-κB	Nuclear factor-κB
IκB	Inhibitor of κB

β-TrCP	β-Transducin repeats-containing protein
JAK/STAT	Janus kinase/signal transducer and activator of transcription
ISGs	IFN-stimulated genes
MVBR	Minimal V protein binding region
TRIM25	Tripartite motif-containing 25
Cul4a	Cullin 4a
CPEs	Cytopathic effects
IL-6	Interleukin-6
IL-8	Interleukin-8
MCP-1	Macrophage chemoattractant protein-1
CCDC50	Coiled-coil domain containing protein 50
DCs	Dendritic cells
rCPIV	Recombinant CPIV
PI	Persistent infection
DVGs	Virus-defective genomes
OVs	Oncolytic viruses
HDAC	Histone deacetylase
DNMTi	DNA methyltransferase inhibitors
NK	Natural killer
ADCC	Antibody-dependent cellular cytotoxicity
ACT	Adoptive cell transfer
CAR-T/NK	Chimeric antigen receptor T/NK cell
TCR-T	T cell receptor-engineered T cell
TIL	Tumor-infiltrating lymphocyte
ICD	Immunogenic cell death
BiTE	Bi-specific T cell engagers
TriTE	Tri-specific T cell engagers
APCs	Antigen-presenting cells
ICIs	Immune checkpoint inhibitors
COVID-19	Coronavirus disease 2019
saRNA	Self-amplifying RNA
GOI	Gene of interest
OAS	2′-5′oligoadenylate synthetase
TLR3	Toll-like receptor 3
TLR7	Toll-like receptor 7
IIPs	Innate inhibiting proteins
HFLC	Human fetal liver cells
HCV	Hepatitis C virus
IL-29	Interleukin-29

frontiers | Frontiers in Microbiology

TYPE Review
PUBLISHED 24 January 2024
DOI 10.3389/fmicb.2023.1291761

OPEN ACCESS

EDITED BY
Shijian Zhang,
Dana–Farber Cancer Institute, United States

REVIEWED BY
Jingqiang Ren,
Wenzhou University, China
Qian Du,
Northwest A&F University, China

*CORRESPONDENCE
Ying Liao
✉ liaoying@shvri.ac.cn

†These authors have contributed equally to this work and share first authorship

RECEIVED 10 September 2023
ACCEPTED 06 November 2023
PUBLISHED 24 January 2024

CITATION
Liao Y, Wang H, Liao H, Sun Y, Tan L, Song C, Qiu X and Ding C (2024) Classification, replication, and transcription of *Nidovirales*. *Front. Microbiol.* 14:1291761. doi: 10.3389/fmicb.2023.1291761

Classification, replication, and transcription of *Nidovirales*

Ying Liao[1*†], Huan Wang[1†], Huiyu Liao[1], Yingjie Sun[1], Lei Tan[1], Cuiping Song[1], Xusheng Qiu[1] and Chan Ding[1,2]

[1]Department of Avian Diseases, Shanghai Veterinary Research Institute, Chinese Academy of Agricultural Sciences, Shanghai, China, [2]Jiangsu Co-Innovation Center for Prevention and Control of Important Animal Infectious Diseases and Zoonoses, Yangzhou, China

Nidovirales is one order of RNA virus, with the largest single-stranded positive sense RNA genome enwrapped with membrane envelope. It comprises four families (*Arteriviдae, Mesoniviridae, Roniviridae, and Coronaviridae*) and has been circulating in humans and animals for almost one century, posing great threat to livestock and poultry，as well as to public health. *Nidovirales* shares similar life cycle: attachment to cell surface, entry, primary translation of replicases, viral RNA replication in cytoplasm, translation of viral proteins, virion assembly, budding, and release. The viral RNA synthesis is the critical step during infection, including genomic RNA (gRNA) replication and subgenomic mRNAs (sg mRNAs) transcription. gRNA replication requires the synthesis of a negative sense full-length RNA intermediate, while the sg mRNAs transcription involves the synthesis of a nested set of negative sense subgenomic intermediates by a discontinuous strategy. This RNA synthesis process is mediated by the viral replication/transcription complex (RTC), which consists of several enzymatic replicases derived from the polyprotein 1a and polyprotein 1ab and several cellular proteins. These replicases and host factors represent the optimal potential therapeutic targets. Hereby, we summarize the *Nidovirales* classification, associated diseases, "replication organelle," replication and transcription mechanisms, as well as related regulatory factors.

KEYWORDS

***Nidovirales*, replication-transcription complex, dis-continuous RNA synthesis, transcription regulatory sequence, replicase, host factor**

1 Introduction

Named after the Latin word "nidus" (meaning nest), *Nidovirales* refers to an order of viruses which produce a 3′ co-terminal nested set of sg mRNAs during infection (Cavanagh, 1997). They are enveloped virus with a single-stranded, positive-sense RNA genome inside, which consists of a 5′ cap and a 3′ poly (A) tail (de Vries et al., 1997; King et al., 2012). They also contains the longest and the most complex RNA genome, which can be distinguished from other RNA viruses by their molecular genetics (Gorbalenya et al., 2006). So far, our knowledge about their molecular biology have mainly originated from the research progress on *Arterividae* and *Coronaviridae*.

Nidovirus infection is initiated by the process of binding between a virus and its receptors, fusing with membranes, and releasing of the virus into the cytoplasm, in which the nucleocapsid protein is degraded to un-coat the viral genome and subsequently the uncoated gRNA is translated into polyproteins 1a and 1ab (Brian and Baric, 2005). Both

polyproteins (pp1a and pp1ab) undergo auto-proteolysis by intrinsic cysteine proteases to yield 13 to 17 non-structural proteins (NSPs) (Ziebuhr et al., 2000; Fang and Snijder, 2010; Snijder et al., 2013). These NSPs are encoded by gene 1, including two proteases and three transmembrane domains (TM) containing proteins, primer synthetases, RNA-dependent RNA polymerase (RdRp), RNA helicase, and endoribonuclease. To be specific, RdRp serves as a key component in the formation of the replication-transcription complex (RTC) and plays a crucial role in the viral RNA synthesis (Hagemeijer et al., 2010; Yan et al., 2021). The RTC interacts with the modified membrane structures such as double-membrane vesicles (DMVs), tiny open double-membrane spherules (DMSs), and convoluted membranes (CMs) to carry out its functions of replication and transcription (Hagemeijer et al., 2010). The DMVs, DMSs, and CMs are derived from the endoplasmic reticulum (ER) membranes by the help of several TM containing viral NSPs (Posthuma et al., 2008; Angelini et al., 2013; van der Hoeven et al., 2016; Oudshoorn et al., 2017). They provide a protective environment for the RTC to efficiently process and synthesize RNA molecules (Roingeard et al., 2022). With the help of RTC, the negative-stranded full-length genomic RNA (-gRNA) and subgenomic RNAs (-sgRNAs) are synthesized, serving as templates to generate gRNA and sg mRNAs, which are further involved in the synthesis of replicases (pp1a and pp1ab), structural proteins, and the accessory proteins. The transmembrane structural proteins are synthesized by ER-associated ribosomes and inserted into the ER membranes, while the nucleocapsid protein (N protein) is synthesized by ribosomes in the cytoplasm. N protein binds to the viral RNA to form a stable structure called RNA-N complex, which enhances the efficiency of replication or translation (Chang et al., 2014; McBride et al., 2014). The assembly process of virion takes place in the membranes located between the ER) and Golgi apparatus (ERGIC), within which specialized compartments are formed when the membrane folds inward to create a small vesicle-like structure (Venkatagopalan et al., 2015; Boson et al., 2021). This assembly process is triggered by the interaction among the viral structural proteins and membranes (Klumperman et al., 1994; Nguyen and Hogue, 1997; de Haan et al., 1998; Wissink et al., 2005; Neuman et al., 2011; Zhang Z. et al., 2022), and the structural proteins subsequently bind to N protein and recruit the gRNA-N complex, during which the structural proteins and membranes form the outer envelope while the gRNA-N nucleocapsid is wrapped inside (Lim and Liu, 2001; Hsieh et al., 2008; Wang et al., 2009; Tseng et al., 2010; Zhang et al., 2015; Rüdiger et al., 2016; Lu et al., 2021). Once the virion assembly is completed within the ERGIC, the mature virus particles are transported out of the cell through a process called exocytosis (Figure 1).

2 Classification and associated diseases of *Nidovirales*

Officially defined by the International Committee on Taxonomy of Viruses (ICTV) at the Xth International Congress of Virology (ICV) held in Jerusalem (Pringle, 1996), *Nidovirales* was classified into four families: *Arterividae, Mesoniviridae, Roniviridae,* and *Coronaviridae,* with the *Coronaviridae* further divided into two sub-families: *Coronavirinae* and *Torovirinae* (Figure 2). However, as a result of the development of virus detection technologies and viral metagenomics, an increasing number of previously unknown viruses have been discovered (Shi et al., 2018). According to the changes to virus taxonomy approved by the ICTV in 2019, currently the order *Nidovirales* is composed of eight suborders: *Abnidovirineae, Arnidovirineae, Coronadovirineae, Mesnidovirineae, Monidovirineae, Nanidovirineae, Ronidovirineae, and Tornidovirineae* (Van Regenmortel, 2000; Walker et al., 2019; Parrish et al., 2021). These eight suborders contain 14 families, 25 subfamilies, 39 genera, 65 subgenera, and 109 species. Because the newly emerged viruses have not yet been comprehensively studied yet, the following introduction on the *Nidovirales* is still based on the original taxonomy (Pringle, 1996).

Nidovirales can infect both vertebrates (*Coronaviridae, Arteriviridae,* and *Roniviridae*) and invertebrates (*Mesoniviridae*) (Table 1), with a wide range of host organisms, from mammal to bird, fish, crustacean, and insect (Cavanagh et al., 1994; Snijder and Meulenberg, 1998; Masters, 2006; Snijder et al., 2013; Hartenian et al., 2020; Ujike and Taguchi, 2021). Classification of viruses within the *Nidovirales* order is primarily based on several factors, including the organization of the viral genome, the homology of the genome sequence, the antigenic characteristics of the viral proteins, the replication strategy, the structure and physicochemical properties of the virus particle, the natural host range. Based on these factors, scientists and researchers are able to understand the characteristics and relationship of such viruses (Masters, 2006; King et al., 2012; Lavi et al., 2012). Compared to DNA viruses, RNA viruses lack proofreading capacity in their RdRp and thus come across more frequent errors or mutations during replication of their genetic materials, which results in their faster genetic drift and their ability to cross species barriers.

2.1 *Coronaviridae*

Coronaviridae is a family of viruses with a single-stranded RNA genome in the size of 25–32 kb. The 5′-proximal two-thirds region encodes two large polyproteins (pp1a and pp1ab) to generate NSPs which are crucial for viral replication, while the 3′-proximal genome encodes 4 structural proteins which are responsible for viral entry and assembly (Brian and Baric, 2005). As well, the virus species specific accessory proteins, which play an important role in modulating the host immune response, are interspersed among the structural protein genes in the 3′-proximal region (Figure 3B).

According to the original classification, the virus family of *Coronaviridae* is further divided into two subfamilies: *Coronavirinae* and *Torovirinae* (Lai and Cavanagh, 1997). The subfamily *Coronavirinae* is named after its crown-like appearance under electron microscopy and characterized by its spherical particle structure with a diameter ranging from 80 nm to 120 nm and its surface adorned with spike (S), membrane (M), and envelope (E) protein. Inside the envelope, there is nucleocapsid which is composed of the viral genomic RNA and N protein (Figure 3A). In contrast, the subfamily *Torovirinae* is named after the Latin word "torus" which means "cushion" or "protuberance" and appears like pleomorphic, elongated particles with a characteristic "cushion-like" or "torus-like" shape, with the particle morphology including rod-shaped, kidney-shaped, and spherical particles (Ujike and Taguchi, 2021).

The subfamily *Coronavirnae* can be further divided into four genera: *α-Coronavirus*, *β-Coronavirus*, *γ-Coronavirus,* and *δ-Coronavirus.* These genera encompass a wide range of coronaviruses that infect human, mammalian animals, and avian species (Lai and Cavanagh, 1997; Masters, 2006; McCluskey et al., 2016). This

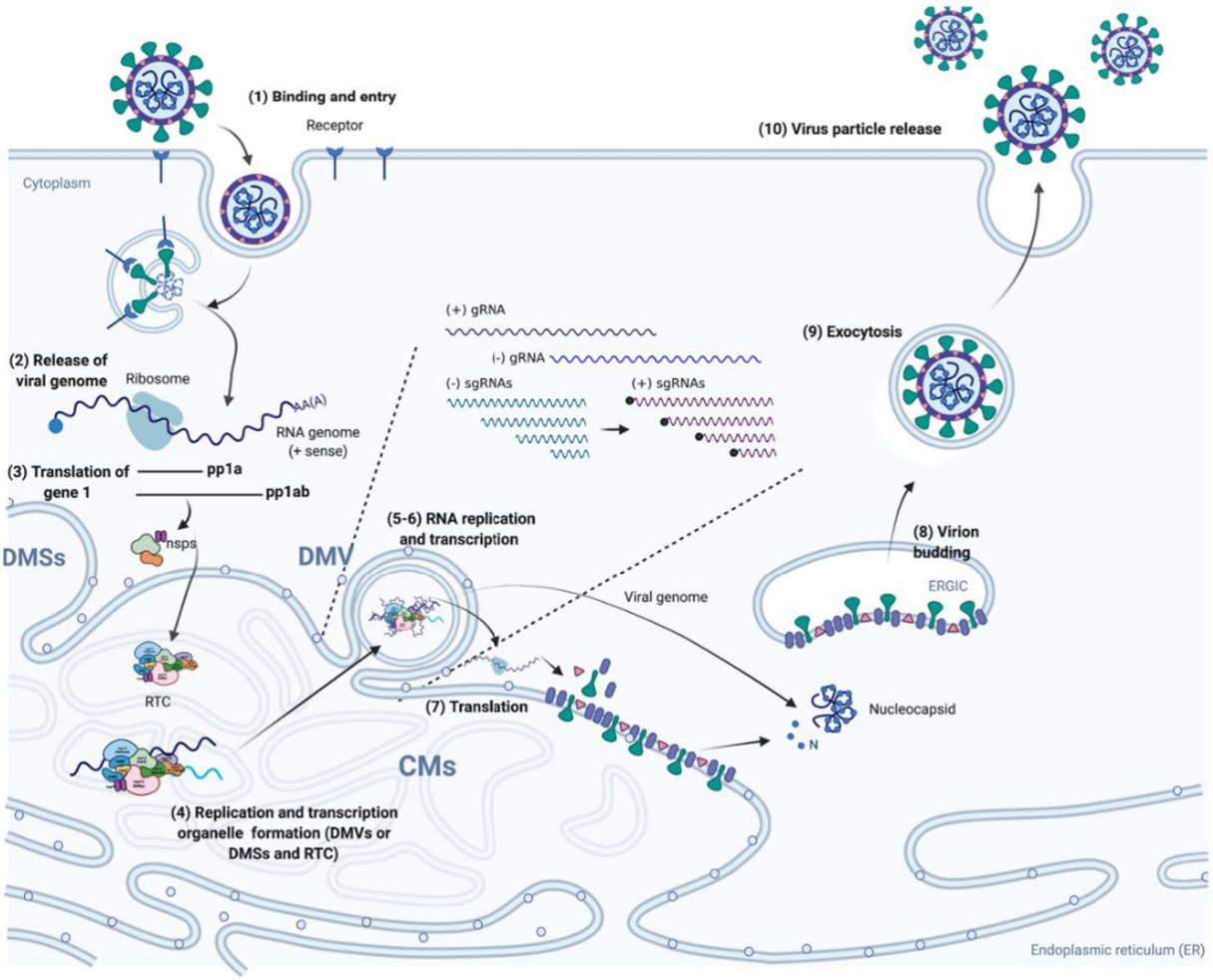

FIGURE 1
Nidovirales life cycle. (1) Virus particles attach to specific receptors on the surface of host cell, which enables the virus to enter into cells through direct fusion with cellular or endosomal membranes; (2–3) The incoming viral genome, a single-stranded RNA molecule, after being released and uncoated serves as template for the synthesis of two polyproteins (pp1a and pp1ab), which are afterwards cleaved by internal papain-like proteases (PLPs) and main protease (Mpro) to generate mature NSPs, including replicases; (4) The formation of viral replication/transcription organelle. The three NSPs containing TM (TM1-3) insert into the intracellular membrane to induce the formation of various membrane structures such as DMVs, CMs, and DMSs, which provide a protective microenvironment for replication and transcription. The NSPs including RdRp, primer synthetases, RNA helicase, endoribonuclease, interact with each other to form the RTC. (5–6) The gRNA and sg mRNAs are synthesized by RTC in the DMVs or DMSs and then transported outside of the DMVs or DMSs; (7) The gRNA and sg mRNAs serve as templates for synthesis of viral proteins by ribosomes; (8) Viral structural proteins are first transported into the ER membrane and then reach the ER-to-Golgi intermediate compartment (ERGIC). Once reaching at the ERGIC, the structural proteins interact with the membranes to curve it and then wrap around the N-gRNA nucleocapsid, resulting in the virion budding into secretory vesicular compartments. (9–10) Mature virus particles are transported out of the cell by exocytosis.

subfamily of viruses mainly causes diseases characterized by symptoms in the respiratory tract, intestinal tract, liver, and central nervous system and poses severe threat not only to human health but also to livestock breeding (Drosten et al., 2003; Woo et al., 2009; Myrrha et al., 2011; Hemida et al., 2014; Zhu et al., 2020). The subfamily can be transmitted from animals to human and differ in terms of their pathogenicity, symptoms and fatality rates. Before the highly pathogenic severe acute respiratory syndrome coronavirus-1 (SARS-CoV-1), middle east respiratory syndrome coronavirus (MERS-CoV), and SARS-CoV-2 emergence, the human coronaviruses usually cause mild or moderate upper respiratory tract diseases, which include HCoV-229E (Hamre and Procknow, 1966), HCoV-OC43 (Hamre and Procknow, 1966; Vabret et al., 2003), HCoV-NL63 (van der Hoek et al., 2004), and HCoV-HKU1 (Woo et al., 2005). These viruses are generally not considered to be highly dangerous or life-threatening (El-Sahly et al., 2000; Falsey et al., 2002; Gagneur et al., 2002). Whereas, MERS-CoV, SARS-CoV-1, and SARS-CoV-2 cause severe symptoms in low respiratory tract, with the typical syndromes of fever and pneumonia (Drosten et al., 2003; Zaki et al., 2012; Salzberger et al., 2021). Among them, MERS-CoV infection is characterized by such symptoms as fever, cough, shortness of breath, and pneumonia, with a fatality rate of 34.4%; SARS-CoV infection is characterized by such symptoms as fever, chills, and body pain, and pneumonia, with a fatality rate of 9.5%; and SARS-CoV-2 infection is characterized by a wide ranges of symptoms, including fever, cough, fatigue, loss of taste or smell, pneumonia and acute respiratory distress syndrome (Petrosillo et al., 2020; Sharma et al., 2020). Since the outbreak of SARS-CoV-2 in December 2019, it has spread globally at an alarming rate, causing more than 771.5 million infections and 6.97 million deaths, with an average mortality rate of 0.9%, as reported to

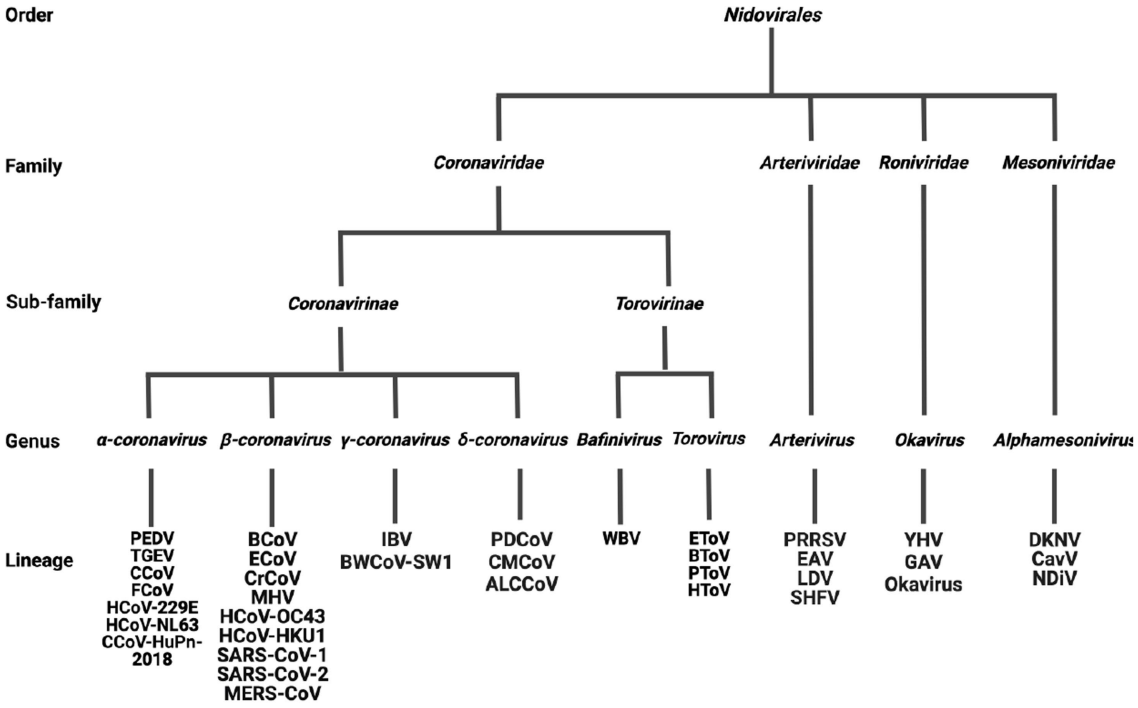

FIGURE 2
The classification of *Nidovirales*. *Nidovirales* consists of 4 families, 2 sub-families, 9 genera and a total of 36 lineages. PEDV, Porcine epidemic diarrhea virus; TGEV, Transmissible gastroenteritis coronavirus; CCoV, Canine coronavirus; FCoV, Feline coronavirus; HCoV-229E, Human coronavirus 229E; HCoV-NL63, Human coronavirus NL63; CCoV-HuPn-2018, Canine coronavirus-human pneumonia-2018; BCoV, Bovine coronavirus; ECoV, Equine coronavirus; CRCoV, Canine respiratory coronavirus; MHV, Mouse hepatitis virus; HCoV-OC43, Human coronavirus OC43; HCoV-HKU1, Human coronavirus HKU1; SARS-CoV-1, Severe acute respiratory syndrome coronavirus-1; SARS-CoV-2, Severe acute respiratory syndrome coronavirus-2; MERS-CoV, Middle east respiratory syndrome coronavirus; IBV, Infectious bronchitis virus; BWCoV-SW1, Beluga whale coronavirus SW1; PDCoV, Porcine delta-coronavirus; CMCoV, Common-moorhen coronavirus; ALCCoV, Asian leopard cat coronavirus; WBV, white bream virus; EToV, Equine torovirus; BToV, Bovine torovirus; PToV, Porcine torovirus; HToV, human torovirus; PRRSV, porcine reproductive and respiratory syndrome virus; EAV, Equine arteritis virus; LDV, Lactate dehydrogenase elevating virus; SHFV, Simian hemorrhagic fever virus; YHV, Yellow head virus; GAV, Gill-associated virus; DKNV, Dak nong virus; CavV, Cavally virus; NDiV, Nam Dinh virus.

WHO by 25 October 2023 (Cheng et al., 2020; Petrosillo et al., 2020; Zhu et al., 2020; Salzberger et al., 2021). In fact, the real infections and deaths number are severely underestimated. As the omicron variant has become the predominant strain and the herd immunity has been established, the mortality rate of SARS-CoV-2 is continuing to decline.

Additionally, *Coronavirinae* turns out an important concern for veterinary. It is currently known that six coronaviruses infect pigs, including transmissible gastroenteritis virus (TEGV), porcine respiratory coronavirus (PRCV), swine acute diarrhea syndrome coronavirus (SADS-CoV), porcine hemagglutinating encephalomyelitis virus (PHEV), porcine epidemic diarrhea virus (PEDV), and porcine δ-coronavirus (PDCoV) (Mora-Díaz et al., 2019; Liu and Wang, 2021; Turlewicz-Podbielska and Pomorska-Mol, 2021). Specifically, TGEV，PRCV, and PHEV have been commonly found in pig herds worldwide for decades, whereas PEDV, SADS-CoV, and PDCoV have been identified more recently and cause clinically indistinguishable acute gastroenteritis, especially lethal to newborn piglets, posing significant challenges to the porcine breeding industry. As the first discovered coronavirus in the 1930's, infectious bronchitis virus (IBV) belongs to the genus of *γ-Coronavirus* and is a highly contagious respiratory virus that causes significant economic loss in the poultry farm. It primarily infects chickens, causing respiratory signs such as depression, coughing, sneezing, nasal discharge, and even death (Najimudeen et al., 2020). Despite routine efforts in its vaccination, this virus is becoming increasingly difficult to prevent and control as a result of its high mutation rate and unpredictable emergence of diverse types throughout the world (Cavanagh, 2007; Khataby et al., 2016; Bande et al., 2017).

With a size of approximately 25–30 kb, the subfamily *Torovirinae* shares similar genome organization with *Coronavirnae* and has two genera: *Torovirus* and *Bafinivirus* (Snijder and Horzinek, 1993; Cavanagh et al., 1994; Koopmans and Horzinek, 1994; de Vries et al., 1997). Four virus species under this genus have been identified to date: equine torovirus (EToV), bovine torovirus (BToV), porcine torovirus (PToV), and human torovirus (HToV), with genetic divergence of 20–40% (Ujike and Taguchi, 2021). Infections of torovirus have been reported worldwide, with cases documented in Europe, America, Asia, New Zealand, and South Africa (Durham et al., 1989; Penrith and Gerdes, 1992; Koopmans and Horzinek, 1994; Cavanagh, 1997; Ujike and Taguchi, 2021). These viruses can cause various gastrointestinal and respiratory symptoms in their respective host species: EToV is known to cause gastrointestinal and respiratory infections in horses and is the only torovirus which has been successfully cultured *in vitro* (Kuwabara et al., 2007); BToV primarily infects cattle and cows with diarrhea and respiratory symptoms (Ito et al., 2009; Aita et al., 2012; Lojkic et al., 2015); PToV mainly brings about gastrointestinal infection in pigs，with its coinfections with other pathogens usually exacerbating the symptoms (Hu et al., 2019); HToV associates with gastroenteritis and diarrhea in children as well as necrotizing enterocolitis in infants (Durham

TABLE 1 The classification of *Nidovirales*.

Family	Sub-family	Genus	Virus species	Host	Genome size (kb)	Genbank accession no
Coronaviridae	*Coronavirinae*	*α-coronavirus*	PEDV	Swine	28.031	MK841495.1
			TGEV	Swine	28.572	DQ811788.1
			CCoV	Canine	29.051	MT114538.1
			FCoV	Feline	29.273	DQ848678.1
			HCoV-229E	Human	27.021	KU291448.1
			HCoV-NL63	Human	27.537	DQ445912.1
			CCoV-HuPn-2018	Human	29.089	MW591993.2
		β-coronavirus	BCoV	Bovine	31.031	U00735.2
			ECoV	Equine	30.943	OL770366.1
			CrCoV	Canine	30.876	KX432213.1
			MHV	Murine	31.291	FJ647225.1
			HCoV-OC43	Human	30.753	KU131570.1
			HCoV-HKU1	Human	29.811	MH940245.1
			SARS-CoV-1	Human	29.746	AY545919.1
			SARS-CoV-2	Human	29.903	NC_045512.2
			MERS-CoV	Human	30.031	MH734115.1
		γ-coronavirus	IBV	Avian	27.608	NC_001451.1
			TCoV	Avian	27.657	NC_010800.1
		δ-coronavirus	PDCoV	Swine	25.370	MN942260.1
			HKU11	Bulbul	26.487	NC_011547.1
			HKU12	Thrush	26.396	NC_011549.1
	Torovirinae	*Bafinivirus*	WBV	White bream	26.660	NC_008516.1
		Torovirus	EToV	Equine	a part of sequence	DQ310701.1
			BToV	Bovine	28.341	MN882587.1
			PToV	Swine	28.305	KM403390.1
			HToV	Human	a part of sequence	KJ645983.1
Arteriviridae		*Arterivirus*	PRRSV	Swine	15.447	AY150312.1
			EAV	Equine	12.704	MG137481.1
			LDV	Murine	14.104	NC_001639.1
			SHFV	Primate (Macaque)	15.717	NC_003092.2
Roniviridae		*Okavirus*	YHV	Shrimp	26.672	FJ848673.1
			GAV	Prawn	26.253	NC_010306.1
			Okavirus	Shrimp	26.662	FJ848674.1
Mesoniviridae		*α-mesonivirus*	DKNV	Culex	20.125	OV054251.1
			CavV	Culex	20.128	NC_015668.1
			NDiV	Vishnui	20.074	NC_020901.1

et al., 1989). The genus of *Bafinivirus* that infects fish was discovered in 2006 (Schütze et al., 2006).

2.2 *Arteriviridae*

The *Arteriviridae* was established as a distinct family in 1996; later on, it was grouped into the order *Nidovirales* because it shares similarities with the family *Coronaviridae* (Cavanagh, 1997; Snijder and Meulenberg, 1998; Gorbalenya et al., 2006; King et al., 2012). Arterivirus particles are spherical and enveloped, with a core housing the RNA genome of approximately 12.7–15.7 kb (Plagemann and Moennig, 1992). Unlike coronaviruses, arteriviruses do not have an obvious spike protein on their surface. Instead, they have relatively small protrusions. The envelope consists of several proteins, including two major envelope proteins GP5-M heterodimer, three minor proteins GP2-GP3-GP4 heterotrimer and GP2-GP4 heterodimer, and two minor protein E and 5a (Snijder et al., 2013). All envelope proteins

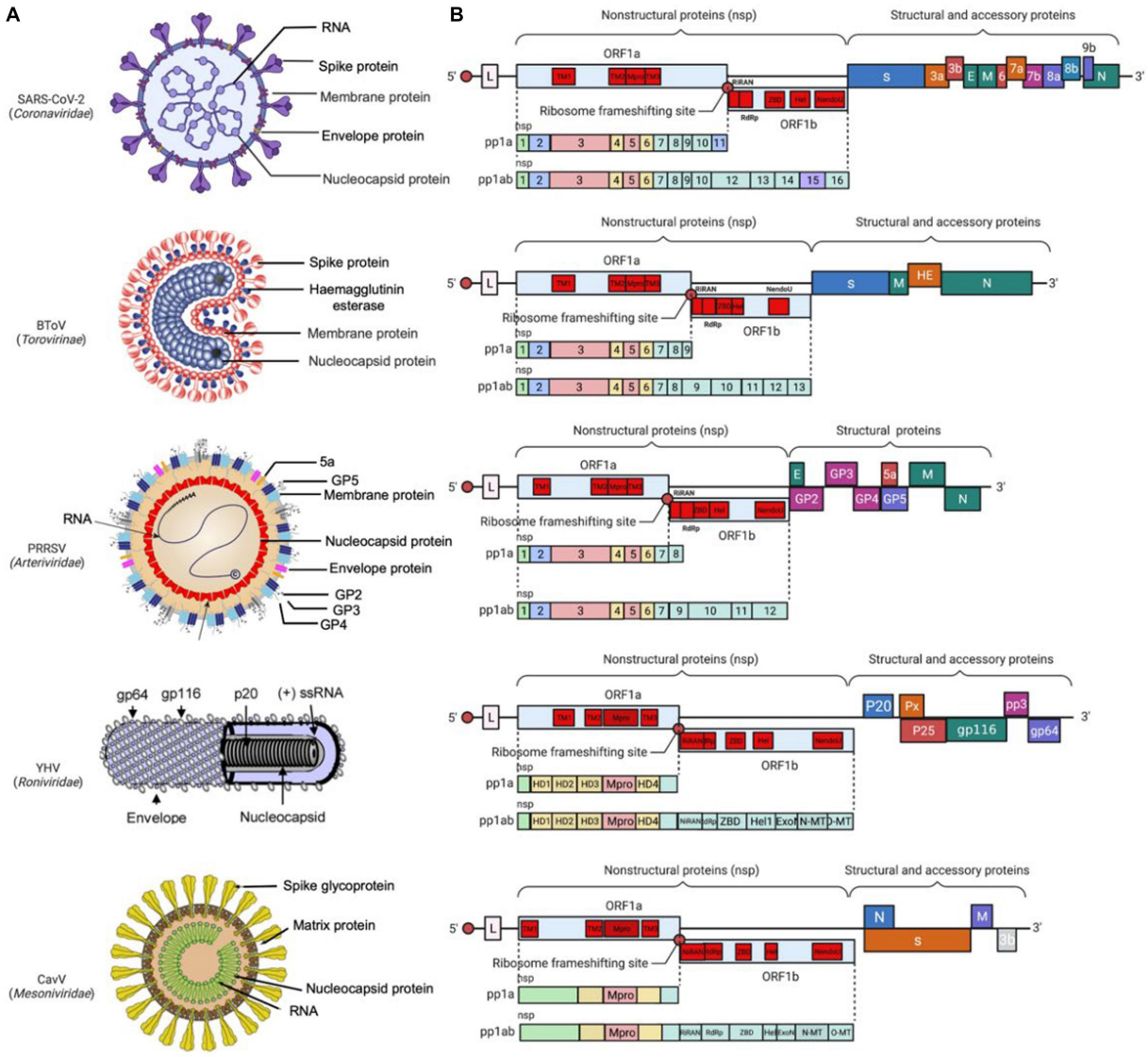

FIGURE 3
Prototype virus particle and genome structure of *Nidovirales*. **(A)** The prototype virus in each family is represented in the diagram, including SARS-CoV-2 from *Coronaviridae,* BToV from *Torovirus*, porcine reproductive and respiratory syndrome virus (PRRSV) from *Arteriviridae,* YHV from *Roniviridae*, and CavV from *Mesoniviridae*. **(B)** Genome organization of the prototype virus (SARS-CoV-2, BToV, PRRSV, YHV, CavV) in each family: the replicase ORF1a and ORF1b are followed by the genes encoding structural and accessory proteins. Red circles represent ribosomal frameshifting sites, and the rectangles represent the open reading frames (ORFs). Colored patterns represent domains common to all nidovirus.

are critical for producing infectious progeny (Dea et al., 2000; Wissink et al., 2005; Music and Gagnon, 2010). Inside the envelope, there is RNA genome wrapped with N protein, which form a pleomorphic core with a mean diameter of 39 nm (Spilman et al., 2009; Dokland, 2010) (Figure 3A). The diame1ter of the virus particles, observed under the cryo-electron microscopy, was approximately 50–60 nm, significantly smaller than coronaviruses (Spilman et al., 2009).

The *Arteriviridae* primarily infect mammals, including equid, swine, opossum, non-human primate, and rodent (Plagemann and Moennig, 1992). One notable member of this family is the prototype equine arteritis virus (EAV), which was firstly discovered in 1957 and is known to infect horses (Bryans et al., 1957; Del Piero, 2000; Balasuriya et al., 2013). Another two species of lactate dehydrogenase-elevating virus (LDV) and simian hemorrhagic fever virus (SHFV), were firstly isolated more than 50 years ago. SHFV is known to cause a highly lethal fever in African non-human primates while LDV infects mice (Riley et al., 1960; Notkins and Shochat, 1963; Plagemann et al., 1995; Snijder and Meulenberg, 1998; Brinton et al., 2015). The porcine reproductive and respiratory syndrome virus (PRRSV) is a highly contagious virus that infect pigs, and its emergence causes significant economic losses to the global swine industry (Neumann et al., 2005; Tian et al., 2007; Lunney et al., 2016; Guo et al., 2018; Zhang H. et al., 2022). Arteriviruses are transmitted through respiratory routes or body fluids; in most cases, they affect macrophages. They can cause a range of symptoms, including persistent or acute asymptomatic infections, miscarriage, respiratory disease, arthritis, fatal hemorrhagic fever, and polio (Snijder et al., 2013). For example, EAV and PRRSV are known to cause mild-to-severe respiratory disease and lead to abortion in pregnant animals (Balasuriya and Carossino, 2017). Due to their veterinary importance,

EAV and PRRSV have been characterized extensively, severing as the basis for our current understanding of arterivirus.

2.3 *Roniviridae*

The family *Roniviridae* include a single genus called *Okavirus* which infect crustacean, mostly shrimp (Cowley et al., 2000; Walker et al., 2021). The virus particles are enveloped with bacilliform geometries and helical symmetry, with a diameter of around 40–60 nm and a genome of 26–27 kb inside (Dhar et al., 2004; Figure 3A). The genus *Okavirus* includes gill-associated virus (GAV) and yellow head virus (YHV), which have been found to associate with mortality in cultured black tiger prawns (*Penaeus monodon*) and white Pacific prawns (*Penaeus vannamei*). It has been reported that these viruses caused economic loss in shrimp farm in Eastern Australia, Thailand, and China (Cowley et al., 2001; Munro and Owens, 2007; Munro et al., 2011; Dong et al., 2017). They have been listed as notifiable pathogens by the World Organization for Animal Health.

2.4 *Mesoniviridae*

Found in 2011, the *Mesoniviridae* has only one genus called *α-Mesonivirus*, which are mosquito-specific virus with a wide geographic distribution (Nga et al., 2011; Zirkel et al., 2011; Lauber et al., 2012; Vasilakis et al., 2014). Belonging to the genus *α-Mesonivirus*, Cavally virus (CavV) and Nam Dinh virus (NDiV) have been the first two characterized mesoniviruses (Nga et al., 2011; Zirkel et al., 2011). These two viruses are closely related and belong to the same species, *α-Mesonivirus* 1. Other phylogenetically diverse mesoniviruses are isolated from a range of mosquito species and geographic locations (Kuwata et al., 2013; Thuy et al., 2013; Zirkel et al., 2013). The mesonivirus particles are about 120 nm in diameter, with rod-shaped spike protein (77 kDa) and differentially glycosylated membrane proteins (17, 18, 19, 20 kDa) on the surface, and a nucleocapsid (25 kDa-N protein and 20 kb-RNA genome) inside (Figure 3A).

3 RNA genome

The *Nidovirales* genome have been studied extensively in recent decades (de Vries et al., 1997; Gorbalenya et al., 2006). Despite variations in genome size and virus particle morphology, *Nidovirales* have been classified primarily based on their common genetic organization, a set of conserved domains and enzyme functions within the polyproteins, and their unique transcription strategy (King et al., 2012). The 5′-proximal genome contains two ORFs (ORF1a and ORF1b), which encompass two-thirds of the genome and encode two giant polyproteins pp1a and pp1ab. These two ORFs possess a conserved domain backbone, including their domains in the sequential order as follows: 5′-TM1-TM2-Mpro-TM3-NiRAN-RdRp-ZBD-HEL-NendoU-3′ (the first four in ORF1a while the remaining in ORF1b) (King et al., 2012). The 3′-proximal genome contains smaller ORFs, which encode structural proteins and accessory proteins, as translated from co-terminal sg mRNAs. These ORFs are different in number, size, and length in different families, and some accessory genes are unique to certain virus species, especially in coronaviruses (de Vries et al., 1997; Figure 3B). In addition, at the 5′- and 3′-termini, there are untranslated regions (UTR) which can regulate the viral RNA replication and transcription.

After virus entry and uncoating, the gRNA is released into the cytosol, and directly serves as a template for transcription, enabling cap-dependent translation of ORF1a to produce pp1a. In addition, an RNA pseudoknot structure is located near the end of ORF1a together with a slippery sequence of "UUUAAC," enabling −1 or −2 ribosomal frameshift and translation on ORF1b to produce a longer pp1ab (Brierley et al., 1989; Plant et al., 2005; Patel et al., 2020). Pp1a and pp1ab are cleaved by intrinsic proteases, either co-translationally or post-translationally, to generate mature NSPs, including papain-like proteases (PLPs), NSPs with TM (TM1, TM2, TM3), 3C-like main protease (Mpro), nucleotidyltransferase (NiRAN), RdRp, superfamily 1 helicase (ZBD-HEL), and endoribonuclease (NendoU) (Gorbalenya et al., 1989; Ziebuhr et al., 2000; Li et al., 2015). The proteins encoded by ORF1a play a significant role in modulation of host gene expression, cleavage and maturation of pp1a and pp1ab (PLP and Mpro) (Ziebuhr et al., 2000), and modification of host membranes so as to create an environment suitable for viral genome synthesis (NSPs with TM1, TM2, or TM3) (van der Hoeven et al., 2016), while the proteins encoded by ORF1b play an important role in RNA replication and transcription, including NiRAN, RdRp, HEL, and NendoU, referred to as replicases (Liu et al., 1994; Thiel et al., 2001; Fang and Snijder, 2010; Lehmann et al., 2015c; Hu et al., 2021). Next, we focus on reviewing these replicases.

4 Replicases

4.1 PLP and 3CLpro (Mpro)

Nidoviruses encode multiple PLPs and a 3CLpro (also called Mpro) (Ziebuhr et al., 2000; Snijder et al., 2013). The PLPs are located in the upstream of TM1 and are present in NSP2 for arteriviruses and in NSP3 for coronaviruses (Snijder et al., 1995; Kanjanahaluethai and Baker, 2000; Ziebuhr et al., 2001; Harcourt et al., 2004). The number of active PLP domains can vary from one virus species to another (Vatter et al., 2014). Structural and enzymatic studies reveal that the PLPs not only cleave peptide bonds (NSP1/NSP2/NSP3 junctions in arteriviruses and NSP1/NSP2/NSP3/NSP4 junctions in coronaviruses) but also act as a deubiquitinating (DUB) enzyme to remove Lys63-linked ubiquitin chains or ubiquitin-like modifiers (ISG15) from host substrates, antagonizing the innate immune response (Frias-Staheli et al., 2007; van Kasteren et al., 2012). Mpro, a chymotrypsin-like protease that plays the main role in the polyprotein processing, is located in NSP4 for arteriviruses and NSP5 for coronaviruses, respectively (Tian et al., 2009). Mpro cleaves all sites downstream of NSP3 for arteriviruses and downstream of NSP4 for coronaviruses (Ziebuhr et al., 2000; Tian et al., 2009). As these proteases facilitate the cleavage of pp1a/pp1ab and maturation of the replicases, the conserved functional enzymatic structures are becoming the optimal therapeutic targets (Dai et al., 2020; Khare et al., 2020; Zhang L. et al., 2020; Banerjee et al., 2021; Capasso et al., 2021). For example, the FDA authorized Paxlovid (nirmatrelvir/ritonavir) specifically targets at the Mpro of SARS-CoV-2 to block the enzymatic function, thereby effectively reducing virus replication and resulting in a great decrease of hospitalization and death among the COVID-19 patients (Graham, 2021; Cokley et al., 2022; Marzolini et al., 2022; Amani and Amani, 2023; Harris, 2023).

4.2 Transmembrane proteins

ORF1a encodes three TM proteins (TM1, TM2, and TM3), namely NSP2, NSP3, NSP5 in arteriviruses and NSP3, NSP4, NSP6 in coronaviruses. TM1 and TM2 reside upstream of the Mpro, while TM3 is located at its downstream (Figure 3B). All of the TM proteins span across the membrane more than once. These TM proteins play a crucial role in modifying intracellular membranes to form DMV, DMS, or CM, which accommodate the RTC and associate with viral RNA synthesis (Bost et al., 2000; Snijder et al., 2006; Posthuma et al., 2008; Angelini et al., 2013; Hagemeijer et al., 2014; van der Hoeven et al., 2016; Oudshoorn et al., 2017). However, their biological significance needs to be further studied.

4.3 RNA-dependent RNA polymerase (RdRp)

RdRp is encoded by the N-terminal region of ORF1b (the enzymatic domain is present in NSP9 for arteriviruses and NSP12 for coronaviruses). It is the critical component of RTC to catalyze the synthesis of RNA with the help of helicase, NendoU, and ribose-2'-O-methyltransferase (O-MTase), and thus plays a crucial role in the replication and transcription (Subissi et al., 2014; Lehmann et al., 2016). Our current knowledge of the structural and enzymatic characteristics of RdRp primarily comes from studies conducted on SARS-CoV and SARS-CoV-2 (Kirchdoerfer and Ward, 2019; Gao et al., 2020). RdRp consists of three domains: a canonical RdRp core domain at C-terminus (occupying two-thirds of the protein), a NiRAN domain at N-terminus, and an interface domain (Figure 4C) (Lehmann et al., 2015a; Posthuma et al., 2017).

The RdRp core domain can be further divided into three subdomains: fingers, palm, and thumb subdomains. In the active site there are multiple functional motifs (6 in arteriviruses and 7 in coronaviruses), named A-G respectively, which are responsible for recognizing the RNA template and substrate, as well as catalyzing the condensation of nucleotides (Poch et al., 1989; Lehmann et al., 2016; Kirchdoerfer and Ward, 2019; Gao et al., 2020). The motif A contains the divalent-cation-binding residues D (D619 and D623 in SARS-CoV-1 NSP12, D618 in and D623 in SARS-CoV-2 NSP12, and D445 and D450 in EAV NSP9), while motif C contains the conserved catalytic residues SDD sequence (residues 759–761 in SARS-CoV-1 and SARS-CoV-2 NSP12, and residues 559–561 in EAV NSP9). The RNA template is supposed to enter the active site in motifs A and C, and the NTP entry channel is within motif F, as determined by the cryo-electron microscopy structure of SARS-CoV-2 NSP12 (Gao et al., 2020). With its key role in viral RNA replication and transcription, RdRp is considered as a primary target for antiviral inhibitors that are designed to mimic nucleotides and inhibit viral RNA replication and transcription. For example, remdesivir is nucleotide analogs which can interfere with the action of RdRp and arrest the RNA synthesis process by delaying the elongation (Gordon et al., 2020a,b). It is the first drugs authorized by FDA for treatment of COVID-19.

As a unique and essential enzymatic domain of *Nidovirales* (Lehmann et al., 2015a), the N-terminal NiRAN domain possesses a self-nucleotidylating activity, which is important for viral RNA replication. It is speculated that the NiRAN might perform multiple functions, for example, it may act as an RNA ligase in mRNA capping (Yan et al., 2021), or serve in protein-primed initiation of RNA synthesis by transferring a NMP to another viral protein NSP9 (Wang B. et al., 2021). These hypotheses have been extensively discussed in a study by Lehmann et al. (2015a).

4.4 Helicase

Based on structural and functional characteristics, helicases can be classified into two subfamilies-SF1 (ZmHEL1) and SF2. The 5′-to-3′ helicase (NSP10 for arteriviruses and NSP13 for coronaviruses) belong to SF1 (ZmHEL1). This helicase domain is exceptionally located downstream of the RdRp in *Nidovirales* (Gorbalenya et al., 1989), while in other families of positive sense single-stranded RNA viruses, it is located upstream of RdRp. As a helicase, ZmHEL1 possesses a conserved N-terminal zinc-binding domain that is commonly found in nidoviruses and is involved in unwinding activity (Seybert et al., 2005; Shi et al., 2020; Tang et al., 2020; Maio et al., 2023). The helicase activity combined with NTP-binding activity plays the vital role in unwinding RNA molecules in the 5′-3′ direction (Seybert et al., 2000a; Ivanov et al., 2004b; Shu et al., 2020; Ren et al., 2021; Fang et al., 2023).

4.5 Endoribonuclease (NendoU)

NendoU is a protein that is specific to *Nidovirales*, including NSP11 for arteriviruses and NSP15 for coronaviruses, a conserved protein that does not have counterparts in other RNA viruses, thus serving as a diagnostic molecular marker for nidovirus (Ivanov et al., 2004a; Gorbalenya et al., 2006; Deng and Baker, 2018). One of its functions of is to cleave the poly (U) sequence which are produced during genome replication/transcription and are found in viral −RNA intermediates, thereby regulating the ratio of −RNA to +RNA and reducing the accumulation of dsRNA. In this way, this protein facilitates the genome replication and synthesis of sg mRNA and also contributes to the evasion of IFN response by reducing the accumulation of dsRNA accumulation (Hackbart et al., 2020; Gao et al., 2021).

4.6 Other replicases

In addition to above conserved replicases, several other conserved replicases that perform RNA synthesis and processing have been identified in some but not all nidoviruses (Posthuma et al., 2017). There are two clades of nidoviruses: one with a large genome size ranging from 25 to 31.7 kb (*Coronaviridae*, *Torovirinae*, and *Roniviridae*), and the other with a small genome size ranging from 12.7 to 15.7 kb (*Arteriviridae*) (Gorbalenya et al., 2006). As a result, the replicase polyproteins of large nidoviruses contain two specific activities that are not found in *Arteriviridae*, namely 3′-5′exoribonuclease (ExoN) encoded by NSP14 (Chen Y. et al., 2009; Tahir, 2021) and O-MTase encoded by NSP16 (Decroly et al., 2011). ExoN is essential for the high fidelity of long RNA synthesis, while O-MTase helps to add the cap structure at the 5′-terminus of viral RNA (Posthuma et al., 2017). The mimicking of host mRNA cap helps the virus to escape the

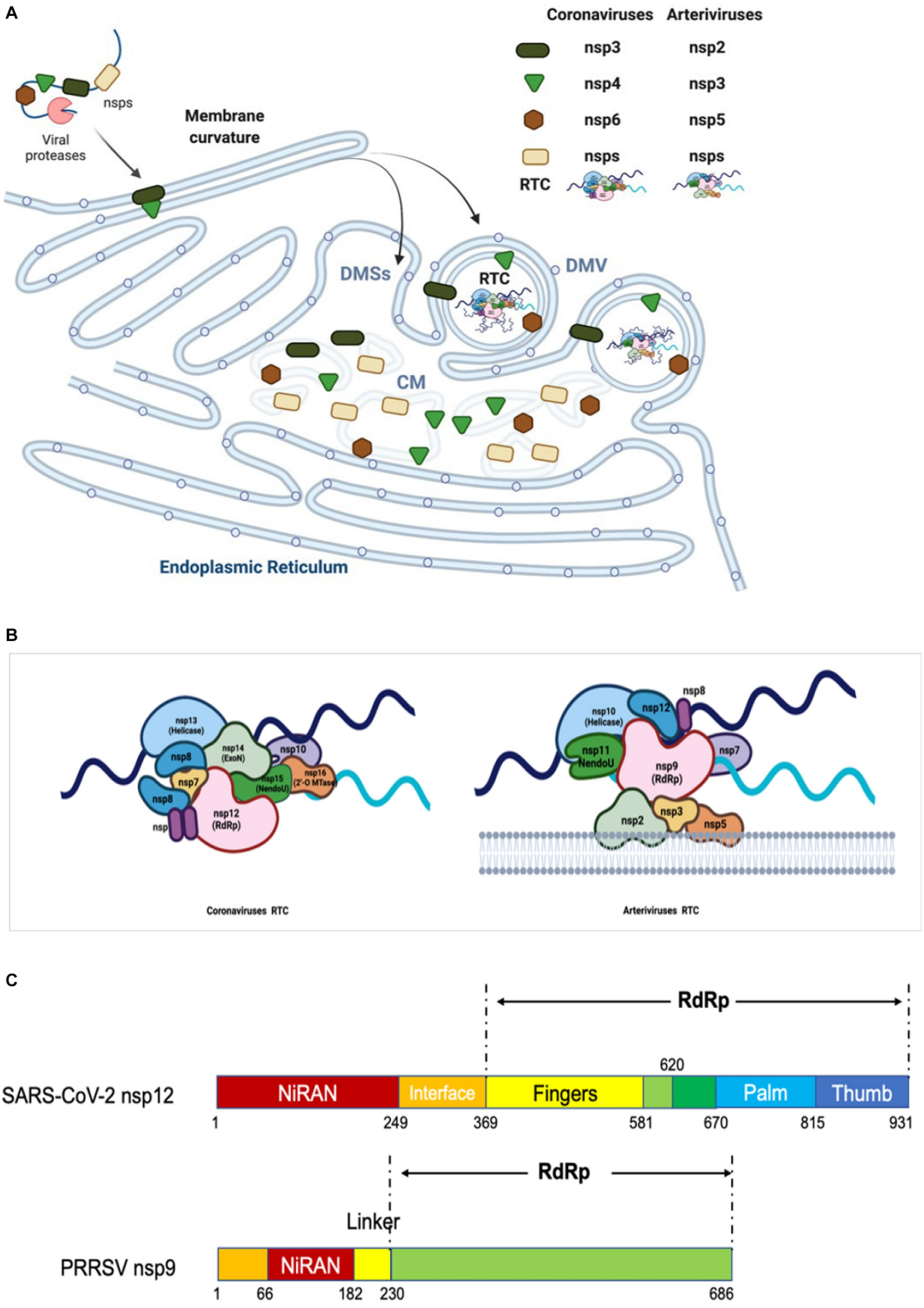

FIGURE 4
Diagram of replication/transcription organelle and RTC. **(A)** Diagram of CMs/DMVs/DMSs. Nidovirus infection leads to the rearrangement of ER membranes and the envelopment of RTC. During this process, the NSPs containing TM are cleaved from pp1a and pp1ab, and then embedded in the ER membrane to form a membrane fold and luminal loops. These interactions yield a complex array of CMs, DMSs or DMVs, which are contiguous with ER membranes. The replicases cleaved from pp1a and pp1ab interact each other and form RTC in DMV. **(B)** Model of RTC. The core RTC is composed of the RdRp (coronavirus: NSP12; arterivirus: NSP9), processivity factors (coronavirus: NSP7-9; arterivirus: NSP12), ExoN complex (coronavirus: NSP10 and NSP14), NendoU (coronavirus: NSP15; arterivirus: NSP11), and helicase (coronavirus: NSP13; arterivirus: NSP10). As shown, for coronavirus, the NendoU is the center of the RTC complex, capped on the two sides by NSP14/NSP16/$(NSP10)_2$, which afterwards recruits NSP12/NSP7/$(NSP8)_2$ to the complex. Helicase is around the ExoN complex. The model is based on the known structure and interactions between the proteins (243). **(C)** The functional domains of RdRp of coronavirus and arterivirus are shown.

host detection, thereby evading the innate immune responses (Chen and Guo, 2016). The importance of NSP16 for coronavirus infection and pathogenesis makes it becoming an attractive target for antiviral therapeutic treatment (Menachery et al., 2014; Chang and Chen, 2021; Tahir, 2021).

The other two RNA-processing domains conserved in *Coronavidae* and *Torovirinae* are ADP-ribose-1′-phosphatase (ADRP) and nucleotide cyclic phosphodiesterase (CPD) respectively (Snijder et al., 2003; Draker et al., 2006). The ADRP domain encoded by ORF1a plays a role in the cellular RNA processing pathway by removing the phosphate from the adenosine diphosphate ribose 1′-phosphate substrate (Michalska et al., 2020). However, the highly specific phosphatase activity is not essential for viral replication, which has been demonstrated by substitutions of active-site residues or complete deletion of the ADRP domain (Putics et al., 2005; Hurst-Hess et al., 2015). The ADRP domain is found in the similar position NSP3 of both families *Coronavidae* and *Torovirinae*, indicating that this region is inherited from a common ancestor. Whereas, the CPD domain is only present in the family *Torovirinae* and *Coronavidae* MHV. In MHV, the CPD domain is expressed by ORF2 though deletion of the CPD-encoding ORF2 does not affect the replication of MHV *in vivo* (Schwarz et al., 1990); however, the other study shows that the mutation of MHV ORF2 causes a attenuated form of the virus in its natural host (Sperry et al., 2005). Thus, the CPD domain of MHV may be one of the determinants of virus pathogenicity. In *Torovirinae*, this enzyme is encoded by the 3′ end of replicase of ORF1a and located immediately upstream of the ORF1a/ORF1b junction, which is involved in the processing of viral RNA (Snijder et al., 1991).

5 RNA synthesis

5.1 Formation of DMVs

Nidovirales replicates its genome in the ER membrane-associated structures known as "replication organelles," which include a complex vesculo-tubular network of CMs, DMVs, and DMSs, partly interconnected through their outer membranes. The SARS-CoV dsRNA is mainly found inside the DMVs (Knoops et al., 2008), while the newly synthesized MHV RNA is located in close proximity to both DMVs and CMs (Gosert et al., 2002); furthermore, the viral RNA positively correlates with the number of DMVs (Ulasli et al., 2010). Above observations suggest that both DMVs and CMs serve as sites for the synthesis of viral RNA.

The rearrangement of the host membranes is important to create a micro-environment appropriate for the synthesis of viral RNA and the recruitment of host factors. The association of viral RNA synthesis with membrane structures exhibits several advantages: (1) An appropriate environment is created by anchoring the viral replicases necessary for replication and transcription; (2) By anchoring viral replication complex to membrane structures, the environment is created for the diffusion of metabolites and macromolecules, so as to facilitate the synthesis process; (3) Compartmentalization helps to separate and organize the process of replication/transcription, translation, and packaging, which ensures that these processes occur in a coordinated manner. It also creates a protected environment for viral RNA replication by eluding recognition and degradation of RNA in the cytosol; (4) The insulation of the RNA replication/transcription intermediates, such as dsRNA, could hinder or delay the host's innate immune response (Neufeldt et al., 2016; van der Hoeven et al., 2016).

The DMVs (about 100 nm) of arterivirus was firstly observed in the perinuclear region of the cell with the electron microscopy since 1970s (Wood et al., 1970), as so observed in other members of this family later on (Stueckemann et al., 1982; Wada et al., 1995; Weiland et al., 1995; Pol et al., 1997; Pedersen et al., 1999). These DMVs are connected to reticular regions of CMs between them, and contiguous with the membrane donor ER. Additionally, the ribosomes are close to the outer membrane of the DMVs (Wood et al., 1970; Stueckemann et al., 1982; van der Hoeven et al., 2016).

The expression of EAV NSP2 and NSP3 (contain TM1 and TM2) is sufficient to induce the DMVs formation and NSP3 plays a key role in the remodeling of membranes (Posthuma et al., 2008); however, the presence of additional NSP5 results in the production of DMVs whose size is more homogenous and closer to those formed in EAV-infected cells ($83 + -21$ nm, $n = 145$) (Figure 4A), indicating a regulatory role for NSP5 in regulating the membranes curvatures and formation of DMVs (van der Hoeven et al., 2016). The NSP2, NSP3 and NSP5 of arterivirus are believed to serve as DMVs scaffolding proteins to recruit other components of RTC to the replicase site (Pedersen et al., 1999; Posthuma et al., 2008; van der Hoeven et al., 2016).

Diverse coronaviruses induce similar membrane structures, including DMVs and DMSs (Snijder et al., 2020; Zhang J. et al., 2020). The DMVs are around twice in the diameter and 8-fold in the volume of those arterivirus-induced DMVs. The SARS-CoV induced DMVs connect with other DMVs and also connect to the ER through their outer membranes (Knoops et al., 2008). 3D electron microscopy reconstructions and living cell imaging also show that SARS-CoV-2 induced DMVs are tethered to the ER, with alteration of the mitochondrial network, remodeling of cytoskeleton elements, and recruitment of peroxisomes to DMVs (Cortese et al., 2020). The *γ-Coronavirus* IBV-induced DMVs are either tethered to the zippered ER with channel connecting the interior of the DMVs with the cytoplasm, or exists as isolated vesicles without DMV-DMV or DMV-ER connections (Maier et al., 2013; Doyle et al., 2018). The use of H3-uridine to metabolically label the newly synthesized molecules enables researcher to reaffirm that DMVs provide an optimal environment for virus RNA synthesis (Snijder et al., 2020), which is further supported by the use of specific antibodies to bind to the target molecules, such as dsRNA and DMVs (Knoops et al., 2008). Recent findings from cryotomography reveal the presence of membrane-spanning hexameric, crown-shaped pore complex in MHV induced DMVs, which makes the viral RNA exporting from DMVs possible. The observation of nucleocapsid structure on the cytosolic side of the DMVs demonstrates that the RNA is exported from DMVs for encapsidation (Wolff et al., 2020).

For coronavirus, the formation of DMVs can be induced by co-expression of NSP3, NSP4, and NSP6 (Angelini et al., 2013; Oudshoorn et al., 2017), which contain three conserved TMs respectively, and are functionally analogous to arterivirus NSP2, NSP3, and NSP5 (Gorbalenya et al., 2006; Figure 4A). The co-expression of three SARS-CoV NSPs (namely NSP3, NSP4, and NSP6) forms both DMVs and other structures resembling the CMs and DMSs presented in SARS-CoV infection (Angelini et al., 2013).

Report also shows that MERS-CoV NSP3 and NSP4 can rearrange the cellular membranes to generate DMVs where the RTC is assembled and anchored (Oudshoorn et al., 2017). Co-expression of SARS-CoV-2 NSP3 and NSP4 also generate DMVs, whereas NSP6 zippers ER membrane and forms the connectors. NSP6 may act as filter in communication between the DMVs and the ER, organizer of DMV cluster, or may mediate contact with lipid droplets (Ricciardi et al., 2022). The co-expression of IBV NSP3, NSP4, NSP6 generates DMVs, and NSP4 alone is sufficient to induce membrane pairing, but not fully resembles DMVs (Doyle et al., 2018).

In both arteriviruses and coronaviruses, it is likely that the proteins containing TM1 and TM2 can induce the formation of DMVs, while the protein comprising TM3 may only modulate the formation of DMVs. Recently, it has been found that ER proteins VMP1 and TMEM41B contribute to DMV formation by facilitating NSP3-NSP4 interaction and ER zipping or subsequent closing of DMVs; the phosphatidylserine (PA) levels is also important for DMV formation (Ji et al., 2023). More and more evidences show that autophagy machinery and ER-associated degradation machinery are hijacked by coronavirus for the DMV formation (Prentice et al., 2004; Twu et al., 2021; Liang et al., 2022; Tan et al., 2023). It should be further investigated whether more host factors are involved in the formation of DMV.

5.2 Formation of RTC

For efficient replication, multiple replicases interact each other to form RTC and then the RTC attaches to modified intracellular membranes, resulting in the formation of a membrane-bound complex which is responsible for RNA synthesis (Sawicki et al., 2005). The association of RTC with modified intracellular membranes is a feature commonly observed in the positive-stranded RNA viruses that infect animals. As for coronavirus, a set of replicases (NSP7, NSP8, NSP9, NSP10, NSP12, NSP13, NSP14, NSP15, and NSP16) assemble into the RTC which is responsible for synthesizing the negative-stranded intermediates, gRNA, and sg mRNAs (Hagemeijer et al., 2010; Subissi et al., 2012; Kirchdoerfer and Ward, 2019; Chen et al., 2020; Hillen et al., 2020; Peng et al., 2020; Wang et al., 2020; Yan et al., 2020, 2021; Mishchenko and Ivanisenko, 2022). The NSP7-NSP8-NSP12 complex plays a central role in the replication/transcription process of coronavirus. NSP12 contains the RdRp domain in its C-terminal region, and serves as the key enzyme for catalyzing the incorporation of NTPs into the growing RNA chain. In collaboration with NSP7 and NSP8, NSP12 forms a holoenzyme RdRp (holo-RdRp) to drive the RNA synthesis in primer-dependent manner (te Velthuis et al., 2010; Ahn et al., 2012; Kirchdoerfer and Ward, 2019; Peng et al., 2020). The primers for the RNA replication/transcription are synthesized by NSP8, which bears a noncanonical RdRp activity and acts as an RNA primase (Imbert et al., 2006; te Velthuis et al., 2012; Biswal et al., 2021). Other subunits have supporting roles in the RTC. When this complex is working, two subunits of NSP13 are positioned above the RTC in which one subunit binds to the 5′ end of the RNA template downstream at the NSP12 RdRp active site for 5′-3′ nucleic acid unwinding (Perry et al., 2021). As a unique ExoN encoded by coronavirus, NSP14 forms an RNA proof reading complex together with NSP10 (Denison et al., 2011; Tahir, 2021). The mismatched base is directed into the shallow active site of the ExoN domain in which it interacts with conserved catalytic residues. Meanwhile, a portion of the dsRNA molecule interacts with both the N-terminus of NSP10 and the residues which are located outside the catalytic site of NSP14-ExoN (Ferron et al., 2018). Associated with RTC, the NSP15 is responsible for cleaving the −RNA intermediates to adjust the ratio of +RNA to −RNA, and reduce the level of dsRNA so as to help the virus escape the host innate immune response (Athmer et al., 2017; Deng and Baker, 2018; Gao et al., 2021; Perry et al., 2021). NSP16 is located in the RTC and responsible for the RNA capping together with NSP10 (Snijder et al., 2016; Benoni et al., 2021). NSP9 inhibits and controls the catalytic activity by inserting into the catalytic center of NSP12 (Slanina et al., 2021; Yan et al., 2021) (Figure 4B).

Similar to coronavirus, the assembly of RTC in arterivirus also requires multiple NSPs to work together. By examining location of PRRSV NSPs during infection, Song et al. found that NSP2, NSP4, NSP7, NSP8, NSP9, NSP10, NSP11, and NSP12 were colocalized well with dsRNA which reveals the virus replication sites, indicating all these NSPs are located to viral RTC (Song et al., 2018). Although NSP3, NSP5, and NSP6 were not examined due to lack of antibodies, the interaction among NSP2, NSP3 and NSP5 suggests that NSP3 and NSP5 are associated with RTC. The core components of arterivirus RTC are possibly composed of all NSPs encoded by ORF1b, including NSP9, NSP10, NSP11, and NSP12 (Snijder et al., 2013). The NSP2, NSP3, NSP5 are responsible for the formation of DMVs and interact with other NSPs to recruit the RTC core components (Nan et al., 2018). The C-terminus of NSP9 involves the function of RdRp, while the N-terminal of NSP9 has been discovered to contain a domain called RdRp-associated NiRAN (Lehmann et al., 2015a, 2016) (Figure 4C). NSP10 is the RNA helicase which can unwind the secondary structure of RNA (Seybert et al., 2000b; Bautista et al., 2002; Lehmann et al., 2015c). Sharing the same/with their own homologs across diverse families of nidoviruses, both NSP9 and NSP10 serve as the key virulence determinants of PRRSV (Li et al., 2014). NSP11 is a protein belonging to the NendoU family and its catalytic sites are highly conserved in *Nidovirales*, although its function remains poorly defined in the arterivirus life cycle (Nedialkova et al., 2009; Zhang et al., 2017). NSP12, a protein that is specific to arterivirus and plays an unexpected key interaction role, can interact with NSP1β, NSP2, NSP9, NSP10, and NSP11, and colocalize well with the DMVs (Lehmann et al., 2015b; Song et al., 2018). During infection, the NSP7 and NSP8 associate with the RTC, and the NSP7 interacts with NSP9; however, their functions in virus replication are poorly understood (Li et al., 2012; Chen et al., 2017). NSP6 has been shown to interact with NSP12; however, due to the unavailability of antibodies and the small size (16 aa), whether NSP6 is involved in RTC has not been determined yet (Kappes and Faaberg, 2015; Song et al., 2018). In all, NSP2, NSP3, and NSP5 form the scaffold of DMVs for supporting the RTC core components in binding to the DMVs, while NSP9 and NSP12 combine together to form a central hub (like a substrate pocket) which is connected to other replicases, including NSP7, NSP8, NSP10, NSP11(Figures 4A,B) (Song et al., 2018).

5.3 Synthesis of RNA

The RNA-dependent RNA synthesis takes place within the cytoplasm of the infected cells and is facilitated by a complex called

RTC that consists of viral replicases and host factors (Lai and Cavanagh, 1997; Enjuanes et al., 2006). During the synthesis process, the viral genome is replicated to produce a full-length gRNA which can play multiple functions: acting as a template for translation of viral replicases (pp1a and pp1ab); serving as a template for synthesis of −RNA intermediates; and working as the genome that will be packaged into new viral particles. Additionally, RTC is also involved in the transcription to yield a nested set of sg mRNAs which are responsible for expressing the viral structural and accessory proteins.

5.3.1 Replication of viral genome

Similar to other +RNA viruses, the replication of nidovirus genome is a continuous process mediated by synthesizing a full-length −RNA (Sola et al., 2015). Firstly, the viral genome acts as a template to translate the viral replicases (pp1a and pp1ab) which are further processed into more than 10 NSPs by internal enzymatic cleavage. The newly synthesized hydrophobic NSPs with TM trigger the formation of DMVs or DMSs, and further recruit other NSPs to form functional RTC. Secondly, the synthesis of −RNA intermetiates begins at the 3′-terminus of the viral genome and is facilitated by the RTC, under the help of the 3′-terminal RNA sequence and the secondary RNA structures. Thirdly, under the help of the catalytic RTC enzyme, the full-length complementary −RNA is synthesized and in turn serves as the template for producing gRNA (Snijder et al., 2016).

5.3.2 Transcription of sg mRNAs

The synthesis of sg mRNAs by discontinuous transcription mechanism and the consequent 5′-3′ co-terminal nested sg mRNAs are distinctive characteristics of the coronavirus and arterivirus (Makino et al., 1988; Jeong and Makino, 1994; van Marle et al., 1999; Miller and Koev, 2000; van Vliet et al., 2002; Mateos-Gomez et al., 2013; Sola et al., 2015). Similar to genome replication, the sg mRNAs synthesis also proceeds within the DMVs. However, this process is more complex, conserved only in some members of *Nidovirales* (coronavirus, bafinivirus, and arterivirus), but not in others (okavirus). The discovery of multiple −sgRNA intermediates in cells infected with TGEV or MHV suggests that the process of negative-strand synthesis is discontinuous (Sawicki and Sawicki, 1990) (Figure 5B). Increasing evidences support the discontinuous transcription mechanism during the synthesis of −sgRNA intermediates plays a role in the generation of sg mRNAs within coronavirus and arterivirus (Sawicki and Sawicki, 1995; Sawicki et al., 2007). This model includes two central principles: (1) discontinuous transcription of −sgRNA intermediates; (2) the process of discontinuous transcription is similar to the mechanism of similarity-assisted or high-frequency copy-choice RNA recombination. The particular mechanical process can be viewed as an event that occurs continuously: (1) the synthesis of −RNA intermediates is facilitated by RTC at the 3′ end of the genome; (2) the extension of newly synthesized −RNA continues until the first functional transcription regulatory sequence (TRS-B) motif is encountered; RTC has two choices: (3) ignore the existence of TRS-B and continue to synthesize until encountering the next TRS-B, or continue to synthesize full-length −RNA intermediates; or (4) stop synthesizing and switch the template to 5′-leader sequence, with homologous leader transcription regulation sequence (TRS-L) to continue the synthesis. The mechanism of template switching is initiated by the complementarity between the 3′-end TRS-B on the newly synthesized −RNA and the TRS-L motif on the gRNA (Figure 5). The new −sgRNA intermediates would act as a template for synthesis of sg mRNAs (Sawicki and Sawicki, 2005; Pasternak et al., 2006). Transfection of *in vitro* synthesized sg mRNAs into cells suggests that long sg mRNAs containing multiple TRSs can also function as templates for synthesizing −sgRNA intermediates (Wu and Brian, 2010).

However, research findings on torovirus EToV and GAV have indicated that not all nidoviruses produces sg mRNAs with a common 5′ leader sequence and 3′ co-terminus (Pasternak et al., 2006). The EToV produces 4 sg mRNAs with 3′ co-terminus. Among these sg mRNAs, only the longest sg mRNA 2 (S gene) carries an 18-nt leader sequence derived from 5′ end of the virus genome via discontinuous RNA synthesis (Smits et al., 2005). In this case, a TRS is absent; fusion of non-continuous sequences appears to be regulated by a specific sequence element, which consists of a hairpin structure and 23-nt 3′ flanking stretches with sequence similar to a region located at the 5′ end of the genome. During the synthesis of −RNA intermediates, it is believed that the presence of hairpin structure can cause the transcriptase complex to detach, and then trigger a template switching mechanism similar to what occurs in arterivirus and coronavirus. The mRNA 3 (M), 4 (HE) and 5 (N) do not process a common 5′ leader sequence, but are fully colinear with the viral genome at 3′ end. They are proceeded by short noncoding regions called "intergenic," which contain the conserved motif with a sequence pattern of 5′-ACN$_{3-4}$CUUUAGA-3′. Representing the torovirus TRS equivalent, the motif does not act as sites for homology-assisted template-switching. Instead, it acts as terminators of transcription during the synthesis of −sgRNAs, and also play as promoters during the synthesis of sg mRNAs (van Vliet et al., 2002; Smits et al., 2005; Stewart et al., 2018). These findings suggest that EToV utilizes both discontinuous and non-discontinuous RNA synthesis mechanisms to generate its sg mRNAs.

The okavirus (GAV and YHV) produces three mRNA: gRNA1, sg mRNA2, and sg mRNA3. These RNAs are all co-terminal at 3′ end, and each possesses a 5′ cap structure and poly (A) tail (Sittidilokratna et al., 2008; Wijegoonawardane et al., 2008). mRNA2 and mRNA3 do not possess a common 5′-leader sequence. Similar to toronavirus mRNA 3 to 5, the okavirus mRNA2 and mRNA3, containing a 5′-GGUCAAUAVAAGGUA-3′ in the intergenic regions (IGRs) preceding gene 2 and gene 3, are produced by a "continuous" transcription strategy (Cowley et al., 2012). In this process, the IGRs serve as a dual function in the genome: whereas, they act as terminators during the synthesis of −RNA intermediates and as the transcriptional promotors during the production of sg mRNAs.

The presence of the common 5′ leader sequence in the −sgRNA intermediates may provide a conserved starting sequence for gRNA and all sg mRNAs synthesis; meanwhile, it may act as a recognition signal for the viral mRNA capping machinery, though no detailed study has been done so far; furthermore, it may enable viral mRNA to escape from virus-induced translation shut off, leading to the translation of viral mRNA as well as the impairment of host gene expression (Banerjee et al., 2020).

6 Regulation of RNA synthesis

Due to the intricate nature of the nidovirus RNA replication and transcription, the study on factors regulating RNA synthesis is still on the early stage compared to knowledge available for some other +RNA viruses. Here, we will provide a summary of the current knowledge

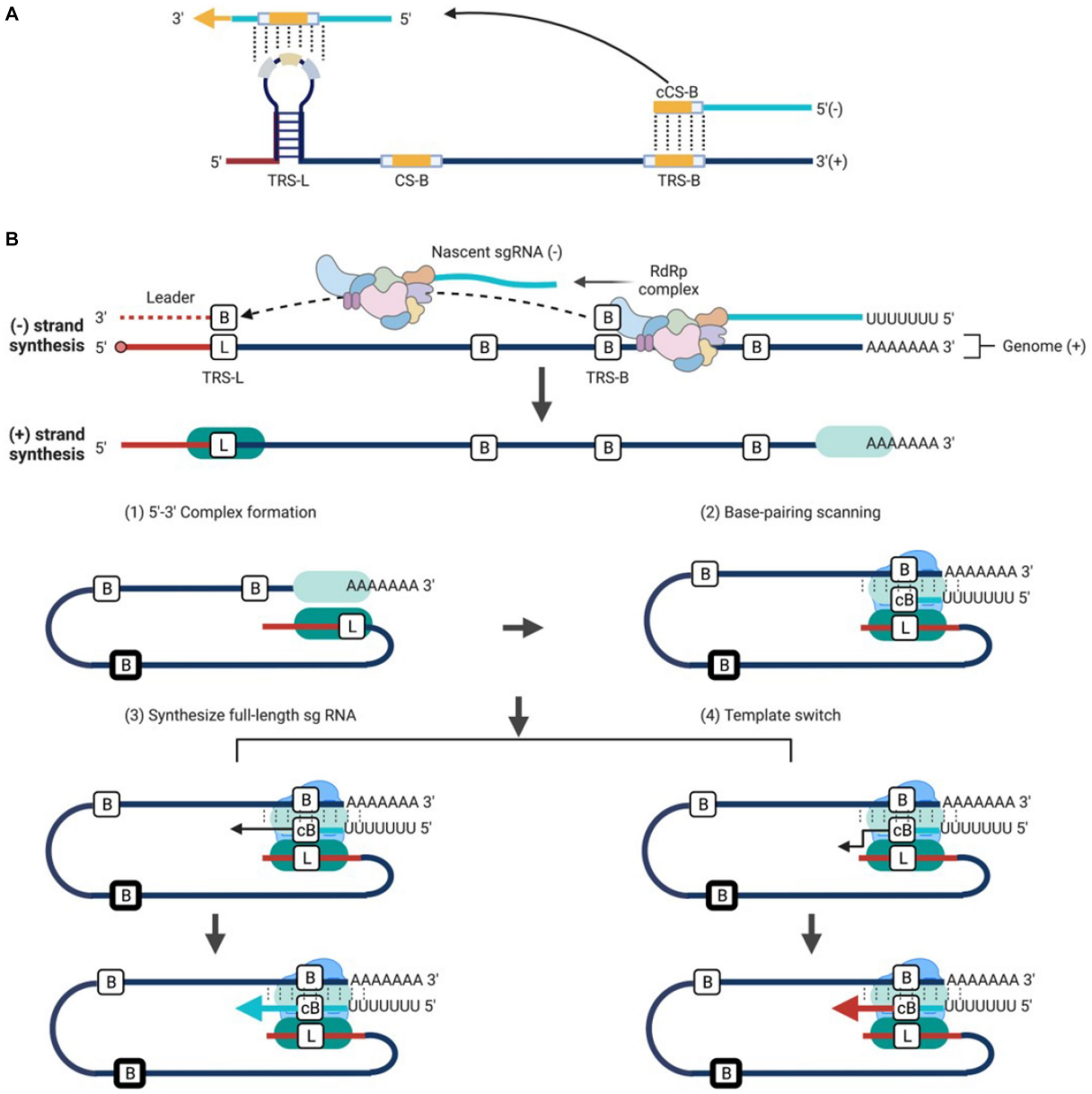

FIGURE 5
Working model of discontinuous transcription for *Nidovirales*. **(A)** TRS contains a conserved 6–7 nt core sequence (CS) flanked by 5′ and 3′ flanking sequences. TRS-B precedes each body gene, containing the core sequence (CS-B) and variable 5′ and 3′ flanking sequence. TRS-L is present at the 5′ end of the genome in an exposed location, with the leader core sequence (CS-L). **(B)** Three-step working model: (1) The components of a functional RTC including the viral NSPs and host proteins are recruited, and the synthesis of −RNA begins at the 3′ end of gRNA; (2) The extension of new synthesis −RNA continues until the first functional TRS motif is encountered. Till now, there are two choices: (3) Ignore the existence of TRS and continue to synthesize full-length −RNA; or (4) Stop synthesizing and switch the template to TRS-L to complete −sgRNAs synthesis. The template is switched by the complementary binding between the 3′ end of the new synthesis −RNA and the TRS-L motif in the 5′ gRNA and the new −sgRNAs in turn acts as a template for the synthesis of sg mRNAs.

regarding the viral and host factors involved in regulating viral RNA synthesis.

6.1 Regulation of RNA synthesis by RNA sequence

Synthesis of nidovirus RNA involves replication of full-length RNA and transcription of sg mRNAs. Many factors are involved in regulating RNA synthesis, with the first being the RNA sequence within the virus genome. These sequences are mainly located at the 5'-UTR and 3'-UTR of the genome or near the upstream of the encoding gene. The minimal sequences essential for TGEV, MHV, and IBV replication have been defined，which include a range of nucleotides located at the 5′ end (466 to 649 nt), at the 3′ end (388 to 493 nt), and at a poly (A) tail. These regions contain secondary and higher-order structures, known as cis-acting RNA elements which interacts with RNA motifs or replicases to initiate the RNA synthesis

(Mukhopadhyay et al., 2009; Chen and Olsthoorn, 2010; Madhugiri et al., 2014).

In coronavirus, the cis-acting RNA elements have a relatively conserved stem-loop (SL) structures (Raman et al., 2003; Kang et al., 2006; Li et al., 2008; Chen and Olsthoorn, 2010; Madhugiri et al., 2014; Figure 6A). Previous studies have demonstrated that SL structures plays a crucial role in the RNA synthesis through either long-distance RNA–RNA or RNA-protein interactions (Li et al., 2008; Yang et al., 2015). The SL structures at the 5′ end were first identified in BCoV, denoted from SL1 to SL6, respectively (Brown et al., 2007; Yang et al., 2015); however, there are seven SLs (SL1–SL7) in MHV (Guan et al., 2011). Among them, the SL1-SL4 are mapped within the 5′-UTR, while the rest SL structures are mapped into an ORF1a coding sequence. For BCoV, the SL5 and SL6 are located at the 5′-terminal 186 nt of NSP1 coding region (Brown et al., 2007). Compared to the two coronaviruses mentioned above, SARS-CoV-2 has one additional SL8 located at the 5′-end of the genome (Alhatlani, 2020). The number of SLs may vary with different coronaviruses, but SL1 to SL2 are conserved among all coronaviruses (Chen and Olsthoorn, 2010; Madhugiri et al., 2014). The SL1 is divided into two parts: the upper and the lower part, with the upper part participating in the coronavirus replication through base pairing. There is a dynamic model proposed for SL1 to mediate the interaction between 5′-UTR and 3′-UTR, thereby promoting the synthesis of −sgRNA intermediates (Li et al., 2008). SL2 is the most conserved 5'-UTR cis-acting RNA element that adopts a YNMG-type or CUYG-type tetraloop conformation (Liu et al., 2009; Lee et al., 2011), and mutation analysis has shown that it is essential for the sgRNAs synthesis (Liu et al., 2007). The leader core sequence (CS-L) and TRS-L, located within the SL3 or SL2, act as receptors for the nascent −RNA during discontinuous transcription (Sola et al., 2011). The conserved TRS-L plays a crucial role in regulating sg mRNAs transcription, which will be detailed in the subsequent TRS section. SL4, located downstream of SL3, is a long hairpin structure that probably functions as a spacer element in controlling the orientation of upstream SLs and TRS, and plays a role in directing sg mRNAs transcription (Yang et al., 2011; Vögele et al., 2021). In *α-Coronavirus*, SL5 is a higher-order structure with three hairpins (SL5a, SL5b, and SL5c) that extends into ORF1a (Chen and Olsthoorn, 2010) and it is also partially conserved in *β-Coronavirus*. Whereas, in IBV, SL5 is predicted to adopt a rod-like structure (Dalton et al., 2001). The structure phylogenetic analysis indicates that SL5 may help RNA interact with N protein and participates in genome packaging, as evidenced by study on TGEV (Morales et al., 2013). SL6 and SL7 are not necessary for coronavirus replication, and their role in RNA synthesis need to be further investigated (Yang et al., 2015).

There are three higher-order structures identified at the 3′-UTR as cis-acting RNA elements, which have been extensively studied in the MHV and BCoV. There are two specific RNA structures downstream of

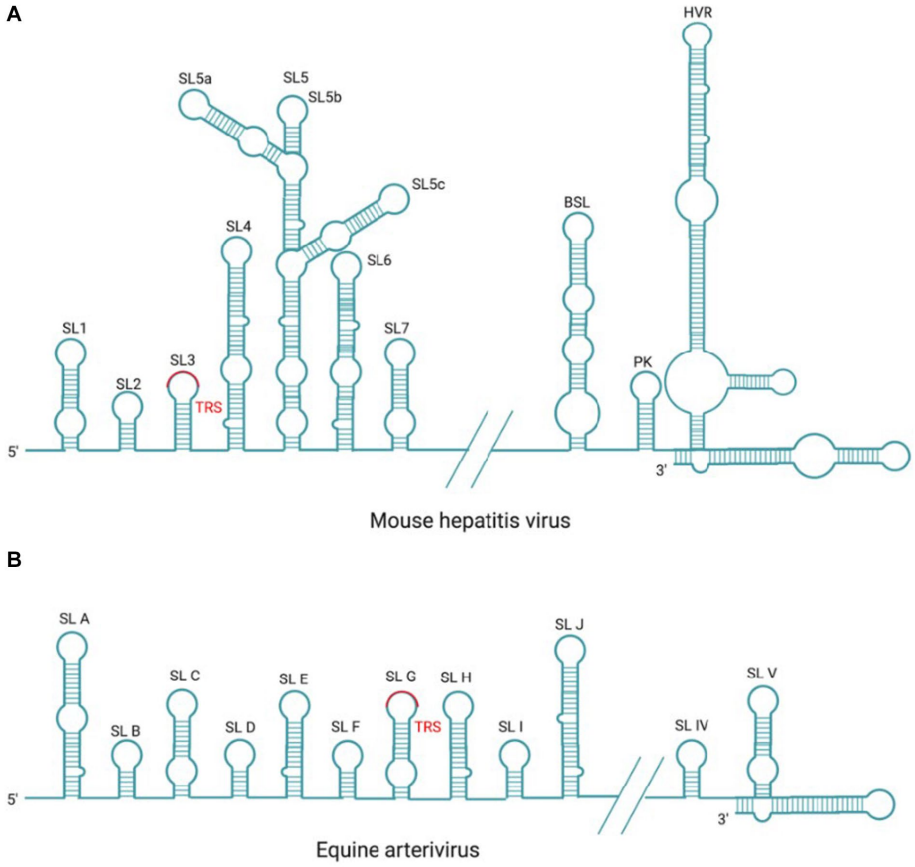

FIGURE 6
Cis-acting RNA element in MHV and EAV. **(A)** There are seven SL structures located in the 5′-UTR and three SL structures of BSL, PK, HVR located in the 3′-UTR within the coronavirus prototype MHV genome. **(B)** There are 10 SL structures located in the 5′-UTR and two SL structures located in the 3′-UTR within the arterivirus prototype EAV genome.

the N gene stop codon, the structurally and functionally conserved bulged stem-loop (BSL) of 68 nt and the hairpin RNA pseudoknot (PK) that consists of 54 nt and overlaps with the BSL of 5 nt. It has been reported that MHV PK loop1 directly interact with the 3′-end of the genome， and also with NSP8 and NSP9 (Zust et al., 2008). In most *β-Coronavirus*, BSL and PK are conserved and play crucial roles in viral RNA synthesis (Stammler et al., 2011; Zhao et al., 2020); however, in SARS-CoV-2 and *γ-coronavirus* IBV, PK is not observed (Dalton et al., 2001; Zhao et al., 2020). Downstream of the PK, there is a hypervariable region (HVR) that is highly divergent in sequence and structure among coronaviruses, but contains a conserved octa-nucleotide sequence 5′-GGAAGAGG-3′ (Goebel et al., 2007). In MHV, the HVR forms multiple SL structures in the last 160 nt of the viral genome, which is not essential in genome replication but affects pathogenicity *in vivo* (Goebel et al., 2007; Zust et al., 2008). Finally, the poly(A) tail functions as a cis-replication signal via interaction with PABPC1, which has been demonstrated in BCoV and MHV (Spagnolo and Hogue, 2000). BCoV and MHV-A59 defective interfering (DI) RNAs with truncated poly (A) tail consisting of 5A or 10 A residues were replicated at delayed kinetics, as compared to (DI) RNAs with wild-type poly (A) tail (>50 A residues; Spagnolo and Hogue, 2000, 2001).

In arterivirus, the cis-acting RNA elements at 5′-UTR and 3′-UTR also play essential roles in the replication and transcription of viral RNA. In EAV and PRRSV, the 5'-UTR cis-acting RNA elements include SLA, SLB, SLC, SLD, SLE, SLF, SLG, SLH, SLI, and SLJ (Figure 6B). SLG contains a conserved TRS-L, which is capable of base-pairing with TRS-B, and this interaction is essential for the −sgRNA intermediates synthesis (Pasternak et al., 2003; van den Born et al., 2005). Mutation analysis in SLB has indicated that the stem of SLB is essential for the synthesis of sg mRNAs during PRRSV infection (Lu et al., 2011); The 3′-UTR cis-acting RNA elements mainly include two putative hairpin structures (SLIV and SLV) and the base-pairing interaction between these two structures plays a role in the synthesis of viral genome and sg mRNAs (Verheije et al., 2001, 2002; Figure 6B). Mutation analysis in SLB has indicated that the stem of SLB is essential for the synthesis of sg mRNAs during PRRSV infection (Lu et al., 2011).

6.2 Transcription regulation sequence (TRS)

The TRS is an important cis-acting RNA element that plays a role in the transcription of nidovirus RNA. Hereby, the role of TRS in regulating RNA synthesis is summarized as following. Previous studies have found that the sg mRNAs of coronavirus, arterivirus, and bafinivirus carry a short 5′ leader sequence of 55–92 nt, 170–210 nt, and 42 nt, respectively (King et al., 2012), which is present at the 5′ end of the genome. This suggests that the sg mRNAs are synthesized by fusing non-contiguous sequence: the leader sequence at the 5′ end of the genome and the 5′ end of each gene coding sequence. Base-pairing is a key step during this non-contiguous fusion transcription process, which has been primarily demonstrated in arterivirus (van Marle et al., 1999; Pasternak et al., 2001) and coronavirus (Zúñiga et al., 2004).

Typically, two specific sequences called TRS-L and TRS-B, located at the 5′ end and proceeding upstream of each gene respectively, are responsible for the base pairing during sg RNA synthesis (Sola et al., 2005; Madhugiri et al., 2016). The TRS in coronavirus and arterivirus sg mRNAs were initially identified by sequencing the junction regions between the leader and body sequences of the sg mRNAs. The conserved sequence of the coronavirus TRS-L and TRS-B is about 7–18 nt, while the corresponding arterivirus TRS is usually about 5–8 nt (Gorbalenya et al., 2006), which is AU-rich. In toronavirus, there is a conserved 12 nt sequence element located upstream of ORF3, ORF4, and ORF5 (Di et al., 2018).

The TRS contains a conserved core sequence (CS) that is typically 6–7 nt in length and several flanking sequences. TRS-L includes the CS-L, while TRS-B includes the CS-B (Sola et al., 2011) (Figure 5A). Since the CS-L downstream of the 5′ leader sequence and all CS-B upstream of each body gene are identical in sequence, the CS-L can be paired with the complementary CS-B base of the newly synthesized −RNA, thus achieving the leader-body connection (Alonso et al., 2002; Sola et al., 2005). The CS-L and CS-B of the *Coronaviridae* and *Arteriviridae* are list in Table 2.

The discontinuous RNA transcription occurs during the synthesis of −sg RNA intermediates. Template switching is an important process during the transcription of sg RNA by RdRp, which needs the base-paring of TRS-L and TRS-B (Posthuma et al., 2017). When encountering the first TRS-B, RdRp stops the synthesis along with the original template and switches to the 5′-leader sequence with homologous TRS-L to complete its synthesis (Sola et al., 2015). This long-distance RNA–RNA interaction promotes the synthesis of −sgRNA intermediates, which in turn serves as a template for sg mRNAs synthesis (Mateos-Gomez et al., 2013).

6.3 Regulation of RNA synthesis by cellular proteins and viral proteins

The factors involved in viral RNA synthesis were identified by studying their binding to viral genome or replicase proteins (Sawicki et al., 2005; Shi and Lai, 2005). Several cellular and viral proteins have been identified to be involved in regulation of nidovirus RNA replication and transcription (van Vliet et al., 2002; Pasternak et al., 2006; Ulferts and Ziebuhr, 2011; Posthuma et al., 2017; de Wilde et al., 2018; Yan et al., 2020). These factors mainly regulate the formation of RTC and the binding of RTC to cis-acting RNA elements through protein-RNA and protein–protein interactions. These host and viral proteins are as well as their interaction proteins are summarized in Table 3.

6.3.1 Protein-RNA interaction

The protein-RNA interaction regulates the RNA synthesis process (Sola et al., 2011). It has been identified that the viral and cellular factors bind to RNA genome or replicases so as to drive the RNA synthesis (Sawicki et al., 2005; Shi and Lai, 2005; Galan et al., 2009; Xu et al., 2010). The common strategies employed to identify the replicase components are: genome wide two-hybrid screening, proteomic analysis, high-throughput functional assay using host cell mutants or siRNA, *in vitro* translation or transcription systems.

Most of the NSPs encoded by ORF1a and ORF1ab, together with N protein and cellular proteins, form the membrane-associated RTC. This complex interacts with viral RNA, and plays a crucial role in mediating the synthesis of viral genome and sg mRNAs. For coronavirus, the enzymes involved in RNA synthesis are the NSP7-NSP8 primase complex, NSP9 dimers, potential molecular switch (NSP10), RdRp (NSP12), helicase (NSP13), ExoN (NSP14), EndoU (NSP15), MTase (NSP16), and some unidentified cellular proteins. Among them, RdRp, helicase, and N protein are essential components

TABLE 2 The CS-L and CS-B of the *Coronaviridae* and *Arteriviridae*.

Family	Viruses	TRS		References
		CS-L	CS-B	
Coronaviridae	TGEV	5′-CUAAAC-3′	5′-GUUUAG-3′	Mateos-Gómez et al. (2011)
	PEDV	5′-AACGTAAA-3′	5′-UUUACGUU-3′	Yang et al. (2021)
	MERS-CoV	5′-AACGAAC-3′	5′-GUUCGUU-3′	Predicted
	HCoV-229E	5′-AACTAAAC-3′	5′-GUUUSGUU-3′	Predicted
	SARS-CoV	5′-ACGAAC-3′	5′-GUUCGU-3′	Thiel et al. (2003) and Hussain et al. (2005)
	SARS-CoV-2	5′-AACGAAC-3′	5′-GUUCGUU-3′	Wang D. et al. (2021)
	IBV	5′-CUUAACAA-3′	5′-UUGUUAAG-3′	Bentley et al. (2013)
	PDCoV	5′-ACACCA-3′	5′-UGGUGU-3′	Fang et al. (2016)
	EToV	5′-CUUUAGA-3′	5′-UVUAAAG-3′	Stewart et al. (2018)
	BCoV	5′-UCUAAA-3′	5′-UUUAGA-3′	Chang et al. (1996)
Arteriviridae	PRRSV	5′-UUAACC-3′	5′-GGUUAA-3′	van den Born et al. (2005) and Sola et al. (2015)
	EAV	5′-UCAACC-3′	5′-GGUUGA-3′	Pasternak et al. (2003)
	SHFV	5′-UCCUUAACC-3′	5′-GGUUAAGGA-3′	Di et al. (2017)

for RTC ; other NSPs and cellular proteins also contribute to the formation of RTC and regulation of RNA synthesis. The role of the replicases encoded by ORF1a and ORF1b in the formation of RTC has been reviewed in section 4 and 5. Hereby, we will focus on how N protein and cellular proteins interact with viral RNA and play a role in the synthesis of viral RNA.

6.3.1.1 N protein

The N protein serves as structural protein within the virion and plays a crucial role in viral transcription and replication. It forms oligomers and binds to gRNA, resulting the formation of helical ribonucleoprotein complexes by wrapping gRNA (Chang et al., 2006; Chen et al., 2007; Lo et al., 2013; Cong et al., 2017; Gui et al., 2017). These complexes are then incorporated into viral particles by interaction with the C-terminus of M proteins (Kuo et al., 2016). In addition to protecting gRNA, N protein regulates the replication and transcription of viral RNA, acting as a chaperone to promote gRNA replication (Almazán et al., 2004; Schelle et al., 2005; Zúñiga et al., 2010). The interaction with NSP3 enables N protein to be recruited to DMVs and associated with RTC (Hurst et al., 2010, 2013; Keane and Giedroc, 2013; Tatar and Tok, 2016; Cong et al., 2020). N protein might be involved in the discontinuous transcription of sg mRNAs, as depletion of N from the replicon reduces the production of sg mRNAs rather than gRNA (Zúñiga et al., 2010). In SARS-CoV-1, the N-terminal domain of N protein binds specifically to TRS-L sequence and enhances the unwinding of TRS duplexes (Grossoehme et al., 2009). In addition, N protein possesses RNA chaperone activity to facilitate the template switching, which is essential for efficient transcription of −sgRNA intermediates (Almazán et al., 2004; Zúñiga et al., 2010). The serine and arginine (SR) rich region, which links N-terminus and C-terminus of N protein, is modified by phosphorylation (Peng et al., 2008; Wu et al., 2009), which results in the differentiation between the binding of viral RNA and cellular mRNA (Chen et al., 2005; Spencer et al., 2008). In IBV, phosphorylation of N protein by GSK-3 also enables the recruitment of cellular RNA helicase DDX1 to RTC, which in turn enables the continuous synthesis of longer sg mRNAs and gRNA by promoting template read-through and transition from discontinuous transcription (Wu et al., 2009, 2014). This mechanism guarantees a proper balance among the synthesis of gRNA, long sg mRNAs, and short sg mRNAs. GSK-3 has been proved to be essential for the phosphorylation of SARS-CoV-2 N protein and the synthesis of viral RNA, serving as a promising target for developing pharmaceuticals to treat COVID-19 (Wu et al., 2014; Liu et al., 2021). A non-redundant dataset containing 495 compounds for GSK3α and 3,070 compounds for GSK3β has been applied to virtual high-throughput screening and two drugs (selinexor and ruboxistaurin) have been selected for further investigation (Pirzada et al., 2023). Therefore, interference with the phosphorylation of N protein by targeting GSK-3 is a feasible strategy to combat against the coronavirus associated diseases.

6.3.1.2 Cellular proteins

Cellular proteins perform their function in viral RNA synthesis via binding to 5′-UTR, internal TRS-B, 3′-UTR, or RTC. The proteins binding to 5′-UTR or 3′-UTR probably participate in viral RNA replication, transcription, translation and stability, while the proteins binding to TRS-B might help the discontinuous transcription.

There are two cellular heterogeneous nuclear ribonucleoproteins, polypyrimidine-tract binding protein (PTB) and hnRNPA1, which participate in the RNA transcription. PTB protein, also known as hnRNP I, plays an important role in regulating the alternative splicing of pre-mRNAs and translating the mRNA (Kaminski et al., 1995; Svitkin et al., 1996; Valcarcel and Gebauer, 1997). During MHV infection, PTB binds to the TRS-L (with UCUAA pentanucleotide

TABLE 3 Summary of host and viral proteins regulating RNA synthesis.

Family	Protein		Interaction proteins	References
Coronaviridae	Host	hnRNPA1	TRS, PTB, N protein,	Stohlman et al. (1988), Zhang and Lai (1995), Li et al. (1999), Wang and Zhang (1999), Shi et al. (2000), and Huang and Lai (2001)
		PTB (hnRNP1)	TRS, hnRNPA1, N protein	Huang and Lai (1999, 2001) and Choi et al. (2002)
		PABP	Poly (A) tail	Spagnolo and Hogue (2000)
		DDX	N protein	Wu et al. (2014)
	Virus	NSP1	NA	Molenkamp et al. (2000), Tijms et al. (2001), Tijms et al. (2007), Sun et al. (2009), and Nedialkova et al. (2010)
		NSP3	NSP4, NSP6	Angelini et al. (2013) and Oudshoorn et al. (2017)
		NSP4	NSP3, NSP6	Angelini et al. (2013) and Oudshoorn et al. (2017)
		NSP9	Single-stranded RNA, NSP12	Egloff et al. (2004), Sutton et al. (2004), Ponnusamy et al. (2008), Snijder et al. (2016), and Yan et al. (2021)
		NSP6	NSP3, NSP4	Angelini et al. (2013) and Oudshoorn et al. (2017)
		NSP12	NSP5, NSP8, NSP9	Brockway et al. (2003)
		NSP13	DDX15	Chen J.-Y. et al. (2009)
		N protein	DDX1, TRS, Poly (A)	Grossoehme et al. (2009), Wu et al. (2014), Snijder et al. (2016), Tsai et al. (2018), and Yan et al. (2021)
Arteriviridae	Host	Cyclophilin	NSP5	de Wilde et al. (2013) and de Wilde et al. (2019)
		Cyclin-dependent kinase 9	NA	Wang M. D. et al. (2021)
		DHX9	N protein, NSP9	Liu et al. (2016)
		Nucleotide-binding oligomerization domain-like receptor (NLR) X1	NSP9	Jing et al. (2019)
		poly(C) binding protein (PCBP)	NSP1β	Napthine et al. (2016)
	Virus	N protein	DHX9	Liu et al. (2016)
		NSP1	P100	Tijms and Snijder (2003)
		NSP2	NSP3	Snijder et al. (2001)
		NSP3	NSP2	Snijder et al. (2001)
		NSP5	NSP2, NSP3	Snijder et al. (2013)
		NSP9	DHX9, NLRX1,	Liu et al. (2016)
		NSP10	NA	Seybert et al. (2000b) and Lehmann et al. (2015c)
		NSP12	NSP11	Song et al. (2018)

repeats) which is located in the 5′-UTR (56–112 nt; Li et al., 1999). Deletion of these leader sequences in DI RNAs results in the reduced RNA transcription, indicating that the binding of PTB to TRS-L might regulate the transcription process. Another study has also demonstrated that PTB binds to the TRS-L sequence of TGEV genome, as identified by the RNA-protein pull-down assay and proteomic analysis (Galan et al., 2009). These findings suggest this protein might play a general role in coronavirus RNA transcription. Interestingly, PTB also interacts with the complementary strand of the 3′-UTR (c3′-UTR), with a strong binding site between 53 and 149 nt and a weak binding site between 270 and 307 nt on the c3′-UTR (Huang and Lai, 1999). The binding of PTB to 53–149 nt leads to a conformational change in the neighboring RNA region. When partial deletion occurs within the PTB-binding sequence, it completely abolishes the conformational change induced by PTB, and impairs the ability of the −RNA to transcribe mRNAs (Huang and Lai, 1999). Thus, the binding of PTB to c3'-UTR may play a crucial role in mRNA transcription by changing the c3′-UTR conformation. PTB has been found to stimulate the internal ribosome entry site (IRES) mediated translation, by interacting with picornavirus IRES elements (Kaminski et al., 1995; Niepmann, 1996; Niepmann et al., 1997). It may exert influence on the IRES-mediated translation of MHV 5b, and IBV 3c, which are ORFs that encode the envelope protein (Thiel and Siddell, 1994; Lai and Cavanagh, 1997; Jendrach et al., 1999). Meanwhile, the interaction between PTB with N protein suggests a potential contribution to the formation of RNP complex (Choi et al., 2002). In summary, according to research findings, the interaction between PTB and MHV RNA leader sequence or sequence complementary to the 3'-UTR is involved in RNA transcription, and the interaction between N protein and PTB also modulates transcription.

As is widely known, another cellular heterogeneous nuclear ribonucleoprotein, hnRNPA1 facilitates the pre-mRNA splicing and transport of cellular RNAs in the nucleus (Dreyfuss et al., 1993), as well as modulates the mRNA translation and turnover in the cytoplasm (Hamilton et al., 1993, 1997; Svitkin et al., 1996). HnRNPA1 was initially found to specifically bind to MHV cTRS-L and cTRS-B present in the −RNA (Furuya and Lai, 1993; Li et al., 1997), which suggests that HnRNPA1 is important for the discontinuous viral RNA transcription. It has been found that mutagenesis of the TRS-B in the DI RNA system will lead to reduced transcription, which was correlated with relative binding affinity of the cTRS-B sequence to hnRNPA1 (Furuya and Lai, 1993; Li et al., 1997; Huang and Lai, 2001). According to another study, a vital hnRNPA1-binding site has been identified within the HRV domain, which is located between 90 and 170 nt from the 3′ end of MHV RNA, while a weak binding site has been identified between 260 and 350 nt (overlapping with the BSL) from the 3′ end (Huang and Lai, 2001). Overexpression of hnRNPA1 results in an acceleration of MHV RNA synthesis, and the expression of dominant-negative hnRNPA1 mutant leads to a global inhibition of viral RNA (Dalton et al., 2001). Additionally, hnRNPA1 interacts with N protein of MHV and forms a component of the RTC (Wang and Zhang, 1999). It also plays a role in facilitating the formation of the RNP complex via binding to the negative-stranded cTRS-L and cTRS-B (Zhang et al., 1999). The extent of hnRNPA1 binding to the cTRS is directly related to the transcription efficiency in the MHV model (Zhang and Lai, 1995). Meanwhile, it has been observed that the hnRNPA1 interacts with the 3′ end of the genome in the TGEV (Luo et al., 2005). In another study, it has been found that hnRNPA1 interacts with N protein of PEDV, and the silenced expression of hnRNPA1 impairs viral replication. The interaction between hnRNPA1 and N protein has also been found in SARS-CoV (Luo et al., 2005), SARS-CoV-2 (Perdikari et al., 2020), IBV (Emmott et al., 2013). Whereas, in the hnRNPA1 defective mouse erythroleukemia cell line CB3 (Ben-David et al., 1992), it has been observed that efficient MHV replication still occurs (Shen and Masters, 2001). The interaction of hnRNP A/B, hnRNP A2/B1, and hnRNP A3 with the MHV negative-stranded leader RNA potentially substitutes for hnRNPA1 in regulating MHV RNA replication (Shi et al., 2003).

It is interesting to note that the hnRNPA1 binding sites on 3′ end of MHV genome are complementary to the sites on the −RNA intermediates that bind to PTB (Huang and Lai, 1999; Li et al., 1999; Huang and Lai, 2001). Mutations that affect PTB binding to the negative strand of the 3'-UTR also hinder hnRNPA1 binding on the positive strand, demonstrating that hnRNPA1 and PTB work together to mediate potential 5′-3′ cross talks in MHV RNA, which plays an important role in RNA replication and transcription.

HnRNP Q, also known as SYNCRIP, is capable of binding to the 5′-UTR or to the complementary sequence c5′-UTR of MHV (Choi et al., 2004). Meanwhile, it has been shown that hnRNP Q bind to TEGV 3′-end genome and positively regulates the synthesis of viral RNA (Galan et al., 2009). As elaborated in a recent study, another hnRNP family member, hnRNP C, is involved in promoting the replication of MERS-CoV and SARS-CoV-2 by regulating the expression of a specific subset of circRNAs and cognitive mRNAs (Zhang X. et al., 2022). The positive role of hnRNPs in viral RNA replication/transcription renders these proteins as broad-spectrum antiviral targets. A hnRNPA2B1 agonist has been demonstrated to effectively inhibit HBV and SARS-CoV-2 omicron *in vivo* (Zuo et al., 2023).

Poly (A)-binding protein (PABP) is a protein that binds to the 3′ poly (A) tail on eukaryotic mRNAs, with its main function being to promote both mRNA translation initiation and mRNA stability. For BCoV, MHV, and TGEV, PABP has been identified as binds to the 3' UTR and poly (A) tail (Lin et al., 1994; Spagnolo and Hogue, 2000; Galan et al., 2009). It has been found that the binding of PABP to 3'-UTR of DI RNA replicons is associated with the replication of DI RNA (Yu and Leibowitz, 1995a,b; Liu et al., 1997; Huang and Lai, 2001). The interaction between PABP and poly (A) tail may have a direct role in coronavirus replication and transcription, which can mediate the interaction between the 5′ and 3′ ends of coronavirus RNA (Kim et al., 1993; Lin et al., 1994, 1996; Lai, 1998), or indirectly modulate the synthesis of viral RNA by affecting the translation process. Wang et al. have illustrated that PABPC1 interacts with the N protein of arterivirus PRRSV and involves in viral replication (Wang et al., 2012); whereas, Tsai et al. have found that the interplay among PABP, N protein and poly(A) tail mainly regulates coronavirus mRNA translation (Tsai et al., 2018).

Other cellular proteins associated with coronavirus RTC include the cellular DEAD box helicase family. This multifunctional protein family is involved in various steps of RNA life cycle, such as transcription, mRNA splicing, RNA transport, translation, RNA decay. The specific interaction between DDX5 and SARS-CoV NSP13 (helicase) is involved in viral RNA synthesis (Chen J.-Y. et al., 2009); and the interaction between DDX1 with IBV and SARS-CoV NSP14 also enhances virus replication (Xu et al., 2010). Interestingly, when the N protein is phosphorylated, it recruits the RNA helicase DDX1 to the phosphorylated-N-containing complex, which in turn facilitates the process of template readthrough and enables the synthesis of longer sg mRNAs; afterwards, the transition from discontinuous to continuous transcription guarantees the balance between sg mRNAs and full-length gRNA (Wu et al., 2014). The N protein of SARS-CoV-2 has been found to interact with several RNA helicases, including DDX1, DDX3, DDX5, DDX6, DDX21, and DDX10; among them, DDX1, DDX5, and DDX6 are essential for virus replication, while DDX21 and DDX10 restrict the viral infection (Ariumi, 2022). All the above studies reveal that the hijacking of host cellular DDX helicases for viral replication and transcription is a general strategy among coronaviruses.

During PRRSV infection, DDX18 redistributes from nucleus to cytoplasm and interacts with NSP2 and NSP10, to promote virus replication (Jin et al., 2017). DDX21 is also translocated from nucleus to cytoplasm and then positively regulates the PRRSV replication by stabilizing the expression of PRRSV NSP1α, NSP1β, and N protein (Li et al., 2022). It has been found that DDX21 interacts with NSP1β, which enhances the expression of DDX21. Another DDX family member, DDX5, has been found to interact with NSP9, the RdRp, thereby positively regulating the replication of PRRSV (Zhao et al., 2015). Moreover, PRRSV infection promotes the DDX10 to translocate from the nucleus to the cytoplasm for macroautophagic/autophagic degradation.

Additionally, the viral E protein interacts with and promotes the selective autophagic degradation of DDX10, to antagonize the antiviral effect of this protein (Li et al., 2023).

6.3.2 Protein–protein interaction

The NSP12 (RdRp), NSP13 (helicase), and N protein are crucial for the replication and transcription of coronavirus RNA. In addition, other viral proteins also contribute to the regulation of RNA synthesis. For example, NSP3, NSP4, and NSP6 are responsible for the formation of DMVs, while NSP3 and NSP5 have the activity to process pp1a and pp1ab so as to produce mature replicases. In MHV, NSP12 (RdRp) has been shown to interact with 3CLpro, NSP8, and NSP9 to perform the RNA synthesis (Brockway et al., 2003). It has been shown that NSP9 forms dimers and binds to single-stranded RNA in a non-sequence-specific manner (Egloff et al., 2004; Sutton et al., 2004; Ponnusamy et al., 2008). Recently, it has been shown that the N terminus of NSP9 inserts into the catalytic center of NiRAN domain of NSP12, which in turn inhibits the activity of NSP12 (Snijder et al., 2016; Yan et al., 2021).

In arterivirus, NSP9 (RdRp), NSP10 (helicase), and N protein play crucial roles in the processes of replication and transcription. NSP2, NSP3, and NSP5 contain TM responsible for remodeling intracellular membranes and recruiting other viral replicases to RTC (Snijder et al., 1994; van der Meer et al., 1998; Snijder et al., 2001; Posthuma et al., 2008). The ability of arterivirus RTC to synthesize RNA *in vitro* is dependent on a host factor (van Hemert et al., 2008).

As a multifunctional protein during EAV infection that contains two papain-like cysteine protease (PCPα and PCPβ) and a zinc-finger motif, NSP1 plays an important role in regulating the viral RNA synthesis and virion biogenesis, as well as in controlling the balance between genome replication and sg mRNAs synthesis (Molenkamp et al., 2000; Tijms et al., 2001, 2007; Nedialkova et al., 2010). In addition, the Zinc-finger motif, located in the N-terminal region of PRRSV NSP1, was involved in regulating sg RNA synthesis (Sun et al., 2009). Therefore, NSP1 protein in arterivirus is a multifunctional protein involved in proteolytic maturation of the replicase and the regulation of RNA transcription.

Paraoxonase-1(PON1), an esterase with specifical paraoxonase activity, interacts with PRRSV RdRp (NSP9) and plays a role in facilitating the NSP9 function in PRRSV replication; moreover, it has been proved to reduce the type I IFN signaling during PRRSV infection (Zhang L. et al., 2022). RBM39, a nuclear protein involved in transcriptional activation and precursor mRNA splicing, relocates from nucleus to cytoplasm to bind with viral RNA, thereby prompting the PRRSV replication (Song et al., 2021).

7 Conclusion

Since the first in-depth analysis on the replication and transcription of *Nidovirales* in 1980 (Evans and Simpson, 1980), significant progress has been made in the understanding of mechanisms and regulation of sg mRNAs generation, and the accurate synthesis mechanism has been determined. During nidovirus infection, a nested set of sg mRNAs were produced, all sharing a common 5′ leader sequence and 3′ co-terminus. It has been demonstrated that the nested −sgRNA intermediates are produced through the discontinuous synthesis mechanism from the gRNA template. Afterwards, these −sgRNA intermediates serve as templates for the synthesis of sg mRNAs. In this process, viral and cellular factors are known to form the RTC and regulate the activities of replicases, such as the N protein, replicases, host cellular hnRNP, PTB, and DDX. In addition, the interactions among RNA–RNA, protein-RNA, and protein–protein play a role in regulating the replication and transcription. The viral transcription and replication machinery represents an attractive target for developing antiviral drugs. For example, the lead compounds, remdesivir and nirmatrelvir, specifically targeting at SARS-CoV-2 RdRp and Mpro respectively, have already been approved for COVID-19 treatment (Gao et al., 2020; Lamb, 2020; Lee et al., 2022; Amani and Amani, 2023; Harris, 2023). Thus, detailed insights provide new opportunities for designing structure-based antiviral drugs, which target at multiple aspects of the RNA synthesis processes.

Author contributions

YL: Conceptualization, Project administration, Supervision, Writing – original draft, Writing – review & editing, Formal analysis, Funding acquisition. HW: Conceptualization, Writing – original draft. HL: Writing – review & editing, Formal analysis. YS: Formal analysis, Supervision, Writing – review & editing. LT: Supervision, Writing – review & editing. CS: Project administration, Writing – review & editing. XQ: Supervision, Writing – review & editing. CD: Funding acquisition, Supervision, Writing – review & editing.

Funding

The author(s) declare financial support was received for the research, authorship, and/or publication of this article. This work was supported by the National Key Research and Development Program (no. 2021YFD1801104), National Natural Science Foundation of China (32172834), and the Shanghai Natural Science Foundation (23ZR1477000).

Conflict of interest

The authors declare that the research was conducted in the absence of any commercial or financial relationships that could be construed as a potential conflict of interest.

The author(s) declared that they were an editorial board member of Frontiers, at the time of submission. This had no impact on the peer review process and the final decision.

Publisher's note

References

Ahn, D.-G., Choi, J.-K., Taylor, D. R., and Oh, J.-W. (2012). Biochemical characterization of a recombinant SARS coronavirus nsp12 RNA-dependent RNA polymerase capable of copying viral RNA templates. *Arch. Virol.* 157, 2095–2104. doi: 10.1007/s00705-012-1404-x

Aita, T., Kuwabara, M., Murayama, K., Sasagawa, Y., Yabe, S., Higuchi, R., et al. (2012). Characterization of epidemic diarrhea outbreaks associated with bovine torovirus in adult cows. *Arch. Virol.* 157, 423–431. doi: 10.1007/s00705-011-1183-9

Alhatlani, B. Y. (2020). *In silico* identification of conserved −acting RNA elements in the SARS-CoV-2 genome. *Futur. Virol.* 15, 409–417. doi: 10.2217/fvl-2020-0163

Almazán, F., Galán, C., and Enjuanes, L. (2004). The nucleoprotein is required for efficient coronavirus genome replication. *J. Virol.* 78, 12683–12688. doi: 10.1128/JVI.78.22.12683-12688.2004

Alonso, S., Izeta, A., Sola, I., and Enjuanes, L. (2002). Transcription regulatory sequences and mRNA expression levels in the coronavirus transmissible gastroenteritis virus. *J. Virol.* 76, 1293–1308. doi: 10.1128/JVI.76.3.1293-1308.2002

Amani, B., and Amani, B. (2023). Efficacy and safety of nirmatrelvir/ritonavir (Paxlovid) for COVID-19: a rapid review and meta-analysis. *J. Med. Virol.* 95:e28441. doi: 10.1002/jmv.28441

Angelini, M. M., Akhlaghpour, M., Neuman, B. W., and Buchmeier, M. J. (2013). Severe acute respiratory syndrome coronavirus nonstructural proteins 3, 4, and 6 induce double-membrane vesicles. *MBio* 4, e00524–e00513. doi: 10.1128/mBio.00524-13

Ariumi, Y. (2022). Host cellular RNA helicases regulate SARS-CoV-2 infection. *J. Virol.* 96:e0000222. doi: 10.1128/jvi.00002-22

Athmer, J., Fehr, A. R., Grunewald, M., Smith, E. C., Denison, M. R., and Perlman, S. (2017). In situ tagged nsp15 reveals interactions with coronavirus replication/transcription complex-associated proteins. *MBio* 8, e02320–e02316. doi: 10.1128/mBio.02320-16

Balasuriya, U. B., and Carossino, M. (2017). Reproductive effects of arteriviruses: equine arteritis virus and porcine reproductive and respiratory syndrome virus infections. *Curr. Opin. Virol.* 27, 57–70. doi: 10.1016/j.coviro.2017.11.005

Balasuriya, U. B., Go, Y. Y., and MacLachlan, N. J. (2013). Equine arteritis virus. *Vet. Microbiol.* 167, 93–122. doi: 10.1016/j.vetmic.2013.06.015

Bande, F., Arshad, S. S., Omar, A. R., Hair-Bejo, M., Mahmuda, A., and Nair, V. (2017). Global distributions and strain diversity of avian infectious bronchitis virus: a review. *Anim. Health Res. Rev.* 18, 70–83. doi: 10.1017/S1466252317000044

Banerjee, A. K., Blanco, M. R., Bruce, E. A., Honson, D. D., Chen, L. M., Chow, A., et al. (2020). SARS-CoV-2 disrupts splicing, translation, and protein trafficking to suppress host defenses. *Cells* 183:4. doi: 10.1016/j.cell.2020.10.004

Banerjee, R., Perera, L., and Tillekeratne, L. M. V. (2021). Potential SARS-CoV-2 main protease inhibitors. *Drug Discov. Today* 26, 804–816. doi: 10.1016/j.drudis.2020.12.005

Bautista, E. M., Faaberg, K. S., Mickelson, D., and McGruder, E. D. (2002). Functional properties of the predicted helicase of porcine reproductive and respiratory syndrome virus. *Virology* 298, 258–270. doi: 10.1006/viro.2002.1495

Ben-David, Y., Bani, M. R., Chabot, B., De Koven, A., and Bernstein, A. (1992). Retroviral insertions downstream of the heterogeneous nuclear ribonucleoprotein A1 gene in erythroleukemia cells: evidence that A1 is not essential for cell growth. *Mol. Cell. Biol.* 12, 4449–4455. doi: 10.1128/mcb.12.10.4449-4455.1992

Benoni, R., Krafcikova, P., Baranowski, M. R., Kowalska, J., Boura, E., and Cahova, H. (2021). Substrate specificity of SARS-CoV-2 Nsp10-Nsp16 Methyltransferase. *Viruses* 13:1722. doi: 10.3390/v13091722

Bentley, K., Keep, S. M., Armesto, M., and Britton, P. (2013). Identification of a noncanonically transcribed subgenomic mRNA of infectious bronchitis virus and other gammacoronaviruses. *J. Virol.* 87, 2128–2136. doi: 10.1128/JVI.02967-12

Biswal, M., Diggs, S., Xu, D., Khudaverdyan, N., Lu, J., Fang, J., et al. (2021). Two conserved oligomer interfaces of NSP7 and NSP8 underpin the dynamic assembly of SARS-CoV-2 RdRP. *Nucleic Acids Res.* 49, 5956–5966. doi: 10.1093/nar/gkab370

Boson, B., Legros, V., Zhou, B., Siret, E., Mathieu, C., Cosset, F. L., et al. (2021). The SARS-CoV-2 envelope and membrane proteins modulate maturation and retention of the spike protein, allowing assembly of virus-like particles. *J. Biol. Chem.* 296:100111. doi: 10.1074/jbc.RA120.016175

Bost, A. G., Carnahan, R. H., Lu, X. T., and Denison, M. R. (2000). Four proteins processed from the replicase gene polyprotein of mouse hepatitis virus colocalize in the cell periphery and adjacent to sites of virion assembly. *J. Virol.* 74, 3379–3387. doi: 10.1128/JVI.74.7.3379-3387.2000

Brian, D. A., and Baric, R. S. (2005). Coronavirus genome structure and replication. *Curr. Top. Microbiol. Immunol.* 287, 1–30. doi: 10.1007/3-540-26765-4_1

Brierley, I., Digard, P., and Inglis, S. C. (1989). Characterization of an efficient coronavirus ribosomal frameshifting signal: requirement for an RNA pseudoknot. *Cells* 57, 537–547. doi: 10.1016/0092-8674(89)90124-4

Brinton, M. A., Di, H., and Vatter, H. A. (2015). Simian hemorrhagic fever virus: recent advances. *Virus Res.* 202, 112–119. doi: 10.1016/j.virusres.2014.11.024

Brockway, S. M., Clay, C. T., Lu, X. T., and Denison, M. R. (2003). Characterization of the expression, intracellular localization, and replication complex association of the putative mouse hepatitis virus RNA-dependent RNA polymerase. *J. Virol.* 77, 10515–10527. doi: 10.1128/JVI.77.19.10515-10527.2003

Brown, C. G., Nixon, K. S., Senanayake, S. D., and Brian, D. A. (2007). An RNA stem-loop within the bovine coronavirus nsp1 coding region is a cis-acting element in defective interfering RNA replication. *J. Virol.* 81, 7716–7724. doi: 10.1128/JVI.00549-07

Bryans, J. T., Doll, E. R., and Knappenberger, R. E. (1957). An outbreak of abortion caused by the equine arteritis virus. *T Cornell Vet.* 47, 69–75.

Capasso, C., Nocentini, A., and Supuran, C. T. (2021). Protease inhibitors targeting the main protease and papain-like protease of coronaviruses. *Expert Opin. Ther. Pat.* 31, 309–324. doi: 10.1080/13543776.2021.1857726

Cavanagh, D. (1997). Nidovirales: a new order comprising Coronaviridae and Arteriviridae. *Arch. Virol.* 142, 629–633.

Cavanagh, D. (2007). Coronavirus avian infectious bronchitis virus. *Vet. Res.* 38, 281–297. doi: 10.1051/vetres:2006055

Cavanagh, D., Brien, D. A., Brinton, M., Enjuanes, L., Holmes, K. V., Horzinek, M. C., et al. (1994). Revision of the taxonomy of the coronavirus, Torovirus and Arterivirus genera. *Arch. Virol.* 135, 227–237. doi: 10.1007/BF01309782

Chang, L. J., and Chen, T. H. (2021). NSP16 2'-O-MTase in coronavirus pathogenesis: possible prevention and treatments strategies. *Viruses* 13:538. doi: 10.3390/v13040538

Chang, C.-K., Hou, M.-H., Chang, C.-F., Hsiao, C.-D., and Huang, T.-H. (2014). The SARS coronavirus nucleocapsid protein--forms and functions. *Antiviral Res.* 103, 39–50. doi: 10.1016/j.antiviral.2013.12.009

Chang, R. Y., Krishnan, R., and Brian, D. A. (1996). The UCUAAAC promoter motif is not required for high-frequency leader recombination in bovine coronavirus defective interfering RNA. *J. Virol.* 70, 2720–2729. doi: 10.1128/jvi.70.5.2720-2729.1996

Chang, C. K., Sue, S. C., Yu, T. H., Hsieh, C. M., Tsai, C. K., Chiang, Y. C., et al. (2006). Modular organization of SARS coronavirus nucleocapsid protein. *J. Biomed. Sci.* 13, 59–72. doi: 10.1007/s11373-005-9035-9

Chen, Y., Cai, H., Pan, J., Xiang, N., Tien, P., Ahola, T., et al. (2009). Functional screen reveals SARS coronavirus nonstructural protein nsp14 as a novel cap N7 methyltransferase. *Proc. Natl. Acad. Sci. U. S. A.* 106, 3484–3489. doi: 10.1073/pnas.0808790106

Chen, C. Y., Chang, C. K., Chang, Y. W., Sue, S. C., Bai, H. I., Riang, L., et al. (2007). Structure of the SARS coronavirus nucleocapsid protein RNA-binding dimerization domain suggests a mechanism for helical packaging of viral RNA. *J. Mol. Biol.* 368, 1075–1086. doi: 10.1016/j.jmb.2007.02.069

Chen, J.-Y., Chen, W.-N., Poon, K.-M. V., Zheng, B.-J., Lin, X., Wang, Y.-X., et al. (2009). Interaction between SARS-CoV helicase and a multifunctional cellular protein (Ddx5) revealed by yeast and mammalian cell two-hybrid systems. *Arch. Virol.* 154, 507–512. doi: 10.1007/s00705-009-0323-y

Chen, H., Gill, A., Dove, B. K., Emmett, S. R., Kemp, C. F., Ritchie, M. A., et al. (2005). Mass spectroscopic characterization of the coronavirus infectious bronchitis virus nucleoprotein and elucidation of the role of phosphorylation in RNA binding by using surface plasmon resonance. *J. Virol.* 79, 1164–1179. doi: 10.1128/JVI.79.2.1164-1179.2005

Chen, Y., and Guo, D. (2016). Molecular mechanisms of coronavirus RNA capping and methylation. *Virol. Sin.* 31:4. doi: 10.1007/s12250-016-3726-4

Chen, J., Malone, B., Llewellyn, E., Grasso, M., Shelton, P. M. M., Olinares, P. D. B., et al. (2020). Structural basis for helicase-polymerase coupling in the SARS-CoV-2 replication-transcription complex. *Cells* 182:33. doi: 10.1016/j.cell.2020.07.033

Chen, S.-C., and Olsthoorn, R. C. L. (2010). Group-specific structural features of the 5′-proximal sequences of coronavirus genomic RNAs. *Virology* 401, 29–41. doi: 10.1016/j.virol.2010.02.007

Chen, J., Xu, X., Tao, H., Li, Y., Nan, H., Wang, Y., et al. (2017). Structural analysis of porcine reproductive and respiratory syndrome virus non-structural protein 7α (NSP7α) and identification of its interaction with NSP9. *Front. Microbiol.* 8:853. doi: 10.3389/fmicb.2017.00853

Cheng, V. C. C., Wong, S. C., To, K. K. W., Ho, P. L., and Yuen, K. Y. (2020). Preparedness and proactive infection control measures against the emerging novel coronavirus in China. *J. Hosp. Infect.* 104, 254–255. doi: 10.1016/j.jhin.2020.01.010

Choi, K. S., Huang, P., and Lai, M. M. (2002). Polypyrimidine-tract-binding protein affects transcription but not translation of mouse hepatitis virus RNA. *Virology* 303, 58–68. doi: 10.1006/viro.2002.1675

Choi, K. S., Mizutani, A., and Lai, M. M. C. (2004). SYNCRIP, a member of the heterogeneous nuclear ribonucleoprotein family, is involved in mouse hepatitis virus RNA synthesis. *J. Virol.* 78, 13153–13162. doi: 10.1128/JVI.78.23.13153-13162.2004

Cokley, J. A., Gidal, B. E., Keller, J. A., and Vossler, D. G.Reviewed and approved by the AES Treatments Committee and Council on Clinical Activities (2022). Paxlovid(TM) information from FDA and guidance for AES members. *Epilepsy Curr* 22, 201–204. doi: 10.1177/15357597221088415

Cong, Y., Kriegenburg, F., de Haan, C. A. M., and Reggiori, F. (2017). Coronavirus nucleocapsid proteins assemble constitutively in high molecular oligomers. *Sci. Rep.* 7:5740. doi: 10.1038/s41598-017-06062-w

Cong, Y., Ulasli, M., Schepers, H., Mauthe, M., V'Kovski, P., Kriegenburg, F., et al. (2020). Nucleocapsid protein recruitment to replication-transcription complexes plays a crucial role in Coronaviral life cycle. *J. Virol.* 94, e01925–e01919. doi: 10.1128/JVI.01925-19

Cortese, M., Lee, J. Y., Cerikan, B., Neufeldt, C. J., Oorschot, V. M. J., Kohrer, S., et al. (2020). Integrative imaging reveals SARS-CoV-2-induced reshaping of subcellular morphologies. *Cell Host Microbe* 28, 853–866 e855. doi: 10.1016/j.chom.2020.11.003

Cowley, J. A., Dimmock, C. M., Spann, K. M., and Walker, P. J. (2000). Gill-associated virus of *Penaeus monodon* prawns: an invertebrate virus with ORF1a and ORF1b genes related to arteri- and coronaviruses. *J. Gen. Virol.* 81, 1473–1484. doi: 10.1099/0022-1317-81-6-1473

Cowley, J. A., Dimmock, C. M., Spann, K. M., and Walker, P. J. (2001). Gill-associated virus of *Penaeus monodon* prawns. Molecular evidence for the first invertebrate nidovirus. *Adv. Exp. Med. Biol.* 494, 43–48. doi: 10.1007/978-1-4615-1325-4_6

Cowley, J. A., Walker, P. J., Flegel, T. W., Lightner, D. V., Bonami, J. R., Snijder, E. J., et al. (2012). "Family—Roniviridae" in *Virus Taxonomy*. eds. A. M. Q. King, M. J. Adams, E. B. Carstens and E. J. Lefkowitz (San Diego: Elsevier), 829–834.

Dai, W., Zhang, B., Jiang, X. M., Su, H., Li, J., Zhao, Y., et al. (2020). Structure-based design of antiviral drug candidates targeting the SARS-CoV-2 main protease. *Science* 368, 1331–1335. doi: 10.1126/science.abb4489

Dalton, K., Casais, R., Shaw, K., Stirrups, K., Evans, S., Britton, P., et al. (2001). Cis-acting sequences required for coronavirus infectious bronchitis virus defective-RNA replication and packaging. *J. Virol.* 75, 125–133. doi: 10.1128/JVI.75.1.125-133.2001

de Haan, C. A., Kuo, L., Masters, P. S., Vennema, H., and Rottier, P. J. (1998). Coronavirus particle assembly: primary structure requirements of the membrane protein. *J. Virol.* 72, 6838–6850. doi: 10.1128/JVI.72.8.6838-6850.1998

de Vries, A. A. F., Horzinek, M. C., Rottier, P. J. M., and de Groot, R. J. (1997). The genome Organization of the Nidovirales: similarities and differences between Arteri-, Toro-, and coronaviruses. *Semin. Virol.* 8, 33–47. doi: 10.1006/smvy.1997.0104

de Wilde, A. H., Boomaars-van der Zanden, A. L., de Jong, A. W. M., Bárcena, M., Snijder, E. J., and Posthuma, C. C. (2019). Adaptive mutations in Replicase Transmembrane subunits can counteract inhibition of equine arteritis virus RNA synthesis by Cyclophilin inhibitors. *J. Virol.* 93, e00490–e00419. doi: 10.1128/JVI.00490-19

de Wilde, A. H., Li, Y., van der Meer, Y., Vuagniaux, G., Lysek, R., Fang, Y., et al. (2013). Cyclophilin inhibitors block arterivirus replication by interfering with viral RNA synthesis. *J. Virol.* 87, 1454–1464. doi: 10.1128/JVI.02078-12

de Wilde, A. H., Snijder, E. J., Kikkert, M., and van Hemert, M. J. (2018). Host factors in coronavirus replication. *Curr. Top. Microbiol. Immunol.* 419, 1–42. doi: 10.1007/82_2017_25

Dea, S., Gagnon, C. A., Mardassi, H., Pirzadeh, B., and Rogan, D. (2000). Current knowledge on the structural proteins of porcine reproductive and respiratory syndrome (PRRS) virus: comparison of the north American and European isolates. *Arch. Virol.* 145, 659–688. doi: 10.1007/s007050050662

Decroly, E., Debarnot, C., Ferron, F., Bouvet, M., Coutard, B., Imbert, I., et al. (2011). Crystal structure and functional analysis of the SARS-coronavirus RNA cap 2'-O-methyltransferase nsp10/nsp16 complex. *PLoS Pathog.* 7:e1002059. doi: 10.1371/journal.ppat.1002059

Del Piero, F. (2000). Equine viral arteritis. *Vet. Pathol.* 37, 287–296. doi: 10.1354/vp.37-4-287

Deng, X., and Baker, S. C. (2018). An "old" protein with a new story: coronavirus endoribonuclease is important for evading host antiviral defenses. *Virology* 517, 157–163. doi: 10.1016/j.virol.2017.12.024

Denison, M. R., Graham, R. L., Donaldson, E. F., Eckerle, L. D., and Baric, R. S. (2011). Coronaviruses: an RNA proofreading machine regulates replication fidelity and diversity. *RNA Biol.* 8, 270–279. doi: 10.4161/rna.8.2.15013

Dhar, A. K., Cowley, J. A., Hasson, K. W., and Walker, P. J. (2004). Genomic organization, biology, and diagnosis of Taura syndrome virus and yellowhead virus of penaeid shrimp. *Adv. Virus Res.* 63, 353–421. doi: 10.1016/S0065-3527(04)63006-5

Di, H., Madden, J. C., Morantz, E. K., Tang, H.-Y., Graham, R. L., Baric, R. S., et al. (2017). Expanded subgenomic mRNA transcriptome and coding capacity of a nidovirus. *Proc. Natl. Acad. Sci. U. S. A.* 114, E8895–E8904. doi: 10.1073/pnas.1706696114

Di, H., McIntyre, A. A., and Brinton, M. A. (2018). New insights about the regulation of Nidovirus subgenomic mRNA synthesis. *Virology* 517, 38–43. doi: 10.1016/j.virol.2018.01.026

Dokland, T. (2010). The structural biology of PRRSV. *Virus Res.* 154, 86–97. doi: 10.1016/j.virusres.2010.07.029

Dong, X., Liu, S., Zhu, L., Wan, X., Liu, Q., Qiu, L., et al. (2017). Complete genome sequence of an isolate of a novel genotype of yellow head virus from *Fenneropenaeus chinensis* indigenous in China. *Arch. Virol.* 162, 1149–1152. doi: 10.1007/s00705-016-3203-2

Doyle, N., Neuman, B. W., Simpson, J., Hawes, P. C., Mantell, J., Verkade, P., et al. (2018). Infectious bronchitis virus nonstructural protein 4 alone induces membrane pairing. *Viruses* 10:477. doi: 10.3390/v10090477

Draker, R., Roper, R. L., Petric, M., and Tellier, R. (2006). The complete sequence of the bovine torovirus genome. *Virus Res.* 115, 56–68. doi: 10.1016/j.virusres.2005.07.005

Dreyfuss, G., Matunis, M. J., Pinol-Roma, S., and Burd, C. G. (1993). hnRNP proteins and the biogenesis of mRNA. *Annu. Rev. Biochem.* 62, 289–321. doi: 10.1146/annurev.bi.62.070193.001445

Drosten, C., Günther, S., Preiser, W., van der Werf, S., Brodt, H.-R., Becker, S., et al. (2003). Identification of a novel coronavirus in patients with severe acute respiratory syndrome. *N. Engl. J. Med.* 348, 1967–1976. doi: 10.1056/NEJMoa030747

Durham, P. J., Hassard, L. E., Norman, G. R., and Yemen, R. L. (1989). Viruses and virus-like particles detected during examination of feces from calves and piglets with diarrhea. *Can. Vet. J.* 30, 876–881.

Egloff, M.-P., Ferron, F., Campanacci, V., Longhi, S., Rancurel, C., Dutartre, H., et al. (2004). The severe acute respiratory syndrome-coronavirus replicative protein nsp9 is a single-stranded RNA-binding subunit unique in the RNA virus world. *Proc. Natl. Acad. Sci. U. S. A.* 101, 3792–3796. doi: 10.1073/pnas.0307877101

El-Sahly, H. M., Atmar, R. L., Glezen, W. P., and Greenberg, S. B. (2000). Spectrum of clinical illness in hospitalized patients with "common cold" virus infections. *Clin. Infect. Dis.* 31, 96–100. doi: 10.1086/313937

Emmott, E., Munday, D., Bickerton, E., Britton, P., Rodgers, M. A., Whitehouse, A., et al. (2013). The cellular interactome of the coronavirus infectious bronchitis virus nucleocapsid protein and functional implications for virus biology. *J. Virol.* 87, 9486–9500. doi: 10.1128/JVI.00321-13

Enjuanes, L., Almazan, F., Sola, I., and Zuniga, S. (2006). Biochemical aspects of coronavirus replication and virus-host interaction. *Annu. Rev. Microbiol.* 60, 211–230. doi: 10.1146/annurev.micro.60.080805.142157

Evans, M. R., and Simpson, R. W. (1980). The coronavirus avian infectious bronchitis virus requires the cell nucleus and host transcriptional factors. *Virology* 105, 582–591. doi: 10.1016/0042-6822(80)90058-6

Falsey, A. R., Walsh, E. E., and Hayden, F. G. (2002). Rhinovirus and coronavirus infection-associated hospitalizations among older adults. *J Infect Dis* 185, 1338–1341. doi: 10.1086/339881

Fang, P., Fang, L., Liu, X., Hong, Y., Wang, Y., Dong, N., et al. (2016). Identification and subcellular localization of porcine deltacoronavirus accessory protein NS6. *Virology* 499, 170–177. doi: 10.1016/j.virol.2016.09.015

Fang, Y., and Snijder, E. J. (2010). The PRRSV replicase: exploring the multifunctionality of an intriguing set of nonstructural proteins. *Virus Res.* 154, 61–76. doi: 10.1016/j.virusres.2010.07.030

Fang, P., Xie, C., Pan, T., Cheng, T., Chen, W., Xia, S., et al. (2023). Unfolding of an RNA G-quadruplex motif in the negative strand genome of porcine reproductive and respiratory syndrome virus by host and viral helicases to promote viral replication. *Nucleic Acids Res.* 51, 10752–10767. doi: 10.1093/nar/gkad759

Ferron, F., Subissi, L., Silveira De Morais, A. T., Le, N. T. T., Sevajol, M., Gluais, L., et al. (2018). Structural and molecular basis of mismatch correction and ribavirin excision from coronavirus RNA. *Proc. Natl. Acad. Sci. U. S. A.* 115, E162–E171. doi: 10.1073/pnas.1718806115

Frias-Staheli, N., Giannakopoulos, N. V., Kikkert, M., Taylor, S. L., Bridgen, A., Paragas, J., et al. (2007). Ovarian tumor domain-containing viral proteases evade ubiquitin-and ISG15-dependent innate immune responses. *Cell Host Microbe* 2, 404–416. doi: 10.1016/j.chom.2007.09.014

Furuya, T., and Lai, M. M. (1993). Three different cellular proteins bind to complementary sites on the 5′-end-positive and 3′-end-negative strands of mouse hepatitis virus RNA. *J. Virol.* 67, 7215–7222. doi: 10.1128/JVI.67.12.7215-7222.1993

Gagneur, A., Sizun, J., Vallet, S., Legr, M. C., Picard, B., and Talbot, P. J. (2002). Coronavirus-related nosocomial viral respiratory infections in a neonatal and paediatric intensive care unit: a prospective study. *J. Hosp. Infect.* 51, 59–64. doi: 10.1053/jhin.2002.1179

Galan, C., Sola, I., Nogales, A., Thomas, B., Akoulitchev, A., Enjuanes, L., et al. (2009). Host cell proteins interacting with the 3′ end of TGEV coronavirus genome influence virus replication. *Virology* 391, 304–314. doi: 10.1016/j.virol.2009.06.006

Gao, B., Gong, X., Fang, S., Weng, W., Wang, H., Chu, H., et al. (2021). Inhibition of anti-viral stress granule formation by coronavirus endoribonuclease nsp15 ensures efficient virus replication. *PLoS Pathog.* 17:e1008690. doi: 10.1371/journal.ppat.1008690

Gao, Y., Yan, L., Huang, Y., Liu, F., Zhao, Y., Cao, L., et al. (2020). Structure of the RNA-dependent RNA polymerase from COVID-19 virus. *Science* 368, 779–782. doi: 10.1126/science.abb7498

Goebel, S. J., Miller, T. B., Bennett, C. J., Bernard, K. A., and Masters, P. S. (2007). A hypervariable region within the 3′ cis-acting element of the murine coronavirus genome is nonessential for RNA synthesis but affects pathogenesis. *J. Virol.* 81, 1274–1287. doi: 10.1128/JVI.00803-06

Gorbalenya, A. E., Enjuanes, L., Ziebuhr, J., and Snijder, E. J. (2006). Nidovirales: evolving the largest RNA virus genome. *Virus Res.* 117, 17–37. doi: 10.1016/j.virusres.2006.01.017

Gorbalenya, A. E., Koonin, E. V., Donchenko, A. P., and Blinov, V. M. (1989). Coronavirus genome: prediction of putative functional domains in the non-structural polyprotein by comparative amino acid sequence analysis. *Nucleic Acids Res.* 17, 4847–4861. doi: 10.1093/nar/17.12.4847

Gordon, C. J., Tchesnokov, E. P., Feng, J. Y., Porter, D. P., and Gotte, M. (2020a). The antiviral compound remdesivir potently inhibits RNA-dependent RNA polymerase from Middle East respiratory syndrome coronavirus. *J. Biol. Chem.* 295, 4773–4779. doi: 10.1074/jbc.AC120.013056

Gordon, C. J., Tchesnokov, E. P., Woolner, E., Perry, J. K., Feng, J. Y., Porter, D. P., et al. (2020b). Remdesivir is a direct-acting antiviral that inhibits RNA-dependent RNA polymerase from severe acute respiratory syndrome coronavirus 2 with high potency. *J. Biol. Chem.* 295, 6785–6797. doi: 10.1074/jbc.RA120.013679

Gosert, R., Kanjanahaluethai, A., Egger, D., Bienz, K., and Baker, S. C. (2002). RNA replication of mouse hepatitis virus takes place at double-membrane vesicles. *J. Virol.* 76, 3697–3708. doi: 10.1128/JVI.76.8.3697-3708.2002

Graham, F. (2021). Daily briefing: Pfizer's COVID pill looks promising. *Nature*. doi: 10.1038/d41586-021-03379-5

Grossoehme, N. E., Li, L., Keane, S. C., Liu, P., Dann, C. E., Leibowitz, J. L., et al. (2009). Coronavirus N protein N-terminal domain (NTD) specifically binds the transcriptional regulatory sequence (TRS) and melts TRS-cTRS RNA duplexes. *J. Mol. Biol.* 394, 544–557. doi: 10.1016/j.jmb.2009.09.040

Guan, B. J., Wu, H. Y., and Brian, D. A. (2011). An optimal cis-replication stem-loop IV in the 5′ untranslated region of the mouse coronavirus genome extends 16 nucleotides into open reading frame 1. *J. Virol.* 85, 5593–5605. doi: 10.1128/JVI.00263-11

Gui, M., Liu, X., Guo, D., Zhang, Z., Yin, C. C., Chen, Y., et al. (2017). Electron microscopy studies of the coronavirus ribonucleoprotein complex. *Protein Cell* 8, 219–224. doi: 10.1007/s13238-016-0352-8

Guo, Z., Chen, X.-X., Li, R., Qiao, S., and Zhang, G. (2018). The prevalent status and genetic diversity of porcine reproductive and respiratory syndrome virus in China: a molecular epidemiological perspective. *Virol. J.* 15:2. doi: 10.1186/s12985-017-0910-6

Hackbart, M., Deng, X., and Baker, S. C. (2020). Coronavirus endoribonuclease targets viral polyuridine sequences to evade activating host sensors. *Proc. Natl. Acad. Sci. U. S. A.* 117, 8094–8103. doi: 10.1073/pnas.1921485117

Hagemeijer, M. C., Monastyrska, I., Griffith, J., van der Sluijs, P., Voortman, J., van Bergen en Henegouwen, P. M., et al. (2014). Membrane rearrangements mediated by coronavirus nonstructural proteins 3 and 4. *Virology* 458-459, 125–135. doi: 10.1016/j.virol.2014.04.027

Hagemeijer, M. C., Verheije, M. H., Ulasli, M., Shaltiel, I. A., de Vries, L. A., Reggiori, F., et al. (2010). Dynamics of coronavirus replication-transcription complexes. *J. Virol.* 84, 2134–2149. doi: 10.1128/JVI.01716-09

Hamilton, B. J., Burns, C. M., Nichols, R. C., and Rigby, W. F. (1997). Modulation of AUUUA response element binding by heterogeneous nuclear ribonucleoprotein A1 in human T lymphocytes. The roles of cytoplasmic location, transcription, and phosphorylation. *J. Biol. Chem.* 272, 28732–28741. doi: 10.1074/jbc.272.45.28732

Hamilton, B. J., Nagy, E., Malter, J. S., Arrick, B. A., and Rigby, W. F. (1993). Association of heterogeneous nuclear ribonucleoprotein A1 and C proteins with reiterated AUUUA sequences. *J. Biol. Chem.* 268, 8881–8887. doi: 10.1016/S0021-9258(18)52955-0

Hamre, D., and Procknow, J. J. (1966). A new virus isolated from the human respiratory tract. *Proceedings of the Society for Experimental Biology and medicine. Soc Exp. Biol. Med.* 121, 190–193. doi: 10.3181/00379727-121-30734

Harcourt, B. H., Jukneliene, D., Kanjanahaluethai, A., Bechill, J., Severson, K. M., Smith, C. M., et al. (2004). Identification of severe acute respiratory syndrome coronavirus replicase products and characterization of papain-like protease activity. *J. Virol.* 78, 13600–13612. doi: 10.1128/JVI.78.24.13600-13612.2004

Harris, E. (2023). FDA Grants full approval to Paxlovid, COVID-19 antiviral treatment. *JAMA* 329:2118. doi: 10.1001/jama.2023.9926

Hartenian, E., Nandakumar, D., Lari, A., Ly, M., Tucker, J. M., and Glaunsinger, B. A. (2020). The molecular virology of coronaviruses. *J. Biol. Chem.* 295, 12910–12934. doi: 10.1074/jbc.REV120.013930

Hemida, M. G., Chu, D. K., Poon, L. L., Perera, R. A., Alhammadi, M. A., Ng, H. Y., et al. (2014). MERS coronavirus in dromedary camel herd, Saudi Arabia. *Emerg. Infect. Dis.* 20, 1231–1234. doi: 10.3201/eid2007.140571

Hillen, H. S., Kokic, G., Farnung, L., Dienemann, C., Tegunov, D., and Cramer, P. (2020). Structure of replicating SARS-CoV-2 polymerase. *Nature* 584, 154–156. doi: 10.1038/s41586-020-2368-8

Hsieh, Y. C., Li, H. C., Chen, S. C., and Lo, S. Y. (2008). Interactions between M protein and other structural proteins of severe, acute respiratory syndrome-associated coronavirus. *J. Biomed. Sci.* 15, 707–717. doi: 10.1007/s11373-008-9278-3

Hu, Y., Ke, P., Gao, P., Zhang, Y., Zhou, L., Ge, X., et al. (2021). Identification of an Intramolecular switch that controls the interaction of helicase nsp10 with membrane-associated nsp12 of porcine reproductive and respiratory syndrome virus. *J. Virol.* 95:e0051821. doi: 10.1128/JVI.00518-21

Hu, Z.-M., Yang, Y.-L., Xu, L.-D., Wang, B., Qin, P., and Huang, Y.-W. (2019). Porcine Torovirus (PToV)-a brief review of etiology, diagnostic assays and current epidemiology. *Front. Vet. Sci.* 6:120. doi: 10.3389/fvets.2019.00120

Huang, P., and Lai, M. M. (1999). Polypyrimidine tract-binding protein binds to the complementary strand of the mouse hepatitis virus 3′ untranslated region, thereby altering RNA conformation. *J. Virol.* 73, 9110–9116. doi: 10.1128/JVI.73.11.9110-9116.1999

Huang, P., and Lai, M. M. (2001). Heterogeneous nuclear ribonucleoprotein a1 binds to the 3′-untranslated region and mediates potential 5′-3′-end cross talks of mouse hepatitis virus RNA. *J. Virol.* 75, 5009–5017. doi: 10.1128/JVI.75.11.5009-5017.2001

Hurst, K. R., Koetzner, C. A., and Masters, P. S. (2013). Characterization of a critical interaction between the coronavirus nucleocapsid protein and nonstructural protein 3 of the viral replicase-transcriptase complex. *J. Virol.* 87, 9159–9172. doi: 10.1128/JVI.01275-13

Hurst, K. R., Ye, R., Goebel, S. J., Jayaraman, P., and Masters, P. S. (2010). An interaction between the nucleocapsid protein and a component of the replicase-transcriptase complex is crucial for the infectivity of coronavirus genomic RNA. *J. Virol.* 84, 10276–10288. doi: 10.1128/JVI.01287-10

Hurst-Hess, K. R., Kuo, L., and Masters, P. S. (2015). Dissection of amino-terminal functional domains of murine coronavirus nonstructural protein 3. *J. Virol.* 89, 6033–6047. doi: 10.1128/JVI.00197-15

Hussain, S., Pan, J., Chen, Y., Yang, Y., Xu, J., Peng, Y., et al. (2005). Identification of novel subgenomic RNAs and noncanonical transcription initiation signals of severe acute respiratory syndrome coronavirus. *J. Virol.* 79, 5288–5295. doi: 10.1128/JVI.79.9.5288-5295.2005

Imbert, I., Guillemot, J.-C., Bourhis, J.-M., Bussetta, C., Coutard, B., Egloff, M.-P., et al. (2006). A second, non-canonical RNA-dependent RNA polymerase in SARS coronavirus. *EMBO J.* 25, 4933–4942. doi: 10.1038/sj.emboj.7601368

Ito, T., Okada, N., Okawa, M., Fukuyama, S., and Shimizu, M. (2009). Detection and characterization of bovine torovirus from the respiratory tract in Japanese cattle. *Vet. Microbiol.* 136, 366–371. doi: 10.1016/j.vetmic.2008.11.014

Ivanov, K. A., Hertzig, T., Rozanov, M., Bayer, S., Thiel, V., Gorbalenya, A. E., et al. (2004a). Major genetic marker of nidoviruses encodes a replicative endoribonuclease. *Proc. Natl. Acad. Sci. U. S. A.* 101, 12694–12699. doi: 10.1073/pnas.0403127101

Ivanov, K. A., Thiel, V., Dobbe, J. C., van der Meer, Y., Snijder, E. J., and Ziebuhr, J. (2004b). Multiple enzymatic activities associated with severe acute respiratory syndrome coronavirus helicase. *J. Virol.* 78, 5619–5632. doi: 10.1128/JVI.78.11.5619-5632.2004

Jendrach, M., Thiel, V., and Siddell, S. (1999). Characterization of an internal ribosome entry site within mRNA 5 of murine hepatitis virus. *Arch. Virol.* 144, 921–933. doi: 10.1007/s007050050556

Jeong, Y. S., and Makino, S. (1994). Evidence for coronavirus discontinuous transcription. *J. Virol.* 68, 2615–2623. doi: 10.1128/jvi.68.4.2615-2623.1994

Ji, M., Li, M., Sun, L., Deng, H., and Zhao, Y. G. (2023). DMV biogenesis during beta-coronavirus infection requires autophagy proteins VMP1 and TMEM41B. *Autophagy* 19, 737–738. doi: 10.1080/15548627.2022.2103783

Jin, H., Zhou, L., Ge, X., Zhang, H., Zhang, R., Wang, C., et al. (2017). Cellular DEAD-box RNA helicase 18 (DDX18) promotes the PRRSV replication via interaction with virus nsp2 and nsp10. *Virus Res.* 238, 204–212. doi: 10.1016/j.virusres.2017.05.028

Jing, H., Song, T., Cao, S., Sun, Y., Wang, J., Dong, W., et al. (2019). Nucleotide-binding oligomerization domain-like receptor X1 restricts porcine reproductive and respiratory syndrome virus-2 replication by interacting with viral Nsp9. *Virus Res.* 268, 18–26. doi: 10.1016/j.virusres.2019.05.011

Kaminski, A., Hunt, S. L., Patton, J. G., and Jackson, R. J. (1995). Direct evidence that polypyrimidine tract binding protein (PTB) is essential for internal initiation of translation of encephalomyocarditis virus RNA. *RNA* 1, 924–938.

Kang, H., Feng, M., Schroeder, M. E., Giedroc, D. P., and Leibowitz, J. L. (2006). Putative cis-acting stem-loops in the 5′ untranslated region of the severe acute respiratory syndrome coronavirus can substitute for their mouse hepatitis virus counterparts. *J. Virol.* 80, 10600–10614. doi: 10.1128/JVI.00455-06

Kanjanahaluethai, A., and Baker, S. C. (2000). Identification of mouse hepatitis virus papain-like proteinase 2 activity. *J. Virol.* 74, 7911–7921. doi: 10.1128/JVI.74.17.7911-7921.2000

Kappes, M. A., and Faaberg, K. S. (2015). PRRSV structure, replication and recombination: origin of phenotype and genotype diversity. *Virology* 479-480, 475–486. doi: 10.1016/j.virol.2015.02.012

Keane, S. C., and Giedroc, D. P. (2013). Solution structure of mouse hepatitis virus (MHV) nsp3a and determinants of the interaction with MHV nucleocapsid (N) protein. *J. Virol.* 87, 3502–3515. doi: 10.1128/JVI.03112-12

Khare, P., Sahu, U., Pandey, S. C., and Samant, M. (2020). Current approaches for target-specific drug discovery using natural compounds against SARS-CoV-2 infection. *Virus Res.* 290:198169. doi: 10.1016/j.virusres.2020.198169

Khataby, K., Fellahi, S., Loutfi, C., and Mustapha, E. M. (2016). Avian infectious bronchitis virus in Africa: a review. *Vet. Q.* 36, 71–75. doi: 10.1080/01652176.2015.1126869

Kim, Y. N., Jeong, Y. S., and Makino, S. (1993). Analysis of cis-acting sequences essential for coronavirus defective interfering RNA replication. *Virology* 197, 53–63. doi: 10.1006/viro.1993.1566

King, A. M. Q. A., Michael, J., Carstens, E. B., and Lefkowitz, E. J. (2012). "Order—Nidovirales" in *Virus Taxonomy*, Ninth Report of the International Committee on Taxonomy of Viruses, 784–794.

Kirchdoerfer, R. N., and Ward, A. B. (2019). Structure of the SARS-CoV nsp12 polymerase bound to nsp7 and nsp8 co-factors. *Nat. Commun.* 10:2342. doi: 10.1038/s41467-019-10280-3

Klumperman, J., Locker, J. K., Meijer, A., Horzinek, M. C., Geuze, H. J., and Rottier, P. J. (1994). Coronavirus M proteins accumulate in the Golgi complex beyond the site of virion budding. *J. Virol.* 68, 6523–6534. doi: 10.1128/jvi.68.10.6523-6534.1994

Knoops, K., Kikkert, M., Worm, S. H. E., Zevenhoven-Dobbe, J. C., van der Meer, Y., Koster, A. J., et al. (2008). SARS-coronavirus replication is supported by a reticulovesicular network of modified endoplasmic reticulum. *PLoS Biol.* 6:e226. doi: 10.1371/journal.pbio.0060226

Koopmans, M., and Horzinek, M. C. (1994). Toroviruses of animals and humans: a review. *Adv. Virus Res.* 43, 233–273. doi: 10.1016/S0065-3527(08)60050-0

Kuo, L., Hurst-Hess, K. R., Koetzner, C. A., and Masters, P. S. (2016). Analyses of coronavirus assembly interactions with interspecies membrane and Nucleocapsid protein chimeras. *J. Virol.* 90, 4357–4368. doi: 10.1128/JVI.03212-15

Kuwabara, M., Wada, K., Maeda, Y., Miyazaki, A., and Tsunemitsu, H. (2007). First isolation of cytopathogenic bovine torovirus in cell culture from a calf with diarrhea. *Clin. Vaccine Immunol.* 14, 998–1004. doi: 10.1128/CVI.00475-06

Kuwata, R., Satho, T., Isawa, H., Yen, N. T., Phong, T. V., Nga, P. T., et al. (2013). Characterization of Dak nong virus, an insect nidovirus isolated from Culex mosquitoes in Vietnam. *Arch. Virol.* 158, 2273–2284. doi: 10.1007/s00705-013-1741-4

Lai, M. M. (1998). Cellular factors in the transcription and replication of viral RNA genomes: a parallel to DNA-dependent RNA transcription. *Virology* 244, 1–12. doi: 10.1006/viro.1998.9098

Lai, M. M., and Cavanagh, D. (1997). The molecular biology of coronaviruses. *Adv. Virus Res.* 48, 1–100. doi: 10.1016/S0065-3527(08)60286-9

Lamb, Y. N. (2020). Remdesivir: first approval. *Drugs* 80, 1355–1363. doi: 10.1007/s40265-020-01378-w

Lauber, C., Ziebuhr, J., Junglen, S., Drosten, C., Zirkel, F., Nga, P. T., et al. (2012). Mesoniviridae: a proposed new family in the order Nidovirales formed by a single species of mosquito-borne viruses. *Arch. Virol.* 157, 1623–1628. doi: 10.1007/s00705-012-1295-x

Lavi, E., Weiss, S. R., and Hingley, S. T. (2012). *The Nidoviruses: (coronaviruses and Arteriviruses)* (Advances in Experimental Medicine and Biology, 494). Softcover reprint of the original 1st ed. 2001. Springer.

Lee, C. W., Li, L., and Giedroc, D. P. (2011). The solution structure of coronaviral stem-loop 2 (SL2) reveals a canonical CUYG tetraloop fold. *FEBS Lett.* 585, 1049–1053. doi: 10.1016/j.febslet.2011.03.002

Lee, T. C., Murthy, S., Del Corpo, O., Senecal, J., Butler-Laporte, G., Sohani, Z. N., et al. (2022). Remdesivir for the treatment of COVID-19: a systematic review and meta-analysis. *Clin. Microbiol. Infect.* 28, 1203–1210. doi: 10.1016/j.cmi.2022.04.018

Lehmann, K. C., Gorbalenya, A. E., Snijder, E. J., and Posthuma, C. C. (2016). Arterivirus RNA-dependent RNA polymerase: vital enzymatic activity remains elusive. *Virology* 487, 68–74. doi: 10.1016/j.virol.2015.10.002

Lehmann, K. C., Gulyaeva, A., Zevenhoven-Dobbe, J. C., Janssen, G. M. C., Ruben, M., Overkleeft, H. S., et al. (2015a). Discovery of an essential nucleotidylating activity associated with a newly delineated conserved domain in the RNA polymerase-containing protein of all nidoviruses. *Nucleic Acids Res.* 43, 8416–8434. doi: 10.1093/nar/gkv838

Lehmann, K. C., Hooghiemstra, L., Gulyaeva, A., Samborskiy, D. V., Zevenhoven-Dobbe, J. C., Snijder, E. J., et al. (2015b). Arterivirus nsp12 versus the coronavirus nsp16 2'-O-methyltransferase: comparison of the C-terminal cleavage products of two nidovirus pp1ab polyproteins. *J. Gen. Virol.* 96, 2643–2655. doi: 10.1099/vir.0.000209

Lehmann, K. C., Snijder, E. J., Posthuma, C. C., and Gorbalenya, A. E. (2015c). What we know but do not understand about nidovirus helicases. *Virus Res.* 202, 12–32. doi: 10.1016/j.virusres.2014.12.001

Li, H. P., Huang, P., Park, S., and Lai, M. M. (1999). Polypyrimidine tract-binding protein binds to the leader RNA of mouse hepatitis virus and serves as a regulator of viral transcription. *J. Virol.* 73, 772–777. doi: 10.1128/JVI.73.1.772-777.1999

Li, L., Kang, H., Liu, P., Makkinje, N., Williamson, S. T., Leibowitz, J. L., et al. (2008). Structural lability in stem-loop 1 drives a 5' UTR-3' UTR interaction in coronavirus replication. *J. Mol. Biol.* 377, 790–803. doi: 10.1016/j.jmb.2008.01.068

Li, Y., Tas, A., Snijder, E. J., and Fang, Y. (2012). Identification of porcine reproductive and respiratory syndrome virus ORF1a-encoded non-structural proteins in virus-infected cells. *J. Gen. Virol.* 93, 829–839. doi: 10.1099/vir.0.039289-0

Li, Y., Tas, A., Sun, Z., Snijder, E. J., and Fang, Y. (2015). Proteolytic processing of the porcine reproductive and respiratory syndrome virus replicase. *Virus Res.* 202, 48–59. doi: 10.1016/j.virusres.2014.12.027

Li, J., Wang, D., Fang, P., Pang, Y., Zhou, Y., Fang, L., et al. (2022). DEAD-box RNA helicase 21 (DDX21) positively regulates the replication of porcine reproductive and respiratory syndrome virus via multiple mechanisms. *Viruses* 14:467. doi: 10.3390/v14030467

Li, H. P., Zhang, X., Duncan, R., Comai, L., and Lai, M. M. (1997). Heterogeneous nuclear ribonucleoprotein A1 binds to the transcription-regulatory region of mouse hepatitis virus RNA. *Proc. Natl. Acad. Sci. U. S. A.* 94, 9544–9549. doi: 10.1073/pnas.94.18.9544

Li, Y., Zhou, L., Zhang, J., Ge, X., Zhou, R., Zheng, H., et al. (2014). Nsp9 and Nsp10 contribute to the fatal virulence of highly pathogenic porcine reproductive and respiratory syndrome virus emerging in China. *PLoS Pathog.* 10:e1004216. doi: 10.1371/journal.ppat.1004216

Li, J., Zhou, Y., Zhao, W., Liu, J., Ullah, R., Fang, P., et al. (2023). Porcine reproductive and respiratory syndrome virus degrades DDX10 via SQSTM1/p62-dependent selective autophagy to antagonize its antiviral activity. *Autophagy* 19, 2257–2274. doi: 10.1080/15548627.2023.2179844

Liang, H., Luo, D., Liao, H., and Li, S. (2022). Coronavirus usurps the autophagy-lysosome pathway and induces membranes rearrangement for infection and pathogenesis. *Front. Microbiol.* 13:846543. doi: 10.3389/fmicb.2022.846543

Lim, K. P., and Liu, D. X. (2001). The missing link in coronavirus assembly. Retention of the avian coronavirus infectious bronchitis virus envelope protein in the pre-Golgi compartments and physical interaction between the envelope and membrane proteins. *J. Biol. Chem.* 276, 17515–17523. doi: 10.1074/jbc.M009731200

Lin, Y. J., Liao, C. L., and Lai, M. M. (1994). Identification of the cis-acting signal for minus-strand RNA synthesis of a murine coronavirus: implications for the role of minus-strand RNA in RNA replication and transcription. *J. Virol.* 68, 8131–8140. doi: 10.1128/jvi.68.12.8131-8140.1994

Lin, Y. J., Zhang, X., Wu, R. C., and Lai, M. M. (1996). The 3′ untranslated region of coronavirus RNA is required for subgenomic mRNA transcription from a defective interfering RNA. *J. Virol.* 70, 7236–7240. doi: 10.1128/jvi.70.10.7236-7240.1996

Liu, D. X., Brierley, I., Tibbles, K. W., and Brown, T. D. (1994). A 100-kilodalton polypeptide encoded by open reading frame (ORF) 1b of the coronavirus infectious bronchitis virus is processed by ORF 1a products. *J. Virol.* 68, 5772–5780. doi: 10.1128/jvi.68.9.5772-5780.1994

Liu, P., Li, L., Keane, S. C., Yang, D., Leibowitz, J. L., and Giedroc, D. P. (2009). Mouse hepatitis virus stem-loop 2 adopts a uYNMG(U)a-like tetraloop structure that is highly functionally tolerant of base substitutions. *J. Virol.* 83, 12084–12093. doi: 10.1128/JVI.00915-09

Liu, P., Li, L., Millership, J. J., Kang, H., Leibowitz, J. L., and Giedroc, D. P. (2007). A U-turn motif-containing stem-loop in the coronavirus 5′ untranslated region plays a functional role in replication. *RNA* 13, 763–780. doi: 10.1261/rna.261807

Liu, L., Tian, J., Nan, H., Tian, M., Li, Y., Xu, X., et al. (2016). Porcine reproductive and respiratory syndrome virus Nucleocapsid protein interacts with Nsp9 and cellular DHX9 To regulate viral RNA synthesis. *J. Virol.* 90, 5384–5398. doi: 10.1128/JVI.03216-15

Liu, X., Verma, A., Garcia, G. Jr., Ramage, H., Lucas, A., Myers, R. L., et al. (2021). Targeting the coronavirus nucleocapsid protein through GSK-3 inhibition. *Proc. Natl. Acad. Sci. U. S. A.* 118:e2113401118. doi: 10.1073/pnas.2113401118

Liu, Q., and Wang, H.-Y. (2021). Porcine enteric coronaviruses: an updated overview of the pathogenesis, prevalence, and diagnosis. *Vet. Res. Commun.* 45, 75–86. doi: 10.1007/s11259-021-09808-0

Liu, Q., Yu, W., and Leibowitz, J. L. (1997). A specific host cellular protein binding element near the 3′ end of mouse hepatitis virus genomic RNA. *Virology* 232, 74–85. doi: 10.1006/viro.1997.8553

Lo, Y. S., Lin, S. Y., Wang, S. M., Wang, C. T., Chiu, Y. L., Huang, T. H., et al. (2013). Oligomerization of the carboxyl terminal domain of the human coronavirus 229E nucleocapsid protein. *FEBS Lett.* 587, 120–127. doi: 10.1016/j.febslet.2012.11.016

Lojkic, I., Kresic, N., Simic, I., and Bedekovic, T. (2015). Detection and molecular characterisation of bovine corona and toroviruses from Croatian cattle. *BMC Vet. Res.* 11:202. doi: 10.1186/s12917-015-0511-9

Lu, J., Gao, F., Wei, Z., Liu, P., Liu, C., Zheng, H., et al. (2011). A 5′-proximal stem-loop structure of 5′ untranslated region of porcine reproductive and respiratory syndrome virus genome is key for virus replication. *Virol. J.* 8:172. doi: 10.1186/1743-422X-8-172

Lu, S., Ye, Q., Singh, D., Cao, Y., Diedrich, J. K., Yates, J. R. 3rd, et al. (2021). The SARS-CoV-2 nucleocapsid phosphoprotein forms mutually exclusive condensates with RNA and the membrane-associated M protein. *Nat. Commun.* 12:502. doi: 10.1038/s41467-020-20768-y

Lunney, J. K., Fang, Y., Ladinig, A., Chen, N., Li, Y., Rowland, B., et al. (2016). Porcine reproductive and respiratory syndrome virus (PRRSV): pathogenesis and interaction with the immune system. *Annu Rev Anim Biosci* 4, 129–154. doi: 10.1146/annurev-animal-022114-111025

Luo, H., Chen, Q., Chen, J., Chen, K., Shen, X., and Jiang, H. (2005). The nucleocapsid protein of SARS coronavirus has a high binding affinity to the human cellular heterogeneous nuclear ribonucleoprotein A1. *FEBS Lett.* 579, 2623–2628. doi: 10.1016/j.febslet.2005.03.080

Najimudeen, S., Hassan, M. S., Cork, S., and Abdul-Careem, M. F. (2020). Infectious bronchitis coronavirus infection in chickens: multiple system disease with immune suppression. *Pathogens* 9:779. doi: 10.3390/pathogens9100779

Madhugiri, R., Fricke, M., Marz, M., and Ziebuhr, J. (2014). RNA structure analysis of alphacoronavirus terminal genome regions. *Virus Res.* 194, 76–89. doi: 10.1016/j.virusres.2014.10.001

Madhugiri, R., Fricke, M., Marz, M., and Ziebuhr, J. (2016). Coronavirus cis-acting RNA elements. *Adv. Virus Res.* 96, 127–163. doi: 10.1016/bs.aivir.2016.08.007

Maier, H. J., Hawes, P. C., Cottam, E. M., Mantell, J., Verkade, P., Monaghan, P., et al. (2013). Infectious bronchitis virus generates spherules from zippered endoplasmic reticulum membranes. *MBio* 4, e00801–e00813. doi: 10.1128/mBio.00801-13

Maio, N., Raza, M. K., Li, Y., Zhang, D. L., Bollinger, J. M. Jr., Krebs, C., et al. (2023). An iron-sulfur cluster in the zinc-binding domain of the SARS-CoV-2 helicase modulates its RNA-binding and -unwinding activities. *Proc. Natl. Acad. Sci. U. S. A.* 120:e2303860120. doi: 10.1073/pnas.2303860120

Makino, S., Soe, L. H., Shieh, C. K., and Lai, M. M. (1988). Discontinuous transcription generates heterogeneity at the leader fusion sites of coronavirus mRNAs. *J. Virol.* 62, 3870–3873. doi: 10.1128/jvi.62.10.3870-3873.1988

Marzolini, C., Kuritzkes, D. R., Marra, F., Boyle, A., Gibbons, S., Flexner, C., et al. (2022). Recommendations for the Management of Drug-Drug Interactions between the COVID-19 antiviral Nirmatrelvir/ritonavir (Paxlovid) and Comedications. *Clin. Pharmacol. Ther.* 112, 1191–1200. doi: 10.1002/cpt.2646

Masters, P. S. (2006). The molecular biology of coronaviruses. *Adv. Virus Res.* 66, 193–292. doi: 10.1016/S0065-3527(06)66005-3

Mateos-Gomez, P. A., Morales, L., Zuniga, S., Enjuanes, L., and Sola, I. (2013). Long-distance RNA-RNA interactions in the coronavirus genome form high-order structures promoting discontinuous RNA synthesis during transcription. *J. Virol.* 87, 177–186. doi: 10.1128/JVI.01782-12

Mateos-Gómez, P. A., Zuñiga, S., Palacio, L., Enjuanes, L., and Sola, I. (2011). Gene N proximal and distal RNA motifs regulate coronavirus nucleocapsid mRNA transcription. *J. Virol.* 85, 8968–8980. doi: 10.1128/JVI.00869-11

McBride, R., van Zyl, M., and Fielding, B. C. (2014). The coronavirus nucleocapsid is a multifunctional protein. *Viruses* 6, 2991–3018. doi: 10.3390/v6082991

McCluskey, B. J., Haley, C., Rovira, A., Main, R., Zhang, Y., and Barder, S. (2016). Retrospective testing and case series study of porcine delta coronavirus in U.S. swine herds. *Vet. Res. Commun.* 123, 185–191. doi: 10.1016/j.prevetmed.2015.10.018

Menachery, V. D., Debbink, K., and Baric, R. S. (2014). Coronavirus non-structural protein 16: evasion, attenuation, and possible treatments. *Virus Res.* 194, 191–199. doi: 10.1016/j.virusres.2014.09.009

Michalska, K., Kim, Y., Jedrzejczak, R., Maltseva, N. I., Stols, L., Endres, M., et al. (2020). Crystal structures of SARS-CoV-2 ADP-ribose phosphatase: from the apo form to ligand complexes. *IUCRJ* 7, 814–824. doi: 10.1107/S2052252520009653

Miller, W. A., and Koev, G. (2000). Synthesis of subgenomic RNAs by positive-strand RNA viruses. *Virology* 273, 1–8. doi: 10.1006/viro.2000.0421

Mishchenko, E. L., and Ivanisenko, V. A. (2022). Replication-transcription complex of coronaviruses: functions of individual viral non-structural subunits, properties and architecture of their complexes. *Vavilovskii Zhurnal Genet Selektsii* 26, 121–127. doi: 10.18699/VJGB-22-15

Molenkamp, R., van Tol, H., Rozier, B. C. D., van der Meer, Y., Spaan, W. J. M., and Snijder, E. J. (2000). The arterivirus replicase is the only viral protein required for genome replication and subgenomic mRNA transcription. *J. Gen. Virol.* 81, 2491–2496. doi: 10.1099/0022-1317-81-10-2491

Mora-Díaz, J. C., Piñeyro, P. E., Houston, E., Zimmerman, J., and Giménez-Lirola, L. G. (2019). Porcine Hemagglutinating encephalomyelitis virus: a review. *Front. Vet. Sci.* 6:53. doi: 10.3389/fvets.2019.00053

Morales, L., Mateos-Gomez, P. A., Capiscol, C., del Palacio, L., Enjuanes, L., and Sola, I. (2013). Transmissible gastroenteritis coronavirus genome packaging signal is located at the 5′ end of the genome and promotes viral RNA incorporation into virions in a replication-independent process. *J. Virol.* 87, 11579–11590. doi: 10.1128/JVI.01836-13

Mukhopadhyay, R., Jia, J., Arif, A., Ray, P. S., and Fox, P. L. (2009). The GAIT system: a gatekeeper of inflammatory gene expression. *Trends Biochem. Sci.* 34, 324–331. doi: 10.1016/j.tibs.2009.03.004

Munro, J., Callinan, R., and Owens, L. (2011). Gill-associated virus and its association with decreased production of *Penaeus monodon* in Australian prawn farms. *J. Fish Dis.* 34, 13–20. doi: 10.1111/j.1365-2761.2010.01209.x

Munro, J., and Owens, L. (2007). Yellow head-like viruses affecting the penaeid aquaculture industry: a review. *Aquacult. Res.* 38, 893–908. doi: 10.1111/j.1365-2109.2007.01735.x

Music, N., and Gagnon, C. A. (2010). The role of porcine reproductive and respiratory syndrome (PRRS) virus structural and non-structural proteins in virus pathogenesis. *Anim. Health Res. Rev.* 11, 135–163. doi: 10.1017/S1466252310000034

Myrrha, L. W., Silva, F. M., Peternelli, E. F., Junior, A. S., Resende, M., and de Almeida, M. R. (2011). The paradox of feline coronavirus pathogenesis: a review. *Adv. Virol.* 2011:109849. doi: 10.1155/2011/109849

Nan, H., Lan, J., Tian, M., Dong, S., Tian, J., Liu, L., et al. (2018). The network of interactions among porcine reproductive and respiratory syndrome virus non-structural proteins. *Front. Microbiol.* 9:970. doi: 10.3389/fmicb.2018.00970

Napthine, S., Treffers, E. E., Bell, S., Goodfellow, I., Fang, Y., Firth, A. E., et al. (2016). A novel role for poly(C) binding proteins in programmed ribosomal frameshifting. *Nucleic Acids Res.* 44, 5491–5503. doi: 10.1093/nar/gkw480

Nedialkova, D. D., Gorbalenya, A. E., and Snijder, E. J. (2010). Arterivirus Nsp1 modulates the accumulation of minus-strand templates to control the relative abundance of viral mRNAs. *PLoS Pathog.* 6:e1000772. doi: 10.1371/journal.ppat.1000772

Nedialkova, D. D., Ulferts, R., van den Born, E., Lauber, C., Gorbalenya, A. E., Ziebuhr, J., et al. (2009). Biochemical characterization of arterivirus nonstructural protein 11 reveals the nidovirus-wide conservation of a replicative endoribonuclease. *J. Virol.* 83, 5671–5682. doi: 10.1128/JVI.00261-09

Neufeldt, C. J., Joyce, M. A., Van Buuren, N., Levin, A., Kirkegaard, K., Gale, M., et al. (2016). The hepatitis C virus-induced membranous web and associated nuclear transport machinery limit access of pattern recognition receptors to viral replication sites. *PLoS Pathog.* 12:e1005428. doi: 10.1371/journal.ppat.1005428

Neuman, B. W., Kiss, G., Kunding, A. H., Bhella, D., Baksh, M. F., Connelly, S., et al. (2011). A structural analysis of M protein in coronavirus assembly and morphology. *J. Struct. Biol.* 174, 11–22. doi: 10.1016/j.jsb.2010.11.021

Neumann, E. J., Kliebenstein, J. B., Johnson, C. D., Mabry, J. W., Bush, E. J., Seitzinger, A. H., et al. (2005). Assessment of the economic impact of porcine reproductive and respiratory syndrome on swine production in the United States. *J. Am. Vet. Med. Assoc.* 227, 385–392. doi: 10.2460/javma.2005.227.385

Nga, P. T., Parquet, M. C., Lauber, C., Parida, M., Nabeshima, T., Yu, F., et al. (2011). Discovery of the first insect nidovirus, a missing evolutionary link in the emergence of the largest RNA virus genomes. *PLoS Pathog.* 7:e1002215. doi: 10.1371/journal.ppat.1002215

Nguyen, V. P., and Hogue, B. G. (1997). Protein interactions during coronavirus assembly. *J. Virol.* 71, 9278–9284. doi: 10.1128/jvi.71.12.9278-9284.1997

Niepmann, M. (1996). Porcine polypyrimidine tract-binding protein stimulates translation initiation at the internal ribosome entry site of foot-and-mouth-disease virus. *FEBS Lett.* 388, 39–42. doi: 10.1016/0014-5793(96)00509-1

Niepmann, M., Petersen, A., Meyer, K., and Beck, E. (1997). Functional involvement of polypyrimidine tract-binding protein in translation initiation complexes with the internal ribosome entry site of foot-and-mouth disease virus. *J. Virol.* 71, 8330–8339. doi: 10.1128/jvi.71.11.8330-8339.1997

Notkins, A. L., and Shochat, S. J. (1963). Studies on the multiplication and the properties of the lactic dehydrogenase agent. *J. Exp. Med.* 117, 735–747. doi: 10.1084/jem.117.5.735

Oudshoorn, D., Rijs, K., Limpens, R. W. A. L., Groen, K., Koster, A. J., Snijder, E. J., et al. (2017). Expression and cleavage of Middle East respiratory syndrome coronavirus nsp3-4 Polyprotein induce the formation of double-membrane vesicles that mimic those associated with Coronaviral RNA replication. *MBio* 8, e01658–e01617. doi: 10.1128/mBio.01658-17

Parrish, K., Kirkland, P. D., Skerratt, L. F., and Ariel, E. (2021). Nidoviruses in reptiles: a review. *Front. Vet. Sci.* 8:733404. doi: 10.3389/fvets.2021.733404

Pasternak, A. O., Spaan, W. J. M., and Snijder, E. J. (2006). Nidovirus transcription: how to make sense. *J. Gen. Virol.* 87, 1403–1421. doi: 10.1099/vir.0.81611-0

Pasternak, A. O., van den Born, E., Spaan, W. J., and Snijder, E. J. (2001). Sequence requirements for RNA strand transfer during nidovirus discontinuous subgenomic RNA synthesis. *EMBO J.* 20, 7220–7228. doi: 10.1093/emboj/20.24.7220

Pasternak, A. O., van den Born, E., Spaan, W. J. M., and Snijder, E. J. (2003). The stability of the duplex between sense and antisense transcription-regulating sequences is a crucial factor in arterivirus subgenomic mRNA synthesis. *J. Virol.* 77, 1175–1183. doi: 10.1128/JVI.77.2.1175-1183.2003

Patel, A., Treffers, E. E., Meier, M., Patel, T. R., Stetefeld, J., Snijder, E. J., et al. (2020). Molecular characterization of the RNA-protein complex directing −2/−1 programmed ribosomal frameshifting during arterivirus replicase expression. *J. Biol. Chem.* 295, 17904–17921. doi: 10.1074/jbc.RA120.016105

Pedersen, K. W., van der Meer, Y., Roos, N., and Snijder, E. J. (1999). Open reading frame 1a-encoded subunits of the arterivirus replicase induce endoplasmic reticulum-derived double-membrane vesicles which carry the viral replication complex. *J. Virol.* 73, 2016–2026. doi: 10.1128/JVI.73.3.2016-2026.1999

Peng, T. Y., Lee, K. R., and Tarn, W. Y. (2008). Phosphorylation of the arginine/serine dipeptide-rich motif of the severe acute respiratory syndrome coronavirus nucleocapsid protein modulates its multimerization, translation inhibitory activity and cellular localization. *FEBS J.* 275, 4152–4163. doi: 10.1111/j.1742-4658.2008.06564.x

Peng, Q., Peng, R., Yuan, B., Zhao, J., Wang, M., Wang, X., et al. (2020). Structural and biochemical characterization of the nsp12-nsp7-nsp8 Core polymerase complex from SARS-CoV-2. *Cell Rep.* 31:107774. doi: 10.1016/j.celrep.2020.107774

Penrith, M. L., and Gerdes, G. H. (1992). Breda virus-like particles in pigs in South Africa. *J. South. Afr. Vet. Assoc.* 63:102.

Perdikari, T. M., Murthy, A. C., Ryan, V. H., Watters, S., Naik, M. T., and Fawzi, N. L. (2020). SARS-CoV-2 nucleocapsid protein phase-separates with RNA and with human hnRNPs. *EMBO J.* 39:e106478. doi: 10.15252/embj.2020106478

Perry, J. K., Appleby, T. C., Bilello, J. P., Feng, J. Y., Schmitz, U., and Campbell, E. A. (2021). An atomistic model of the coronavirus replication-transcription complex as a hexamer assembled around nsp15. *J. Biol. Chem.* 297:101218. doi: 10.1016/j.jbc.2021.101218

Petrosillo, N., Viceconte, G., Ergonul, O., Ippolito, G., and Petersen, E. (2020). COVID-19, SARS and MERS: are they closely related? *Clin. Microbiol. Infect.* 26, 729–734. doi: 10.1016/j.cmi.2020.03.026

Pirzada, R. H., Ahmad, B., Qayyum, N., and Choi, S. (2023). Modeling structure-activity relationships with machine learning to identify GSK3-targeted small molecules as potential COVID-19 therapeutics. *Front. Endocrinol.* 14:1084327. doi: 10.3389/fendo.2023.1084327

Plagemann, P. G., and Moennig, V. (1992). Lactate dehydrogenase-elevating virus, equine arteritis virus, and simian hemorrhagic fever virus: a new group of positive-strand RNA viruses. *Adv. Virus Res.* 41, 99–192. doi: 10.1016/s0065-3527(08)60036-6

Plagemann, P. G., Rowland, R. R., Even, C., and Faaberg, K. S. (1995). Lactate dehydrogenase-elevating virus: an ideal persistent virus? *Springer Semin. Immunopathol.* 17, 167–186. doi: 10.1007/BF00196164

Plant, E. P., Pérez-Alvarado, G. C., Jacobs, J. L., Mukhopadhyay, B., Hennig, M., and Dinman, J. D. (2005). A three-stemmed mRNA pseudoknot in the SARS coronavirus frameshift signal. *PLoS Biol.* 3:e172. doi: 10.1371/journal.pbio.0030172

Poch, O., Sauvaget, I., Delarue, M., and Tordo, N. (1989). Identification of four conserved motifs among the RNA-dependent polymerase encoding elements. *EMBO J.* 8, 3867–3874. doi: 10.1002/j.1460-2075.1989.tb08565.x

Pol, J. M., Wagenaar, F., and Reus, J. E. (1997). Comparative morphogenesis of three PRRS virus strains. *Vet. Microbiol.* 55, 203–208. doi: 10.1016/S0378-1135(96)01329-6

Ponnusamy, R., Moll, R., Weimar, T., Mesters, J. R., and Hilgenfeld, R. (2008). Variable oligomerization modes in coronavirus non-structural protein 9. *J. Mol. Biol.* 383, 1081–1096. doi: 10.1016/j.jmb.2008.07.071

Posthuma, C. C., Pedersen, K. W., Lu, Z., Joosten, R. G., Roos, N., Zevenhoven-Dobbe, J. C., et al. (2008). Formation of the arterivirus replication/transcription complex: a key role for nonstructural protein 3 in the remodeling of intracellular membranes. *J. Virol.* 82, 4480–4491. doi: 10.1128/JVI.02756-07

Posthuma, C. C., Te Velthuis, A. J. W., and Snijder, E. J. (2017). Nidovirus RNA polymerases: complex enzymes handling exceptional RNA genomes. *Virus Res.* 234, 58–73. doi: 10.1016/j.virusres.2017.01.023

Prentice, E., Jerome, W. G., Yoshimori, T., Mizushima, N., and Denison, M. R. (2004). Coronavirus replication complex formation utilizes components of cellular autophagy. *J. Biol. Chem.* 279, 10136–10141. doi: 10.1074/jbc.M306124200

Pringle, C. R. (1996). Virus taxonomy 1996—a bulletin from the Xth international congress of virology in Jerusalem. *Arch. Virol.* 141, 2251–2256. doi: 10.1007/BF01718231

Putics, A., Filipowicz, W., Hall, J., Gorbalenya, A. E., and Ziebuhr, J. (2005). ADP-ribose-1-monophosphatase: a conserved coronavirus enzyme that is dispensable for viral replication in tissue culture. *J. Virol.* 79, 12721–12731. doi: 10.1128/JVI.79.20.12721-12731.2005

Raman, S., Bouma, P., Williams, G. D., and Brian, D. A. (2003). Stem-loop III in the 5′ untranslated region is a cis-acting element in bovine coronavirus defective interfering RNA replication. *J. Virol.* 77, 6720–6730. doi: 10.1128/JVI.77.12.6720-6730.2003

Ren, J., Ding, Z., Fang, P., Xiao, S., and Fang, L. (2021). ATPase and helicase activities of porcine epidemic diarrhea virus nsp13. *Vet. Microbiol.* 257:109074. doi: 10.1016/j.vetmic.2021.109074

Ricciardi, S., Guarino, A. M., Giaquinto, L., Polishchuk, E. V., Santoro, M., Di Tullio, G., et al. (2022). The role of NSP6 in the biogenesis of the SARS-CoV-2 replication organelle. *Nature* 606, 761–768. doi: 10.1038/s41586-022-04835-6

Riley, V., Lilly, F., Huerto, E., and Bardell, D. (1960). Transmissible agent associated with 26 types of experimental mouse neoplasms. *Science* 132, 545–547. doi: 10.1126/science.132.3426.545

Roingeard, P., Eymieux, S., Burlaud-Gaillard, J., Hourioux, C., Patient, R., and Blanchard, E. (2022). The double-membrane vesicle (DMV): a virus-induced organelle dedicated to the replication of SARS-CoV-2 and other positive-sense single-stranded RNA viruses. *Cell. Mol. Life Sci.* 79:425. doi: 10.1007/s00018-022-04469-x

Rüdiger, A.-T., Mayrhofer, P., Ma-Lauer, Y., Pohlentz, G., Müthing, J., von Brunn, A., et al. (2016). Tubulins interact with porcine and human S proteins of the genus Alphacoronavirus and support successful assembly and release of infectious viral particles. *Virology* 497, 185–197. doi: 10.1016/j.virol.2016.07.022

Salzberger, B., Buder, F., Lampl, B., Ehrenstein, B., Hitzenbichler, F., Holzmann, T., et al. (2021). Epidemiology of SARS-CoV-2. *Infection* 49, 233–239. doi: 10.1007/s15010-020-01531-3

Sawicki, S. G., and Sawicki, D. L. (1990). Coronavirus transcription: subgenomic mouse hepatitis virus replicative intermediates function in RNA synthesis. *J. Virol.* 64, 1050–1056. doi: 10.1128/jvi.64.3.1050-1056.1990

Sawicki, S. G., and Sawicki, D. L. (1995). Coronaviruses use discontinuous extension for synthesis of subgenome-length negative strands. *Adv. Exp. Med. Biol.* 380, 499–506. doi: 10.1007/978-1-4615-1899-0_79

Sawicki, S. G., and Sawicki, D. L. (2005). Coronavirus transcription: a perspective. *Curr. Top. Microbiol. Immunol.* 287, 31–55. doi: 10.1007/3-540-26765-4_2

Sawicki, S. G., Sawicki, D. L., and Siddell, S. G. (2007). A contemporary view of coronavirus transcription. *J. Virol.* 81, 20–29. doi: 10.1128/JVI.01358-06

Sawicki, S. G., Sawicki, D. L., Younker, D., Meyer, Y., Thiel, V., Stokes, H., et al. (2005). Functional and genetic analysis of coronavirus replicase-transcriptase proteins. *PLoS Pathog.* 1:e39. doi: 10.1371/journal.ppat.0010039

Schelle, B., Karl, N., Ludewig, B., Siddell, S. G., and Thiel, V. (2005). Selective replication of coronavirus genomes that express nucleocapsid protein. *J. Virol.* 79, 6620–6630. doi: 10.1128/JVI.79.11.6620-6630.2005

Schütze, H., Ulferts, R., Schelle, B., Bayer, S., Granzow, H., Hoffmann, B., et al. (2006). Characterization of white bream virus reveals a novel genetic cluster of nidoviruses. *J. Virol.* 80, 11598–11609. doi: 10.1128/JVI.01758-06

Schwarz, B., Routledge, E., and Siddell, S. G. (1990). Murine coronavirus nonstructural protein ns2 is not essential for virus replication in transformed cells. *J. Virol.* 64, 4784–4791. doi: 10.1128/jvi.64.10.4784-4791.1990

Seybert, A., Hegyi, A., Siddell, S. G., and Ziebuhr, J. (2000a). The human coronavirus 229E superfamily 1 helicase has RNA and DNA duplex-unwinding activities with 5′-to-3′ polarity. *RNA* 6, 1056–1068. doi: 10.1017/s1355838200000728

Seybert, A., Posthuma, C. C., van Dinten, L. C., Snijder, E. J., Gorbalenya, A. E., and Ziebuhr, J. (2005). A complex zinc finger controls the enzymatic activities of nidovirus helicases. *J. Virol.* 79, 696–704. doi: 10.1128/JVI.79.2.696-704.2005

Seybert, A., van Dinten, L. C., Snijder, E. J., and Ziebuhr, J. (2000b). Biochemical characterization of the equine arteritis virus helicase suggests a close functional relationship between arterivirus and coronavirus helicases. *J. Virol.* 74, 9586–9593. doi: 10.1128/JVI.74.20.9586-9593.2000

Sharma, A., Tiwari, S., Deb, M. K., and Marty, J. L. (2020). Severe acute respiratory syndrome coronavirus-2 (SARS-CoV-2): a global pandemic and treatment strategies. *Int. J. Antimicrob. Agents* 56:106054. doi: 10.1016/j.ijantimicag.2020.106054

Shen, X., and Masters, P. S. (2001). Evaluation of the role of heterogeneous nuclear ribonucleoprotein A1 as a host factor in murine coronavirus discontinuous transcription and genome replication. *Proc. Natl. Acad. Sci. U. S. A.* 98, 2717–2722. doi: 10.1073/pnas.031424298

Shi, S. T., Huang, P., Li, H. P., and Lai, M. M. (2000). Heterogeneous nuclear ribonucleoprotein A1 regulates RNA synthesis of a cytoplasmic virus. *EMBO J.* 19, 4701–4711. doi: 10.1093/emboj/19.17.4701

Shi, S. T., and Lai, M. M. C. (2005). Viral and cellular proteins involved in coronavirus replication. *Curr. Top. Microbiol. Immunol.* 287, 95–131. doi: 10.1007/3-540-26765-4_4

Shi, M., Lin, X.-D., Chen, X., Tian, J.-H., Chen, L.-J., Li, K., et al. (2018). The evolutionary history of vertebrate RNA viruses. *Nature* 556, 197–202. doi: 10.1038/s41586-018-0012-7

Shi, Y., Tong, X., Ye, G., Xiu, R., Li, L., Sun, L., et al. (2020). Structural characterization of the helicase nsp10 encoded by porcine reproductive and respiratory syndrome virus. *J. Virol.* 94, e02158–e02119. doi: 10.1128/JVI.02158-19

Shi, S. T., Yu, G. Y., and Lai, M. M. (2003). Multiple type a/B heterogeneous nuclear ribonucleoproteins (hnRNPs) can replace hnRNP A1 in mouse hepatitis virus RNA synthesis. *J. Virol.* 77, 10584–10593. doi: 10.1128/JVI.77.19.10584-10593.2003

Shu, T., Huang, M., Wu, D., Ren, Y., Zhang, X., Han, Y., et al. (2020). SARS-Coronavirus-2 Nsp13 possesses NTPase and RNA helicase activities that can be inhibited by bismuth salts. *Virol. Sin.* 35, 321–329. doi: 10.1007/s12250-020-00242-1

Sittidilokratna, N., Dangtip, S., Cowley, J. A., and Walker, P. J. (2008). RNA transcription analysis and completion of the genome sequence of yellow head nidovirus. *Virus Res.* 136, 157–165. doi: 10.1016/j.virusres.2008.05.008

Slanina, H., Madhugiri, R., Bylapudi, G., Schultheiss, K., Karl, N., Gulyaeva, A., et al. (2021). Coronavirus replication-transcription complex: vital and selective NMPylation of a conserved site in nsp9 by the NiRAN-RdRp subunit. *Proc. Natl. Acad. Sci. U. S. A.* 118:e2022310118. doi: 10.1073/pnas.2022310118

Smits, S. L., van Vliet, A. L. W., Segeren, K., el Azzouzi, H., van Essen, M., and de Groot, R. J. (2005). Torovirus non-discontinuous transcription: mutational analysis of a subgenomic mRNA promoter. *J. Virol.* 79, 8275–8281. doi: 10.1128/JVI.79.13.8275-8281.2005

Snijder, E. J., Bredenbeek, P. J., Dobbe, J. C., Thiel, V., Ziebuhr, J., Poon, L. L. M., et al. (2003). Unique and conserved features of genome and proteome of SARS-coronavirus, an early split-off from the coronavirus group 2 lineage. *J. Mol. Biol.* 331, 991–1004. doi: 10.1016/S0022-2836(03)00865-9

Snijder, E. J., Decroly, E., and Ziebuhr, J. (2016). The nonstructural proteins directing coronavirus RNA synthesis and processing. *Adv. Virus Res.* 96, 59–126. doi: 10.1016/bs.aivir.2016.08.008

Snijder, E. J., den Boon, J. A., Horzinek, M. C., and Spaan, W. J. (1991). Comparison of the genome organization of Toro- and coronaviruses: evidence for two nonhomologous RNA recombination events during Berne virus evolution. *Virology* 180, 448–452. doi: 10.1016/0042-6822(91)90056-H

Snijder, E. J., and Horzinek, M. C. (1993). Toroviruses: replication, evolution and comparison with other members of the coronavirus-like superfamily. *J. Gen. Virol.* 74, 2305–2316. doi: 10.1099/0022-1317-74-11-2305

Snijder, E. J., Kikkert, M., and Fang, Y. (2013). Arterivirus molecular biology and pathogenesis. *J. Gen. Virol.* 94, 2141–2163. doi: 10.1099/vir.0.056341-0

Snijder, E. J., Limpens, R. W. A. L., de Wilde, A. H., de Jong, A. W. M., Zevenhoven-Dobbe, J. C., Maier, H. J., et al. (2020). A unifying structural and functional model of the coronavirus replication organelle: tracking down RNA synthesis. *PLoS Biol.* 18:e3000715. doi: 10.1371/journal.pbio.3000715

Snijder, E. J., and Meulenberg, J. J. (1998). The molecular biology of arteriviruses. *J. Gen. Virol.* 79, 961–979. doi: 10.1099/0022-1317-79-5-961

Snijder, E. J., van der Meer, Y., Zevenhoven-Dobbe, J., Onderwater, J. J. M., van der Meulen, J., Koerten, H. K., et al. (2006). Ultrastructure and origin of membrane vesicles associated with the severe acute respiratory syndrome coronavirus replication complex. *J. Virol.* 80, 5927–5940. doi: 10.1128/JVI.02501-05

Snijder, E. J., van Tol, H., Roos, N., and Pedersen, K. W. (2001). Non-structural proteins 2 and 3 interact to modify host cell membranes during the formation of the arterivirus replication complex. *J. Gen. Virol.* 82, 985–994. doi: 10.1099/0022-1317-82-5-985

Snijder, E. J., Wassenaar, A. L., and Spaan, W. J. (1994). Proteolytic processing of the replicase ORF1a protein of equine arteritis virus. *J. Virol.* 68, 5755–5764. doi: 10.1128/jvi.68.9.5755-5764.1994

Snijder, E. J., Wassenaar, A. L., Spaan, W. J., and Gorbalenya, A. E. (1995). The arterivirus Nsp2 protease. An unusual cysteine protease with primary structure similarities to both papain-like and chymotrypsin-like proteases. *J. Biol. Chem.* 270, 16671–16676. doi: 10.1074/jbc.270.28.16671

Sola, I., Almazán, F., Zúñiga, S., and Enjuanes, L. (2015). Continuous and discontinuous RNA synthesis in coronaviruses. *Ann Rev Virol* 2, 265–288. doi: 10.1146/annurev-virology-100114-055218

Sola, I., Mateos-Gomez, P. A., Almazan, F., Zuñiga, S., and Enjuanes, L. (2011). RNA-RNA and RNA-protein interactions in coronavirus replication and transcription. *RNA Biol.* 8, 237–248. doi: 10.4161/rna.8.2.14991

Sola, I., Moreno, J. L., Zuniga, S., Alonso, S., and Enjuanes, L. (2005). Role of nucleotides immediately flanking the transcription-regulating sequence core in coronavirus subgenomic mRNA synthesis. *J. Virol.* 79, 2506–2516. doi: 10.1128/JVI.79.4.2506-2516.2005

Song, Y., Guo, Y., Li, X., Sun, R., Zhu, M., Shi, J., et al. (2021). RBM39 alters phosphorylation of c-Jun and binds to viral RNA to promote PRRSV proliferation. *Front. Immunol.* 12:664417. doi: 10.3389/fimmu.2021.664417

Song, J., Liu, Y., Gao, P., Hu, Y., Chai, Y., Zhou, S., et al. (2018). Mapping the nonstructural protein interaction network of porcine reproductive and respiratory syndrome virus. *J. Virol.* 92, e01112–e01118. doi: 10.1128/JVI.01112-18

Spagnolo, J. F., and Hogue, B. G. (2000). Host protein interactions with the 3′ end of bovine coronavirus RNA and the requirement of the poly(a) tail for coronavirus defective genome replication. *J. Virol.* 74, 5053–5065. doi: 10.1128/JVI.74.11.5053-5065.2000

Spagnolo, J. F., and Hogue, B. G. (2001). Requirement of the poly(a) tail in coronavirus genome replication. *Adv. Exp. Med. Biol.* 494, 467–474. doi: 10.1007/978-1-4615-1325-4_68

Spencer, K. A., Dee, M., Britton, P., and Hiscox, J. A. (2008). Role of phosphorylation clusters in the biology of the coronavirus infectious bronchitis virus nucleocapsid protein. *Virology* 370, 373–381. doi: 10.1016/j.virol.2007.08.016

Sperry, S. M., Kazi, L., Graham, R. L., Baric, R. S., Weiss, S. R., and Denison, M. R. (2005). Single-amino-acid substitutions in open reading frame (ORF) 1b-nsp14 and ORF 2a proteins of the coronavirus mouse hepatitis virus are attenuating in mice. *J. Virol.* 79, 3391–3400. doi: 10.1128/JVI.79.6.3391-3400.2005

Spilman, M. S., Welbon, C., Nelson, E., and Dokland, T. (2009). Cryo-electron tomography of porcine reproductive and respiratory syndrome virus: organization of the nucleocapsid. *J. Gen. Virol.* 90, 527–535. doi: 10.1099/vir.0.007674-0

Stammler, S. N., Cao, S., Chen, S.-J., and Giedroc, D. P. (2011). A conserved RNA pseudoknot in a putative molecular switch domain of the 3′-untranslated region of coronaviruses is only marginally stable. *RNA* 17, 1747–1759. doi: 10.1261/rna.2816711

Stewart, H., Brown, K., Dinan, A. M., Irigoyen, N., Snijder, E. J., and Firth, A. E. (2018). Transcriptional and translational landscape of equine Torovirus. *J. Virol.* 92, e00589–e00518. doi: 10.1128/JVI.00589-18

Stohlman, S. A., Baric, R. S., Nelson, G. N., Soe, L. H., Welter, L. M., and Deans, R. J. (1988). Specific interaction between coronavirus leader RNA and nucleocapsid protein. *J. Virol.* 62, 4288–4295. doi: 10.1128/jvi.62.11.4288-4295.1988

Stueckemann, J. A., Holth, M., Swart, W. J., Kowalchyk, K., Smith, M. S., Wolstenholme, A. J., et al. (1982). Replication of lactate dehydrogenase-elevating virus in macrophages. 2. Mechanism of persistent infection in mice and cell culture. *J. Gen. Virol.* 59, 263–272. doi: 10.1099/0022-1317-59-2-263

Subissi, L., Decroly, E., Bouvet, M., Gluais, L., Canard, B., and Imbert, I. (2012). Les enzymes de la replication/transcription chez les coronavirus. *Virologie* 16, 199–209. doi: 10.1684/vir.2012.0455

Subissi, L., Posthuma, C. C., Collet, A., Zevenhoven-Dobbe, J. C., Gorbalenya, A. E., Decroly, E., et al. (2014). One severe acute respiratory syndrome coronavirus protein complex integrates processive RNA polymerase and exonuclease activities. *Proc. Natl. Acad. Sci. U. S. A.* 111, E3900–E3909. doi: 10.1073/pnas.1323705111

Sun, Y., Xue, F., Guo, Y., Ma, M., Hao, N., Zhang, X. C., et al. (2009). Crystal structure of porcine reproductive and respiratory syndrome virus leader protease Nsp1alpha. *J. Virol.* 83, 10931–10940. doi: 10.1128/JVI.02579-08

Sutton, G., Fry, E., Carter, L., Sainsbury, S., Walter, T., Nettleship, J., et al. (2004). The nsp9 replicase protein of SARS-coronavirus, structure and functional insights. *Structure* 12, 341–353. doi: 10.1016/j.str.2004.01.016

Svitkin, Y. V., Ovchinnikov, L. P., Dreyfuss, G., and Sonenberg, N. (1996). General RNA binding proteins render translation cap dependent. *EMBO J.* 15, 7147–7155. doi: 10.1002/j.1460-2075.1996.tb01106.x

Tahir, M. (2021). Coronavirus genomic nsp14-ExoN, structure, role, mechanism, and potential application as a drug target. *J. Med. Virol.* 93, 4258–4264. doi: 10.1002/jmv.27009

Tan, X., Cai, K., Li, J., Yuan, Z., Chen, R., Xiao, H., et al. (2023). Coronavirus subverts ER-phagy by hijacking FAM134B and ATL3 into p62 condensates to facilitate viral replication. *Cell Rep.* 42:112286. doi: 10.1016/j.celrep.2023.112286

Tang, C., Deng, Z., Li, X., Yang, M., Tian, Z., Chen, Z., et al. (2020). Helicase of type 2 porcine reproductive and respiratory syndrome virus strain HV reveals a unique structure. *Viruses* 12:215. doi: 10.3390/v12020215

Tatar, G., and Tok, T. T. (2016). Clarification of interaction mechanism of mouse hepatitis virus (MHV) N and nsp3 protein with homology modeling and protein-protein docking analysis. *Curr. Comput. Aided Drug Des.* 12, 98–106. doi: 10.2174/1573409912666160226131253

te Velthuis, A. J. W., Arnold, J. J., Cameron, C. E., van den Worm, S. H. E., and Snijder, E. J. (2010). The RNA polymerase activity of SARS-coronavirus nsp12 is primer dependent. *Nucleic Acids Res.* 38, 203–214. doi: 10.1093/nar/gkp904

te Velthuis, A. J. W., van den Worm, S. H. E., and Snijder, E. J. (2012). The SARS-coronavirus nsp7+nsp8 complex is a unique multimeric RNA polymerase capable of both de novo initiation and primer extension. *Nucleic Acids Res.* 40, 1737–1747. doi: 10.1093/nar/gkr893

Thiel, V., Herold, J., Schelle, B., and Siddell, S. G. (2001). Viral replicase gene products suffice for coronavirus discontinuous transcription. *J. Virol.* 75, 6676–6681. doi: 10.1128/JVI.75.14.6676-6681.2001

Thiel, V., Ivanov, K. A., Putics, Á., Hertzig, T., Schelle, B., Bayer, S., et al. (2003). Mechanisms and enzymes involved in SARS coronavirus genome expression. *J. Gen. Virol.* 84, 2305–2315. doi: 10.1099/vir.0.19424-0

Thiel, V., and Siddell, S. G. (1994). Internal ribosome entry in the coding region of murine hepatitis virus mRNA 5. *J. Gen. Virol.* 75, 3041–3046. doi: 10.1099/0022-1317-75-11-3041

Thuy, N. T., Huy, T. Q., Nga, P. T., Morita, K., Dunia, I., and Benedetti, L. (2013). A new nidovirus (NamDinh virus NDiV): its ultrastructural characterization in the C6/36 mosquito cell line. *Virology* 444, 337–342. doi: 10.1016/j.virol.2013.06.030

Tian, X., Lu, G., Gao, F., Peng, H., Feng, Y., Ma, G., et al. (2009). Structure and cleavage specificity of the chymotrypsin-like serine protease (3CLSP/nsp4) of porcine reproductive and respiratory syndrome virus (PRRSV). *J. Mol. Biol.* 392, 977–993. doi: 10.1016/j.jmb.2009.07.062

Tian, K., Yu, X., Zhao, T., Feng, Y., Cao, Z., Wang, C., et al. (2007). Emergence of fatal PRRSV variants: unparalleled outbreaks of atypical PRRS in China and molecular dissection of the unique hallmark. *PloS One* 2:e526. doi: 10.1371/journal.pone.0000526

Tijms, M. A., Nedialkova, D. D., Zevenhoven-Dobbe, J. C., Gorbalenya, A. E., and Snijder, E. J. (2007). Arterivirus subgenomic mRNA synthesis and virion biogenesis depend on the multifunctional nsp1 autoprotease. *J. Virol.* 81, 10496–10505. doi: 10.1128/JVI.00683-07

Tijms, M. A., and Snijder, E. J. (2003). Equine arteritis virus non-structural protein 1, an essential factor for viral subgenomic mRNA synthesis, interacts with the cellular transcription co-factor p100. *J. Gen. Virol.* 84, 2317–2322. doi: 10.1099/vir.0.19297-0

Tijms, M. A., van Dinten, L. C., Gorbalenya, A. E., and Snijder, E. J. (2001). A zinc finger-containing papain-like protease couples subgenomic mRNA synthesis to genome translation in a positive-stranded RNA virus. *Proc. Natl. Acad. Sci. U. S. A.* 98, 1889–1894. doi: 10.1073/pnas.98.4.1889

Tsai, T.-L., Lin, C.-H., Lin, C.-N., Lo, C.-Y., and Wu, H.-Y. (2018). Interplay between the poly(a) tail, poly(a)-binding protein, and coronavirus Nucleocapsid protein regulates gene expression of coronavirus and the host cell. *J. Virol.* 92, e01162–e01118. doi: 10.1128/JVI.01162-18

Tseng, Y. T., Wang, S. M., Huang, K. J., Lee, A. I., Chiang, C. C., and Wang, C. T. (2010). Self-assembly of severe acute respiratory syndrome coronavirus membrane protein. *J. Biol. Chem.* 285, 12862–12872. doi: 10.1074/jbc.M109.030270

Turlewicz-Podbielska, H., and Pomorska-Mol, M. (2021). Porcine coronaviruses: overview of the state of the art. *Virol. Sin.* 36, 833–851. doi: 10.1007/s12250-021-00364-0

Twu, W. I., Lee, J. Y., Kim, H., Prasad, V., Cerikan, B., Haselmann, U., et al. (2021). Contribution of autophagy machinery factors to HCV and SARS-CoV-2 replication organelle formation. *Cell Rep.* 37:110049. doi: 10.1016/j.celrep.2021.110049

Ujike, M., and Taguchi, F. (2021). Recent Progress in Torovirus molecular biology. *Viruses* 13:435. doi: 10.3390/v13030435

Ulasli, M., Verheije, M. H., de Haan, C. A. M., and Reggiori, F. (2010). Qualitative and quantitative ultrastructural analysis of the membrane rearrangements induced by coronavirus. *Cell. Microbiol.* 12, 844–861. doi: 10.1111/j.1462-5822.2010.01437.x

Ulferts, R., and Ziebuhr, J. (2011). Nidovirus ribonucleases: structures and functions in viral replication. *RNA Biol.* 8, 295–304. doi: 10.4161/rna.8.2.15196

Vabret, A., Mourez, T., Gouarin, S., Petitjean, J., and Freymuth, F. (2003). An outbreak of coronavirus OC43 respiratory infection in Normandy, France. *Clin. Infect. Dis.* 36, 985–989. doi: 10.1086/374222

Valcarcel, J., and Gebauer, F. (1997). Post-transcriptional regulation: the dawn of PTB. *Curr. Biol.* 7, R705–R708. doi: 10.1016/S0960-9822(06)00361-7

van den Born, E., Posthuma, C. C., Gultyaev, A. P., and Snijder, E. J. (2005). Discontinuous subgenomic RNA synthesis in arteriviruses is guided by an RNA hairpin structure located in the genomic leader region. *J. Virol.* 79, 6312–6324. doi: 10.1128/JVI.79.10.6312-6324.2005

van der Hoek, L., Pyrc, K., Jebbink, M. F., Vermeulen-Oost, W., Berkhout, R. J. M., Wolthers, K. C., et al. (2004). Identification of a new human coronavirus. *Nat. Med.* 10, 368–373. doi: 10.1038/nm1024

van der Hoeven, B., Oudshoorn, D., Koster, A. J., Snijder, E. J., Kikkert, M., and Bárcena, M. (2016). Biogenesis and architecture of arterivirus replication organelles. *Virus Res.* 220, 70–90. doi: 10.1016/j.virusres.2016.04.001

van der Meer, Y., van Tol, H., Locker, J. K., and Snijder, E. J. (1998). ORF1a-encoded replicase subunits are involved in the membrane association of the arterivirus replication complex. *J. Virol.* 72, 6689–6698. doi: 10.1128/JVI.72.8.6689-6698.1998

van Hemert, M. J., de Wilde, A. H., Gorbalenya, A. E., and Snijder, E. J. (2008). The in vitro RNA synthesizing activity of the isolated arterivirus replication/transcription complex is dependent on a host factor. *J. Biol. Chem.* 283, 16525–16536. doi: 10.1074/jbc.M708136200

van Kasteren, P. B., Beugeling, C., Ninaber, D. K., Frias-Staheli, N., van Boheemen, S., García-Sastre, A., et al. (2012). Arterivirus and nairovirus ovarian tumor domain-containing Deubiquitinases target activated RIG-I to control innate immune signaling. *J. Virol.* 86, 773–785. doi: 10.1128/JVI.06277-11

van Marle, G., Dobbe, J. C., Gultyaev, A. P., Luytjes, W., Spaan, W. J., and Snijder, E. J. (1999). Arterivirus discontinuous mRNA transcription is guided by base pairing between sense and antisense transcription-regulating sequences. *Proc. Natl. Acad. Sci. U. S. A.* 96, 12056–12061. doi: 10.1073/pnas.96.21.12056

Van Regenmortel, M. (2000). *International committee on taxonomy of viruses. Virus taxonomy: Classification and nomenclature of viruses: Seventh report of the international committee on taxonomy of viruses*. San Diego: Academic.

van Vliet, A. L. W., Smits, S. L., Rottier, P. J. M., and de Groot, R. J. (2002). Discontinuous and non-discontinuous subgenomic RNA transcription in a nidovirus. *EMBO J.* 21, 6571–6580. doi: 10.1093/emboj/cdf635

Vasilakis, N., Guzman, H., Firth, C., Forrester, N. L., Widen, S. G., Wood, T. G., et al. (2014). Mesoniviruses are mosquito-specific viruses with extensive geographic distribution and host range. *Virol. J.* 11:97. doi: 10.1186/1743-422X-11-97

Vatter, H. A., Di, H., Donaldson, E. F., Radu, G. U., Maines, T. R., and Brinton, M. A. (2014). Functional analyses of the three simian hemorrhagic fever virus nonstructural protein 1 papain-like proteases. *J. Virol.* 88, 9129–9140. doi: 10.1128/JVI.01020-14

Venkatagopalan, P., Daskalova, S. M., Lopez, L. A., Dolezal, K. A., and Hogue, B. G. (2015). Coronavirus envelope (E) protein remains at the site of assembly. *Virology* 478, 75–85. doi: 10.1016/j.virol.2015.02.005

Verheije, M. H., Kroese, M. V., Rottier, P. J. M., and Meulenberg, J. J. M. (2001). Viable porcine arteriviruses with deletions proximal to the 3′ end of the genome. *J. Gen. Virol.* 82, 2607–2614. doi: 10.1099/0022-1317-82-11-2607

Verheije, M. H., Olsthoorn, R. C., Kroese, M. V., Rottier, P. J., and Meulenberg, J. J. (2002). Kissing interaction between 3′ noncoding and coding sequences is essential for porcine arterivirus RNA replication. *J. Virol.* 76, 1521–1526. doi: 10.1128/JVI.76.3.1521-1526.2002

Vögele, J., Ferner, J.-P., Altincekic, N., Bains, J. K., Ceylan, B., Fürtig, B., et al. (2021). H, C, N and P chemical shift assignment for stem-loop 4 from the 5'-UTR of SARS-CoV-2. *Biomol. NMR Assign.* 15, 335–340. doi: 10.1007/s12104-021-10026-7

Wada, R., Fukunaga, Y., Kondo, T., and Kanemaru, T. (1995). Ultrastructure and immuno-cytochemistry of BHK-21 cells infected with a modified Bucyrus strain of equine arteritis virus. *Arch. Virol.* 140, 1173–1180. doi: 10.1007/BF01322744

Walker, P. J., Cowley, J. A., Dong, X., Huang, J., Moody, N., Ziebuhr, J., et al. (2021). ICTV virus taxonomy profile. *J. Gen. Virol.* 102:jgv001514. doi: 10.1099/jgv.0.001514

Walker, P. J., Siddell, S. G., Lefkowitz, E. J., Mushegian, A. R., Dempsey, D. M., Dutilh, B. E., et al. (2019). Changes to virus taxonomy and the international code of virus classification and nomenclature ratified by the international committee on taxonomy of viruses (2019). *Arch. Virol.* 164, 2417–2429. doi: 10.1007/s00705-019-04306-w

Wang, X., Bai, J., Zhang, L., Wang, X., Li, Y., and Jiang, P. (2012). Poly(a)-binding protein interacts with the nucleocapsid protein of porcine reproductive and respiratory syndrome virus and participates in viral replication. *Antiviral Res.* 96, 315–323. doi: 10.1016/j.antiviral.2012.09.004

Wang, J., Fang, S., Xiao, H., Chen, B., Tam, J. P., and Liu, D. X. (2009). Interaction of the coronavirus infectious bronchitis virus membrane protein with beta-actin and its implication in virion assembly and budding. *PloS One* 4:e4908. doi: 10.1371/journal.pone.0004908

Wang, D., Jiang, A., Feng, J., Li, G., Guo, D., Sajid, M., et al. (2021). The SARS-CoV-2 subgenome landscape and its novel regulatory features. *Mol. Cell* 81, 2135–2147.e5. doi: 10.1016/j.molcel.2021.02.036

Wang, B., Svetlov, D., and Artsimovitch, I. (2021). NMPylation and de-NMPylation of SARS-CoV-2 nsp9 by the NiRAN domain. *Nucleic Acids Res.* 49, 8822–8835. doi: 10.1093/nar/gkab677

Wang, Q., Wu, J., Wang, H., Gao, Y., Liu, Q., Mu, A., et al. (2020). Structural basis for RNA replication by the SARS-CoV-2 polymerase. *Cells* 182:34. doi: 10.1016/j.cell.2020.05.034

Wang, M. D., Yang, L., Meng, J. J., Pan, J. J., Zhang, C., Wan, B., et al. (2021). Functionally active cyclin-dependent kinase 9 is essential for porcine reproductive and respiratory syndrome virus subgenomic RNA synthesis. *Mol. Immunol.* 135, 351–364. doi: 10.1016/j.molimm.2021.05.004

Wang, Y., and Zhang, X. (1999). The nucleocapsid protein of coronavirus mouse hepatitis virus interacts with the cellular heterogeneous nuclear ribonucleoprotein A1 in vitro and in vivo. *Virology* 265, 96–109. doi: 10.1006/viro.1999.0025

Weiland, F., Granzow, H., Wieczorek-Krohmer, M., and Weiland, E. (1995). "Electron microscopic studies on the morphogenesis of PRRSV in infected cells—comparative studies", in Immunobiology of viral infections. In: *Proceedings of the 3rd Congress of the European Society of Veterinary Virology*, 499–502.

Wijegoonawardane, P. K. M., Cowley, J. A., Phan, T., Hodgson, R. A. J., Nielsen, L., Kiatpathomchai, W., et al. (2008). Genetic diversity in the yellow head nidovirus complex. *Virology* 380, 213–225. doi: 10.1016/j.virol.2008.07.005

Wissink, E. H. J., Kroese, M. V., van Wijk, H. A. R., Rijsewijk, F. A. M., Meulenberg, J. J. M., and Rottier, P. J. M. (2005). Envelope protein requirements for the assembly of infectious virions of porcine reproductive and respiratory syndrome virus. *J. Virol.* 79, 12495–12506. doi: 10.1128/JVI.79.19.12495-12506.2005

Wolff, G., Limpens, R. W. A. L., Zevenhoven-Dobbe, J. C., Laugks, U., Zheng, S., de Jong, A. W. M., et al. (2020). A molecular pore spans the double membrane of the coronavirus replication organelle. *Science* 369, 1395–1398. doi: 10.1126/science.abd3629

Woo, P. C. Y., Lau, S. K. P., Chu, C.-M., Chan, K.-H., Tsoi, H.-W., Huang, Y., et al. (2005). Characterization and complete genome sequence of a novel coronavirus, coronavirus HKU1, from patients with pneumonia. *J. Virol.* 79, 884–895. doi: 10.1128/JVI.79.2.884-895.2005

Woo, P. C., Lau, S. K., Huang, Y., and Yuen, K. Y. (2009). Coronavirus diversity, phylogeny and interspecies jumping. *Exp. Biol. Med.* 234, 1117–1127. doi: 10.3181/0903-MR-94

Wood, O., Tauraso, N., and Liebhaber, H. (1970). Electron microscopic study of tissue cultures infected with simian haemorrhagic fever virus. *J. Gen. Virol.* 7, 129–136. doi: 10.1099/0022-1317-7-2-129

Wu, H. Y., and Brian, D. A. (2010). Subgenomic messenger RNA amplification in coronaviruses. *Proc. Natl. Acad. Sci. U. S. A.* 107, 12257–12262. doi: 10.1073/pnas.1000378107

Wu, C. H., Chen, P. J., and Yeh, S. H. (2014). Nucleocapsid phosphorylation and RNA helicase DDX1 recruitment enables coronavirus transition from discontinuous to continuous transcription. *Cell Host Microbe* 16, 462–472. doi: 10.1016/j.chom.2014.09.009

Wu, C. H., Yeh, S. H., Tsay, Y. G., Shieh, Y. H., Kao, C. L., Chen, Y. S., et al. (2009). Glycogen synthase kinase-3 regulates the phosphorylation of severe acute respiratory syndrome coronavirus nucleocapsid protein and viral replication. *J. Biol. Chem.* 284, 5229–5239. doi: 10.1074/jbc.M805747200

Xu, L., Khadijah, S., Fang, S., Wang, L., Tay, F. P., and Liu, D. X. (2010). The cellular RNA helicase DDX1 interacts with coronavirus nonstructural protein 14 and enhances viral replication. *J. Virol.* 84, 8571–8583. doi: 10.1128/JVI.00392-10

Yan, L., Ge, J., Zheng, L., Zhang, Y., Gao, Y., Wang, T., et al. (2021). Cryo-EM structure of an extended SARS-CoV-2 replication and transcription complex reveals an intermediate state in cap synthesis. *Cells* 184, 184–193 e110. doi: 10.1016/j.cell.2020.11.016

Yan, L., Zhang, Y., Ge, J., Zheng, L., Gao, Y., Wang, T., et al. (2020). Architecture of a SARS-CoV-2 mini replication and transcription complex. *Nat. Commun.* 11:5874. doi: 10.1038/s41467-020-19770-1

Yang, D., Liu, P., Giedroc, D. P., and Leibowitz, J. (2011). Mouse hepatitis virus stem-loop 4 functions as a spacer element required to drive subgenomic RNA synthesis. *J. Virol.* 85, 9199–9209. doi: 10.1128/JVI.05092-11

Yang, D., Liu, P., Wudeck, E. V., Giedroc, D. P., and Leibowitz, J. L. (2015). SHAPE analysis of the RNA secondary structure of the mouse hepatitis virus 5′ untranslated region and N-terminal nsp1 coding sequences. *Virology* 475, 15–27. doi: 10.1016/j.virol.2014.11.001

Yang, Y., Yan, W., Hall, A. B., and Jiang, X. (2021). Characterizing transcriptional regulatory sequences in coronaviruses and their role in recombination. *Mol. Biol. Evol.* 38, 1241–1248. doi: 10.1093/molbev/msaa281

Yu, W., and Leibowitz, J. L. (1995a). A conserved motif at the 3′ end of mouse hepatitis virus genomic RNA required for host protein binding and viral RNA replication. *Virology* 214, 128–138. doi: 10.1006/viro.1995.9947

Yu, W., and Leibowitz, J. L. (1995b). Specific binding of host cellular proteins to multiple sites within the 3′ end of mouse hepatitis virus genomic RNA. *J. Virol.* 69, 2016–2023. doi: 10.1128/JVI.69.4.2016-2023.1995

Zaki, A. M., van Boheemen, S., Bestebroer, T. M., Osterhaus, A. D. M. E., and Fouchier, R. A. M. (2012). Isolation of a novel coronavirus from a man with pneumonia in Saudi Arabia. *N. Engl. J. Med.* 367, 1814–1820. doi: 10.1056/NEJMoa1211721

Zhang, X., Chu, H., Chik, K. K., Wen, L., Shuai, H., Yang, D., et al. (2022). hnRNP C modulates MERS-CoV and SARS-CoV-2 replication by governing the expression of a subset of circRNAs and cognitive mRNAs. *Emerg. Microbes Infect.* 11, 519–531. doi: 10.1080/22221751.2022.2032372

Zhang, X., and Lai, M. M. (1995). Interactions between the cytoplasmic proteins and the intergenic (promoter) sequence of mouse hepatitis virus RNA: correlation with the amounts of subgenomic mRNA transcribed. *J. Virol.* 69, 1637–1644. doi: 10.1128/jvi.69.3.1637-1644.1995

Zhang, J., Lan, Y., and Sanyal, S. (2020). Membrane heist: coronavirus host membrane remodeling during replication. *Biochimie* 179, 229–236. doi: 10.1016/j.biochi.2020.10.010

Zhang, M., Li, X., Deng, Z., Chen, Z., Liu, Y., Gao, Y., et al. (2017). Structural biology of the Arterivirus nsp11 Endoribonucleases. *J. Virol.* 91, e01309–e01316. doi: 10.1128/JVI.01309-16

Zhang, X., Li, H. P., Xue, W., and Lai, M. M. (1999). Formation of a ribonucleoprotein complex of mouse hepatitis virus involving heterogeneous nuclear ribonucleoprotein A1 and transcription-regulatory elements of viral RNA. *Virology* 264, 115–124. doi: 10.1006/viro.1999.9970

Zhang, L., Lin, D., Sun, X., Curth, U., Drosten, C., Sauerhering, L., et al. (2020). Crystal structure of SARS-CoV-2 main protease provides a basis for design of improved α-ketoamide inhibitors. *Science* 368, 409–412. doi: 10.1126/science.abb3405

Zhang, Z., Nomura, N., Muramoto, Y., Ekimoto, T., Uemura, T., Liu, K., et al. (2022). Structure of SARS-CoV-2 membrane protein essential for virus assembly. *Nat. Commun.* 13:4399. doi: 10.1038/s41467-022-32019-3

Zhang, L., Pan, Y., Xu, Y., Zhang, W., Ma, W., Ibrahim, Y. M., et al. (2022). Paraoxonase-1 facilitates PRRSV replication by interacting with viral nonstructural Protein-9 and inhibiting type I interferon pathway. *Viruses* 14:1203. doi: 10.3390/v14061203

Zhang, H., Sha, H., Qin, L., Wang, N., Kong, W., Huang, L., et al. (2022). Research Progress in porcine reproductive and respiratory syndrome virus-host protein interactions. *Animals* 12:1381. doi: 10.3390/ani12111381

Zhang, X., Shi, H., Chen, J., Shi, D., Dong, H., and Feng, L. (2015). Identification of the interaction between vimentin and nucleocapsid protein of transmissible gastroenteritis virus. *Virus Res.* 200, 56–63. doi: 10.1016/j.virusres.2014.12.013

Zhao, S., Ge, X., Wang, X., Liu, A., Guo, X., Zhou, L., et al. (2015). The DEAD-box RNA helicase 5 positively regulates the replication of porcine reproductive and respiratory syndrome virus by interacting with viral Nsp9 in vitro. *Virus Res.* 195, 217–224. doi: 10.1016/j.virusres.2014.10.021

Zhao, J., Qiu, J., Aryal, S., Hackett, J. L., and Wang, J. (2020). The RNA architecture of the SARS-CoV-2 3'-Untranslated region. *Viruses* 12:1473. doi: 10.3390/v12121473

Zhu, N., Zhang, D., Wang, W., Li, X., Yang, B., Song, J., et al. (2020). A novel coronavirus from patients with pneumonia in China, 2019. *N. Engl. J. Med.* 382, 727–733. doi: 10.1056/NEJMoa2001017

Ziebuhr, J., Snijder, E. J., and Gorbalenya, A. E. (2000). Virus-encoded proteinases and proteolytic processing in the Nidovirales. *J. Gen. Virol.* 81, 853–879. doi: 10.1099/0022-1317-81-4-853

Ziebuhr, J., Thiel, V., and Gorbalenya, A. E. (2001). The autocatalytic release of a putative RNA virus transcription factor from its polyprotein precursor involves two paralogous papain-like proteases that cleave the same peptide bond. *J. Biol. Chem.* 276, 33220–33232. doi: 10.1074/jbc.M104097200

Zirkel, F., Kurth, A., Quan, P.-L., Briese, T., Ellerbrok, H., Pauli, G., et al. (2011). An insect nidovirus emerging from a primary tropical rainforest. *MBio* 2, e00077–e00011. doi: 10.1128/mBio.00077-11

Zirkel, F., Roth, H., Kurth, A., Drosten, C., Ziebuhr, J., and Junglen, S. (2013). Identification and characterization of genetically divergent members of the newly established family Mesoniviridae. *J. Virol.* 87, 6346–6358. doi: 10.1128/JVI.00416-13

Zúñiga, S., Cruz, J. L. G., Sola, I., Mateos-Gómez, P. A., Palacio, L., and Enjuanes, L. (2010). Coronavirus nucleocapsid protein facilitates template switching and is required for efficient transcription. *J. Virol.* 84, 2169–2175. doi: 10.1128/JVI.02011-09

Zúñiga, S., Sola, I., Alonso, S., and Enjuanes, L. (2004). Sequence motifs involved in the regulation of discontinuous coronavirus subgenomic RNA synthesis. *J. Virol.* 78, 980–994. doi: 10.1128/JVI.78.2.980-994.2004

Zuo, D., Chen, Y., Cai, J. P., Yuan, H. Y., Wu, J. Q., Yin, Y., et al. (2023). A hnRNPA2B1 agonist effectively inhibits HBV and SARS-CoV-2 omicron in vivo. *Protein Cell* 14, 37–50. doi: 10.1093/procel/pwac027

Zust, R., Miller, T. B., Goebel, S. J., Thiel, V., and Masters, P. S. (2008). Genetic interactions between an essential 3′ cis-acting RNA pseudoknot, replicase gene products, and the extreme 3′ end of the mouse coronavirus genome. *J. Virol.* 82, 1214–1228. doi: 10.1128/JVI.01690-07

Frontiers in Microbiology

Explores the habitable world and the potential of microbial life

The largest and most cited microbiology journal which advances our understanding of the role microbes play in addressing global challenges such as healthcare, food security, and climate change.

Discover the latest Research Topics

See more →

Frontiers

Avenue du Tribunal-Fédéral 34
1005 Lausanne, Switzerland
frontiersin.org

Contact us

+41 (0)21 510 17 00
frontiersin.org/about/contact